AD-A012 495

SHIP MOTIONS AND CAPSIZING IN ASTERN SEAS

S. J. Chou, et al

California University

Prepared for:

Coast Guard

December 1974

210083

Report No. CG-D-103-75

ADA012495

SHIP MOTIONS AND CAPSIZING IN ASTERN SEAS

S. J. CHOU

O. H. OAKLEY

J. R. PAULLING

R. VAN SLYKE

P. D. WOOD

P. F. ZINK

FINAL REPORT FOR PERIOD

AUGUST 1970 - DECEMBER 1974

DECEMBER 1974

Document is available to the public through the National Technical Information Service, Springfield, Virginia 22151

Prepared for

DEPARTMENT OF TRANSPORTATION
UNITED STATES COAST GUARD
Office of Research and Development
Washington, D.C. 20590

2 JUN 1975

The work reported herein was accomplished for the U.S. Coast Guard's Office of Research and Development, Marine Safety Technology Division, as part of its program in Commercial Vessel Safety.

The contents of this report reflect the views of S. J. Chou, O. H. Oakley, Jr., J. R. Paulling, R. Van Slyke, P. D. Wood, P. F. Zink, who are responsible for the facts and the accuracy of the data presented herein. The contents do not necessarily reflect the official views or policy of the Coast Guard. This report does not constitute a standard, specification, or regulation.

Reviewed By : J. R. AMY
Project Officer

Submitted By: J. M. CECE, Ph.D.
CDR, U.S. Coast Guard
Chief, Marine Safety Projects Branch

Released By : W. D. MARKLE, JR.
CAPT, U.S. Coast Guard
Chief, Marine Safety Technology Division
Office of Research and Development
U.S. Coast Guard Headquarters
Washington, D..C 20590

Technical Report Documentation Page

1. Report No. CG-D-103-75	2. Government Accession No.	3. Recipient's Catalog No.
4. Title and Subtitle: Ship Motions and Capsizing in Astern Seas		5. Report Date: December 1974
		6. Performing Organization Code
7. Author(s): S. J. Chou, O. H. Oakley, Jr., J. R. Paulling, R. Van Slyke, P. D. Wood, P. F. Zink		8. Performing Organization Report No.
9. Performing Organization Name and Address: Department of Naval Architecture, University of California, Berkeley, California		10. Work Unit No. (TRAIS)
		11. Contract or Grant No. DOT-CG-84,545-A
12. Sponsoring Agency Name and Address: Department of Transportation, United States Coast Guard, Washington, D.C.		13. Type of Report and Period Covered: Final Report for Period August 1970 - December 1974
		14. Sponsoring Agency Code
15. Supplementary Notes		

16. Abstract

An analytical and experimental study of ship motions and capsizing in extreme seas has been conducted. The analysis of linear and quasi-linear one-dimensional roll models has revealed motion anomalies not apparent from the usual linearized ship motion theory. Extensive tests have been conducted using two radio-controlled models in the wind generated seas of San Francisco Bay. Directional spectra were computed, using a variety of techniques, from the wave measurements by an array of wave gages. Comparisons of the experimentally determined motions and a linear strip theory prediction are presented. A time domain numerical simulation program for motions and capsizing has been used to investigate motions in a variety of wave group configurations. The results show good agreement with observed capsizing phenomena and have revealed a number of important characteristics associated with large geometry changes in waves.

17. Key Words: Ship Motions; Capsizing; Wave Group Analysis; Directional Wave Spectra	18. Distribution Statement: Document is available to the public through the National Technical Information Service, Springfield, Va. 22151

PRICES SUBJECT TO CHANGE

19. Security Classif. (of this report)	20. Security Classif. (of this page)	21. No. of Pages	22. Price
Unclassified	Unclassified	341	9.50 2.25

Form DOT F 1700.7 (8-72) Reproduction of completed page authorized

SHIP MOTIONS AND CAPSIZING IN ASTERN SEAS

FINAL REPORT

by

S. J. Chou[3]
O. H. Oakley, Jr.[2]
J. R. Paulling[1]
R. Van Slyke[3]
P. D. Wood[3]
P. F. Zink[3]

Department of Naval Architecture
University of California
Berkeley, California

December 1974

Final Report for Period August 1970 - December 1974

Prepared for

DEPARTMENT OF TRANSPORTATION
UNITED STATES COAST GUARD
WASHINGTON, D.C.

Contract DOT-CG-84,549-A

1. Professor of Naval Architecture
2. Associate Research Engineer
3. Graduate Student

ia

ABSTRACT

An analytical and experimental study of ship motions and capsizing in extreme seas has been conducted. The analysis of linear and quasi-linear one-dimensional roll models has revealed motion anomalies not apparent from the usual linearized ship motion theory. Extensive tests have been conducted using two radio-controlled models in the wind generated seas of San Francisco Bay. Directional spectra were computed, using a variety of techniques, from the wave measurements by an array of wave gages. Comparisons of the experimentally determined motions and a linear strip theory prediction are presented. A time domain numerical simulation program for motions and capsizing has been used to investigate motions in a variety of wave group configurations. The results show good agreement with observed capsizing phenomena and have revealed a number of important characteristics associated with large geometry changes in waves.

TABLE OF CONTENTS

List of Figures

LIST OF TABLES

I. INTRODUCTION

Stability against capsizing in heavy seas is one of the most fundamental requirements considered by the naval architect when designing a ship. At the same time it is one of the least understood phenomena in the realm of ship motion theory. By its very nature, stability is concerned with extreme motion both of ship and waves. Therefore, the linearized methods of wave and ship motion analysis which have received so much attention in recent years cannot be applied here with any expectation of obtaining directly useable results, but may be used only for general guidance. Statistically, capsizing falls into the category of events of rare occurence, again calling for special techniques in studying its probability distributions.

The basic purpose of studying capsizing is to establish prediction techniques which may be used by naval architects during the design process. Even though traditional empirical methods have apparently been successful in insuring adequate stability of conventional ships built in the past, it is expected that the future will see more rapid evolution in ship size, speed, geometry, and performance requirements. Some of the new, high performance ship types may be expected to experience motion, control, and even stability problems when operating in severe seas which are not susceptible to prediction or remedy by traditional empirical methods. The more general goal of our study, therefore, is to establish a basis of understanding of phenomena associated with the operation of ships in severe seas and to relate these ship behavior phenomena to the geometrical and operational characteristics of the ship.

Model experiments conducted under conditions which are as realistic as possible in simulating a severe storm sea environment offer the best initial means of gaining this understanding. At the present time, there are no towing tanks which have the capability of producing realistic short-crested seas of sufficient severity. Further, the infrequent nature of the capsizing event indicates that experimental runs of considerable length will be required, especially in following seas where the frequency of wave encounter is low. The testing of free-running radio-controlled models in an open water area in natural wind-generated waves is an alternative to tank testing that has been successfully used for this purpose in the past.

As is the case of all experiments conducted in a natural environment, there is the difficulty of controlling the conditions of the test. However, the two principal requirements enumerated above: steep short-crested waves and virtually unlimited length of run are available only in this way.

The first experiments of this type were conducted by a group working under the direction of Professor Kurt Wendel at the universities of Hamburg and Hannover in Germany. Their work clearly pointed out the value of open water testing as a means of studying capsizing. Partly as a result of the success of Wendel, the present capsizing study was initiated in 1969 at the University of California under the sponsorship of the U.S. Coast Guard. This research started with a program of model testing in the open waters of San Francisco Bay. Concurrently with the model experiments, analytical work has been carried out in two general areas:

1. Work supporting the experiments themselves, e.g., the development of procedures for data processing.
2. Studies of certain aspects of ship motion complementary to the experiments as an aid in the design of the experiments or as a means of explaining experimental results. Especially noteworthy of work conducted in the first category, a thorough evaluation has been made of available techniques for the directional analysis of wave spectra using measurements made with sparse wave gage arrays. This has led to the development of a new method of analysis of directional spectra.

In the second category, several reports (in the form of student theses) have investigated areas of nonlinear ship motion analysis by either new techniques or in greater detail than before in an attempt to obtain insight and understanding of ship behavior anomalies observed experimentally. Some of these results may be found in Haddara (1971), Perez (1972) Oakley (1973), Paulling and Wood (1973), and later sections of the present report. A paper presented before the Tenth Naval Hydrodynamics Symposium, Oakley, *et al.* (1974) forms the nucleus for the present report.

Experiments have now been completed with two models, one a conventional cargo ship and the other, a fast twin screw container ship. As a result of these experiments and concurrent analytical work,a great deal has been learned about the mechanism of capsizing. This understanding has led to the development of a numerical simulation of the large amplitude motion of the ship in certain capsizing situations . It is now possible to duplicate on a computer certain important aspects of the motion of the model observed during the experiments. The numerical computation, however, has one drawback in common with other time-domain simulation techniques — it has an exorbitant appetite for computer time. It does not appear economically feasible using present-generation machines to numerically simulate a complete experimental run, not to mention a ship lifetime of experience. However, an important observation made during the experiments suggests how this difficulty may be overcome. It was observed that severe motions, control difficulties and capsizings of the model almost invariably occurred when the model encountered a wave group consisting of several especially steep and nearly regular waves. Such wave groups characteristically occur from time to time in the midst of a random seaway. While the statistics of their occurrence apparently have not been extensively studied, there is some indication that it is possible to derive the expressions relating the frequency of occurrence of groups having specified characteristics to the energy spectrum of the seaway.

The experimental observation then suggests that the probability of capsizing may be related to the probability of the ship encountering a wave group having the characteristics necessary to cause capsizing. The numerical simulation technique noted above would be used only to study the ship behavior in wave groups consisting of a small number of individual waves in order to define the critical group characteristics for capsizing. The long term statistics associated with the prediction of capsizing would then be divorced from the mechanism of capsizing and would be concerned only with the prediction of the probability of the ship encountering wave groups having the critical characteristics. Thus long computer simulation runs would be unnecessary.

Since the problem of predicting the occurrence of wave groups has received so little attention in the past, it forms a subject for study under the present work. Evaluations of some previously proposed prediction techniques are given using experimental wave data obtained in the present study. Also, some suggestions are made for the future direction which this work should take.

II. LINEAR AND QUASI-LINEAR MOTION COMPUTATIONS

As noted in the INTRODUCTION modern ship motion research has been mostly concerned with small amplitude motion which is amenable to a linearized dynamic-hydrodynamic analysis. The The practical implementation of such procedures has been most successfully obtained in the strip-method of computation as exemplified by the work of Salvesen, Tuck, and Faltinsen (1970). It is safe to say that the strip calculation now provides a workable design tool for predicting the average seakeeping performance of a proposed ship early in the design process.

Performance predictions, however, are usually concerned with the average behavior of the ship over long periods of time encompassing, e.g., the length of a voyage and tens of thousands or hundreds of thousands of wave encounters, rather than the short intervals which the ship spends in extremely severe seas. Performance characteristics which have been successfully described by linear procedures are ship motions, structural loads, stresses and even occurrence of seemingly nonlinear large-amplitude phenomena such as the frequency of slamming and bow immersion. Prerequisite to a study of performance but not part of it is survivability. In contrast to the average conditions with which performance estimates are concerned, a study of survivability addresses itself to the extreme sea and motion conditions having a very low probability of occurrence. Thus, by definition, in studying capsizing of ships in extreme seas, we are concerned with the largest, steepest waves which the ship may encounter during her lifetime (sometimes at its very end!), and with motions of such large amplitude, that they are well beyond the range of a linear ship motion analysis. Nevertheless, it is useful to review some of the features of linear motion theory in hopes that its results may provide some guidance and insight into certain phenomena of concern in a study of capsizing. Further insight and new phenomena may also be revealed by certain nonlinear theoretical procedures which have been developed to augment linear ship motion theory.

In a study of capsizing, what results of interest may be obtained from linear motion theory? The first which suggests itself is resonant rolling. Although a linear analysis of roll does not accurately describe the details of the motion at large amplitudes, some of the properties of this mode of motion may be revealed. For example, there is substantial evidence that rolling motion in beam seas in the absence of other effects is not likely to result in danger to the ship. The vessel may roll to very large angles if the frequency content of the sea is in the right relationship to the natural frequency of the ship, but in order for her to be placed in danger of capsizing, additional factors must be present. These may include strong wind heeling moments, damage to the watertight envelope of the ship resulting in the flooding of a portion of the interior and the entrapment of large quantities of water on deck by bulwarks.

Tests of the range of applicability of the linear ship motion technique have been made by Dalzell, and some of his results for the Mariner-type ship were reported in a discussion to a paper by Ochi (1964). Pitch and heave motions were measured in regular waves of various steepness. For waves more than 1.75 times the model length these motions show a linear behavior with wave height for values of wave height to length ratio up to 1/12. In the shorter waves, the pitch motion appeared to drop somewhat below a straight line relationship for the higher waves, i.e. the graph of pitch versus wave height was concave downward in these waves.

Figure II-1 shows some results obtained at the University of California from experiments and corresponding calculations of the relative rolling motion between the ship model and wave surface. The experiments and calculations were carried to moderately large angles and show reasonably good correlation. The important characteristic of this motion is its tendency to

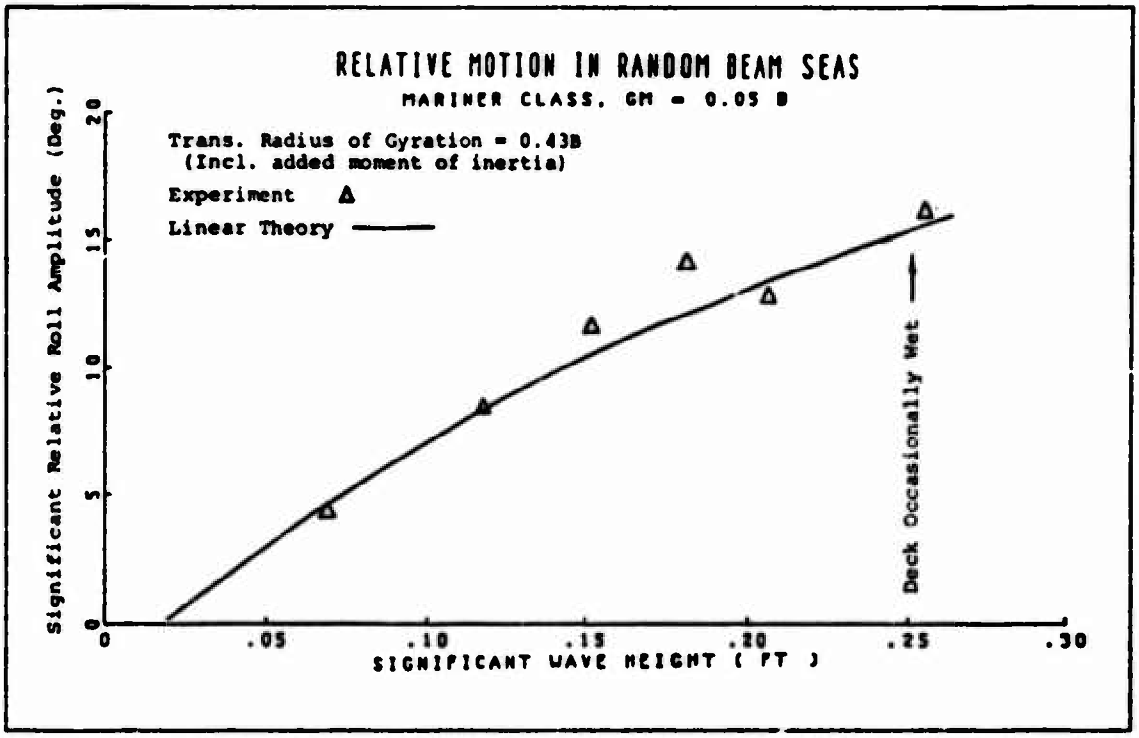

Figure II-1

level off in increasingly higher sea states. Since the relative rolling motion is more important than the absolute roll in relation to such effects as water entrapment on deck, this suggest that the effects of increasingly severe sea states tends to level off.

These calculations were made using a linear approximation to the ship righting arm curve equal to displacement times the initial metacentric height. The quadratic roll damping was approximated by an equivalent linear damping coefficient. The trend of this curve illustrates the degree of agreement that may be expected in comparing linear calculations with experiments. The maximum wave steepness, however, is not in the extreme or survival range.

It is also useful, at this point, to look at some results of nonlinear ship motion theory. Two topics of ship dynamics have been studied using nonlinear equations of motion: maneuvering in calm water, and rolling in beam seas. In both cases, the procedure has been to include terms in the equations of motion representing forces which depend in a nonlinear manner upon some of the unknown motion variables. Most commonly, these have been damping forces assumed to vary as the square of velocity or more general forces which, by reason of symmetry , behave as odd functions and may therefore be expressed by cubic terms in all velocities and accelerations. In principle, these terms represent higher order terms in a Taylor series expansion of the total force on the ship, where the force is assumed to depend in some unknown way upon the relevant instantaneous motion variables. Many of the terms can, in fact, be related to specific physical effects, e.g., the above noted viscous drag which varies in a nonlinear manner with velocity.

The results of including nonlinear terms in the equations of motion are twofold . First, behavior which might be obtained by a conventional linear analysis is modified somewhat without changing its basic nature. Second, new phenomena may be revealed which are not present in the linear results. We shall look at examples of each of these cases and attempt to relate them to the capsizing problem.

In studying the large amplitude rolling motion of ships in beam seas, the method of equivalent linearization has been utilized by several investigators, e.g. Vassilopoulos (1971) and St. Denis (1967). Equivalent linearization is a method which is generally suitable for describing a dynamic system in which large deviations from linear behavior are not anticipated, (weak nonlinearity). A reasonable approximation to the exact behavior of the real system, therefore, is given by an equivalent linear system having linear coefficients appropriately selected. The principal shortcoming to the method, in common with most approximation methods, is that the limits of applicability or degree of approximation are difficult to estimate.

In applying equivalent linearization, one writes a set of linear differential equations to describe the behavior of the real nonlinear system. The coefficients of the linear equations are then chosen in such a way that the behavior of the solution is, in some way, equivalent to the behavior of the real system. To illustrate this technique let us consider

$$I_x\ddot{\phi}+D(\dot{\phi})+R(\phi)=K_e(t) \quad , \tag{II-1}$$

where $D(\dot{\phi})$ and $R(\phi)$ are the damping and restoring moments respectively. Let us further restrict the problem by assuming sinusoidal excitation and an exact damping moment which varies quadratically with roll velocity

$$D(\dot{\phi})=C_q\dot{\phi}|\dot{\phi}| . \tag{II-2}$$

The equivalent linear damping coefficient, C_L, for this case has been derived by Blagoveshchensky and is

$$C_L=\frac{8\omega}{3\pi}\dot{\phi}_{\circ}C_q \quad , \tag{II-3}$$

where $\phi_{\circ}$ is the amplitude, and ω the frequency of the rolling motion. This expression is obtained by requiring that the linear damping results in the same dissipation of energy per cycle of motion as the quadratic resisting moment.

In the case of random seas, the concept of energy interchange "per cycle" is not meaningful since the motion is no longer periodic. Rather, one must deal with time averages, but the concept of equivalent energy interchange still applies. Both St. Denis and Vassilopoulos estimated equivalent linear coefficients for roll motion in random beam seas by the following procedure. Assume that the actual force (moment) which is function of motion variable X_j, is given by $F_i(X_j)$. This is to be approximated by an equivalent force consisting of a linear term in the appropriate motion variable plus an error term, E

$$F_i(X_j)=C_iX_j+E. \tag{II-4}$$

We shall require that C_i be selected such that the time average of the mean square of the error term, E, will be a minimum.

$$\frac{\partial \langle E^2 \rangle}{\partial C_i} = 0 \tag{II-5}$$

For the case of quadratic damping this leads to the following expression

$$\sqrt{8/\pi}\ \sigma_{\dot{\phi}} C_q \ . \tag{II-6}$$

Thus it is seen that the evaluation of (II-5) leads to an equivalent linear force coefficient for random motion which, as in the case of sinusoidal motion, is a function of the motion amplitude itself, in this case, $\sigma_{\dot{\phi}}$, the RMS value of the velocity.

Applying the same reasoning to a nonlinear restoring moment, let us represent the righting moment curve by a fifth-order, odd polynomial in the roll angle ϕ,

$$R(\phi)=C_1\phi+C_3\phi^3+C_5\phi^5. \tag{II-7}$$

Designating the equivalent linear restoring moment by an error term plus $C_E\phi$, and again assuming the roll motion to be a zero mean, Gaussian process, having an RMS amplitude given by σ_ϕ, minimization of the error term, equation (II-5) leads to

$$C_E=C_1+3C_3\sigma_\phi^2+15C_5\sigma_\phi^4 \ . \tag{II-8}$$

By introducing equivalent linear forces and moments for the "exact" nonlinear terms, we see that we have obtained a linear system in which these forces depend on the mean amplitude of the motion. The solution, for a given amplitude of the excitation, must therefore be obtained by iteration. That is, one begins with an estimate of $\sigma_{\dot{\phi}}$, and computes the moment coefficients by (II-6) and (II-8). These are then inserted into the roll equation of motion. The solution for roll amplitude is then obtained and its RMS value compared with the assumed σ_ϕ. Convergence is usually quite rapid.

Now consider the nature of the coefficients appearing in (II-8) for a typical ship. Referring to Figure A-3 it is noted that C_1 will normally be positive and is, in fact, the product of the metacentric height and displacement, C_3 will be positive corresponding to the concave upward nature of the initial part of the curve, and C_5 is negative corresponding to the reversal of the curvature beyond approximately 30°. Thus, it is seen that if the RMS roll is in the medium range, the equivalent linear coefficient will be greater than the small angle linear value (stiff restoring spring) and the ship will have maximum roll response to wave component frequencies higher than the small angle natural frequency. For large average roll amplitude however, C_5 predominates resulting in a soft equivalent effective spring constant, and the maximum response is to wave frequencies lower than the small angle natural frequency.

This, qualitatively, describes a situation in which the consideration of certain nonlinear forces in the equations of motion has the effect of modifying the results that might have been obtained by a linear analysis, but without introducing any radical changes in the behavior.

Let us now consider another kind of nonlinear term which may be included in the roll equation of motion. Recall that the higher order damping and restoring terms in (II-2) and (II-7) may be considered as higher order derivatives in a Taylor Series expansion of the perturbation force about a mean state of motion of the ship. In such an expansion, there will be higher order mixed derivatives as well, exemplified by a roll restoring moment term of the following form

$$R(\phi,y)=K_{\phi y}\phi y. \qquad \text{(II-9)}$$

This may be thought of as expressing the change in the linear restoring moment coefficient, C_1, with changes in the heave position of the ship designated by y. The method of calculating $K_{\phi y}$, as well as details of the analysis whose results are given here, are found in a paper by Paulling and Rosenberg (1959). Including just this nonlinear term, the roll equation of motion (II-1) becomes

$$I_x\ddot{\phi}+C_L\dot{\phi}+C_1\phi+K_{\phi y}\phi y=K_e(t). \qquad \text{(II-10)}$$

Let us now assume that the ship is proceeding in regular head or following seas so that, by symmetry, the roll excitation, $K_e(t)$ is zero. In this case, the heave motion is sinusoidal and is given by $y_o \cos \omega t$. Equation (II-10) then becomes

$$I_x\ddot{\phi}+C_L\dot{\phi}+\phi(C_1+K_{\phi y}y_o\cos \omega t)=0 \qquad \text{(II-11)}$$

For the time being, ignore the damping, C_L. The resulting equation is known as Mathieu's equation and has solutions expressible in the form of special functions. It should be noted that this is a linear differential equation in ϕ. The unique feature of the equation is the presence of a time-dependent coefficient of the roll motion variable ϕ.

The solutions to Mathieu's equation have a property of considerable importance in ship rolling problems in that for certain values of the frequency, ω, the solution is unstable. Physically, this implies that if the roll motion described by (II-11) is taking place in an unstable region, the amplitude will grow until limited by a physical constraint not included in this equation. The unstable frequency may be found as follows.

Introducing the change of variable $\tau=\omega t$, equation (II-11) (with C_L neglected) may be rewritten

$$\frac{d^2\phi}{d\tau^2}+(\delta+\varepsilon\cos\tau)\phi=0 \qquad \text{(II-12)}$$

where

$$\delta=\frac{C_1}{I_x\omega^2}=\frac{\omega_n^{\ 2}}{\omega^2}$$

$$\varepsilon = \frac{K_{\phi y} y_o}{I_x \omega^2}$$

$\omega_n = \sqrt{C_1 / I_x}$ = natural frequency in roll.

Figure II-2 is a graph of ε versus δ for the Mathieu equation in which regions corresponding to stable solutions have been shaded. It is seen that for small values of ε, corresponding to small heave motion, y_o, we have unstable solutions of Mathieu's equation and therefore, unstable rolling motion occurring for

$$\delta = 1/4,\ 4/4,\ 9/4, \ldots = (n/2)^2; n = 1, 2, 3 \ldots$$

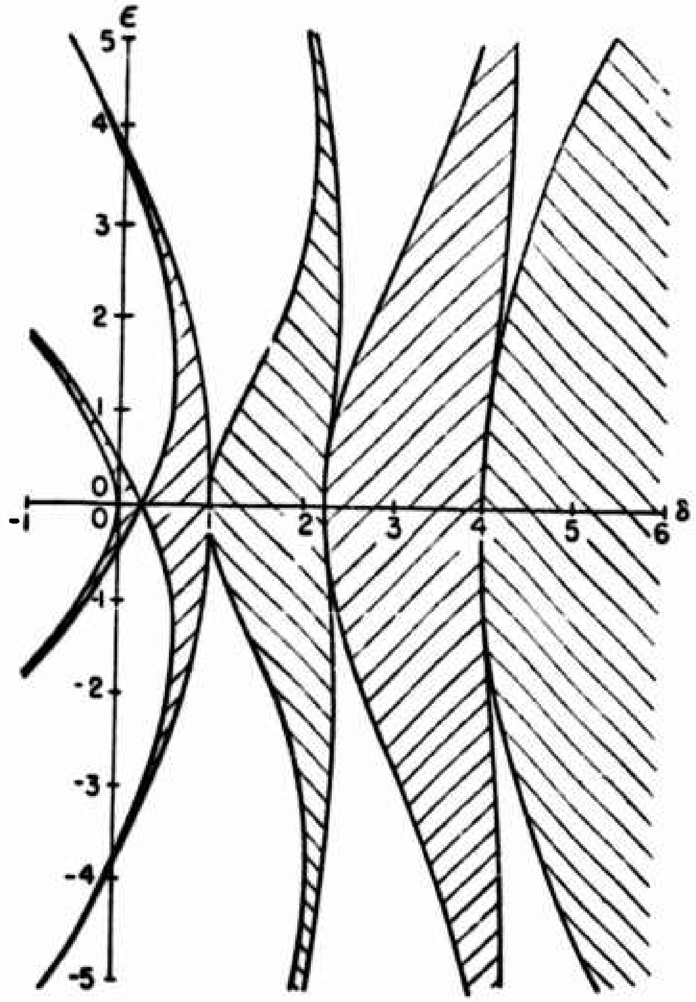

STABLE REGIONS SHADED

FIG. II-2 STABLE AND UNSTABLE REGIONS FOR THE MATHIEU EQUATION

Since δ is the square of the ratio of the natural frequency to exciting frequency, this means that unstable roll occurs when this frequency ratio takes on half-integer values. The lowest and widest unstable region occurs at an exciting frequency of twice the natural frequency. Thus, unstable roll will be excited if the ship encounters head or following seas with a frequency of encounter equal to twice the natural frequency of roll. For usual ship-wave proportions in which capsizing is likely, this occurs only in following seas. Note also that the instability may occur at an encounter frequency equal to the natural frequency of roll, 2/3 times the natural frequency and so on. The width of the unstable region for these higher frequencies is less,however,than that at the lowest frequency with the practical result that for unstable motion to be excited at the higher frequency, the amplitude of the variable term, ε, and therefore y_o, must be greater. For practical purposes, only the two lower unstable frequencies have any significance.

The existance of this parametrically induced unstable motion has been investigated theoretically and experimentally by Grim (1952), Kerwin (1955), and Paulling and Rosenberg (1959). The former two utilized a ship model equipped with a pair of weights which rotated at constant angular velocity in the vertical plane. In this way, the vertical position of the center of gravity, thus the metacentric height was forced to vary sinusoidally. The latter performed a constrained model experiment in which the ship model was mechanically forced to oscillate vertically in heave but with mechanical attachment to the oscillating mechanism which allowed freedom in roll. Thus the condition of sinusoidal heave was induced artificially in calm water. In both types of experiments, an unstable rolling motion was found to be set up at frequencies predicted by the Mathieu instability chart. Grim showed that the motion would ultimately reach a steady state value determined by nonlinear damping. Kerwin, in addition to his experiments, carried out a numerical integration of the equation of roll motion. He concluded from this solution that the transient behavior in the region of instability was quite sluggish and that a large number of oscillations would be experienced before the amplitude of roll, starting from a small arbitrary disturbance, would grow to appreciable magnitude. This conclusion is not in accord with observations of the model behavior during some of the experiments which form the subject of later parts of the present paper and we shall return to this point.

The above discussions has described the phenomenon of parametrically induced unstable roll motion. The excitation consists of the periodic variations in static transverse stability which result from the variation in geometry of the immersed hull during periodic heave oscillation of the ship. When the ship moves through head or following seas, the immersed geometry variations result from the changing water profile along the ship or wave surface, as well as from the ship motion. The relationship between transverse stability and the wave proportions in following seas has been investigated by Paulling (1961). It is shown that significant variations in the righting arm curve are caused by the changes in the immersed geometry as the ship is overtaken by successive crests and troughs in following or head seas. In general, for waves of length nearly equal to the ship length the ordinates of the righting arm curve are increased if a wave trough is near amidships and decreased when a crest is near amidships. The effect is most pronounced in steep waves and for ships of low freeboard. Typical curves of righting arms for these two conditions, crest amidships, and trough amidships are shown in Figure A-4.

If the entire righting arm curve shown in Figure A-4 rather than just the initial slope is considered in a Mathieu type analysis, one obtains an equation of the form

$$I_x\ddot{\phi}+C_L\dot{\phi}+RM(\phi,t)=0. \qquad \text{(II-13)}$$

Here, $RM(\phi,t)$ represents the time-dependent variation between the extreme righting arm curves, trough amidships to crest amidships, as waves move past the ship. Neither a solution nor a motion stability chart is available for (II-13). Some characteristics of the large-amplitude motion under the influence of typical ship righting moment curves have been obtained by numerically integrating the following differential equation

$$I_x\ddot{\phi}+C_L\dot{\phi}+ C_o(\phi)+C_1(\phi)\cos\omega_e t=0. \qquad \text{(II-14)}$$

In this equation $C_o(\phi)$ is the mean of the trough amidship and crest amidships righting moment curves, and $C_1(\phi)$ is one-half their difference. Two important features of the resulting motion were obtained in these studies:

(1) Motion instabilities were obtained, just as in the case of the linear Mathieu equation, resulting in a growth of motion from an initial small disturbance. As the motion grew however, the "effective stiffness" of the restoring moment (see Equation II-8) changed from its small-angle value. The system therefore became "detuned" from the exciting frequency and the motion would tend to limit itself. With a different value for the initial disturbance, the instability would be found at a somewhat different frequency corresponding to the altered effective stiffness associated with this amplitude.

(2) In Figure A-4 it is observed that the variations in stability with wave position are not symmetrically arranged about the still water curve. The crest amidships curve nearly coincides with the still water curve up to about twenty degrees, while the trough amidships curve is significantly higher than the other two. This asymmetry is less pronounced in ships with low freeboard amidships and relatively little flare in the ends.

The effect of the asymmetrical nature of the righting arm curves is to make the ship respond to parametrically excited motion as though the mean restoring moment initial slope were greater than the still water value. Thus, for the case illustrated in Figure A-4, the first Mathieu unstable frequency will be somewhat higher than that predicted by using the still water metacentric height. Further, since the stability variation between trough and crest varies with wave height, this unstable frequency will also be different for different wave heights.

This departure of the Mathieu instability frequency is thought to explain certain important differences in the observed motion response of the two different ship models which were tested. It will, therefore, be referred to again in a later chapter in which the experimental results are discussed.

If the ship is moving through a following sea, it is apparent that the ship will experience periodic variations in its transverse stability, and these variations will affect the roll motion of the ship. Although the preceeding discussion was concerned with regular waves, a somewhat similiar phenomenon but perhaps of a transient nature might be expected if the ship encounters a wave group having sufficient regularity and steepness. Such behavior has, in fact, been observed during some experiments to be described in the next section and the nature of this observed motion suggests that the wave induced stability changes and resulting parametrically induced roll play an important role in extreme motions and capsizing.

The examples just described illustrate the point that contemporary linear and nonlinear ship motion theory can reveal many features of ship behavior of interest to a study of capsizing, but it falls short of describing all aspects of the problem. This suggests that experiments, conducted in conditons which are as realistic as possible, offer the best possibility for an initial study of capsizing. The primary objective will be to gain insight and understanding of the basic phenomena. A second purpose will be to gather some data upon which to base conclusions and to be used as calibration for theoretical studies of the motion.

As noted in the INTRODUCTION, experiments utilizing radio-controlled free running ship models have been conducted several times in the past to study aspects of ship behavior and control for which adequate theory is lacking or for which conventional towing tanks are inadequate. In order to conduct free running experiments, one requires, in addition to a suitable test site, certain hardware items.

These include the test model itself, complete with radio controls, scaled autopilot steering systems, self-contained propulsion and monitoring instrumentation to record the pertinent motion variables, apparatus for recording the wave conditions in the test area, and some kind of floating platform from which to conduct the experiment. Such experiments performed in San Francisco Bay during the past three years are described in the following section.

III. EXPERIMENTS

A. Sea Spectra Measurement & Analysis

If the model tests are to reflect realistic extreme sea situations, it is obviously important that the waves at model scale adequately represent full scale conditions. An important part of the program has therefore been the recording and analysis of the seaway. The following sections provide a brief analysis of the measured wave data and a qualitative comparison with full scale storm conditions. Appendicies D and E contain detailed tabulations of wave statistics and plots of both point and directional sea spectra. Chapter VI contains a discussion of wave encounter and wave group phenomena.

1. Test Site, Array, and Procedures

The test area, known as the "Berkeley Flats", is a region of gradually shoalling water with an average depth of from eight to twelve feet and a mud bottom. Tidal currents are generally under one knot and the test area is outside of the regular commercial traffic lanes.

During the summer months, the overall wind pattern is extremely stable and repeats itself day after day. The hot air rising in the central valley draws the cooler ocean air through the Golden Gate. The test site is located down wind and slightly off to one side. The fetch is between three and six nautical miles in the form of a diverging funnel, two miles wide at the Gate and over four just before the test area. The overall geometry of the area is shown in Figure III-1. On a typical test day, the winds would be light in the early morning and build gradually to about fifteen knots, depending on location, by mid afternoon. The waves are a typical "wind sea." Ocean swell is rarely noticeable in the Bay and is of no consequence in the test area.

The waves were measured using an array of step type wave gages (Haddara, 1971 and Chou *et al.*, 1972). Three of the gages were mounted on arms extending from a wave buoy and the fourth gage was located at the center. The wave buoy is of the tension leg variety, each interconnected column being held down with its own anchor line. The buoy is very stable and has virtually no motion in heave and probably less than ten degrees in yaw in extreme conditions. Since the support vessel supplied electrical power and carried the tape recorder, it was necessary to anchor and connect with the buoy via a long electrical cable on the bottom. The wave measurements were monitored with a strip chart recorder and the observed wind and sea conditions recorded. The analog records were later digitized at 0.2 second intervals.

2. Point Spectra and Statistics

The waves were recorded for fifteen minutes approximately every hour to hour and one-half or when there was a significant change in conditions. Observations of wind, tide, currents, wave height and direction, and other potentially useful data were noted on the data sheets. Statistics were computed from the digitized time series and derived from the spectrum computations. Appendicies D and E contain the summaries of the runs and statistical information for both the 1972 and 1973 test seasons. The 1973

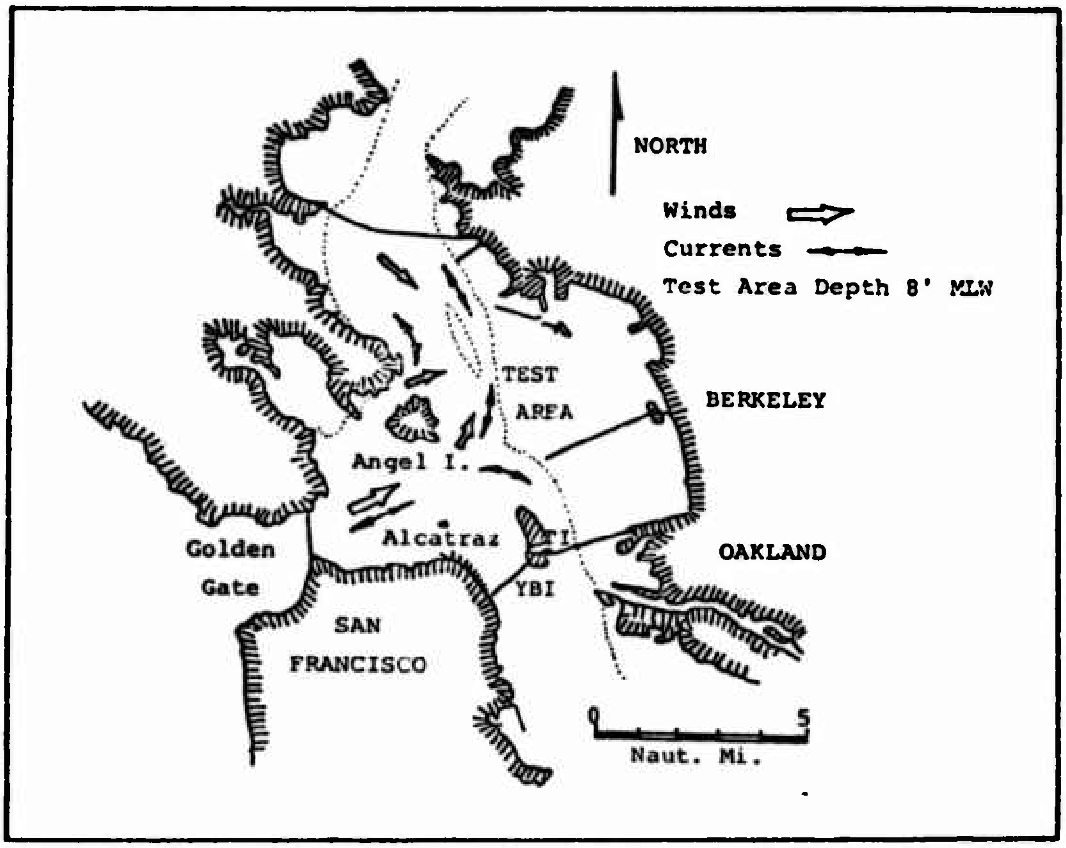

Figure III-1 Test Site and San Francisco Bay Area overview tabulation, Table E- 1, contains a summary of the notes taken during the tests. Figure III-2 shows the distribution of wave recordings with respect to significant wave height (4*RMS) for both 1972 and 1973.

The spectral analysis was conducted using a fast Fourier analysis technique with 2048 points and a 0.4 second time interval. Smoothing was done by block averaging over eight or sixteen frequencies.

An outline of the method is given in Appendix H of Haddara, *et al.* (1971). The point spectra of one probe recorded on each day are shown in Figure E-2. The growth of the spectra appears to follow the general description of a fetch limited sea as reported by JONSWAP, The Joint North Sea Wave Project (Hasselman, et al, 1973).

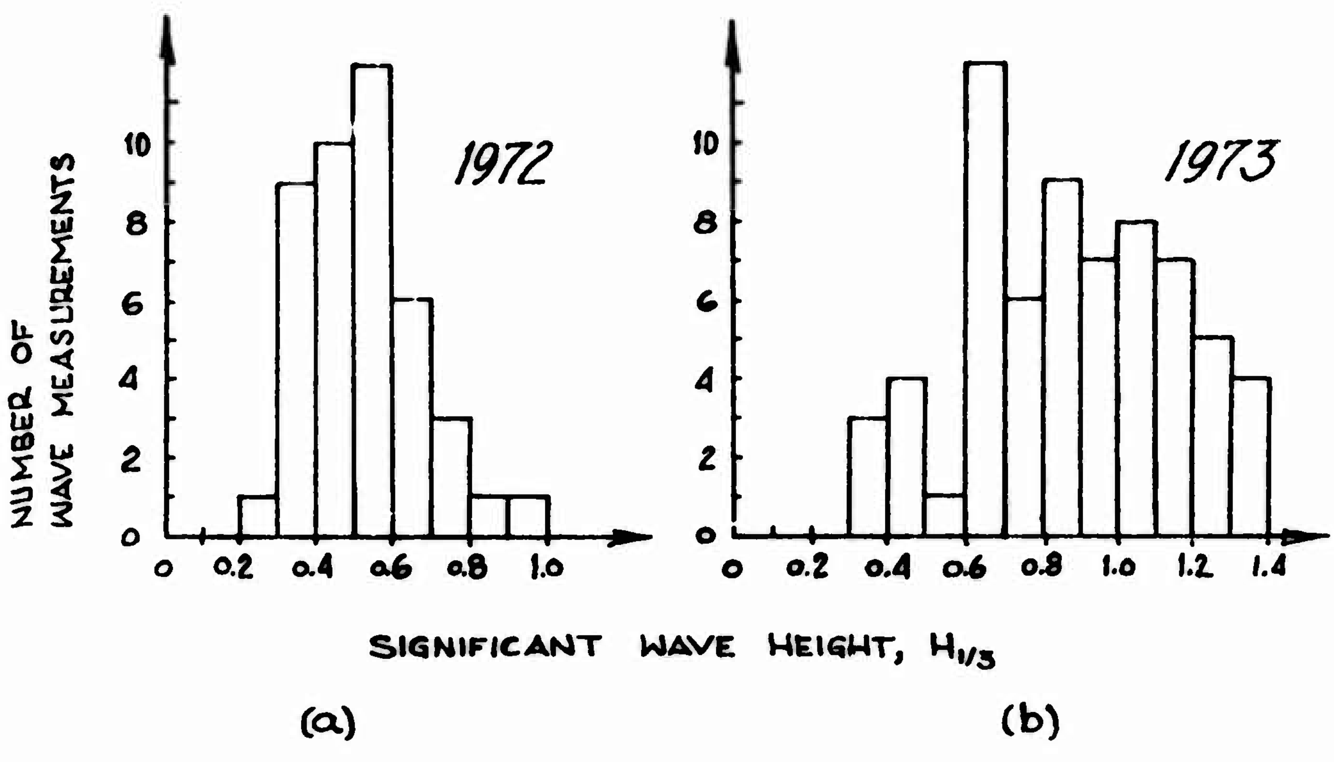

Figure III-2 Distribution of Significant Wave Height, 1972 and 1973.

A parameterized one-dimensional spectrum was used to fit that data. The spectrum was given as the product of a Pierson-Moskowitz (1964) type spectrum with parameters α and f_m:

$$S^{PM}(f)=\alpha g^2(2\pi)^{-4}f^{-5}exp[-1.25(f_m/f)^4] , \qquad \text{(III-1)}$$

and a "peak enhancement" factor:

$$\gamma\ exp\ [-(f - f_m)^2/2\sigma^2 f_m^{\ 2}], \qquad \text{(III-2)}$$

where

$$\sigma = \begin{cases} \sigma_a & \text{for } f \leq f_m \\ \sigma_b & \text{for } f \geq f_m \end{cases} \quad \text{width of the spectral peak}$$

f_m = frequency of the peak

$\gamma = S^{OBS}\ (f_m)/S^{PM}(f_m)$

Typical values of the constants can be estimated from the non-dimensional fetch

$$\tilde{x} = xg/U_{10}^{\ 2}$$

where x is fetch and U_{10} is the wind velocity at ten meters, using

$$f_m = \frac{g}{U_{10}}\ 3.5\ \tilde{x}^{-0.33}\ ,\ \alpha = 0.076\ x^{-0.22} \qquad \text{(III-3)}$$

the (JONSWAP) estimates of γ, σ_a, and σ_b showed much scatter but were assumed to be approximately 3.3, 0.07, and 0.05, respectively. The fetch derived from Equation III-3, given the spectral peak f_m and the measured wind velocity $U_5 = U_{10}/1.11$, ranged from approximately one nautical mile at low wind speeds to about seven nautical miles at the higher wind speeds. The scatter in the present data is due in part to inaccuracies in wind speed measurements since these were not taken over the full fifteen minute wave recording period. However, the derived fetch appears to correlate with the direction of the current in the generating area.

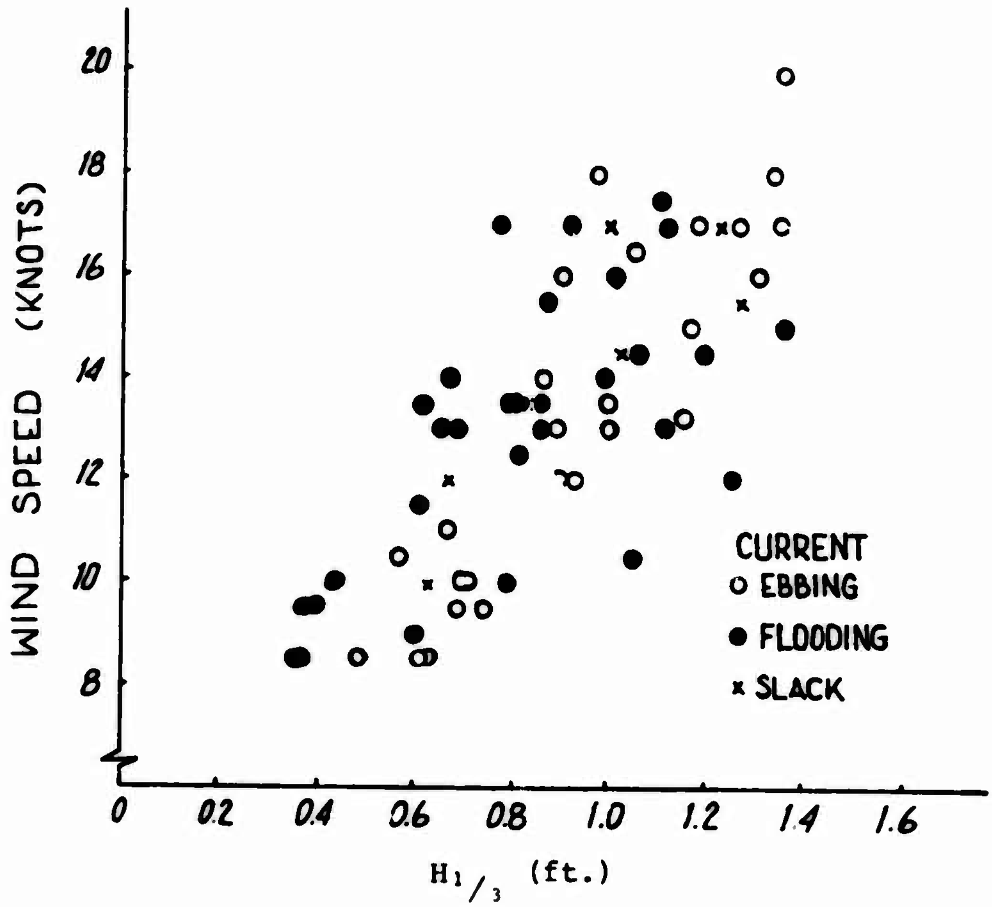

Figure III-3 Wind Speed vs Significant Wave Height

The significant wave height versus wind speed is shown in Figure III-3. As expected, an ebb current produces larger waves since it opposes the mean ·ind direction. The anomalous low wind speed and high significant wave heights are usually associated with decaying spectra and cross sea situations. The peak ratio γ, unlike JONSWAP, varied smoothly from approximately 3.3 for low spectra to 0.98 for the highest. The fit of the parameterized model with the experimental spectrum is shown in Figure III-4. The parameterized model was computed using the observed peak frequency f_m and amplitude $S^{OBS}(f_n)$ and appears to agree reasonably well. It may be possible to use such models as aids in interpolating for spectra at times other than those measured.

On one occasion, nine wave recordings were made during a four hour period in order to investigate wave stationarity. Consecutive records yield similar spectra with amplitude and directional properties that correlate very well with the observed values. Futhermore, the changes appeared to be smooth functions

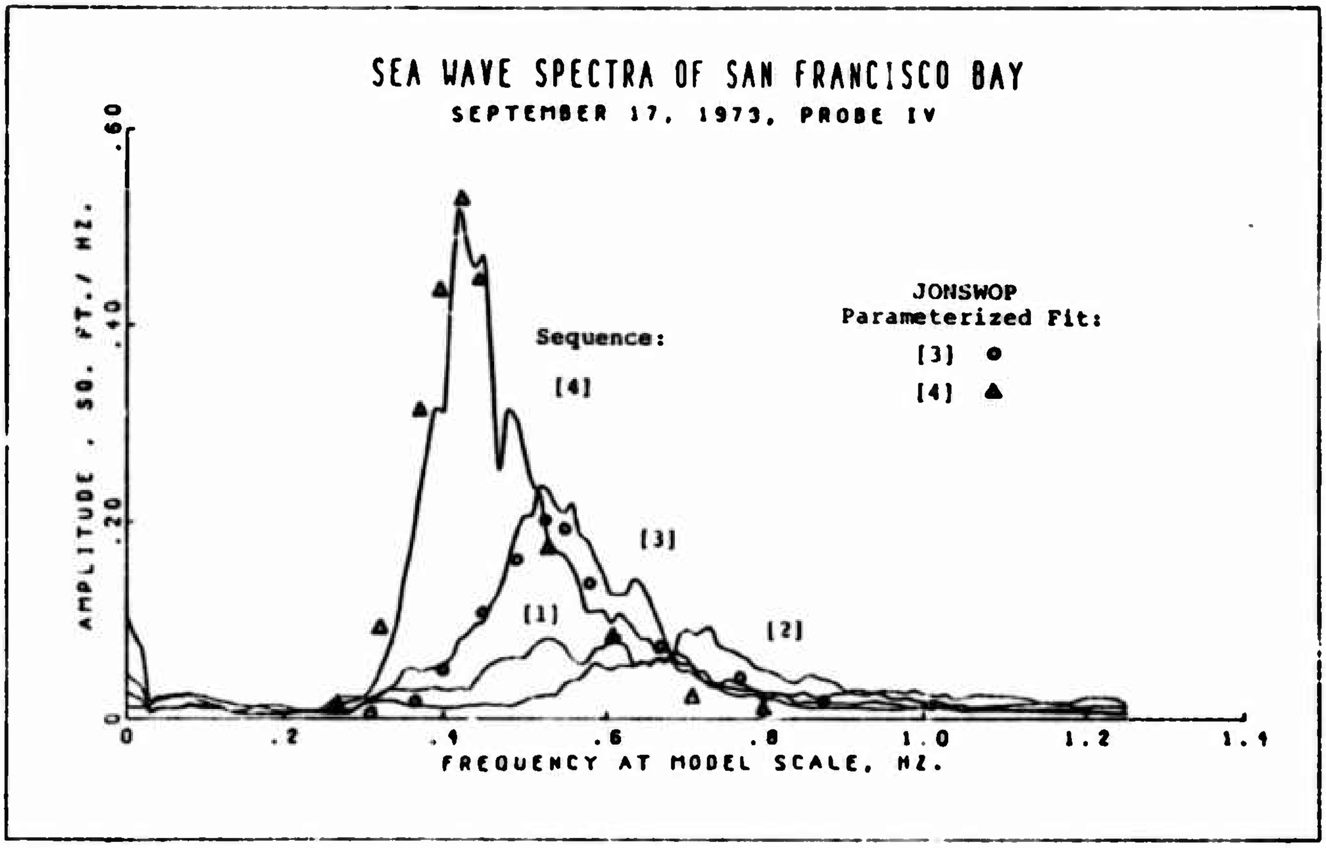

Figure III-4 Point Spectra for 17 September 1973

of time. If there were no unusual changes in the observed wind and wave characteristics, it is therefore probably reasonable to interpolate between consecutive measurements for an estimate of intermediate sea conditions.

All of the spectra peaked at $f = 0.38$ *Hz* or above with one exception which peaks at approximately 0.32 *Hz*. The large spectrum on that day is the only one with any energy at $f = 0.3$ *Hz*, which corresponds to a deep water wave-length of 56.9 feet. Even at this frequency there is only a nine percent decrease in the wavelength due to shallow water. Since this is still 3.1 times longer than the models being tested, the effect of the shallow water is not considered to be significant.

Some spectra exhibited a small spike below $f = 0.03$ *Hz* peaking at zero frequency. These correlate well with rapid changes in the tide at the time of recording.

The significant wave height computed from the point spectrum differs considerably from the analysis of the time series. The spectral statistics agree with those of time series, however, if any zero frequency spike is removed from the spectral area and the significant wave height is corrected using the broadness facter (Loukakis, 1970).

$$H_{1/3_{\text{time series}}} = H_{1/3_{\text{spectrum}}} * \sqrt{1-\varepsilon^2/2}$$

where

$$\varepsilon^2 = 1-m_2^2/(m_0 m_4)$$

$$m_n = \int_0^\infty \omega^n S(\omega)\, d\omega.$$

As noted earlier, the measured spectra do not appear to be significantly distorted due to the limited fetch or water depth. The amplitude and frequency content also seem to scale reasonably well. Figure III-5 is a plot of a number of scaled San Francisco Bay point spectra assuming a scale ratio of $\lambda=30$. Figure III-6 is a collection of full scale storm spectra recorded at a number of locations. These represent a variety of shapes and, it might be noted, are not the largest available. The model and full scale spectra are seen to agree quite well. These are admittedly rather severe conditions that occur only rarely, but they probably represent the very situations where capsizing becomes an important danger. Figure III-7 gives the equivalent Pierson-Moskowitz spectra for comparison purposes. Our knowledge of the shape of storm sea spectra, let alone the detailed time history of the wave elevation, is woefully lacking. The detailed experimental information provided in the

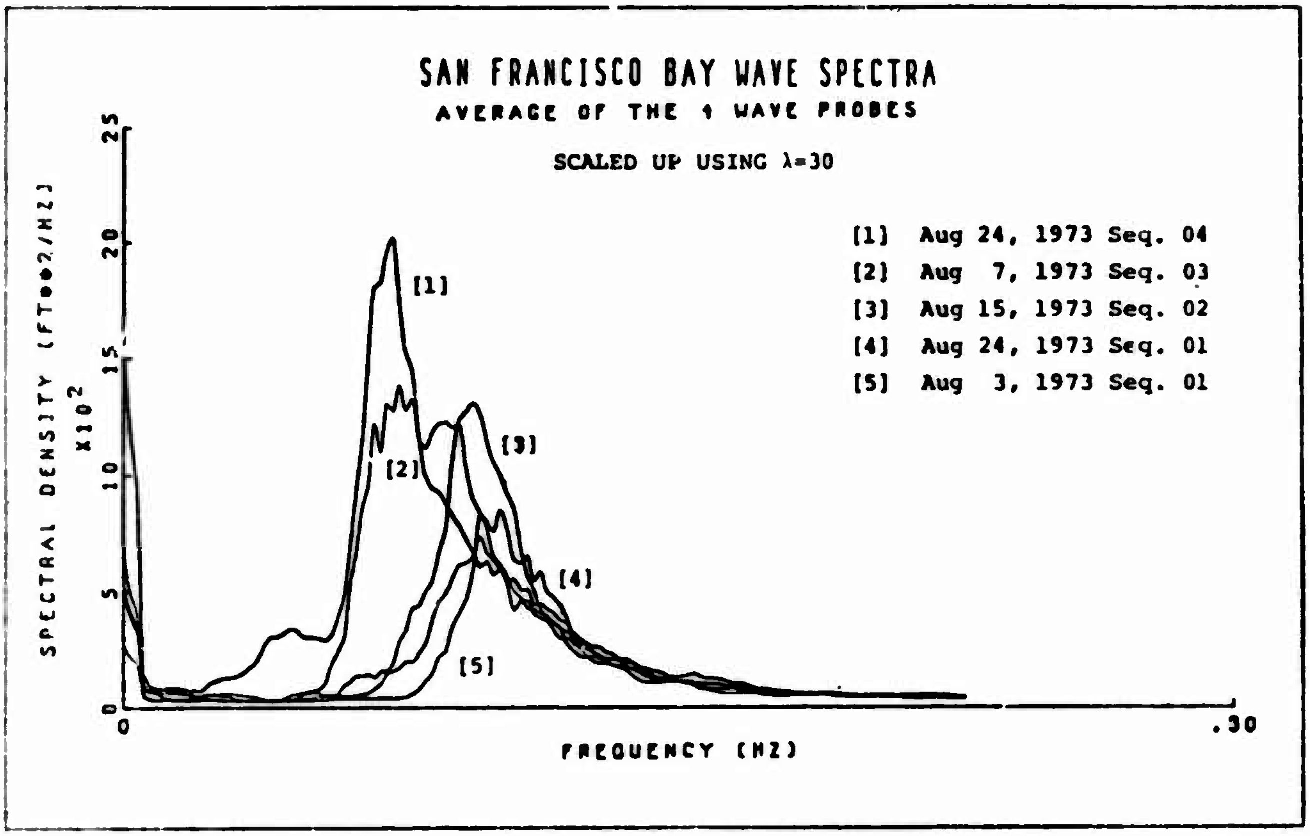

Figure III-5 Typical San Francisco Bay Spectra Scaled using λ=30

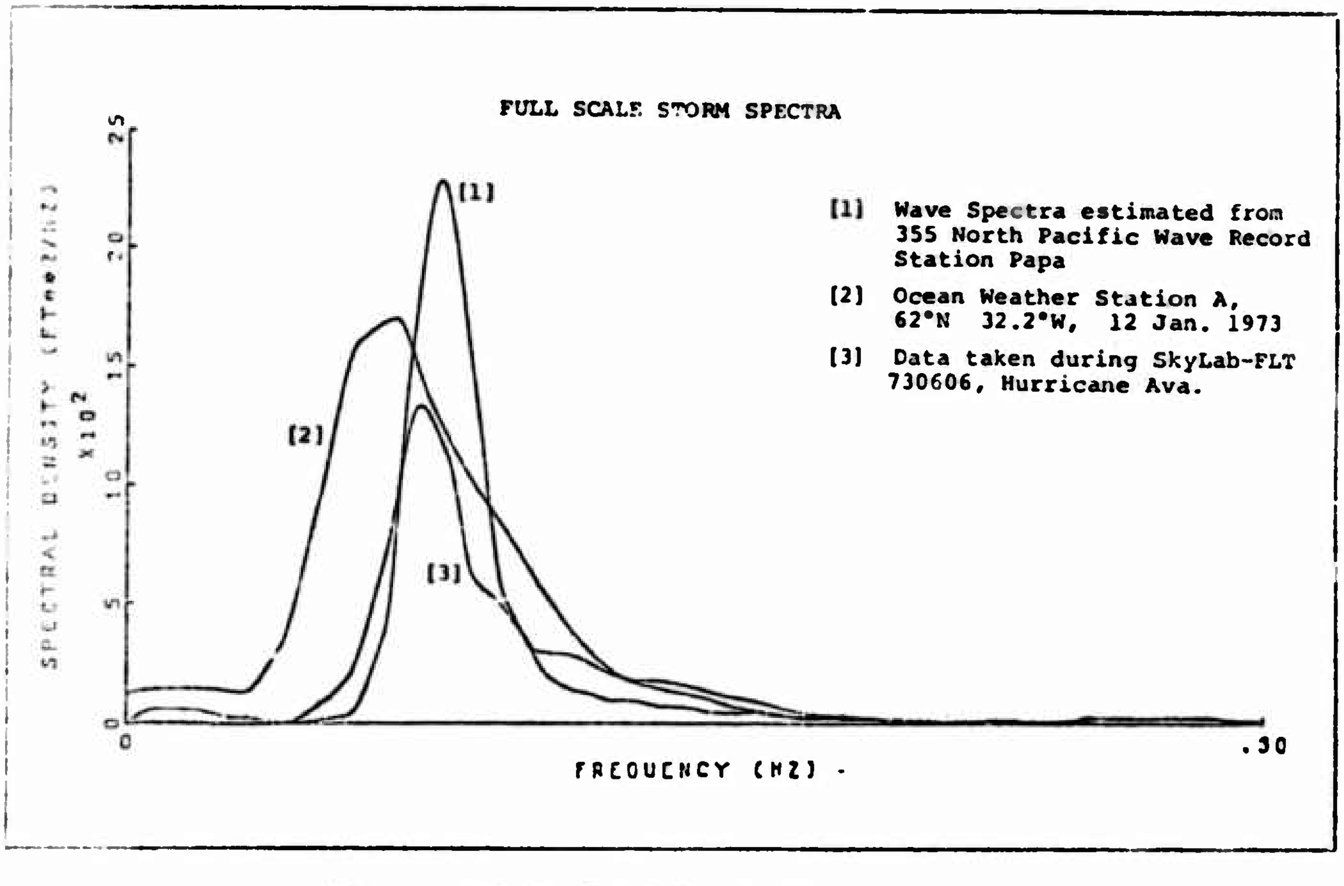

Figure III-6 Full Scale Storm Spectra

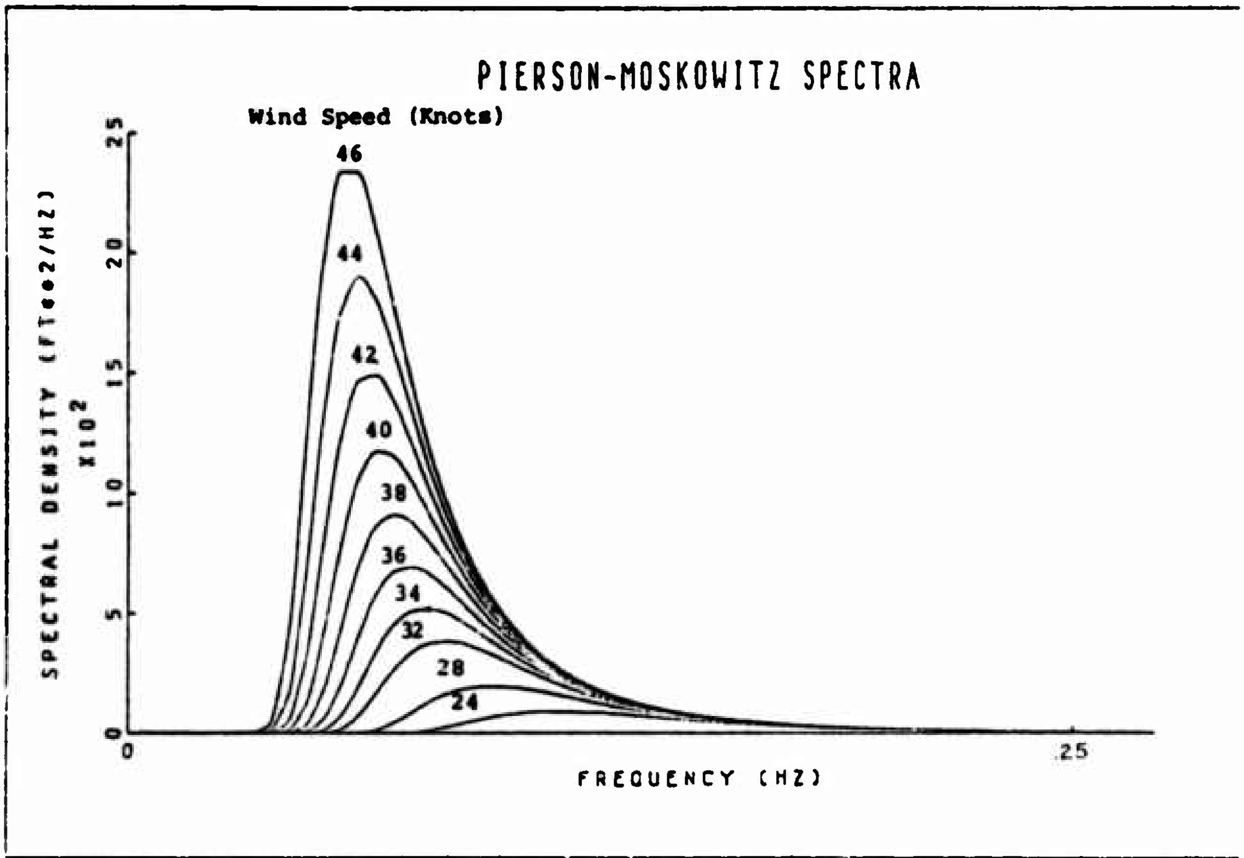

Figure III-7 Pierson Moskowitz Spectra

appendix cannot be adequately judged since comparable full scale data is just not available. On the other hand, this may not be the case in the near future. Long range monitoring of the sea surface using radar reflections off of the ionosphere and other sophisticated measuring techniques are currently under development. These show promise of providing sufficient data to evaluate quantitatively the adequacy of these experimental spectra and the often employed "Standard" sea spectra.

3. Directional Spectra

The major reason for experimenting in the open waters of San Francisco Bay was the desire to investigate ship capsizing in more or less "reasonable extreme" sea conditions. This of course implies the possibility that the sea spectrum could be multi-directional. A measure of the directionality was therefore considered vital for the interpretation of the resulting motions.

A number of analysis techniques were evaluated. The first method involved computing the first few terms of a Fourier series expansion of the directional spreading function at each frequency (Oakley, 1973). This method has not proven to be well suited to the analysis of a small number of gages. Spurious peaks and negative spectral estimates are frequent problems. The peak direction can be accurately computed but not the amount of spreading. Knowing the peak direction, θ_o, a $\cos^n(\theta-\theta_o)$ spreading function could be assumed. The current literature on the subject of directional spreading advocates a cosine squared spreading function within the generating area. A narrower spreading relation is more appropriate the farther one moves from the region of wave generation. The test area appears to be within the wind wave generating region so a moderately broad spreading function should be applicable. However, this does not appear to be the case from observations. The waves appear to be quite unidirectional and relatively narrow banded in character. Another analysis technique investigated was the maximum likelihood filter developed by Capon (1969). This procedure requires only the inverse of the cross-spectral matrix and is therefore rather simple to use. The wave number-frequency spectrum estimate is given by

$$\hat{S}(k,f) = \sum_{j,l=1}^{K} [\hat{Q}_{jl}(f)\exp(-i\underset{\sim}{k}\cdot\underset{\sim}{X}_{jl})]^{-1}$$

where

$[\hat{Q}_{jl}(f)]$ = inverse of the cross spectral matrix with elements corresponding to the gage pair j-l.

$\underset{\sim}{k}$ = wave number (directional) for water of depth h.

$\underset{\sim}{X}_{jl}$ = distance between gage pair j-l in an array of K gages.

This method offers significantly improved resolution over the Fourier series method and yields positive definite spectral estimates. Cross plots of the directional spectrum $S(\theta,f)$ for September 17, 1973, run number 3, at selected frequencies are shown in Figure III-9. The directions are shown relative to the buoy. The peak direction and relative narrowness agree very well with observation. The narrowest peak corresponds to a cosine spreading function raised to the 6.8 power. Resolution appears to be acceptable for wavelengths up to an order of magnitude longer than the average distance between gage pairs. Note however that with only four gages, resolution is not unlimited. The filter is only able to achieve complete separation of a pair of sine waves if they are separated by at least 15 or more degrees in azimuth. Since the spectral estimate is given by the inverse of a trigonometric series, there is a tendency to spread energy into all directions. The amount of spreading increases with a decrease in frequency or the number of gages. Spreading also increases with the amplitude of the peak of the distribution with such a small array. Care must therefore be taken in applying the results. Small amounts of spurious energy, relative to the peak, going in the wrong direction may show up in the prediction of ship accelerations, for example.

Improved resolution is possible using a linear programming approach (Oakley, 1973). This technique attempts to minimize the largest deviation between the measured cross spectrum and a parameterized estimate. The method is capable of achieving a very high degree of resolution, even for a limited number of gages, by looking only at those directions containing energy. If pushed too far, however, the directional distribution estimate begins to resemble a distribution of spikes even if the actual distribution is smooth. Some care in interpreting the results is therefore in order. If the spectrum is known to be "smooth", a smoother parameterization than the tent functions used in Oakley (1973) should be considered. The linear programming technique was used to check the results using Capon's analysis. The results support the previous observation that the directional distributions tend to be very narrow, especially for the higher seastates and lower frequencies.

The point spectra and directional spectra for the 1973 test season are plotted in Appendix E. The directional spectra are presented as contour plots relative to magnetic North. These are somewhat easier to interpret than the cluttered cross-

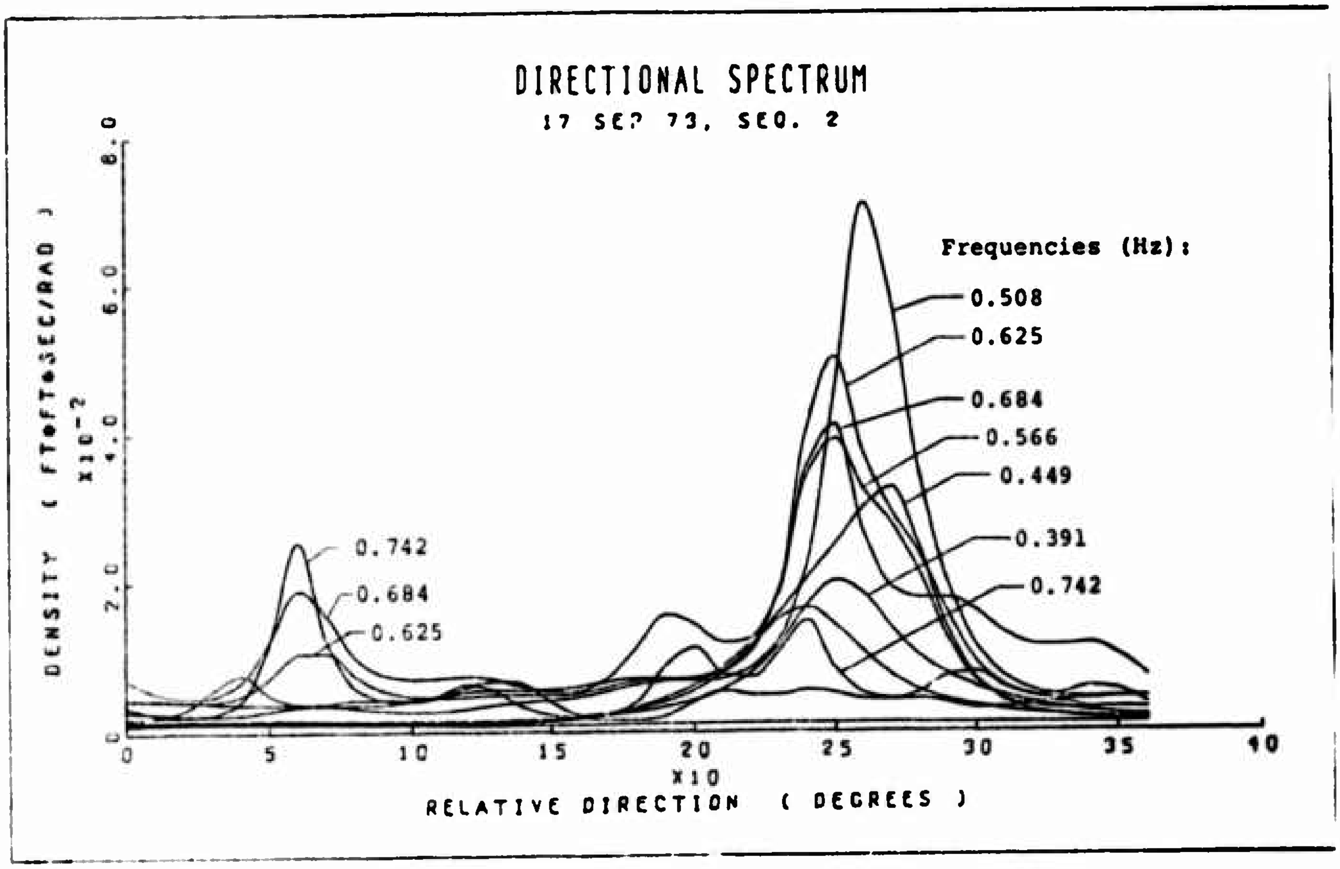

Figure III-8 Directional Spectrum Cross-Plot

plots of spectral density versus direction. Note however that the amount of directional spreading is deceptive. The contour plots obscure the relative narrowness of the peaks of the larger spectra. Note also that the contouring levels differ from run to run.

Run 4 on August 24, 1973 offers a particularly dramatic example of the power of the directional analysis. The winds were rather light and erratic during the morning and early afternoon at the initial test location. Potentially better westerly wind and sea conditions were apparently developing in the test area closer to the Berkeley pier. Upon arrival at this new location a West or Northwesterly breeze had also developed to the north of the previous test site. The resulting seaway was a classic example of two wave trains crossing at right angles, both of approximately the same amplitude and wave length. The two spectral peaks are clearly shown in the contour plot. The connecting lines, Figure F-3.27 are spurious directional spreading at constant frequency.

The wave buoy direction was not recorded on three occasions. Since the wind direction and spectral peak were always in good agreement, the buoy orientation was assumed to be the value required to bring them into line. This fact is noted on the contour plots. The wave array and model headings are probably reliable only to within ± 10 degrees due to reading errors and variable amounts of deviation.

An additional seaway topic of importance is that of wave groups. A discussion of the theoretical and experimental statistics is presented in Chapter VI.

B. Model Experiments

Extensive experiments have been conducted in the open waters of San Francisco Bay for over three seasons. Two seventeen foot models were tested. The first was a medium speed, full hull form ($\lambda=30$, *American Challenger*) of wood construction (Haddara, et al, 1971). The second model represented a high speed, narrow hull form ($\lambda=55$, *Sealand-7 Container Class*), (Chou, et al, 1973) and was the more fully instrumented. Body plans and principal dimensions of the two models are given in Appendix A. Comparisons given in this report are based upon the same assumed scale ratio, $\lambda=30$ for both.

The second model is a fiberglass reinforced epoxy sandwich construction with a balsa core. Large hatches with O-ring seals were provided for easy access and proved to be completely water-tight. Table A-I lists the particulars of the two models. These models were self-propelled, using a 24 volt DC PM field motor, and were radio controlled. The rechargeable battery circuitry is divided to provide power to the instruments and propulsion separately. Four batteries are also used as movable ballast for GM changes in the second model.

An analog tape recorder in the model was used to record four, and later seven, channels of data selected from the following:

a.) pitch, roll, yaw, and yaw rate angles (gyros)

b.) heave, sway and surge accelerations for a location near the CG of the model.

c.) motor RPM, relative water speed, and rudder angle.

The autopilot system was designed to simulate a typical full scale system with heading error and yaw rate feedback, a dead band and time lag. A detailed description is presented in Haddara, *et al.* (1972), and an analysis of the actual system characteristics is given in Appendix C of this report.

The righting arm curves for the two models in calm water and in waves are given in Figures A-3 and A-4.

After recording the waves, the wave buoy cable was disconnected and left with the anchored dinghy. The model was then launched such that the wave buoy would be passed close aboard at approximately half way through the run. The compass heading of the model was recorded but the heading characterizations, i.e., following, quartering, or beam, were selected strictly by eye. During the course of the run the model would occasionally deviate from the desired heading due to initial heading errors during uncaging, drift of the yaw gyro, or a change in the observed principal direction of the seas. Course corrections were radioed to the model in the form of two degree steps in the yaw gyro heading angle. If the model was able to maintain course, the relative heading was held substantially constant. Since the sea conditions were often extreme, the model would occasionally experience a broach or a series of large yaw forces and would be thrown off course into a large quartering or even beam sea heading. At high speeds there was sufficient directional control for the rudder (generally hard over) to bring the model slowly back on course as soon as the large group of waves had passed. At the lowest Froude number and largest seas, the model on a number of occasions was unable to recover for long periods and wallowed in beam seas until a long lull arrived. The spectral analysis of these runs generally show very large values at low frequencies in the yaw and rudder angles.

If a capsize occurred before the end of a fifteen minute run, the model was recovered, the yaw gyro re-caged, and the procedure repeated until there was a noticeable change in sea conditions or approximately one hour had elasped since the last wave measurements. Launching and recovery in high seas was a tricky operation requiring both skill and time. Two long runs or three to four short runs were generally all that could be done between wave measurements. Nevertheless, a substantial number of experiments were conducted in a variety of sea conditions, speeds, GM's, and headings.

Tables D-V and E-III provide an overview and summary of the model runs during the 1972 and 1973 test season. The statistics were derived from an analysis of the time series rather than from the spectrum of motions.

At the completion of the day's testing the onboard model tape recorder was removed and the analog signal inspected on a strip chart recorder. The data were digitized each week and the results preserved in both analog and digital form.

Many runs were too short to make either a statistical or spectral analysis meaningful. Only runs over seven minutes have been selected for statistical analysis, the majority being over ten minutes. Many of these involve rather violent motions, especially in roll, yaw, and rudder deflections. These are necessary conditions for a capsize to be likely, but this makes a comparison with a linear theory analysis rather difficult.

The mean relative speed between the model and water was measured on numerous runs using a paddle wheel type speedometer. Figure III-9 is a plot of the mean speed versus significant wave height (interpolated to the time of the run) for the various headings. The measured speed is seen to decrease with increasing significant wave height, even in following seas. If there were significant surge motions, the speedometer would be expected to read a lower value due to the decreased relative velocity between the model and water velocity on the face of the wave. Computations were made using the linear motions program, using both the calm water speeds and the lower speeds reported by the speedometer. Due to the nature of the folding of the motion spectra for conversion to the encounter domain, the frequency distribution is quite sensitive to speed changes. Better frequency agreement was found for speeds close to the speedometer readings, rather than the calm water speeds. This would suggest that the mean velocity did indeed decrease and that in the mean surging was not too significant. This agrees with the observations made in the Bay. An estimate of surging is possible by using the surge accelerometer data taken on about a third of the runs. The RMS surge motion and RMS surge velocity were obtained by integrating inverse moments of the acceleration spectrum. Typical motion amplitudes were less than 0.5 feet and speed deviation less than eight percent about the mean in the larger seastates.

The principal cause of the speed decrease is presumably the large rudder deflections required to keep the model on course in the following and quartering seas. A plot of the RMS rudder deflections versus significant wave height, speed, and headings showed a large amount of scatter. This points to the need for some further experiments expressly to evaluate the speed decrement due to rudder motions.

Motor RPM was not regularly recorded due to channel limitations. It was checked, however, and found to be sufficiently constant.

The heave and sway accelerometers ($\pm$ $2g$) were adjusted to have ranges of approximately two-thirds of a g. Subsequent analysis suggests that there may have been somewhat more structural damping involved in the heave acceleration measurements at high frequencies than anticipated. The surge accelerometer ($\pm$ $1g$) had a higher gain factor and is believed to have worked well.

Pitch and roll angle measurements appear to be accurate. The full scale yaw range needs to be large, and it should be remembered that very small yaw motions are only a small percentage of the recorded range.

In order to compare the experimental results with calculations using an inviscid linear theory, the actual roll damping of the model is required. The damping coefficient was computed from two sets of experiments, one at zero speed and one at forward speed. The analytical procedure and results are reported in Appendix B.

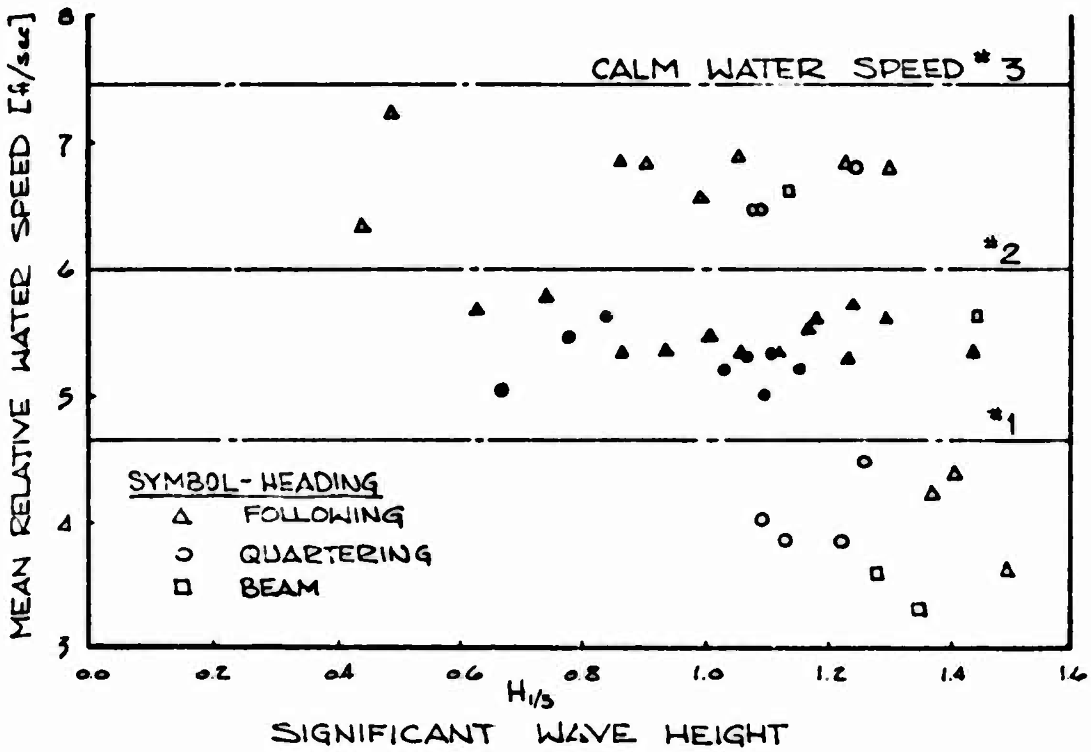

Figure III-9 Model Speed vs Significant Wave Height

C. Observations

A pronounced difference was observed between the two models at the relative frequency of occurrence of low cycle resonance at the first Mathieu frequency. This first unstable frequency (of encounter) it will be recalled is equal to twice the natural frequency of roll. During the experiments, it was observed that the *Challenger* model experienced low cycle resonance at this frequency relatively frequently, in perhaps one-third to one half of all capsizes. The *SL-7* model on the other hand experienced virtually no capsizes at the first Mathieu unstable frequency.

The explanation is obtained by reference to Figures III-10 (a) and (b) where righting arm curves in still water and waves of various heights are plotted for the two models. A pronounced difference is seen in the nature of the curves for the two different hull forms. In the case of the *Challenger*, the trough amidship and crest amidship curves are relatively symmetrically disposed about the still water curve. That is, the increase in righting arm for the trough amidships case is about equal to the decrease in righting arm for the crest amidships position of the wave of the same height. In contrast, for the *SL-7* the entire family of crest amidships curves nearly coincide with the still water curve up to an angle of heel of about 18 degrees, while all of the trough amidships curves are much steeper and higher over the entire range . It appears from the nature of these curves that the *SL-7* operating in regular following seas would experience a mean righting arm curve lying midway between the trough amidships and crest amidships curves, which would have higher values than the still water curve. In other words, for the *SL-7* model, the apparent mean ordinates of the righting arm curve in following seas are greater than the calm water values.

This, in turn, influences the frequency of wave encounter at which Mathieu type resonance is experienced. While the *Challenger* displayed such resonant behavior in the roll motion at an encounter

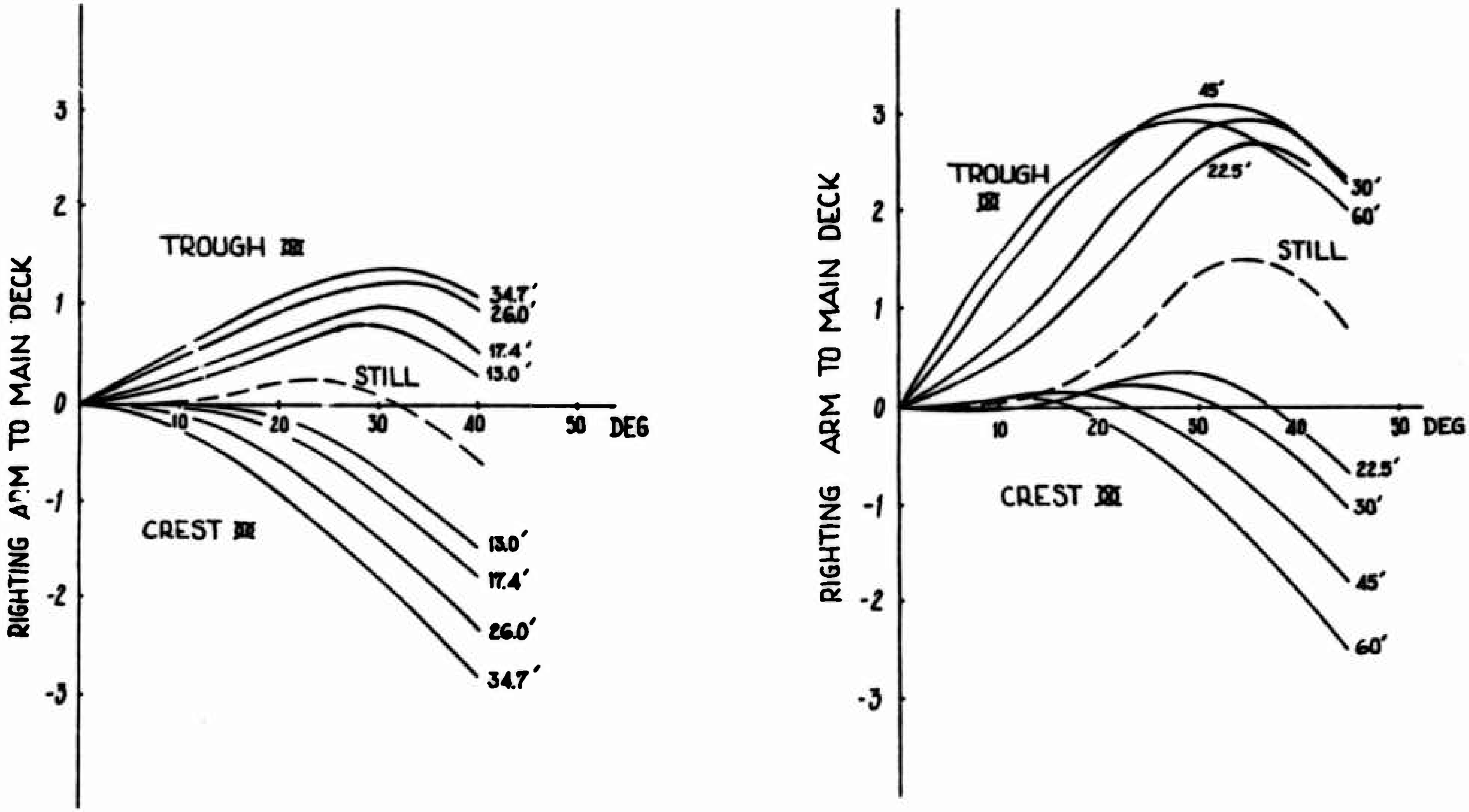

(a) (b)

Figure III-10

frequency of almost exactly twice the natural roll frequency in calm water. The *SL-7* model, on the other hand, experienced almost no cases of roll motion at half the encounter frequency, but did show large motion and frequent capsizes at a roll frequency equal to the encounter frequency. The explanation is given by the difference between the two vessels righting arm curves in following seas. The *Challenger's* natural frequency in waves is nearly equal to that in calm water because of the symmetry in the righting arm curves for the crest and trough amidships positions. Mathieu resonance at the first unstable frequency was observed to occur quite frequently during the experiments because the combination of model speed and average wave lengths resulted in the occurrence of encounter frequencies in this range. For the *SL-7* on the other hand, the mean effective righting arms in waves was generally substantially greater than in still water. This resulted in a relatively high "apparent" natural frequency of roll in waves. The combinations of model speeds and wave lengths in which tests were conducted resulted in frequencies of encounter which were more nearly equal to, rather than twice, the natural frequency of roll.

This observation was borne out by the results obtained by numerically integrating the approximate equation of motion (II-14) which was described in an earlier section. Mathieu instability in the results of the numerical solution was observed to occur at a frequency of excitation equal to twice the (small angle) natural frequency which would be computed by using the mean initial slope of the trough amidships and crest amidships righting arm curves rather than the still water GM.

All capsizes observed in the course of our experiments occurred in following or quartering seas, and these, as was pointed out in an earlier section, are the headings of the ship relative to waves in which the stability is most strongly affected by the waves. From observing the capsizes and the motion picture records of them, it was clear that the attenuation of stability by the waves played a very important role in nearly all capsizes. Further, it was possible to distinguish three distinct modes of capsizing which may be described as follows.

Mode 1: Low Cycle Resonance. This refers to an oscillatory rolling motion which builds up rapidly, i.e., in two to five cycles, to a very large amplitude, culminating in a capsize.

The phenomenon appears to occur in approximately the following sequence. The model, while operating in following or quartering seas, encounters a group of especially steep and regular waves. When the crest of a wave is about amidships, the stability of the model is greatly reduced and it takes a large roll. This wave moves on past the model and a trough comes into the amidships position while the model is heeled over, resulting in sharply increased stability. This causes the model to "snap" back upright, acquiring a high roll angular velocity by the time it reaches the upright position. Another wave crest, meanwhile, is moving into the amidships position, resulting in diminished stability once again as the ship starts rolling past upright and to the other side. The ship then rolls far over to the side against a diminished restoring moment. If now another trough moves into the amidships position with the correct timing, the roll will be stopped and the model snaps upright again. This process continues until either the model capsizes or it moves out of the wave group and the motion dies down. This mode of capsize is seen to be related to the Mathieu motion instability. It results directly from the periodic stability variations experienced by the ship moving through waves and in its most pronounced form takes place at one-half the encounter frequency, thus at the first Mathieu unstable frequency.

Mode 2: Pure Loss of Stability.

This usually occurs in a following sea at high speed. The model is observed to encounter one or more very steep and high waves and, with little or no preliminary rolling motion, simply loses all stability when a crest moves into the amidships position and "flops" over. The essential prerequisite for this to occur is a model speed nearly equal to the wave phase velocity so that the model remains almost stationary relative to the crest for a sufficient length of time to capsize. The necessary wave would be of about the same length as the model and the height would be sufficient to immerse the deck in the crest with the model upright. This, of course, implies a high model speed since a Froude number of 0.4 is required for the model speed to be exactly equal to wave speed in waves of length equal to model length. From motion picture records of several capsizes of this nature, it appeared that a model speed lying between the group velocity (one-half the phase velocity) and the phase velocity could result in this mode of capsize.

Mode 3: Broaching. This is the most dynamic mode in appearance, and has received the most attention in the previous literature. In this mode of capsize, the model is struck from astern by three or four steep breaking seas in succession. As each wave strikes it, the model is forced to yaw off course to such an extent that the steering system is unable to correct the heading in the time interval between waves. The breaking seas striking the model, combined with the dynamic heeling moment resulting from the turn, combine to cause capsizing, again with the crest of a wave amidships. The essential features of broaching are the breaking waves striking the model in series, and the large heading deviation and associated angular velocity.

On several occasions, broaching was observed to occur without capsizing but with such total loss of directional control that the model swung through ninety degrees from a following sea course to beam seas. This was observed to occur most frequently in the light displacement condition where the rudder was less deeply immersed and therefore less effective. On several occasions, at low speed, the model was totally unable to regain it original course, but remained in the beam sea condition even with the rudder hard over.

IV. LINEAR ANALYSIS AND EXPERIMENTAL COMPARISONS

This chapter is an attempt to investigate the applicability of linear ship motions theory to the case of extreme following seas. There are a number of obvious reasons for pursuing a linear analysis. No other three-dimensional theory is so well developed. Strip theory has yielded surprisingly good comparisons with measurements despite a flagrant disregard of the restrictions on the input wave frequency, wavelength, and amplitude. Capsizing is a rare event and should be viewed in a probablistic sense. A spectral description of the motions is far more amenable to long term extreme motion prediction than a time series derived from a nonlinear model.

On the other hand, there are a number of reasons why one should not expect particularly good agreement. Strip theory requires the input wavelength to be of the order of the beam. For a ship operating under conditions varying from beam to following seas, the significant responses stem largely from the excitation of waves ranging in wavelength from the order of the beam to the length of the vessel. The solution is singular for the unrestored motions in stern seas when $\omega_e=0$. Significant variations of the roll hydrostatic restoring coefficient are not included in the computations since linearized hydrostatics are determined from the calm water properties of the waterplane section. A rudder-autopilot system, having important nonlinear properties, may be of some consequence in large following seas. Obtaining a good linearized estimate of the roll damping (including the viscous contribution) and a measure of the waves actually encountered also introduce complications.

These are all potential problems. The significance of each one must be evaluated under actual test conditions. The aim here is to see if there is sufficient agreement between theory and experiment to warrant further refinements in the linear prediction procedure and to determine if an estimate may be made as to the bounds to which this theory may be applied.

Linear motion predictions were made using the Salvesen, Tuck, Faltinsen theory (1970). The six degree of freedom ship motions program, SEAWAY, developed at U.C.Berkeley, uses a modified version of the Frank close-fit method for calculating the two-dimensional hydrodynamic coefficients. The first and second "irregular frequencies" have been removed. Coefficients at the desired encounter frequencies are obtained by interpolation from a computed table. The program will generate a Pierson-Moskowitz sea spectrum or accept either a point or a directional empirical spectra as input. The point spectrum can be spread using a cosine to the power r distribution if desired. An additional feature is the Froude-Krylov computation of surge motion. Surge is assumed to be a second order quantity in most linear, head sea ship motion predictions. This is not the case, however, for long waves in following and quartering seas where the surge exciting force can be significant.

Before proceeding directly into the evaluation of the experimental results and theoretical predictions, it is of value to comment upon a few of the previously mentioned potential theoretical problems and to discuss examples of the calculated linear transfer functions with regard to sensitivity and possible singularities.

Experimental research and analysis carried on within the last 20 years has clearly shown that linear strip theory may be used to predict pitch and heave motions in head and bow seas with reasonable accuracy even at high Froude numbers and large sea states. The success of the theory is believed to stem largely from the predominance of the reasonable linear pitch and heave hydrostatic restoring coefficients in the solution of these coupled equations of motion. Variations in the geometry of the waterplane due to waves or a heel angle induce dramatic changes in the roll hydrostatic restoring moment so that as indicated in Figure A-3, the righting arm curve is not linearly related to the roll angle. In a following seaway the restoring moment will actually vary sinusoidally between the two extremes. It is necessary then to choose a suitable value for the $\overline{GM}$ so that $\overline{GM}\theta$ will give a reasonable approximation of the righting arm up to 15 degrees or some appropriate figure of the RMS roll amplitude.

Viscous effects become apparent in roll in the neighborhood of resonance. To account for this, a constant is added to the computed wave damping coefficient which is equal to the difference between the total measured damping and the computed damping at resonance. Experiments conducted elsewhere have demonstrated that roll damping is increased at forward speed. To verify this change and to determine the incremental variation with speed, values for the total damping were determined from roll decay experiments conducted with the *SL-7* model in calm water at zero speed and at the three speed settings. The linear damping term at forward speed was approximately three times greater than the zero speed estimate. Large irregular variations in the total damping occurred between the three Froude numbers. Values for the increased damping calculated from a relationship which was linear in forward speed approximated the general increase which was measured. As can be expected changes due to $\overline{GM}$ were significant due to the predominance of the roll period in the calculations. A more complete discussion of the roll decay experiments and of the calculations of the total roll damping term is presented in Appendix B.

During experimental runs in San Francisco Bay, the *SL-7* model was observed to experience large heel angles due to the effect of the rudder, particularly at high speed. If the model broached, as it was prone to do in a large following or quartering seaway, and if its speed was not greatly reduced, then the model would heel significantly as the rudder-autopilot system tried to correct the course. This induced roll moment coupled with a succeeding large wave was often sufficient to capsize the model. Clearly, the effect of a rudder-autopilot system is important in ship motion calculations in large seas, at least for a time domain solution. But how would such a system affect linear ship motion predictions? Intuitively, it was felt that the magnitude of the related motions would be reduced. To verify this assumption, a linear rudder-autopilot system was added to SEAWAY.

Normally, any autopilot system is designed to operate in a linear manner. The rudder force or lift is proportional to the rudder angle, δ, which in turn is a function of the yaw gain and the yaw rate gain.

$$\delta = k_1\psi + k_2\dot{\psi}$$

The nonlinearities arise due to any deadband in the system, due to time lags inherent in the mechanical system and due to a maximum limitation of the rudder angle.

It is possible, though, to use a least squares fit method to determine values for k_1 and k_2 which give a better approximation of the actual operation of the rudder-autopilot system. See Appendix C. With acceptable values for k_1 and k_2, the rudder coefficient of lift, and the center of pressure of the rudder, the appropriate coefficients may be determined and added to the coupled equations of motion in roll, yaw, and sway.

The response amplitude operators (RAO) are the motion components computed for unit wave amplitudes. These were calculated for one condition of the *SL-7* model with and without an equivalent linear rudder-autopilot system. Results are presented in Figures IV-1.1 through IV-2.3. As anticipated, the yaw and sway motions were decreased. Surprisingly, the roll RAO's showed a small but definite increase. Note that the results are presented for wave frequencies and not for encounter frequencies. The latter would require a folding of the spectra or a concentration of the energy within a narrower band.

Calculation of the RAO's using SEAWAY was limited by a maximum of 24 wave frequencies. In order to avoid missing resonant peaks in the spectra and to assure that linear interpolation between spectral ordinates would be reasonable, a maximum wave frequency of 8.0 radians per second was chosen. Selection of this upper limit was due to the fact that most of the measured wave point spectra contained very little energy beyond this frequency. Even so, some of the RAO's do show a somewhat "squarish" peak which would indicate that the peak was rather narrow and that the resonant frequency occurred midway within the interval.

The heave and pitch RAO's shown in Figures IV-3.1 and IV-3.2 display a gradual change in shape and magnitude between different headings with respect to the wave direction. The largest variations occur near beam seas. For $\chi = 90°$ the response is very broad and therefore susceptible to excitation from higher frequencies, even after folding, since for this condition $\omega_e = \omega$. This point is significant for theoretical predictions for a quartering seas course when the directional spectrum is reasonably broad. Resulting motion spectra may be heavily influenced by high frequency components from the beam direction.

In order to check SEAWAY's output, comparisons were made with published experimental data. Good agreement was obtained for pitch and heave RAO's for all directions and a range of speeds.

Unfortunately, there is a lack of experimental results for sway, yaw and roll RAO's which does not permit a reasonable comparison to be made with SEAWAY's output. Sway and yaw RAOs (Figures IV-1.1 and IV-1.3) are generally characterized by sharp peaks at the resonant frequency for each heading or direction. The roll RAOs are also closely related to the natural frequency. However, the spectra shown in Figure IV-1.2 exhibit much broader qualities and often a second peak due to the coupling effects of yaw and sway.

One aspect of linear strip theory predictions which has not been touched upon is the seaway or directional wave spectra. This is, of course, along with speed and direction, one of the major variables in linear theory predictions. The directional spectra used as input for SEAWAY were computed by Capon's maximum likelihood filter from the point spectra measured with the four probe wave buoy between various experimental runs. As discussed in Chapter III the measurement and computation of the directional spectra has been very successful. Possible inaccuracies may arise due to the step-measurement of the wave height or due to the spreading or smoothing which is done in calculating a 360 degree spectra from a number of point spectra. However, these points are of relatively minor importance compared with two other considerations. First, point spectra were measured at one location while the model during a very long run may have covered a distance of 2/3 of a mile or more. Second, the seaway was not measured simultaneously with each run but rather at infrequent intervals between runs. All model runs were bracketed by wave spectral measurements. Interpolation between wave spectra for the time of the model run should be possible for many of these experiments. However, little is known about the changes in spectral shape with time. Comparisons of linear theory predictions with experimental results are made using the directional spectra before and after. Good agreement would require that the computed model motions bracket the experimental motions in a manner consistent with the time intervals between measured events.

The magnitude of the variation in the seaway during a long run is somewhat difficult to assess. Courses were chosen so that the model would pass near the wave buoy approximately half way through a 900 second long run. Disregarding the necessary interpolation in time, the wave spectra may be assumed to represent the mean wave conditions of a long run. Judging from the time histories of the measured motions and from observations of the waves during experiments this assumption is not altogether unreasonable.

The significance of using the seaway measured before and after a run instead of an interpolated spectrum between the two will be discussed later on in light of the actual comparisons between theory and experiment.

One of the aims of studying and comparing linear theory predictions with measured experimental motions was to attempt to determine an upper bound or limit to which the theory may be applied. Certainly the comparisons will not represent a complete range of the input variables, particularly the sea state. Virtually all of the experiments were conducted in rather large following and quartering seas. Comparisons with linear computations in many cases are not particularly fair since large waves and motions present a totally new geometry and substantially altered stability characteristics. The model's speed and heading were subject to variation such as a real ship might experience in heavy seas. Courses and speeds used for linear calculations represent the best possible choice for the mean conditions of a run. In spite of the seeming inability to determine the input parameters exactly due to their variation and of the general disregard for some of the basic restrictions of linear theory, it was hoped that the predictions would still give reasonable estimates of the measured motions or values which showed a definite comparable trend that might possibly be explained and therefore corrected. Comparisons of the computations for all six degrees of freedom with measured values have shown a large amount of scatter. In fact, the agreement in general has been poor. In order to indicate the degree of agreement, to point out some possible sources of error and to assess qualitatively the value or usefulness of the theory for predictions of ship motions in extreme seas, a few experimental runs will be discussed.

Rather than pick a number of experimental runs at random for comparison, a matrix of the runs was formulated, based upon a minimum length of 500 seconds and the "reasonableness" of the data recorded, to facilitate an analysis over a range of seastates. The seastate used to characterize a run and determine its place in the matrix was found by a linear interpolation between the seastate measured before and after the run. Most of the long runs with the *SL-7* model were made for speeds 2 and 3 at $\overline{GM}$ conditions 4 and 6. At lower speeds the model was less likely to capsize and therefore many of the long runs for large seaways occur at low speeds. However, for such conditions it was observed that the model often experienced difficulty in maintaining its prescribed course and once knocked about to beam seas could not return to a quartering or following seas heading. Linear motions were calculated for speed 2 *GM4* and for speed 3 *GM6* of the matrix. Generally the results from the two conditions were

were similar. For the sake of brevity only the surge, pitch, heave, roll and yaw motions for a few runs for the former condition will be discussed. The results are presented in Figures IV-4.1 through IV-4.22.

Translational surge and heave motions were calculated as displacements. In order to compare them with the measured accelerations their spectra were multiplied by ω_e^4, thus emphasizing any motions at higher frequencies.

Surge accelerations were measured for only three of the six runs and are presented in Figures IV-4.5, 4.13, and 4.18. The computed surge motions, which were determined solely from the Froude-Krylov forces, display two very distinct peaks. The first peak occurs at fairly low encounter frequencies and is significantly larger than the second. Note that no similar experimental motions were measured; thus pointing out that neglect of the damping due to the forced motion of the model is a serious omission. The second peak shows a slight agreement both in magnitude and in frequency range with the measured peak.

Both measured and calculated heave accelerations showed an upward trend toward the higher frequencies. See Figures IV-4.1, 4.9, 4.14 and 4.19. This characteristic is readily attributable to beam sea components of the directional spectra. Elimination of the ramps from computed results could be effected by truncating the directional spectra to remove all input from these directions. In general comparison between measured and calculated heave results were disappointingly poor. Unfortunately, no reasonable explanation may be offered for these anomalies, particularly in lieu of the fact that good agreement between measured and calculated heave motions was obtained for head sea tests. As mentioned earlier, comparison with other published heave measurements has also been good even for a wide range of speeds and headings.

Agreement between measured and calculated pitch motions was reasonable for most runs. The computed spectra usually exhibited a much narrower spectral peak.

The encounter frequency at which the computed pitch spectrum peaks is a useful measure of the speed of the model. This value together with the results obtained from the relative velocity transducer permitted an estimation to be made of the decrease in speed due the waves. In essence the speed input to SEAWAY was varied for a number of runs until the peaks of the measured and calculated pitch spectra coincided. The influence of the magnitude of the seaway upon the speed of the model is presented as a graph of relative water speed measured versus significant wave height in Figure III-9. Due to the scatter obtained, a constant speed loss was assumed for each speed setting. For the *SL-7* model in the light condition, the speeds assumed for linear computations were 4.40, 5.75, and 7.10 fps., corresponding to reductions of 0.25, 0.25 and 0.35 fps. for speed settings 1, 2, and 3 respectively.

The calculated pitch spectra for run 11.05 (Figure IV-4.4) differ significantly due to a very large increase in the seaway between successive measurements. The development of the seaway was probably not gradual. As such, interpolation between the directional spectra would probably not have been valid. Figure E-1.10 gives a time sequence of the runs and wave records for the day and some insight as to the growth of the seaway.(See Figure E-2.11)

Like pitch, the measured roll spectra, shown in Figures IV-4.2, 4.6, 4.10, 4.15 and 4.20 exhibited broader peaks than those predicted by linear theory. The total energy or area under the curve was often approximately double. Peak values for the examples were reasonable though consistently low. This is believed attributable to the use of a damping coefficient which was calculated using the natural period of small roll rather than the period of roll at large angles. The latter is approximately 10 percent smaller and would have produced a similar 10 percent reduction in the damping coefficient which in turn would have increased the calculated roll peaks slightly. See Appendix B for a more detailed discussion of the roll damping.

Both measured and computed yaw spectra displayed peaks at the low frequency end of the spectrum. However, the difference in magnitude was quite large so that any further comparisons are seemingly impractical. In fact, only run 18.03 shown in Figure IV-4.16 displays some correlation in shape between the measured and computed spectral curves.

Based upon the foregoing results, linear theory does not appear to be a useful tool for predicting motions for all six degrees of freedom in extreme following seas. Unfortunately the aim of assessing the bounds or limitations of the theory has not been realized except to conclude that it is inadequate for the aforementioned conditions. To accomplish the latter task would require a controlled series of experiments in which the effect of each variable might be determined separately.

Although it may not be feasible to use a computed spectrum for a statistical analysis of roll in extreme following seas due to the discrepancy in spectral area, it would appear that a useful value for the maximum roll angle may be determined from linear theory provided that a reasonable "adjusted" value for the GM is chosen and that the damping coefficient include the effect of forward speed and is calculated for large roll angles as proposed in Appendix B.

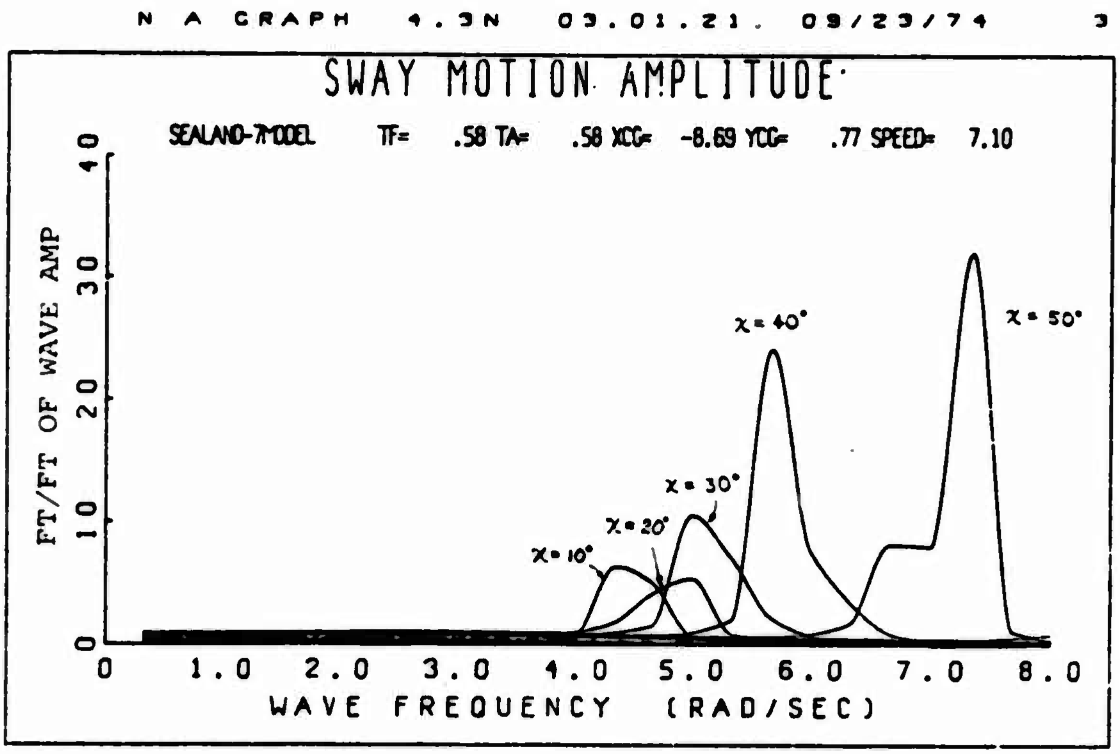

Figure IV-1.1

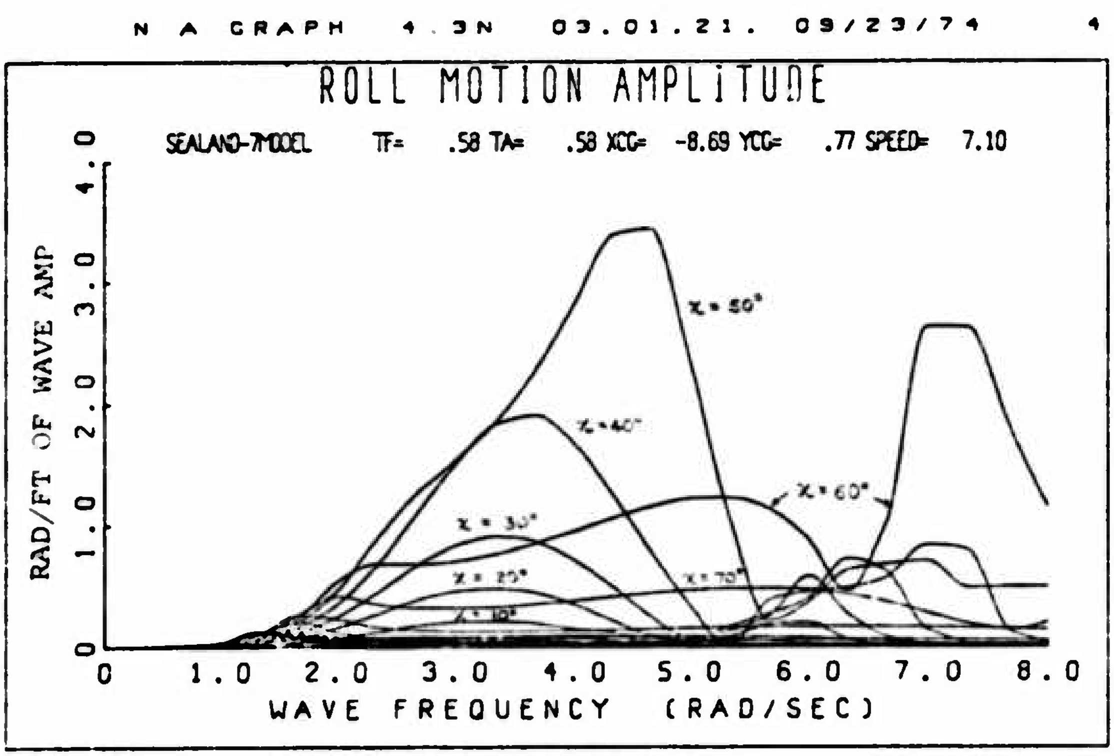

Figure IV-1.2

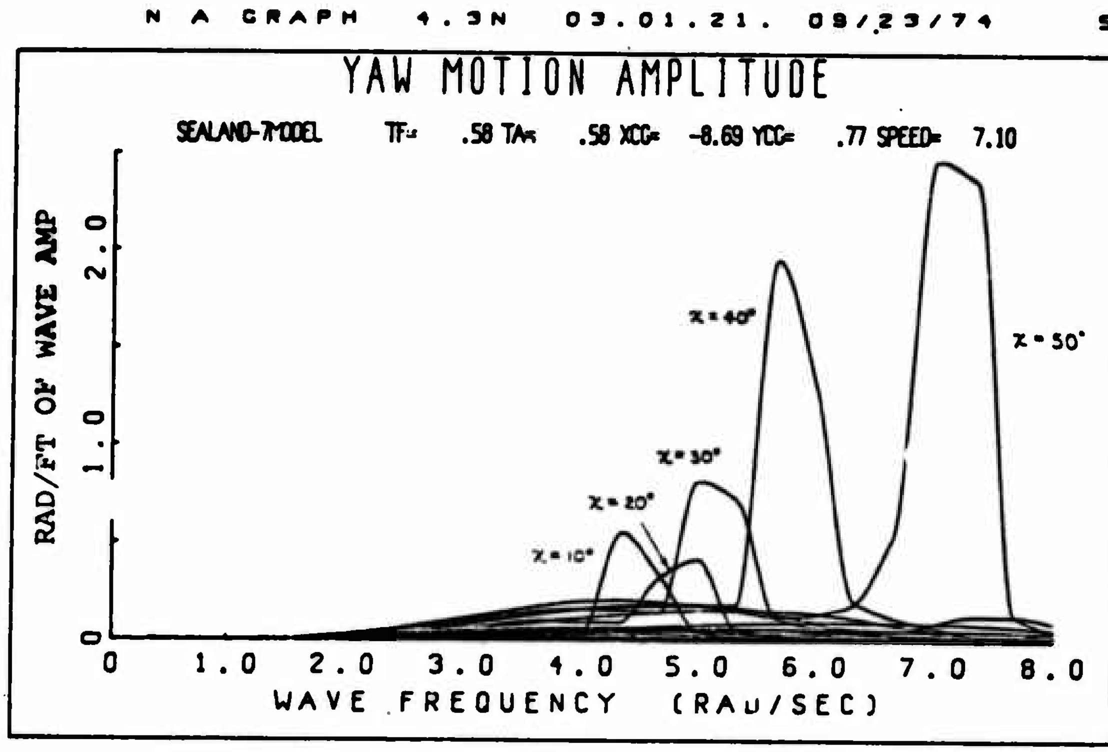

Figure IV-1.3

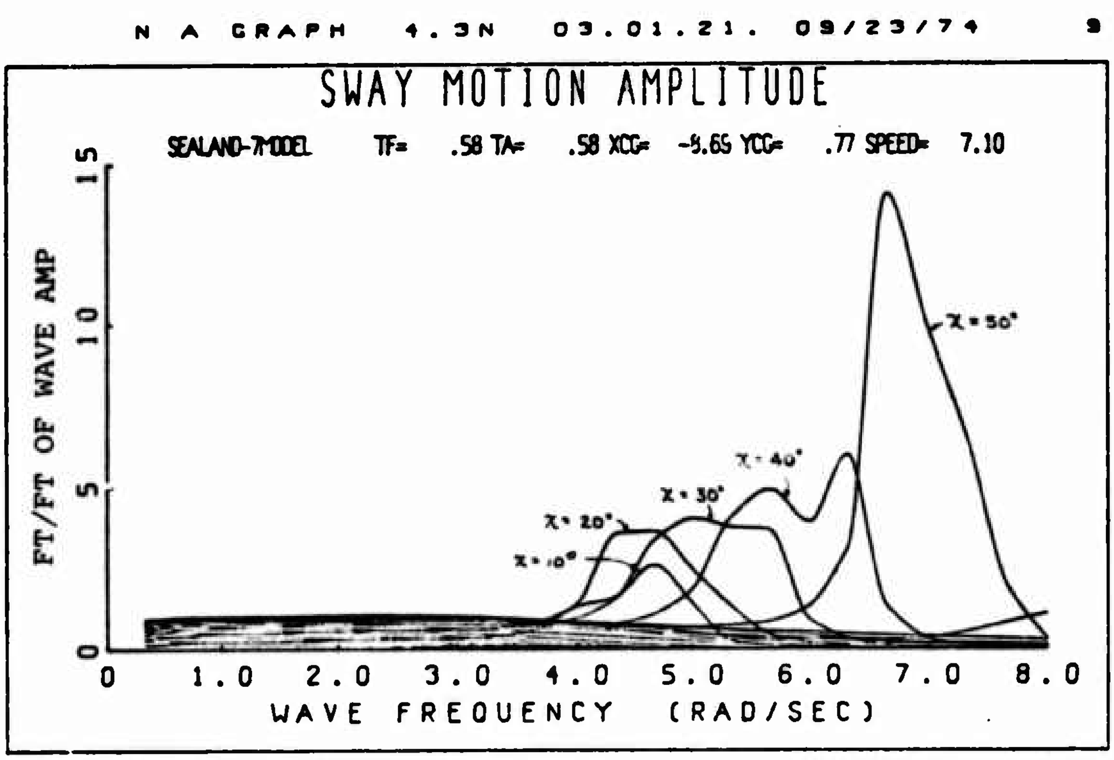

Figure IV-2.1

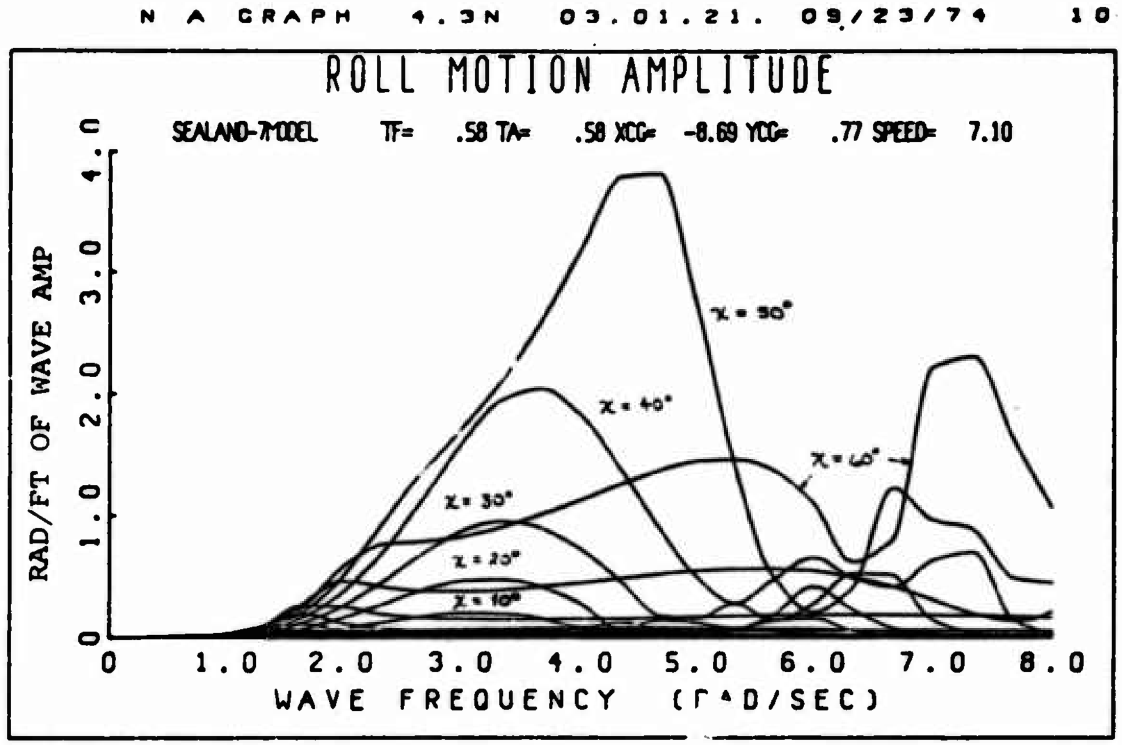

Figure IV-2.2

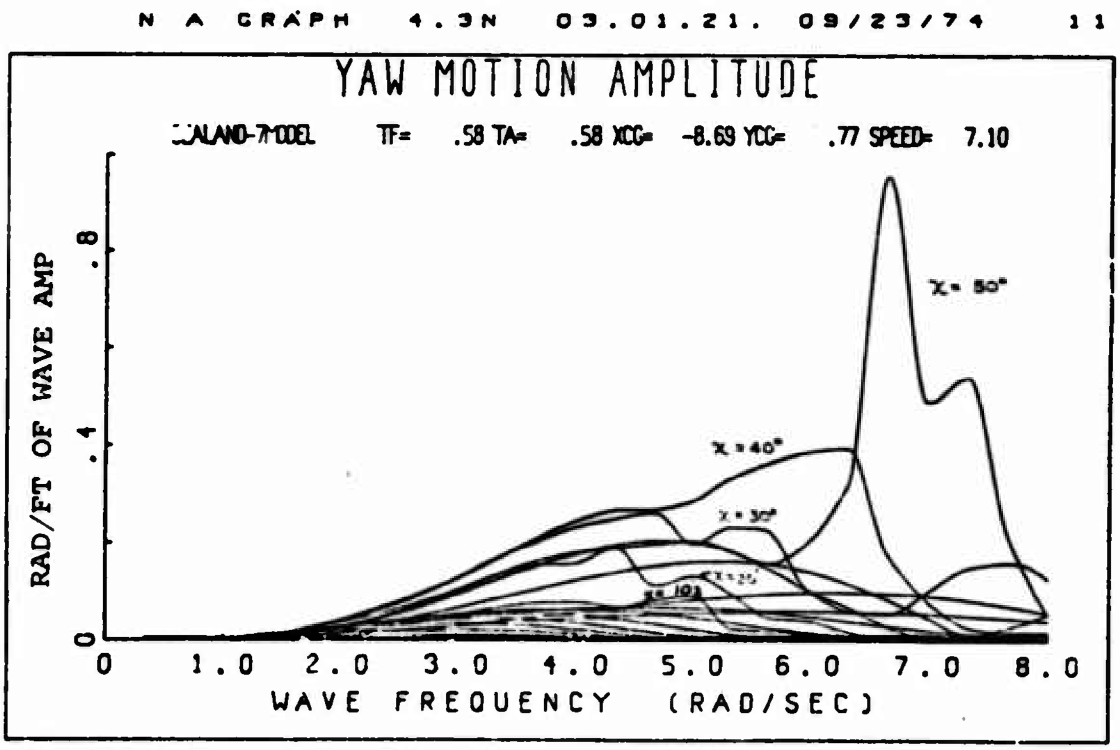

Figure IV-2.3

N A GRAPH 4.3N 03.01.21. 09/23/74 2

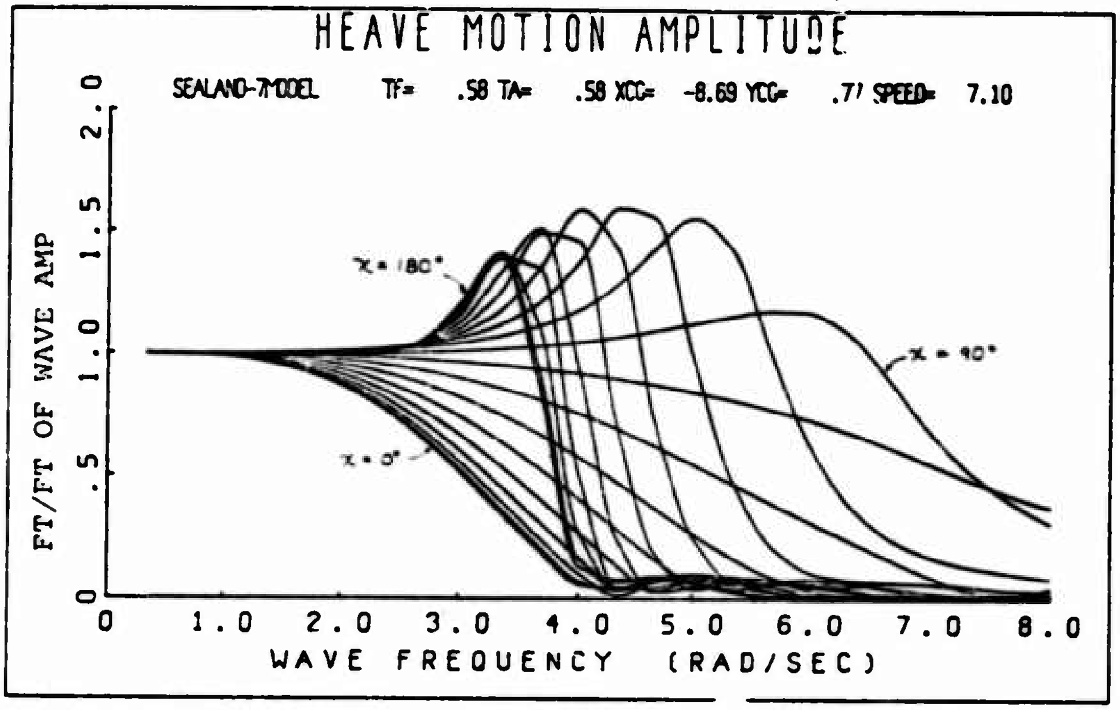

Figure IV-3.1

N A GRAPH 4.3N 03.01.21. 09/23/74 6

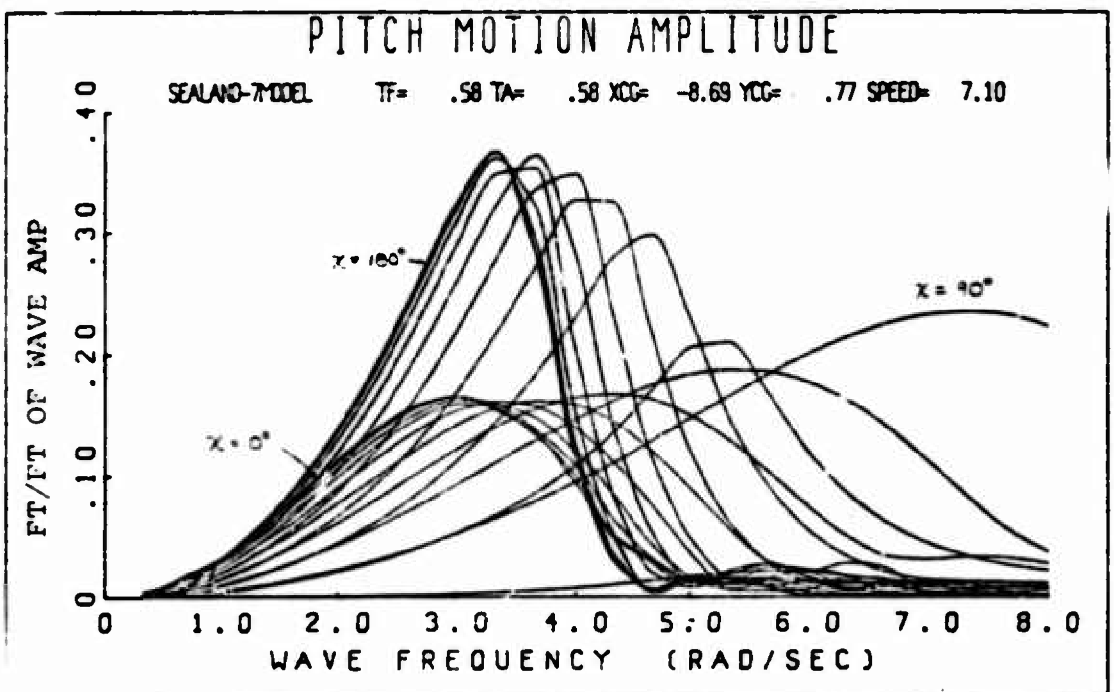

Figure IV-3.2

N A GRAPH 4.3P 02.12.34. 09/28/74 3

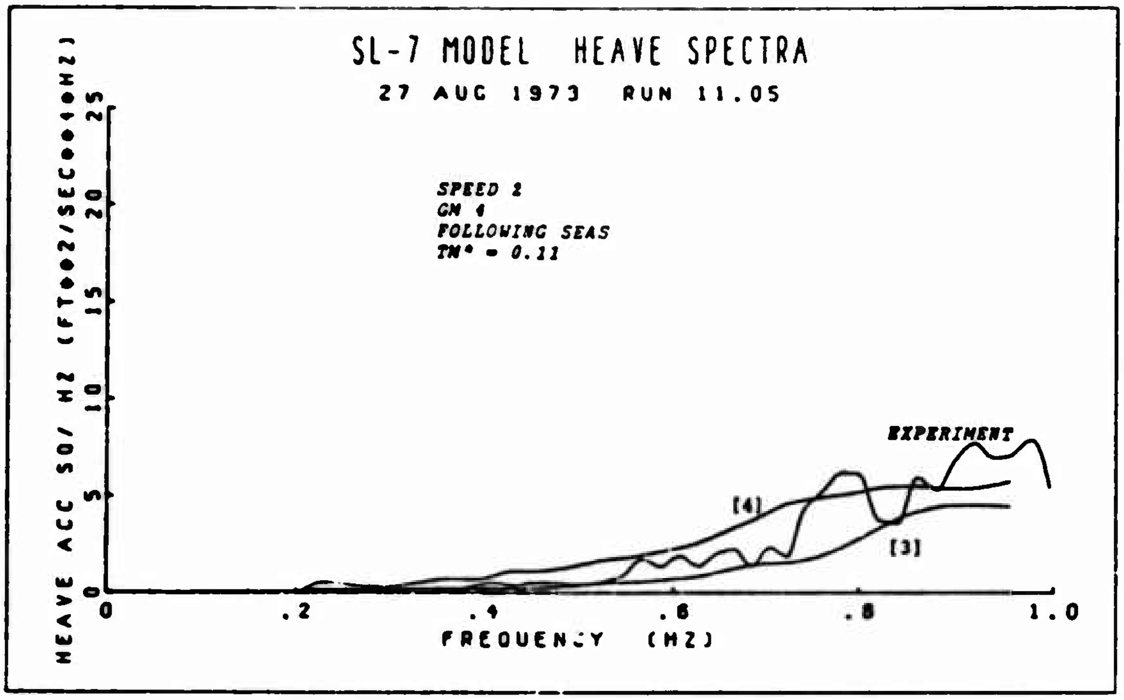

* TM = Time of the model run as a percentage of the time between seaway records

Figure IV-4.1

N A GRAPH 4.3P 02.12.34. 09/28/74 2

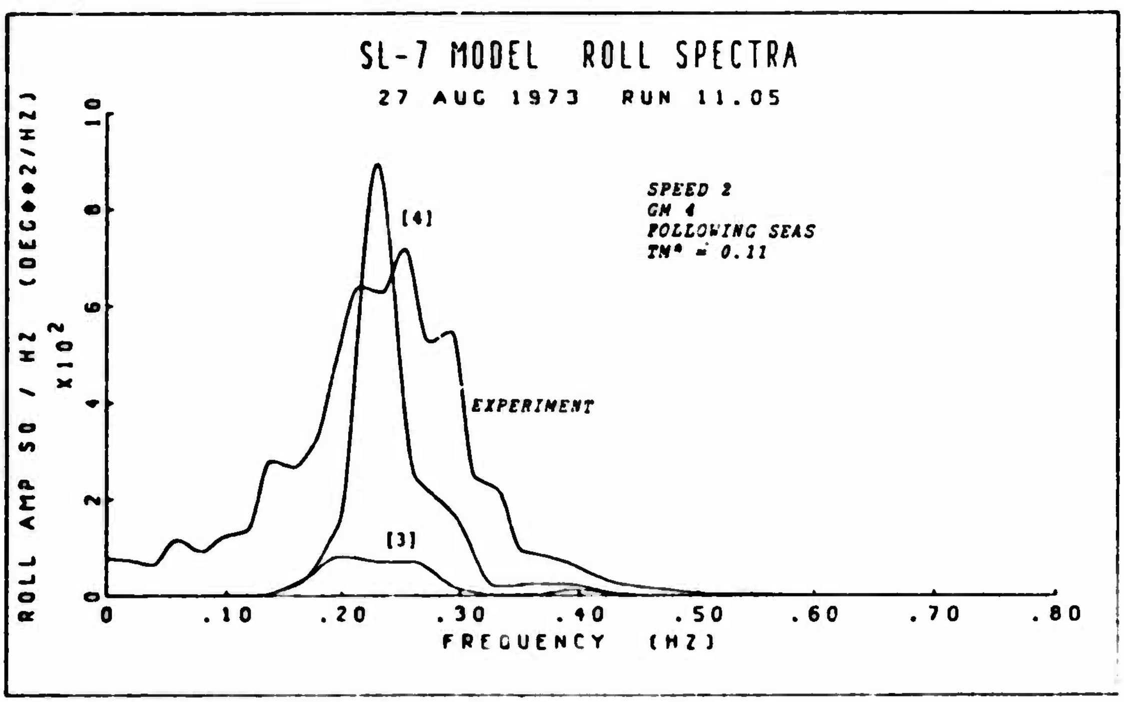

* TM = Time of the model run as a percentage of the time between seaway records.

Figure IV-4.2

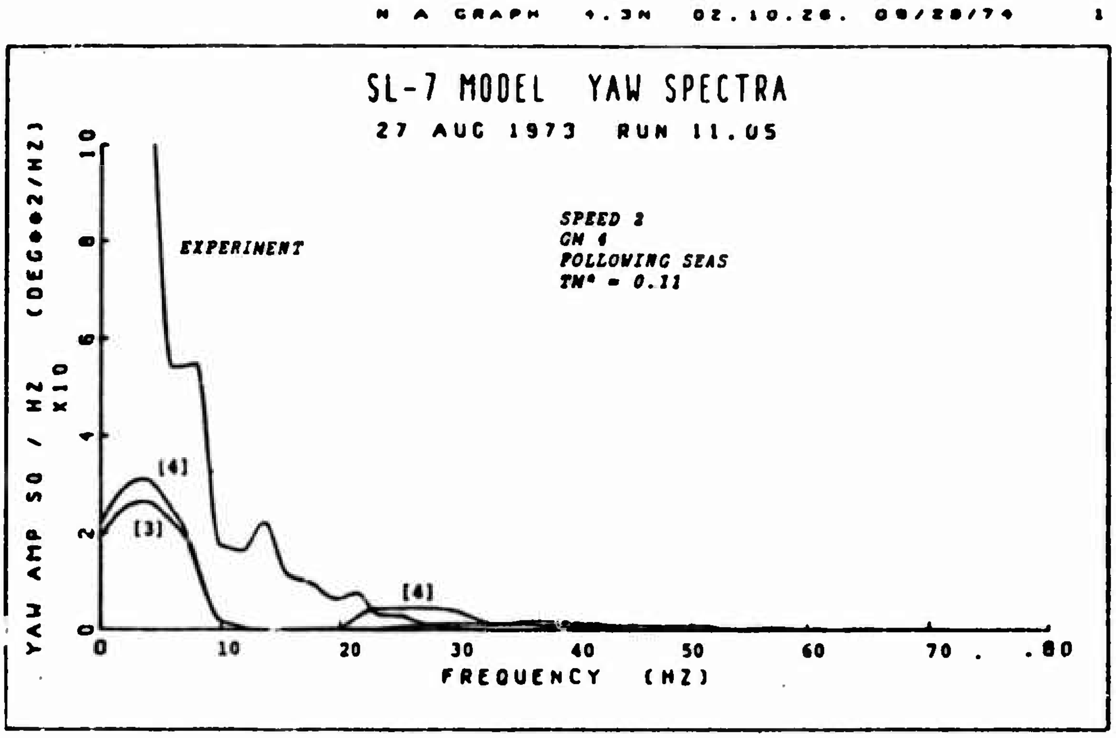

* TM = Time of the model run as a percentage of the time between seaway records.

Figure IV-4.3

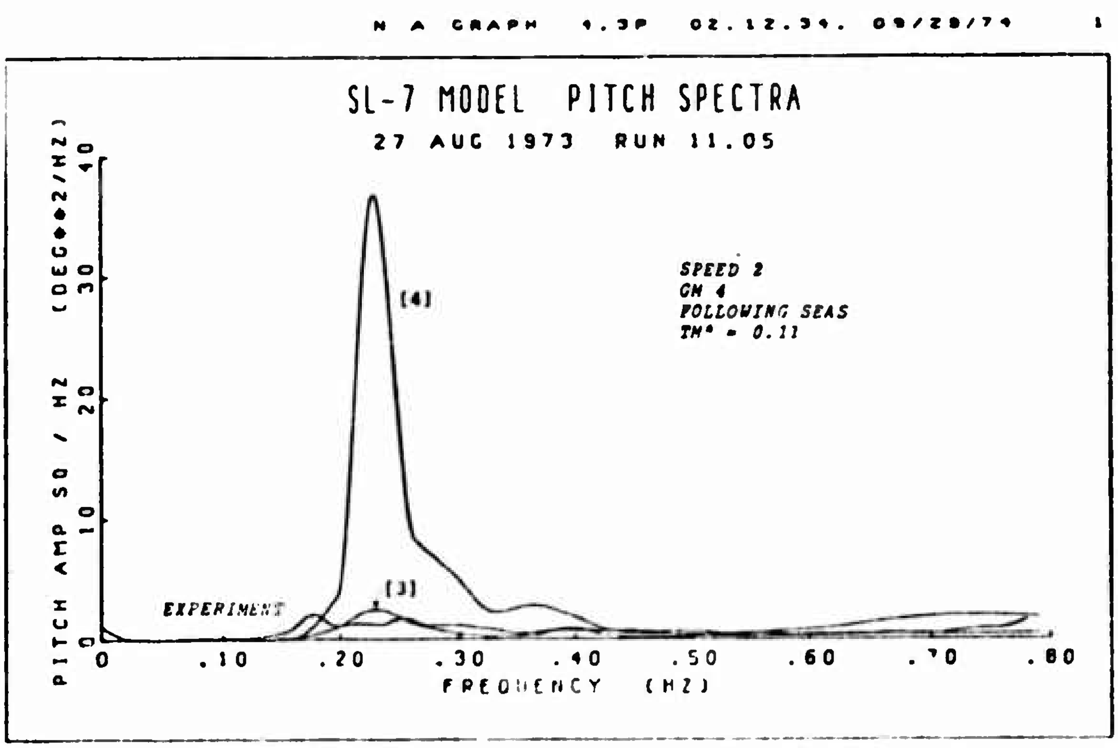

* TM = Time of the model run as a percentage of the time between seaway records.

Figure IV-4.4

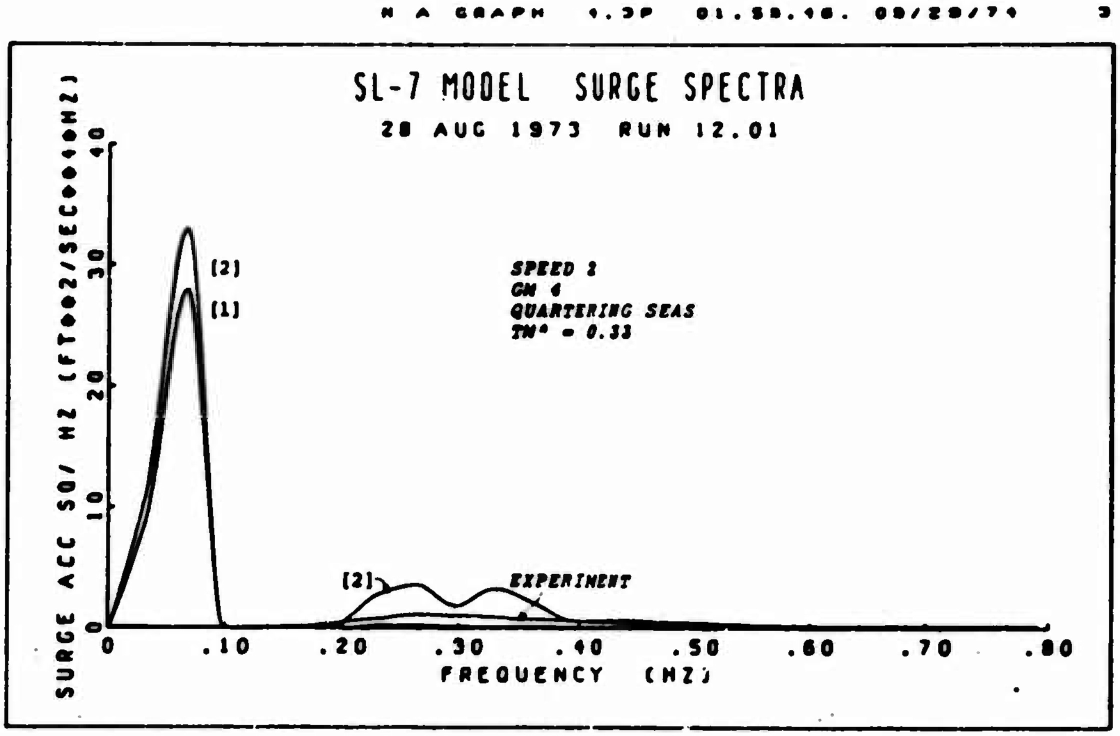

* TM = Time of the model run as a percentage of the time between seaway records.

Figure IV-4.5

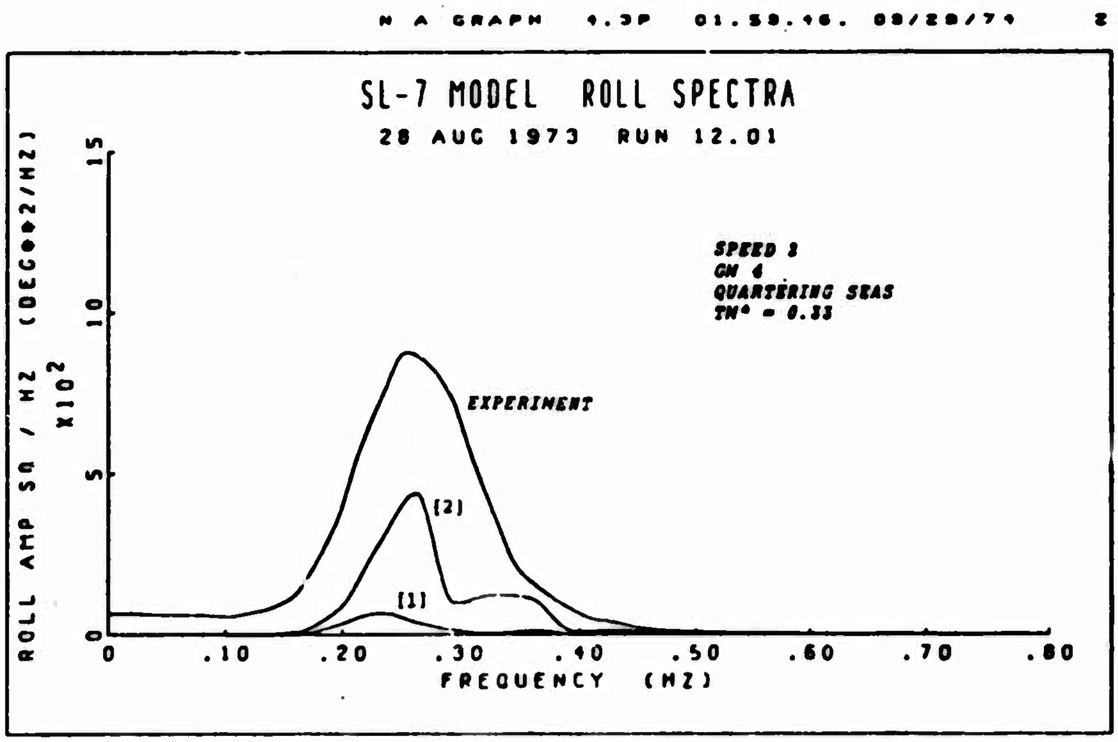

* TM = Time of the model run as a percentage of the time between seaway records.

Figure IV-4.6

N A GRAPH 4.3N 01.57.40. 08/28/74 1

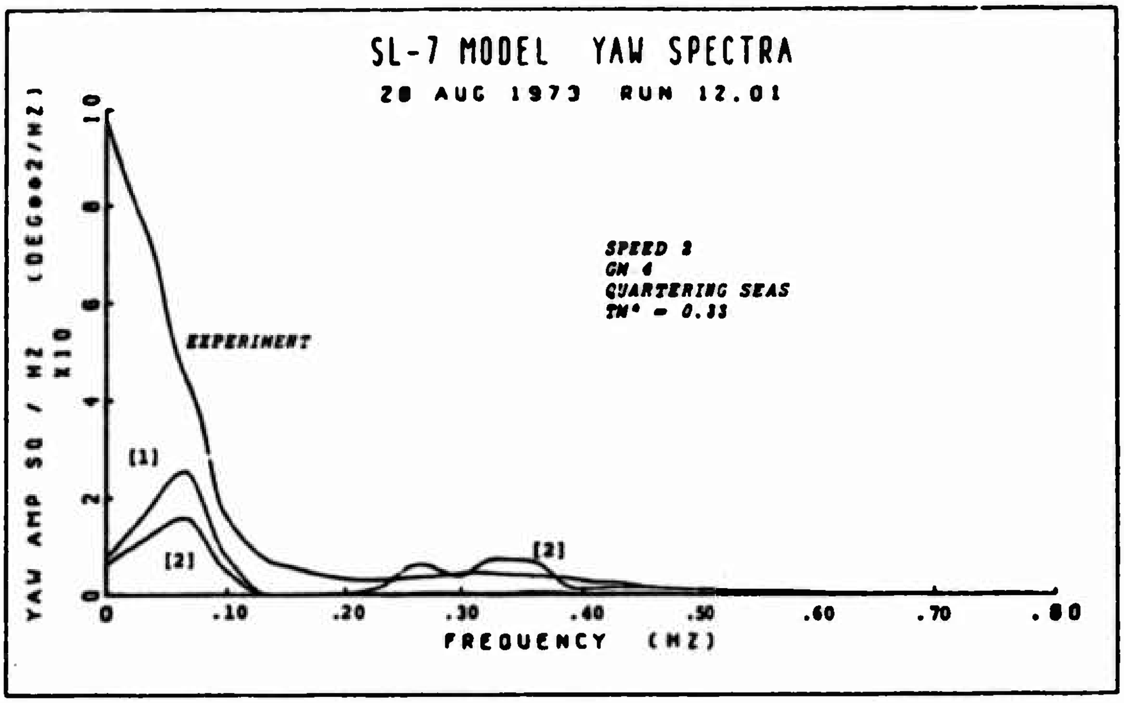

* TM = Time of the model run as a percentage of the time between seaway records.

Figure IV-4.7

N A GRAPH 4.3P 01.59.46. 08/28/74 1

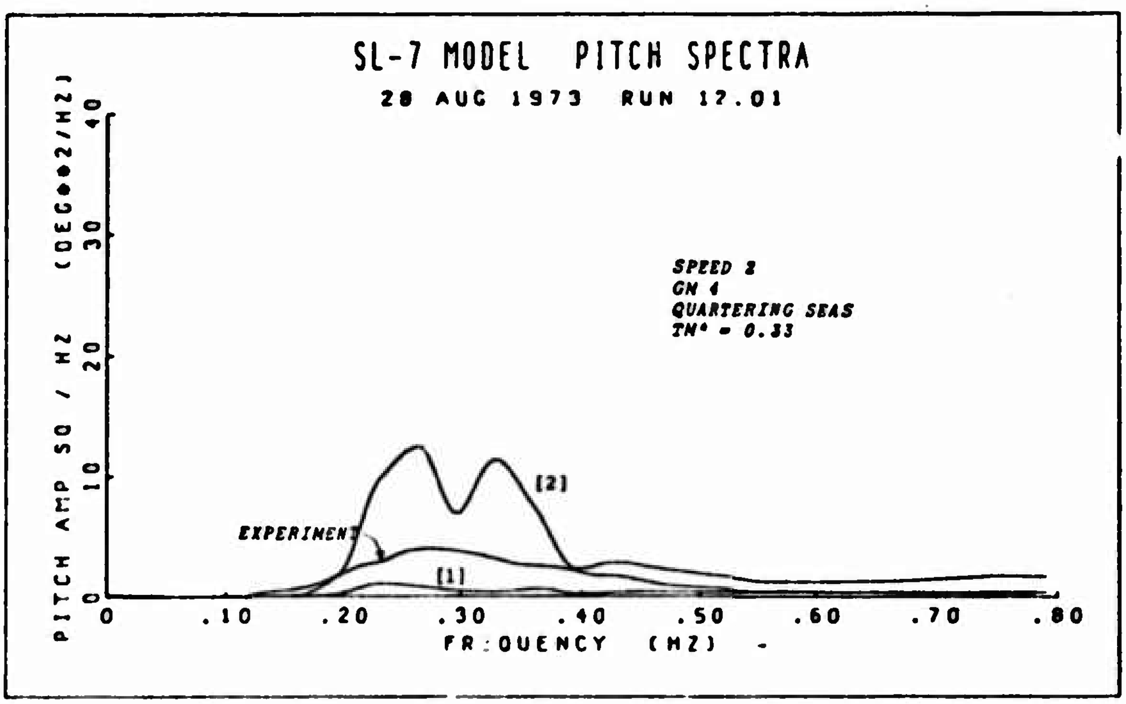

* TM = Time of the model run as a percentage of the time between seaway records.

Figure IV-4.8

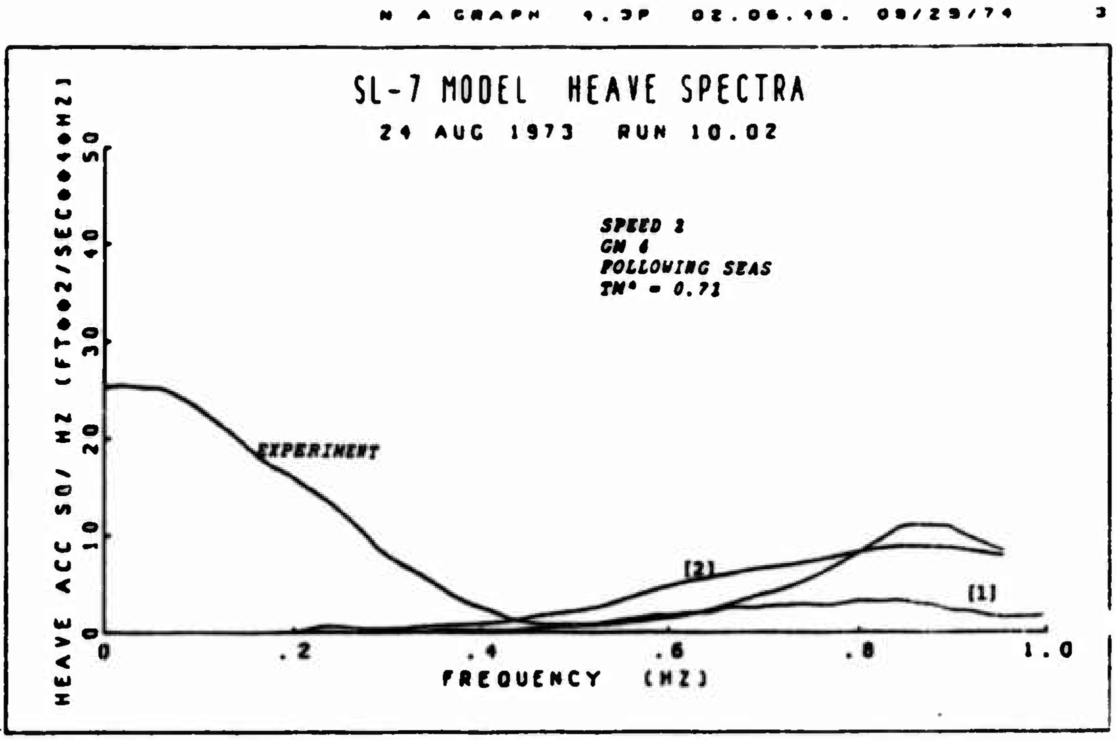

* TM = Time of the model run as a percentage of the time between seaway records.

Figure IV-4.9

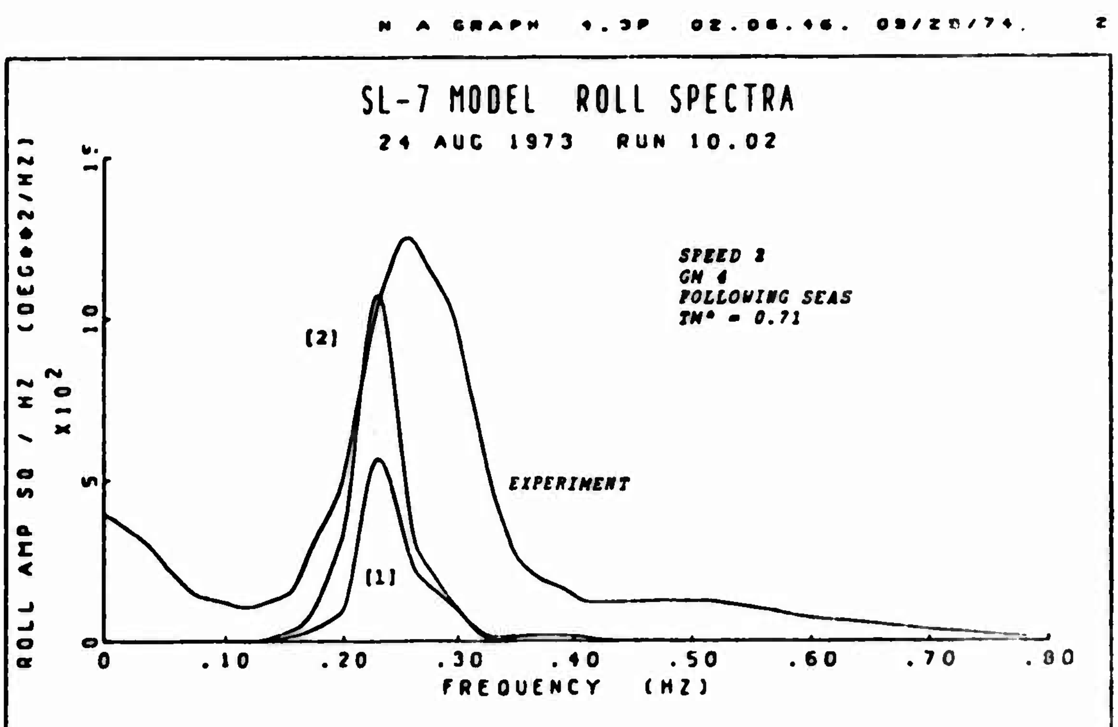

* TM = Time of the model run as a percentage of the time between seaway records.

Figure IV-4.10

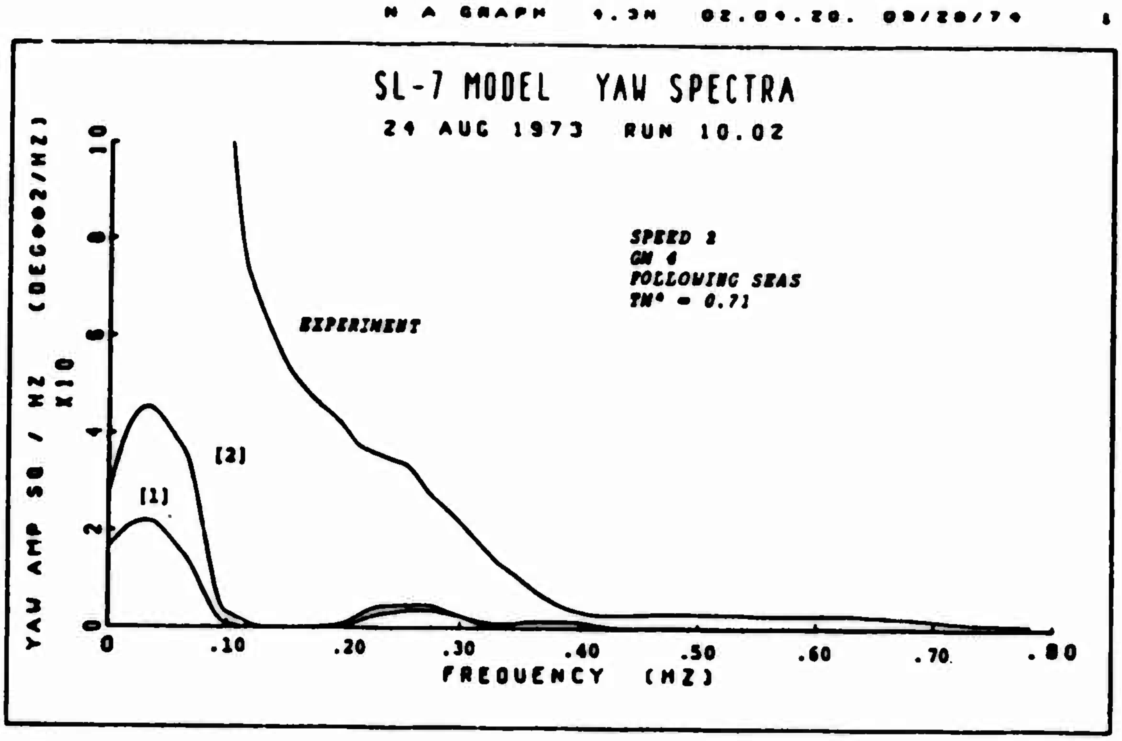

* TM = Time of the model run as a percentage of the time between seaway records.

Figure IV-4.11

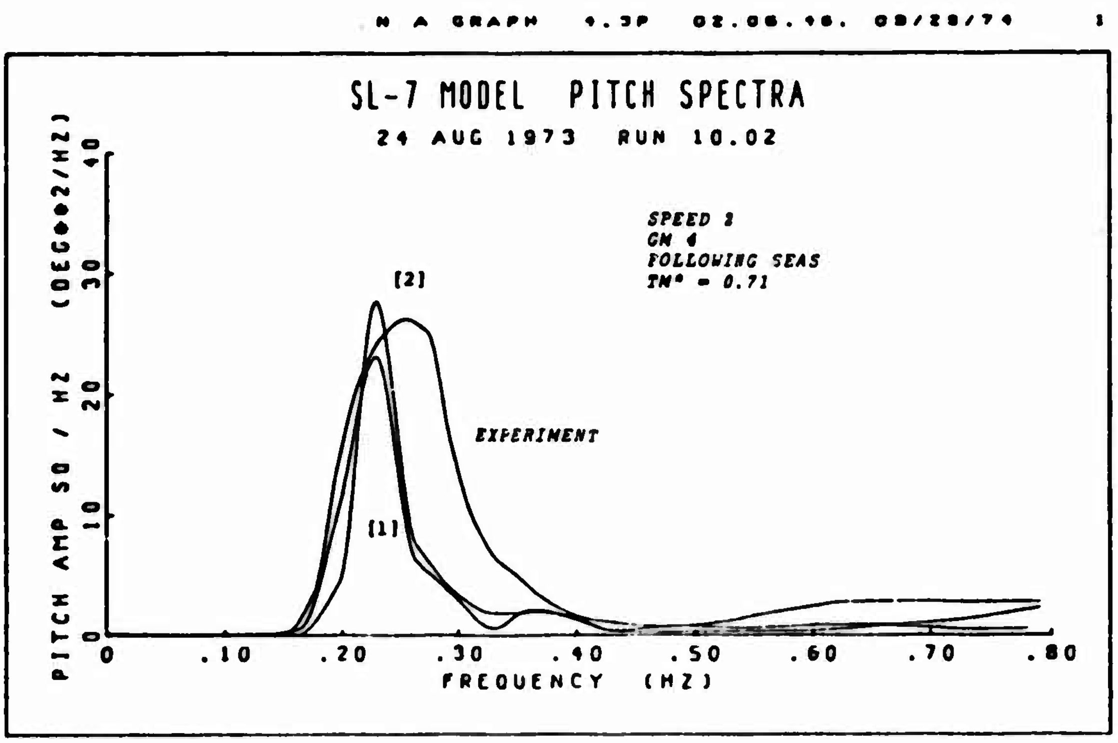

* TM = Time of the model run as a percentage of the time between seaway records.

Figure IV-4.12

N A GRAPH 4.3N 01.42.32. 08/28/74 5

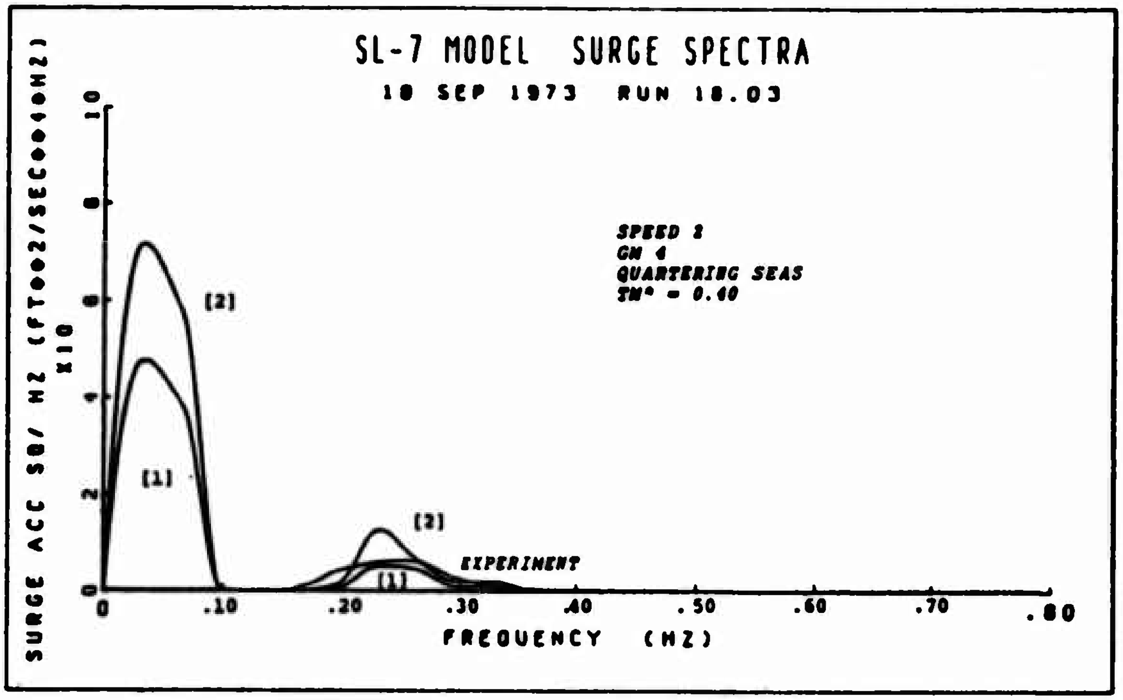

* TM = Time of the model run as a percentage of the time between seaway records.

Figure IV-4.13

N A GRAPH 4.3P 01.44.20. 08/28/74 3

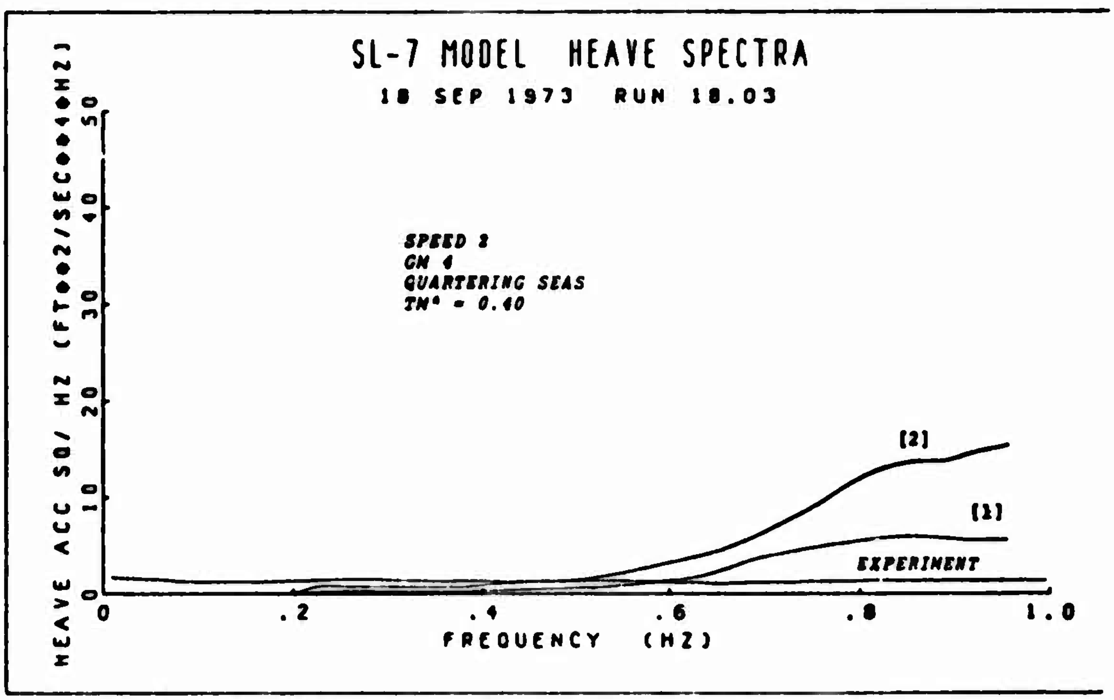

* TM = Time of the model run as a percentage of the time between seaway records.

Figure IV-4.14

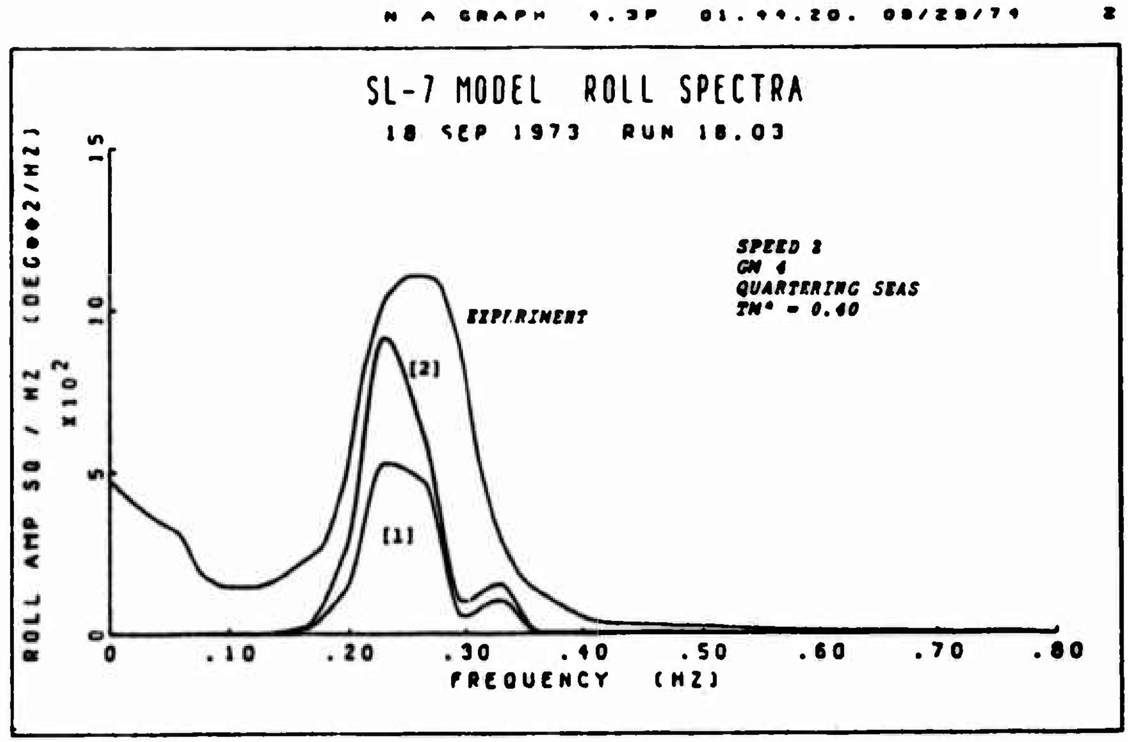

* TM = Time of the model run as a percentage of the time between seaway records.

Figure IV-4.15

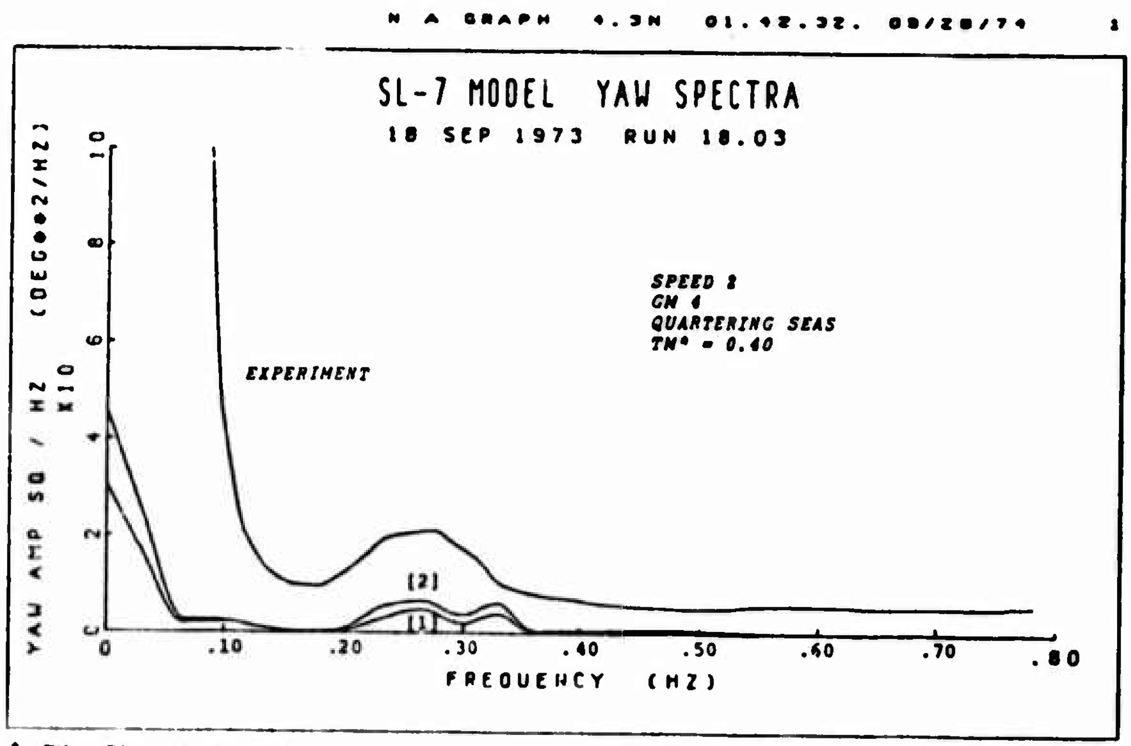

* TM = Time of the model run as a percentage of the time between seaway records.

Figure IV-4.16

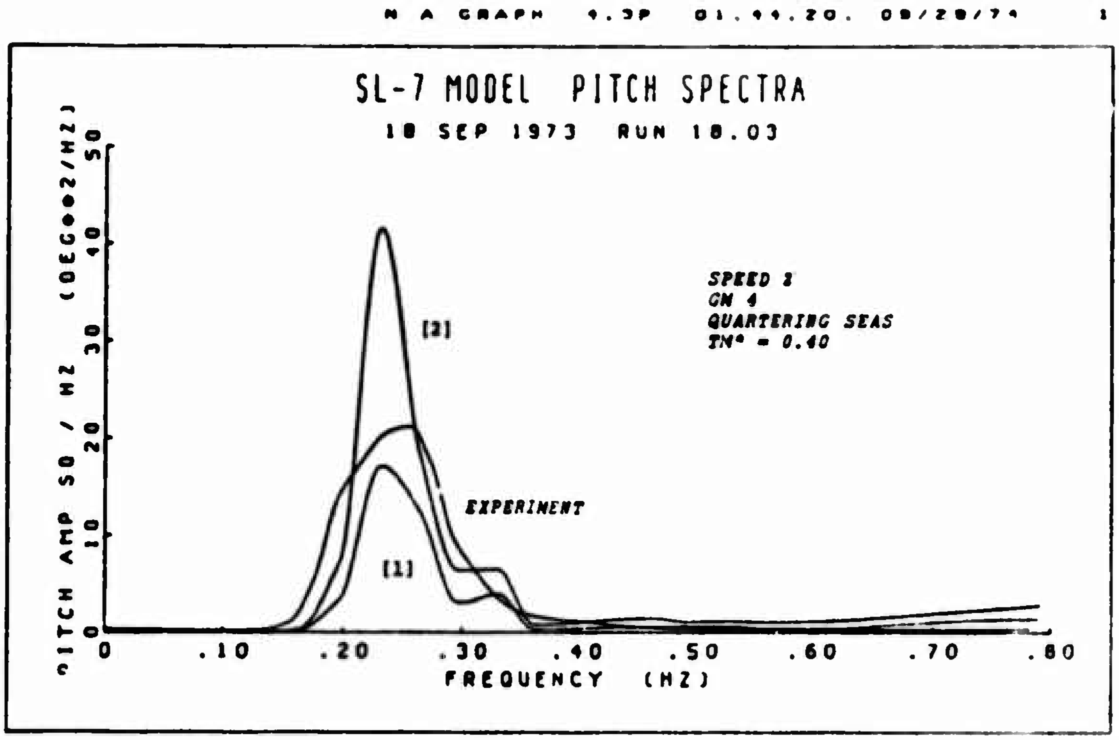

* TM = Time of the model run as a percentage of the time between seaway records.

Figure IV-4.17

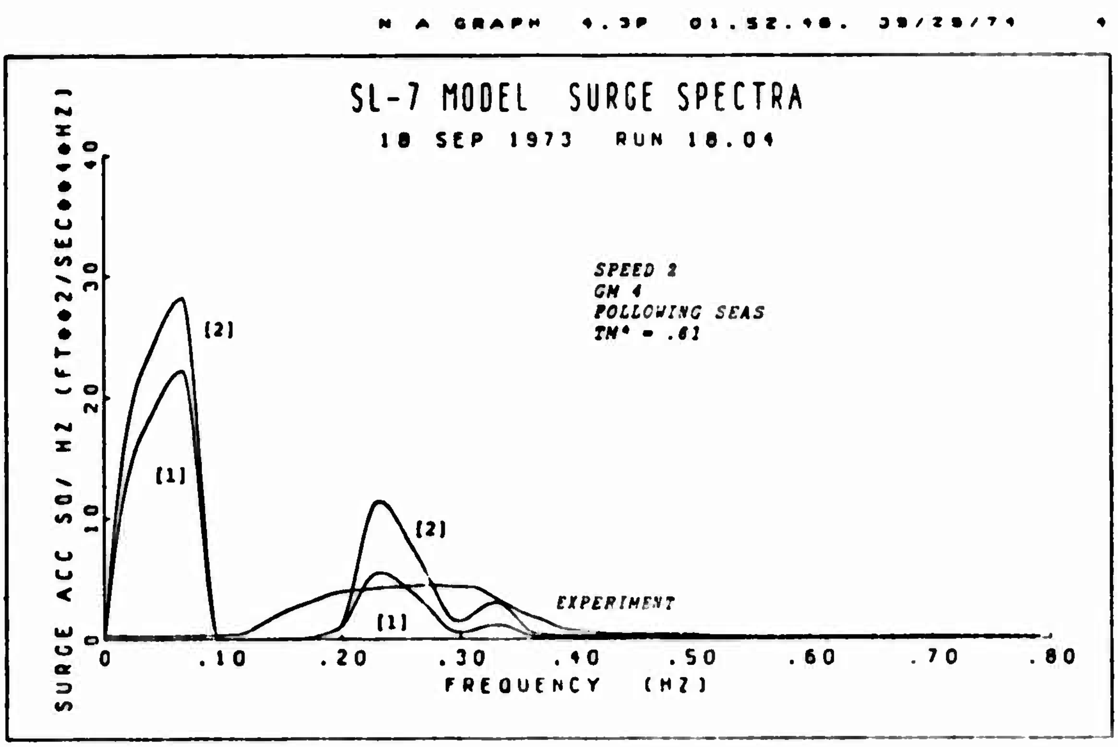

* TM = Time of the model run as a percentage of the time between seaway records.

Figure IV-4.18

N A GRAPH 4.3P 01.52.46. 08/28/74 3

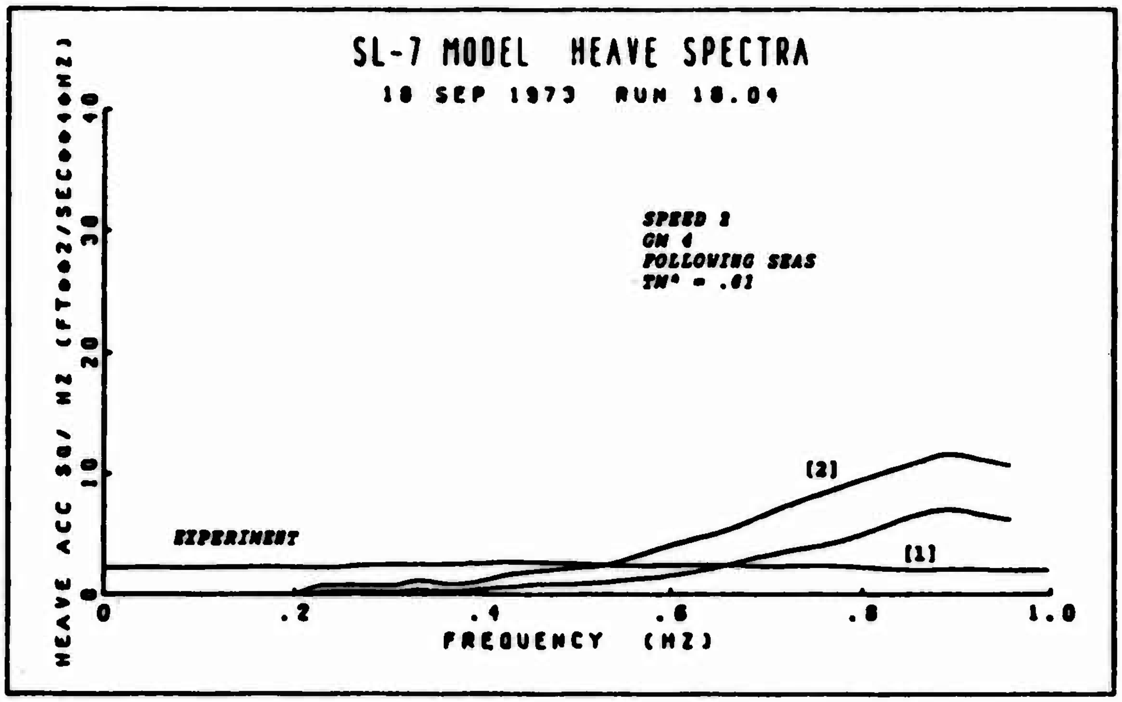

* TM = Time of the model run as a percentage of the time between seaway records.

Figure IV-4.19

N A GRAPH 4.3P 01.52.46. 08/28/74 2

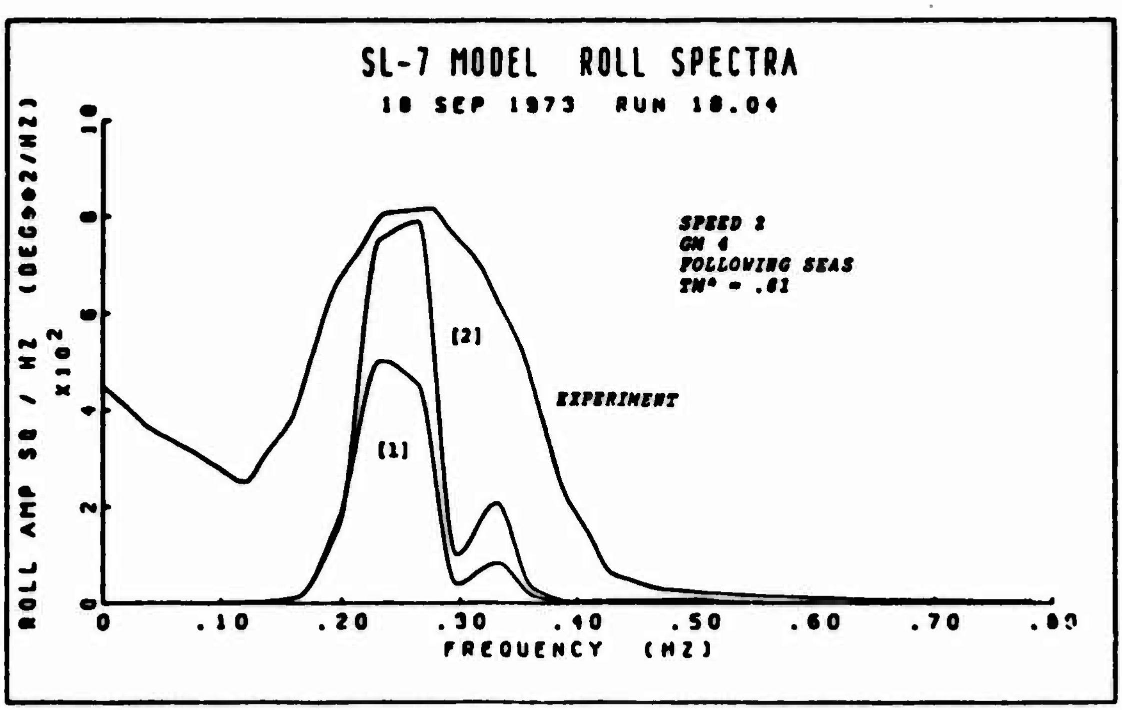

* TM = Time of the model run as a percentage of the time between seaway records.

Figure IV-4.20

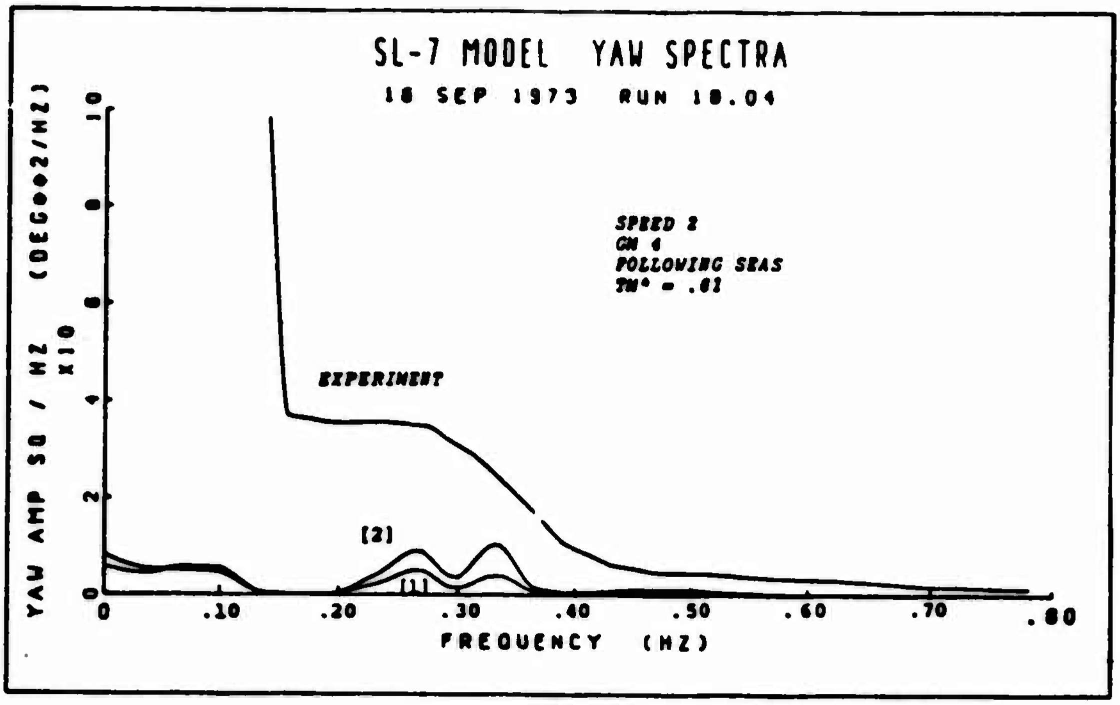

* TM = Time of the model run as a percentage of the time between seaway records.

Figure IV-4.21

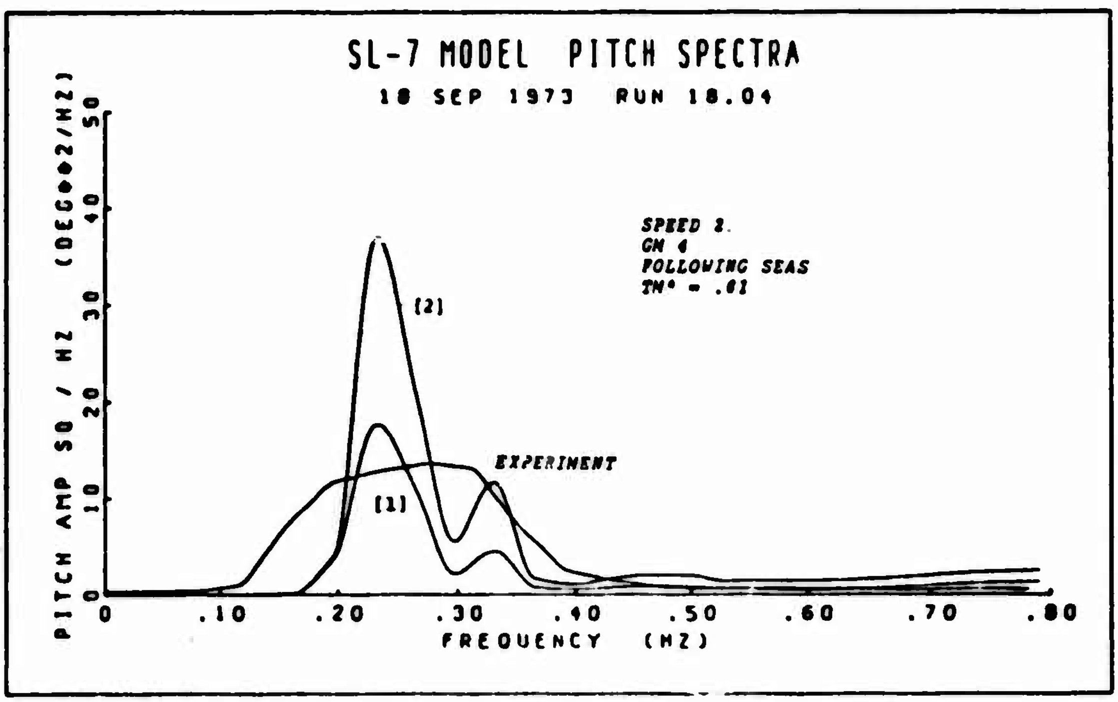

* TM = Time of the model run as a percentage of the time between seaway records.

Figure IV-4.22

V. NUMERICAL SIMULATION OF THE MOTION IN ASTERN SEAS

A complete analytical solution for the motion of a ship in waves requires first that the hydrodynamic forces acting on the ship be found. Solutions of the hydrodynamic problems have heretofore been obtained only under the assumption of small motion amplitudes, in which case the forces acting on the ship are computed as though the instantaneous position of the ship differs but little from its mean position. Such an assumption cannot be used in the present case where large deviations in position from the mean are an essential feature of the phenomenon. Instead, we observe that at high speed in following and quartering seas the frequency of wave encounter will be low and the ship motion will be determined largely by the hydrostatic forces. This enables us to retreat from the necessity of determining the hydrodynamic forces with great accuracy but to concentrate instead on the hydrostatic forces which may be computed for the exact position of ship and waves. These forces, plus additional external forces representing, e.g., the steering and controls, plus a simplified approximation to the relatively unimportant hydrodynamic terms then are used as the right hand side of the rigid body equations of motion. A standard numerical procedure is employed to integrate the equations of motion leading to a step-by-step approximation of the vessel's motion.

A. Formulation of the Problem

The ship is assumed to behave as a rigid body having six degrees of freedom. Newton's second law may be written for the body in the form

$$\frac{d}{dt} m \underset{\sim}{v} = \underset{\sim}{f} \qquad \text{(V-1)}$$

and

$$\frac{d}{dt} \underset{\sim}{I} \, \underset{\sim}{\omega} = \underset{\sim}{g} \qquad \text{(V-2)}$$

where

t = time,

m = mass of the body (ship),

$\underset{\sim}{v}$ = velocity vector of the mass center,

$\underset{\sim}{f}$ = force vector,

$\underset{\sim}{I}$ = inertia matrix,

$\underset{\sim}{\omega}$ = angular velocity vector, and

$\underset{\sim}{g}$ = moment of the force about the mass center.

The force and moment result from the gravitational force acting at the mass center and the interaction between the ship and the sea. The force and moment, in general, depend on the time history of the position of the ship in the sea. Under appropriate circumstances, however, this history may be characterized by the instantaneous position, velocity, and acceleration of the ship. The general problem is nonlinear in the motion variables in that the force and moment are nonlinear functions of the motion of the ship, and the rate of change of angular momentum in equation (V-2) contains nonlinear terms. As noted previously, we shall focus on an exact computation only of the hydrostatic part of the force.

B. Coordinate Systems

Since large amplitude motions are to be computed, it is necessary to clearly define the relationships between several coordinate systems to be used in describing the ship and water motion. The coordinate systems described below are right hand Cartesian systems.

A Newtonian reference frame is formed by the $\bar{O}\bar{x}\bar{y}\bar{z}$ system which is fixed in space and so oriented that the $\bar{x}\bar{z}$-plane is the equilibrium sea surface, and the $\bar{y}$-axis is directed upwards.

A body coordinate system $Gxyz$ is fixed in the ship such that the origin, G, coincides with the center of gravity of the ship. In a ship of usual form, the x-axis is parallel to the baseline and directed forward, the xy-plane is parallel to the centerplane of the ship, the y-axis is directed upward and the z-axis to starboard.

The position of the ship mass center, G, may be specified in the fixed coordinate system by

$$\bar{x} = x_G$$
$$\bar{y} = y_G$$
$$\bar{z} = z_G .$$

This may be represented by the vector

$$\bar{\underset{\sim}{x}} = \begin{Bmatrix} x_G \\ y_G \\ z_G \end{Bmatrix} \qquad \text{(V-3)}$$

The velocity of the mass center is represented by the vector

$$\bar{\underset{\sim}{v}} = \frac{d}{dt}\,\bar{\underset{\sim}{x}} = \begin{Bmatrix} \frac{d}{dt}\,x_G \\ \frac{d}{dt}\,y_G \\ \frac{d}{dt}\,z_G \end{Bmatrix} \qquad \text{(V-4)}$$

Any rotation of the ship coordinate system is uniquely defined by the modified set of Eulerian angles described below. These angles are similar to the ones given by Blagoveshchensky (1962), but differ from the ones used by Euler. The angles are defined as follows.

Consider the ship coordinates in a position before rotation with the x, y, and z-axes parallel to the fixed $\bar{x}$, $\bar{y}$, $\bar{z}$-axes. This is the orientation of $Gx_1y_1z_1$ in Figure V-1. Rotate the triad about the y_1-axis to the yaw angle ϕ. This postions the frame as $Gx_2y_1z_2$ in the figure. Next, rotate about the z_2-axis to the pitch angle ψ. The figure shows the yawed and pitched orientation as Gxy_3z_2. The final rotation is about the x-axis to the roll angle θ. The orientation of the ship coordinates, $Gxyz$, is indicated in the figure.

The Eulerian angles ϕ, ψ and θ are represented by the vector

$$\underset{\sim}{\alpha} = \begin{Bmatrix} \theta \\ \phi \\ \psi \end{Bmatrix} \qquad \text{(V-5)}$$

The angular volocities about the ship coordinate axes are denoted by p, q, and r corresponding to components of the angular velocity vector along the x, y, and z-axes. These angular velocities may be expressed in terms of the Eulerian angles and their derivatives:

$$\begin{aligned} p &= \frac{d\theta}{dt} + \frac{d\phi}{dt}\sin\psi \\ q &= \frac{d\phi}{dt}\cos\theta\cos\psi + \frac{d\psi}{dt}\sin\theta \\ r &= \frac{d\psi}{dt}\cos\theta - \frac{d\phi}{dt}\sin\theta\cos\psi \end{aligned} \qquad \text{(V-6)}$$

The notation is simplified by representing the angular velocities by the vector

$$\underset{\sim}{\omega} = \begin{Bmatrix} p \\ q \\ r \end{Bmatrix} . \qquad \text{(V-7)}$$

If we define the matrix

$$\underset{\sim}{B} = \begin{bmatrix} 1 & \sin\psi & 0 \\ 0 & \cos\theta\cos\psi & \sin\theta \\ 0 & -\sin\theta\cos\psi & \cos\theta \end{bmatrix} , \qquad \text{(V-8)}$$

and note that

$$\frac{d\tilde{\alpha}}{dt} = \begin{Bmatrix} \frac{d\theta}{dt} \\ \\ \frac{d\phi}{dt} \\ \\ \frac{d\psi}{dt} \end{Bmatrix}, \qquad \text{(V-9)}$$

then equations (V-6) are represented by

$$\underset{\sim}{B} \frac{d\tilde{\alpha}}{dt} = \underset{\sim}{\omega} \quad . \qquad \text{(V-10)}$$

The moments and products of inertia in the angular momentum equation (V-2) are represented by the matrix

$$\underset{\sim}{I} = \begin{bmatrix} I_{xx} & -I_{xy} & -I_{xz} \\ -I_{xy} & I_{yy} & -I_{yz} \\ -I_{xz} & -I_{yz} & I_{zz} \end{bmatrix}, \qquad \text{(V-11)}$$

The moments of inertia are defined as

$$I_{xx} = \Sigma\, m'\, (y^2 + z^2),$$

$$I_{yy} = \Sigma\, m'\, (z^2 + x^2), \qquad \text{(V-12)}$$

and

$$I_{zz} = \Sigma\, m'\, (x^2 + y^2),$$

where the summations are taken over all particles of mass m

comprising the ship. The products of inertia are

$$I_{xy} = \Sigma\ m'\ xy,$$
$$I_{xz} = \Sigma\ m'\ xz, \qquad \text{(V-13)}$$

and

$$I_{yz} = \Sigma\ m'\ yz.$$

These moments and products of inertia are constants in the moving ship coordinate system, $Gxyz$.

In the $Gxyz$ coordinate system, the rate of change of angular momentum is given by

$$\frac{d}{dt} \underset{\sim}{I}\, \underset{\sim}{\omega} = \underset{\sim}{I} \frac{d}{dt} \underset{\sim}{\omega} + \underset{\sim}{\omega} \times \underset{\sim}{I}\underset{\sim}{\omega}, \qquad \text{(V-14)}$$

C. Time Domain Integration

The equations of motion are solved by numerical integration in the time domain. In order to perform the integration using standard algorithms, the equations of motion are rewritten as first order ordinary differential equations.

The position of the ship's center of gravity is determined by the linear momentum equation (V-1). This equation and equation (V-4) are rewritten as

$$\frac{d}{dt} \underset{\sim}{\bar{v}} = \frac{1}{m} \underset{\sim}{f} \qquad \text{(V-15)}$$

and

$$\frac{d}{dt} \underset{\sim}{\bar{x}} = \underset{\sim}{\bar{v}}\ . \qquad \text{(V-16)}$$

In equations (V-15) and (V-16) the vectors are referred to the Newtonian reference frame, $\bar{O}\bar{x}\bar{y}\bar{z}$.

The rotations of the ship are governed by the angular momentum equation (V-2). Combining equations (V-2) and (V-14) and rewriting equation (V-10) give

$$\frac{d}{dt} \underset{\sim}{\omega} = \underset{\sim}{I}^{-1} [\underset{\sim}{g} - \underset{\sim}{\omega} \times \underset{\sim}{I}\underset{\sim}{\omega}] \tag{V-17}$$

and

$$\frac{d}{dt} \underset{\sim}{\alpha} = \underset{\sim}{B}^{-1} \underset{\sim}{\omega} . \tag{V-18}$$

In equation (V-17) the moment vector is referred to the ship coordinate system, $Gxyz$.

The vector equations (V-15), (V-16), (V-17), and (V-18) form a system of twelve simultaneous first order ordinary differential equations which may be integrated by standard numerical procedures. The current version of the program uses a fifth-order Adams type predictor-corrector algorithm developed by Glauz (1960). This features a variable time step to control integration error and an interpolation procedure to avoid the calculation of derivatives at the times chosen for the output of results. At each time step in the integration, the algorithm predicts values for the instantaneous position of the ship and its velocity. The remainder of the program is devoted to the computation of the force and moment used to evaluate (V-15) and (V-17). The integration routine corrects the position and velocity based on the values of the derivatives (V-15) through (V-18), but if the error is small these derivatives are not recomputed.

For computation purposes equations (V-15) and (V-17) are combined. The generalized force vector includes both force and moment:

$$\underset{\sim}{f} = \begin{Bmatrix} f_1 \\ f_2 \\ f_3 \\ g_1 \\ g_2 \\ g_3 \end{Bmatrix} = \begin{Bmatrix} f_1 \\ f_2 \\ f_3 \\ f_4 \\ f_5 \\ f_6 \end{Bmatrix} \tag{V-19}$$

The changing angular momentum in the rotating ship coordinates is included in

$$\underset{\sim}{f}' = \begin{Bmatrix} f_1 \\ f_2 \\ f_3 \\ g_1' \\ g_2' \\ g_3' \end{Bmatrix} \tag{V-20}$$

where the moment components are

$$\underset{\sim}{g}' = \begin{Bmatrix} g_1' \\ g_2' \\ g_3' \end{Bmatrix} = \underset{\sim}{g} - \underset{\sim}{\omega} \times \underset{\sim}{I}\,\underset{\sim}{\omega} .$$

In (V-19) and (V-20) the first three elements are components of force in ship coordinates, and the last three are components of the moment. The generalized acceleration vector is

$$\underset{\sim}{a} = \frac{d}{dt} \begin{Bmatrix} u \\ v \\ w \\ p \\ q \\ r \end{Bmatrix} . \tag{V-21}$$

The inertia of the ship is represented by the matrix

$$\underset{\sim}{A}' = \begin{bmatrix} m & 0 & 0 & 0 & 0 & 0 \\ 0 & m & 0 & 0 & 0 & 0 \\ 0 & 0 & m & 0 & 0 & 0 \\ 0 & 0 & 0 & I_{xx} & -I_{xy} & -I_{xz} \\ 0 & 0 & 0 & -I_{xy} & I_{yy} & -I_{yz} \\ 0 & 0 & 0 & -I_{xz} & -I_{yz} & I_{zz} \end{bmatrix} \qquad \text{(V-22)}$$

Using this notation the momentum equations (V-15) and (V-17) are

$$\underset{\sim}{A}' \underset{\sim}{a} = \underset{\sim}{f}' . \qquad \text{(V-23)}$$

After determining the force this may be solved for the acceleration, $\underset{\sim}{a}$. For the integration, the first three components of $\underset{\sim}{a}$, the linear accelerations, are transformed into the fixed coordinate system to provide velocity derivatives (V-15), and the derivatives of the angular velocity (V-17) are the last three elements of $\underset{\sim}{a}$.

D. Computation of Force and Moment

The present version of the computer program for the time-domain simulation of large amplitude ship motions assumes that the force and moment acting on the ship may be modeled using an accurate computation of the hydrostatic or Froude-Krylov forces plus approximations to the hydrodynamic forces.

Since large amplitude motions and finite amplitude waves are assumed, the hydrostatic restoring and coupling coefficients computed for the equilibrium position cannot be used. It has been shown by Paulling (1961) and others that there can be significant variations in the roll restoring moment as a wave progresses alc 'he ship's length as well as the change in this moment caused ل large amplitude roll angles. The Froude-Krylov force that is computed by the numerical simulator includes both the motion exciting force and the restoring force and moment that result from the situation of the ship in the system of waves at any time step during the simulation.

The sea surface elevation is given by the sum of sinusoidal waves in the fixed, $\bar{O}\bar{x}\bar{y}\bar{z}$, coordinate system. The water surface is given by

$$\bar{\eta}(\bar{t},\bar{x},\bar{z}) = \sum_{i=1}^{N} \eta_i(\bar{t},\bar{x},\bar{z}) \qquad \text{(V-24)}$$

where

$\bar{\eta}$ = the $\bar{y}$ coordinate of the surface,

and

N = the number of wave components (in the present version of the program $0 \leq N \leq 20$).

The component wave amplitude is:

$$\eta_i = A_i \cos(\bar{x}k_i \cos\delta_i - \bar{z}k_i \sin\delta_i + \phi_i - \sigma_i t)$$

where

A_i = the amplitude of the i-th wave,

σ_i = the circular frequency,

ϕ_i = initial phase angle,

$k_i = \sigma_i^2/g$ = wave number,

g = the gravitational acceleration,

and

δ_i = the direction of the wave propagation.

The wave pressure is

$$p(t,\bar{x},\bar{y},\bar{z}) = -\rho g\bar{y} + \sum_{i=1}^{N} p_i(t,\bar{x},\bar{y},\bar{z})$$
$$p_i = \rho g e^{k_i\bar{y}} \eta_i \tag{V-25}$$

where

ρg = the specific weight of the water.

The Froude-Kyrlov force and moment may be obtained by integrating the pressure over the entire wetted surface of the ship. By applying Gauss' Theorem the force and moment are given by integrals of the pressure gradient over the submerged volume of the ship. The components of the force and moment in the ship coordinate system, $Gxyz$, are

$$\begin{aligned}
f_1 &= - \iiint \frac{\partial p}{\partial x}\, dV \\
f_2 &= - \iiint \frac{\partial p}{\partial y}\, dV \\
f_3 &= - \iiint \frac{\partial p}{\partial z}\, dV \\
f_4 &= \iiint \left(z\frac{\partial p}{\partial y} - y\frac{\partial p}{\partial z}\right) dV \\
f_5 &= \iiint \left(x\frac{\partial p}{\partial z} - z\frac{\partial p}{\partial x}\right) dV \\
f_6 &= \iiint \left(y\frac{\partial p}{\partial x} - x\frac{\partial p}{\partial y}\right) dV
\end{aligned} \tag{V-26}$$

which may be represented by the generalized force vector, $\underset{\sim}{f}$. In equation (V-26) the volume element is dV; f_1, f_2 and f_3 are forces in the x, y, and z-directions; and f_4, f_5 and f_6 are moments about these x, y, and z - axes. The integrals are taken over all volume up to the instantaneous sea surface within the envelope of the ship.

The ship hull is approximated by a number of polygons representing the stations of the ship. Each polygon is in a plane defined by a constant value of x in the ship coordinate system. A maximum of 24 line segments are used for each closed polygon station in the ship and a maximum of 25 stations may be used. The stations may be unsymmetrical and unequal station spacings are permitted. The position of the center of gravity may be in any fixed position relative to the ship.

The integrals of the pressure gradients, velocities and accelerations over each station made up with straight line segments are evaluated exactly, but with two restrictions on the angle of pitch. First, the pitch angle must not become so large as to cause the intersection of a station plane and the instantaneous sea surface to define multiple regions or a closed contour in the station plane. Second, the magnitude of a quantity like the product of the pitch angle and the slope of all component waves must be "small". These two restrictions are satisfied for vessels of usual proportions in waves with realistic slopes.

The two-dimensional forces and moment at each station are evaluated as functions of the form

$$f(x) = V' + \sum_{i=1}^{N} [C_i \cos (k_i' x) + S_i \sin (k_i' x)] \tag{V-27}$$

where

V' is obtained from the static $(\rho g \bar{y})$ part of the pressure,

C_i and S_i result from the sinusoidal pressure fluctuation for the i-th wave component, and

k_i' is a projection of the wave number onto the x-axis of the ship.

The relative magnitude of C_i and S_i depends on the phase of the waves relative to the center of ship coordinates at each instant of time. The integrals and moments of the functions like (V-27) along the length of the ship are evaluated with the assumption that V', C_i, and S_i vary linearly in x between adjacent stations of the ship.

E. Wave Diffraction, Added Mass and Damping

Approximations are used for the hydrodynamic forces resulting from the diffraction of the incident waves and motion of the ship. These forces are computed using constant two-dimensional added mass and linear damping coefficients for each station combined with averages of the water acceleration and velocity relative to the stations. The hydrodynamic approximations are not expected to lead to serious errors if the Froude-Krylov force is dominant. This, as noted, is expected to be the case in the most severe capsizing situations in following or quartering seas.

The hydrodynamic force resulting from the diffraction of the waves is approximated in the following manner. Two dimensional added mass and damping coefficients for heave, sway, roll and roll-sway coupling are entered into the program as constants for each station of the ship. Each time the sectional Froude-Krylov forces are computed by integrating the pressure gradient over a station of the ship, average values of vertical, hortizontal and "roll" water velocities and accelerations are also evaluated for the station. The "roll" velocity and acceleration components are the first and second time derivatives of the slopes of constant pressure lines in the plane of the station. The two-dimensional coefficients are scaled by the instantaneous submerged area of the station, and the products of the average water velocities and accelerations with these coefficients yield two-dimensional diffraction forces which are added to the two-dimensional Froude-Krylov forces before the longitudinal integrations are performed.

The force resulting from ship velocities in heave, sway, roll, yaw and pitch are computed in the above manner using the scaled damping coefficients and the components of ship velocity at each station. Since the linear and angular accelerations of the ship are unknown when the forces are being computed, the force resulting from the ship acceleration cannot be computed with the same procedure. Instead, a matrix of three-dimensional added mass coefficients is computed using the scaled two-dimensional added mass coefficients. The product of this added mass matrix and the vector of accelerations, gives the required force vector. The generalized acceleration vector, $\underset{\sim}{a}$, is defined by equation (V-21). The hydrodynamic force and moment resulting from this acceleration is

$$\underset{\sim}{h} = -\underset{\sim}{A}'' \underset{\sim}{a} \qquad \text{(V-28)}$$

where $\underset{\sim}{A}''$ is the added mass matrix. The use of longitudinal moments of the two-dimensional added mass coefficients leaves the elements, A''_{ij}, which are related to surge (i or j equal to 1) undefined. They are taken as zero.

In order to use this hydrodynamic force, the momentum equation (V-23) is rewritten as

$$\underset{\sim}{A}' \underset{\sim}{a} = \underset{\sim}{f}' + \underset{\sim}{h} \qquad \text{(V-29)}$$

where the right hand side is the sum of all forces on the ship. The inertia matrix for the ship is $\underset{\sim}{A}'$.

The substitution of equation (V-28) into equation (V-29) gives the momentum equation including added mass:

$$\underset{\sim}{A} \underset{\sim}{a} = \underset{\sim}{f}' \qquad \text{(V-30)}$$

where

$$\underset{\sim}{A} = \underset{\sim}{A}'' + \underset{\sim}{A}'.$$

Equation (V-30) is solved to obtain the accelerations required for integration.

F. Steering System

The steering system of a typical ship consists of three components--an autopilot, steering machinery and the rudder. The autopilot computes a rudder angle which should correct or prevent errors in the ships heading. The machinery attempts to rotate the rudder to the angle specified by the autopilot. This rotation is mechanically limited to some maximum rate of rotation and some maximum rudder deflection angles. The rudder acts as a lifting surface in the water which generates forces and moments on the ship which are used to maintain the desired course. The steering system for the numerical simulation incorporates these three components.

The autopilot model computes a required rudder angle which is a linear combination of the yaw rate, the yaw angle (heading error), and the time integral of the yaw angle. The proportionality factor or "gain parameter" for any of these heading functions may be set to zero resulting in a simpler autopilot. For example, the yaw integral gain parameter is zeroed to simulate the autopilots used for the *Challenger* and *SL-7* models that were run on San Francisco Bay. The yaw angle used for the heading error and yaw integral is the angle ϕ which is always measured about a fixed vertical axis. The yaw rate is measured in the ship coordinates rather than about a fixed vertical axis. This is the same as used in the ship model autopilots but it may differ from that used in some full sized autopilots. Two "dead band" parameters are provided in the simulated autopilot. If the magnitude of the heading error is less than the first dead band parameter, the autopilot will require a zero rudder angle rather than the value computed using the gain parameters. This type of dead band is typical of the "weather" adjustment of ship autopilots. The other dead band available in the simulation was incorporated in the ship model autopilots. With this form of dead band the magnitude of the required rudder angle is reduced by the value of this dead band parameter.

The steering machinery is modeled with constant values for the rate of rotation of the rudder and limits to the magnitude of rudder deflection. If the autopilot requires a rudder deflection rate that is less than the machinery rate and an angle that is less than the mechanical stops, the machinery simulation sets the rudder to the autopilot angle. Otherwise, the rudder angle lags that computed by the autopilot.

The rudder is simulated by a vertical line (in ship coordinates) through an effective center of the rudder. The average of the water velocity relative to points on this line is computed at each time step. The water velocity across this line is the superposition of the motion of the ship, the motion of the water particles in the waves, and a constant wake velocity. The lift and drag forces on the rudder are assumed to be proportional to the instantaneous submerged rudder area, the square of the average relative water velocity, and to the angle of incidence between the rudder and the average water velocity. Rudder lift is limited by a stall angle. The lift and drag forces are resolved into force and moment components in the ship coordinate system.

G. Other Forces

An additional damping force may be computed for any of the six motion components. Let f_i be one of the components of the force or moment in the ship coordinate system, and let v_i be the corresponding component of linear or angular velocity. The force or moment is computed from

$$f_i = f_i^* - v_i L_i - v_i |v_i| Q_i \qquad \text{(V-31)}$$

where

f_i^* = force or moment due to the waves and steering system,

L_i = coefficient of linear damping for the particular motion component, and

Q_i = coefficient of quadratic damping for the particular motion component.

There are three force and three moment equations using these three-dimensional linear and quadratic damping constants, but in practice the only non-zero coefficients are for surge and roll.

Surge damping may be controlled by equation (V-31) or by an optional table of resistance versus speed data. When this option is used, a surge damping (or accelerating) force is obtained by interpolation in the resistance table. This surge force is equal to the resistance at the desired speed minus the resistance for the velocity predicted at each time step.

H. Examples of Numerical Simulations

Several examples of motions simulated by the numerical time domain integration are presented here. These computations were performed for the *American Challenger* class of cargo ship for which a model was previously tested on San Francisco Bay. Details of the experiments with this vessel are given in the reports by Haddara, *et al.* (1971) and Paulling, *et al.* (1972). Characteristics of the vessel and its displacement condition for the simulations are given in Table V-I. Table A-I in Appendix A contains a detailed compilation of the vessel's characteristics. A bodyplan is also included in that appendix as Figure A-1. The offsets for the simulations were limited to 13 stations. Motion calculations were carried out at ship scale rather than at the scale of the model used for the experiments. The ratio of ship length to model length is 30.189, and the time scale for Froude number similarity is about 5.5. Metacentric heights corresponding to model ballast weight positions 2 and 3 were used for the simulations. The righting arm curves for the *Challenger* are shown in Figure A-3 in Appendix A. In addition to the curve for still water, the righting arms for the ship in a longitudinal wave with crest amidship and trough amidship are plotted.

Three simulations with a single sinusoidal wave are shown in Figures V-2 through V-7. The wave is overtaking the ship from dead astern. The circular wave frequency is 0.575 radians per second, corresponding to a wave length of 610 feet.

The first example is for a wave amplitude of 6.5 feet. The initial roll angle is 15 degrees to starboard. To decrease the effect of starting transients caused by the choice of initial conditions, all forces applied to the ship are multiplied by a ramp function which increases linearly with time from zero to one for the first 10 seconds of the integration. The roll history is plotted as Figure V-2, and that for pitch is Figure V-3. The pitch record may be used to judge the number of wave encounters. In this example the rolling occurs as one-half of the wave encounter frequency, and the roll amplitude builds up rapidly. The first roll to port has an amplitude of about 19 degrees, and the last starboard roll is to an amplitude of 28 degrees. The ship capsizes to port.

The next example is for the same wave condition, but the initial roll angle is 5 degrees to starboard. The roll record is Figure V-4, and pitch is Figure V-5. Rolling again occurs at one half the pitch and wave encounter frequency. The roll motion peaks at eleven degrees after 130 seconds, and it appears to stabilize thereafter.

The third example repeats the initial conditions of the previous one with the five degree initial roll, but the wave amplitude is increased to 7.5 feet. The roll and pitch responses are Figures V-6 and V-7. The interesting thing here is that the resulting roll amplitude is smaller for this case with a larger wave amplitude. The roll amplitude for this run is about eight degrees.

The remaining examples are for a wave system consisting of two sinusoidal waves traveling in the same direction. The circular frequencies of the waves are 0.433 and 0.601 radians per second, which correspond to wave lengths of 1076 and 558 feet. The amplitudes of both wave components were equal in magnitude. Three simulation runs for following seas and this two-component sea are shown in Figures V-8 through V-10, and V-12 through V-17. The metacentric height for these runs is 0.558 feet (GM position 3).

To initiate rolling, the waves approach the ship from the direction of ten degrees to starboard of dead astern. The amplitude of each component wave is five feet making a twenty foot maximum wave height in the group. The first simulation begins with the two wave components in phase at the position of the ships center of gravity. The starting ramp is applied to the first 60 seconds of the run. Figure V-8 shows the wave amplitude at the position of the center of gravity of the ship. The roll record is displayed in Figure V-9. After about 120 seconds the rolling begins to take place at one half of the frequency of wave encounter. As the wave amplitude builds, the rolling becomes erratic: rolling alternates with the encounter frequency and one half of that frequency. Figure V-10 shows the pitch record for this run. The ramp function used for starting the simulation results in the attenuation of the pitch at the beginning of the record. Note that the pitch angle gives a good indication of the wave slope for these waves which are longer than ship length. The pitch and roll experiment records for the *SL-7* model shown in Figure V-11 exhibit this same erratic rolling with the roll motion occurring at the wave encounter frequency and then at one half of this frequency.

Figures V-12 through V-14 show the wave, roll, and pitch records for a simulation with the same initial conditions as before, except that the phase angles of the two waves are initially one half cycle apart causing the amplitudes to cancel. The starting ramp is reduced to 30 seconds. In this run the rolling is at the same frequency as the wave encounter, and the amplitude is less than half that of the previous example.

The last example, for the two-component following seas, shows the wave, roll and pitch records in Figures V-15 through V-17. The initial conditions are the same as for the previous example except that an initial roll angle of fifteen degrees to starboard has been added. Rolling begins at one half the encounter frequency which is close to the natural roll frequency for calm water and this roll amplitude. As the wave amplitude and roll exciting moment build up the ship is forced to roll at the encounter frequency.

Figure V-18 shows a *Challenger* model experiment in following seas for the corresponding speed and GM condition. Although the experiment ended in a capsize with low cycle resonance and these simulations did not, both the experiment and the first and last following sea calculations show a tendency for the roll frequency to switch back and forth between the encounter frequency and one half the encounter frequency.

Two examples of capsize simulations in quartering seas are shown in Figures V-19 through V-25. The two-component wave system that was used for the following sea runs is used here, but the direction is such that the waves approach the ship from 35 degrees to starboard of dead astern. At the beginning of the runs the two wave components are in phase.

The first quartering example is for a metacentric height of 0.257 ft (GM position 2). The wave record for this run is shown in Figure V-19. The starting ramp was 60 seconds in length, and ended near the end of the first wave group. Roll and pitch records are in Figures V-20 and V-21. At about forty seconds from the start a wave crest comes amidship and vessel rolls 14 degrees to port. The next wave crest comes amidships at about sixty seconds and a starboard roll into the wave of 4 degrees is reached. The next roll is 22 degrees to port just after the next crest passes. The ship rolls to starboard as the waves begin to build in the second wave group. The maximum starboard roll of 23 degrees is reached as the next crest moves away. The roll momentum imparted the ship by the increased righting arm of the next trough coming amidship together with the reduced stability in the crest that follows causes the ship to capsize to port--clearly an example of low cycle resonance.

Figure V-22 shows the last two and a half minutes of a model run corresponding to the same speed, heading relative to the waves and GM condition. The experiment also ended with a capsizing to port caused by low cycle resonance.

An example of pure loss of stability is shown in Figures V-23 through V-25. The metacentric height was 0.557 ft. (GM position 3). The wave amplitude at the center of gravity of the ship is shown in Figure V-23. Roll and pitch are in Figures V-24 and V-25. Rolling is at one half the frequency of wave encounter between 40 and 110 seconds into the run. After that the wave amplitude and the roll moment are so large that the ship is forced to roll at the encounter frequency. The vessel finally capsizes with the combination of a large port roll and a wave crest amidships.

TABLE V - I

CHARACTERISTICS OF THE *AMERICAN CHALLENGER*

USED FOR THE TIME DOMAIN SIMULATION

	SHIP	MODEL
Length Between Perpendiculars	529.0 ft	17.523 ft
Characteristic length	521.0 ft	17.258 ft
Beam	75.0 ft	2.484 ft
Depth[a]	46.5 ft	18.484 ft
Mean Draft	29.75 ft	11.827 in
Displacement	19652.5 tons	1600 lbs
Speed	27.7 ft/sec	2.99 ft/sec
Froude number	0.215	0.215
Metacentric heights:		
GM position 2	0.257 ft	0.102 in.
GM position 3	0.558 ft	0.222 in.

[a]This depth is greater than the depth of the actual ship because the model was constructed up to the level of the top of the bulwark rather than to the main deck level of the ship.

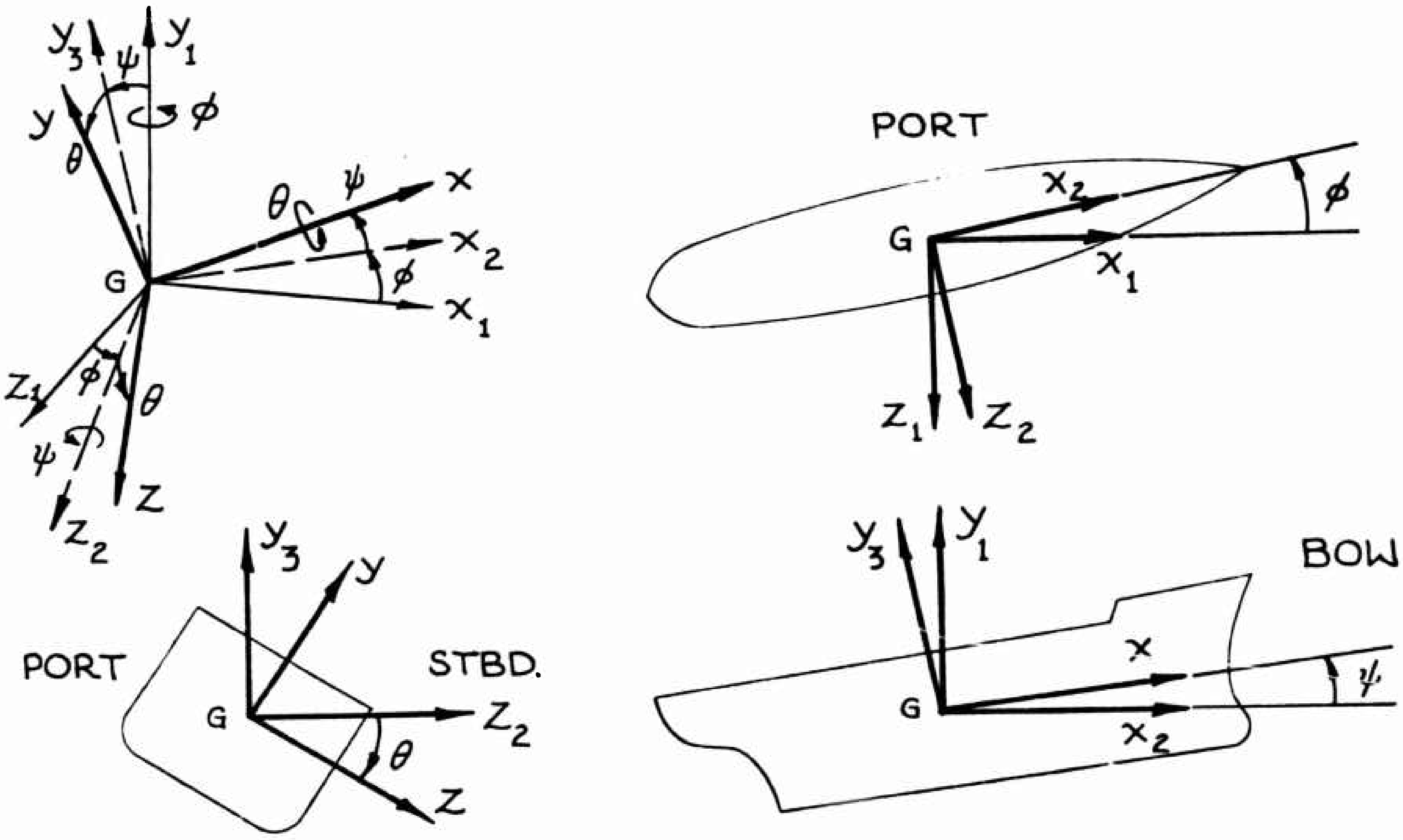

Figure V-1 Coordinate Rotations

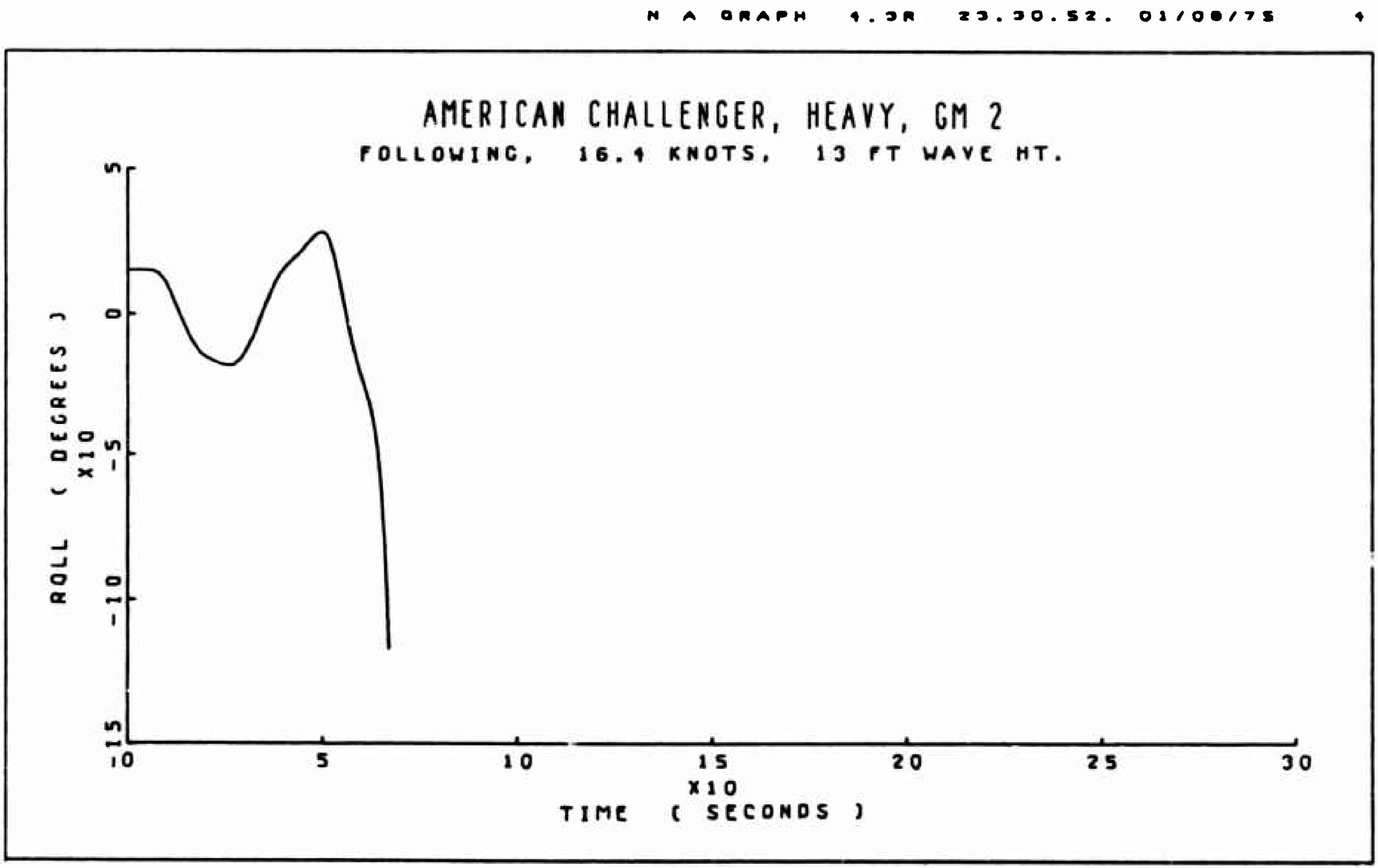

Figure V-2 Roll Simulation

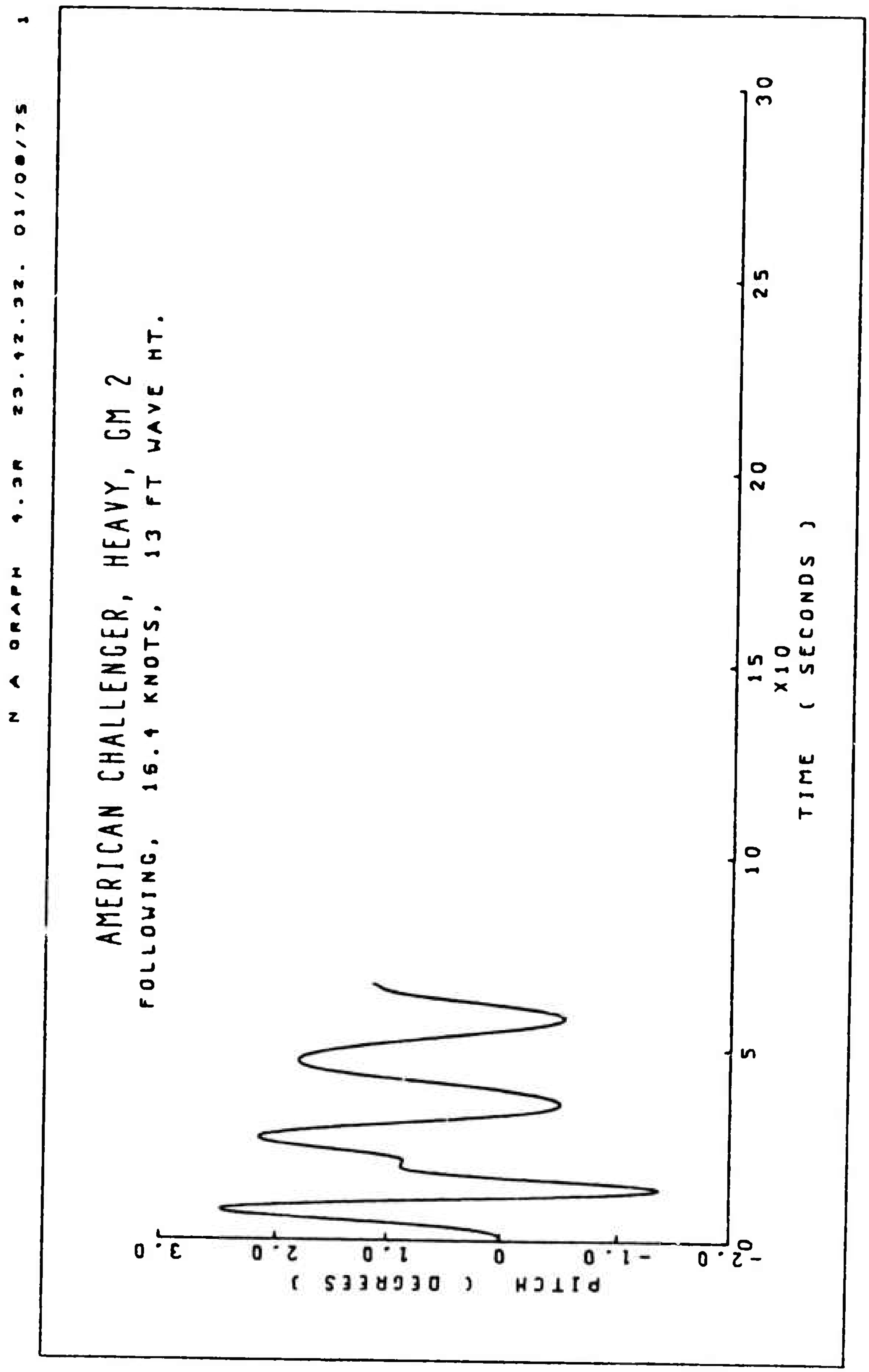

Figure V-3 Pitch Simulation

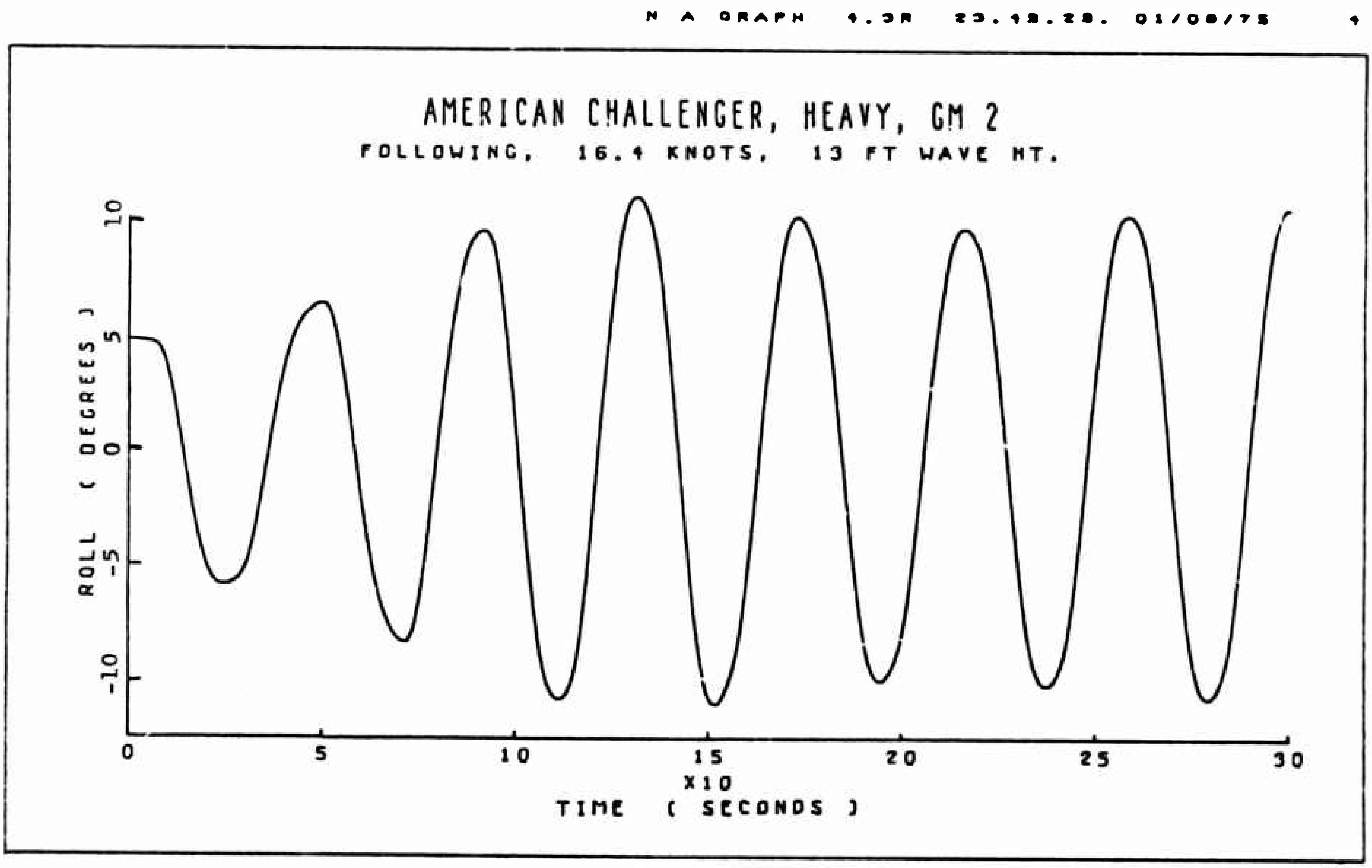

Figure V-4 Roll Simulation

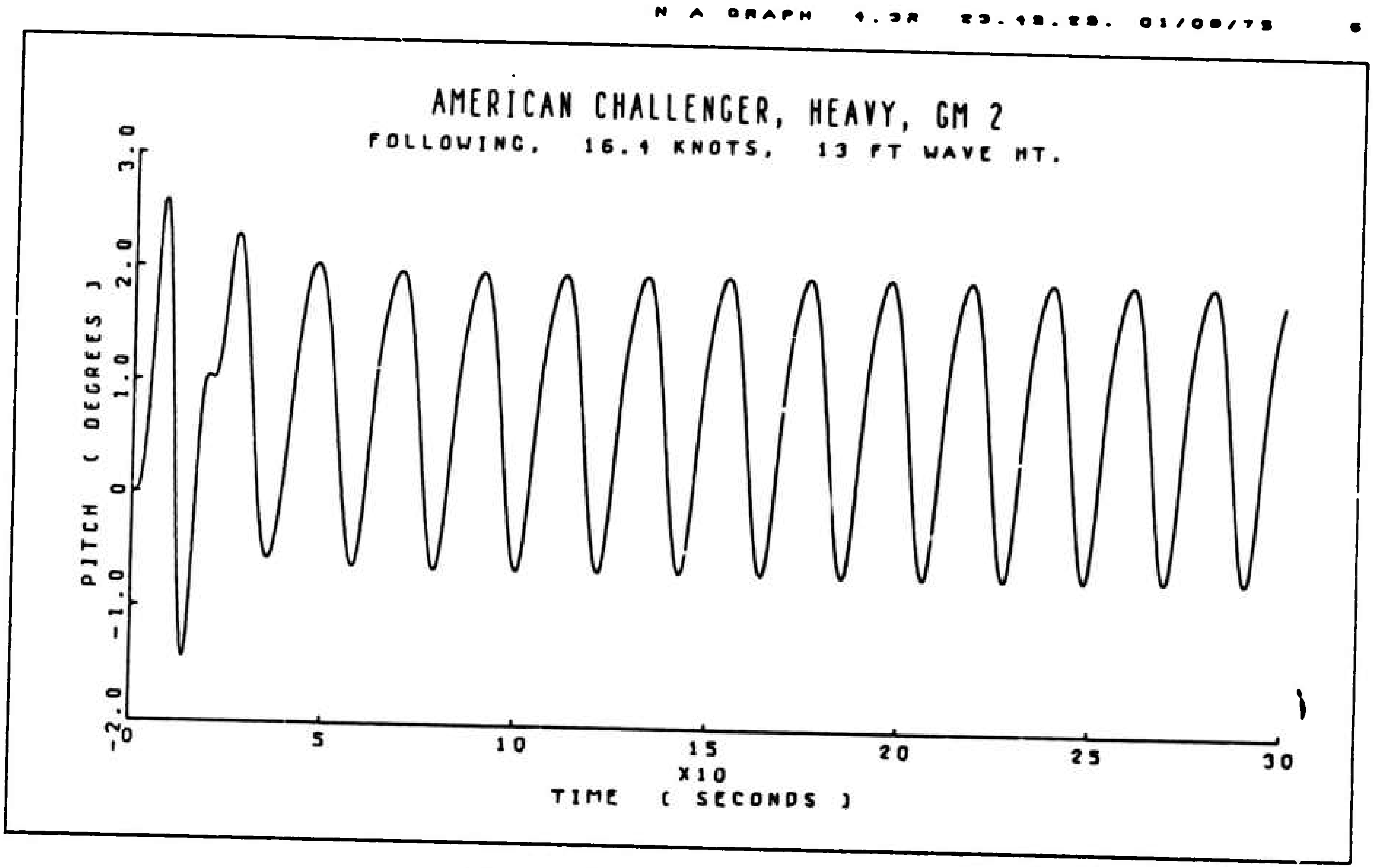

Figure V-5 Pitch Simulation

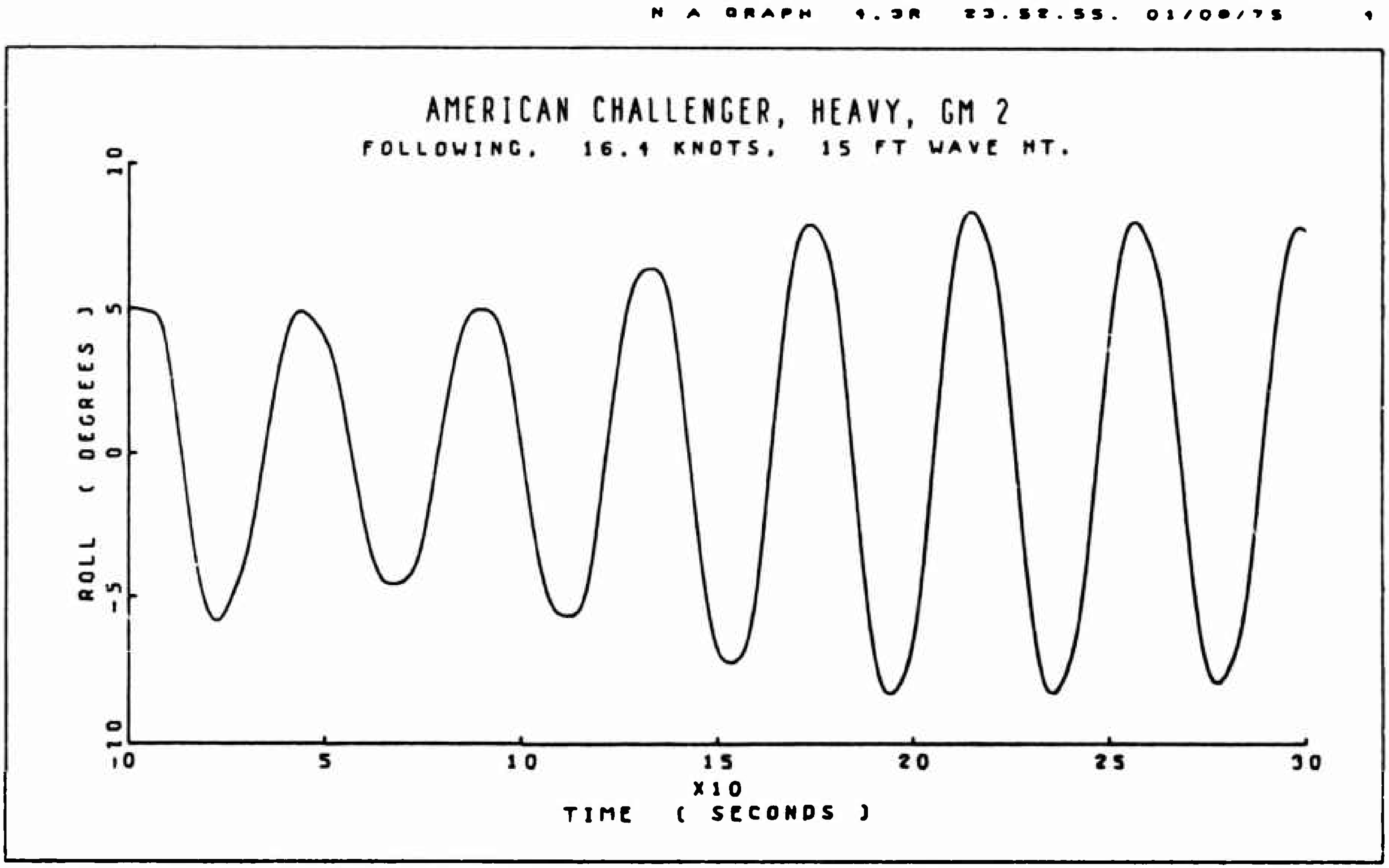

Figure V-6 Roll Simulation

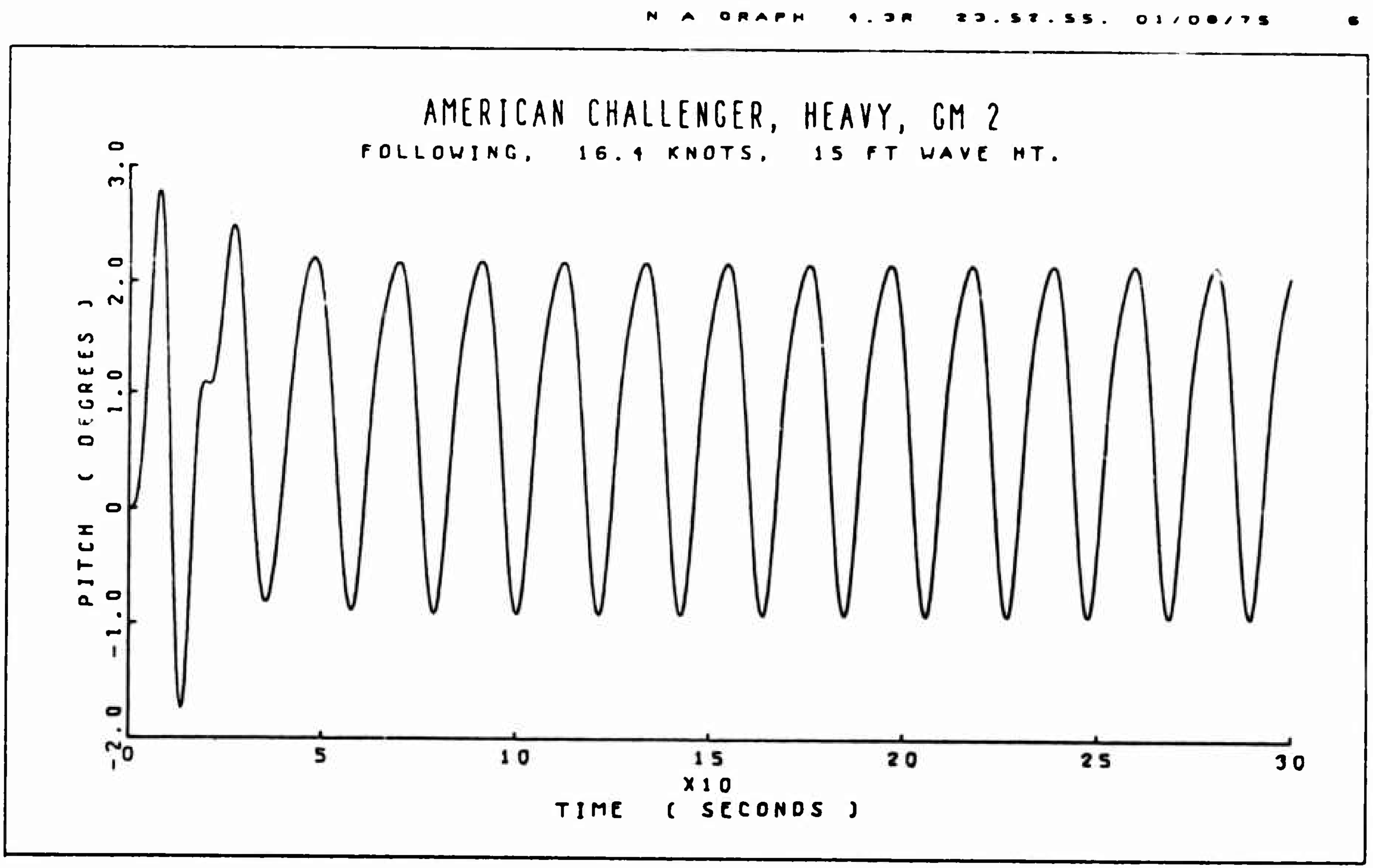

Figure V-7 Pitch Simulation

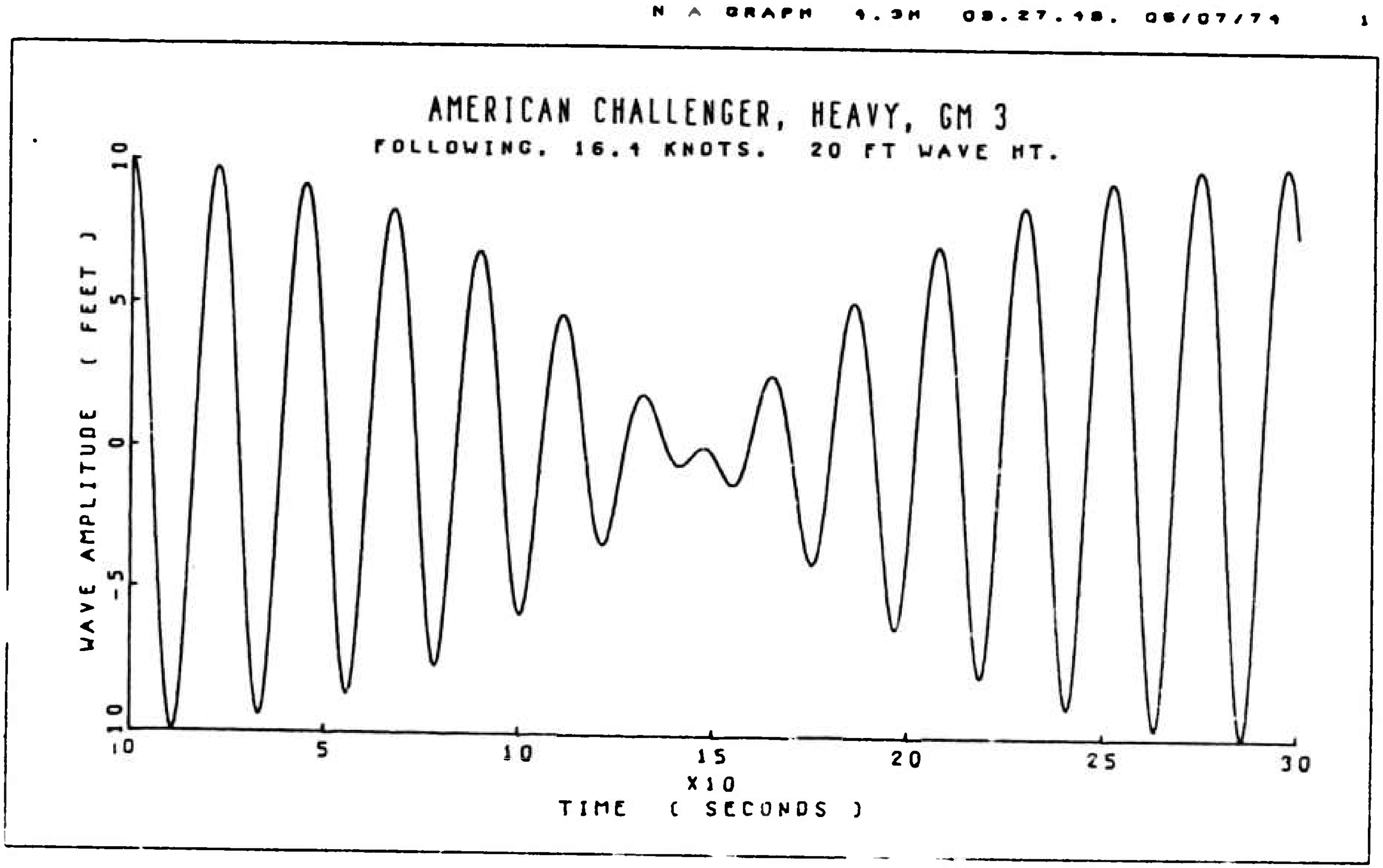

Figure V-8 Wave Simulation

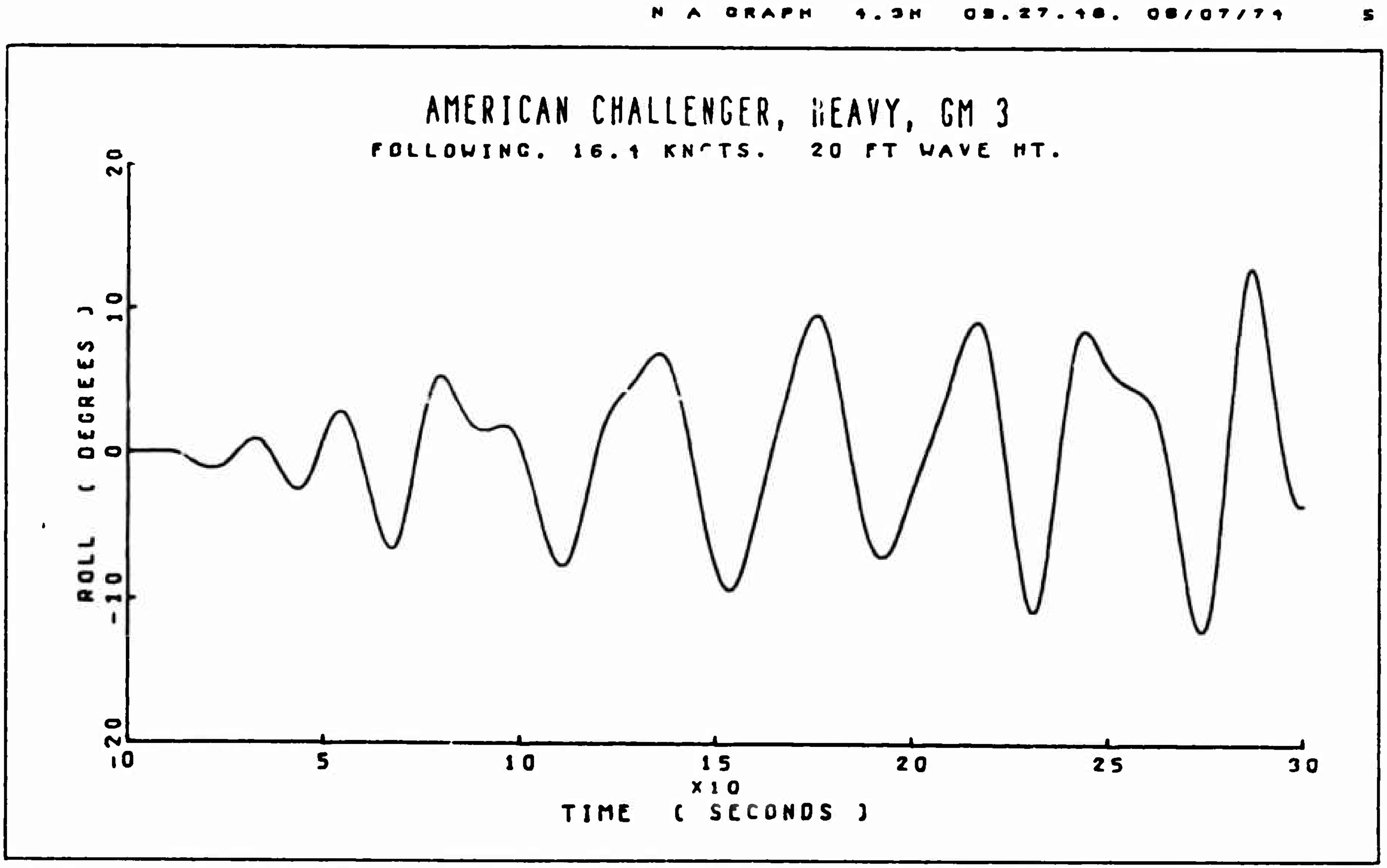

Figure V-9 Roll Simulation

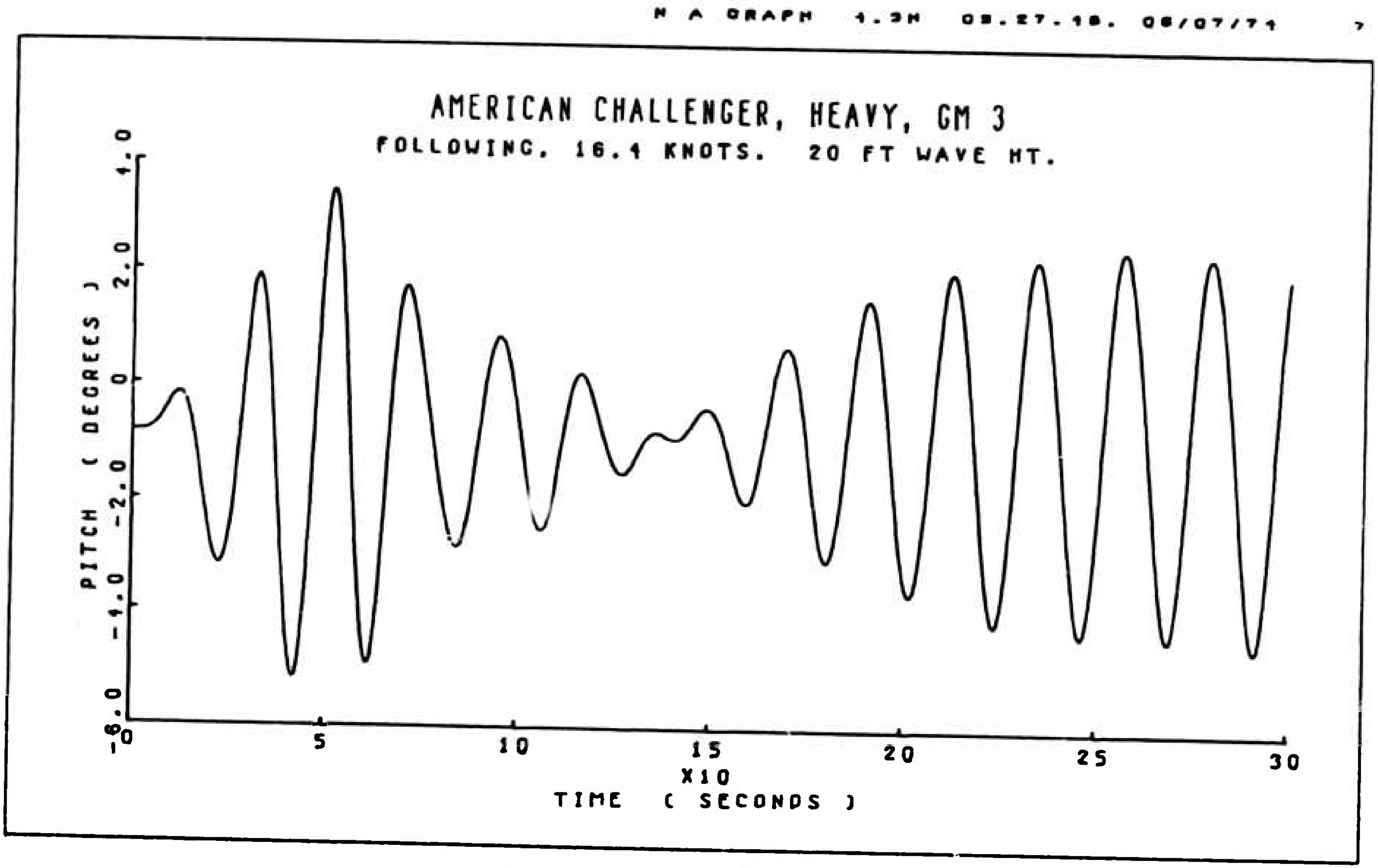

Figure V-10 Pitch Simulation

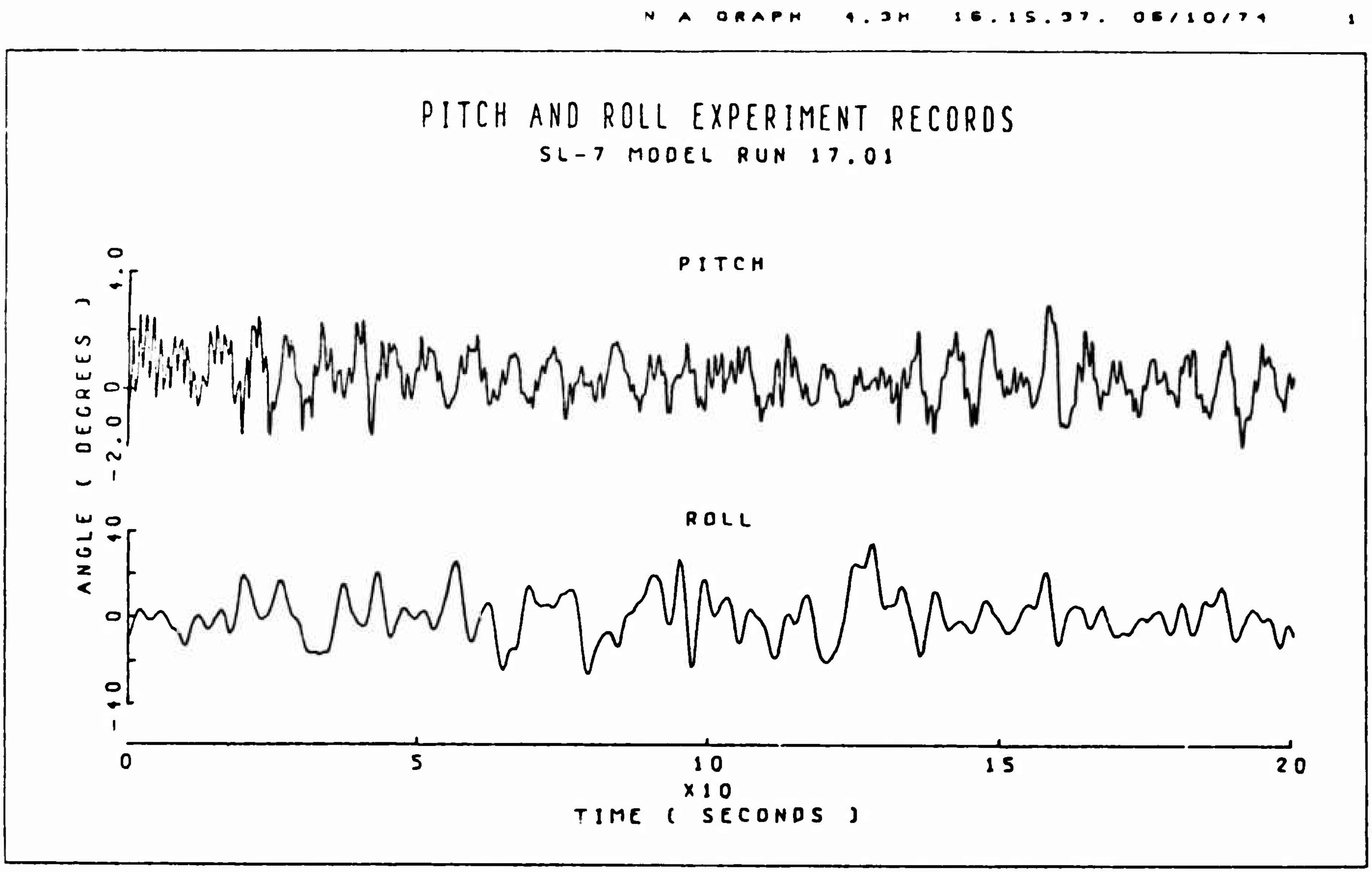

Figure V-11 *SL-7* Model Experiment Records

N A GRAPH 4.3M 22.12.20. 08/08/74 1

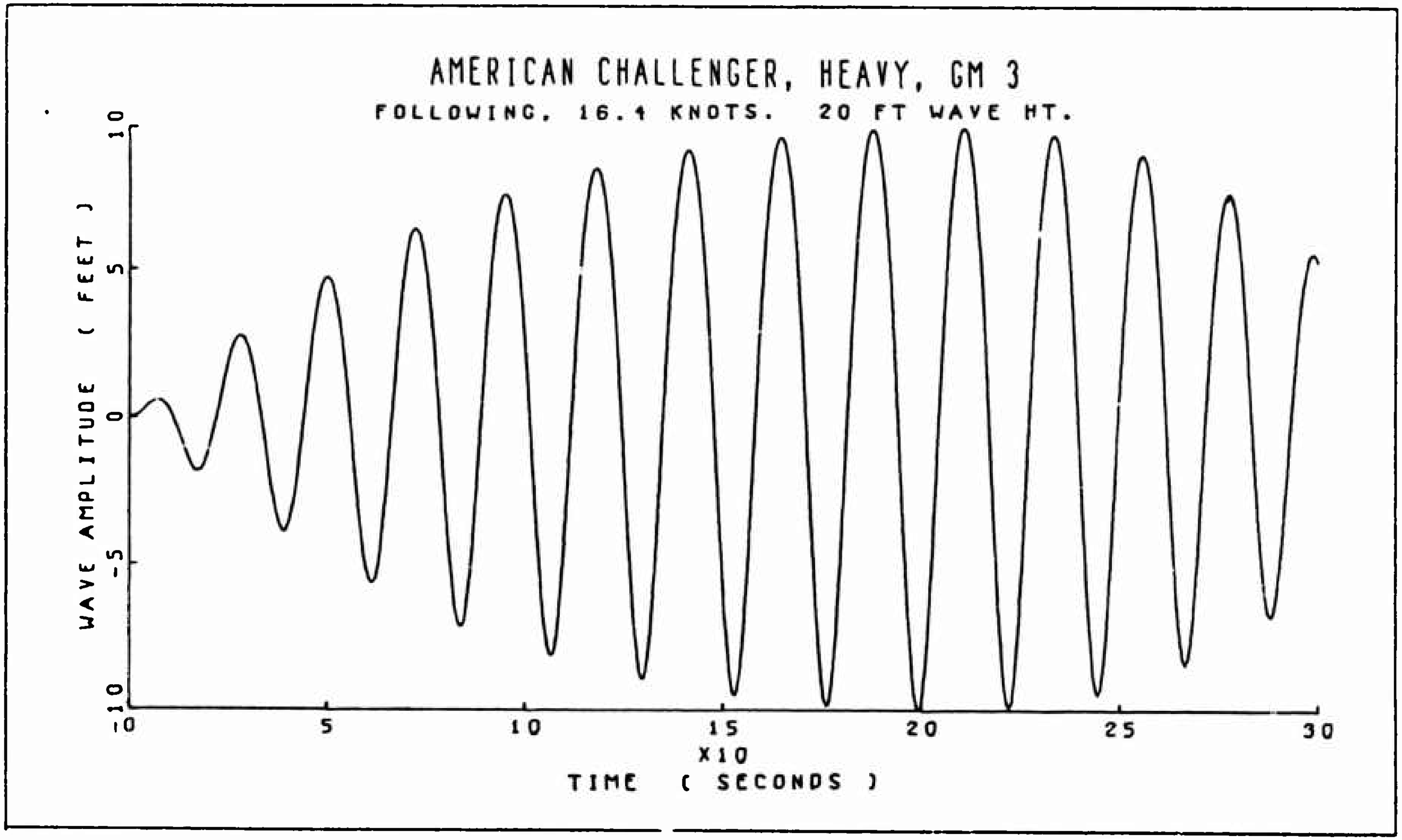

Figure V-12 Wave Simulation

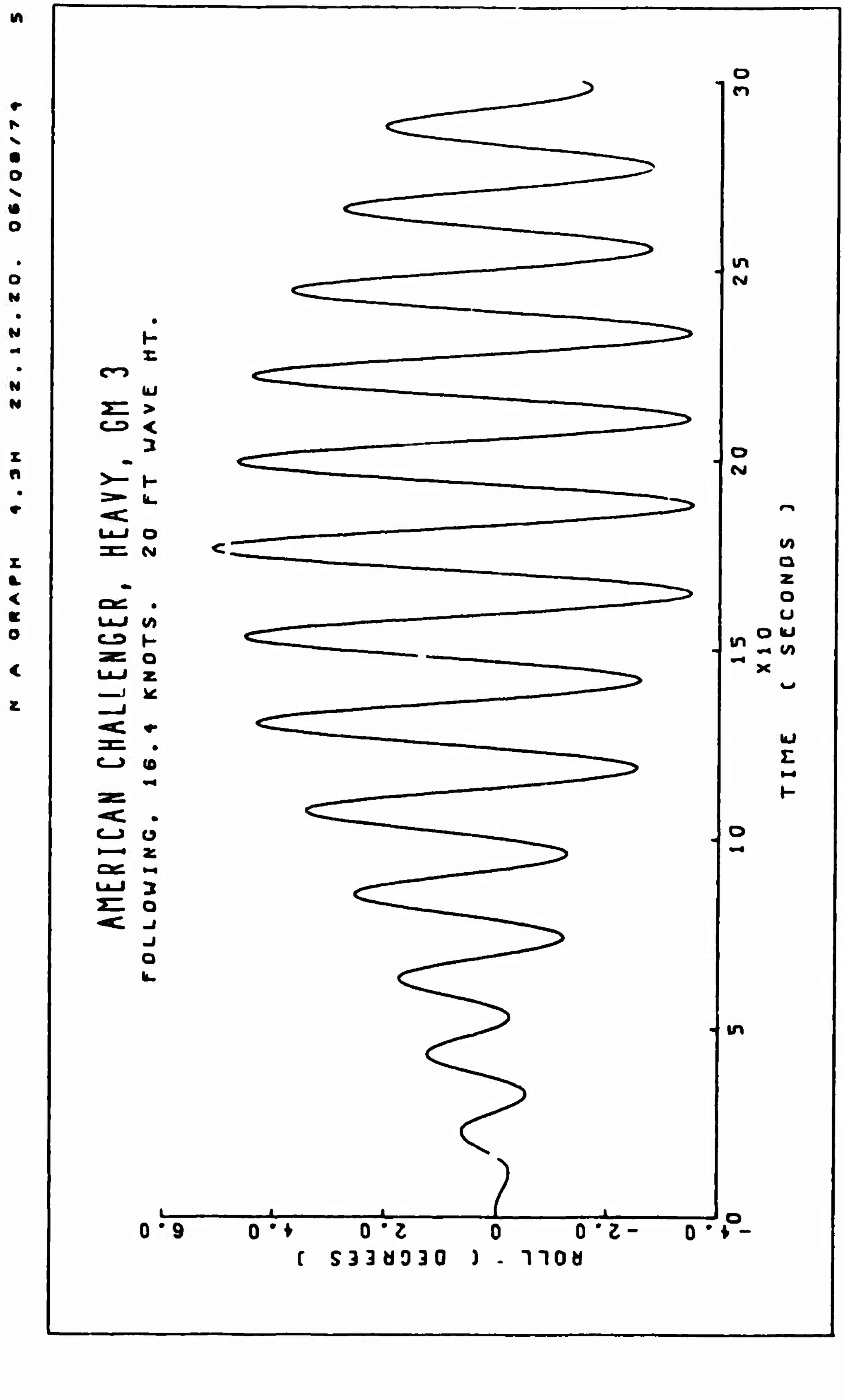

Figure V-13 Roll Simulation

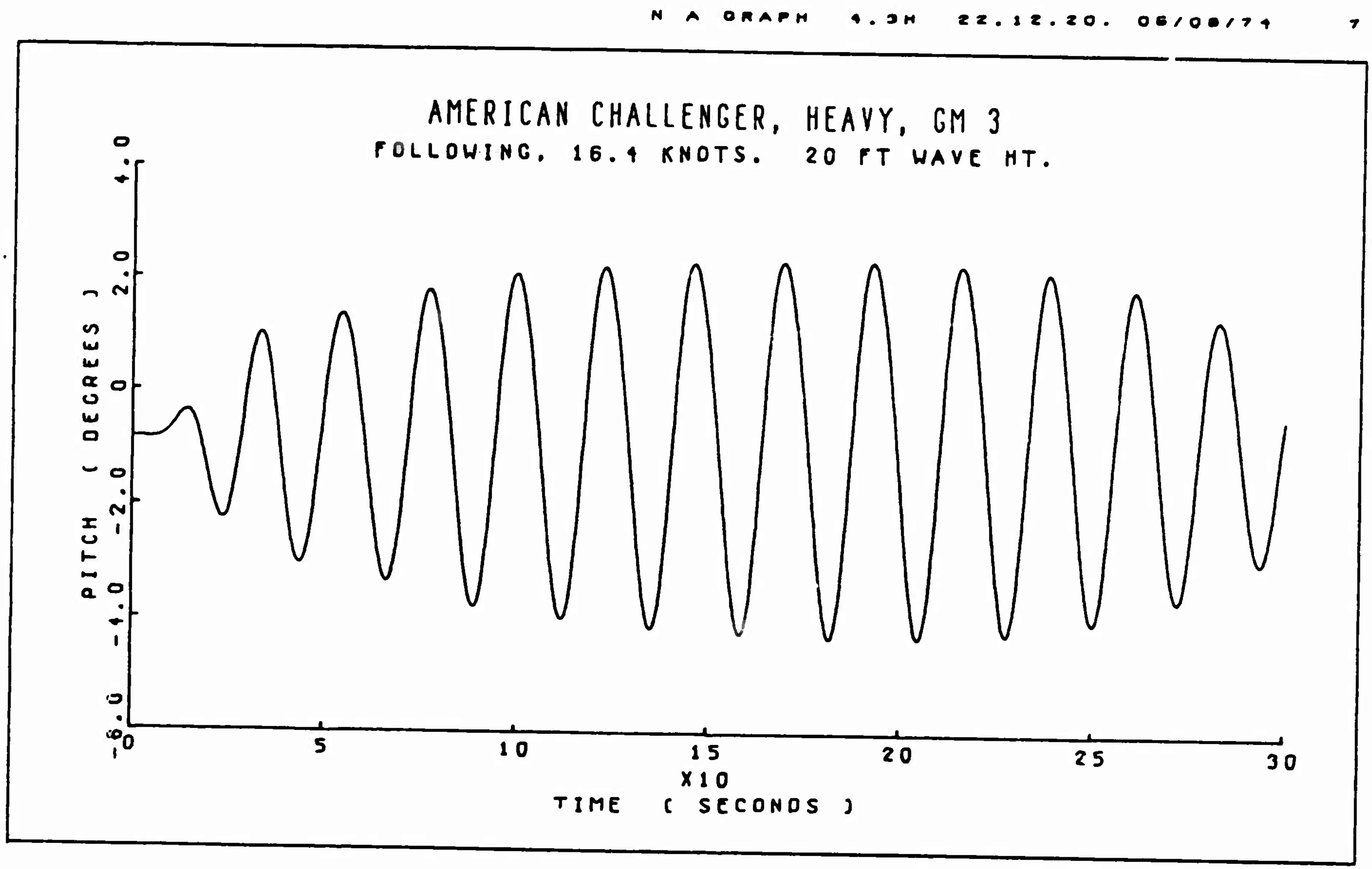

Figure V-14 Pitch Simulation

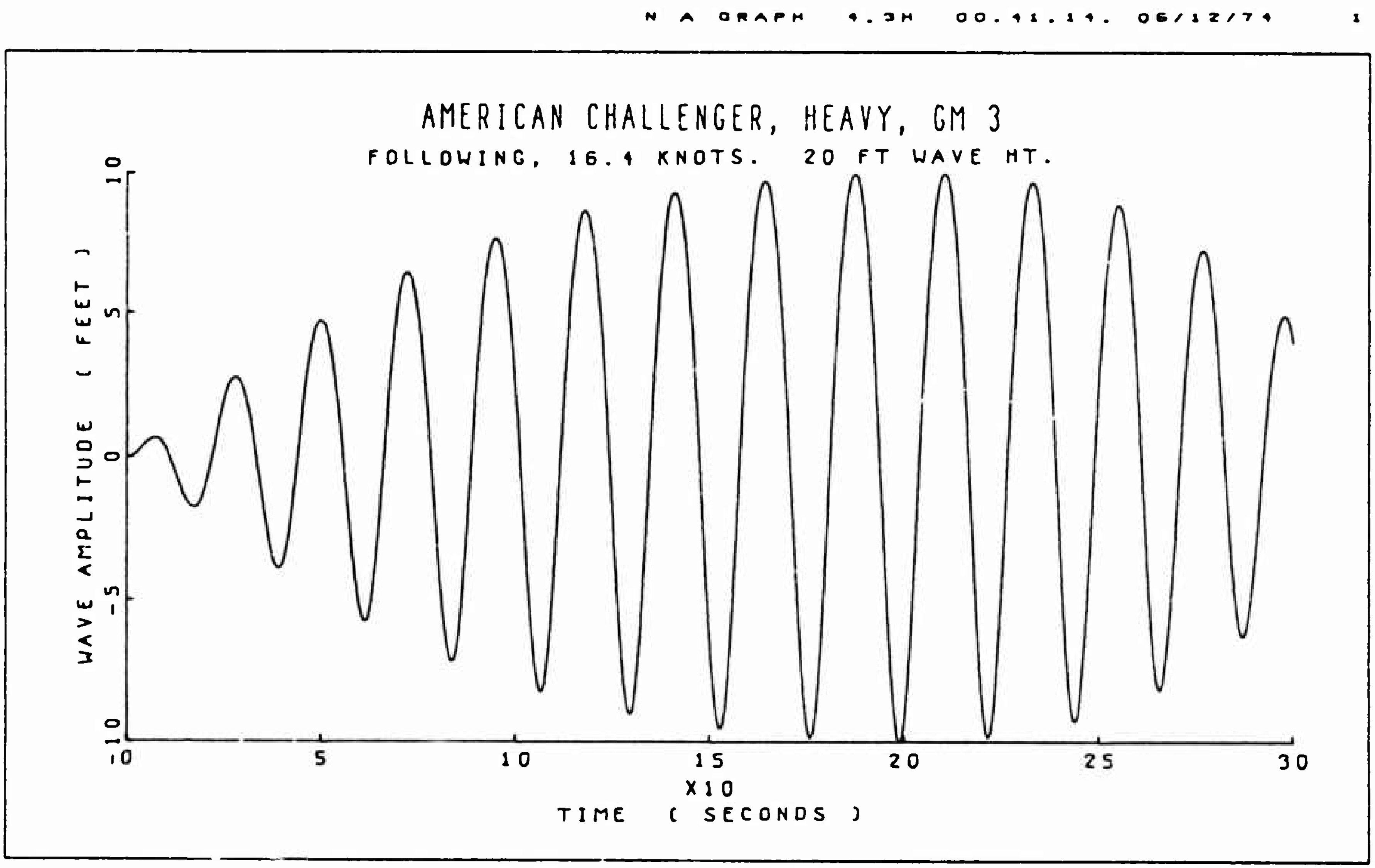

Figure V-15 Wave Simulation

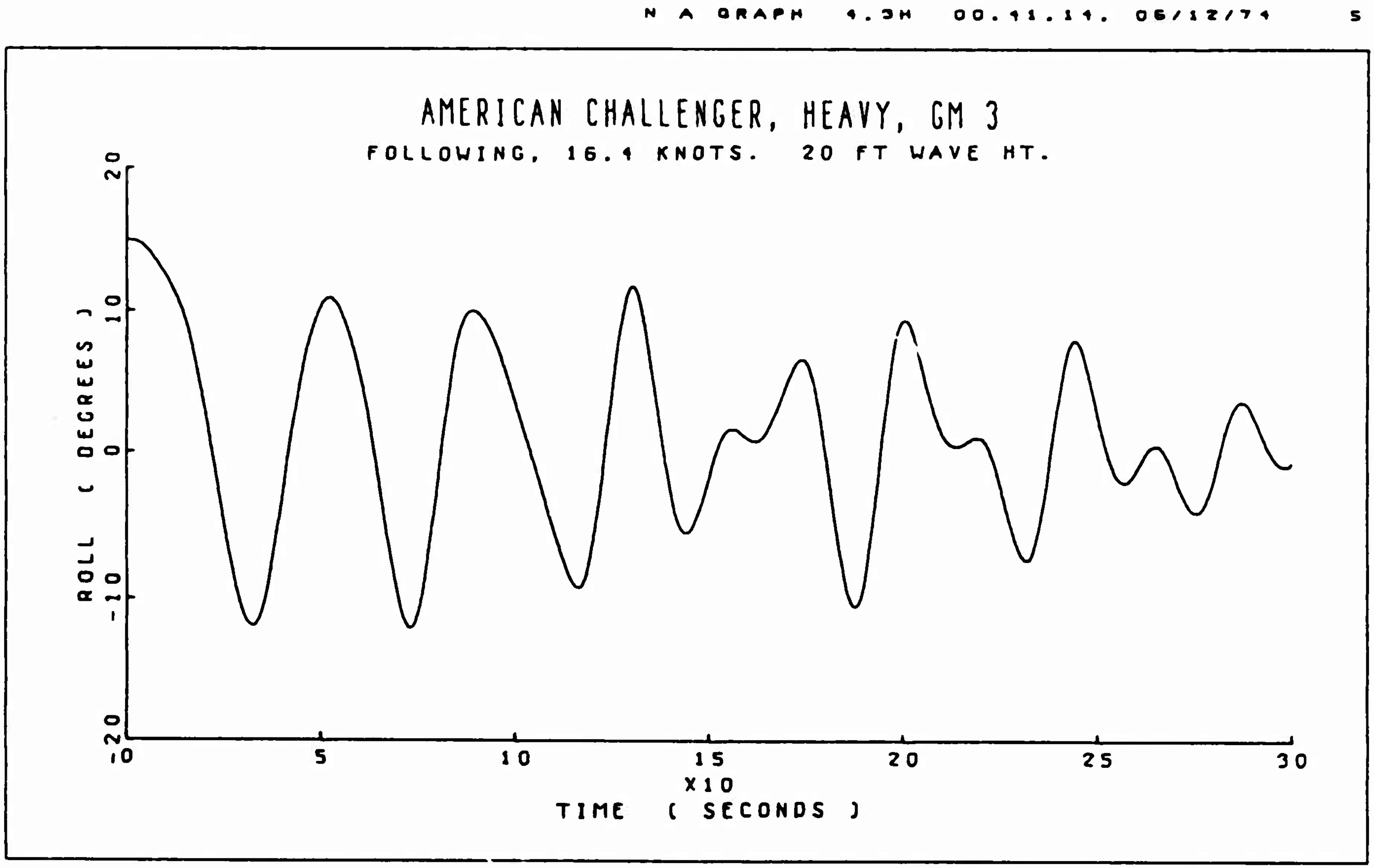

Figure V-16 Roll Simulation

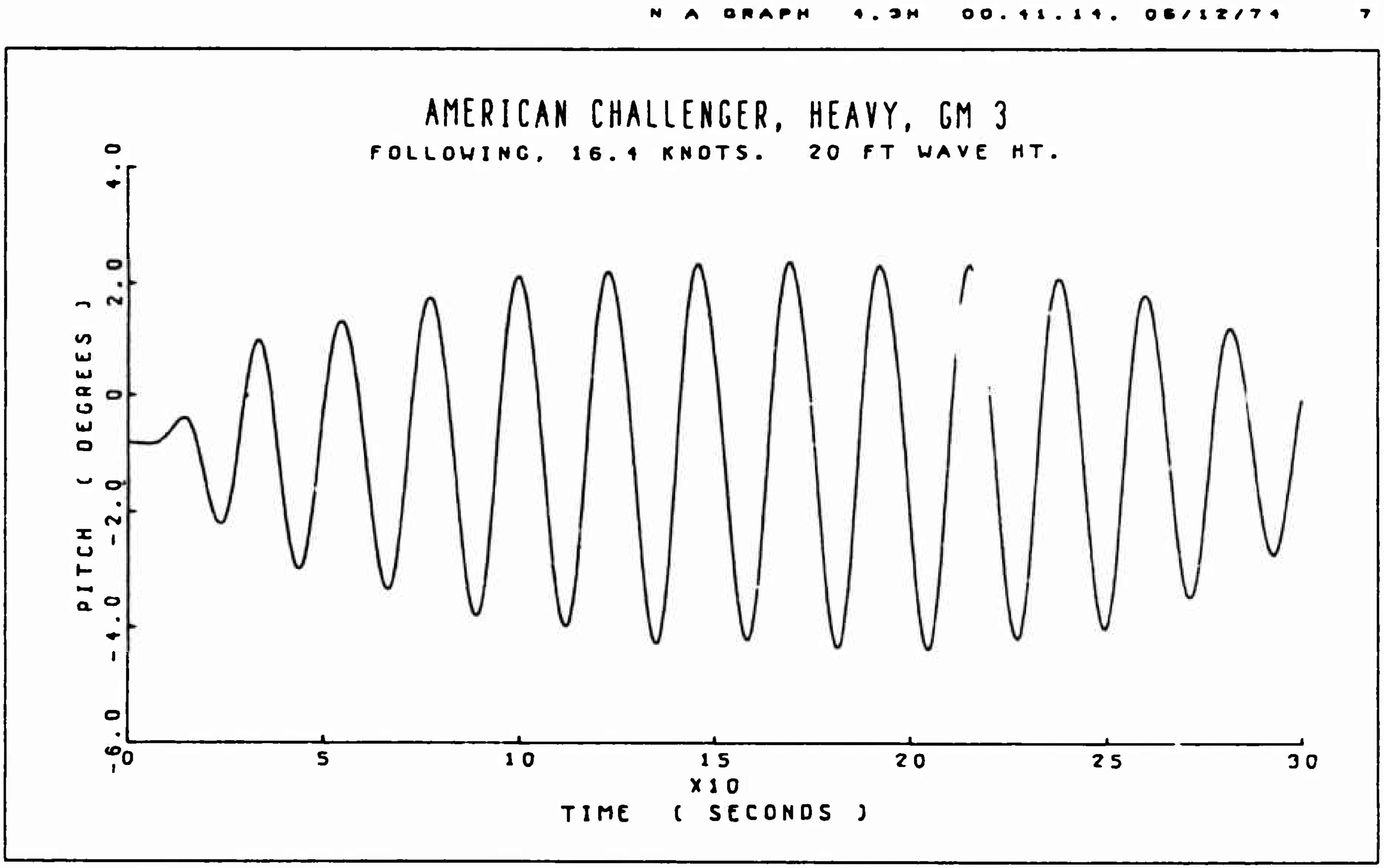

Figure V-17 Pitch Simulation

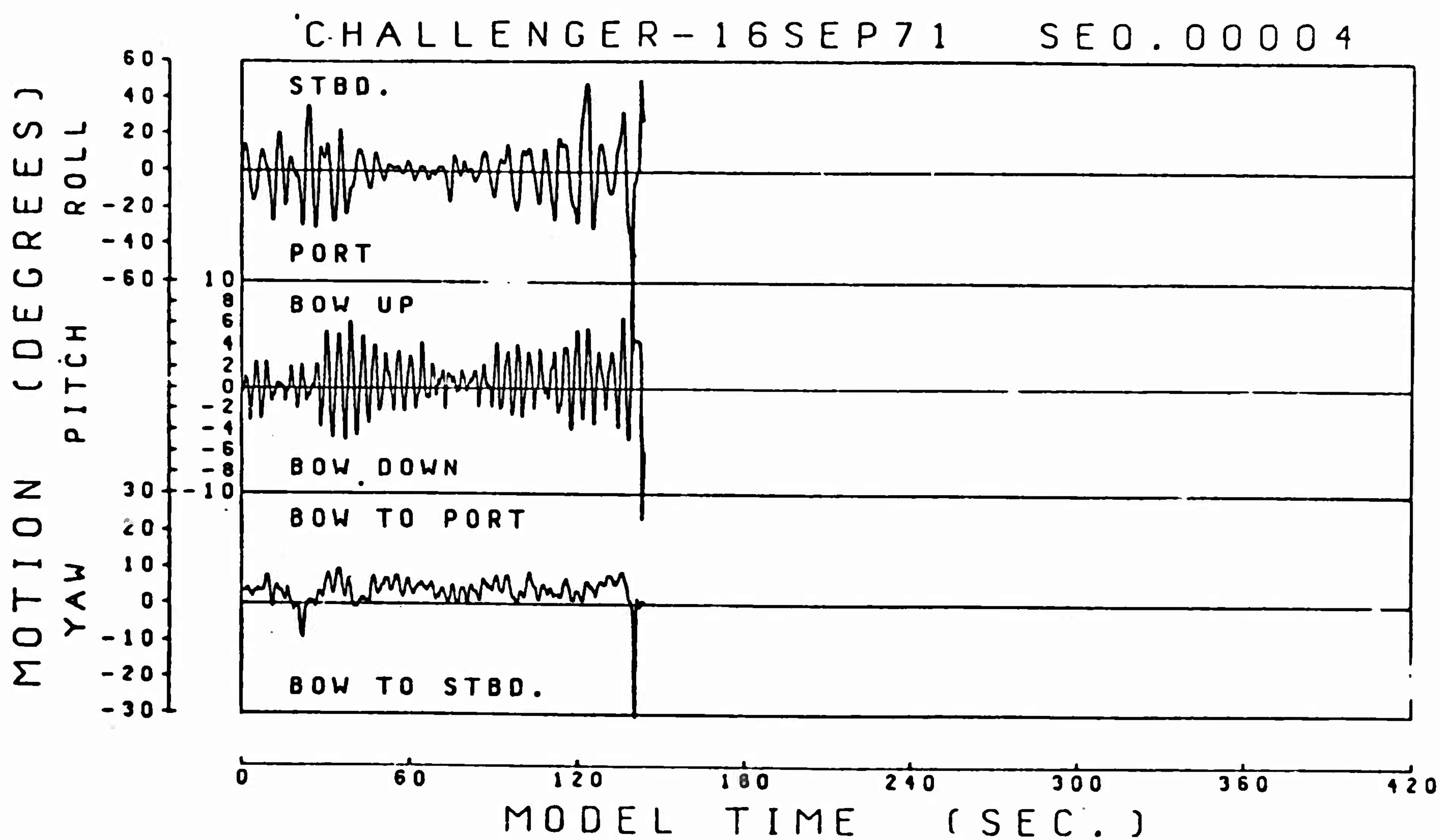

Figure V-18 *American Challenger* Model Experiment

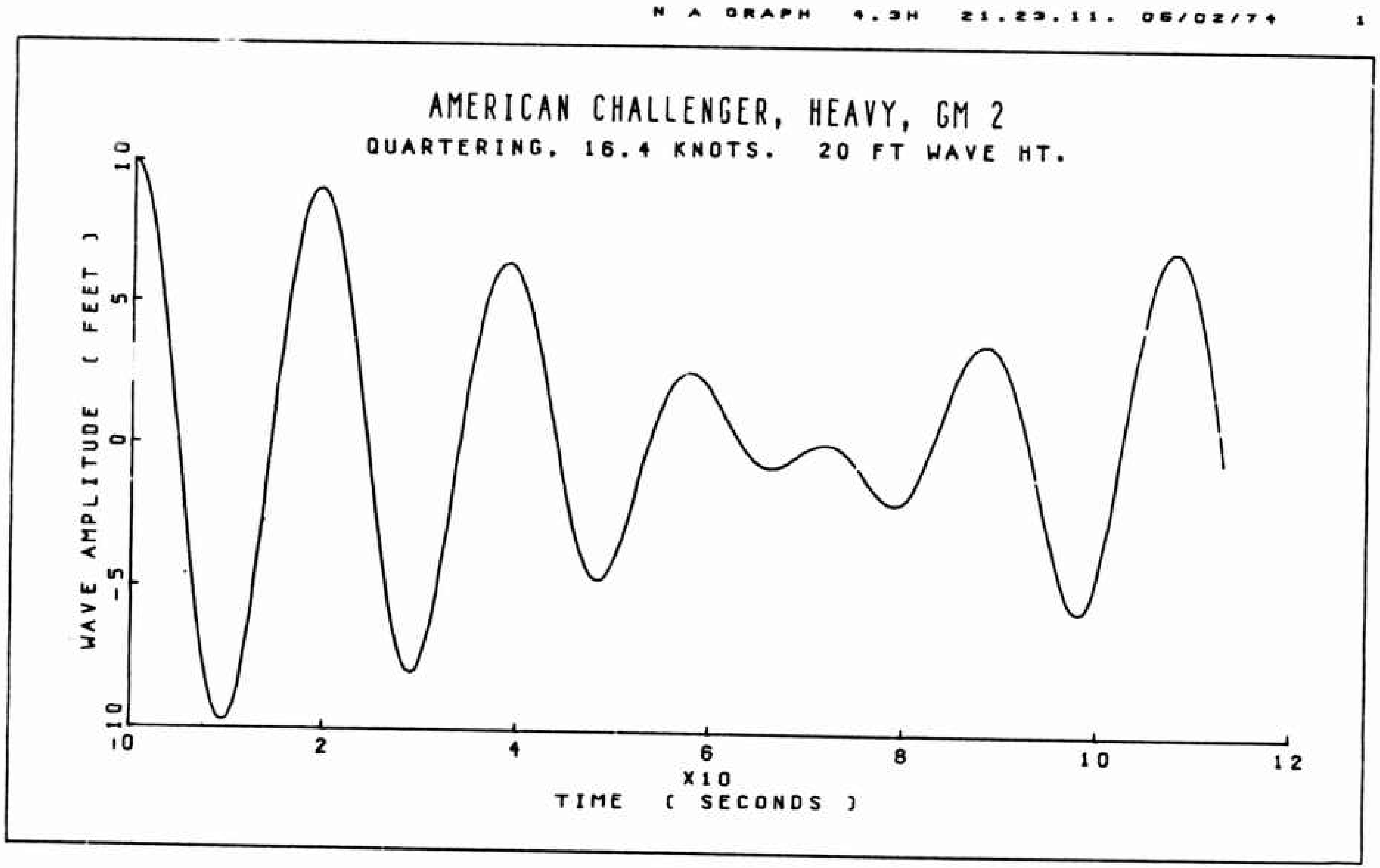

Figure V-19 Wave Simulation

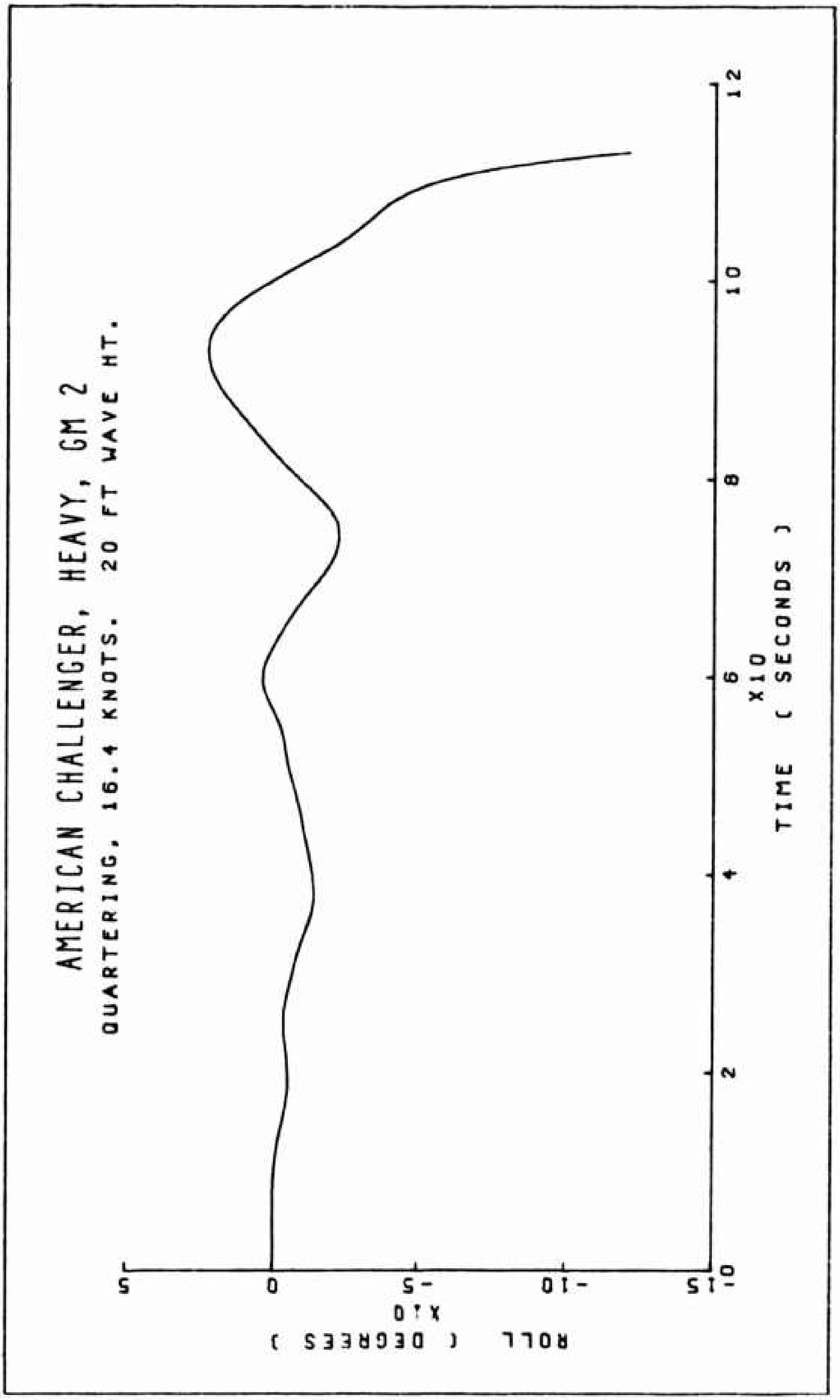

Figure V-20 Roll Simulation

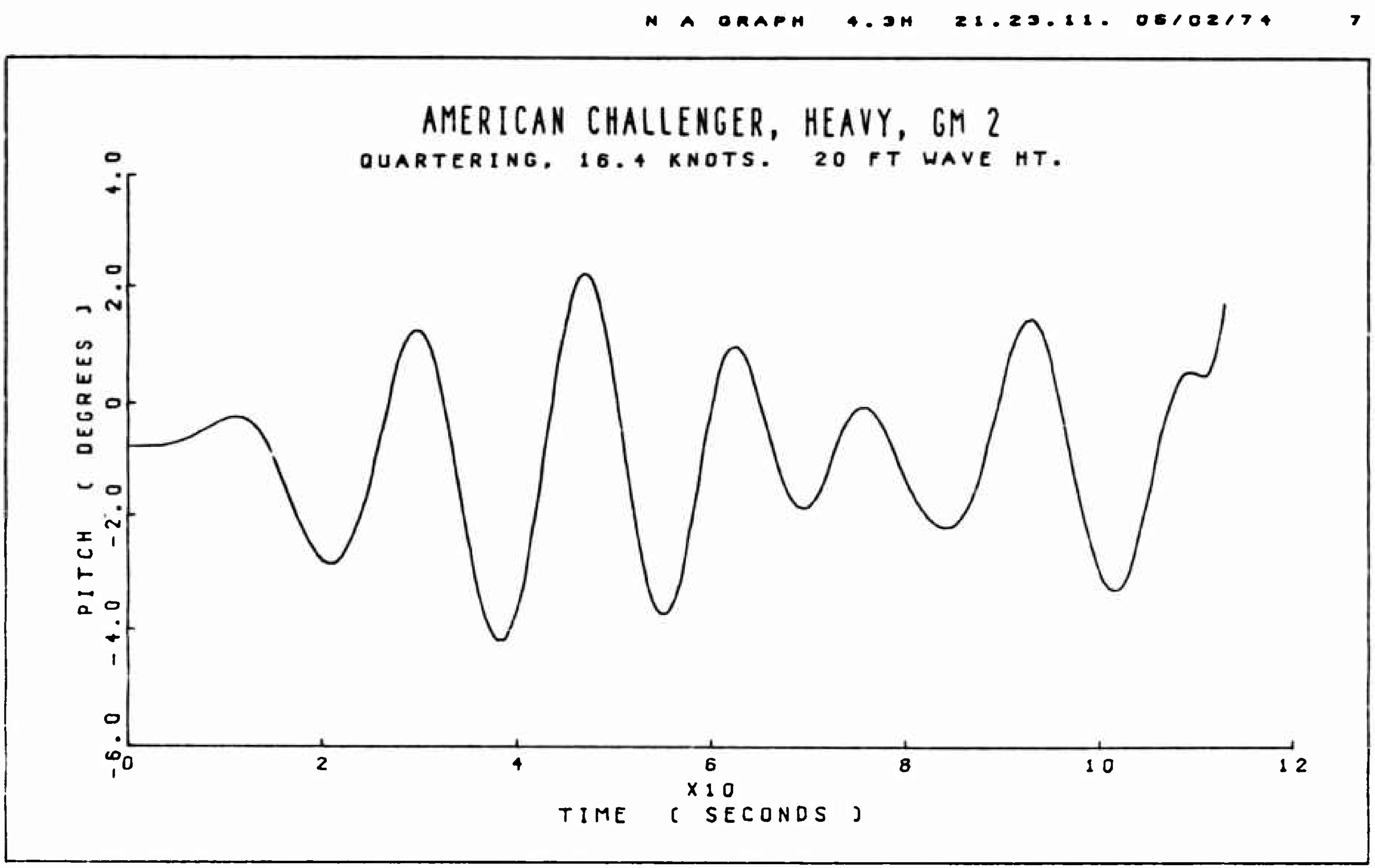

Figure V-21 Pitch Simulation

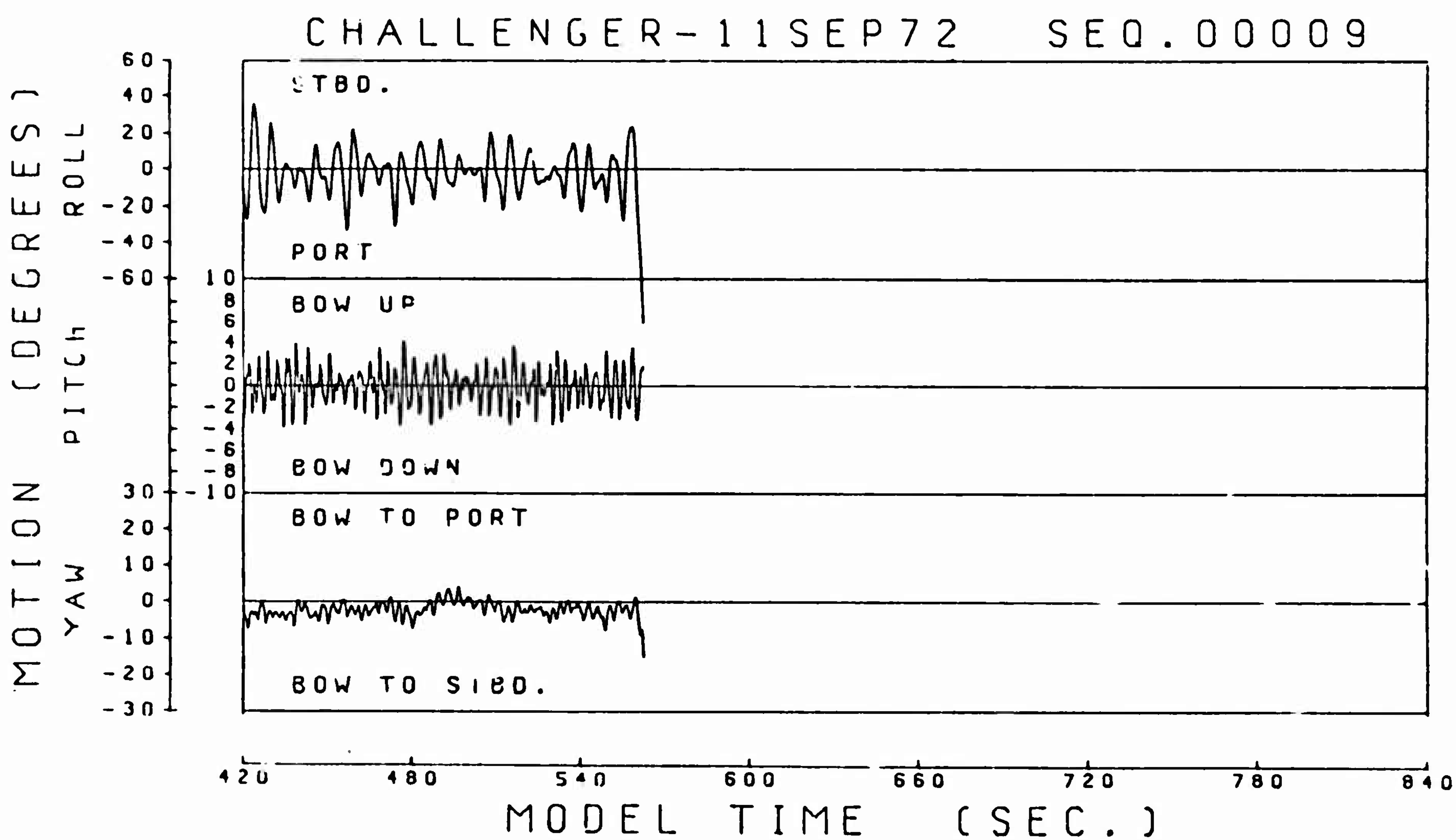

Figure V-22 *American Challenger* Experiment

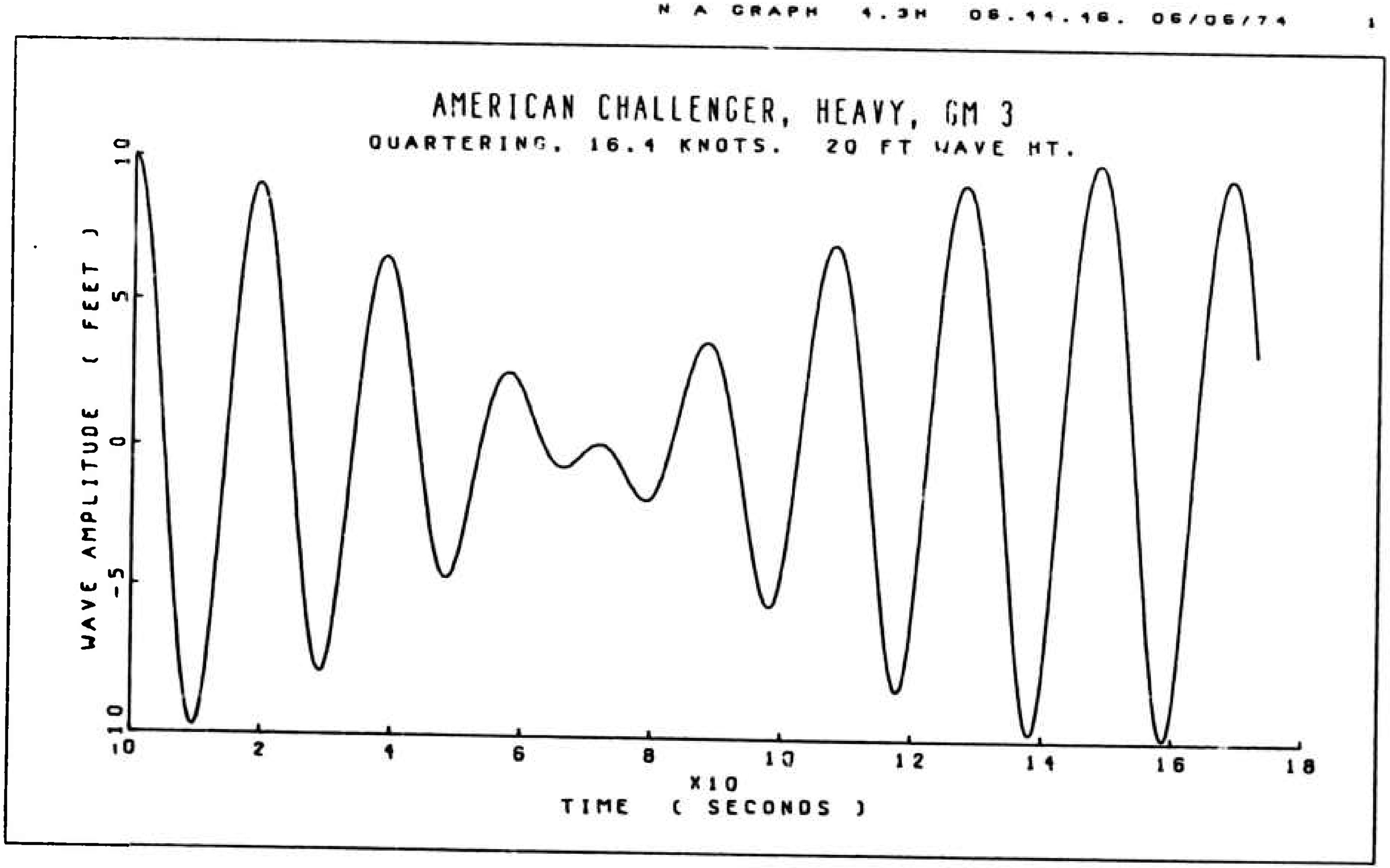

Figure V-23 Wave Simulation

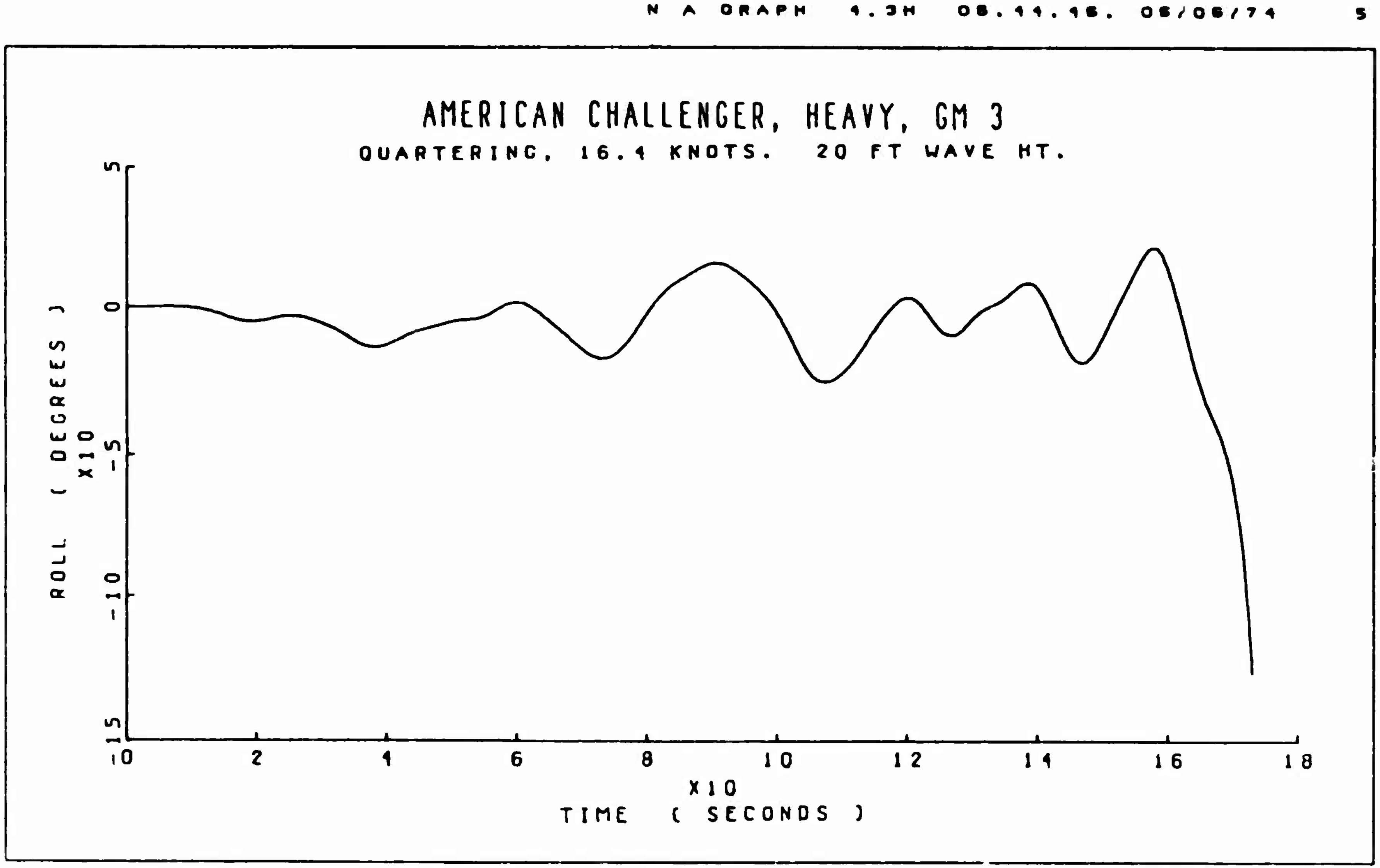

Figure V-24 Roll Simulation

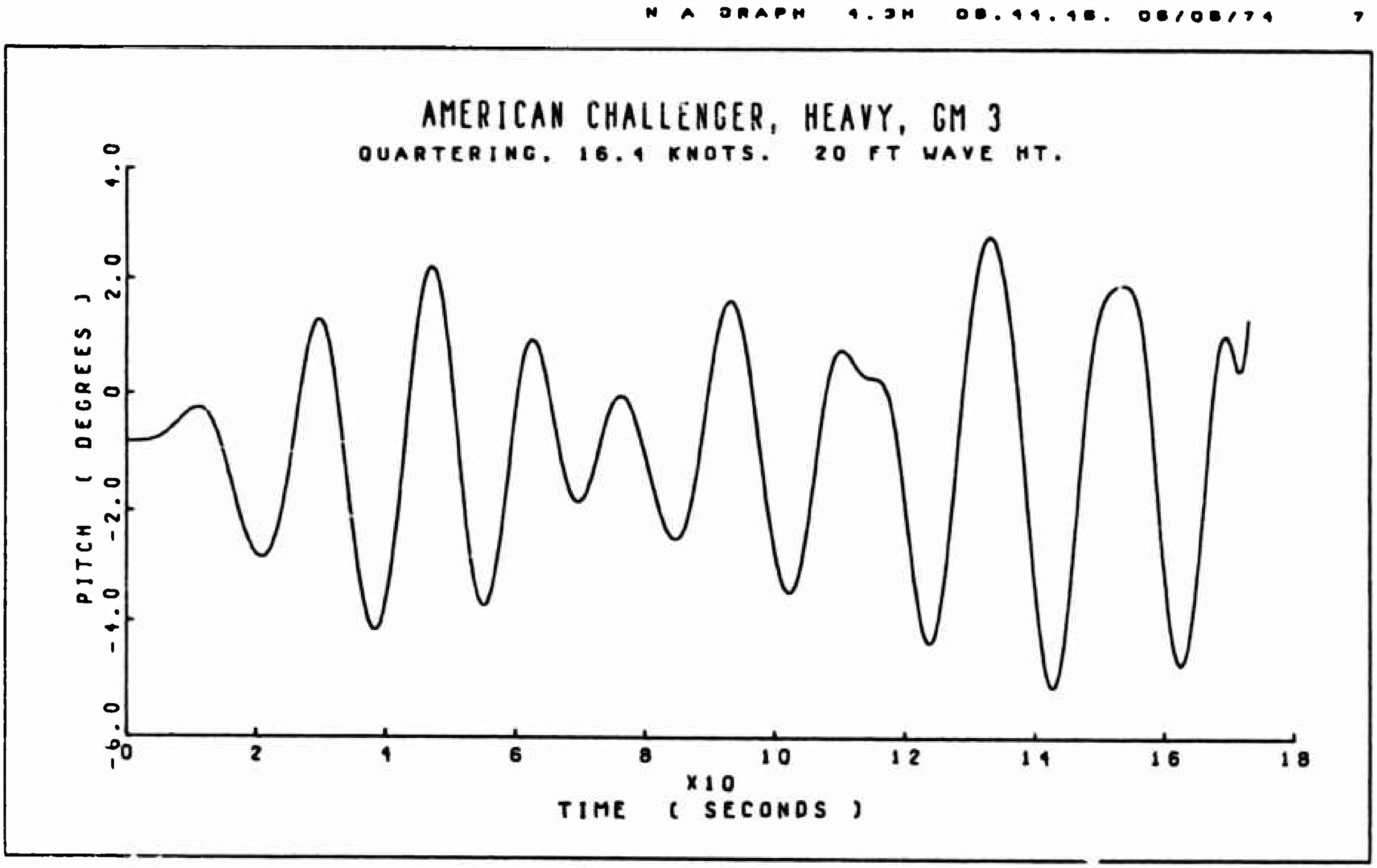

Figure V-25 Pitch Simulation

VI ENCOUNTER PHENOMENA, WAVE GROUPS, AND PREDICTION

It is obvious that intact ship capsizing is due, in large part, to the configuration of the waves encountered by the ship. There is a great deal of difference, however, between the wave shape observed in a fixed coordinate system and the resulting excitation experienced by the moving vessel in following seas. The following discussion is intended as a review of some simple wave encounter relations and an exploration of the potential usefulness of wave group statistics.

A. Wave Encounter Phenomena

A number of striking phenomena are observed in the wave pattern encountered by a vessel moving in following seas. None of these observations are new, yet some discussions of waves in the encounter domain is in order in light of the capsize modes discussed in previous chapters.

The most dramatic event in the encounter domain occurs at zero frequency. A vessel moving at or near the velocity of a wave crest may experience a significant non-oscillating force and a critical loss of stability. Capsizing due to broaching or to a pure loss of stability can result. The zero occurs at an absolute wave frequency of $g/(U\cos\chi)$ where $U \cos \chi$ is the ship velocity in the direction of wave travel. A singularity appears at this frequency in the prediction of the unrestored motions using linear theory. Normally few displacement vessels move at such large Froude numbers. Exceptions might be forthcoming as the speed of containerships increases and fast vessels are driven at their limit. Small craft, such as fishing boats and tugs, can experience problems when they operate in shallow water. The phase speed of wave travel can be reduced to sufficiently small values that such craft have no difficulty in running with a crest amidships. For example, a modern tuna seiner 144 feet on the waterline with a design speed of approximately 15 knots travels at the phase speed of a 125-foot wave. In thirty feet of water, a deep water wave of 160 feet will have a length of approximately 140 feet, it will be steeper, and will run at this same ship speed.

The folding of the wave spectrum in the encounter domain is also familiar. Figure VI-1 shows a typical experimental wave spectrum in the absolute and in the frequency of encounter domain for two speeds. The collapse of virtually all of the energy to a narrow band of rather low frequencies should be noted and is potentially significant for purposes of mathematical simulation. The frequency collapse with respect to wave length is dramatically shown in Figure VI-2 presented by Kastner (1973). It is evident that, for a given ship speed U , a quartering situation may involve the most serious concentration of energy. The situation could be serious if this frequency is near the natural frequency of rolling or in the neighborhood of the frequency for low cycle resonance. It has often been stated that the seaway appears to be a confused collection of waves with random phasing and the only thing regular about the sea is its irregularity. Intuition would therefore suggest that extended excitation at a single frequency or a very narrow frequency band is unlikely, especially when the spectrum tends to be rather broad banded. It is apparent, however, that in following seas the picture is radically altered.

Excitation by a series of large waves at or near a single frequency appears to be a requirement for capsizing due to low cycle resonance. These conditions may be a far more common event than might first be assumed. For purposes of discussion, it will be convenient to consider a wave group or packet formed by the superposition of two regular wave components:

$$\eta(x,t) = \frac{1}{2}\{\cos(k_1 x - \omega_1 t) + \cos(k_2 x - \omega_2 t)\}.$$

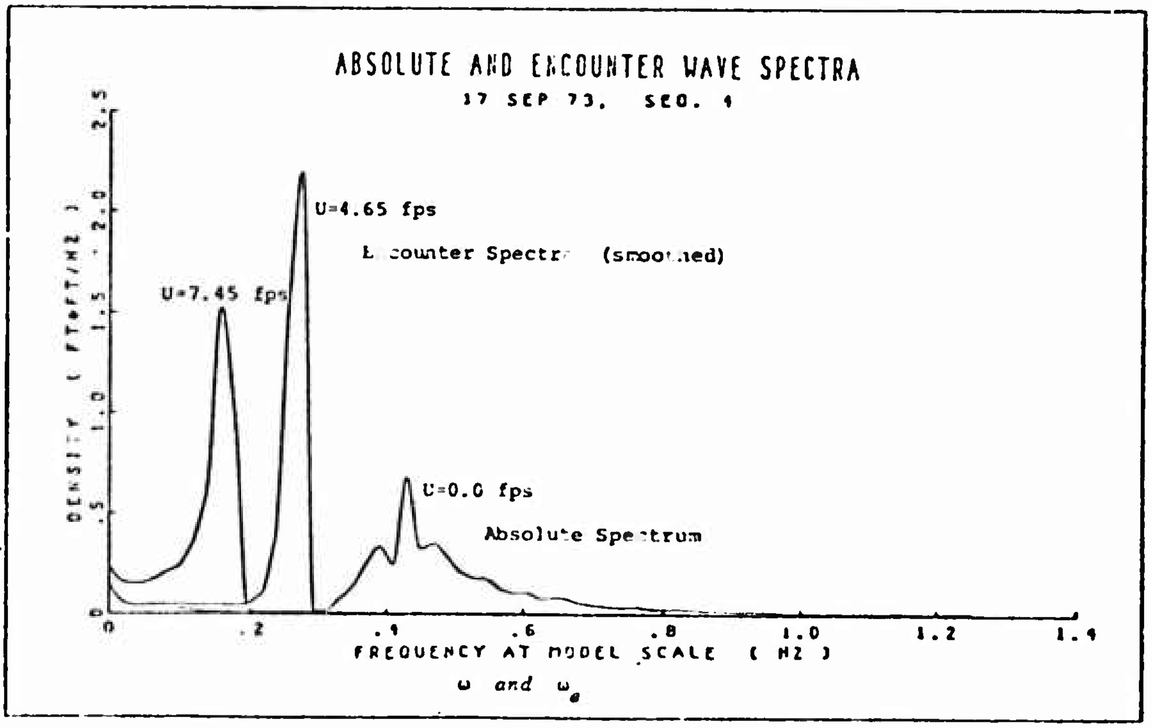

Figure VI-1 Absolute and Encounter Wave Spectra

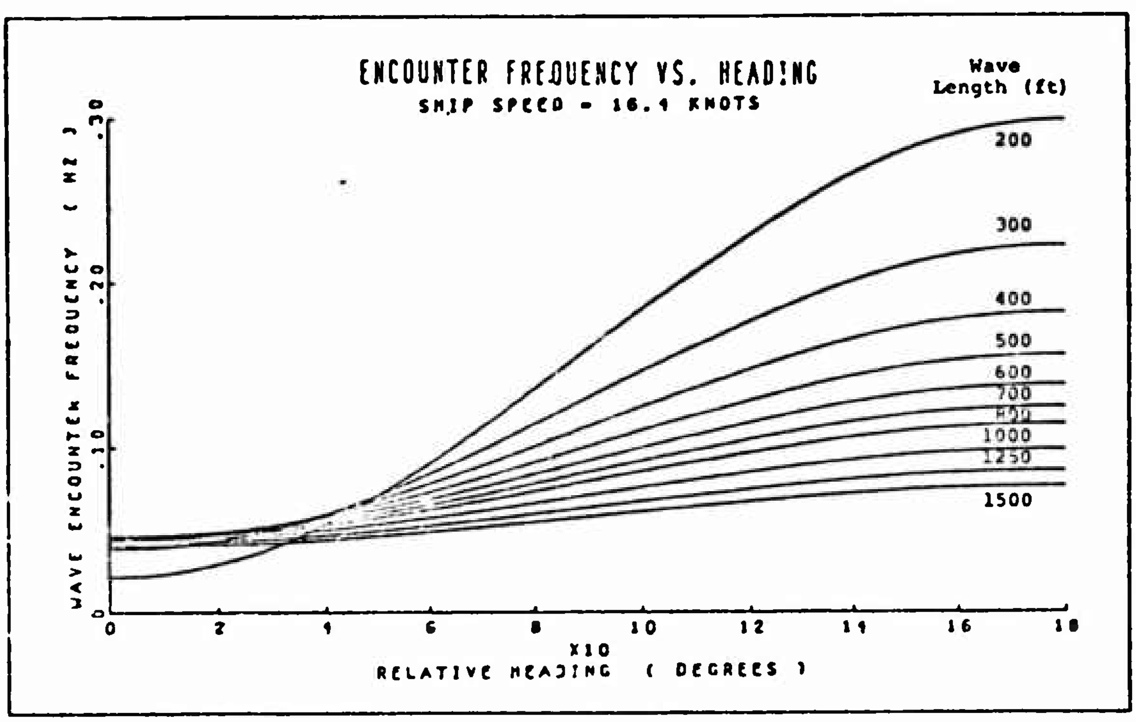

Figure VI-2 Encounter Frequency vs Heading

The number of waves in a group at any instant of time is given by

$$N[t=o] = \frac{k_1 + k_2}{2(k_1 - k_2)}$$

and is the number that would be observed from a photograph or film. This is not the same group size obtained from a record made at a fixed point, however. A wave probe located at $x=0$ would observe

$$N[x=0] = \frac{\omega_1 + \omega_2}{2(\omega_1 - \omega_2)}$$

waves in each group. Figure VI-3 (a) is a plot of the sum of two waves of frequency 0.433 and 0.601 rad/sec. The number of waves in each group therefore represents an increase by a factor of 1.9 over the number that would be observed at a fixed instant. This discrepency is often overlooked when comparing wave records with motion records.

A dramatic change occurs with forward speed in following seas. The number of waves encountered by a vessel moving at a speed $U \cos \chi$ is

$$N[x=Ut\cos\chi] = \frac{(k_1+k_2)U\cos\chi - (\omega_1+\omega_2)}{2\{(k_1-k_2)U\cos\chi-(\omega_1-\omega_2)\}}$$

Here the observed wave frequency is

$$f_e=\{(k_1+k_2)U\cos\chi - (\omega_1+\omega_2)\}/(4\pi)$$

which is zero when

$$U\cos\chi = \frac{\omega_1+\omega_2}{(k_1+k_2)}$$

As noted earlier, this is often a very high speed for more dangerous waves of sufficient length and amplitude. The ratio of the number of waves encountered at forward speed to the number observed at any

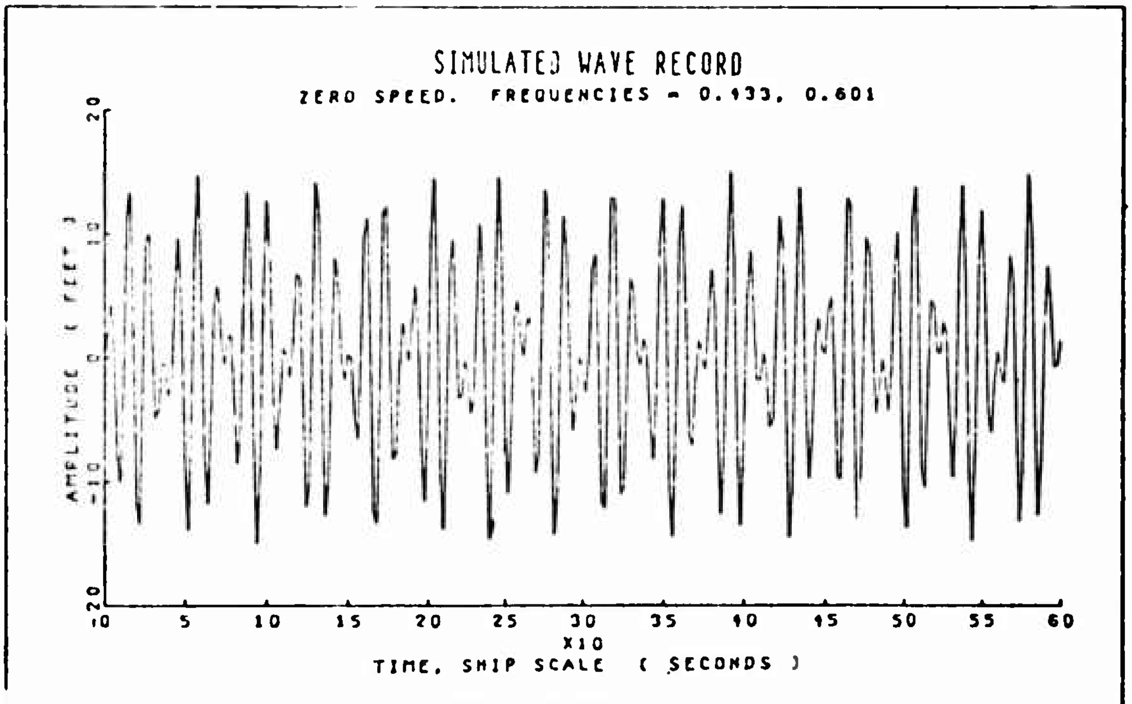

Figure VI-3a Simulated Wave Records

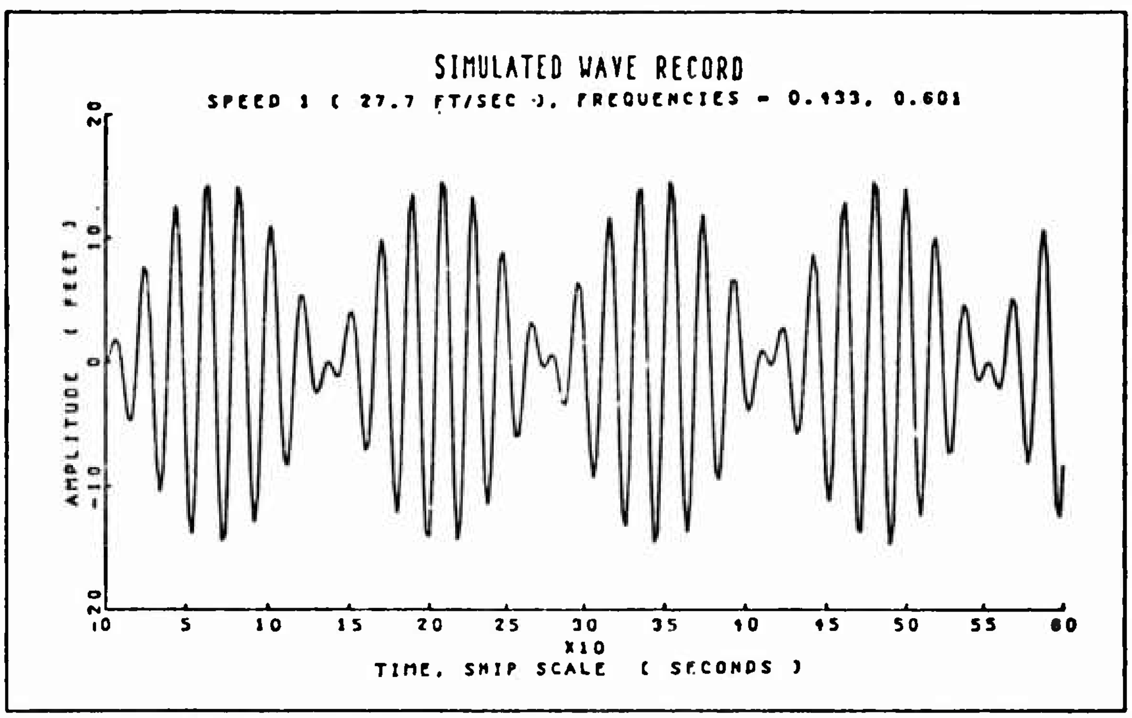

Figure VI-3b Simulated Wave Records

one instant is therefore

$$\frac{U\cos\chi - \dfrac{(\omega_1 + \omega_2)}{(k_1 + k_2)}}{U\cos\chi - \dfrac{(\omega_1 - \omega_2)}{(k_1 + k_2)}}\ .$$

Figure VI-3 (b) shows the same set of waves pictured above but viewed in the encounter domain where $U\cos\chi = 22.7$ fps. There is a gain by a factor of 4.5 in the number of waves in each group over an observation at fixed time and a gain of 3.1 over an observation at a fixed point. These facts are well known but need to be repeated to be appreciated. If the ship moves at or near the group velocity it will encounter a very large number of waves even when the observed wave group or packet appears to be rather small. This also implies that the frequency of encounter could be very pure during such a wave group. If the wave group contains one or more large waves, their repeated encounter in the moving domain could become a favorable situation for low cycle resonance or a combination of resonance and large stability loss.

B. Wave Group Statistics

The experiments described in Chapter III provided ample evidence of the importance of "wave groups" in the process of broaching and capsizing. Further insight was gained by the numerical simulation and analysis of Chapter V. It was also obvious that numerical simulations of long runs, though faster and less costly than open water experiments, are also very expensive. Yet some sort of time domain simulation is required due to the nonlinear nature of the phenomena. The statistical results from many long runs would probably provide the most accurate data base for extrapolation. The success of such numerical simulation depends upon the knowledge of the wave system actually encountered by the vessel. Running a finite number of capsize simulations for rather specific wave configurations appear to be the only practical approach. This of course does not permit a complete coverage of all relevant wave configurations which means that a statistical analysis based solely on the runs executed is not possible (Paulling, et al, 1972). However, the complexity of the wave system and the apparent irregularity suggest that only a probabilistic description of the seaway and approach to extreme motion prediction will be successful. Attempting to assign probabilities to any but the most simple wave events is presently out of the question. Until seastate monitoring techniques can provide sufficiently detailed and accurate information of extreme values, the possibility of using a simplified description of wave events leading to extreme motions or capsizing should not be overlooked. This is where the concept of wave groups may permit engineering estimates of the probability of capsizing and a measure of ship safety.

Ideally it would be possible to separate the study of capsizing from the occurrence of relevant wave configurations. For example, it may be possible to exercise the simulator to determine those wave group parameters that result in a capsize or nearly so. This might be referred to as the "capsize surface". The probability of capsizing would then be expressible as the product of the probability of capsizing in a given wave group (zero or one) and the probability of encountering such a wave group. The required contributions of the naval architect and the oceanographer thereby become somewhat more clearly defined.

Two questions must be answered if such an approach is worth pursuing. The first is whether a relatively smooth capsize surface exists and is determinable. The second question is whether the probability of occurence of any given wave group configuration can be estimated.

Chapter V presented a short analysis of the sensitivity of capsizing to changes in wave configuration. Though by no means exhaustive, the first indications of the study were that moderate changes in the input wave group resulted in smooth changes in the motions.

The second question involved the determination of the probability of encountering a given wave group. Theoretical and experimental studies of wave group statistics to date are not sufficiently complete for practical use. However, the following review and analysis suggests that practical results may be possible and forthcoming.

The exact definition of a wave group has yet to be given. The definition is in fact somewhat arbitrary and depends on its uses. Most investigators have employed the most convenient form for their own purposes. Each definition aims to characterize the beat-like appearance of the wave amplitude which is often visible in an irregular wave train. Low frequency components and asymmetry are usually removed prior to statistical analysis by using the wave height or the envelope of the process as the basic parameter. A group is usually defined by employing one or more of the following parameters:

Hg	the largest wave height in a sequence
H_L	the level which a sequence of N waves exceed
N	the number of waves in the group
Tg	the average period of the component waves
T_1	the period of the envelope exceeding the level H_L
T_2	the period between up-crossings of level H_L by the envelope
H	the height measured between a crest and the average of neighboring troughs

A group may be defined as a series of waves for which the wave height envelope exceeds a specified level. An alternative definition might involve the period of each individual wave component. The group defined by Thompson (1974) was based on the height of the largest wave in a sequence where the approximate period of each wave component was within a given range of the average period for the group. The largest height, H_g, had to be greater than or equal to one third the significant wave height.

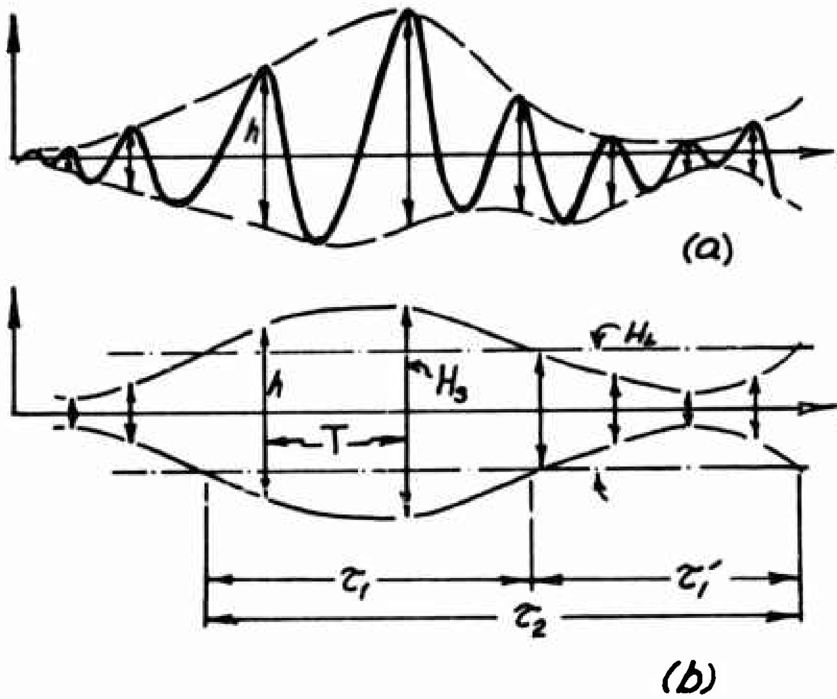

Figure VI-4 Wave Group Definition Sketch

Other definitions can be easily constructed. The largest wave in a group is likely to be the most important parameter for prediction of capsizing due to pure loss of stability. On the other hand, the average period, overall level H_L, and length of run T, should be more relevant for studies of resonant buildup of motions. Additional experience with numerical simulation should help to clarify the important parameters.

Once the parameters are chosen, it is necessary to construct the joint probability distribution, e.g. P (H, Hg, Tg, N). This can be done by fitting curves to the actual data records. Some parameters have been studied in this way (Thompson, 1974). Assistance from theory is also available, but there is not enough, as yet, to construct the entire joint probability for typical wave spectra. A detailed study of wave groups is necessary. As a first step, a brief review of some of the theoretical highlights and the correlation with data recorded in San Francisco Bay will be given.

Several of the references listed at the end of this report contain discussions of certain aspects of "wave groups". Among them, two different approaches were used for the analysis. For a given level, the first approach considers the number of waves in a group while the second approach considers the elapsed time of the envelope above the level.

The first approach is represented by Goda (1970) and Ewing (1972 and 1973). Ewing dealt with the mean number of waves in or between groups of waves in a record for a given level. Mean value statistics however, are not likely to be sufficient for the above purposes.

C. The Probability of Having a Given Number of Waves in a Group

In Goda's (1970) analysis of "wave groups", he defined the length, j, of a run of height, h, as the wave heights exceeding h for $j-1$ consecutive waves after one exceedence and then a failure to exceed the level at the $j+1$ wave. Let the probability that each wave height will exceed h be p, then the probability that the wave will not exceed h is

$$q = 1 - p. \tag{VI-1}$$

If the wave heights are independent of each other, then the probability of having j_1 consecutive waves with a height greater than h after the first up-crossing of level h is

$$p_1(j_1) = p^{j_1 - 1}\, q \, . \tag{VI-2}$$

The mean and variance of the length of runs in a record are:

$$E(j_1) = \frac{1}{q} \tag{VI-3}$$

$$\sigma^2(j_1) = \frac{p}{q^2} \tag{VI-4}$$

Next, he defined the recurrence interval for wave groups as a total run at level h , which is the number of waves between two successive groups. The probability of a total run with a length of j_2 is given by

$$P_2(j_2) = \frac{pq}{p-q} \left(p^{j_2-1} - q^{j_2-1}\right). \qquad \text{(VI-5)}$$

The mean and variance of the length of a total run are calculated as

$$E(j_2) = \frac{1}{p} + \frac{1}{q}\,, \qquad \text{(VI-6)}$$

$$\sigma^2(j_2) = \frac{p}{q^2} + \frac{q}{p^2}. \qquad \text{(VI-7)}$$

For comparison of this theory with his simulated wave record, three definitions of runs were used: waves exceeding the median wave height H_{median}, waves exceeding the significant wave height $H_{1/3}$, and the total run length from the two successive wave groups exceeding $H_{1/3}$. His results are shown on Figure VI-5. The spectrum M-9 has almost uniform spectral density and exhibits run lengths that are similar to those predicted by this independent random process. The other extreme, namely a narrow banded, highly peaked spectrum, is represented by spectrum M-5. The distribution of the length of runs differs significantly from that represented by this process. On the other hand, a more realistic wave spectrum is represented by spectrum F-4 which is of Pierson-Moskowitz or wind wave form. The distribution characteristics of the length of runs of this spectrum follows, in general, the shape of that represented by this independent wave process, but the magnitude is so different that this process cannot describe it accurately.

The same analysis has been performed for waves measured in San Francisco Bay. A typical result for a wave record at various heights is shown on Figure VI-6 and Figure VI-7. These resemble the results shown in Figures VI-5 from spectrum F-4.

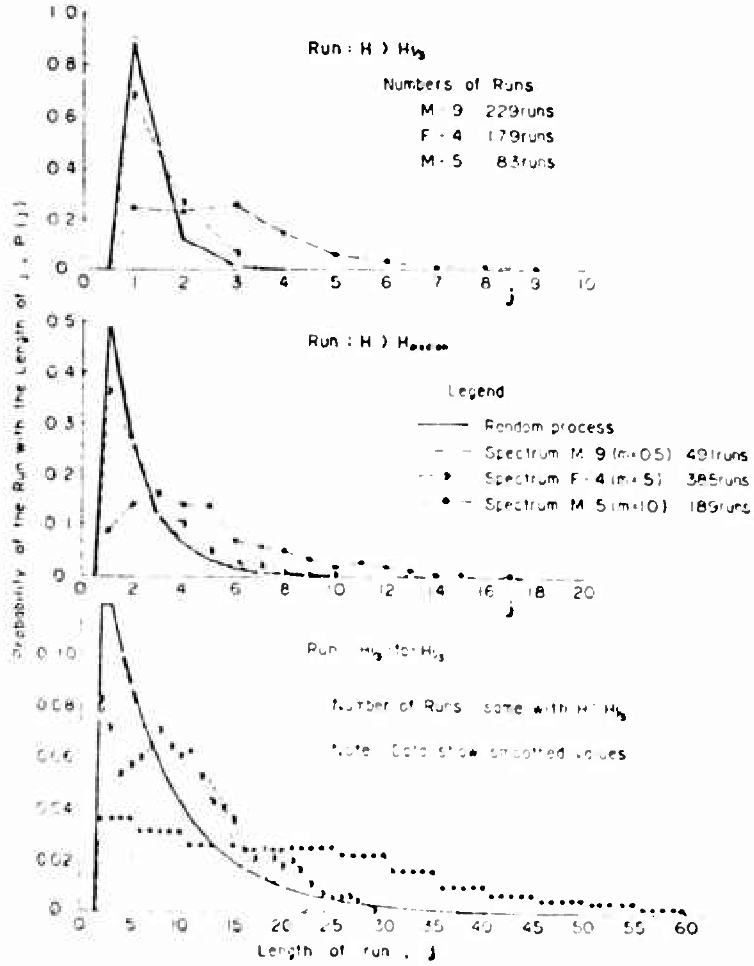

Figure VI-5 Length of Run vs. Wave Height

Note that the agreement between wave data and the results of predictions by this method is better at lower levels than at higher levels. The latter, however, are of more interest. Also, note that for wind waves, as represented by the San Francisco Bay wave data or spectrum F-4, the probability of only one wave in a group is always smaller than that predicted by Goda's method while the probability that there are more waves in a group is always larger. Therefore it can be concluded that:

1. larger waves tended to come in groups,
2. successive wave heights are correlated with each other,

3. the distribution of the length of runs described by this independent random process can represent only the shape of the curve.

D. The Probability of the Elapsed Time of the Envelope Being Above a Given Level.

This approach is performed by Nolte and Hsu (1973), (to be published), and Vanmarcke (1971). Again, Vanmarcke discussed mainly the mean values of various parameters. Although useful, his analysis will not be pursued further here.

Nolte and Hsu (1973) assumed that the probability that the envelope height will cross a level h_o during an interval of time can be described by a Poisson process. The assumptions associated with using the Poisson model are stated by them as follows:

1. The probability of the envelope's crossing the level h_o in any non overlapping time interval is independent and time invariant.
2. The probability of crossing the level h_o in a small time interval is proportional to the size of the interval.
3. The probability of multiple crossings in a small time interval is negligible relative to the probability of a single crossing.

They then define the time duration for a group of level h_o as the elapsed time beginning when the envelope crosses above the level, h_o, and ending when the envelope crosses below the level h_o. This time duration is shown on Figure VI-4 as τ_1. The probability that the time duration is greater than t is expressed by them as an exponential

$$P(\tau_1 > t | h_o) = \exp[-t/\tau(h_o)] \qquad \text{(VI-8)}$$

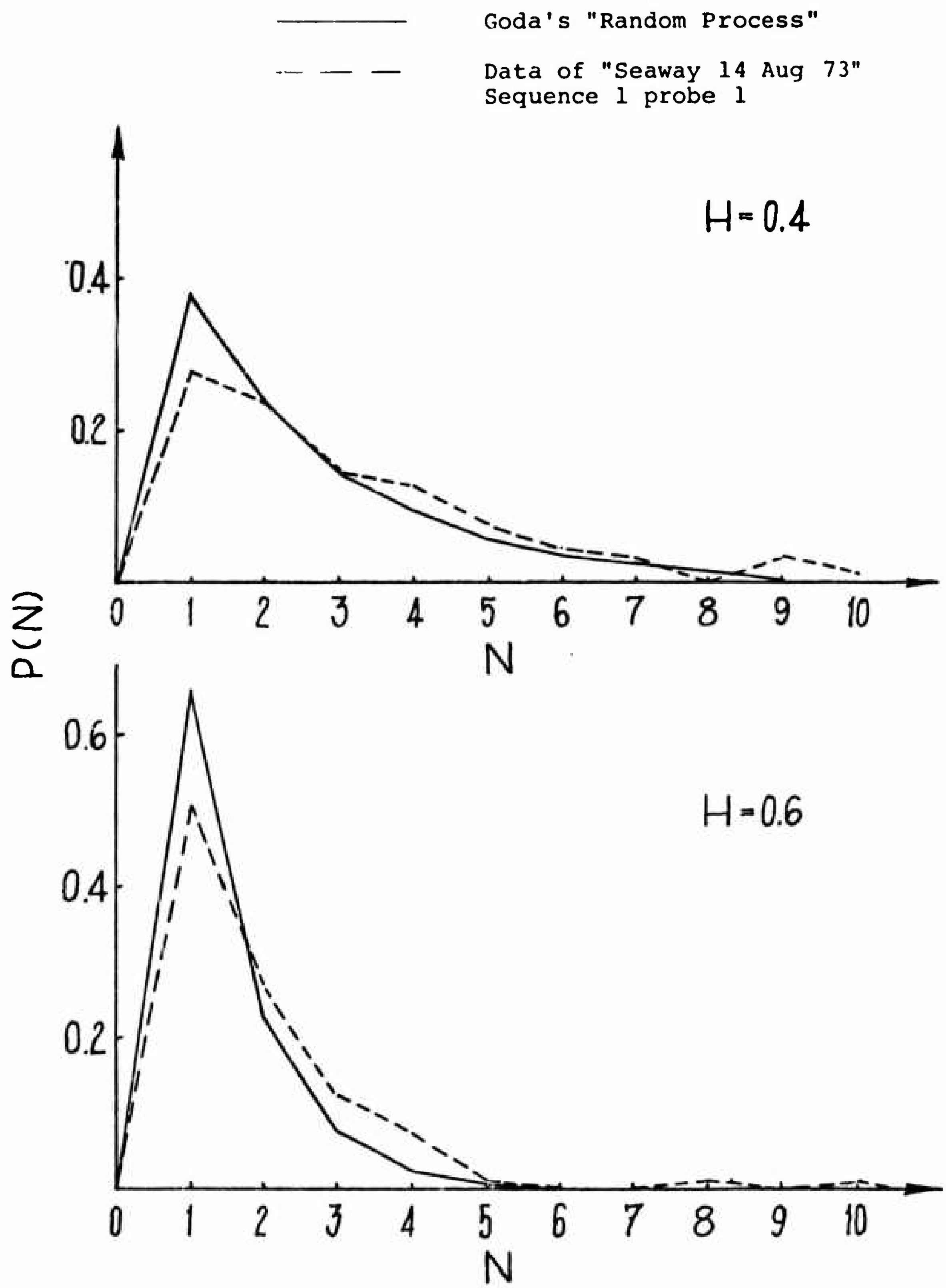

Figure VI-6. D·stribution of N Waves in a Group Above Level H=0.4ft. and H=0.6ft.

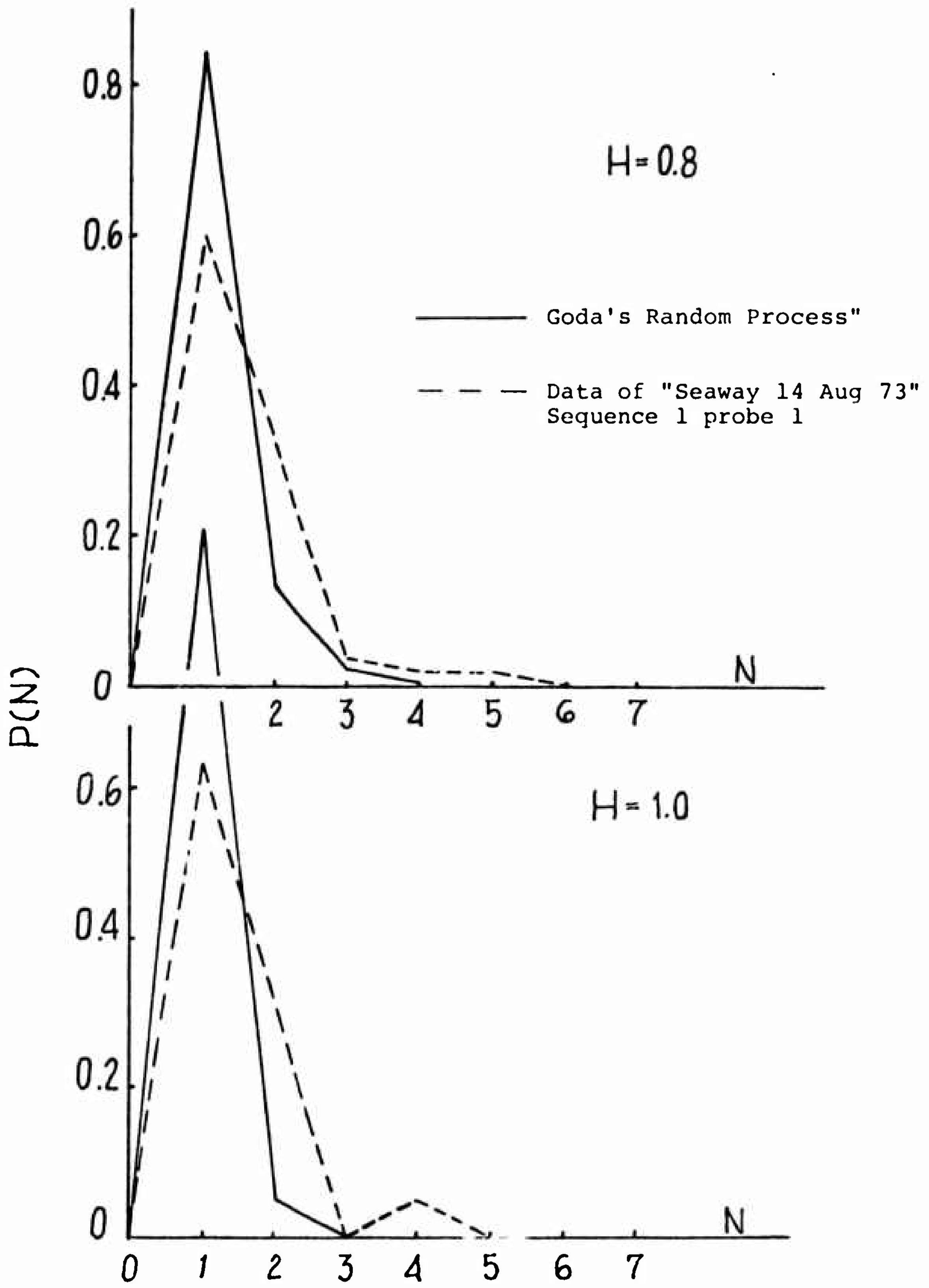

Figure VI-7. Distribution of N Waves in a Group Above Level H=0.8ft. and H=1.0ft.

where $\tau(h_o)$ is the average time duration for groups of level h_o. They derived this mean time duration as

$$\tau(h_o) = \frac{1}{2\sqrt{2\pi}h_o}\left[\frac{1}{f_e^2 - \bar{f}^2}\right]^{1/2} \qquad \text{(VI-9)}$$

in which h_o is the level of the envelope height divided by the significant wave height. f_e is the average wave frequency defined by

$$f_e^2 = \frac{\int_o^\infty S(f) f^2 df}{\int_o^\infty S(f)\, df} = \frac{m_2}{m_o}\,. \qquad \text{(VI-10)}$$

$S(f)$ is the wave energy spectrum, $\bar{f}$ is the centroid of the wave energy spectrum defined as

$$\bar{f} = \frac{\int_o^\infty S(f) f\, df}{\int_o^\infty S(f)\, df} = \frac{m_1}{m_o}\,, \qquad \text{(VI-11)}$$

and m_i is the i^{th} moment of the energy spectrum.

With these known, they further derive the average frequency of occurrence for wave groups of level h_o as

$$\nu(h_o) = \frac{\exp(-2h_o^2)}{\tau(h_o)} \qquad \text{(VI-12)}$$

If the number of waves in a group is denoted by N, then the probability that a wave group contains more than n waves higher than the level h_o is

$$P(N{>}n|h_o) = \exp[-nT/\tau(h_o)] \qquad \text{(VI-13)}$$

where T is the average wave period.

Since the number of groups in a record of time L is assumed to be described by a Poisson process, the probability of having M groups of waves of level h_o can be expressed as

$$P(M|h_o) = \frac{[\nu(h_o)L]^M}{M!} \exp[-\nu(h_o)L]. \qquad \text{(VI-14)}$$

If the highest wave height in a group of N waves exceeding the level h_o is denoted by H^1, then the probability that H^1 is less than h is derived as

$$P(H^1<h|h_o,N) = 1-\exp[-2(h^2-h_o^2)]^N. \qquad \text{(VI-15)}$$

In normalized form, the energy spectra for the envelope and the square of the envelope are shown to be equal and can be expressed as

$$E(f) = \frac{\int_0^\infty S(x)S(f+x)dx}{\int_0^\infty S^2(x)dx} \qquad \text{(VI-16)}$$

where $S(x)$ is the energy spectrum for the wave trace and x is a dummy variable representing frequency.

The assumption of a Poisson model is shown by Nolte and Hsu to agree very well with data collected during one storm in the Gulf of Mexico. Similar statistics have been determined for the waves measured in San Francisco Bay. Some results are shown in Figures VI-8, VI-9, and VI-10 for different levels of the same wave record.

In comparing their results with the data they collected, Nolte and Hsu noted that because of the finite wave population of the record, $\tau(h_o)$ obtained from Equation (VI-9) cannot represent the mean time duration properly.

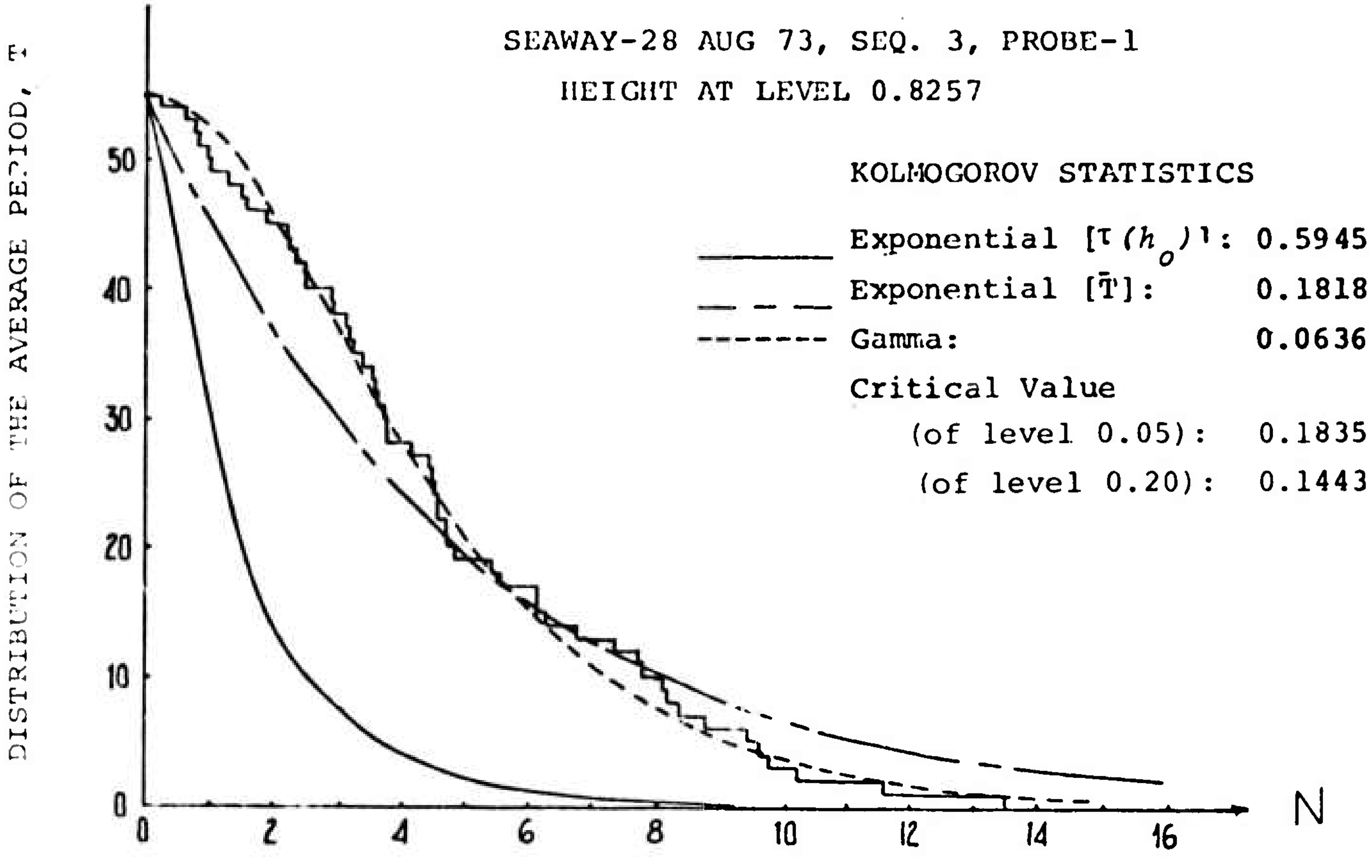

Figure VI-8

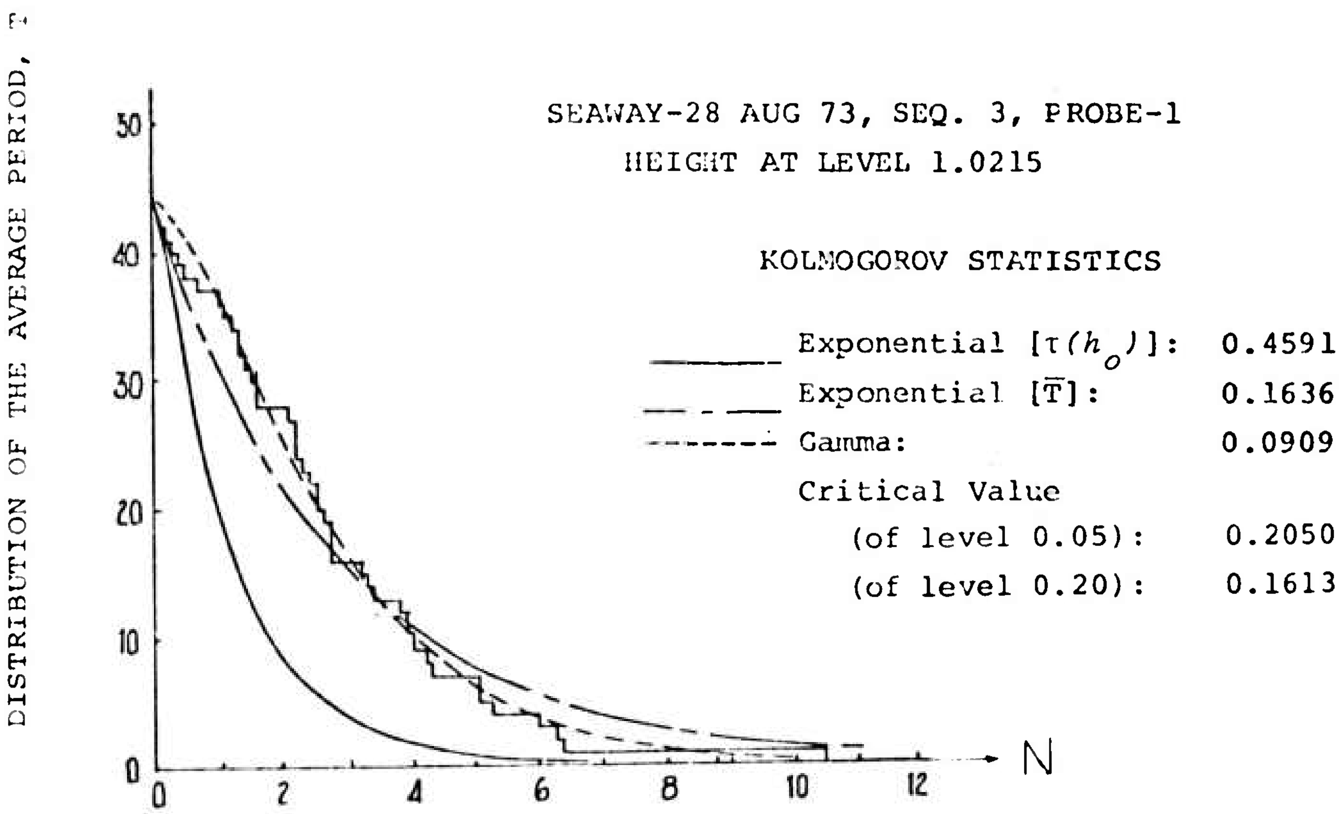

Figure VI-9

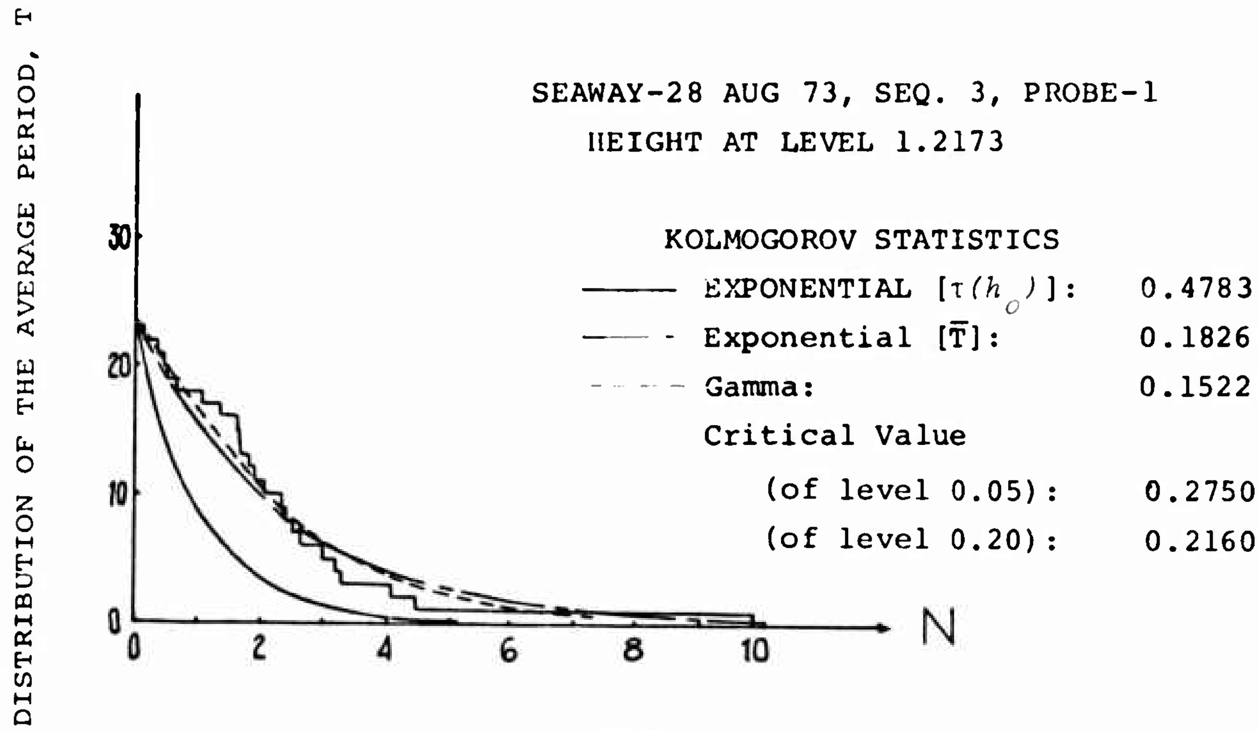

Figure VI-10

(This fact was clearly shown by the San Francisco Bay wave data.) Further study showed that

$$\tau(h_o) = \frac{\int_{h_o}^{\infty} P(h)\,dh}{P(h_o)} \left(\bar{\dot{h}}\right)^{-1}, \qquad \text{(IV-17)}$$

where

$$\bar{\dot{h}} = \int_0^{\infty} \dot{h}\, P(\dot{h})\, d\dot{h} \, . \qquad \text{(IV-18)}$$

Since $\bar{\dot{h}}$ is a constant for a given wave record, then

$$\tau(h_o) \propto \frac{\int_{h_o}^{\infty} P(h)\,dh}{P(h_o)} . \qquad \text{(IV-19)}$$

This relation may then be used to obtain the mean time duration

$\tau(h_o)$. It is not obvious that we can ignore $\bar{\dot{h}}$ and obtain the same statistics. On the other hand, the main concern at this point is to find out the statistical characteristics of τ_1 , rather than the actual mean time duration. The actual data mean is therefore used in the plots. The results seem to follow the exponential curve reasonably well. Kolmogorov statistics have been calculated to evaluate the quality of fit and have been shown to accept the hypothesis that the data is exponentially distributed at a level of 0.2 .

A Poisson process is a very handy assumption to make in many situations. It is formed by the so called streams of random events with a continuous time parameter (Cramer and Leadbetter, 1967). In most applications we are concerned with events, such as calls on a telephone line or arrivals of customers in a shop, which occur successively in time. A Poisson process is usually assumed for these events because in some cases the Poisson model will give an approximation of the true situation and in others it will at least provide a starting point for various generalizations (Cramer & Leadbetter, 1967). The time interval between events for a Poisson process is an exponentially distributed random variable as was implied by equation (VI-8). In the time series for a given level h_o , if we consider any crossing of the envelope as an "event" then we should count τ_1' as well as τ_1 in Figure VI-4 as the time intervals between events. On the other hand if we consider only up-crossings as "events", then it would be more appropriate to consider τ_2 as the time intervals between events. In this case the number of events in a time interval is the same as the number of wave groups in that interval. The distribution curve for τ_2 has been calculated and the results shown in Figures VI-11, VI-12, and VI-13 also agree reasonably well with an exponential curve.

It should be noted that Vanmarcke (1974) had also made the assumption that τ_1 is exponentially distributed. A more complicated exponential type curve had been suggested by Davidan *et. al.*

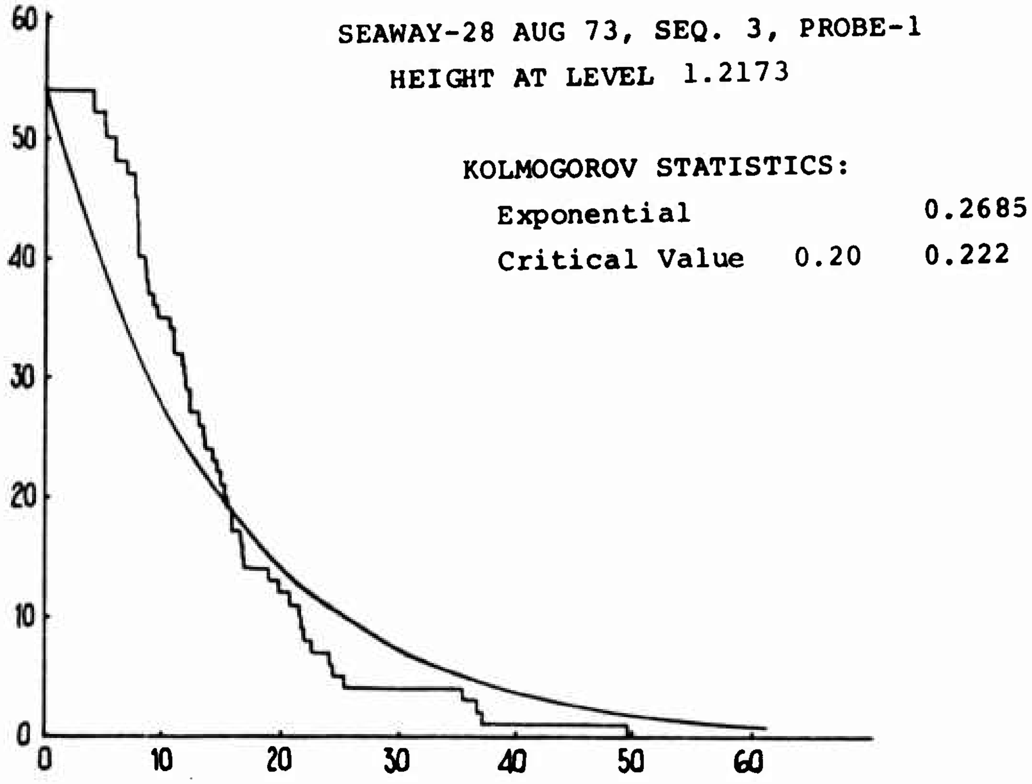

Figure VI-11

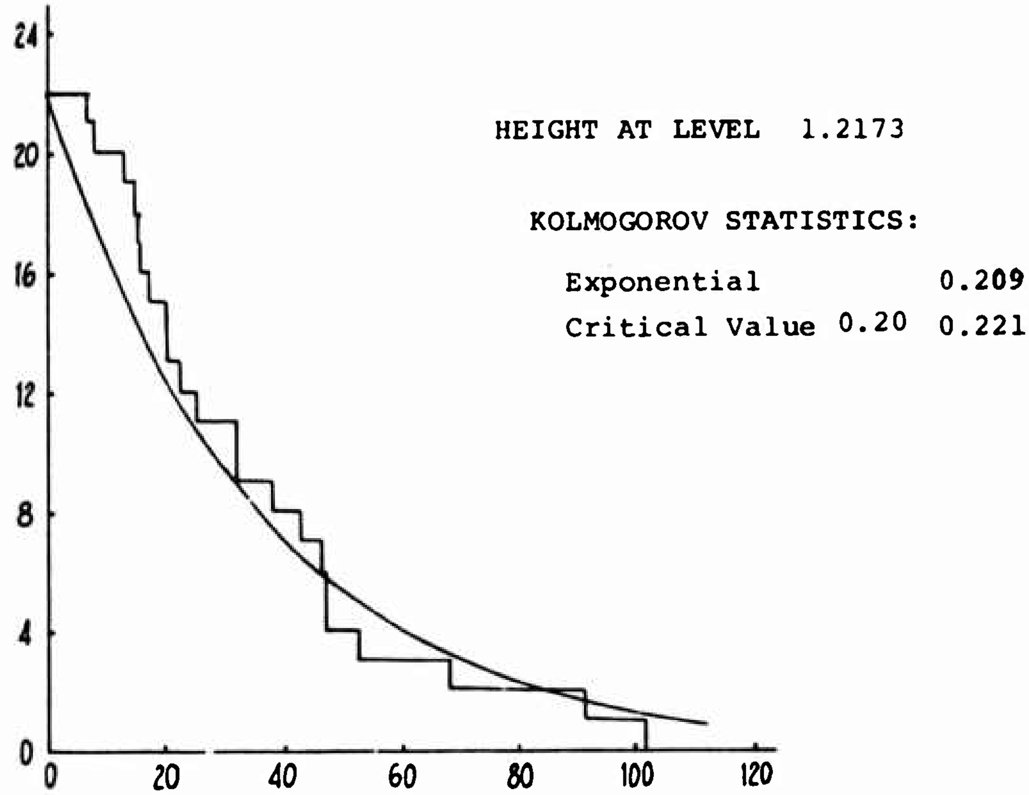

Figure VI-12

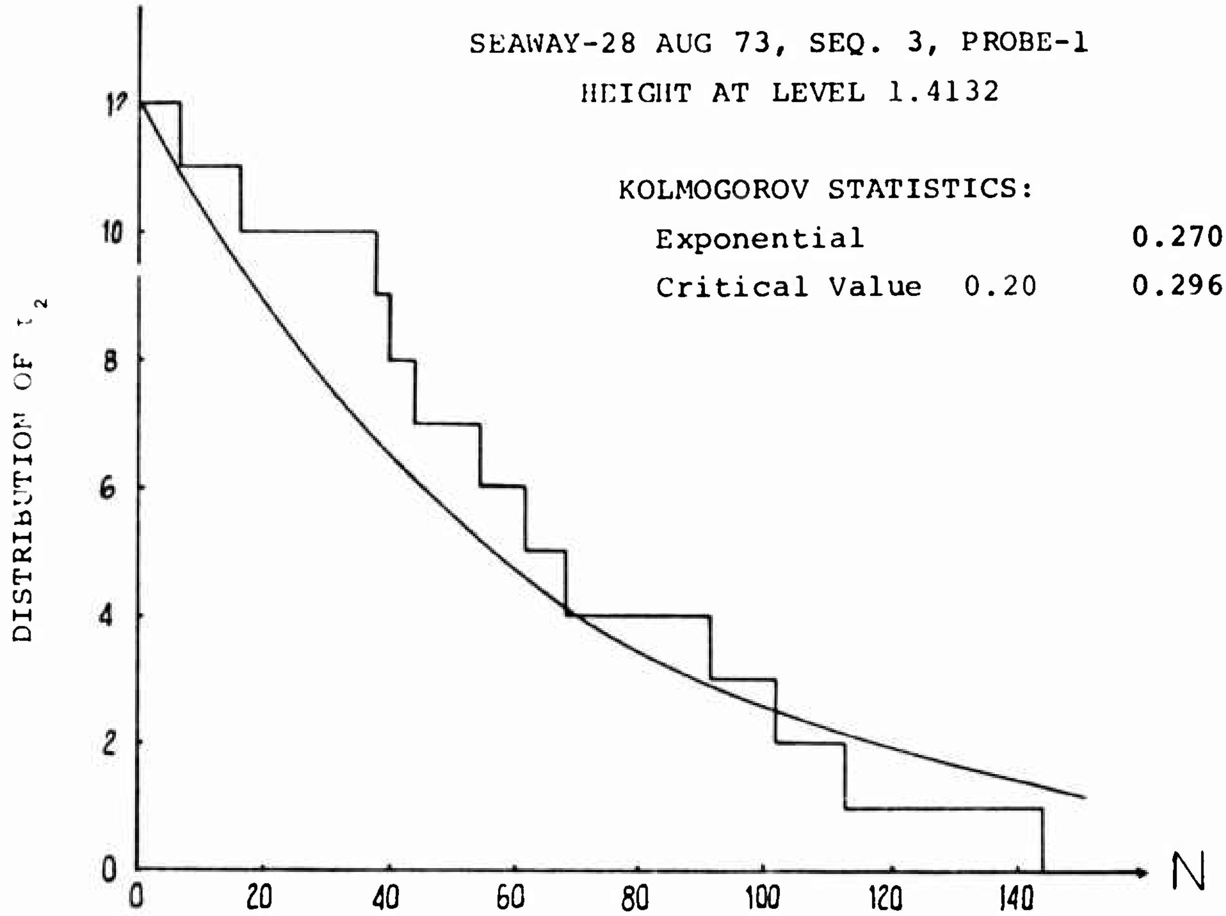

Figure VI-13

E. DISCUSSIONS

As can be seen from the comparisons of wave data, improvements on both of the above approaches are necessary so that more accurate probabilities can be predicted. For the elapsed time τ_1 of the envelope above a given level, a gama curve can be shown to better fit the data than an exponential curve.

On the other hand, as stated earlier, the purpose of this section is to obtain the probability of occurance for a deterministic wave configuration. In practice, a design wave is usually described by a height and a period. For most engineering purposes, especially for inputs to a ship capsize simulator, the most important parameters needed to describe a wave group seems to be the number of waves in a group N, the level H, and the mean period of waves in the group T. The joint probability of these three parameters is therefore desired. Due to the complex nature of multi-dimensional joint probabilities, it would be desirable to separate this joint probability so that each parameter can be studied individually. Using Bayes' rule, this joint probability can be written as

$$P(H,N,T) = P(H)P(N|H)P(T|H,N). \qquad \text{(VI-20)}$$

Now if a time series is interpreted as consecutive outcomes of individual waves, each having its own height and period, this joint probability can then be established.

The analysis of wave record "SEAWAY 14 AUG 73", sequence 1, probe I, will be discussed. In this example, a wave in the time series is defined as one cycle starting and ending with a trough. The height and period of the wave is defined as the distance from the peak to the average of two troughs and time interval between the two troughs respectively. The results of the analysis are shown on Figures VI-14 through IV-18.

$P(H)$, as shown on Figure VI-14, is approximately a Rayleigh distribution. $P(N|H)$, at four different levels H, is shown in Figure VI-15. As stated earlier this can be represented by Goda's method reasonably well although improvement is necessary. $P(T|H,N)$ is shown on Figures VI-16 through VI-18. This conditional probability is likely to cause the most difficulty. When H and/or N is large, there will not be enough data points to estimate this probability properly. However, from these figures, a normal curve seems to be a reasonable suggestion.

A detailed study of these conditional probabilities, both theoretically and experimentally is in order. The parameters needed to describe each conditional probability also should be investigated so that the joint probability, Equation (VI-20), can be estimated from the spectrum rather than the time series.

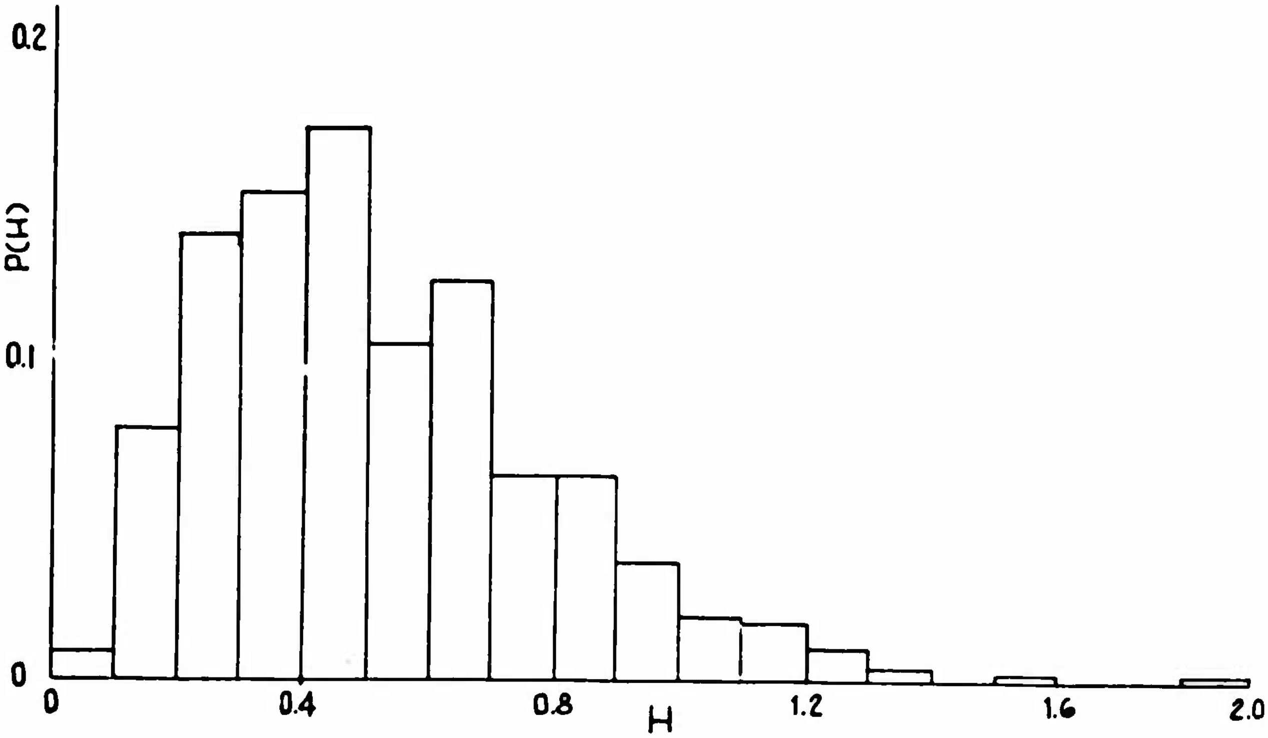

Figure VI-14

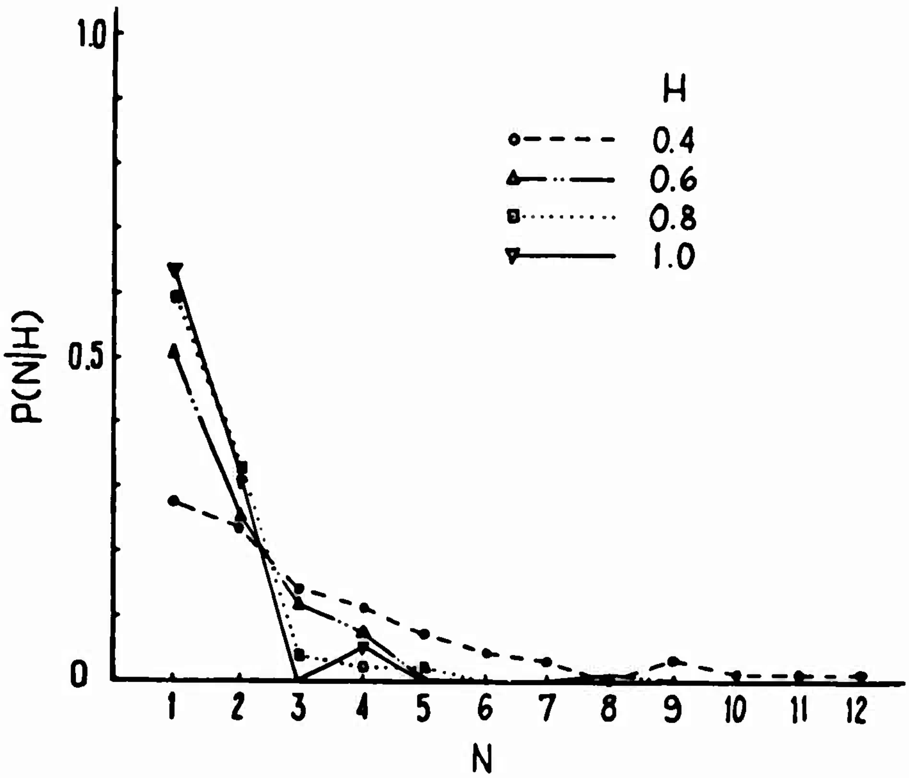

Figure VI-15

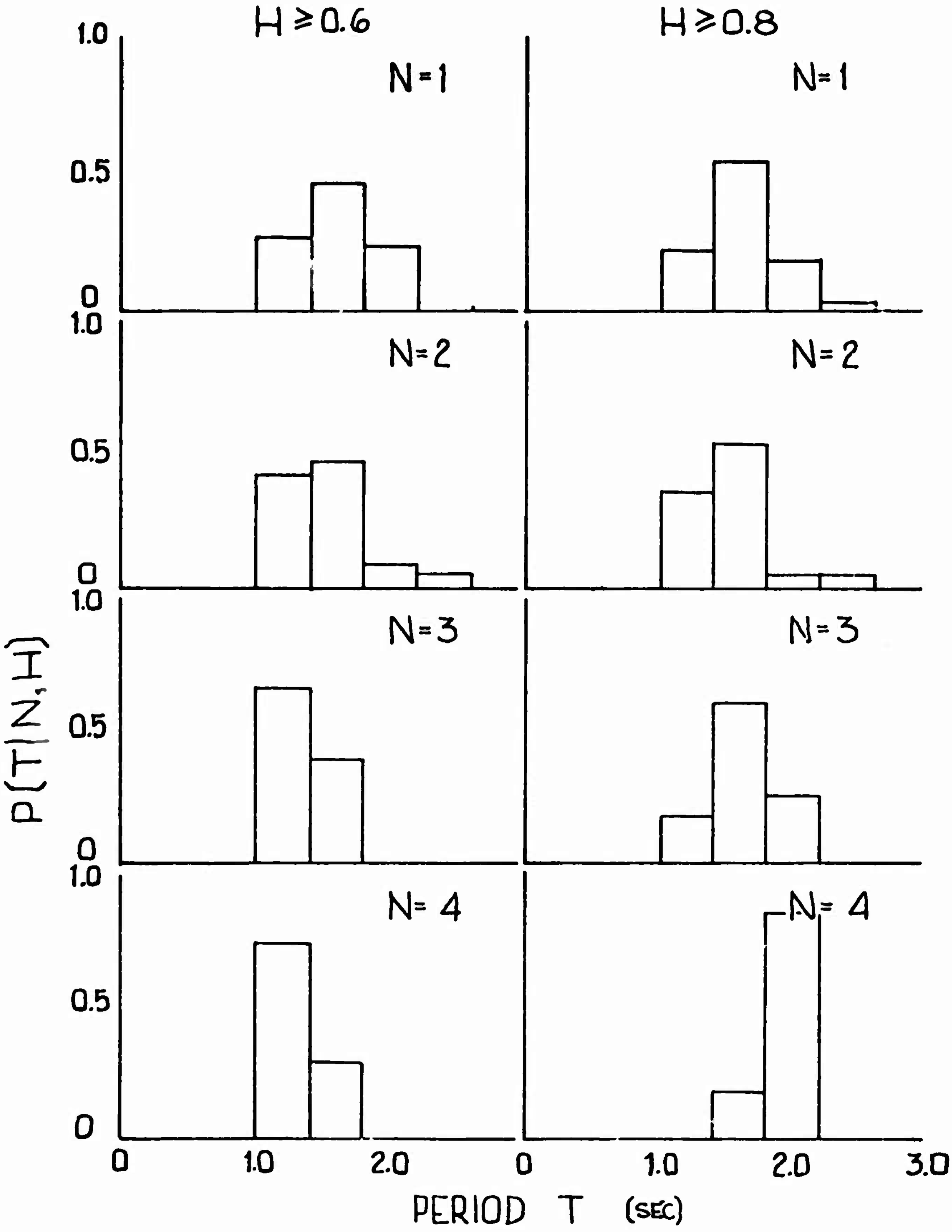
H ≥ 0.6
H ≥ 0.8
N=1
N=1
N=2
N=2
N=3
N=3
N=4
N=4
1.0
0.5
0
P(T|N,H)
0
1.0
2.0
0
1.0
2.0
3.0
PERIOD T (SEC)

Figure VI-16

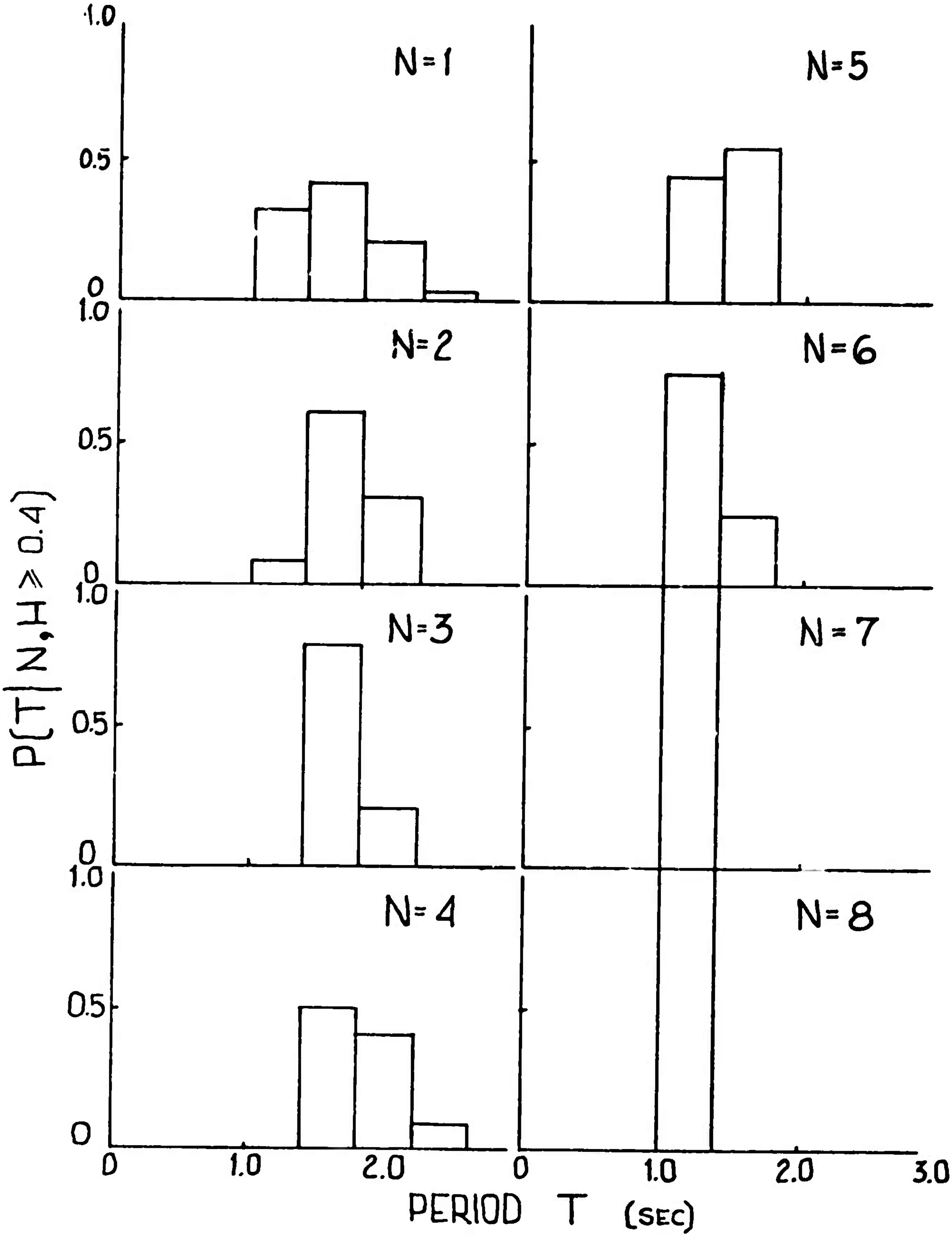

Figure VI-17

Figure VI-18

VII CONCLUSIONS

Since this is the final comprehensive project report, it is felt worthwhile to include a large body of detailed information which might otherwise not have been reported. In several places in the report, it is noted that the present results are tentative and that further comparisons and analysis are definitely indicated, especially when new full-scale data, e.g., storm wave statistics, become available.

The study was initiated with the optimistic hope of gaining both insight into the fundamental nature of ship capsizing and gathering statistics upon which to base stability criteria. As a secondary objective it was hoped to be able to develop analytical methods by means of which capsizing could be predicted and parametric studies could be performed. Some of these objectives have been fulfilled only to a limited extent. While the fundamental nature of capsizing of intact ships in heavy seas has been fairly well revealed, the ability to obtain reliable statistical estimates of the probability of capsizing of a specific ship is still lacking. As a specific example, it is clear now that neither long experimental runs nor long time-domain computer simulation provide a feasible means of amassing the statistical base needed for such predictions. On the other hand, it appears possible to simulate on a computer the short-term large amplitude motion of a ship in steep quartering or following seas. At the same time, other analytic techniques have been developed which make it possible to study certain nonlinear motions characteristic of capsizing situations. These techniques offer the possibility of associating ship capsizing with the occurrence of a relatively small family of wave patterns. The probabilistic nature of capsizing is then divorced from the mechanism of ship motion and is derivable solely from the statistics of the waves.

In Summary

1. Linear ship motion can only broadly outline areas of speed, heading, and ship characteristics which may lead to trouble.

2. Classical ship motion theories which are augmented by some nonlinear terms may reveal phenomena, not apparent in results of linear theory, which may lead to severe motion. The ability to predict capsizing is still not available through such theories but they are useful in parametric studies of ship characteristics in relation to stability.

3. The open water experiments mentioned above yield great insight into the mechanics of capsizing. The phenomenon is a "rare event" in the statistical sense however, and very extensive experimental programs would be required to adequately describe the probability of capsize of just one ship configuration.

4. An important side benefit of these experiments has been the development of methods of deducing the directional properties of wind generated waves from measurements made by a sparse gage array. These measurements show that good similarity exists between the wave conditions in the model test area and full scale storm waves at sea.

5. The knowledge gained in the experiments has led to the development of a time-domain numerical simulation of the large amplitude motion of a ship in following and quartering seas. Records of severe motions including capsizes have been computed by this technique, and the computed motions resemble, quite closely, the motions of the model under similar sea conditions. This technique appears tobe useful in defining the regions of wave properties which may cause capsizing.

6. The characteristics of wave groups encountered by the model have considerable influence on the tendency to capsize. The prediction of wave group occurrence has not received much attention in the literature yet it seems to play a fundamental role in the prediction of the probability of ship capsizing. It appears that the statistics of wave groups can be derived from the conventional representation of the random seaway and therefore, the study of wave groups is a fruitful subject for future work.

ACKNOWLEDGEMENTS

A large number of individuals and organizations have been instrumental in aiding this work by their direct participation or by contributing data, information or helpful suggestions. The list is quite long and it is hoped that none are overlooked. Project engineers and graduate students who were associated with the study in its earlier stages were M. R. Haddara, S. Kastner, and L. Pérez y Pérez. Their contributions have, in general, been documented in earlier reports and publications under the contract. The assistance of Mr. Ralph M. Payne and his staff of the University of California Engineering Shops has been invaluable in the fabrication of instruments and equipment. Similarly, Lyn Magel, Naval Architecture Department Principal Electronic Technician has been a vital member of the team throughout the entire project where so much reliance has been placed on electronic instrumentation.

Several agencies and individuals from outside the University of California assisted the work by contributing data, facilities and hardware. We would especially like to thank the following:

The Sea Land Company for making available the *SL-7* model and corresponding data.

The Richmond Yacht Club for permitting the use of the guest dock and small boat launching crane as a base of experiment operations.

Several individuals and laboratories made full scale wave data available for comparison with data measured here, including:

P. Kruseman of the Koninkljk Nederlands Meteorologisch Instituut;

John Garrett of the Pacific Region Marine Sciences Directorate, Water Management, Dept. of the Environment, Canada;

J. R. Wilson of the Marine Environmental Data Service, Marine Sciences Directorate, Dept. of the Environment, Canada;

W. Brown of the Jet Propulsion Laboratory, Pasadena, California;

F. H. Hsu of the Amoco Production Company;

Don B. Young of the Lockheed Shipbuilding and Construction Company;

B. Au of the Naval Research Laboratory, Washington, D.C.;

J. McFadden and Duncan Ross of the U.S. Dept. of Commerce, National Oceanic and Atmospheric Administration, Miami, Florida.

The project's computations were carried out using the facilities of the University of California Computer Center and the Lawrence Berkeley Laboratory Computer Center.

Finally, grateful acknowledgement is made of the great assistance rendered by several department secretaries in typing this and the other reports produced during the courses of the work. They are Helen Strauch, Doris Victory, Marylou Newby and Lydia Briedis.

The work was sponsored by the U. S. Coast Guard under Contract DOT-CG-849A.

REFERENCES

Blagoveshchensky, S. N.

Theory of Ship Motions, Translation ed. by L. Landweber, Dover, Vol. 1, 1962.

Capon, J.

"High-Resolution Frequency Wave Number Spectrum Analysis," *Proc. IEEE*, Vol. 57, No. 8, Aug. 1969.

Chou, S. J.; Magel, L. F.; Oakley, O. H.; Paulling, J. R.; Wood, P. D.

"Capsizing Experiments in San Francisco Bay -- Annual Report 1973," Dept. of Naval Architecture, Univ. of Calif., Berkeley, June, 1973.

Cramer, H.; Leadbetter, M. R.

Stationary and Related Stochastic Processes, John Wiley and Sons, Inc. 1967.

Davidan, I. N.; Kublanov, Y. M.; Lopatukhin, L. I.; Rozhkov, V. A.

"The Results of Experimental Studies on the Probabilistic Characteristics of Wind Waves," *International Symposium on the Dynamics of Marine Vehicles and Structures in Waves*, Paper 39.

Ewing, J. A.

"A Review of Recent Work on the Length of Groups of High Wave Heights." IMCO, December, 1972.

Ewing, J. A.

"Mean Length of Runs of High Waves," *Journal of Geophysical Research*, Vol. 78, No. 12, April, 1973.

Goda, Yoshimi

"Numerical Experiments on Wave Statistics with Spectral Simulation." Report of the Port and Harbour Research Institute, Vol. 9, No. 3, Sept. 1970.

Glauz, R. D.

"Adams Method of Integration of Differential Equations," Computing Services Report No. 13, Aerojet-General, Sacramento, Calif., May 12, 1960.

Grim, O.

"Rollschwingungen, Stabilitat und Sicherheit in Seegang," *Schiffstechnik*, Vol. 1, pp. 10-21, 1952.

Haddara, M. R.; Kastner, S.; Magel, L. F.; Paulling, J. R.; Pérez y Pérez, L.; Wood, P. D.

"Capsizing Experiments with a Model of a Fast Cargo Liner in San Francisco Bay," U.S. Coast Guard Project 723411, Naval Architecture Department, Univ. of Calif., Berkeley, Jan. 1972.

Hasselmann, K., et al.

"Measurements of Wind-Wave Growth and Swell Decay During the North Sea Wave Project (JONSWOP)," Report by the Deutsches Hydrographisches Institut, Hamburg, 1973.

Kastner, S.

"Analysis and Evaluation of Capsizing Experiments in San Francisco Bay 1971," Department of Naval Architecture, Univ. of Calif., Berkeley, Mar. 1973.

Kerwin, J. E.

"Notes on Rolling in Longitudinal Waves," *International Shipbuilding Progress*, Vol. 2, pp. 597-614, 1955.

Loukakis, T. A.

"Experimental and Theoretical Determination of Waveform and Ship Response Extremes," MIT Dept. of NA and ME Report No. 69-7, May 1970.

Nolte, K. G.; Hsu, F. H.

"Statistics of Ocean Wave Groups," Offshore Technology Conference Paper No. OTC 1688, 1972, also published in *Society of Petroleum Engineers Journal*, Vol. 13, No. 3, June 1973.

Nolte, K. G.; Hsu, F. H.

"The Statistical Distribution of the Larger Wave Heights of a Sea-State," to be published.

Oakley, Jr., O. H.

"Directional Wave Spectra Measurement and Analysis Systems," SNAME Panel H-7 Seakeeping Symposium, Webb Institute of Naval Architecture, Oct. 1973.

Ochi, K. M.

"Extreme Behavior of a Ship in Rough Seas," *Trans.* SNAME Vol. 72, pp. 143-202, 1964.

Paulling, J. R.

"The Transverse Stability of a Ship in a Longitudinal Seaway", *Journal of Ship Research*, Vol. 4, No. 4, pp. 37-49, March 1961.

Paulling, J. R.

"Stability and Ship Motions in a Seaway," USCG Office of Research and Development Project 713111, Dept. of Naval Architecture, Univ. of Calif., Berkeley, Sept. 1970.

Paulling, J. R.; Kastner, S.; Schaffran, S. D.

"Experimental Studies of Capsizing of Intact Ships in Heavy Seas", Technical Report. Dept. of Trans., U.S. Coast Guard, Contract DOT-CG-84, 549-A, Project 5940.1 .1/GDST-3411, Nov. 1972.

Paulling, J. R.; Rosenberg, R. M.

"On Unstable Ship Motion Resulting from Nonlinear Coupling", *Journal of Ship Research*, Vol. 3, No. 1, pp. 36-46, June 1959.

Pierson, W. J., Jr and L. Moskowitz

"A Proposed Spectral Form for Fully Developed Wind Seas Based on the Similarity Theory of S. A. Kitaigorskii," *Journal of Geophysical Research*, Vol. 69, 5181, 1964.

Salvesen, N.; Tuck, E. O.; Faltinsen, O.

"Ship Motions and Sea Loads", *Trans.*SNAME, Vol. 78, pp. 250-269, 1970.

St. Denis, M.

"On a Problem in the Theory of Nonlinear Oscillations of Ships", *Schiffstechnik*, Bd 14, H 70, pp. 11-14, 1967.

St. Denis, M.

"Some Cautions on the Employment of the Spectral Technique to Describe the Waves of the Sea and the Response Thereto of Oceanic Systems", OTC 1819, Offshore Technology Conference, Houston, pp. 827-840, 1973.

Thompson, W. C.; Smith, R. C.

"Wave Groups in Ocean Swell", *Proceedings of the International Symposium on Ocean Wave Measurement and Alalysis*, ASCE, New Orleans, Vol. 1, pp. 338-351, Sept. 1974.

Vanmarcke, E. H.

"Properties of Spectral Moments with Application to Random Vibration", ASCE National Structural Engineering Meeting Baltimore, Maryland, April, 1971.

Vassilopoulos, L.

"Ship Rolling at Zero Speed in Random Beam Seas with Nonlinear Damping and Restoration", *Journal of Ship Research*, Vol. 15, No. 4, pp. 289-294, Dec. 1971.

Vugts, J. H.

"Cylinder Motions in Beam Waves", Netherlands Ship Research Centre TNO Shipbuilding Dept., Leeghwaterstraat 5, Delft Report No. 115 S, Dec. 68, pp. 25.

REPORTS AND PUBLICATIONS ISSUED UNDER THIS PROJECT

Chou, S. J.; Magel, L.F. ; Oakley, O. H.; Paulling, J. R. and Wood, P. D.

"Capsizing Experiments in San Francisco Bay." Dept. of Naval Architecture, University of Calif., Berkeley, June 1973. (Dept. of Transportation -U.S.C.G. Report No. CG-D-18-73)

Haddara, M. R.

"On Nonlinear Rolling of Ships in Random Seas." Dept. of Naval Architecture, University of Calif., Berkeley, May 1971. (Dept. of Transportation -U.S.C.G. Project. No. 713111)

Haddara, M. R.

"On Nonlinear Rolling of Ships in Random Seas." *International Shipbuilding Progress.* Vol. 20, No. 230, October 1973, pp. 377-387

Haddara, M. R.

"On The Stability of Ship Motion in Regular Oblique Waves." *International Shipbuilding Progress.* Vol. 18, No. 207, November 1971, pp. 416-434

Haddara, M. R.; Kastner, S.; Magel, L. F.; Paulling, J. R.; Pérez y Pérez, L.; and Wood, P. D.

"Capsizing Experiments with a Model of a Fast Cargo Liner in San Francisco Bay." Dept. of Naval Architecture, University of Calif., Berkeley. January 1972. (Dept. of Transp. U.S.C.G. Project No. 723411)

Oakley, O. H., Jr.

"Directional Wave Spectra Measurement and Analysis Systems," SNAME T&R Symposium S-3, Seakeeping 1953-1973. Webb Inst. of Naval Architecture, Glen Cove, N. Y., Oct. 1973.

Oakley, O. H., Jr.; Paulling, J. R.; and Wood, P. D.

"Ship Motions and Capsizing in Astern Seas." *Tenth Symposium on Naval Hydrodynamics*, Massachusetts Inst. of Tech., Cambridge, Mass., June 24-28, 1974

Paulling, J. R.

"Stability and Ship Motion in a Seaway." Dept. of Naval Architecture, University of California, Berkeley, September 1970. (Dept. of Transportation - U.S.C.G.- Project 713111)

Paulling, J. R.; Kastner, S.; and Schaffran, S. D.

"Experimental Studies of Capsizing of Intact Ships in Heavy Seas." Dept. of Naval Architecture, University of Calif., November 1972. (Dept. of Transportation - U.S.C.G. Project 5940.1.1/GDST-3411)

Paulling, J. R.; and Wood, P. D.

"Numerical Simulation of Large-Amplitude Ship Motions in Astern Seas." SNAME T&R Symposium S-3, Seakeeping 1953-1973, Webb Inst. of Naval Architecture, Glen Cove, N. Y., October 1973.

Pérez y Pérez, L.

"A Time Domain Solution to the Motions of a Steered Ship in Waves," Dept. of Naval Architecture, Univ. of California, Berkeley, November 1972. (Dept. of Transportation - U.S.C.G Report No. CG-D-19-73)

Pérez y Pérez, L.

"A Time-Domain Solution to the Motions of a Steered Ship in Waves," *Journal of Ship Research*, Vol. 18, No. 1, March 1974, pp. 32-45

APPENDIX A

SHIP AND MODEL CHARACTERISTICS

EXPERIMENTAL CALIBRATIONS

WAVE ARRAY DIMENSIONS

TABLE A-I

CHARACTERISTICS OF MODELS IN TEST CONDITIONS

MODEL	CHALLENGER		SEALAND-7	
CONDITION	LIGHT	HEAVY	LIGHT	HEAVY
Length Over All, LOA			17.12 ft	17.12 ft
Length Between Perpendiculars, LBP	17.52 ft	17.52 ft	16.36 ft *	16.36 ft
Breadth, B	29.81 in.	29.81 in.	23.125 in. **	23.125 in.
Depth, D	14.84 in.	14.84 in.	13.375 in. ***	13.375 in.
Draft at Amidship, T	7.95 in.	11.83 in.	7.00 in.	8.49 in.
Draft at Forward Perpendicular	7.48 in.	10.34 in.	7.00 in.	8.49 in.
Draft at After Perpendicular	8.42 in.	13.32 in.	7.00 in.	8.49 in.
Freeboard, F	10.53 in.	6.66 in.	6.375 in.	4.885 in.
LBP/B	7.05	7.05	8.53	8.53
T/D	0.430	0.640	0.523	0.635
T/B	0.267	0.397	0.303	0.367
F/D	0.570	0.360	0.477	0.365
F/B	0.353	0.233	0.276	0.211
Displacement	984 lb	1600 lb	630 lb	814 lb
Midship Section Coefficient	0.976	0.984	0.935	0.946
			0.944 @ sta 11	0.954 @ sta 11
Block Coefficient	0.533	0.571	0.533	0.561
Prismatic Coefficient	0.546	0.580	0.570	0.593
Waterplane Coefficient	0.625	0.689	0.668	0.718
$\delta \overline{GM}$	0.120 in.	0.120 in.	0.113 in.	0.0905
Number of Steps	7 (0-7)	7 (0-7)	6 (1-7)	6 (1-7)
GM Position No. 2 Salt Water	0.214 in.	0.102 in.	0.102 in.	0.090 in.
GM Position No. 4 Salt Water	0.454 in.	0.342 in.	0.328 in.	0.271 in.
GM Position No. 6 Salt Water	0.694 in.	0.582 in.	0.554 in.	0.453 in.
KM Salt Water	12.203	12.460 in.	9.827 in.	9.796 in.
Speed Setting No. 1	3.97 fps (.169 Fn)	3.96 fps (.169 Fn)	4.65 fps (.203 Fn)	4.53 fps (.197 Fn)
Speed Setting No. 2	5.83 fps (.249 Fn)	5.04 fps (.215 Fn)	6.00 fps (.261 Fn)	6.10 fps (.266 Fn)
Speed Setting No. 3	7.10 fps (.303 Fn)	6.13 fps (.261 Fn)	7.45 fps (.325 Fn)	7.58 fps (.330 Fn)

The coefficients presented above were calculated with a hydrostatics program using trapezoidal rule and therefore differ slightly from the actual.

* This length is equivalent to a full scale ship length of 900 feet, taken from J.J. Henry Co. drawing. no. 5576-1B, for 20 stations. It is not the length between the forward perpendicular and the center line of the rudder stock (roughly 880 feet).

** The beam at ⊠ on main deck is approximately 0.1 inch greater than it should be due to an error in construction.

*** This depth is equivalent to a full scale ship depth of 61.25 feet.

AMERICAN CHALLENGER

BODY PLAN

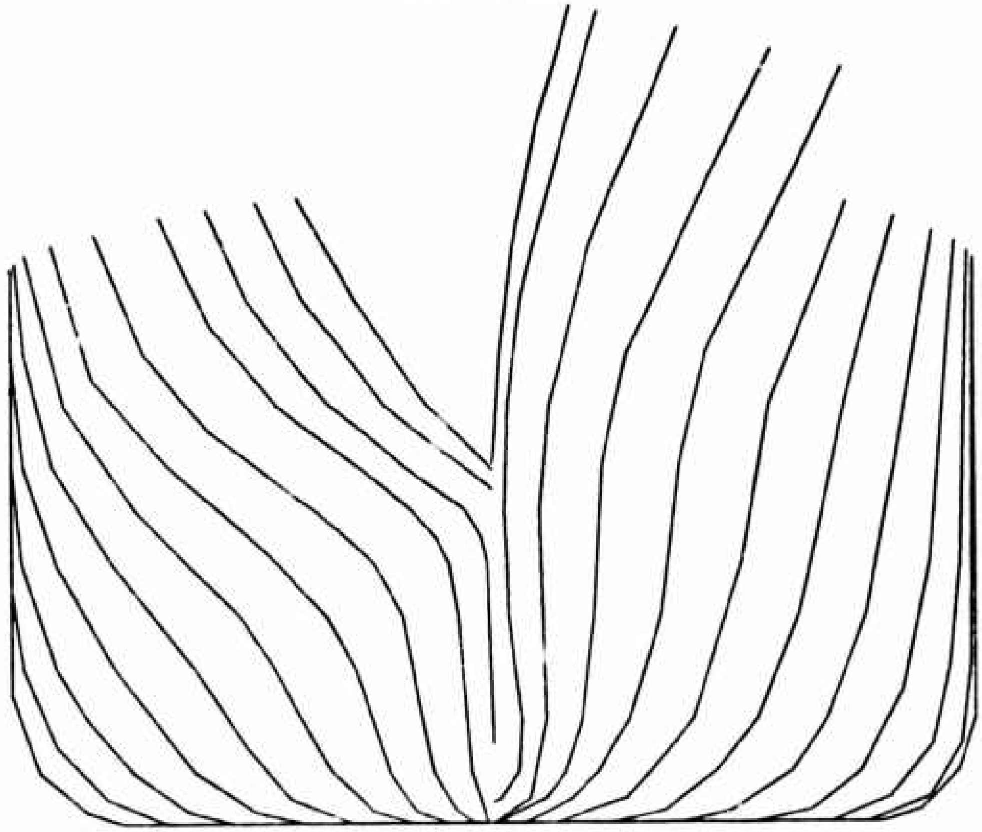

PRINCIPAL CHARACTERISTICS (Ship Scale)

L.B.P.	529'-0"
BEAM, molded	75'-0"
DEPTH, molded	46'-6" *
DESIGN DRAFT	27'-6"
DISPLACEMENT, molded	17716 L.T
BLOCK COEFFICIENT	.5775
PRISMATIC COEFFICIENT	.5863
MIDSHIP SECTION COEFFICIENT	.9849
WATERPLANE COEFFICIENT	.6983

* This depth is measured from the baseline to the top of the bulwark.

Figure A-1

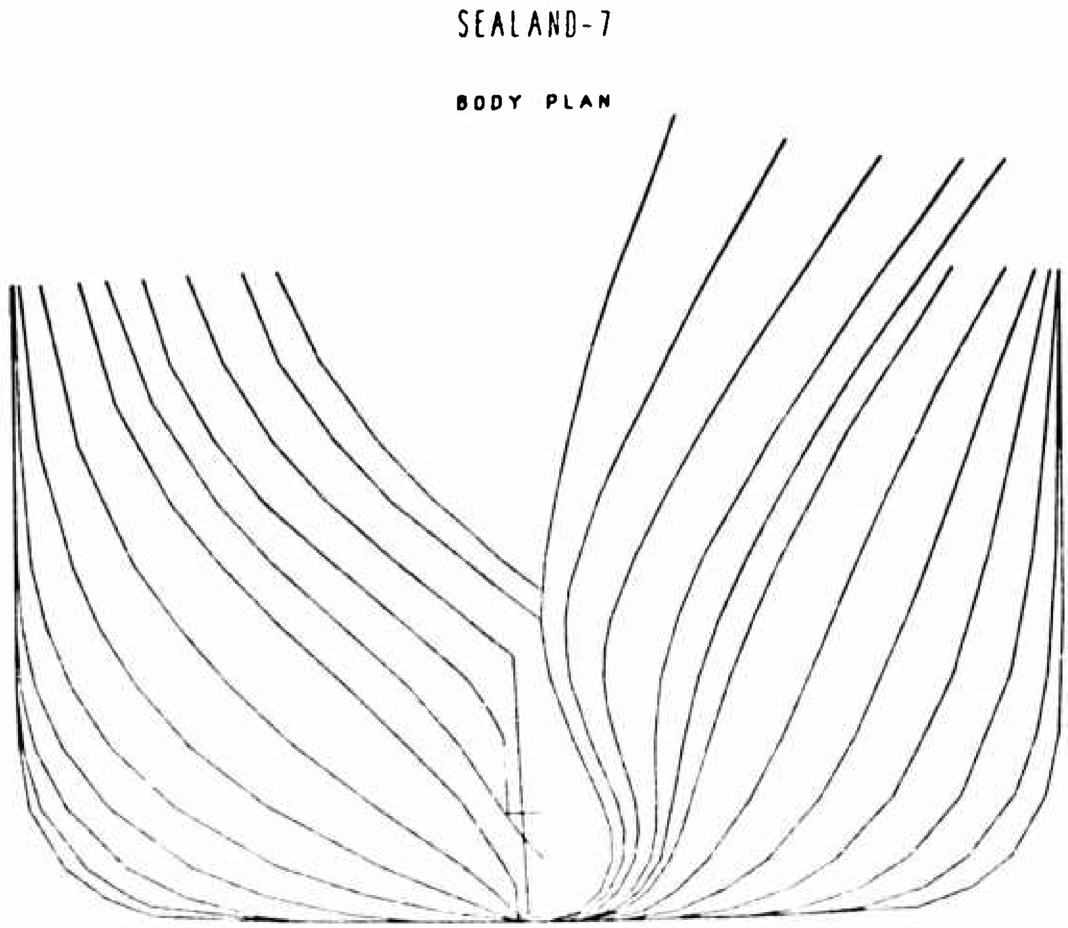

PRINCIPLE CHARACTERISTICS
(full scale)

L.B.P.	900'-0"
BEAM, molded	105'-5"
DEPTH, molded	64'-0"
DESIGN DRAFT	32'-0"
DISPLACEMENT, molded	46,740 LT
BLOCK COEFFICIENT	.538
PRISMATIC COEFFICIENT	.568
MIDSHIP SECTION COEFFICIENT	.947

* From preliminary design done by J. J. Henry - Drawing No. 5576 1B

Figure A-2

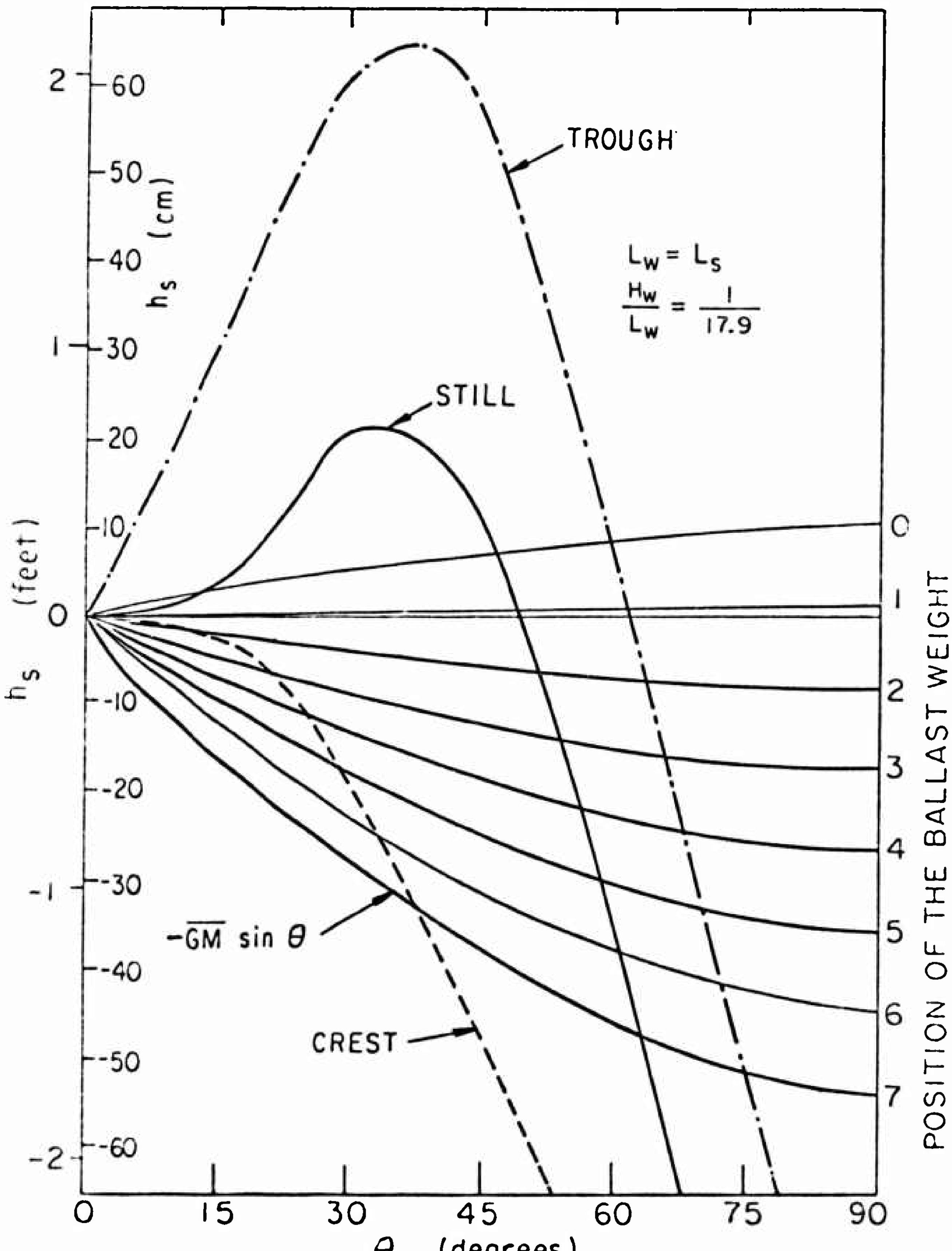

Figure A-3 Righting Arm Curves for the *Challenger* in the Heavy Condition

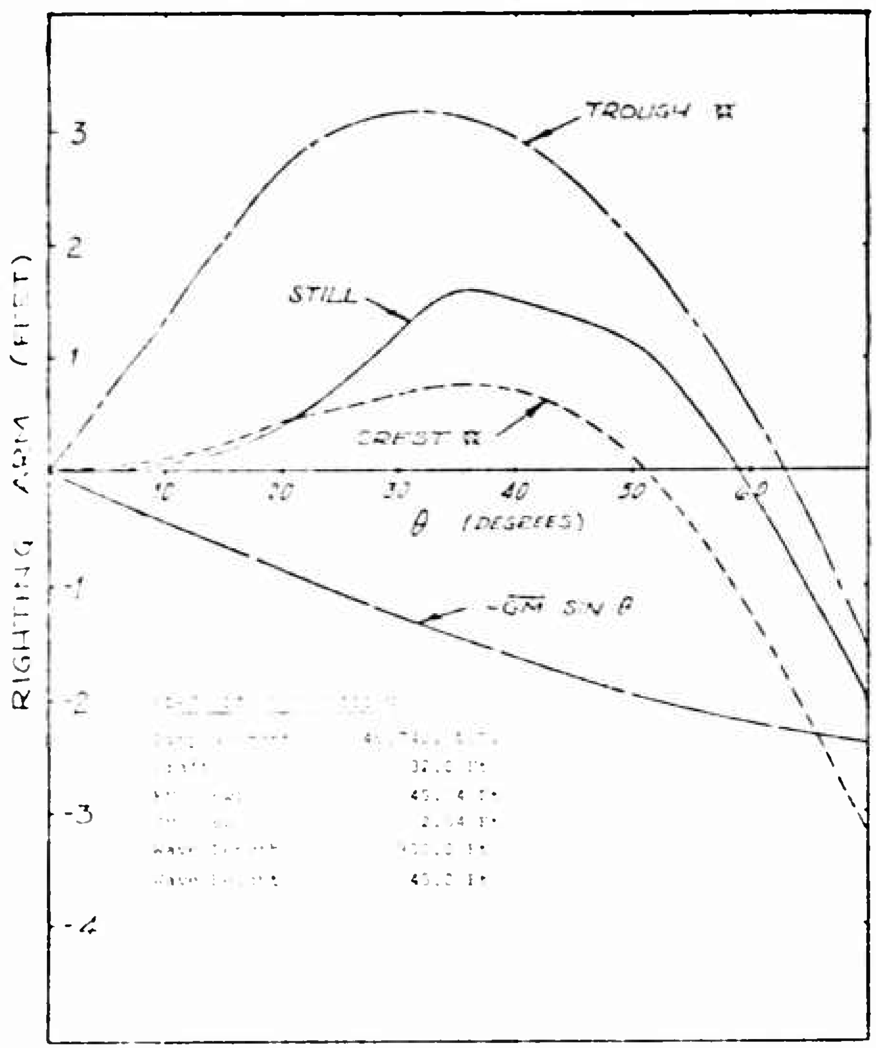

Figure A-4.1

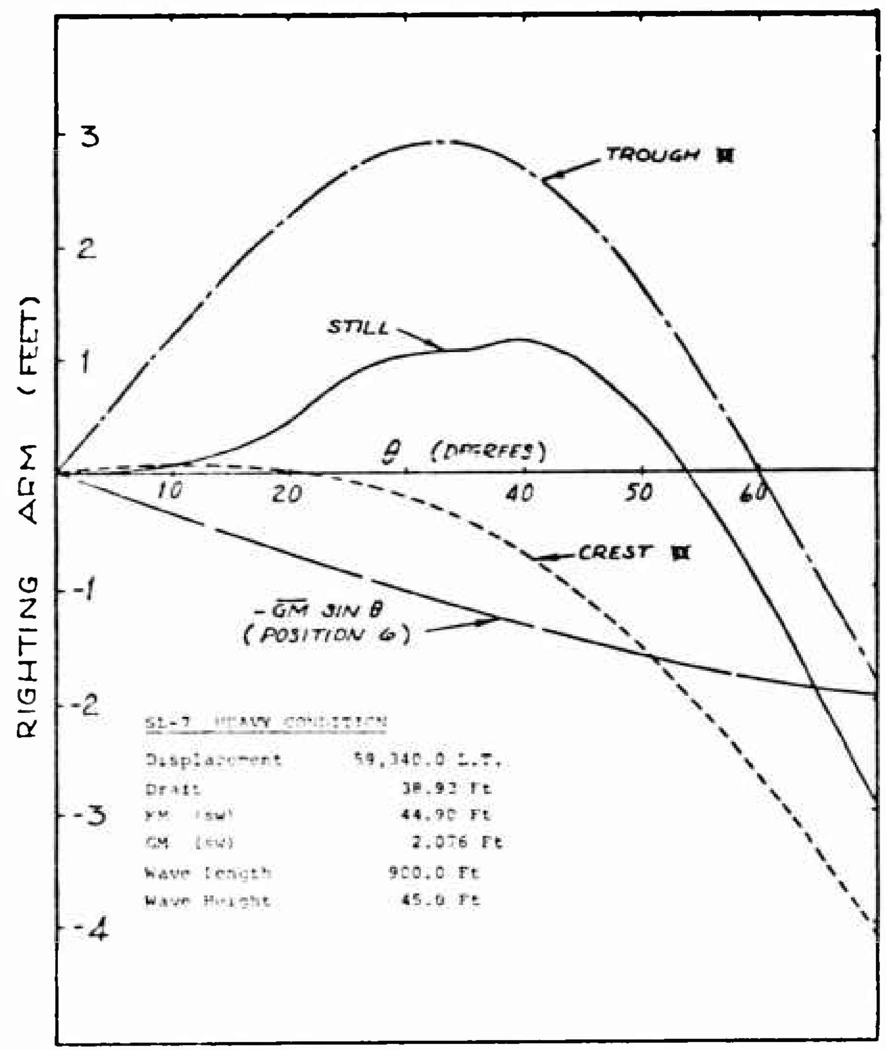

Figure A-4.2

Righting Arm Curves for the *Sealand-7*
(full scale).

TABLE A-2

SL-7 CALIBRATION FACTORS FOR 1973

ROLL	± 83.750 degrees	/	± 1.35 volts
YAW	± 66.466 degrees	/	± 1.35 volts
PITCH	± 22.620 degrees	/	± 1.35 volts
RUDDER	± 47.750 degrees	/	± 1.35 volts
SWAY	± 20.285 ft/sec^2	/	± 1.35 volts
SURGE	± 7.333 ft/sec^2	/	± 1.35 volts
HEAVE	± 19.731 ft/sec^2	/	± 1.35 volts
RPM	± 1088.71 RPM	/	± 1.35 volts
SPEED	± 8.6 ft/sec	@	1.35 volts
	± 2.2 ft/sec	@	0.00 volts

TABLE A-3

1973 WAVE PROBE ARRAY GEOMETRY

PROBE NO.	DISTANCE (ft)	BEARING (compass deg.)
1	0.0	0.0
2	9.208	0.0
3	9.292	60.0
4	5.125	25.8

APPENDIX B

Roll Damping

The coefficients and wave exciting forces necessary for linear ship motion predictions may be computed using potential flow theory for an ideal inviscid fluid. Values, thus obtained, have been found to be reasonably accurate when compared to experimental results, except the roll damping term, for which the viscous contribution is considerable. Roll damping affects the motion response only in a very narrow range bracketing roll resonance. An acceptable value for the roll damping coefficient, $q_{\phi\phi}$, may therefore be determined from experiments in which the model is allowed to roll at its natural frequency. The theory and procedure for evaluating $q_{\phi\phi}$ from roll extinction experiments, summarized briefly below, are given in (Vugts, 1968).

Vugts' analysis deals with the motions of a cylinder and will be assumed applicable to a hull form. The equation of motion in roll about the center of gravity for no wave excitation and no induced sway is

$$P_{\phi\phi}\ddot{\phi} + q_{\phi\phi}\dot{\phi} + r_{\phi\phi}\phi = 0 \tag{B-1}$$

where $r_{\phi\phi}$ is the hydrostatic restoring moment and $P_{\phi\phi}$ is a term including the effects of the transverse moment of inertia and the roll added mass about the center of gravity. $r_{\phi\phi}$ is easily calculated by:

$$r_{\phi\phi} = \rho g \, \nabla \, \overline{GM} \tag{B-2}$$

and $P_{\phi\phi}$ may be approximated from the natural period of rolling from the following equation,

$$T_{\phi} = \frac{4\pi P_{\phi\phi}}{\sqrt{4P_{\phi\phi}r_{\phi\phi} - q_{\phi\phi}^{2}}} \tag{B-3}$$

with the assumption that the motion is lightly damped or that term $4p_{\phi\phi}\,r_{\phi\phi}$ is much larger than $q_{\phi\phi}$. This gives

$$p_{\phi\phi} = \frac{r_{\phi\phi}T_{\phi}^{2}}{4\pi^{2}}\,. \tag{B-4}$$

The roll damping term is determined from the measured decrease in the oscillations or the logarithmic decrement,

$$\delta = \ln\phi_A - \ln\phi_B = -\frac{q_{\phi\phi}T_{\phi}}{2p_{\phi\phi}} \tag{B-5}$$

where ϕ_A, ϕ_B, and the relationship between δ and $q_{\phi\phi}$ are defined in Figure B-1, taken from Vugts (1968).

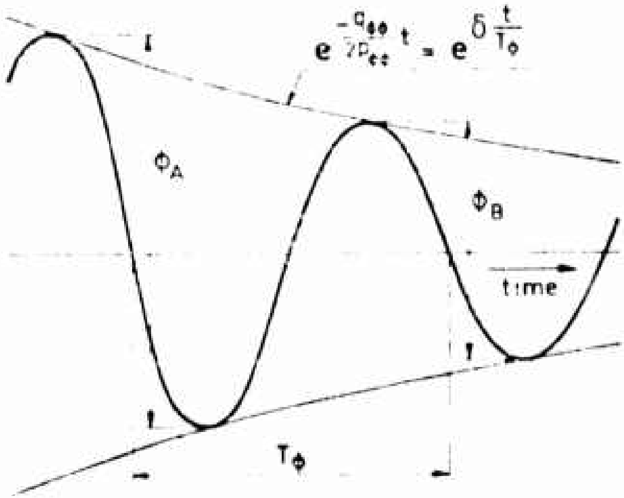

Figure B-1 Roll Decrement

Substituting equation (B-3) in (B-5) for the value of T_{ϕ} and solving for $q_{\phi\phi}$ results in

$$q_{\phi\phi} = \left[\frac{p_{\phi\phi}r_{\phi\phi}\delta^{2}}{\pi^{2}+{}^{1}/_{4}\,\delta^{2}}\right]^{1/2}. \tag{B-6}$$

A significant parameter which is often overlooked in determining the roll damping is forward speed. Blagoveshchensky proposes that as a rolling ship moves ahead it imparts more energy into the fluid and that the resulting increase in damping is linearly proportional with forward speed. The significance of the increase is readily noted from a comparison of the roll extinction curves at zero speed and at forward speed for the *SL-7* model in the same condition shown in Figures B-2 and B-3.

An increase in roll damping due to the forward speed is taken into account in the theory presented by Salvesen, Tuck, and Faltinsen (1970) in the calculations dealing with the blunt stern effect on the ship. To use this feature in SEAWAY for a ship like the *SL-7* which has a very small portion of its transom below the load waterline, it would be necessary to approximate the point along the hull where separation occurs and to remove the stations aft of this point from the calculations. The *SL-7* offsets for SEAWAY calculations were not modified for flow separation. Rather the measured increased damping due to forward speed was added to that which was determined from the integral of the two-dimensional damping coefficients along the hull.

Experiments were performed to determine the increase in roll damping at forward speed with the twofold purpose of ascertaining a better figure for linear theory computations and of determining a reasonable relationship between these two variables.

The same analysis was applied to the forward speed roll decay tests as for the still water, though with some reservation. Imparting an initial roll angle or impulsive roll moment to the free running model was somewhat difficult to do without also engendering some sway or yawing motion. This task was actually accomplished by following the model in the rubber boat and pushing one deck edge of the model down at about amidship by means of a fairly long pole. From an observation of this procedure, it was noted that any resulting yaw or sway motions were damped out very quickly so that any such motion could be considered negligible after only one half of one roll cycle.

Before commenting upon the results, one point should be clarified. It was desired to determine a value for B_{44} which

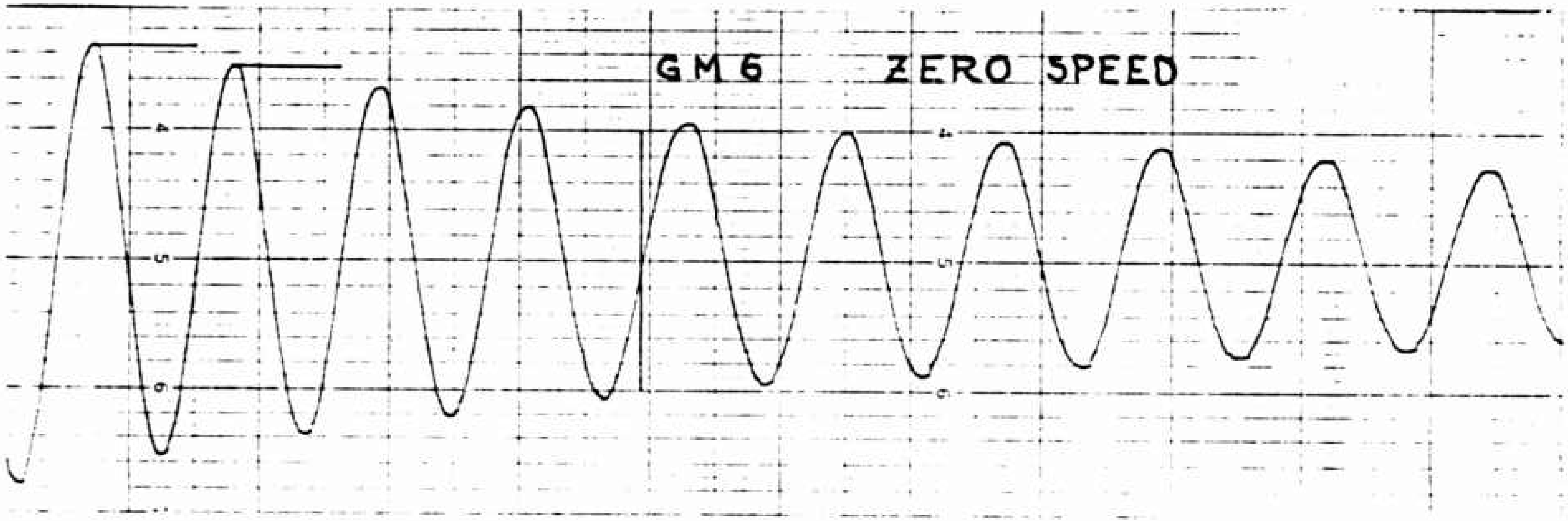

Figure B-2 Zero Speed Roll Decay for SL-7

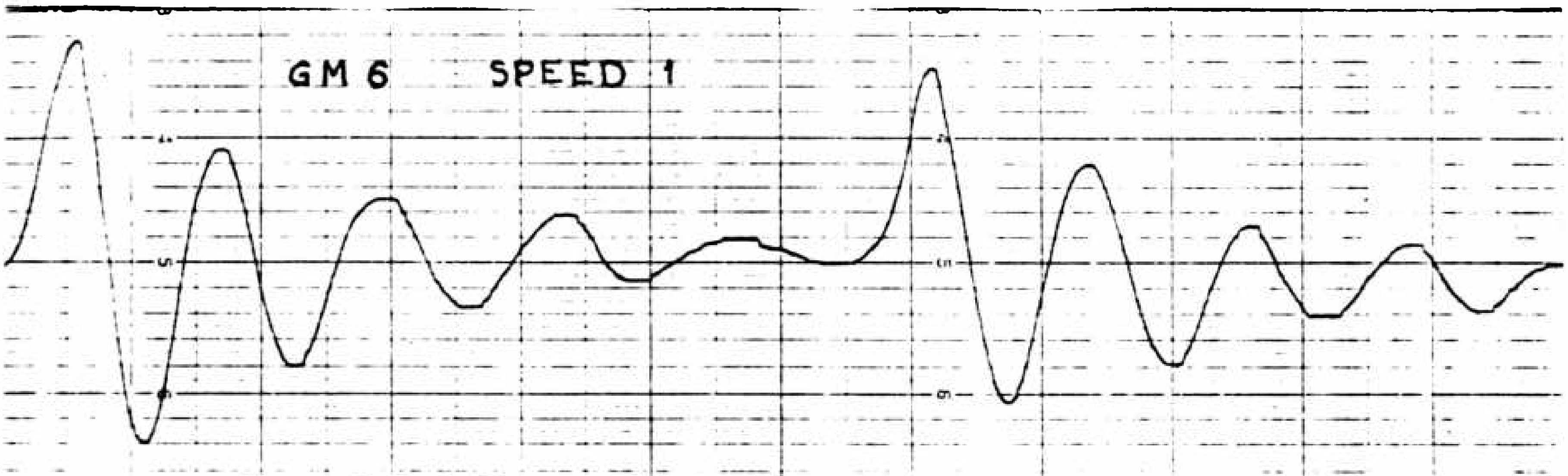

Figure B-3 Roll Decay for SL-7 at Forward Speed Setting No. 1

would give a good linear approximation of the model's motions in the extreme seaway (scaled) in San Francisco Bay. However, for large roll amplitudes the restoring moment is not linear and indeed the period between successive cycles is changing. Since the results were to be used as input for the linear ship motions program, SEAWAY, in order to be consistent, all calculations were made using a value of T_ϕ determined from zero speed roll extinction curves after the motion had diminished significantly and the period was fairly constant. Generally, the roll period for the initial roll cycles (roughly a 15 degree amplitude) was about 10% less than the natural period of roll.

Values of the roll double amplitude were plotted against the number of cycles. A constant ϕ_A, approximately equal to 30 degrees, was chosen and appropriate values of ϕ_B picked off the curves for an increment of one cycle. An example is given in Figure B-4.

Roll decay experiments were run at zero forward speed and at all three speed settings for the *SL-7* in the heavy condition and in the light condition with and without bilge keels. The results of these tests are listed in Table B-I and presented schematically in Figures B-5 and B-6.

A nondimensional coefficient, β is used to compare roll damping at different speeds for the different model test conditions. It was computed from the following relationship

$$\beta = \frac{q_{\phi\phi}}{2\sqrt{I_{xx_{air}} r_{\phi\phi}}} \tag{B-7}$$

$q_{\phi\phi}$ is the total roll damping including both viscous and hydrodynamic contributions, $r_{\phi\phi}$ is the roll restoring moment, and $I_{xx_{air}}$ is the moment of inertia of the model in air about a longitudinal axis through the center of gravity. For these computations $I_{xx_{air}}$ is the difference between the total moment of

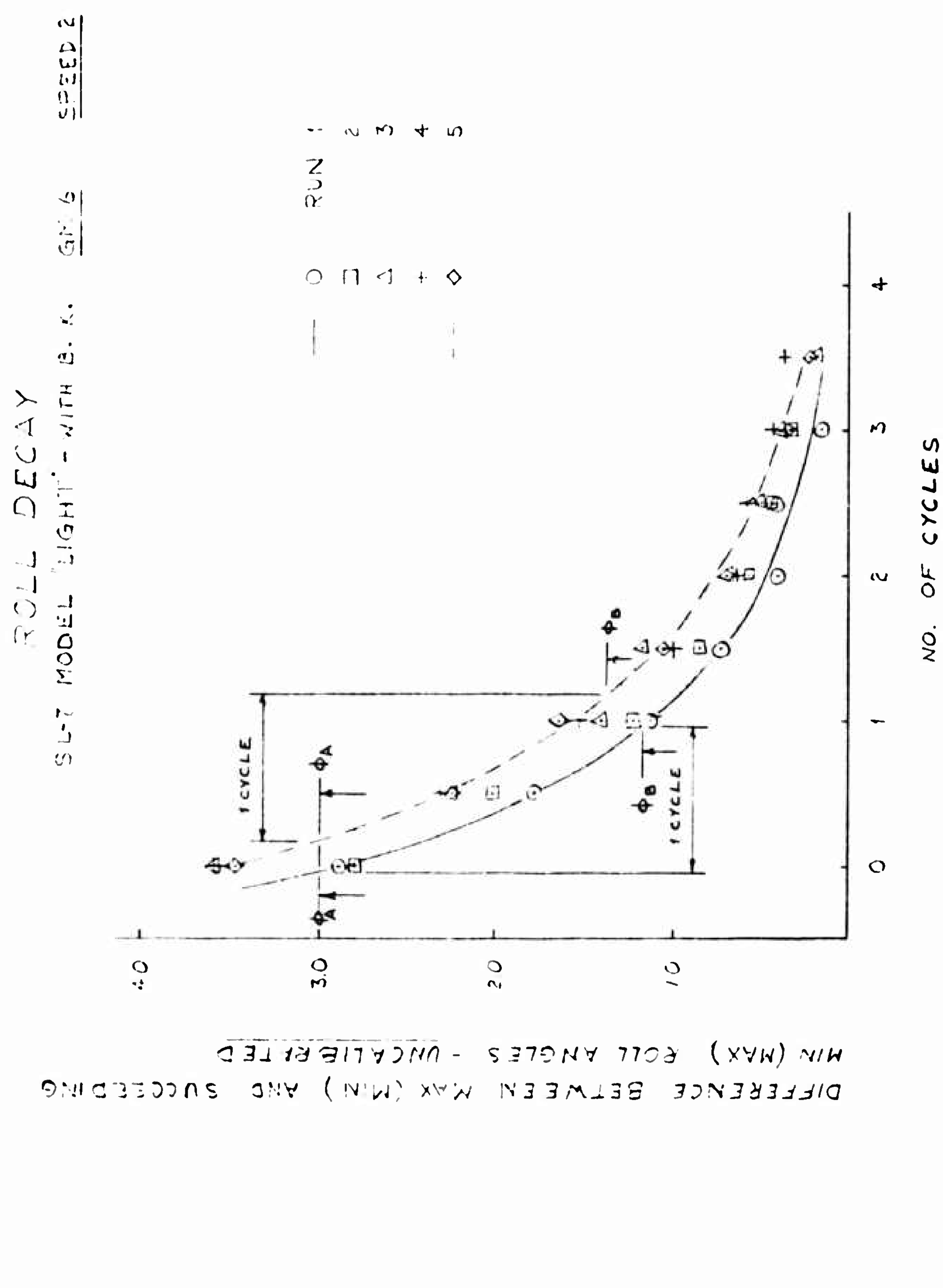
ROLL DECAY
SL-7 MODEL 'LIGHT' - WITH B. K.
SPEED 2
RUN 1
2
3
4
5
1 CYCLE
1 CYCLE
0
1
2
3
4
NO. OF CYCLES
4.0
3.0
2.0
1.0
DIFFERENCE BETWEEN MAX (MIN) AND SUCCEEDING
MIN (MAX) ROLL ANGLES - UNCALIBRATED

Figure B-4

TABLE B-I

ROLL DECAY TEST RESULTS

DATE	MODEL COND.	GM NO.	GM %B	T_ϕ sec.	q_{hyd}	ZERO SPEED			SPEED 1*			SPEED 2*			SPEED 3*		
						δ_{avg}	$q_{\phi\phi}$	β	δ_{avg}	$q_{\phi\phi}$	β	δ_{avg}	$q_{\phi\phi}$	β	δ_{avg}	$q_{\phi\phi}$	β
14 SEP 73	L	3	.93	5.83	.002	-.210	.700	.038									
		4	1.42	5.00	.004	-.193	.845	.034									
		6	2.40	3.97	.013	-.180	1.06	.032									
28 SEP 73	H	2	.39	7.84	.001	-.178	.432	.031									
		4	1.18	5.18	.004	-.188	.904	.032									
		6	1.96	4.20	.007	-.205	1.346	.035	-.727	4.74	.123	-.743	4.83	.126	-.632	4.125	.107
29 JUL 74	L	3	.93	5.83	.002				-.887	2.90	.155	-1.118	3.63	.195	-1.088	3.54	.189
		4	1.42	5.00	.004												
		6	2.40	3.97	.013				-.823	4.79	.143	-.819	4.77	.143	-.823	4.79	.143
02 AUG 74	L W/O B.K.	3	.93	5.27	.003	-.122	.369	.022	-.642	1.93	.116	-.761	2.28	.137	-.679	2.04	.123
		4	1.42	4.58	.007	-.148	.592	.026									
		6	2.40	3.62	.021	-.145	.775	.026	-.639	3.41	.113	NOT RECORDED			-.486	2.60	.086

* The actual speed will differ depending upon the condition of the model, light or heavy. See Table A-I .

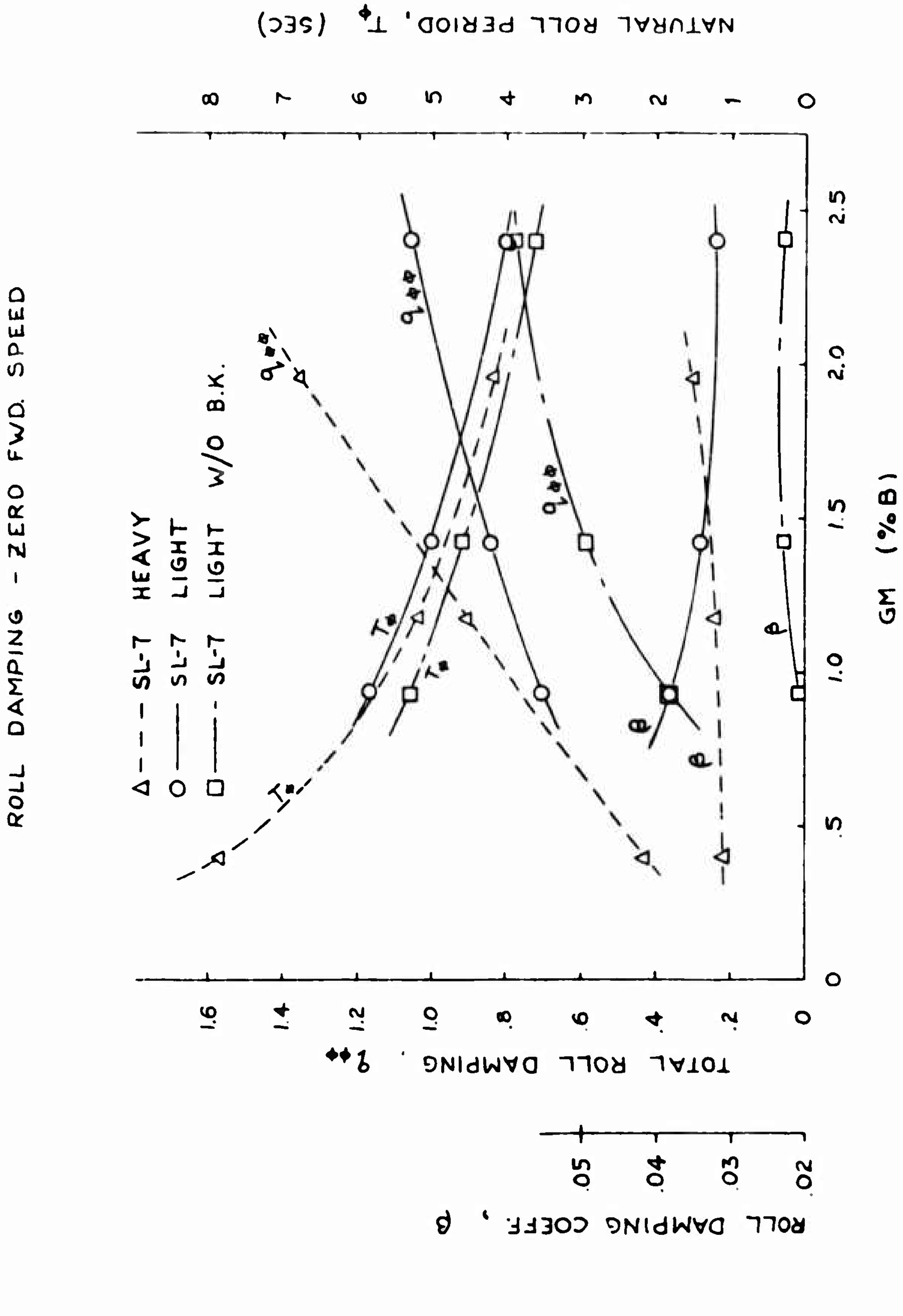

Figure IV-5 Roll Damping vs $\overline{GM}$

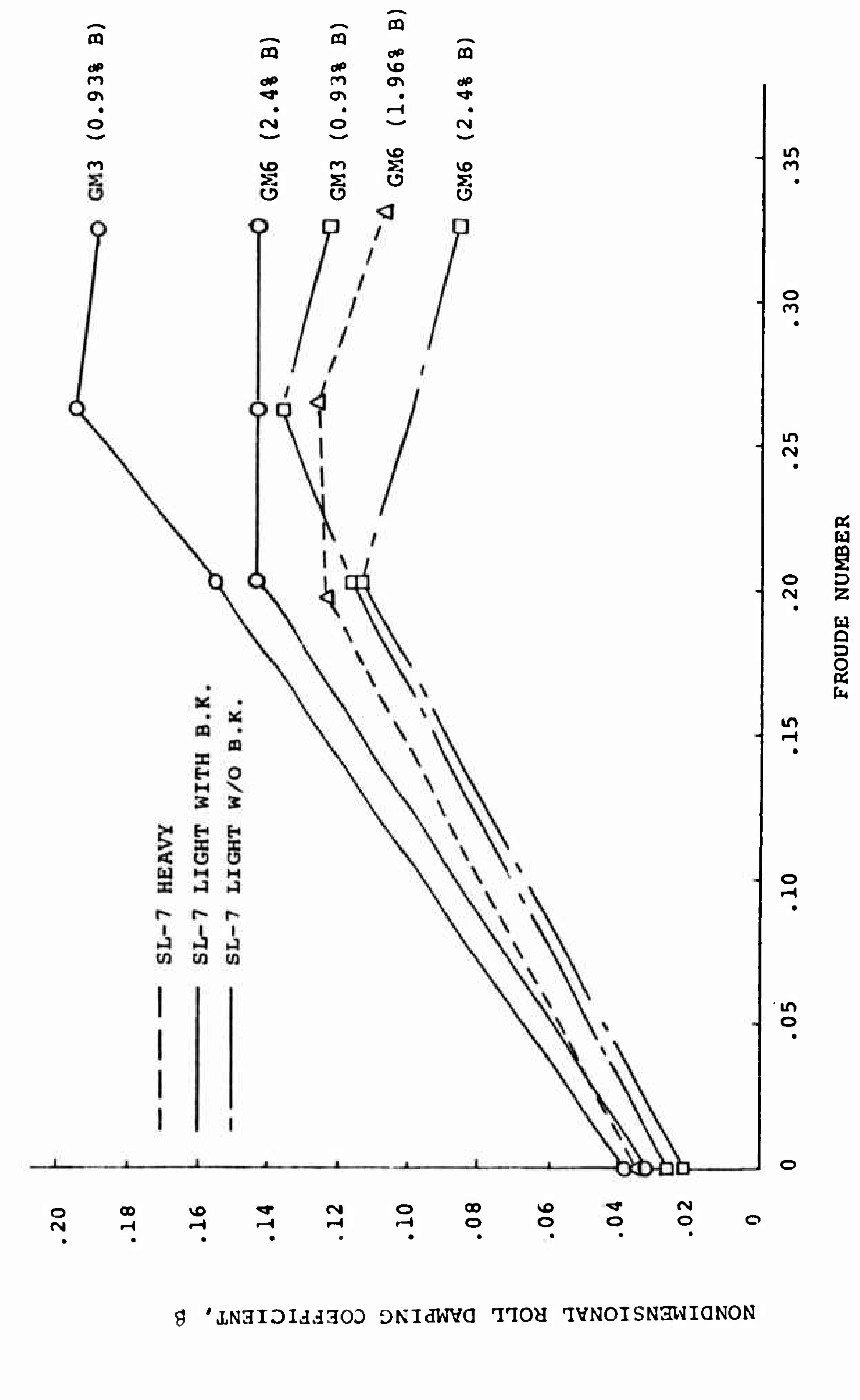

Figure IV-6 Roll Damping vs Forward Speed inertia computed with the GM and the roll period in salt water and the hydrodynamic added mass. Note that the values for the hydrodynamic damping given in Table B-I, are small compared to the total, $q_{;\phi}$. These were computed by the linear ship motions program "SEAWAY" with an offset deck which did not include the bilge keels and therefore are somewhat misrepresentative of the actual hydrodynamic damping. For the light condition without bilge keels, though B is a useful measure of the total viscous damping.

The increase in roll damping with forward speed is believed to be attributable to a transverse moment developed from sway-lift forces on the submerged portion of the hull. The sway involved here is not that of the center of gravity. Rather it is the horizontal motion of a point on the hull due to rolling and therefore porportional to the vertical distance from the center of roll. If the lift force of the bare hull is assumed to act at a vertical height equal to the center of buoyancy, and the effect of the rudder is included, the equation for the damping moment would appear as follows:

$$M_2 = \frac{1}{2} \rho v^2 \left[\theta_h A_h \left(\frac{C_L}{\alpha}\right)_h d_h + \theta_r A_r \left(\frac{C_L}{\alpha}\right)_r d_r \right] \qquad \text{(B-8)}$$

where

θ_h = hull angle of attack

A_h = one-half the submerged surface area of the hull and will be assumed to be equal to the length, L times the draft, T.

$\left(\frac{C_L}{\alpha}\right)_h$ = the coefficient of lift of the hull per unit angle of attack

d_h = the vertical distance from the center of buoyancy to the center of roll

θ_r = rudder angle of attack

A_r = the surface area of one side of the rudder

$\left(\frac{C_L}{\alpha}\right)_r$ = the coefficient of lift of the rudder per unit angle of attack

d_r = the vertical distance from the center of pressure of the rudder to the center of roll.

v = the forward velocity

ρ = the density of salt water

Since the angles of attack,

$$\theta_h = \frac{\dot{\phi} d_h}{v} \; ; \; \theta_r = \frac{\dot{\phi} d_r}{v}$$

$$M_2 = \frac{1}{2} \rho v \dot{\phi} \left[A_h \left(\frac{C_L}{\alpha}\right)_h d_h^2 + A_r \left(\frac{C_L}{\alpha}\right)_r d_r^2 \right] \qquad \text{(B-9)}$$

If the above expression is equated to a first order damping term which is linear in forward velocity,

$$M_2 = D_2 v \dot{\phi} \; ,$$

and

$$q_{\phi\phi} = (D_1 + D_2 v) \dot{\phi}$$

where D_1 is the zero speed linear damping coefficient, then,

$$D_2 = \frac{1}{2} \rho \left[A_h \left(\frac{C_L}{\alpha}\right)_h d_h^2 + A_r \left(\frac{C_L}{\alpha}\right)_r d_r^2 \right] \qquad \text{(B-10)}$$

Comparisons were made between the measured increase in damping with forward speed and that calculated using equation B-9. In general, the theoretical increase in damping approximated quite closely the average increase which was measured.

Generally, the experimental results show a great deal of scatter for relatively few points. Fortunately, some useful qualitative conclusions may be drawn. The curves of $q_{\phi\phi}$ for zero forward speed showed little correlation except in general magnitude between the light and heavy conditions. β values were fairly close and would appear to be a more reasonable measure for comparison between different ships or conditions. Removal of the bilge keels resulted in a general decrease in roll damping of about 25 to 30 percent. Damping was significantly greater at forward speed by a factor of 3 or 4. The large variations between points illustrated in Figure B-5 indicate the desirability for plotting the points with a series of straight lines rather than a faired curve. Due to the relatively good agreement between the calculated and measured increases in roll damping associated with forward velocity, it is reasonable to assume a linear relationship between roll damping and forward speed. These results are far from conclusive and clearly demonstrate the need for a series of experiments which better covers the range of important variables and from which a valuable confidence interval may be determined.

APPENDIX C

COMPARISON AND DETERMINATION OF AUTO PILOT PARAMETERS

The autopilot control for the *SL-7* model is a Proportional Differential (PD) control circuit with a dead band or "weather adjustment". A block diagram of the autopilot for the model is shown in Figure C-1.

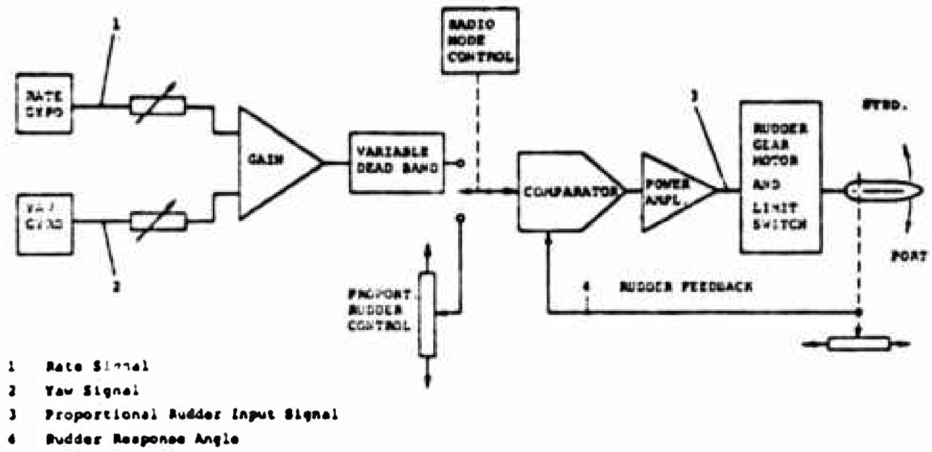

Figure C-1 Block Diagram Autopilot Model

The system is setup such that the rudder angle is proportional to the yaw and the yaw rate as in the following equations:

$$\delta = \delta_1 + \delta_2 = a_1\beta + a_2\dot{\beta} \qquad |\beta| \geq \beta_0$$

$$\delta = 0 \qquad |\beta| < \beta_0$$

where

δ = rudder angle

δ_1 = yaw proportional rudder response

δ_2 = yaw rate proportional rudder response

β = yaw angle

β_0 = dead band (weather adjustment)

a_1, a_2 are constant coefficients

The yaw angle is positive when the bow of the model turns to port; and the rudder angle is positive when the rudder turns to starboard.

The purpose of the dead band or "weather adjustment" is to stop excessive rudder motions, particularly in rough seas. It is generally recommended for ship autopilots that

$\beta_0 = 0$	in good weather
$\beta_0 > 0$	in rough seas, in order to prevent unnecessary or excessive rudder motion

The value of the coefficients a_1 and a_2 depend on the type of ship and the operating conditions. They are generally determined by experiment. Typical values for β_0, a_1 and a_2 are:

β_0	3/4° to 4°	
a_1	1 to 4	*deg / deg*
a_2	4 to 20	*deg • sec / deg*
$\frac{a_2}{a_1}$	4 to 5	*sec*

During the 1973-74 test season, yaw and rudder motions were recorded as functions of time. Based upon this data we wish to do two things:

1. Compare the static calibration constants with the coefficients (a_1, a_2) obtained from a linear equation, describing the experimental rudder motion as a function of the yaw and yaw rate.

2. Determine a more realistic equation representing the experimental rudder motion as a function of the yaw and it's derivatives.

The calibration of the autopilot was done in air and the complete description of the procedure is reported in Haddara (1971). A similar procedure was used for the 1972 and 1973 experiments.

The linear equation used to determine the response of the rudder as a function of yaw and yaw rate was:

$$\delta = a_1 \beta + a_2 \dot{\beta}$$

The yaw rate, $\dot{\beta}$, was determined by fitting a parabolic curve through every three points of the yaw vs time record and calculating the slope at each of these points. The method of Least Squares was used to calculate a_1 and a_2. Up to 200 points (δ_n, β_n, $\dot{\beta}_n$, n = 1,200) were used. Since most of the model runs had more than 200 samples, a number (200) of evenly spaced points (same time interval) were used. The results and the calibrated values are shown in Table C-I

TABLE C-I

AUTO PILOT COEFFICIENTS FOR A LINEAR RUDDER EQUATION

DATE	RECORD #	SPEED	$H_{1/3}$	HEAD-ING	a_1	a_2
SEPT 17	1	3	0.54	F	1.10	.66
	2	3	0.59	F	1.04	.61
	3	2	0.69	Q	1.34	.59
	4	2	0.75	F	1.15	.76
	5					
	6	2	0.82	Q	1.12	.31
	7	3	0.93	F	.95	-.03
	8	2	0.97	F	.98	.28
	9	1	1.02	F	1.16	.41
CALIBRATION					1.96	

The 17th of September was chosen for analysis because it is a very representative day and included many runs at different speeds.

The a_1 and a_2 obtained from the calibration were a good deal larger than the a_1 and a_2 obtained from the linear equation. Possible reasons for this would be:

1. The rudder motion lags the yaw by some time interval

2. The dead band was not accounted for in the equation. This could significantly alter the constants a_1 and a_2

3. If the rudder is hard over, the rudder angle is constant and no longer dependent on β or $\dot{\beta}$. If such were the case, then again, the accuracy of a_1 and a_2 would be limited.

Examination of experimental values of the rudder, yaw and yaw rate show that the value obtained for the a_1 and a_2 by the Least Squares method are consistent with the data. It appears that of the three reasons given for possible error in the coefficients, the third may be discarded, as this does not happen in the data to any great extent.

Another equation was tried incorporating a time lag, τ. Assuming that the response of the rudder lags the yaw, we assumed that

$$\delta = a_1 \beta(t-\tau) + a_2 \dot{\beta}(t-\tau)$$

$$t = \text{time}$$

$$\tau = \text{time lag}$$

Expanding the above equation in a Taylor's series we obtain

$$\delta = a_1 \left(\beta - \tau\dot{\beta} + \ddot{\beta}\frac{\tau^2}{2!} - \dddot{\beta}\frac{\tau^3}{3!} \ldots.\right) + a_2 \left(\dot{\beta} - \tau\ddot{\beta} + \dddot{\beta}\frac{\tau^2}{2!} \ldots.\right)$$

which can be approximated as:

$$\delta = a_1\beta + (a_2 - \tau a_1)\dot{\beta}_1 + \left(\frac{\tau^2}{2!} a_1 - \tau a_2\right)\ddot{\beta}$$

$$+ \left(\frac{\tau^2}{2!} a_2 - \frac{\tau a_1}{3!}\right)\dddot{\beta}$$

$\ddot{\beta}$ and $\dddot{\beta}$ were calculated by taking the derivative of the yaw rate ($\dot{\beta}$). The method of Least Squares was used to calculate the coefficients a_1, a_2, and τ. Again a maximum of 200 sets of points was allowed.

The results of this equation are shown in Table C-II.

TABLE C-II

AUTOPILOT COEFFICIENTS FOR A PARABOLIC RUDDER EQUATION

DATE	RECORD #	SPEED	$H_{1/3}$	HEAD-ING	a_1	a_2	τ
SEPT 17	1	3	0.54	F	1.10	.99	.32
	2	3	0.59	F	1.02	.90	.25
	3	2	0.69	Q	1.32	1.13	.32
	4	2	0.75	F	1.10	1.04	.28
	5						
	6	2	0.82	Q	1.12	.40	.07
	7	3	0.93	F	.94	.75	.70
	8	2	0.97	F	.97	.59	.29
	9	1	1.02	F	1.14	.80	.29

In going from the linear equation to the parabolic equation the a_1's remained essentially the same, while the a_2's changed in the neighborhood of 50%. It appears that the calculated time lag is smaller than that estimated from the model runs by up to factor of 3. The parabolic fit seems to indicate that τ is almost insignificant for this day. The increased a_2's are probably due, however, to the fact that τ is included.

It must be remembered that the dead band was not included in either of the fitted equations. But as pointed out, the computed values of a_1, a_2, and τ are reasonably consistent with the data.

APPENDIX D

SUMMARY OF MODEL RUNS AND SEASTATE INFORMATION FOR 1972

FIGURE D-1

SUMMARY OF MODEL RUNS AND SEASTATE INFORMATION

VS. TIME OF RECORDING - 1972

GM No.	See Table A-I for the American Challenger.
SPEED No.	See Table A-I for the American Challenger.
Seaway Records	Sequence of recordings including bad starts, etc.
— — —	Assumed Seaway Energy or Wave Amplitude
— — — —	90% Confidence Bound
1.02	Model Run Number Time and Duration of a Model Run
X	Model Run Ending in a Capsize

SUMMARY OF MODEL RUNS AND SEASTATE INFORMATION

VS. TIME OF RECORDING - 1972

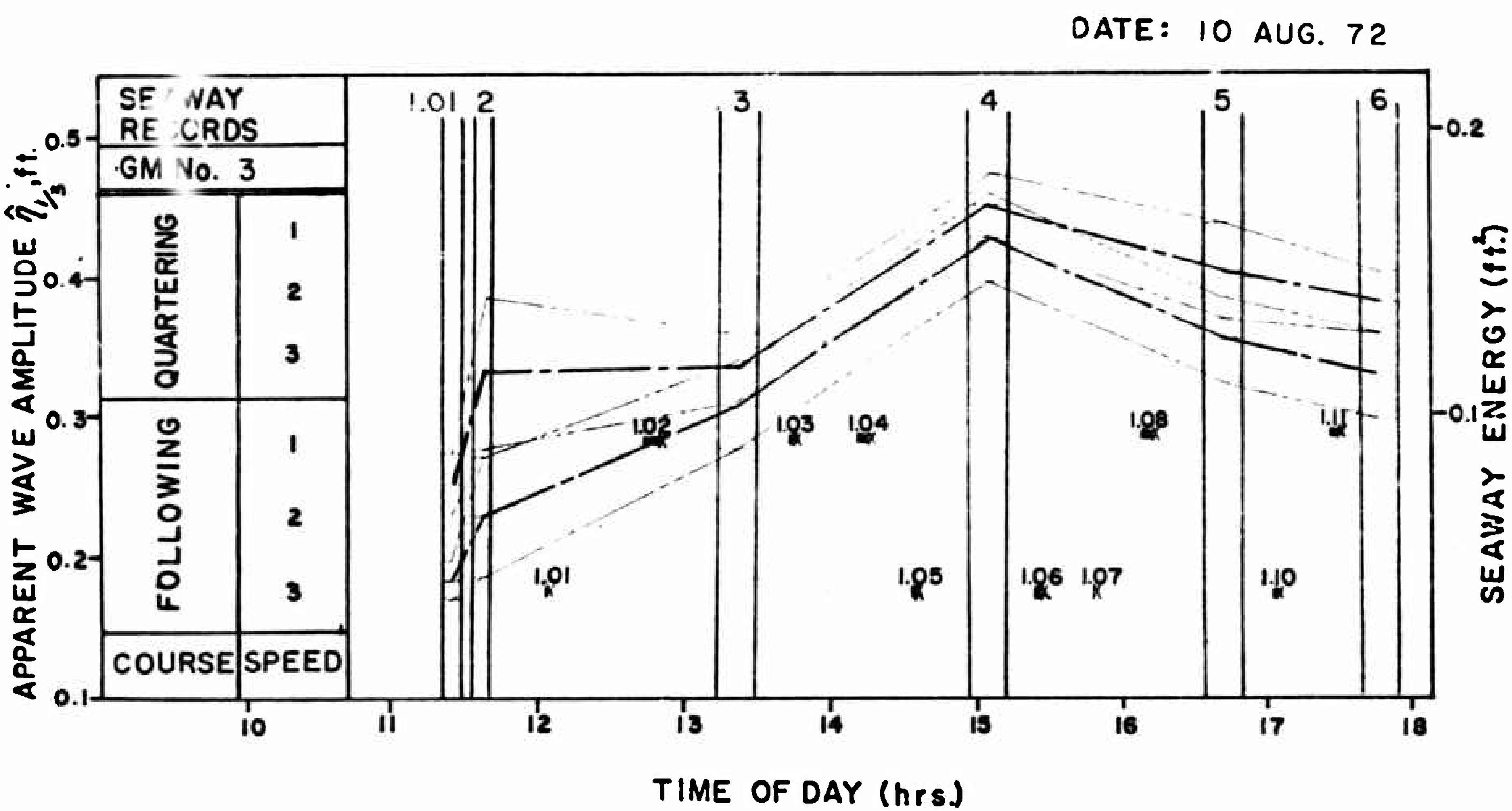

FIGURE D1.1

SUMMARY OF MODEL RUNS AND SEASTATE INFORMATION

VS. TIME OF RECORDING - 1972

DATE: 5 SEPT. 72

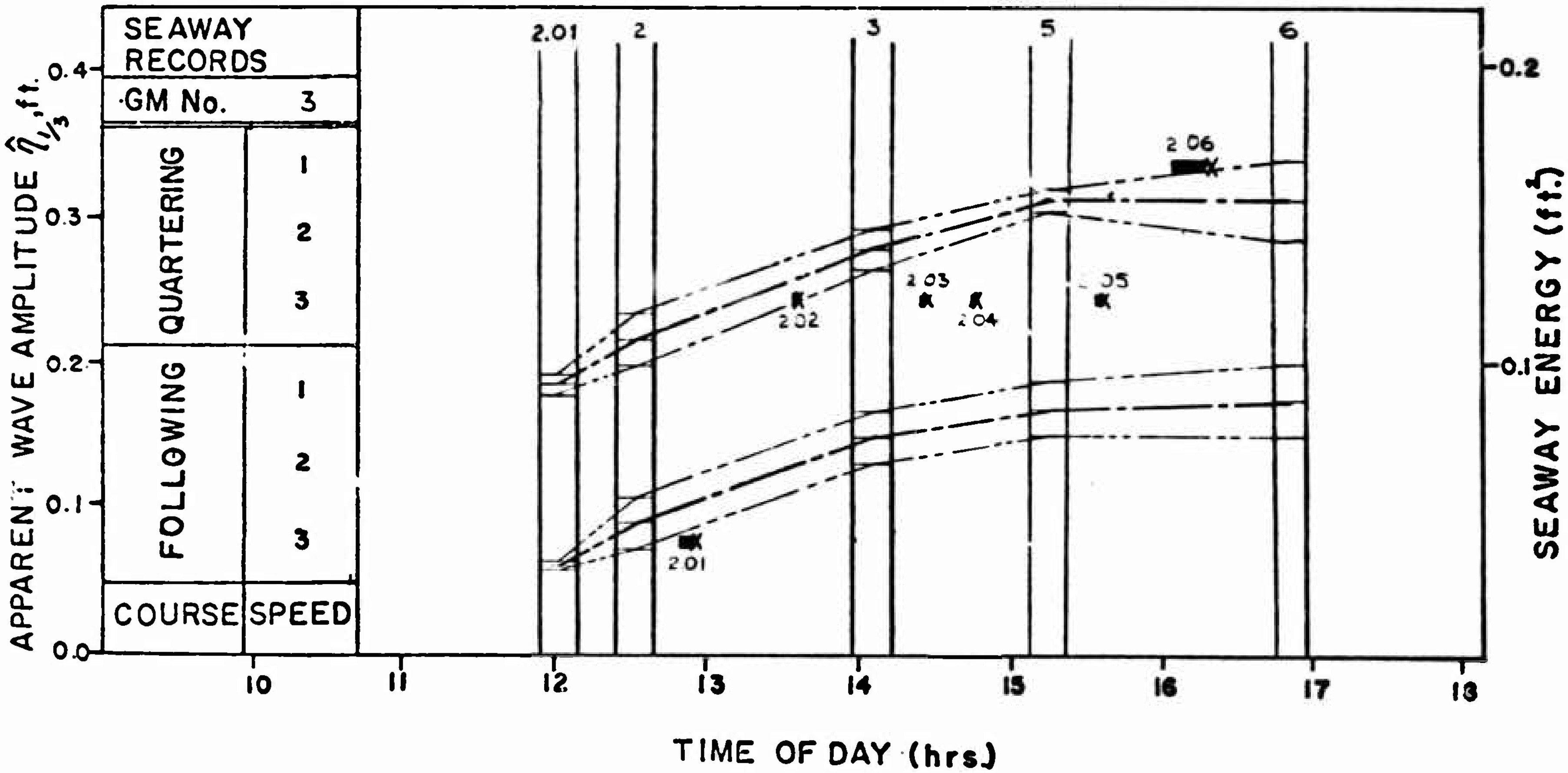

FIGURE D 1.2

VS. TIME OF RECORDING - 1972

DATE: 7 SEPT. 72

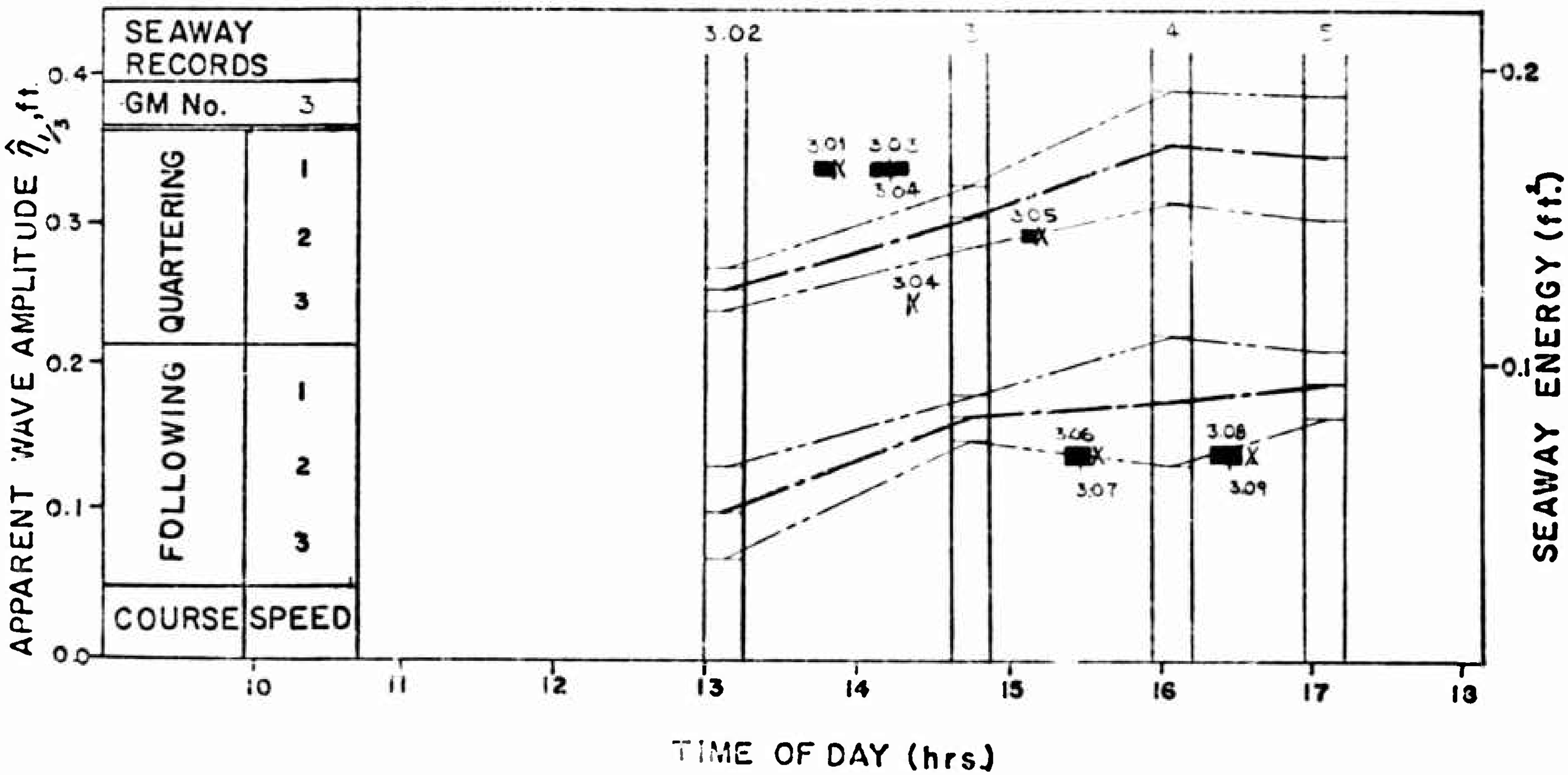

FIGURE D 1.3

SUMMARY OF MODEL RUNS AND SEASTATE INFORMATION

VS. TIME OF RECORDING - 1972

DATE: 11 SEPT. 72

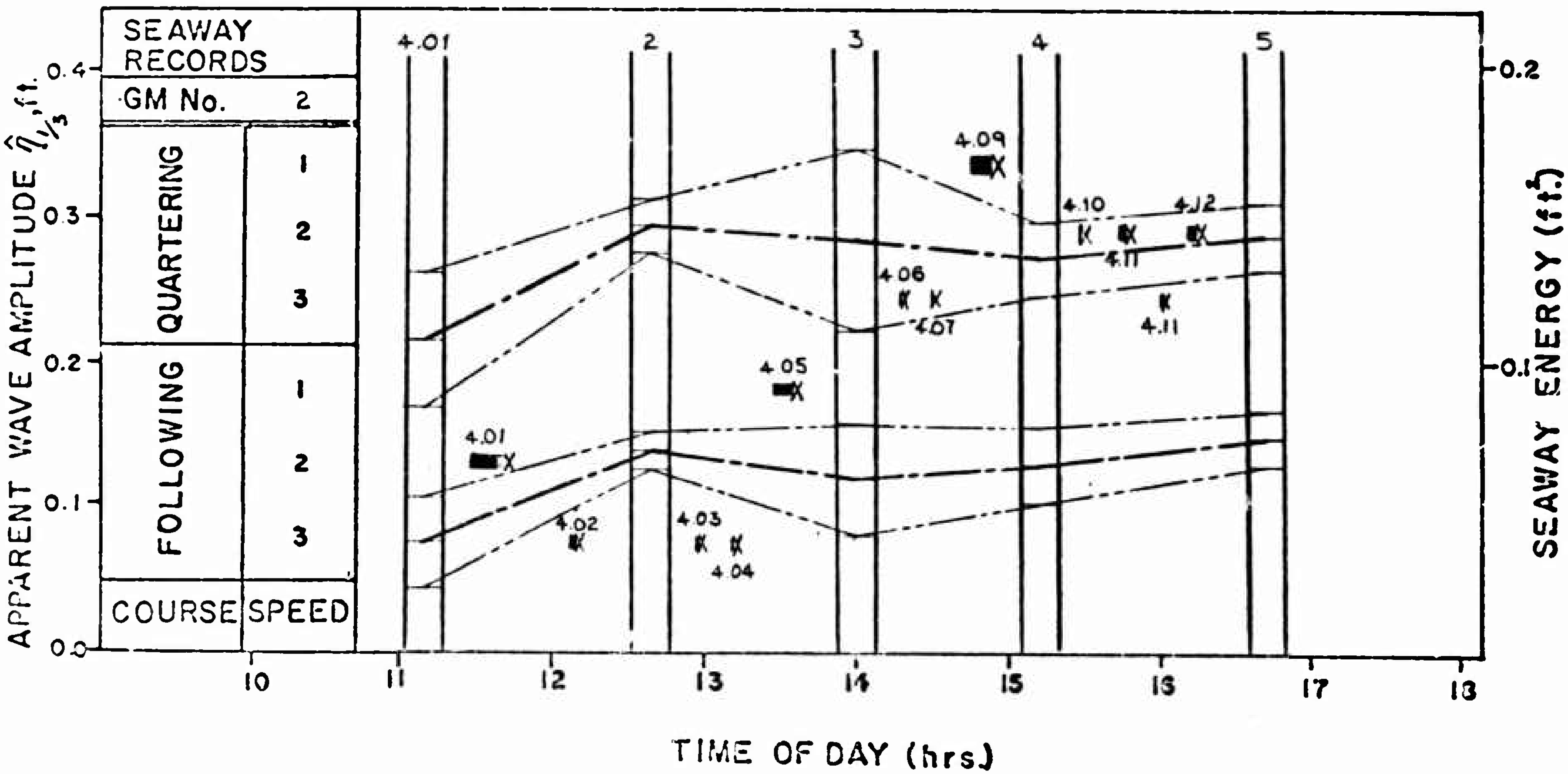

FIGURE D 1.4

SUMMARY OF MODEL RUNS AND SEASTATE INFORMATION

VS. TIME OF RECORIDNG - 1972

DATE: 13 SEPT. 72

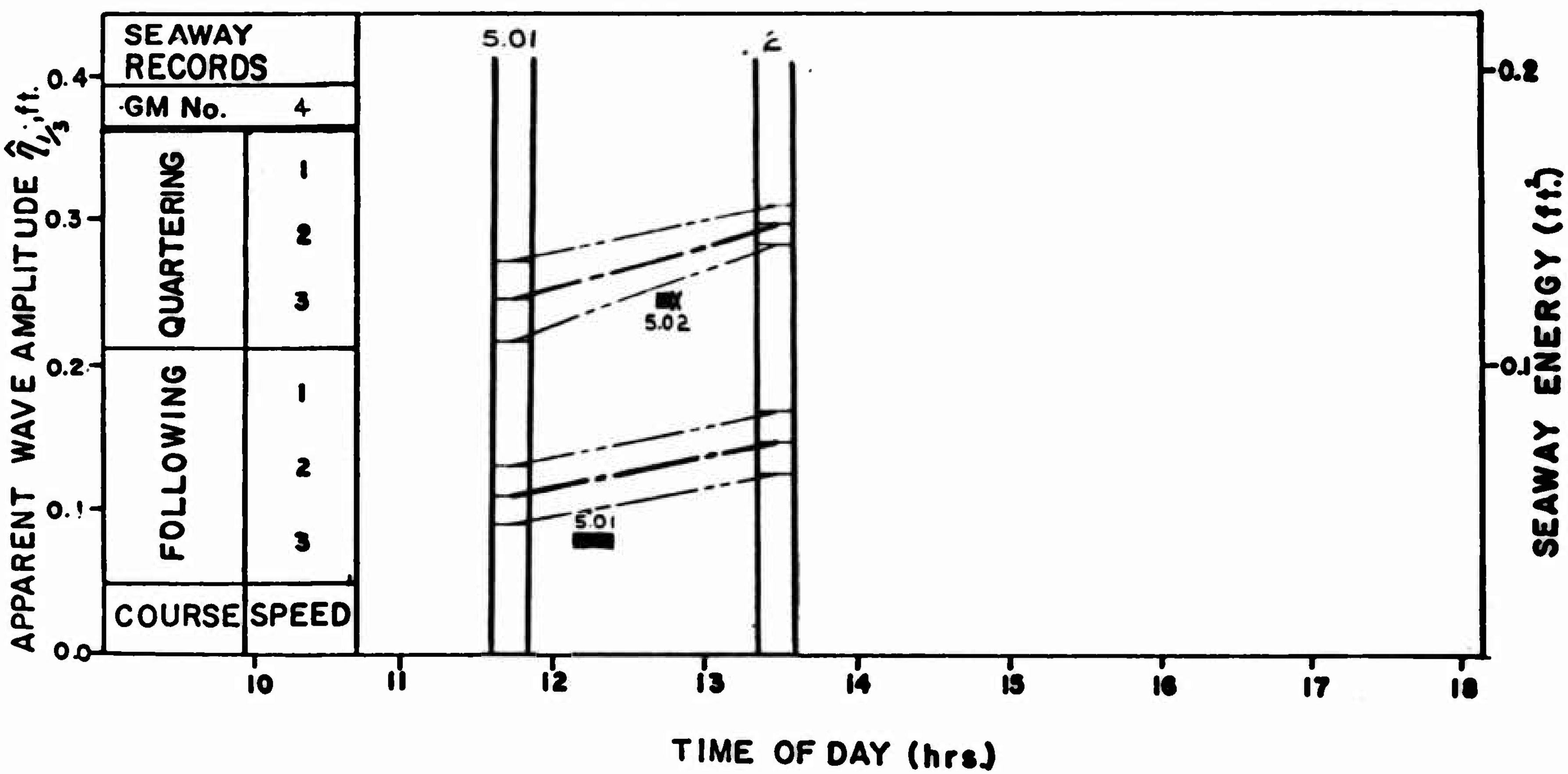

FIGURE D 1.5

SUMMARY OF MODEL RUNS AND SEASTATE INFORMATION

VS. TIME OF RECORDING - 1972

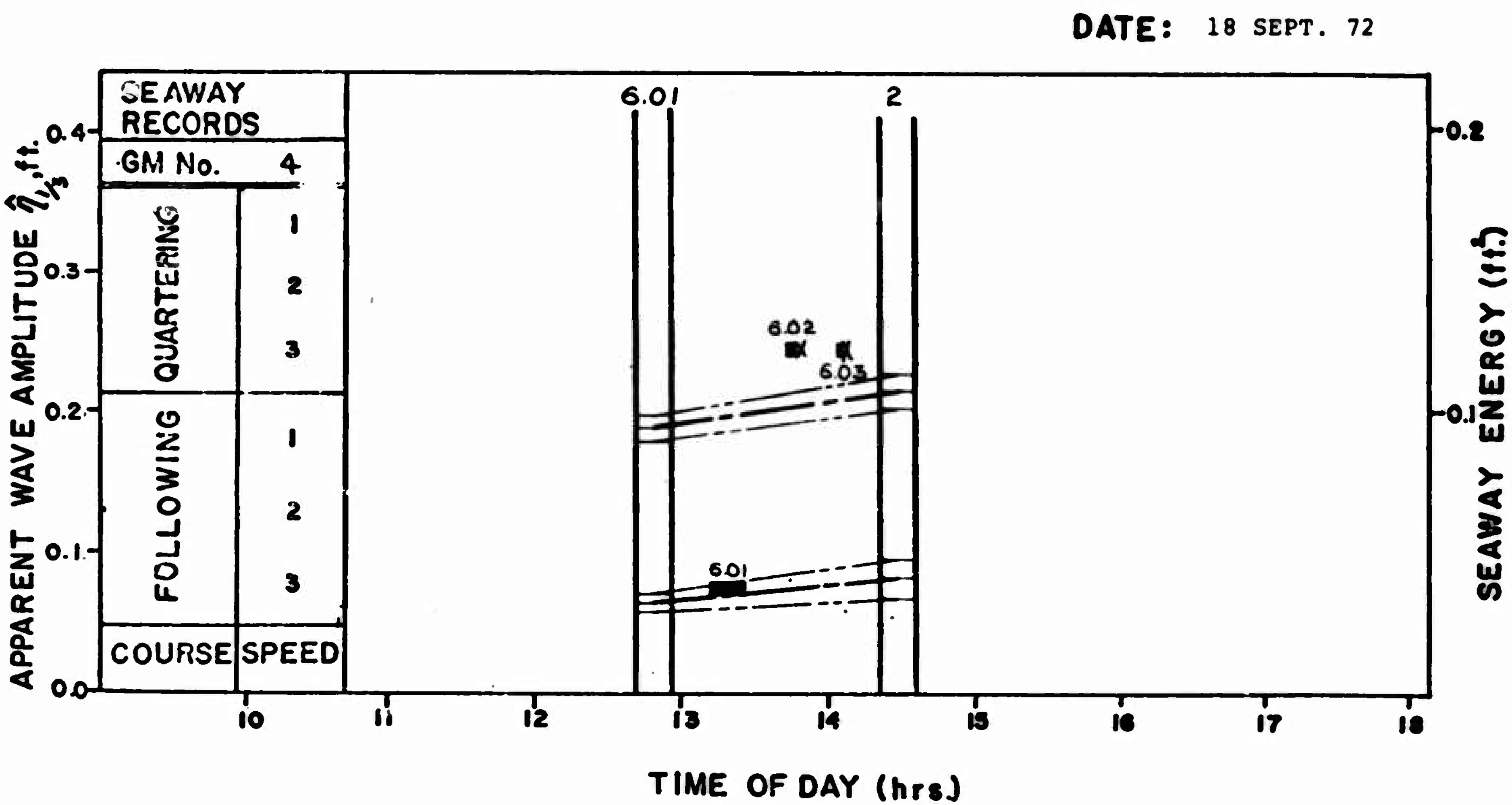

FIGURE D 1.6

SUMMARY OF MODEL RUNS AND SEASTATE INFORMATION

VS. TIME OF RECORDING - 1972

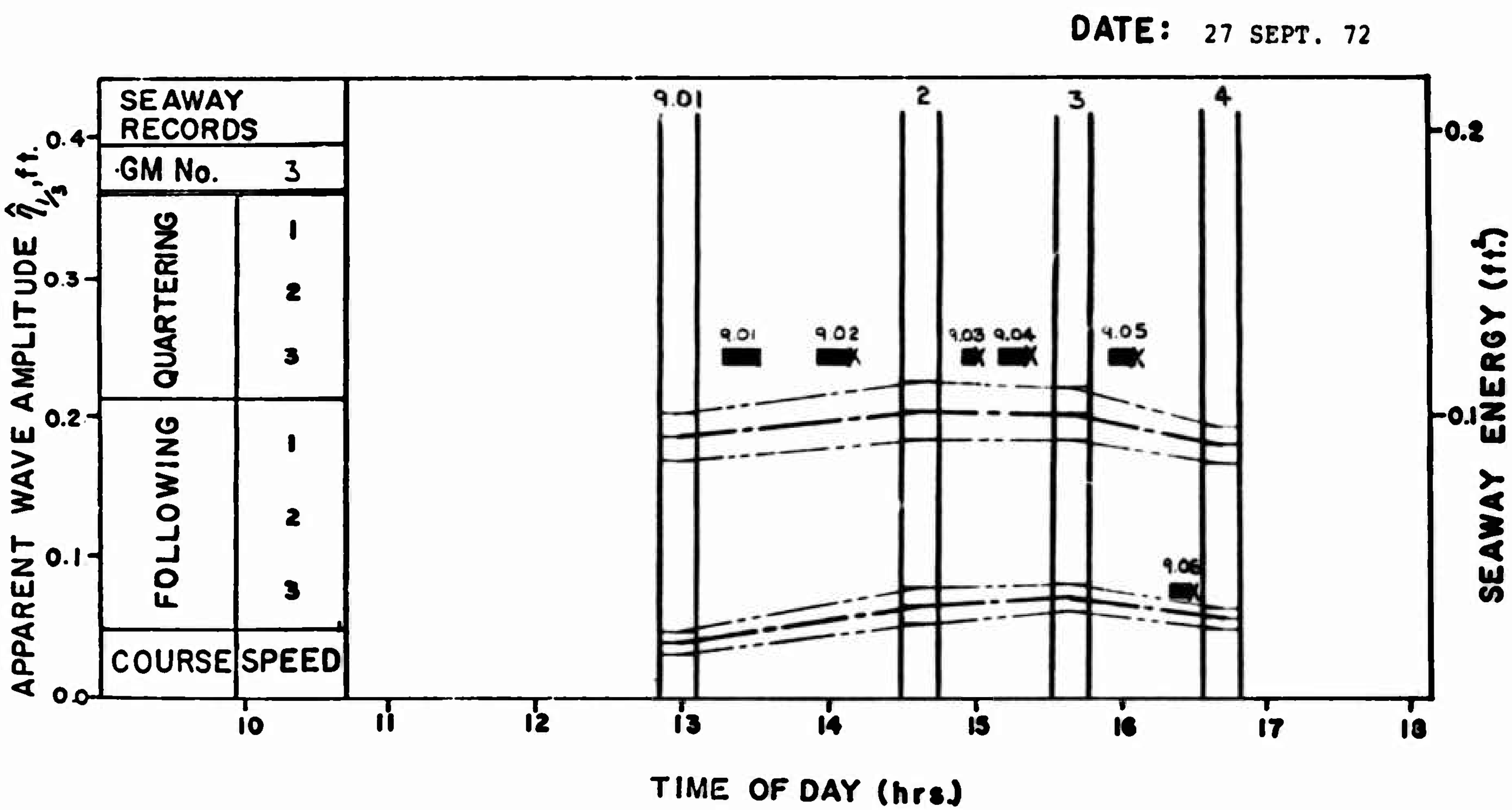

FIGURE D 1.9

SUMMARY OF MODEL RUNS AND SEASTATE INFORMATION

VS. TIME OF RECORDING - 1972

DATE: 21 SEPT 72

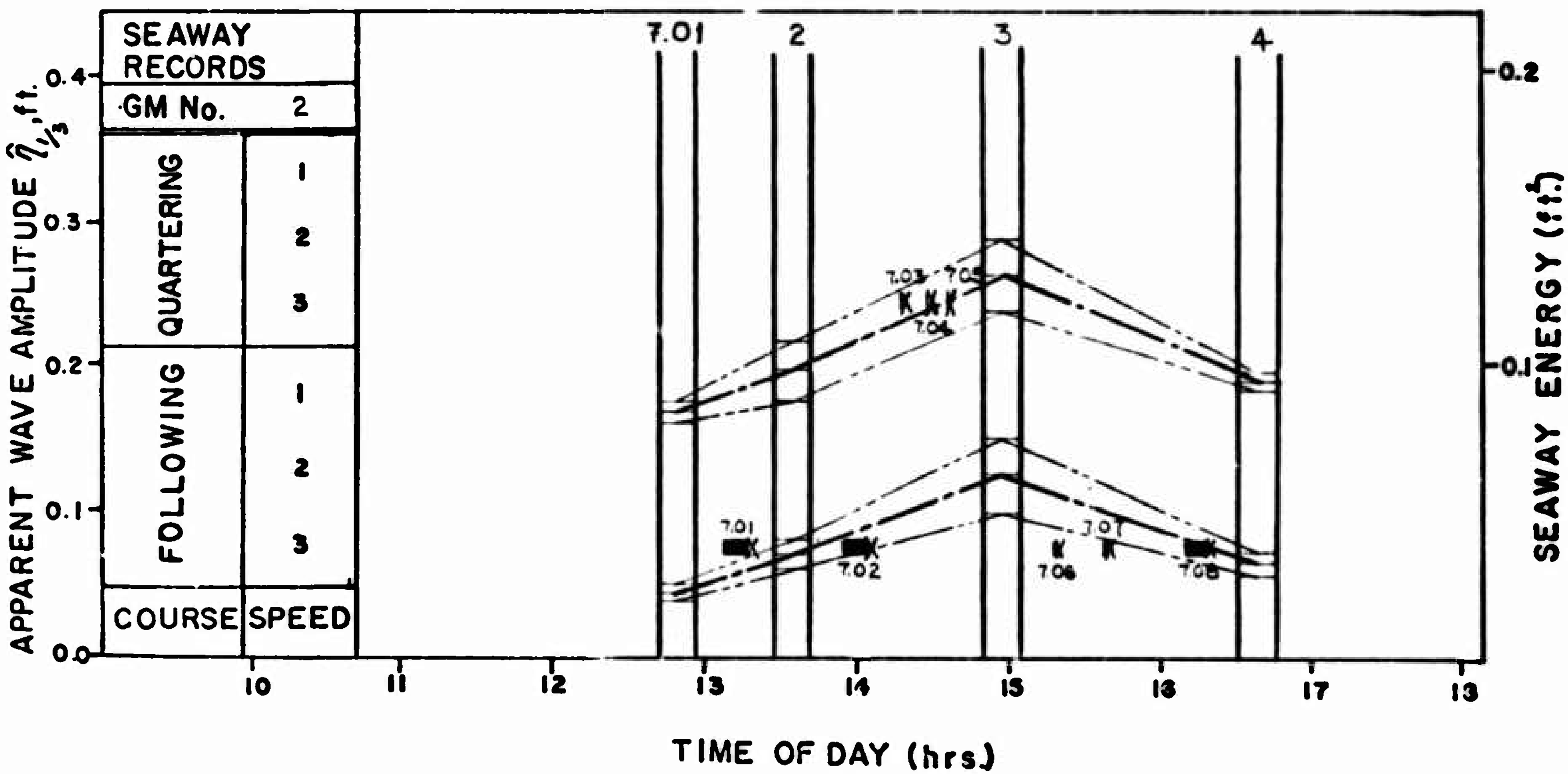

FIGURE D 1.7

SUMMARY OF MODEL RUNS AND SEASTATE INFORMATION

VS. TIME OF RECORDING - 1972

DATE: 25 SEPT. 72

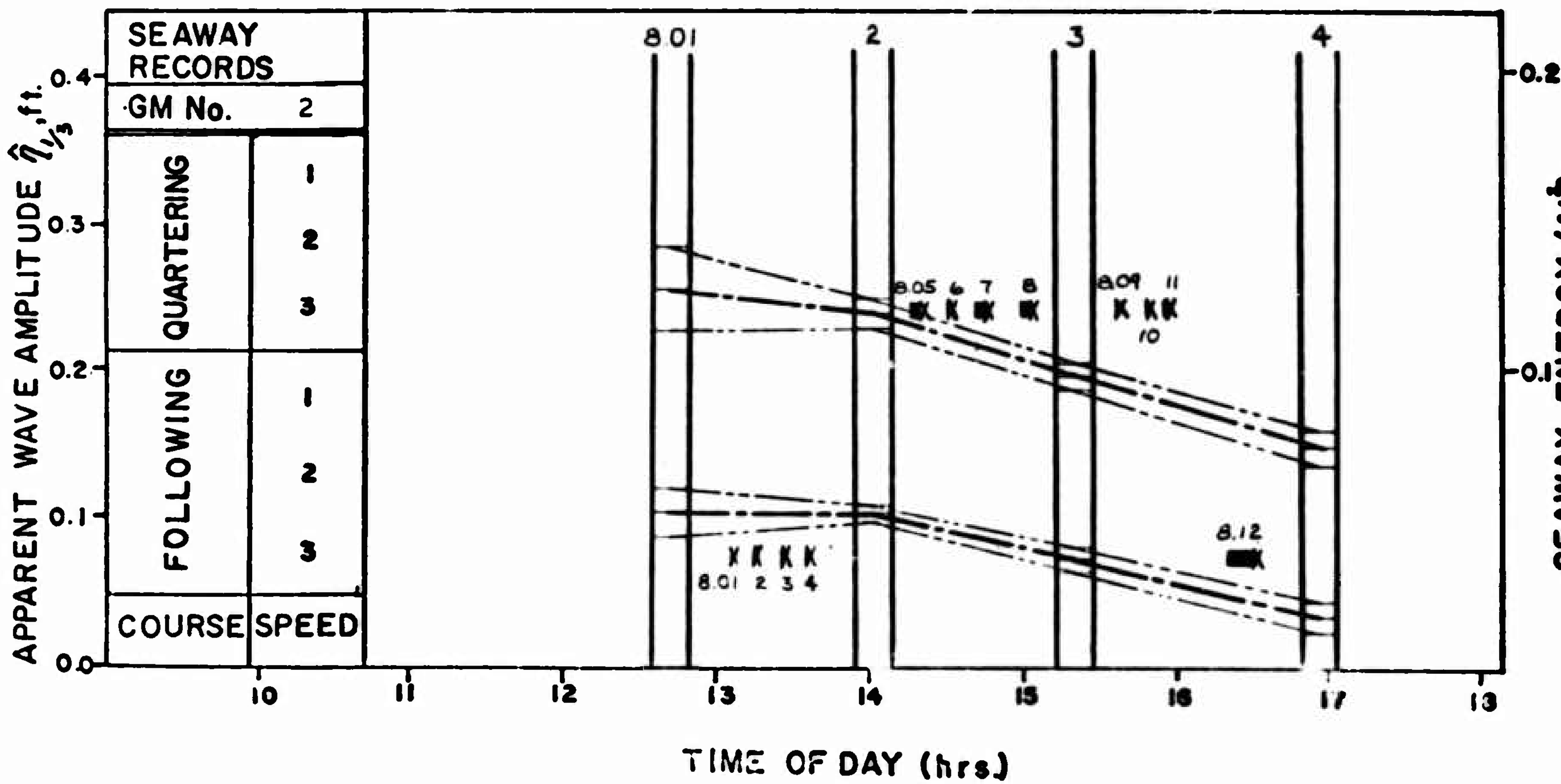

FIGURE D 1.8

SUMMARY OF MODEL RUNS AND SEASTATE INFORMATION

VS. TIME OF RECORDING - 1972

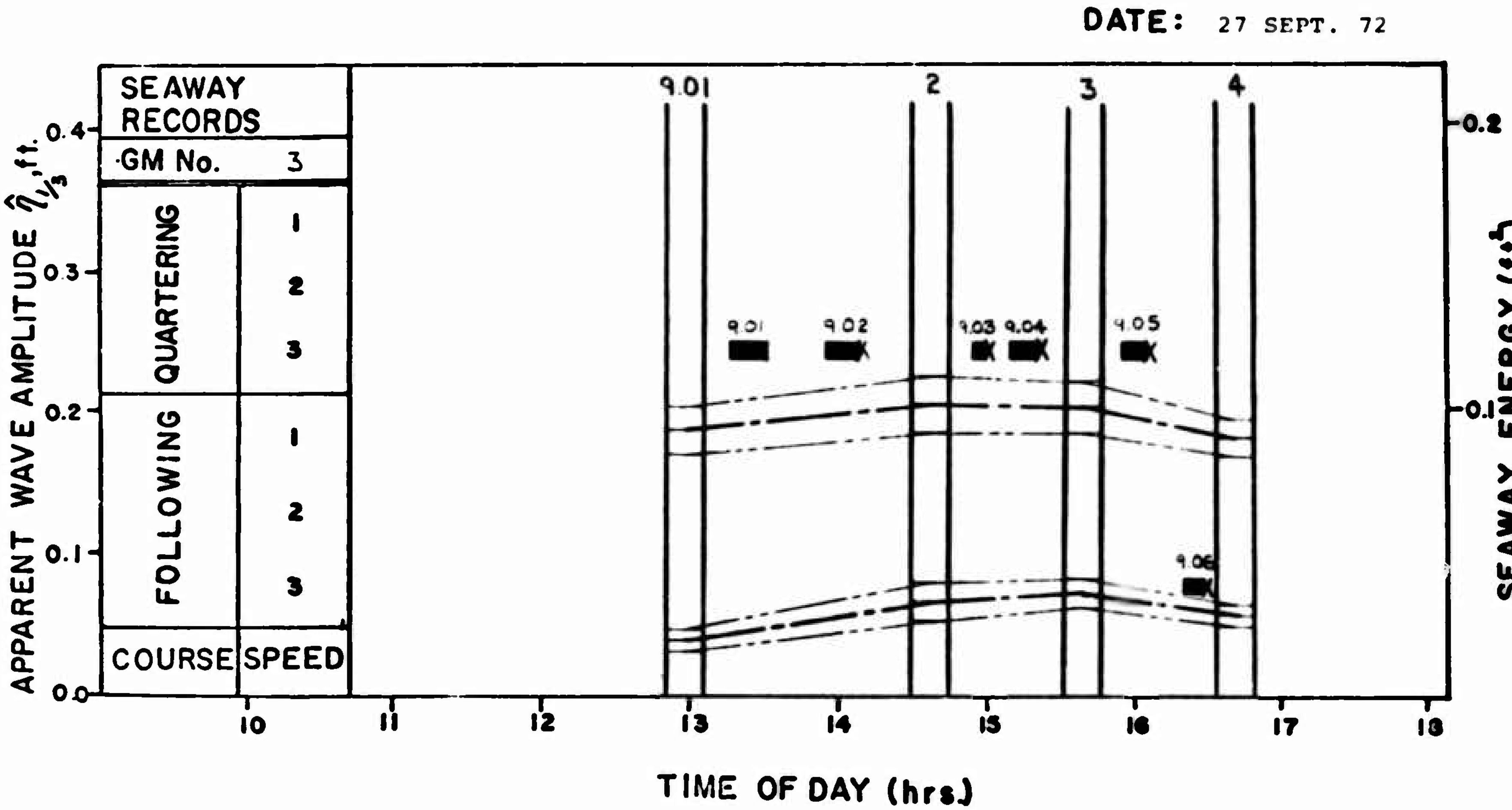

FIGURE D 1.9

SUMMARY OF MODEL RUNS AND SEASTATE INFORMATION

VS. TIME OF RECORDING - 1972

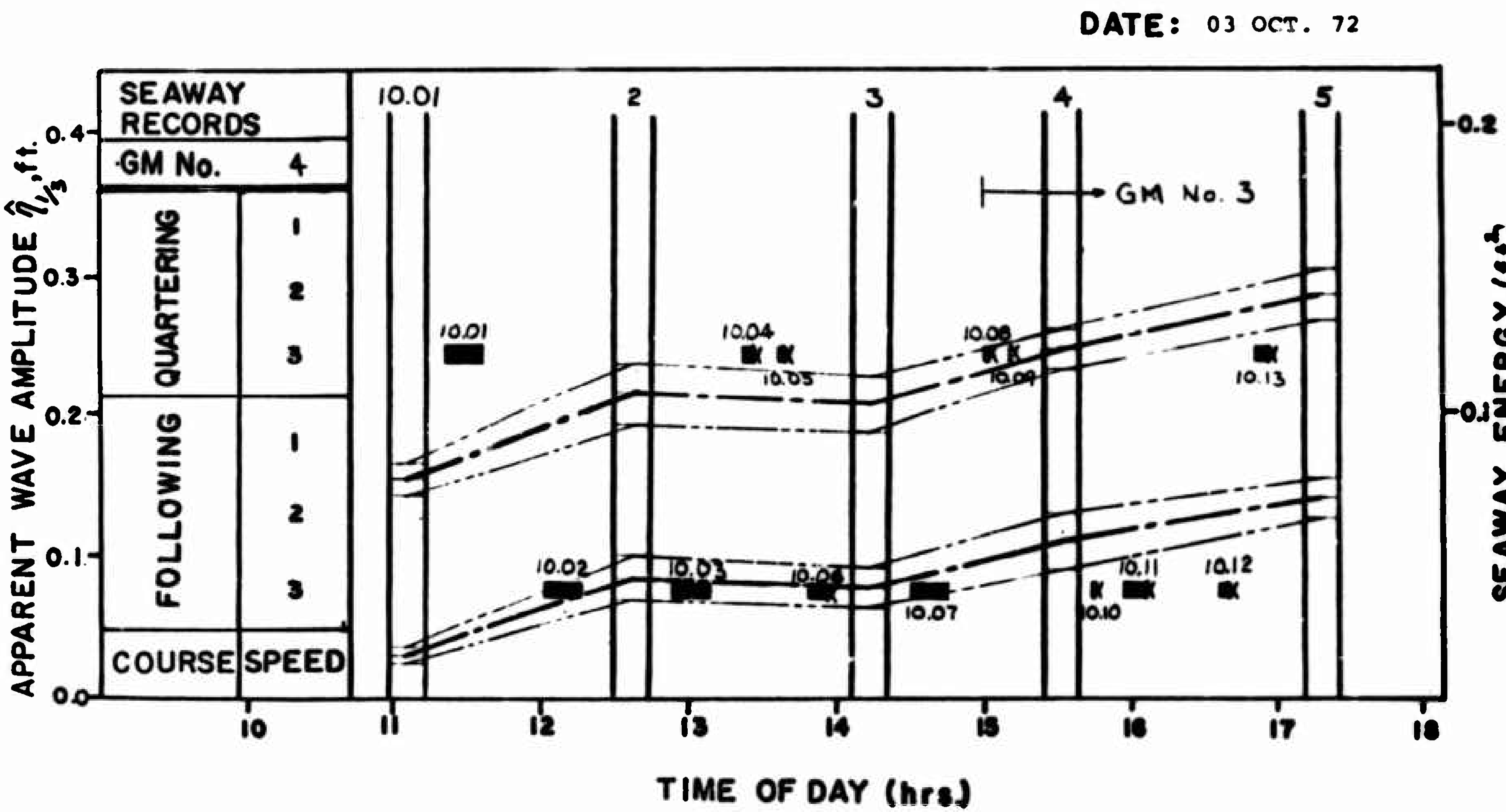

FIGURE D 1.10

TABLE D-I

STATISTICAL VALUES FOR ALL WAVE

RECORDS FROM FFT SPECTRA 1972

RMS Amplitude Computed from the Spectra using the Fast Fourier Transform Method of Analysis for the Four Wave Probes.

TABLE D-I

Statistical Values for All Wave Records From FFT Spectra

RMS Amplitude Ft. (Deviation from Mean)

DATE	TIME	I	II	III	IV
Aug. 10, 1972	11.20	0.2015	0.2232	0.2051	0.2190
	11.34	0.2207	0.2523	0.2936	0.2729
	1.14	0.3037	0.3301	0.3154	0.3382
	2.57	0.3948	0.4099	0.4040	0.4256
	4.35	0.3497	0.3635	0.3817	0.3813
	5.40	0.3159	0.3395	0.3461	0.3532
Sept. 5, 1972	11.55	0.1818	0.1826	0.1768	0.1752
	12.25	0.2248	0.2231	0.2048	0.2046
	1.59	0.2908	0.3126	0.2793	0.2698
	3.08	0.3115	0.2949	0.2924	0.2871
	4.43	0.3068	0.2997	0.2767	0.2860
Sept. 7, 1972	1.00	0.2634	0.2316	0.2327	0.2408
	2.37	0.3141	0.2978	0.3062	0.2949
	3.55	0.3526	0.3201	0.3206	0.3289
	4.58	0.3280	0.3071	0.2987	0.3133
Sept. 11, 1972	11.03	0.2345	0.1925	0.1729	0.2080
	12.32	0.2707	0.2753	0.2551	0.2606
	1.52	0.2840	0.2644	0.2261	0.2629
	3.04	0.2764	0.2570	0.2362	0.2517
	4.34	0.3018	0.2740	0.2929	0.2846
Sept. 13, 1972	11.34	0.2622	0.2370	0.2334	0.2399
	1.22	0.2894	0.2687	0.2591	0.2732
Sept. 18, 1972	12.40	0.1785	0.1838	0.1948	0.1875
	2.21	0.1940	0.1978	0.2186	0.2076
Sept. 21, 1972	12.41	0.1532	0.1566	0.1698	0.1605
	1.27	0.2015	0.2095	0.2168	0.2188
	2.52	0.2424	0.2803	0.2707	0.2726
	4.31	0.1712	0.1846	0.1970	0.1830
Sept. 25, 1972	12.36	0.2221	0.2246	0.2400	0.2429
	1.54	0.2309	0.2297	0.2385	0.2356
	3.12	0.2038	0.2041	0.2178	0.2074
	4.51	0.1929	0.1507	0.1928	0.1804

TABLE D-I

Statistical Values for All Wave Records from FFT Spectra

RMS Amplitude Ft. (Deviation from Mean)

DATE	TIME	I	II	III	IV
Sept. 27, 1972	12.52	0.1427	0.1315	0.1602	0.1330
	2.29	0.1880	0.1650	0.1949	0.1855
	3.31	0.1970	0.1833	0.2046	0.1904
	4.38	0.1822	0.1947	0.1970	0.1887
Oct. 3, 1972	10.58	0.1423	0.1345	0.1259	0.1328
	12.29	0.2280	0.1983	0.2292	0.2140
	2.06	0.2237	0.2063	0.2255	0.2162
	3.23	0.2474	0.2213	0.2430	0.2435
	5.10	0.2797	0.2717	0.2665	0.2616

TABLE D-II

STATISTICAL MEANS OF SEAWAY SIGNIFICANT AMPLITUDES, RECORDED IN SAN FRANCISCO BAY 1972

$\acute{\eta}_{1/3}$	Significant Amplitude, i.e. 2*RMS derived from the time series.
$\bar{\acute{\eta}}_{1/3}$	Average of the four probes.
$S_{\acute{\eta}}$	Standard Deviation of the Mean.

TABLE D-II

Statistical Means of Seaway Significant Amplitudes, Recorded in San Francisco Bay 1972

PROBE NO. →		$\hat{h}_{1/3}$, Ft.				$\bar{\hat{h}}_{1/3}$ Ft.	$s_{\hat{h}}$ Ft.	$\frac{s_{\hat{h}}}{\bar{\hat{h}}_{1/3}}$	Seq. No.
		1	2	3	4				
DATE	SAMPLE No.	←amplitudes→				mean amplit.	*		
8/8/72	0.01	.3746	.3618	.3262	.3722	.3587	.0112	.0312	1.
8/10/72	1.01	.2487	.2711	.2400	.2669	.2567	.0074	.0288	1.
	1.02	.2929	.3057	.3655	.3547	.3297	.0179	.0542	2.
	1.03	.3161	.3490	.3274	.3480	.3351	.0081	.0241	11.
	1.04	.4474	.4485	.4403	.4748	.4527	.0076	.0167	12.
	1.05	.3694	.4014	.4165	.4219	.4023	.0118	.0293	13.
	1.06	.3585	.3816	.3840	.3969	.3802	.0080	.0210	14.
9/5/72	2.01	.1898	.1876	.1875	.1789	.1859	.0024	.0130	1.
	2.02	.2304	.2253	.2097	.2031	.2171	.0064	.0296	2.
	2.03	.2859	.2817	.2757	.2641	.2768	.0047	.0171	3.
	2.06	.3186	.3095	.3126	.3066	.3118	.0026	.0082	4.
	2.05	.3142	.3367	.2925	.3133	.3142	.0090	.0287	5.
9/7/72	3.02	.2711	.2517	.2499	.2462	.2547	.0056	.0219	1.
	3.03	.3284	.3050	.3060	.2969	.3091	.0068	.0219	2.
	3.04	.3878	.3416	.3296	.3487	.3519	.0126	.0358	3.
	3.05	.3798	.3416	.3125	.3379	.3429	.0139	.0405	4.
9/11/72	4.01	.2527	.1937	.1868	.2306	.2159	.0156	.0721	1.
	4.02	.3006	.3031	.2758	.2874	.2917	.0063	.0217	2.
	4.03	.3177	.2823	.2389	.3010	.2850	.0170	.0596	3.
	4.04	.2954	.2620	.2595	.2627	.2699	.0085	.0316	4.
	4.05	.2995	.2691	.3029	.2842	.2889	.0078	.0269	5.
9/13/72	5.01	.2698	.2515	.2458	.2259	.2462	.0090	.0364	1.
	5.02	.2997	.2946	.2784	.2899	.2906	.0045	.0156	2.
9/18/72	6.01	.1838	.1826	.1948	.1796	.1852	.0033	.0179	1.
	6.02	.2041	.2117	.2242	.2164	.2141	.0042	.0197	2.

TABLE D-II

<u>Statistical Means of Seaway Significant Amplitudes, Recorded in San Francisco Bay 1972</u> (cont.)

PROBE NO.→		$\hat{\eta}_{1/3}$, Ft. 1	2	3	4	$\bar{\hat{\eta}}_{1/3}$ Ft.	$s_{\hat{\eta}}$ Ft.	$\dfrac{s_{\hat{\eta}}}{\bar{\hat{\eta}}_{1/3}}$	Seq. No.
DATE	SAMPLE No.	← amplitudes →				mean amplit.	*		
9/21/72	7.01	.1606	.1642	.1794	.1678	.1680	.0041	.0243	1.
	7.02	.1806	.1973	.2007	.2144	.1982	.0069	.0350	2.
	7.03	.2403	.2791	.2685	.2681	.2640	.0083	.0314	3.
	7.04	.1848	.2004	.2020	.1925	.1949	.0040	.0203	4.
9/25/72	8.01	.2424	.2368	.2602	.2792	.2546	.0096	.0376	1.
	8.02	.2413	.2313	.2474	.2366	.2391	.0034	.0143	2.
	8.03	.1902	.1916	.2034	.1936	.1947	.0030	.0153	3.
	8.04	.1569	.1453	.1438	.1395	.1464	.0037	.0254	5.
9/27/72	9.01	.1902	.1703	.1982	.1813	.1850	.0060	.0324	1.
	9.02	.2120	.1881	.2215	.2118	.2083	.0071	.0342	2.
	9.03	.2155	.1682	.2154	.2037	.2057	.0065	.0314	3.
	9.04	.1687	.1862	.1829	.1715	.1773	.0043	.0240	5.
10/3/72	10.01	.1628	.1554	.1488	.1420	.1522	.0045	.0293	1.
	10.02	.2334	.2016	.2237	.2030	.2154	.0078	.0364	2.
	10.03	.2187	.1896	.2183	.2136	.2100	.0069	.0329	3.
	10.04	.2576	.2344	.2487	.2424	.2458	.0049	.0200	5.
	10.05	.3066	.2883	.2956	.2764	.2917	.0063	.0217	6.

* s = Standard Deviation of the Mean

TABLE D-III

STATISTICAL MEANS OF SEAWAY ENERGIES,

RECORDED IN SAN FRANCISCO BAY 1972

η_{RMS}	Root Mean Square Wave Amplitude
$\overline{\eta}^2_{RMS}$	Average Mean Square Value
S_E	Standard Deviation of the Mean

Mean Energy Ship Scale assuming λ =30.

TABLE D-III

Statistical Means of Seaway Energies, Recorded in San Francisco Bay 1972

PROBE NO. →		η_{RMS}, Ft.				$\overline{\eta^2_{RMS}}$ Ft.²	s_E Ft.²	$\frac{s_E}{\eta^2}$	mean energy ship scale Ft.²	Seq. No.
		1	2	3	4					
DATE	SAMPLE No.	← ordinates →				mean energy	*			
8/8/72	0.01	.290	.278	.268	.308	.0821	.0049	.0599	74.82	1.
8/10/72	1.01	.198	.222	.201	.218	.0441	.0025	.0558	40.19	1.
	1.02	.217	.248	.282	.268	.0649	.0070	.1085	59.15	2.
	1.03	.302	.328	.315	.337	.1030	.0049	.0475	93.87	11.
	1.04	.393	.408	.399	.423	.1646	.0054	.0329	150.01	12.
	1.05	.337	.353	.367	.368	.1271	.0052	.0409	115.84	13.
	1.06	.315	.337	.344	.351	.1136	.0051	.0447	103.53	14.
9/5/72	2.01	.179	.178	.173	.173	.0309	.0006	.0186	28.16	1.
	2.02	.221	.220	.199	.200	.0443	.0025	.0566	40.37	2.
	2.03	.278	.275	.262	.257	.0721	.0027	.0379	65.71	3.
	2.04	.302	.285	.284	.277	.0825	.0031	.0371	75.19	4.
	2.05	.305	.299	.275	.285	.0848	.0040	.0467	77.28	5.
9/7/72	3.02	.182	.230	.231	.238	.0490	.0054	.1099	44.66	1.
	3.03	.300	.282	.287	.280	.0826	.0026	.0319	75.28	2.
	3.04	.259	.305	.307	.315	.0884	.0073	.0825	80.57	3.
	3.05	.322	.302	.291	.307	.0934	.0039	.0421	85.12	4.
9/11/72	4.01	.225	.178	.170	.198	.0376	.0049	.1300	34.27	1.
	4.02	.268	.272	.254	.258	.0692	.0023	.0328	63.07	2.
	4.03	.211	.264	.225	.262	.0583	.0064	.1098	53.13	3.
	4.04	.275	.256	.234	.250	.0647	.0043	.0670	58.97	4.
	4.05	.285	.257	.276	.268	.0737	.0032	.0429	67.17	5.
9/13/72	5.01	.253	.226	.225	.232	.0548	.0032	.0575	49.94	1.
	5.02	.285	.264	.255	.269	.0723	.0035	.0490	65.89	2.
9/18/72	6.01	.174	.180	.186	.182	.0326	.0009	.0267	29.71	1.
	6.02	.194	.198	.218	.207	.0418	.0023	.0545	38.10	2.
9/21/72	7.01	.144	.149	.159	.150	.0226	.0009	.0408	20.60	1.
	7.02	.178	.190	.195	.197	.0361	.0016	.0434	32.90	2.
	7.03	.226	.266	.255	.257	.0630	.0042	.0665	57.42	3.
	7.04	.171	.185	.187	.183	.0328	.0013	.0387	29.89	4.

TABLE D-III

Statistical Means of Seaway Energies,

Recorded in San Francisco Bay 1972 (cont.)

PROBE NO. →		η_{RMS}, Ft. 1	2	3	4	$\overline{\eta^2_{RMS}}$ Ft.²	s_E Ft.²	$\frac{s_E}{\overline{\eta^2}}$	mean energy ship scale Ft.²	Seq. No.
DATE	SAMPLE No.	← ordinates →				mean energy	*			
9/25/72	8.01	.220	.220	.238	.241	.0527	.0026	.0500	48.03	1.
	8.02	.227	.226	.234	.231	.0526	.0008	.0155	47.94	2.
	8.03	.188	.189	.200	.191	.0368	.0011	.0295	33.54	3.
	8.04	.154	.131	.138	.128	.0191	.0017	.0878	17.41	5.
9/27/72	9.01	.142	.130	.150	.133	.0193	.0013	.0666	17.59	1.
	9.02	.188	.165	.194	.185	.0336	.0023	.0672	30.62	2.
	9.03	.195	.182	.200	.189	.0366	.0015	.0420	33.36	3.
	9.04	.160	.175	.176	.167	.0288	.0013	.0453	26.25	5.
10/3/72	10.01	.139	.121	.124	.121	.0160	.0011	.0680	14.58	1.
	10.02	.215	.190	.216	.201	.0423	.0025	.0596	38.55	2.
	10.03	.208	.180	.205	.196	.0391	.0024	.0617	35.63	3.
	10.04	.245	.216	.240	.240	.0554	.0030	.0541	50.49	5.
	10.05	.278	.269	.259	.259	.0709	.0024	.0332	64.62	6.

* s = Standard Deviation of the Mean

TABLE D-IV

STATISTICAL MEANS OF SEAWAY ZERO CROSSING PERIODS, RECORDED IN SAN FRANCISCO BAY 1972

τ	Zero crossing periods obtained from the time series
$\bar{\tau}$	Mean period
S_E	Standard Deviation of the Mean

TABLE D-IV

Statistical Means of Seaway Zero Crossing Periods,

Recorded in San Francisco Bay 1972

PROBE NO. →		τ, Sec. 1	2	3	4	$\bar{\tau}$ Sec.	s_E Sec.	$\frac{s_E}{\bar{\tau}}$	Seq. No.
DATE	SAMPLE No.	← periods →				mean period	*		
8/8/72	0.01	2.0000	1.7121	1.6377	1.8226	1.7931	0.0787	0.0439	1.
8/10/72	1.01	1.6359	1.4902	1.5701	1.5464	1.5606	0.0302	0.0193	1.
	1.02	1.7393	1.6351	1.6031	1.6483	1.6564	0.0292	0.0176	2.
	1.03	2.0078	1.9007	1.8767	1.9669	1.9380	0.0301	0.0155	11.
	1.04	2.3779	2.3141	2.3473	2.3473	2.3466	0.0130	0.0056	12.
	1.05	2.5052	2.5721	2.4601	2.4787	2.5040	0.0245	0.0098	13.
	1.06	2.4545	2.3956	2.4453	2.3956	2.4227	0.0158	0.0065	14.
9/5/72	2.01	1.6368	1.6483	1.6016	1.6516	1.6346	0.0114	0.0070	1.
	2.02	1.7301	1.8004	1.7965	1.7926	1.7799	0.0167	0.0094	2.
	2.03	2.1558	2.2661	2.2630	2.3174	2.2506	0.0340	0.0151	3.
	2.04	2.2536	2.2915	2.3207	2.3011	2.2917	0.0141	0.0061	4.
	2.05	2.1473	2.1874	2.1962	2.1701	2.1752	0.0108	0.0050	5.
9/7/72	3.02	1.8471	1.9029	1.8703	1.8703	1.8726	0.0115	0.0061	1.
	3.03	2.2883	2.2322	2.2201	2.2567	2.2493	0.0151	0.0067	2
	3.04	2.4165	2.3849	2.3574	2.4094	2.3920	0.0134	0.0056	3.
	3.05	2.2475	2.3044	2.3076	2.2413	2.2752	0.0178	0.0078	4.
9/11/72	4.01	1.5650	1.7847	1.7264	1.7246	1.7252	0.0244	0.0142	1.
	4.02	1.8471	1.8725	1.8597	1.8513	1.8576	0.0056	0.0030	2.
	4.03	1.7393	1.8084	1.8576	1.8144	1.8049	0.0245	0.0136	3.
	4.04	2.0054	1.9669	2.0871	1.9883	2.0119	0.0263	0.0131	4.
	4.05	2.1586	2.1758	2.1904	2.1816	2.1766	0.0067	0.0031	5.
9/13/72	5.01	1.7542	1.7174	1.7693	1.8225	1.7658	0.0218	0.0123	1.
	5.02	1.7809	1.8388	1.9366	1.9692	1.8814	0.0434	0.0231	2.
9/18/72	6.01	1.8388	1.8534	1.8327	1.8044	1.8323	0.0103	0.0056	1.
	6.02	1.8347	1.8388	1.8985	1.9029	1.8687	0.0185	0.0099	2.
9/21/72	7.01	1.6926	1.6566	1.6583	1.6368	1.6611	0.0116	0.0070	1.
	7.02	1.9716	1.9140	1.9669	1.9575	1.9525	0.0132	0.0067	2.
	7.03	2.1501	2.2171	2.1558	2.1195	2.1606	0.0204	0.0095	3.
	7.04	1.9669	1.9908	1.9321	1.9622	1.9630	0.0121	0.0061	4.

TABLE D-IV

Statistical Means of Seaway Zero Crossing Periods,

Recorded in San Francisco Bay 1972 (cont.)

PROBE NO. →		τ, Sec. 1	2	3	4	$\bar{\tau}$ Sec.	s_E Sec.	$\frac{s_E}{\bar{\tau}}$	Seq. No.
DATE	SAMPLE No.	← periods →				mean period	*		
9/25/72	8.01	1.7067	1.7598	1.6770	1.6351	1.6946	0.0262	0.0155	1.
	8.02	1.8450	1.8746	1.7828	1.8492	1.8379	0.0195	0.0106	2.
	8.03	1.9859	1.9811	1.9253	1.9575	1.9624	0.0139	0.0071	3.
	8.04	1.9932	1.9908	1.9389	1.9208	1.9609	0.0183	0.0093	5.
9/27/72	9.01	1.5142	1.5545	1.5004	1.5341	1.5258	0.0118	0.0077	1.
	9.02	1.6961	1.7542	1.6735	1.6335	1.6893	0.0252	0.0149	2.
	9.03	1.7828	1.8164	1.7467	1.7712	1.7793	0.0145	0.0081	3.
	9.04	1.9118	1.9482	1.9366	1.9230	1.9299	0.0079	0.0041	5.
10/3/72	10.01	1.6000	1.8492	1.6839	1.6400	1.6933	0.0547	0.0323	1.
	10.02	2.0531	2.0609	2.0078	2.0687	2.0476	0.0137	0.0067	2.
	10.03	2.0153	2.1141	1.9787	2.0353	2.0358	0.0286	0.0140	3.
	10.04	1.9789	2.0177	2.0128	2.0029	2.0030	0.0087	0.0043	5.
	10.05	1.8854	1.9185	2.0103	1.9645	1.9447	0.0272	0.0140	6.

* s = Standard Deviation of the Mean

TABLE D-V

OVERVIEW OF MODEL TESTS IN SAN FRANCISCO BAY 1972

GM No.	See Table A-I for the *American Challenger*.
Heading	Visual description of the model heading vs. the apparent wave direction.
Speed No.	See Table A-I for the *American Challenger*.
Duration	Length of the Model Run.
δ_t	Digitized Rate.
Seq. No.	Sequence Number assigned during Calibration of the Digitized data.

MOTION DATA RECORDED FOR THE CHALLENGER MODEL IN THE HEAVY CONDITION DURING THE 1972 SEASON.

	YAW	RUDDER	ROLL	PITCH	RPM
13 SEP - 03 OCT	1*	2	3	4	

* The number refers to the channel on which the data was recorded.

TABLE D-V

Overview for Model Tests in San Francisco Bay 1972

DATE	RUN No.	GM. No.	HEADING	SPEED No.	DURATION [sec.]	CAP-SIZE	δ_t [sec.]	NO. OF SAMPLES	SEQ. NO.
8/10/71	1.01	3	following	1		← NO RECORD →			
	1.02	3	following	1	350.0	PORT	.200	1734	02
	1.03	3	following	1	132.0	PORT	.200	649	03
	1.04	3	following	1	194.0	STBD.	.200	972	04
	1.05	3	following	3	56.4	STBD.	.200	302	05
	1.06	3	following	3	114.0	PORT	.200	567	06
	1.07	3	following	3		← NO RECORD →			07
	1.08	3	following	3	233.8	STBD.	.200	1178	08
	1.10	3	following	3	23.7	PORT	.200	103	09
	1.11	3	following	3	141.8	PORT	.200	708	10
9/5/72	2.01	3	following	3	266.3	PORT	.400	653	02
	2.02	3	quartering	3	37.7	PORT	.400	91	03
	2.03	3	quartering	3	56.9	PORT	.400	141	04
	2.04	3	quartering	3	29.3	PORT	.400	70	05
	2.05	3	quartering	3	60.9	PORT	.400	147	06
	2.06	3	quartering	1	834.7	PORT	.400	2048	07
9/7/72	3.01	3	quartering	1		← NO RECORD →			
	3.02	3	quartering	1	450.0		.200	2048	02
	3.03	3	quartering	1	450.0		.200	2048	03
	3.04	3	quartering	3	14.9	PORT	.200	72	04
	3.05	3	quartering	2	327.3	PORT	.200	1769	05
	3.06	3	following	2	450.0		.200	2048	06
	3.07	3	following	2	145.8	PORT	.200	891	07
	3.08	3	following	2	450.0		.200	2048	08
	3.09	3	following	2	361.1	STBD.	.200	1794	09

TABLE D-V

Overview for Model Tests in San Francisco Bay 1972 (cont.)

DATE	RUN No.	GM. No.	HEADING	SPEED No.	DURATION [sec.]	CAP-SIZE	δ_t [sec.]	NO. OF SAMPLES	SEQ. NO.
9/11/72	4.01	2	following	2	880.0	STBD.	.400	2068	02
	4.02	2	following	3	110.0	STBD.	.400	282	03
	4.03	2	following	3	67.0	PORT	.400	149	04
	4.04	2	following	3	50.0	PORT	.400	123	05
	4.05	2	following	1	460.0		.400	1193	06
	4.06	2	quartering	3	55.0	PORT	.400	127	07
	4.07	2	quartering	3	7.0	← NO RECORD →			08
	4.08	2	quartering	1	555.0	PORT	.400	1407	09
	4.09	2	quartering	2	20.0	PORT	.400	44	10
	4.10	2	Q-F*	2	172.0	STBD.	.400	577	11
	4.11	2	quartering	3	25.0	PORT	.400	61	12
	4.12	2	quartering	2	194.0	PORT	.400	486	13
9/13/72	5.01	4	following	3	900.0		.400	2048	02
	5.02	4	quartering	3	318.0	PORT	.400	799	03
9/18/72	6.01	4	following	3	900.0		.400	2048	02
	6.02	4	quartering	3	111.7	PORT	.400	276	03
	6.03	4	quartering	3	75.3	PORT	.400	181	04
9/21/72	7.01	2	following	3	361.4	STBD.	.400	892	02
	7.02	2	following	3	423.6	STBD.	.400	1047	03
	7.03	2	quartering	3	28.0	STBD.	.400	61	04
	7.04	2	quartering	3	30.0	STBD.	.400	66	05
	7.05	2	quartering	3		← NO RECORD →			06
	7.06	2	following	3	46.6	PORT	.400	110	07
	7.07	2	following	3	54.6	STBD.	.400	129	08
	7.08	2	following	3	405.6	STBD.	.400	1003	09

* From quartering to almost following at the end.

TABLE D-V

Overview for Model Tests in San Francisco Bay 1972 (cont.)

DATE	RUN No.	GM. No.	HEADING	SPEED No.	DURATION [sec.]	CAPSIZE	δ_t [sec.]	NO. OF SAMPLES	SEQ. NO.
9/25/72	8.01	2	following	3		← NO RECORD →			02
	8.02	2	following	3	19.6	STBD.	.400	48	03
	8.03	2	following	3	39.0	PORT	.400	96	04
	8.04	2	following	3	28.6	STBD.	.400	69	05
	8.05	2	quartering	3	137.0	PORT	.400	345	06
	8.06	2	quartering	3	33.5	PORT	.400	80	07
	8.07	2	quartering	3	175.4	STBD.	.400	436	08
	8.08	2	quartering	3	136.2	PORT	.400	339	09
	8.09	2	quartering	3	10.4	PORT	.400	23	10
	8.10	2	quartering	3	36.3	PORT	.400	88	11
	8.11	2	quartering	3	56.0	PORT	.400	138	12
	8.12	2	following	3	672.0	STBD.	.400	1689	13
9/27/72	9.01	3	quartering	3	900.0		.400	2048	02
	9.02	3	quartering	3	864.8	PORT	.400	2048	03
	9.03	3	quartering	3	244.0	PORT	.400	607	04
	9.04	3	quartering	3	827.8	PORT	.400	2048	05
	9.05	3	quartering	3	672.8	PORT	.400	1696	06
	9.06	3	following	3	505.4	STBD.	.400	1261	07
10/3/72	10.01	4	quartering	3	960.0		.400	2048	02
	10.02	4	following	3	900.0		.400	2048	03
	10.03	4	following	3	915.0		.400	2048	04
	10.04	4	quartering	3	140.0	PORT	.400	321	05
	10.05	4	quartering	3	60.0	X	.400	110	06
	10.06	4	following	3	838.0	PORT	.400	926	07
	10.07	3	following	3	900.0		.400	2048	08
	10.08	3	quartering	3	58.0	PORT	.400	114	09
	10.09	3	quartering	3	30.0	PORT	.400	69	10
	10.10	3	following	3	40.0	PORT	.400	114	11
	10.11	3	following	3	600.0	STBD	.400	1567	12
	10.12	3	quartering	3	107.0	PORT	.400	242	13
	10.13	3	quartering	3	154.0	PORT	.400	357	14

TABLE D-VI

STATISTICAL RESULTS FROM MEASURED
MODEL DATA 1972

The highest amplitude statistics were computed from an analysis of the time series.

The seaway statistics were interpolated to the time of the model run and are intended only as a guide.

TABLE D-VI

Statistical Results from Measured Model Data 1972

DATE & RUN NO.	Seq No. Cal	1. YAW DEGREES MEAN	RMS	1/3	1/10	1/100	2. RUDDER, DEGREES MEAN	RMS	1/3	1/10	1/100	3. ROLL, DEGREES MEAN	RMS	1/3	1/10	1/100	4. PITCH, DEGREES MEAN	RMS	1/3	1/10	1/100	5. SEAWAY (Interpolated) $\overline{\eta^2}$ Ft²	$\eta_{1/3}$ Ft	$\bar{T}$ Sec.
		of ordinates		highest amplitude			of ordinates		highest amplitude			of ordinates		highest amplitude			of ordinates		highest amplitude					
8/10																								
1.01									← NO RECORD →													.073	.329	1.74
1.02	02	-4.8	5.1	5.6	11.3	44.7	4.2	4.1	5.4	9.2	17.5	-1.0	16.9	21.2	42.8	154.9	-0.2	1.4	2.2	3.1	3.9	.091	.332	1.83
1.03	03	1.3	8.8	9.7	25.2	77.0	0.3	5.6	5.5	11.6	37.9	2.2	20.1	29.2	69.6	0.0*	-0.1	1.9	3.1	4.3	5.3	.117	.360	2.01
1.04	04	-2.1	10.7	10.9	25.1	62.6	2.3	5.5	5.0	10.0	38.0	2.2	22.0	46.3	115.7	156.5	-0.1	2.9	4.7	7.5	34.0	.134	.395	2.13
1.05	05	0.0	30.4	52.3	102.6	0.0*	4.8	14.6	18.7	38.3	0.0*	8.5	44.5	107.3	149.6	0.0*	1.1	6.5	14.5	30.0	0.0*	.144	.420	2.20
1.06	06	-1.1	11.5	15.8	38.3	78.8	3.1	6.7	7.1	12.5	18.7	-1.2	26.0	51.4	114.2	0.0*	0.2	1.8	3.0	3.9	4.9	.153	.445	2.35
1.07	07									← NO RECORD →												.147	.435	2.39
1.08	08	1.3	13.1	9.6	20.1	96.5	3.0	8.8	7.0	16.5	64.7	2.5	20.7	19.5	43.3	148.2	0.5	3.6	4.8	8.7	33.1	.138	.422	2.44
1.10	09	-10.4	14.7	23.1	30.0	0.0*	7.0	9.0	12.1	15.9	0.0*	-10.4	59.3	135.5	172.2	0.0*	-0.1	2.2	3.5	4.6	0.0	.123	.400	2.46
1.11	10	-4.2	7.5	8.9	16.9	43.2	4.6	5.8	7.3	12.8	23.0	-1.0	23.4	24.6	52.1	156.9	0.0	2.4	4.1	5.5	6.8	.117	.388	2.42
9/5																								
2.01	02	2.9	4.8	7.0	9.8	13.6	2.0	5.7	7.5	13.4	23.2	3.9	15.8	23.6	31.0	46.8	0.2	1.8	2.4	3.3	4.0	.049	.229	1.89
2.02	03	1.7	8.7	6.3	8.8	0.0*	4.9	6.9	11.2	18.1	0.0*	-5.4	27.6	39.8	44.8	0.0*	0.3	2.1	2.9	4.0	0.0*	.063	.257	2.07
2.03	04	-2.3	9.7	10.1	21.1	0.0*	6.1	7.9	8.3	15.0	0.0*	-4.4	21.1	34.5	73.7	0.0*	0.3	1.5	1.8	2.5	0.0*	.074	.289	2.25
2.04	05	4.6	18.8	42.5	74.3	0.0*	6.1	6.7	8.8	15.3	0.0*	-5.3	35.2	63.4	172.4	0.0*	0.3	1.5	1.9	2.6	0.0*	.078	.299	2.26
2.05	06	-1.6	10.2	8.7	12.8	0.0*	8.0	9.3	12.3	18.8	0.0*	-8.1	24.8	32.3	38.8	0.0*	0.1	1.9	2.4	3.4	0.0*	.083	.312	2.26
2.06	07	-2.7	3.1	4.3	6.7	12.2	6.4	5.8	7.1	10.4	20.7	-3.3	10.1	16.1	22.6	35.3	0.1	1.0	2.6	3.7	5.2	.083	.313	2.22
9/7																								
3.01									← NO RECORD →													.055	.268	1.95
3.02	02	-1.5	2.7	4.1	5.9	9.1	5.4	4.7	6.4	9.9	16.3	-3.4	9.0	15.7	21.0	28.8	0.1	1.8	2.9	3.9	5.3	.065	.278	2.07
3.03	03	-2.6	2.3	3.5	4.9	7.4	6.5	4.8	6.3	9.3	14.1	-3.8	9.3	16.9	22.1	29.5	0.1	1.9	3.1	4.1	5.7	.067	.281	2.10
3.04	04	-4.9	8.3	11.2	13.7	0.0*	11.6	10.5	16.0	21.9	0.0*	-9.7	49.4	142.0	0.0**	0.0*	-0.1	2.5	4.0	6.5	0.0*	.073	.290	2.15
3.05	05	-2.2	4.7	5.3	10.3	48.3	5.1	5.7	6.6	11.0	26.1	-2.6	17.4	30.7	50.3	155.5	-0.1	2.0	3.3	4.2	5.4	.083	.318	2.27
3.06	06	-1.2	2.6	3.8	5.4	7.1	2.6	3.6	4.7	7.3	13.5	2.8	10.1	17.2	23.6	38.8	-0.0	1.9	3.0	4.2	5.7	.085	.332	2.33
3.07	07	0.5	3.9	4.7	8.0	13.2	2.3	3.4	3.7	7.4	14.4	2.6	14.5	21.7	32.0	0.0*	-0.1	1.9	3.0	4.1	4.9	.086	.336	2.34
3.08	08	-2.7	3.0	4.4	6.1	8.6	4.6	5.6	7.9	11.5	17.9	-0.8	12.8	23.3	29.2	37.3	-0.1	2.0	3.4	4.4	5.4	.089	.350	2.35
3.09	09	-1.4	3.8	5.4	8.5	16.1	3.6	6.4	8.1	13.3	27.1	-1.6	16.6	29.3	37.4	61.5	-0.2	2.4	4.0	5.3	6.9	.090	.348	2.33

* Model oscillates less than one hundred times before capsizing
** Model oscillates less than ten times before capsizing

TABLE D-VI

Statistical Results from Measured Model Data 1972 (cont.)

DATE & RUN NO.	Seq No. Cal	1. YAW DEGREES MEAN	RMS	1/3	1/10	1/100	2. RUDDER, DEGREES MEAN	RMS	1/3	1/10	1/100	3. ROLL, DEGREES MEAN	RMS	1/3	1/10	1/100	4. PITCH, DEGREES MEAN	RMS	1/3	1/10	1/100	5. SEAWAY (Interpolated) η^2 Ft^2	$h_{1/3}$ Ft	$\bar{T}$ Sec.
		of ordinates		highest amplitude			of ordinates		highest amplitude			of ordinates		highest amplitude			of ordinates		highest amplitude					
9/11																								
4.01	02	-0.3	2.6	4.0	5.4	7.6	1.5	2.3	2.8	4.9	8.4	3.9	10.1	16.9	22.4	29.6	-0.2	1.1	1.4	1.9	2.8	.045	.232	1.75
4.02	03	-2.4	9.3	12.3	24.1	0.0*	4.5	7.4	7.3	11.0	16.6	0.6	24.1	42.6	90.2	0.0*	-0.1	1.3	1.6	2.3	3.1	.052	.268	1.83
4.03	04	0.2	8.2	5.2	8.6	0.0*	2.9	7.0	8.4	16.7	0.0*	-5.7	17.8	28.7	50.0	0.0*	-0.2	1.0	1.4	1.6	0.0*	.067	.291	1.85
4.04	05	0.3	2.0	10.6	30.4	0.0*	2.5	4.5	3.6	7.0	0.0*	-5.3	25.3	45.9	165.3	0.0*	0.0	1.4	1.8	2.7	0.0*	.064	.289	1.84
4.05	06	-2.1	4.5	3.9	6.9	26.9	2.4	5.8	4.3	8.6	38.4	-0.1	12.7	17.9	25.8	42.2	-0.1	1.2	1.4	1.9	2.6	.060	.287	1.82
4.06	07	-3.9	8.3	5.8	8.8	0.0*	6.1	6.5	7.2	11.6	0.0*	-9.0	22.3	27.9	39.3	0.0*	-0.1	1.3	1.8	2.5	0.0*	.059	.283	1.84
4.07	08									← NO RECORD →												.060	.280	1.88
4.08	09	-2.4	2.4	3.5	5.0	8.0	4.3	4.3	5.3	7.5	14.1	-1.8	11.7	18.7	25.1	35.5	-0.2	1.5	1.8	2.5	3.8	.063	.275	1.95
4.09	10	-3.7	10.2	6.0	7.2	0.0*	6.1	8.8	6.8	10.9	0.0*	-10.5	24.3	32.7	0.0**	0.0*	-0.3	1.2	1.6	2.6	0.0*	.066	.273	2.03
4.10	11	-1.5	5.6	4.4	7.0	12.1	3.4	5.0	5.8	10.0	16.7	-2.1	14.8	21.1	30.0	0.0*	-0.1	1.5	1.9	2.8	4.2	.068	.278	2.06
4.11	12	-2.3	4.5	8.3	9.0	0.0*	5.3	7.1	9.1	14.2	0.0*	-4.7	35.7	60.9	129.0	0.0*	-0.1	1.8	2.2	2.8	0.0*	.069	.283	2.10
4.12	13	-2.2	4.9	3.5	4.8	5.8	3.8	4.7	4.8	7.6	11.1	-1.3	12.7	20.4	28.8	0.0*	-0.2	1.9	2.5	3.4	5.1	.071	.286	2.13
9/13																								
5.01	02	0.4	3.7	5.7	7.8	11.9	2.7	4.4	5.0	9.1	22.5	2.5	10.9	18.0	24.0	42.6	0.1	1.1	1.4	2.0	2.8	.059	.258	1.79
5.02	03	0.1	13.2	13.1	33.2	123.6	4.9	8.0	8.8	18.5	74.6	-2.6	23.7	39.0	82.4	160.6	0.3	2.5	2.2	4.5	30.6	.064	.270	1.83
9/18																								
6.01	02	0.1	3.4	5.0	7.2	10.1	3.3	4.5	5.7	9.8	18.3	1.6	12.4	20.6	27.4	39.3	0.2	1.2	1.6	2.3	3.3	.035	.193	1.83
6.02	03	-1.1	3.4	4.3	5.5	0.0*	5.0	4.5	5.9	9.4	18.0	-2.6	15.4	22.2	28.4	0.0*	0.3	1.3	1.7	2.4	0.0*	.038	.202	1.85
6.03	04	-0.6	4.4	6.2	8.7	0.0*	4.5	6.5	6.2	9.5	0.0*	-3.9	22.5	30.3	37.2	0.0*	0.2	1.7	2.3	2.3	0.0*	.040	.206	1.86
9/21																								
7.01	02	1.2	4.8	6.4	9.3	18.0	3.1	5.3	5.9	11.2	28.6	5.2	15.4	24.2	31.0	48.3	0.3	0.9	1.2	1.8	2.5	.029	.183	1.80
7.02	03	0.9	6.8	7.5	12.9	51.2	2.9	6.2	7.3	13.9	41.3	1.6	16.9	26.5	35.4	69.6	0.2	1.2	1.6	2.3	4.8	.043	.215	2.00
7.03	04	2.7	6.6	8.0	11.7	0.0*	2.5	9.7	12.6	20.9	0.0*	5.1	26.4	35.3	0.0**	0.0*	0.4	1.8	2.4	3.0	0.0*	.050	.232	2.06
7.04	05	0.0	3.5	6.1	8.3	0.0*	3.2	4.5	6.1	10.1	0.0*	1.2	25.1	34.6	51.5	0.0*	0.2	1.4	2.0	2.7	0.0*	.053	.241	2.08
7.05	06									← NO RECORD →												.056	.248	2.11
7.06	07	3.1	10.4	5.2	6.5	0.0*	0.2	6.5	4.9	7.1	0.0*	4.0	18.1	28.3	31.7	0.0*	0.3	1.6	2.1	2.7	0.0*	.057	.250	2.12
7.07	08	6.1	11.5	7.1	9.2	0.0*	3.6	8.2	7.0	14.5	0.0*	12.8	21.3	19.4	23.6	0.0*	1.5	1.6	2.0	2.8	0.0*	.051	.236	2.07
7.08	09	0.6	4.0	5.8	8.9	13.9	4.3	4.8	6.0	10.0	19.4	4.1	17.8	26.5	47.5	151.7	0.6	1.2	1.5	2.1	2.8	.040	.210	2.01

* Model oscillates less than one hundred times before capsizing
** Model oscillates less than ten times before capsizing

TABLE D-VI

Statistical Results from Measured Model Data 1972 (cont.)

DATE & RUN NO.	Seq No. Cal	1. YAW DEGREES MEAN of ordinates	RMS	1/3 highest amplitude	1/10	1/100	2. RUDDER, DEGREES MEAN of ordinates	RMS	1/3 highest amplitude	1/10	1/100	3. ROLL, DEGREES MEAN of ordinates	RMS	1/3 highest amplitude	1/10	1/100	4. PITCH, DEGREES MEAN of ordinates	RMS	1/3 highest amplitude	1/10	1/100	5. SEAWAY (Interpolated) $\overline{\eta^2}$ Ft²	$\eta_{1/3}$ Ft	$\overline{T}$ Sec.
9/25																								
8.01									← NO RECORD →															
8.02	03	-2.9	9.3	5.6	0.0**	0.0*	2.5	3.7	5.1	6.5	0.0*	8.8	23.5	35.0	0.0**	0.0*	0.1	1.0	1.2	1.5	0.0*	.053	.251	1.74
8.03	04	-2.3	3.5	3.6	4.4	0.0*	3.2	5.2	6.0	9.0	0.0*	1.3	19.5	31.4	40.3	0.0*	0.0	1.2	1.8	2.2	0.0*	.053	.249	1.75
8.04	05	1.7	4.1	3.7	5.2	0.0*	-1.1	4.6	6.3	11.7	0.0*	9.4	20.4	27.3	31.8	0.0*	0.0	1.2	1.6	1.9	0.0*	.053	.245	1.78
8.05	06	-2.5	6.3	5.4	8.9	15.4	3.6	6.7	7.2	12.3	21.2	-7.7	21.5	31.2	36.4	0.0*	-0.1	1.3	1.6	2.3	3.4	.050	.230	1.86
8.06	07	-2.7	4.5	7.1	9.0	0.0*	5.2	7.5	13.1	15.8	0.0*	-9.2	24.1	32.0	42.0	0.0*	-0.2	2.1	2.9	3.2	0.0*	.047	.222	1.87
8.07	08	-2.7	6.2	6.6	13.0	74.7	3.6	6.1	7.1	10.8	15.3	-4.4	20.3	30.0	36.8	0.0*	-0.2	1.4	1.8	2.6	3.5	.043	.214	1.90
8.08	09	-2.9	5.0	5.3	7.7	0.0*	3.6	7.0	7.7	11.9	24.5	-3.5	19.0	31.5	36.4	0.0*	-0.2	1.8	2.2	3.2	4.5	.040	.202	1.92
8.09	10	-3.6	11.2	7.9	0.0**	0.0*	7.2	6.0	8.9	0.0**	0.0*	-19.1	22.1	26.8	0.0**	0.0*	-0.5	1.6	2.1	2.5	0.0*	.033	.187	1.96
8.10	11	-5.1	7.5	5.8	6.2	0.0*	5.5	8.6	8.2	10.3	0.0*	-5.6	19.2	24.2	29.9	0.0*	-0.2	1.2	1.5	2.2	0.0*	.030	.181	1.96
8.11	12	-3.0	8.3	12.3	34.1	0.0*	3.4	5.9	8.1	13.2	0.0*	-4.6	22.8	38.8	70.9	0.0*	-0.2	1.0	1.4	2.1	0.0*	.028	.178	1.96
8.12	13	-2.7	3.0	4.1	5.9	8.9	1.8	3.9	5.0	7.8	11.6	1.4	14.3	24.0	29.8	42.3	-0.3	0.9	1.1	1.6	2.5	.025	.162	1.96
9/27																								
9.01	02	-2.1	2.5	3.7	5.5	8.4	3.1	3.3	4.2	6.7	12.5	-2.4	10.9	18.7	22.9	27.7	-0.1	0.6	0.7	1.0	1.4	.023	.191	1.57
9.02	03	-1.9	3.4	4.9	7.3	12.1	3.4	4.6	5.9	9.8	17.7	-2.2	12.5	20.7	27.2	43.6	-0.2	0.8	1.1	1.5	2.2	.029	.200	1.63
9.03	04	-2.9	3.0	4.0	5.4	7.2	4.3	4.6	5.3	8.0	11.8	-3.3	14.5	22.4	27.7	32.8	-0.2	0.8	1.1	1.5	2.3	.035	.207	1.72
9.04	05	-2.0	3.9	5.2	8.3	19.7	3.5	5.8	6.3	10.4	22.3	-3.1	14.4	23.3	31.8	51.8	-0.2	0.9	1.2	1.7	2.2	.036	.206	1.74
9.05	06	-2.6	7.3	7.0	15.3	101.4	4.9	6.3	7.8	13.4	49.8	-3.7	18.7	30.9	54.0	158.8	-0.1	2.0	1.6	2.8	11.2	.034	.196	1.83
9.06	07	-2.3	4.5	4.4	7.8	31.5	3.4	5.0	5.7	8.4	13.6	-0.4	14.0	20.4	25.9	63.0	-0.2	0.9	1.2	1.8	2.7	.031	.186	1.88
10/3																								
10.01	02	-2.4	2.9	4.2	6.3	9.3	3.2	4.0	4.8	7.7	15.6	-4.1	12.2	20.2	26.8	39.7	0.0	0.8	1.0	1.5	2.2	.022	.168	1.78
10.02	03	-1.5	3.4	5.1	7.4	11.6	2.4	4.1	4.9	8.5	17.7	1.6	10.7	18.2	23.4	31.7	0.1	1.0	1.3	1.8	2.5	.036	.199	1.96
10.03	04	-1.0	3.4	5.2	7.4	10.2	2.6	4.5	5.1	9.0	19.6	0.7	11.6	19.2	24.8	35.1	0.0	1.4	1.8	2.5	3.5	.041	.214	2.05
10.04	05	-2.3	5.5	5.6	8.4	0.0*	5.2	7.1	7.6	12.6	19.4	-5.6	18.2	25.5	30.7	0.0*	0.1	1.7	2.3	3.0	3.2	.040	.213	2.05
10.05	06	-5.9	12.1	13.7	34.3	0.0*	9.5	11.2	16.7	26.5	0.0*	-6.8	30.2	31.7	43.1	0.0*	0.1	1.9	2.9	3.6	0.0*	.039	.212	2.04
10.06	07	-2.3	7.2	7.4	14.0	71.6	5.1	7.6	8.6	15.5	43.0	-3.6	20.7	39.2	74.9	160.4	0.0	2.2	2.3	3.5	10.1	.039	.211	2.04
10.07	08	-1.9	3.5	5.0	7.2	12.1	3.0	5.1	5.7	10.0	20.3	0.5	13.0	21.5	27.8	38.3	0.0	1.1	1.5	2.2	3.2	.044	[illegible]	2.03
10.08	09	-0.4	5.1	5.6	6.7	0.0*	2.7	8.1	10.9	20.2	0.0*	-5.3	22.0	30.9	37.8	0.0*	0.2	1.7	2.4	3.1	0.0*	.049	.232	2.01
10.09	10	-5.1	7.4	5.0	7.9	0.0*	5.9	7.5	6.9	9.0	0.0*	-10.1	19.1	22.0	23.9	0.0*	0.0	1.5	2.1	2.5	0.0*	.051	.236	2.01
10.10	11	-5.8	8.6	6.5	8.2	0.0*	5.9	9.8	12.3	22.4	0.0*	-7.4	19.4	25.2	34.5	0.0*	0.0	1.4	1.8	2.1	0.0*	.057	.249	1.99
10.11	12	-3.1	5.4	6.2	11.5	59.6	2.2	5.4	6.4	10.8	25.5	1.7	15.7	27.1	43.5	150.2	-0.1	1.2	1.7	2.4	3.6	.060	.258	1.98
10.12	13	-5.2	8.0	9.8	21.8	0.0*	4.7	9.3	10.9	18.9	0.0*	-6.2	26.1	45.0	78.8	0.0*	-0.3	1.6	2.4	3.3	0.0*	.066	.281	1.96
10.13	14	-3.7	4.6	5.7	9.3	0.0*	3.0	7.4	8.7	15.5	25.3	-4.2	19.4	30.3	42.6	0.0*	-0.2	1.6	2.2	2.9	3.9	.067	.275	1.95

* Model oscillates less than one hundred times before capsizing

** Model oscillates less than ten times before capsizing

APPENDIX E

SUMMARY OF MODEL RUNS AND SEASTATE INFORMATION FOR 1973 AND 1974

Figures E-1

SUMMARY OF MODEL RUNS AND SEASTATE INFORMATION VS. TIME OF RECORDS 1973 and 1974

Model runs are indicated by symbols:

GM No. - See Table A-I for the SL-7 Model.

SPEED - See Table A-I for the SL-7 Model.

COURSE F - Folowing seas (visual observation)

Q - Quartering seas

B - Beam seas

H - Head seas

1.01 - Experiment run number

- Model run without capsize:

vertical position corresponds to course and speed;

horizontal position indicates time of day;

horizontal length indicates duration of run.

- Model run with capsize.

Linear interpolutions of seaway measurements are indicated by lines:

——————— Significant wave height.

— — — Direction of spectrum peak.

SUMMARY OF MODEL RUNS AND SEASTATE INFORMATION

VS. TIME OF RECORDS - 1973 & 1974

SL-7 MODEL CONDITION: LIGHT DATE: 03 AUG 73

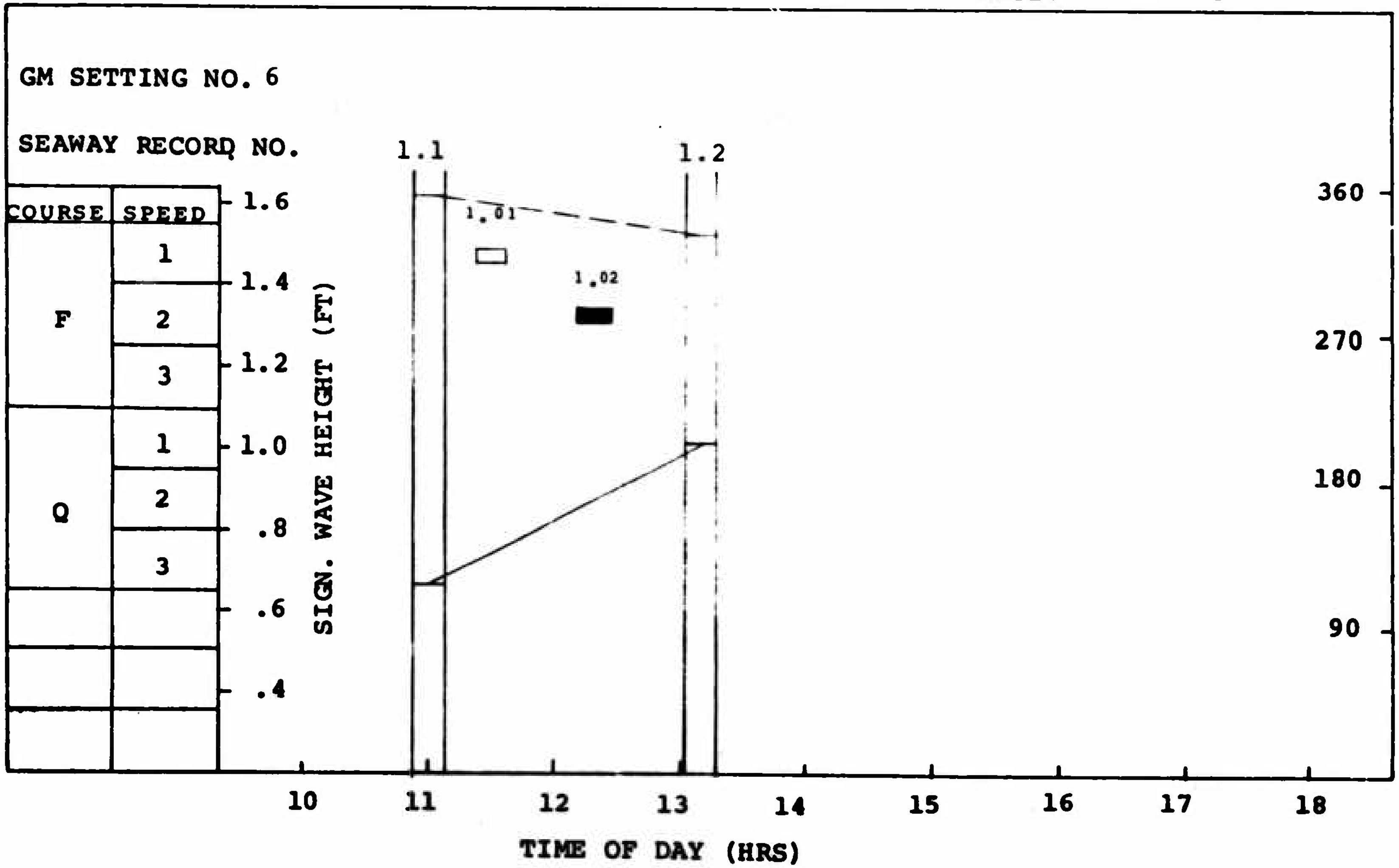

FIGURE E-1.1

SUMMARY OF MODEL RUNS AND SEASTATE INFORMATION

VS. TIME OF RECORDS - 1973 & 1974

SL-7 MODEL CONDITION: LIGHT DATE: 07 AUG 73

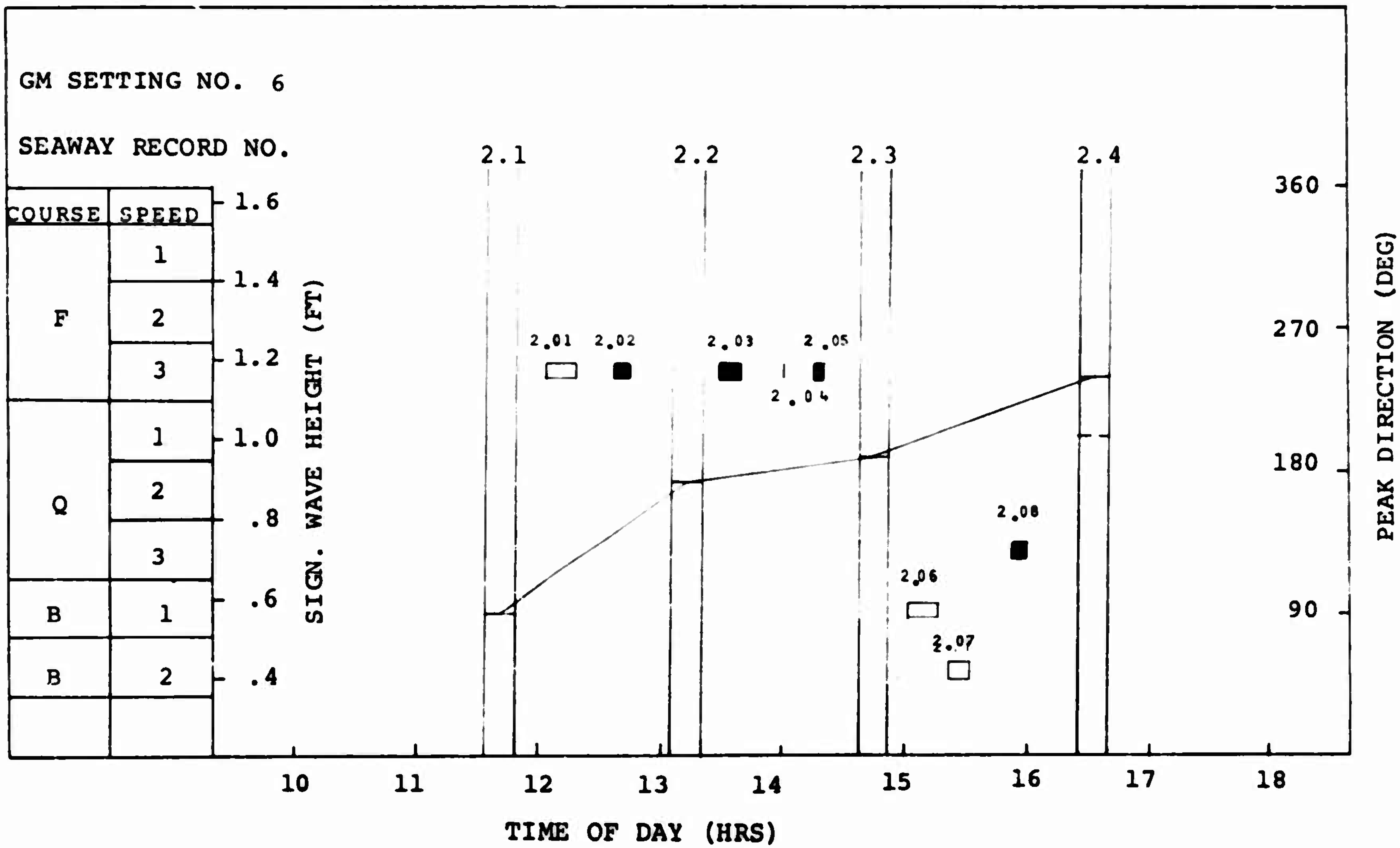

FIGURE E-1.2

SUMMARY OF MODEL RUNS AND SEASTATE INFORMATION

VS. TIME OF RECORDS - 1973 & 1974

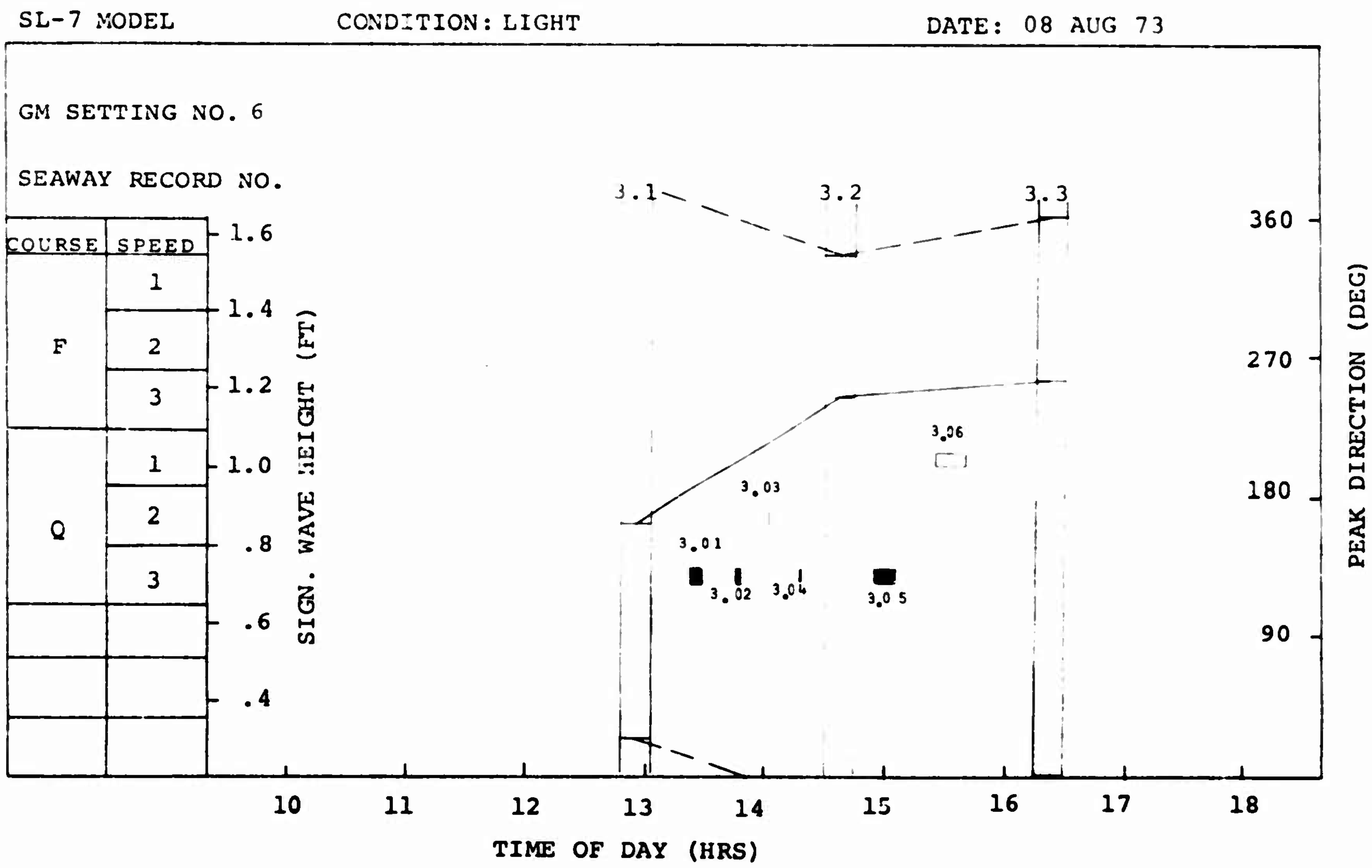

FIGURE E-1.3

SUMMARY OF MODEL RUNS AND SEASTATE INFORMATION

VS. TIME OF RECORDS - 1973 & 1974

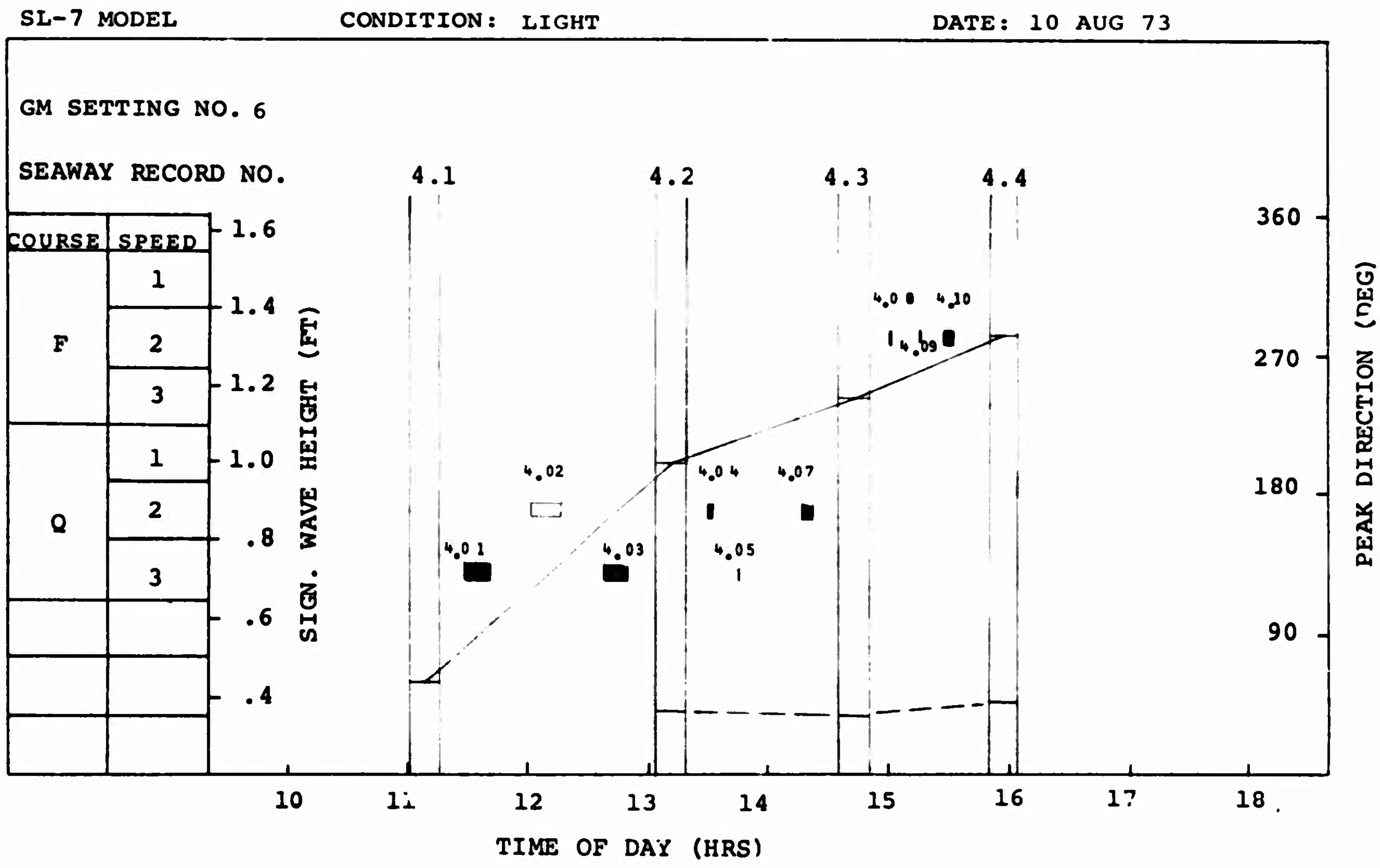

FIGURE E-1.4

SUMMARY OF MODEL RUNS AND SEASTATE INFORMATION

VS. TIME OF RECORDS - 1973 & 1974

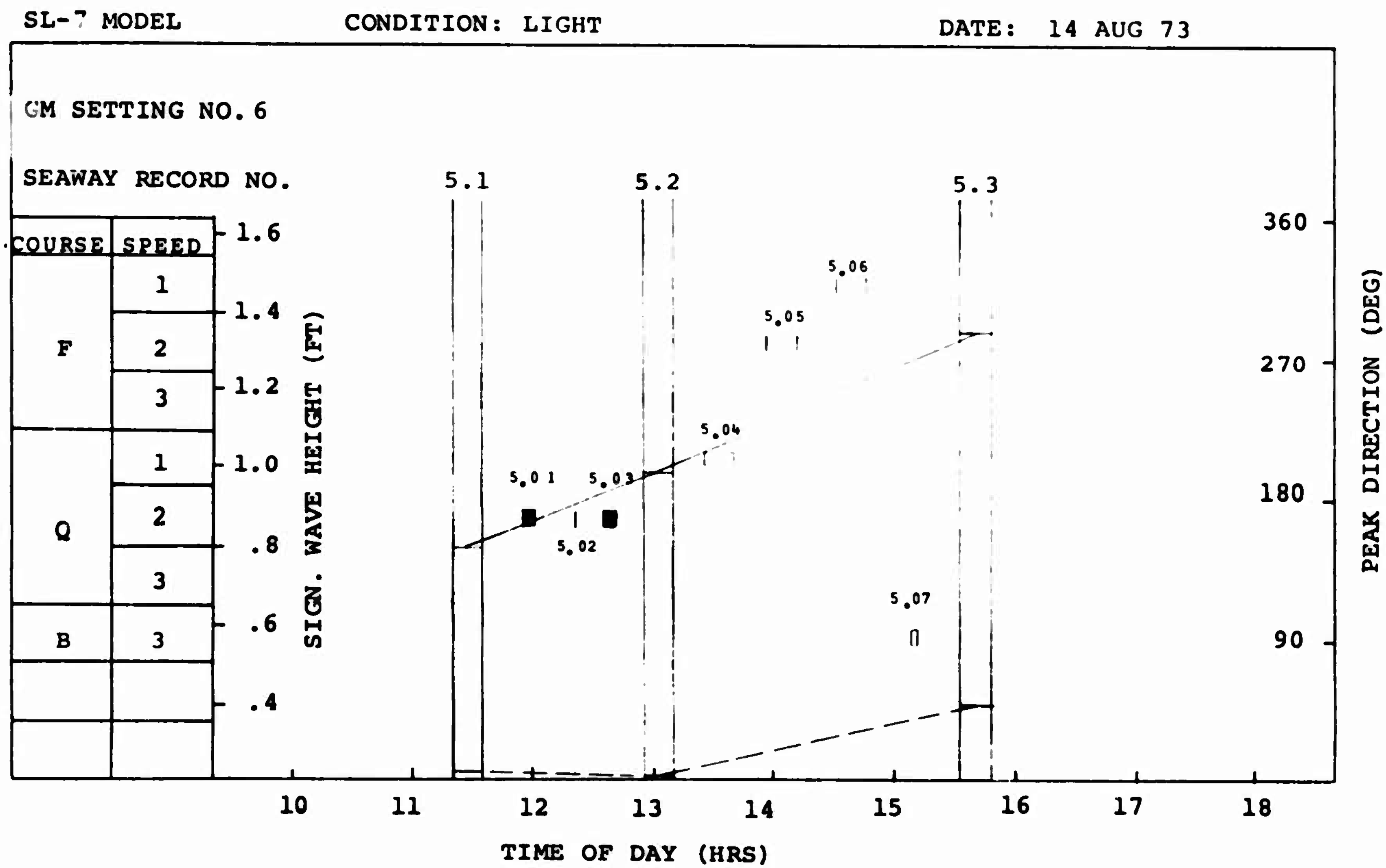

FIGURE E-1.5

SUMMARY OF MODEL RUNS AND SEASTATE INFORMATION

VS. TIME OF RECORDS - 1973 & 1974

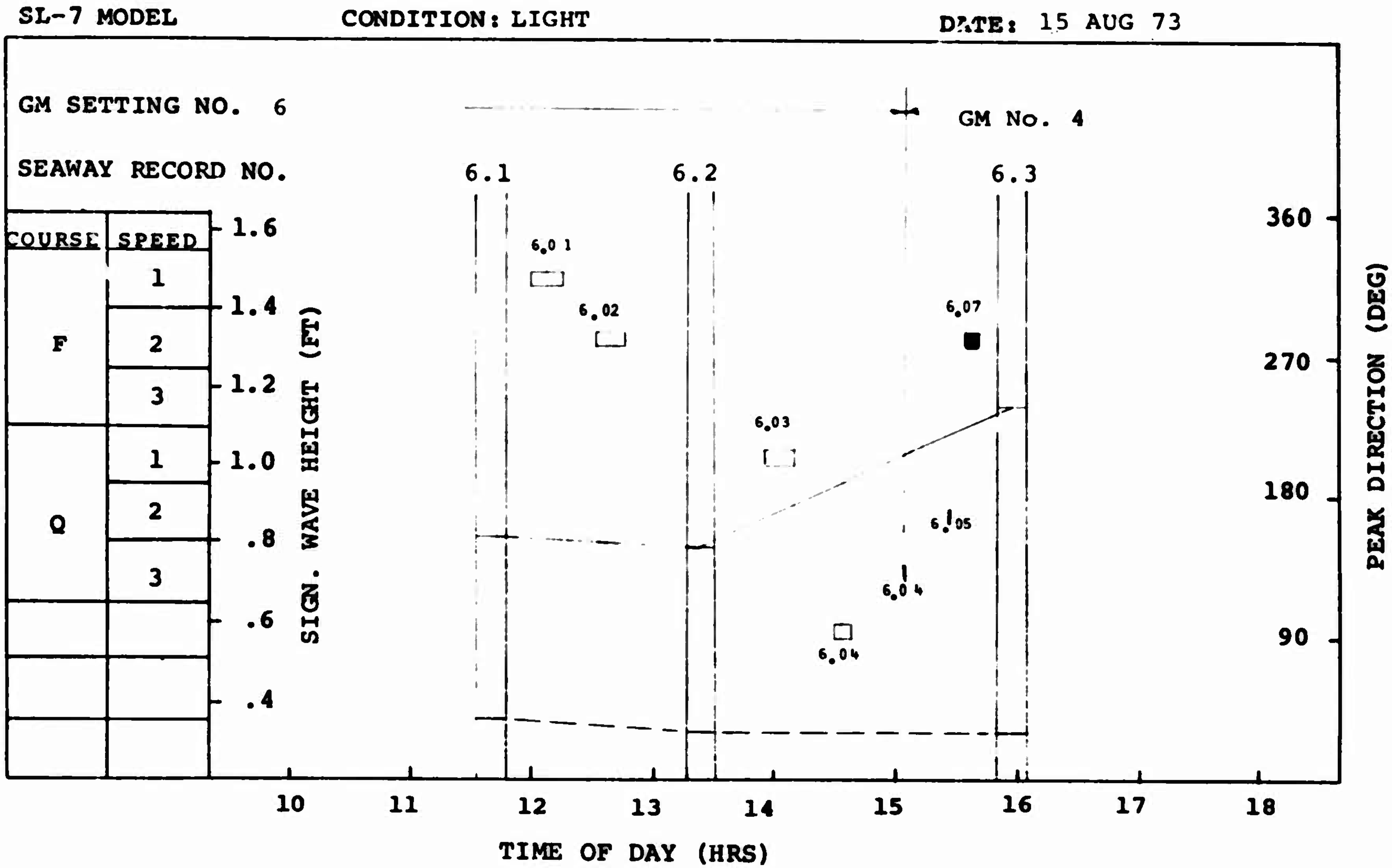

FIGURE E-1.6

SUMMARY OF MODEL RUNS AND SEASTATE INFORMATION

VS. TIME OF RECORDS - 1973 & 1974

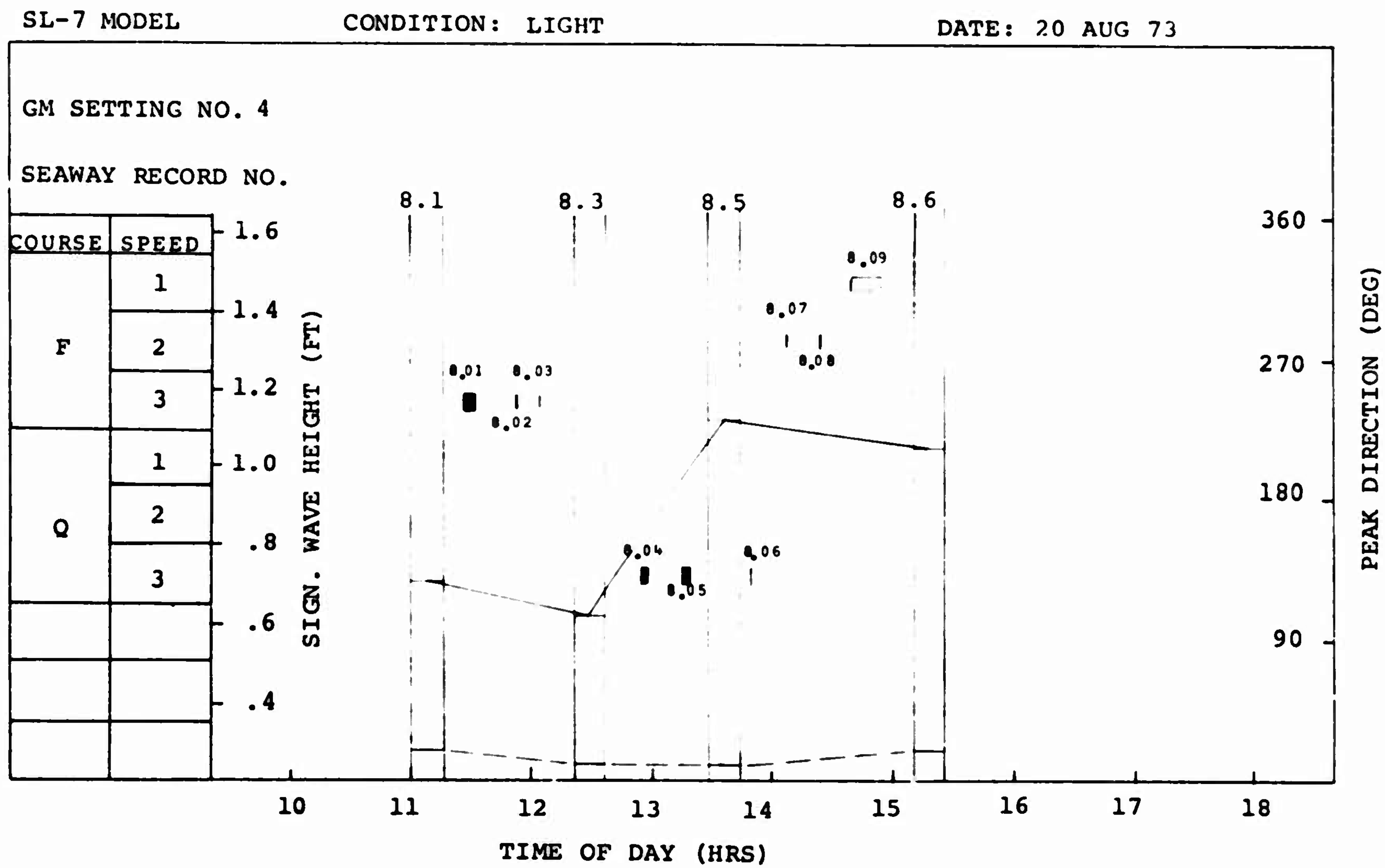

FIGURE E-1.7

SUMMARY OF MODEL RUNS AND SEASTATE INFORMATION

VS. TIME OF RECORDS - 1973 & 1974

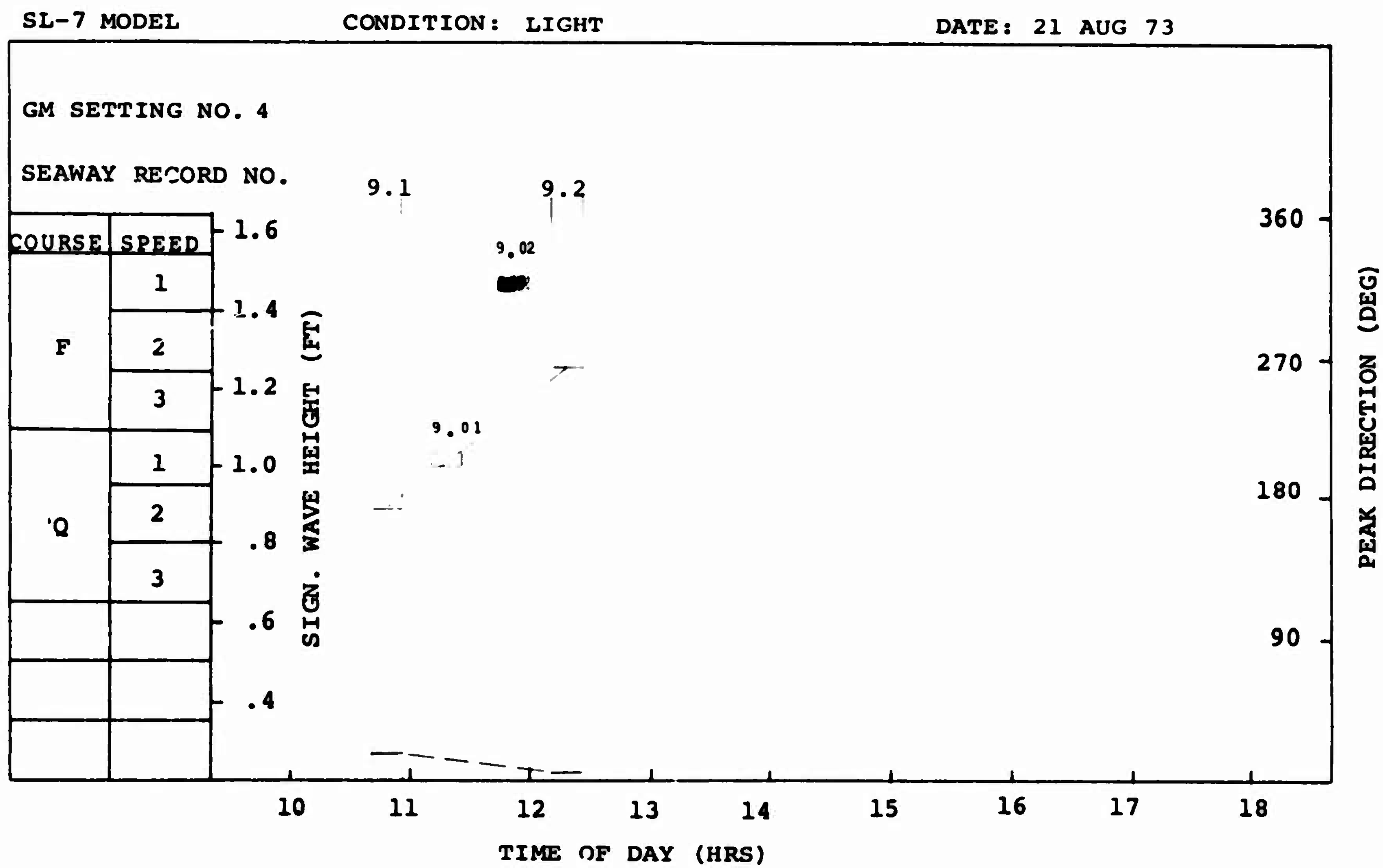

FIGURE E-1.8

SUMMARY OF MODEL RUNS AND SEASTATE INFORMATION

VS. TIME OF RECORDS - 1973 & 1974

SL-7 MODEL CONDITION: LIGHT DATE: 24 AUG 73

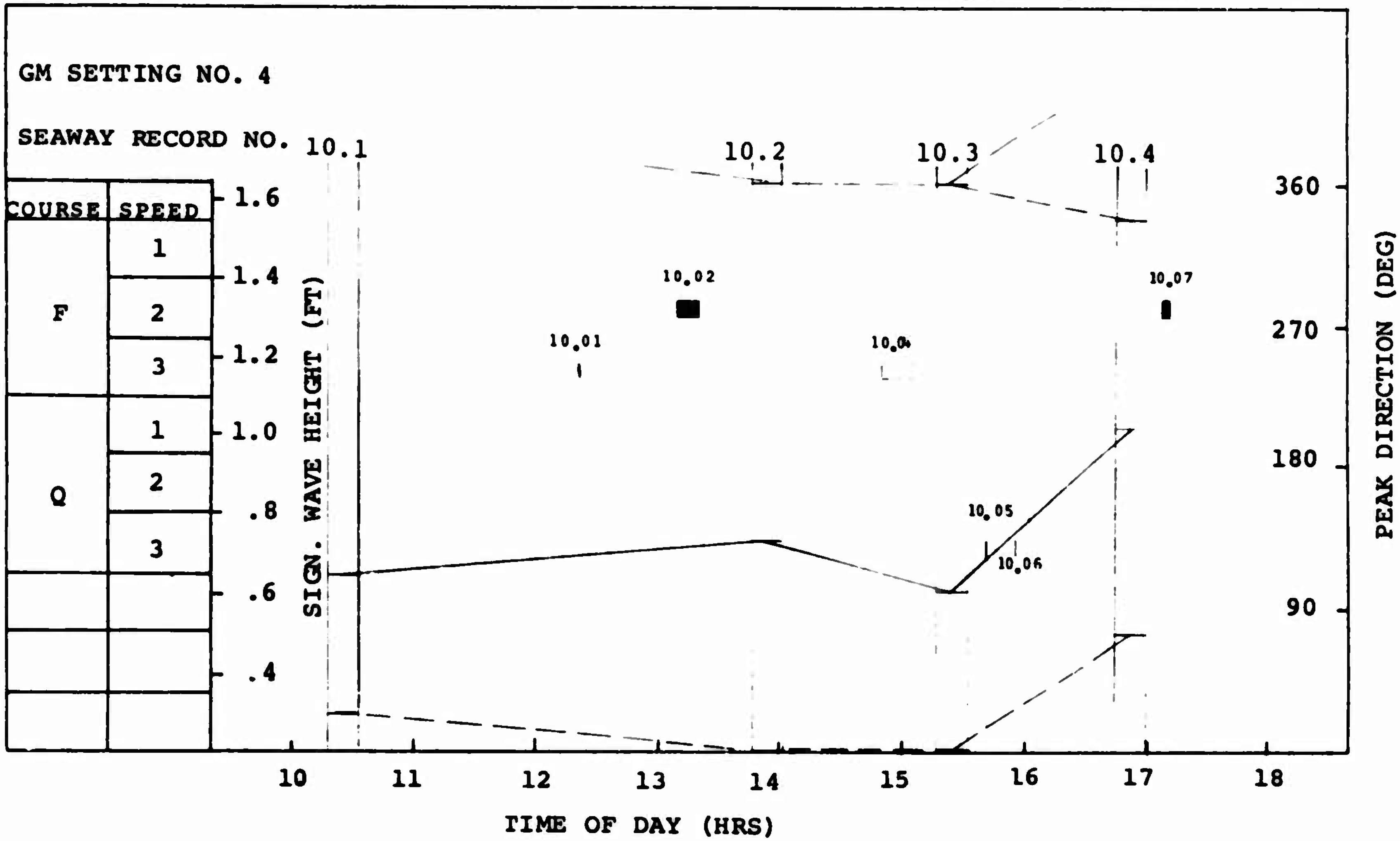

FIGURE E-1.9

SUMMARY OF MODEL RUNS AND SEASTATE INFORMATION

VS. TIME OF RECORDS - 1973 & 1974

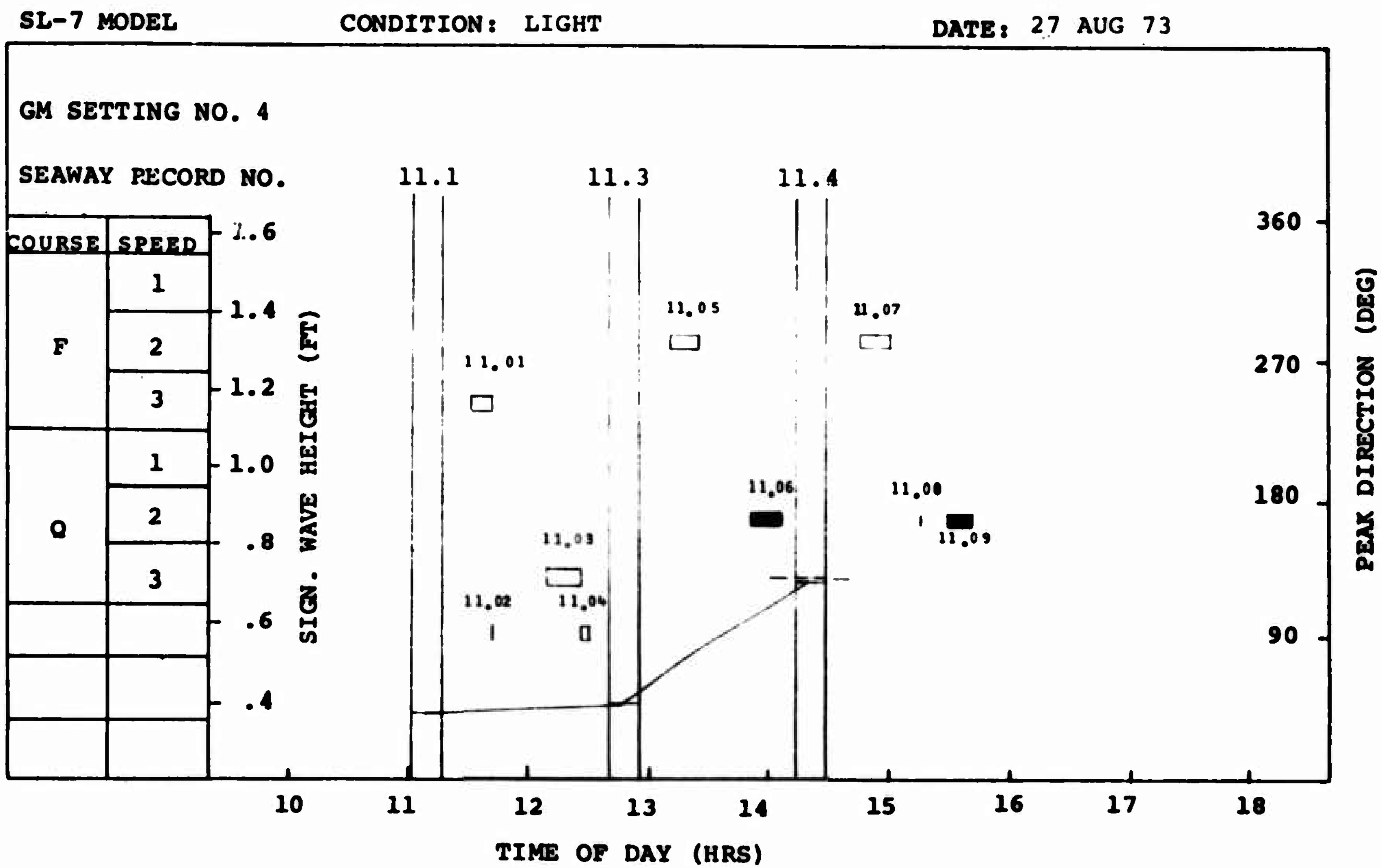

FIGURE E-1.10

SUMMARY OF MODEL RUNS AND SEASTATE INFORMATION

VS. TIME OF RECORDS - 1973 & 1974

SL-7 MODEL CONDITION: LIGHT DATE: 28 AUG 73

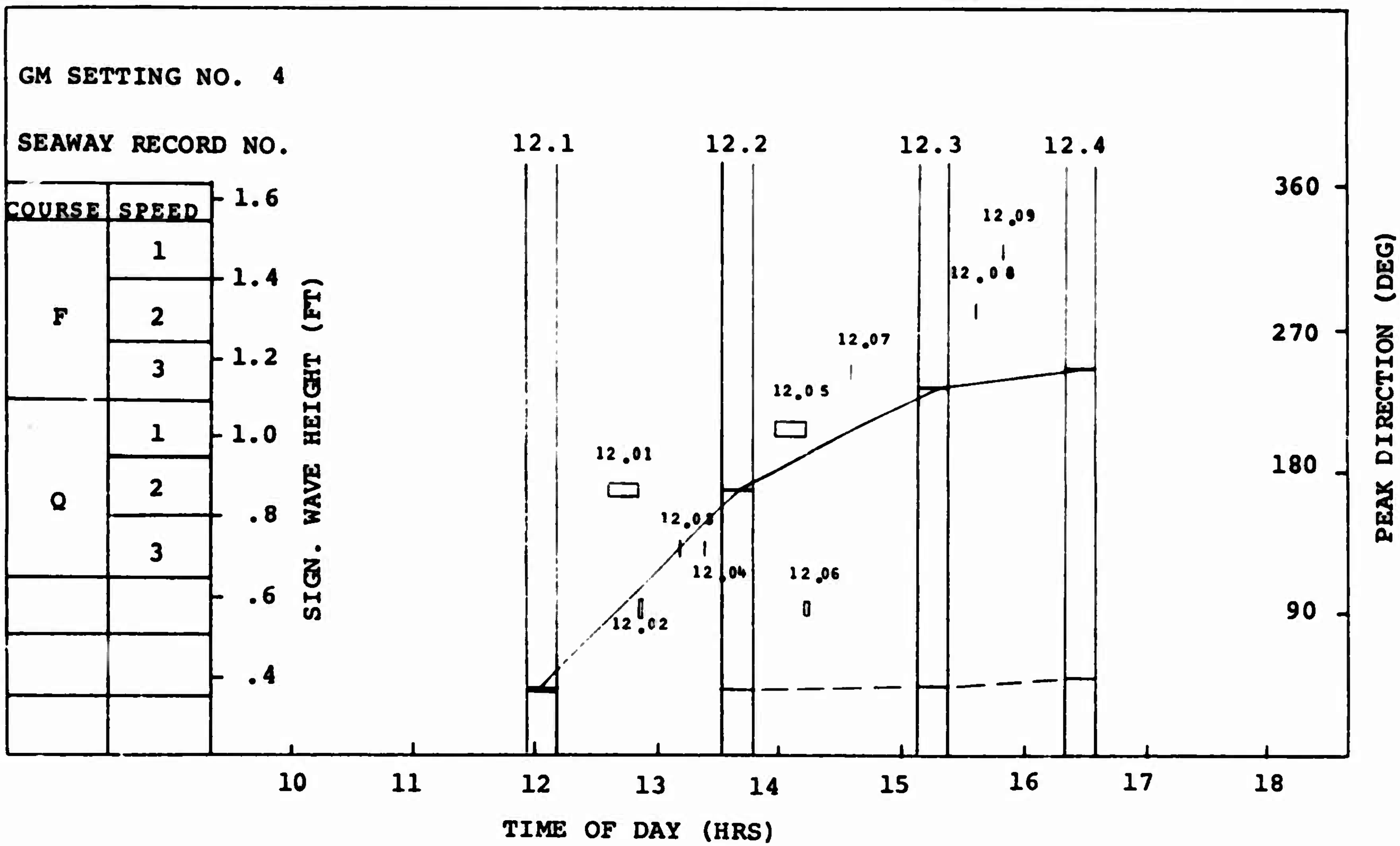

FIGURE E-1.11

SUMMARY OF MODEL RUNS AND SEASTATE INFORMATION

VS. TIME OF RECORDS - 1973 & 1974

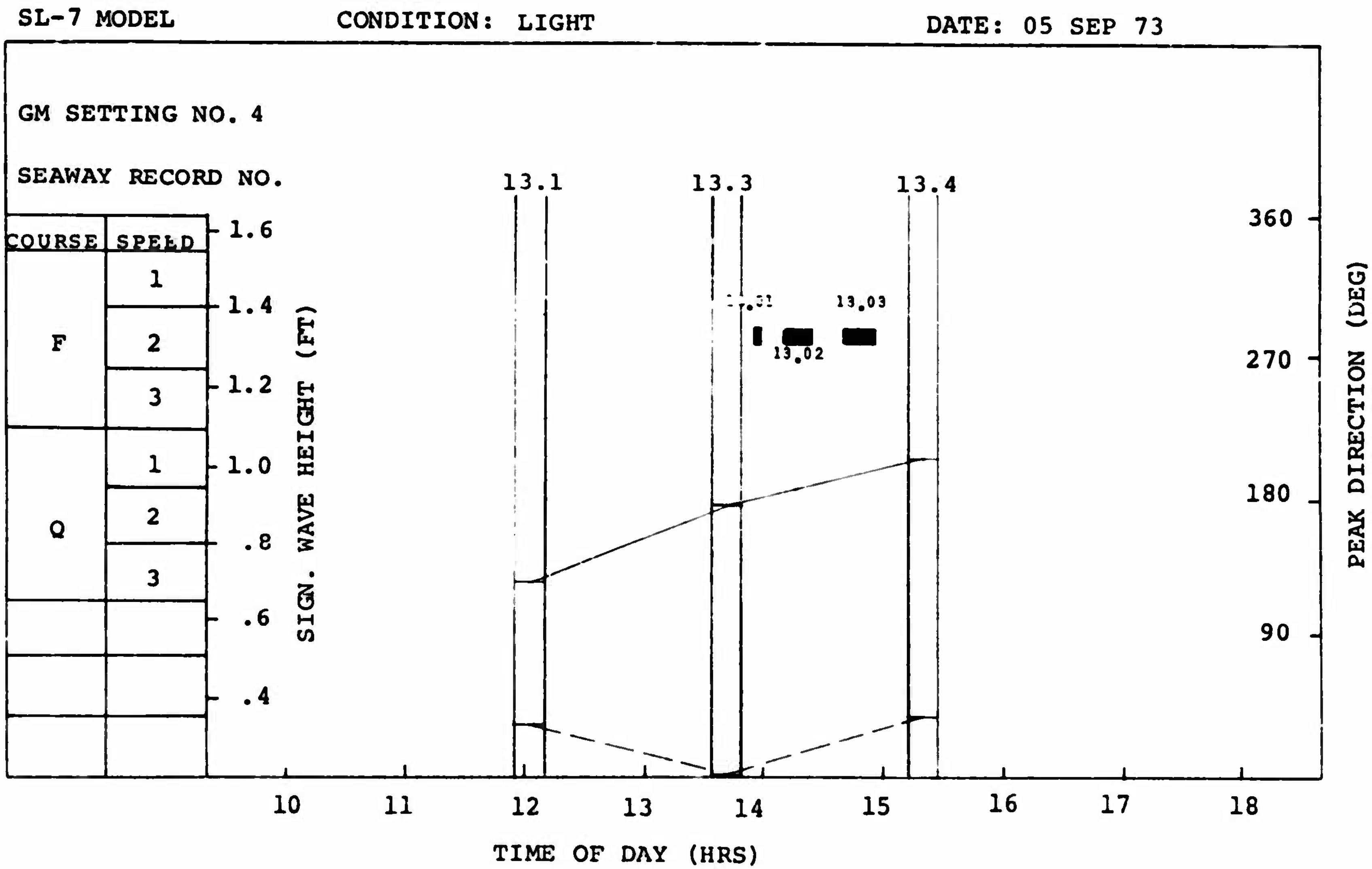

FIGURE E-1.12

SUMMARY OF MODEL RUNS AND SEASTATE INFORMATION

VS. TIME OF RECORDS - 1973 & 1974

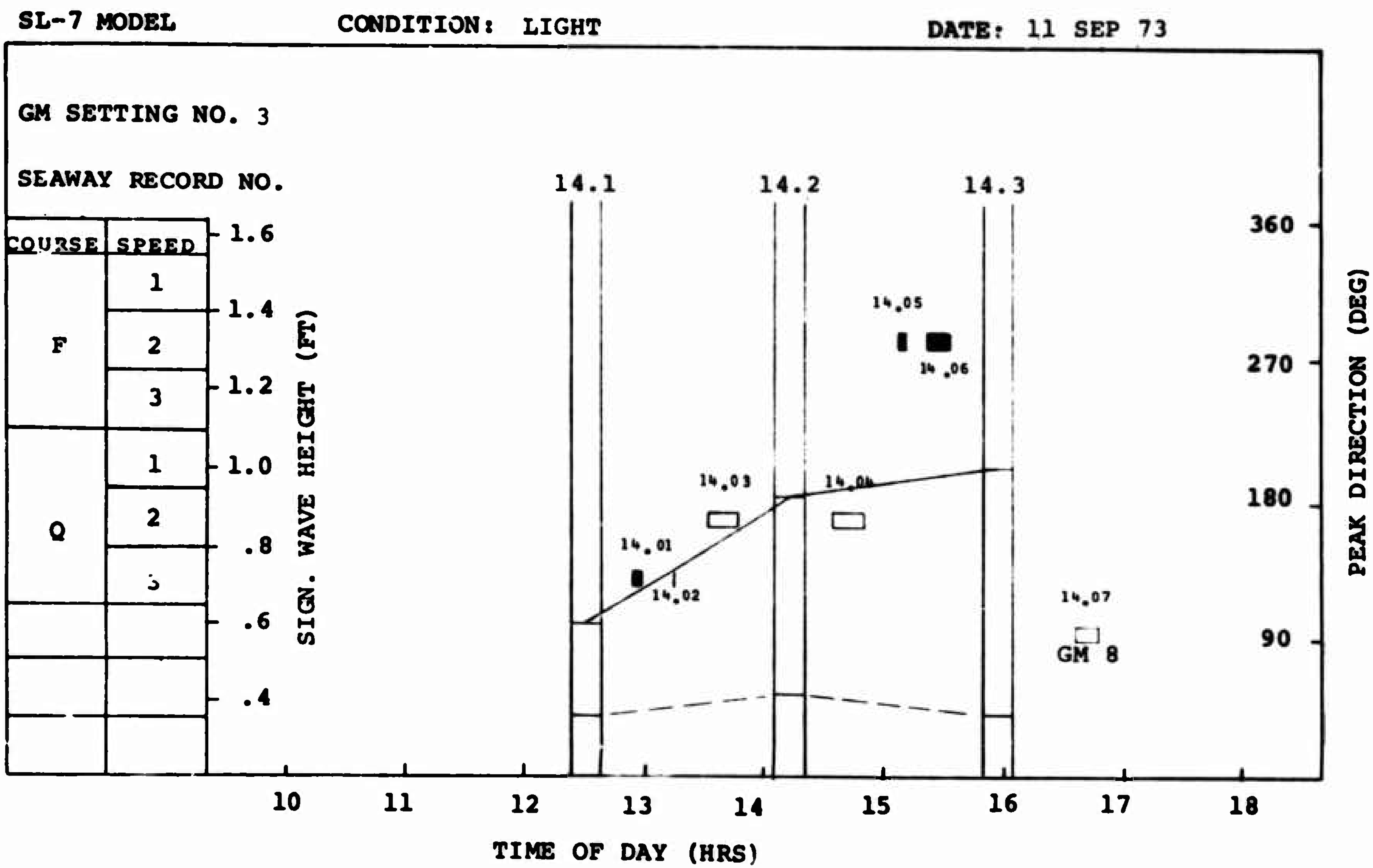

FIGURE E-1.13

SUMMARY OF MODEL RUNS AND SEASTATE INFORMATION

VS. TIME OF RECORDS - 1973 & 1974

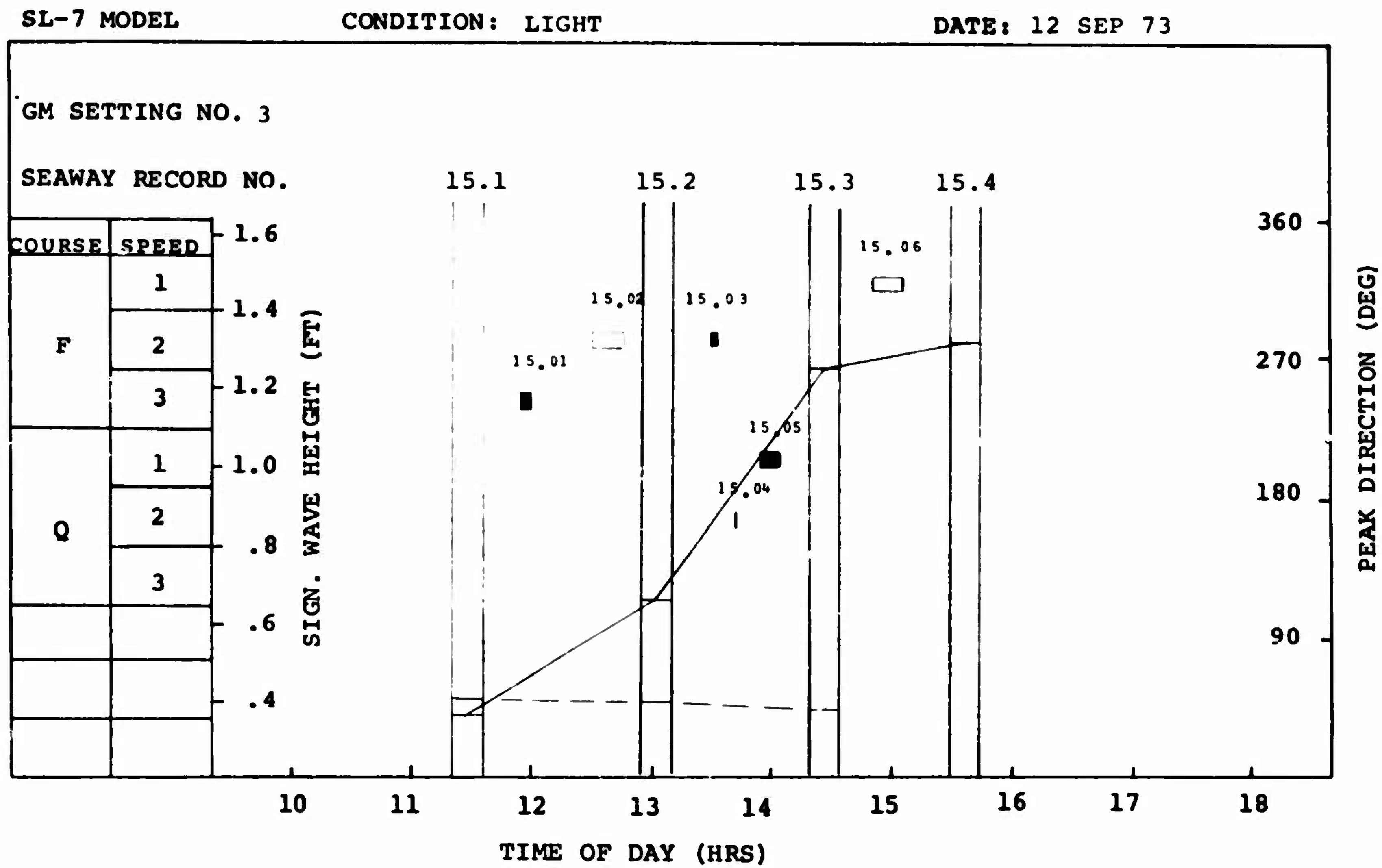

FIGURE E-1.14

SUMMARY OF MODEL RUNS AND SEASTATE INFORMATION

VS. TIME OF RECORDS - 1973 & 1974

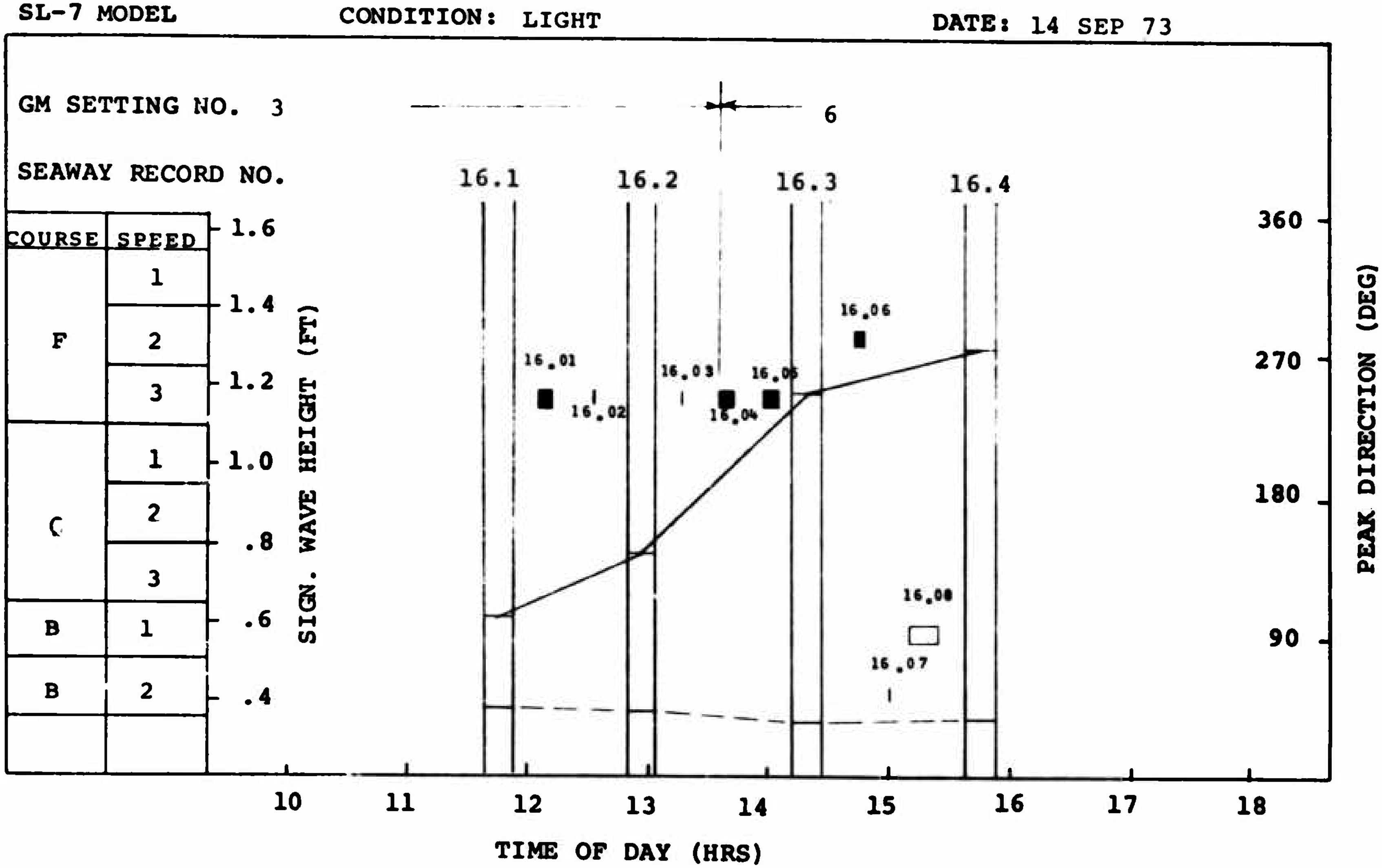

FIGURE E-1.15

SUMMARY OF MODEL RUNS AND SEASTATE INFORMATION

VS. TIME OF RECORDS - 1973 & 1974

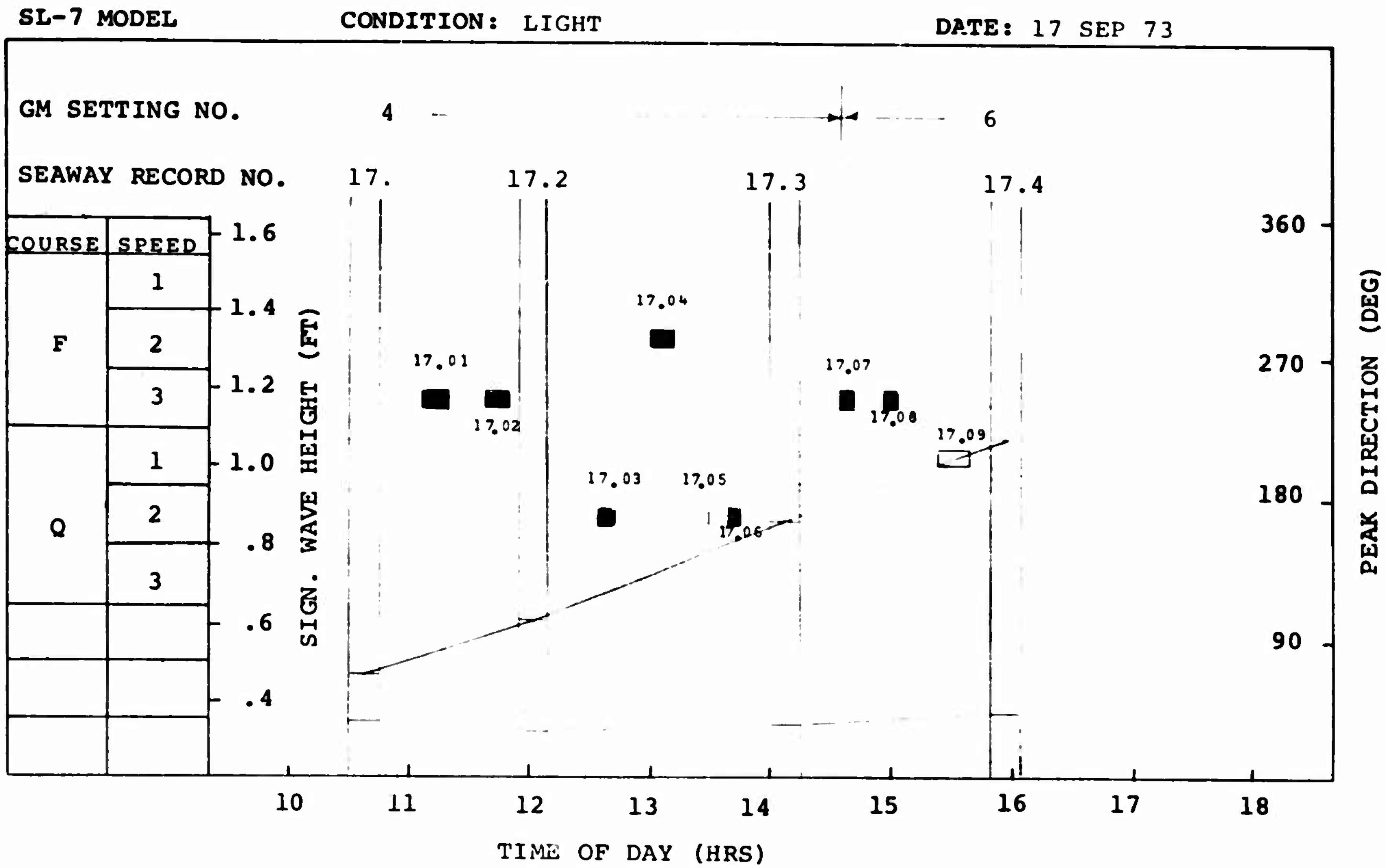

FIGURE E-1.16

SUMMARY OF MODEL RUNS AND SEASTATE INFORMATION

VS. TIME OF RECORDS - 1973 & 1974

SL-7 MODEL CONDITION: LIGHT DATE: 18 SEP 73

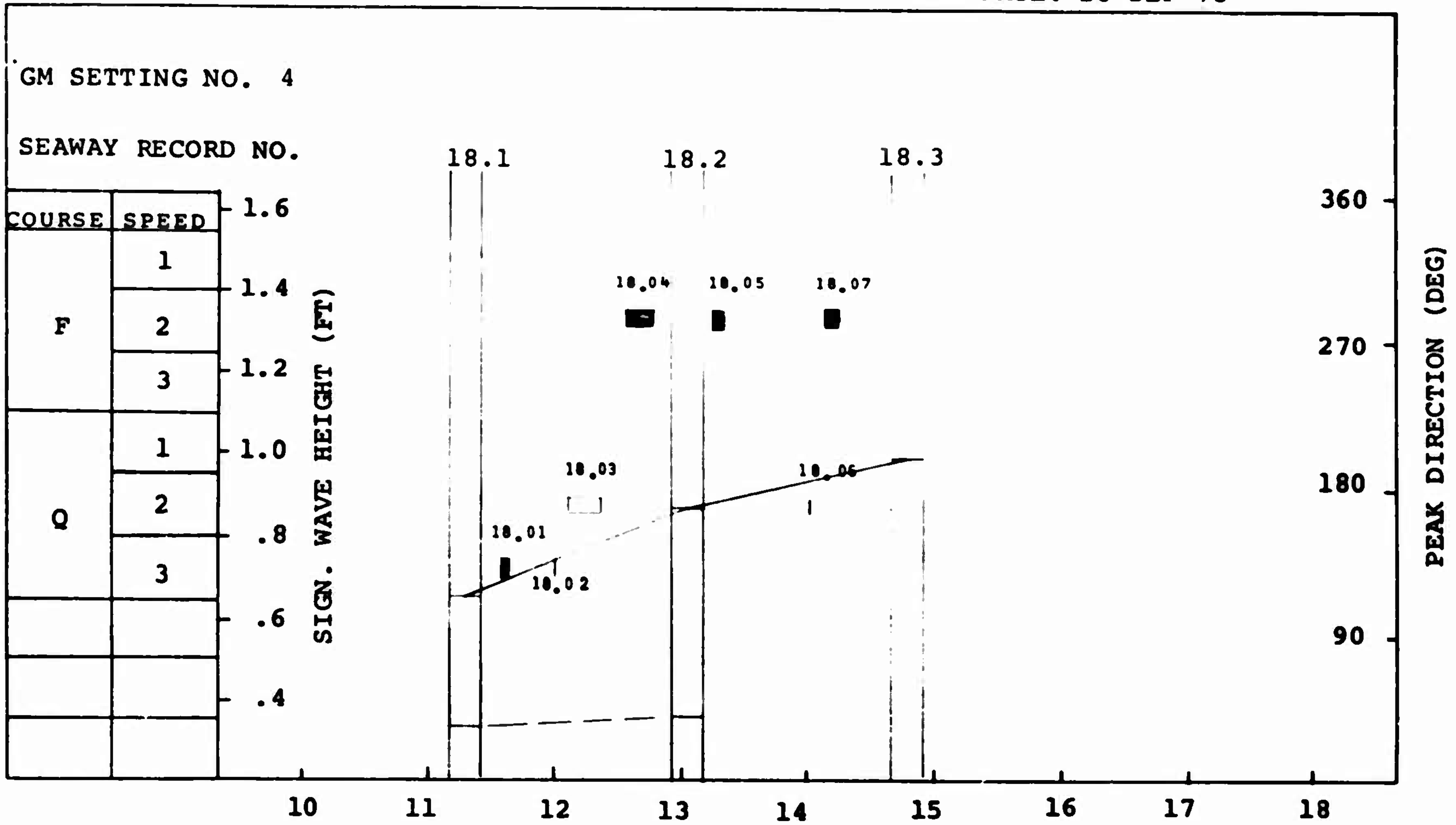

FIGURE E-1.17

SUMMARY OF MODEL RUNS AND SEASTATE INFORMATION

VS. TIME OF RECORDS - 1973 & 1974

SL-7 MODEL CONDITION: LIGHT DATE: 19 SEP 73

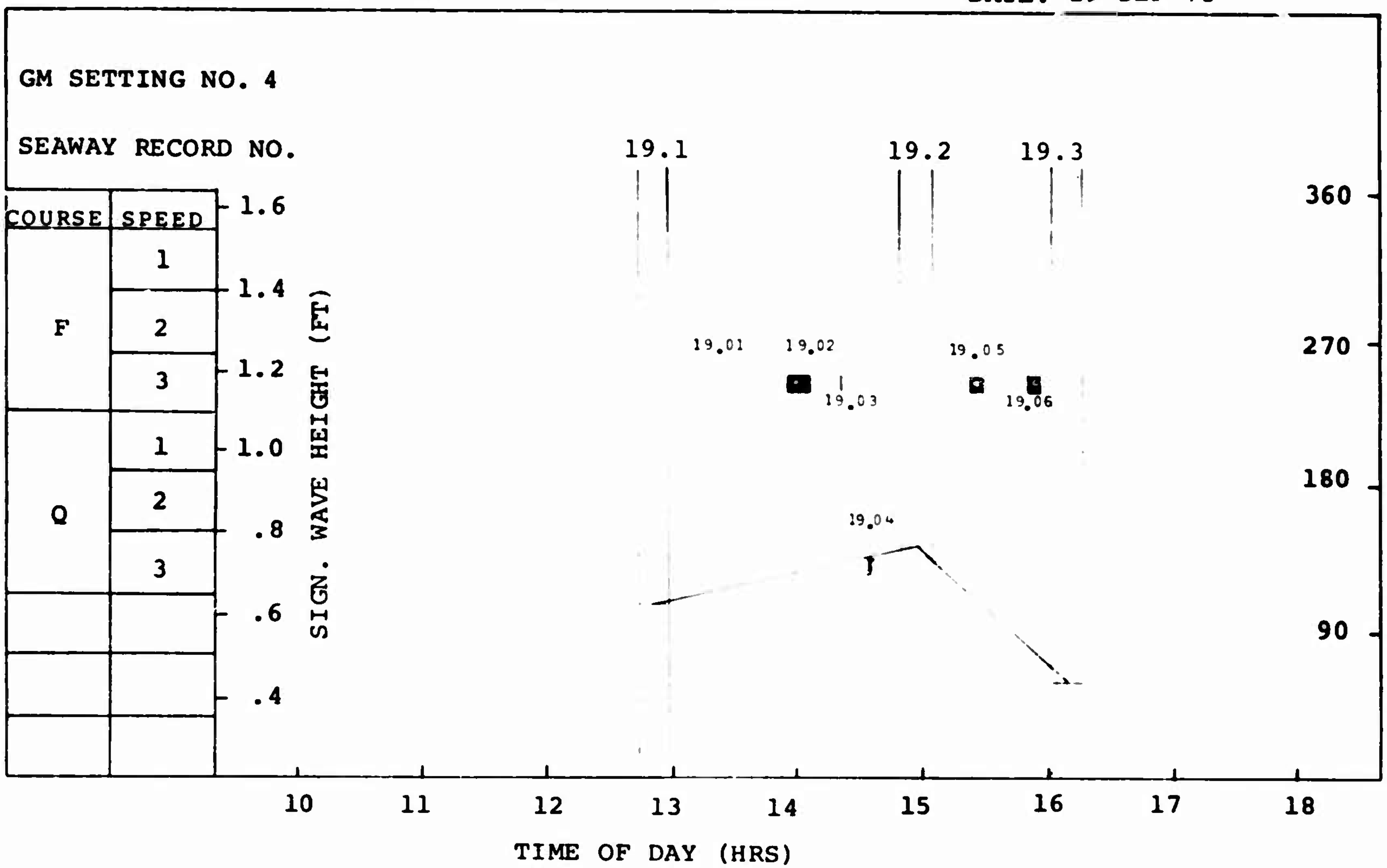

FIGURE E-1.18

SUMMARY OF MODEL RUNS AND SEASTATE INFORMATION

VS. TIME OF RECORDS - 1973 & 1974

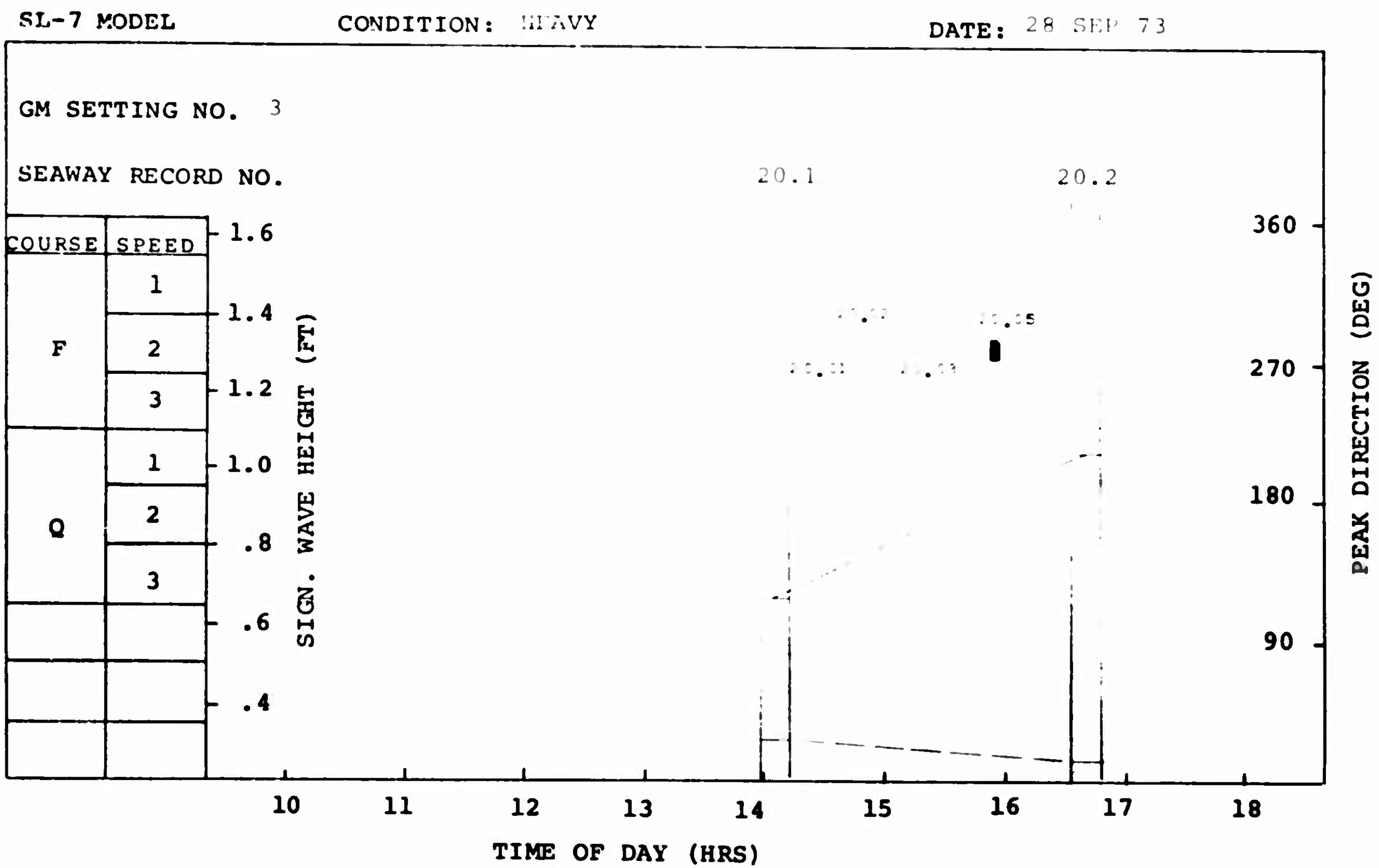

FIGURE E-1.19

SUMMARY OF MODEL RUNS AND SEASTATE INFORMATION

VS. TIME OF RECORDS - 1973 & 1974

SL-7 MODEL CONDITION: HEAVY DATE: 04 OCT 73

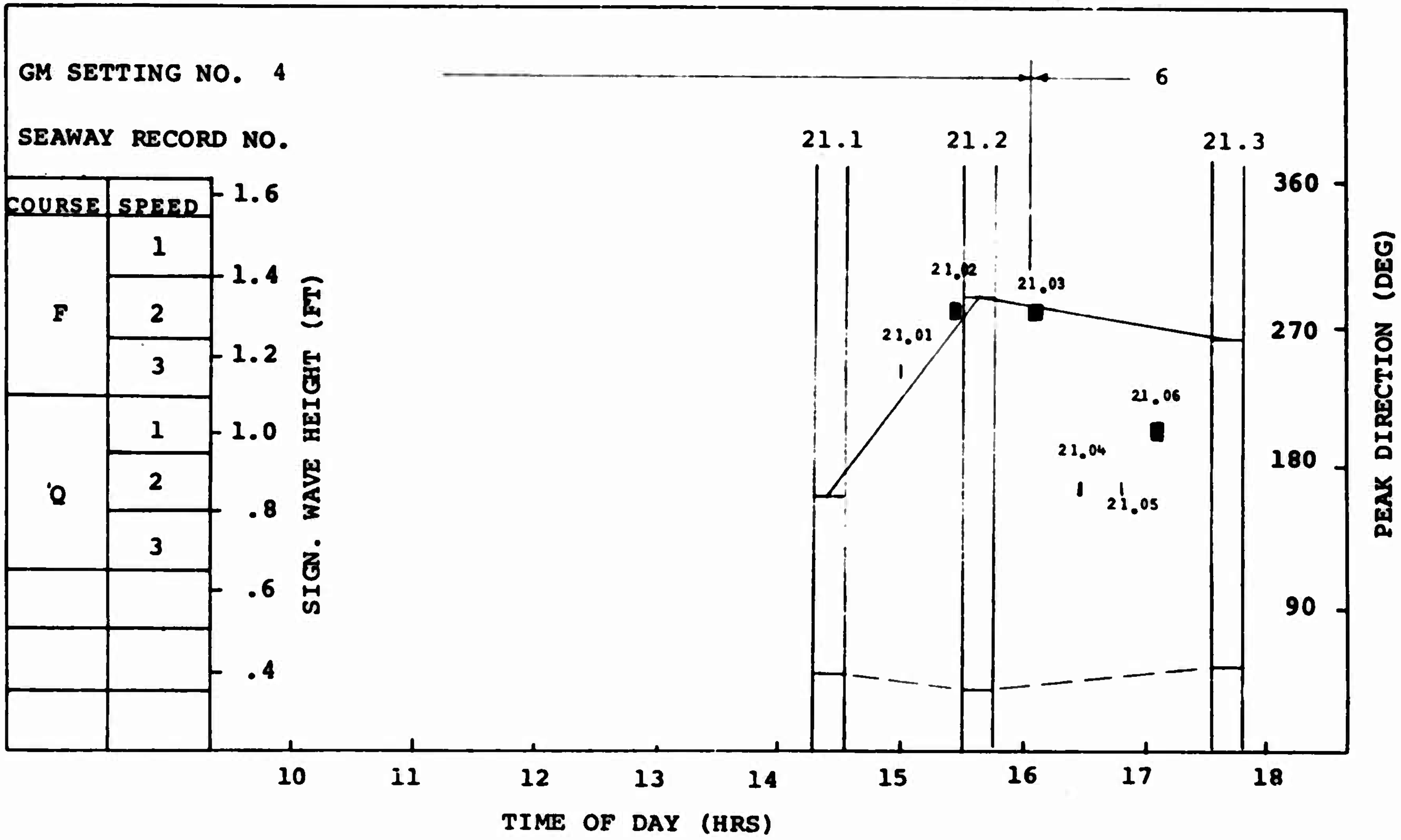

FIGURE E-1.20

SUMMARY OF MODEL RUNS AND SEASTATE INFORMATION

VS. TIME OF RECORDS - 1973 & 1974

SL-7 MODEL CONDITION: HEAVY DATE: 10 MAY 74

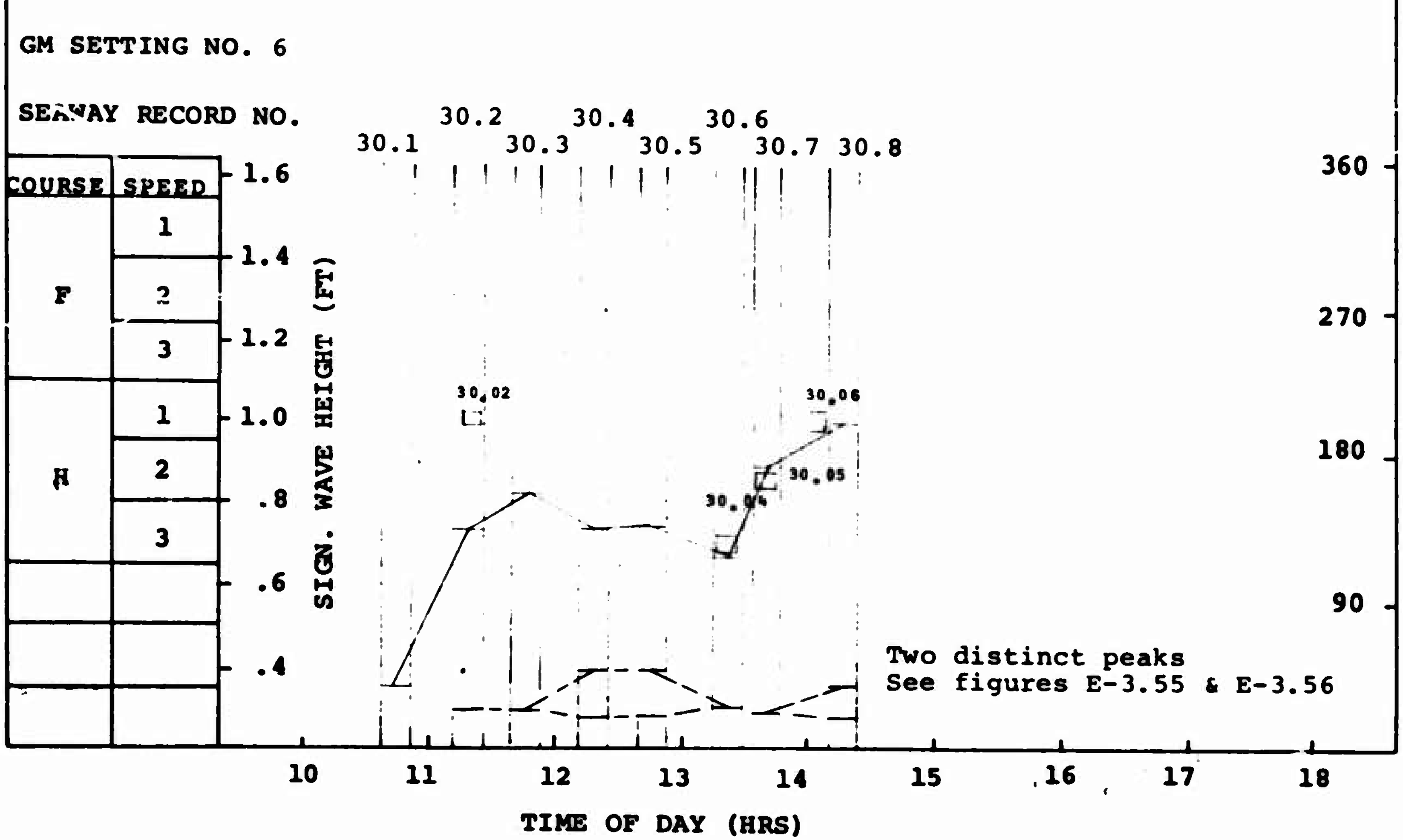

FIGURE E-1. 21

SUMMARY OF MODEL RUNS AND SEASTATE INFORMATION

VS. TIME OF RECORDS - 1973 & 1974

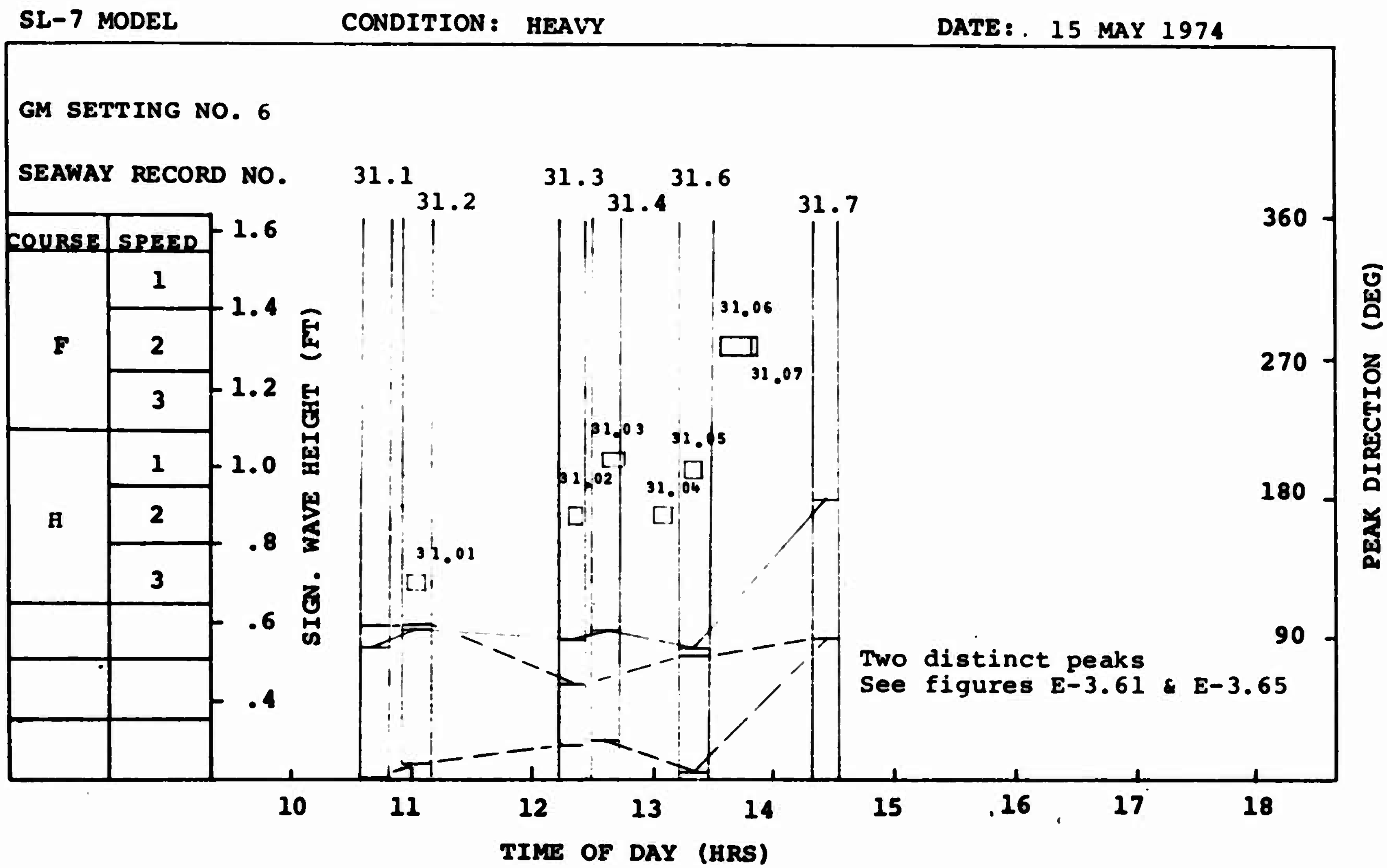

FIGURE E-1.22

FIGURES E-2

POINT SPECTRA OF PROBE-IV FOR 1973 and 1974

The plots contain the wave spectra of probe IV measured on a single day in order to show the spectral growth (or decay) throughout the test period.

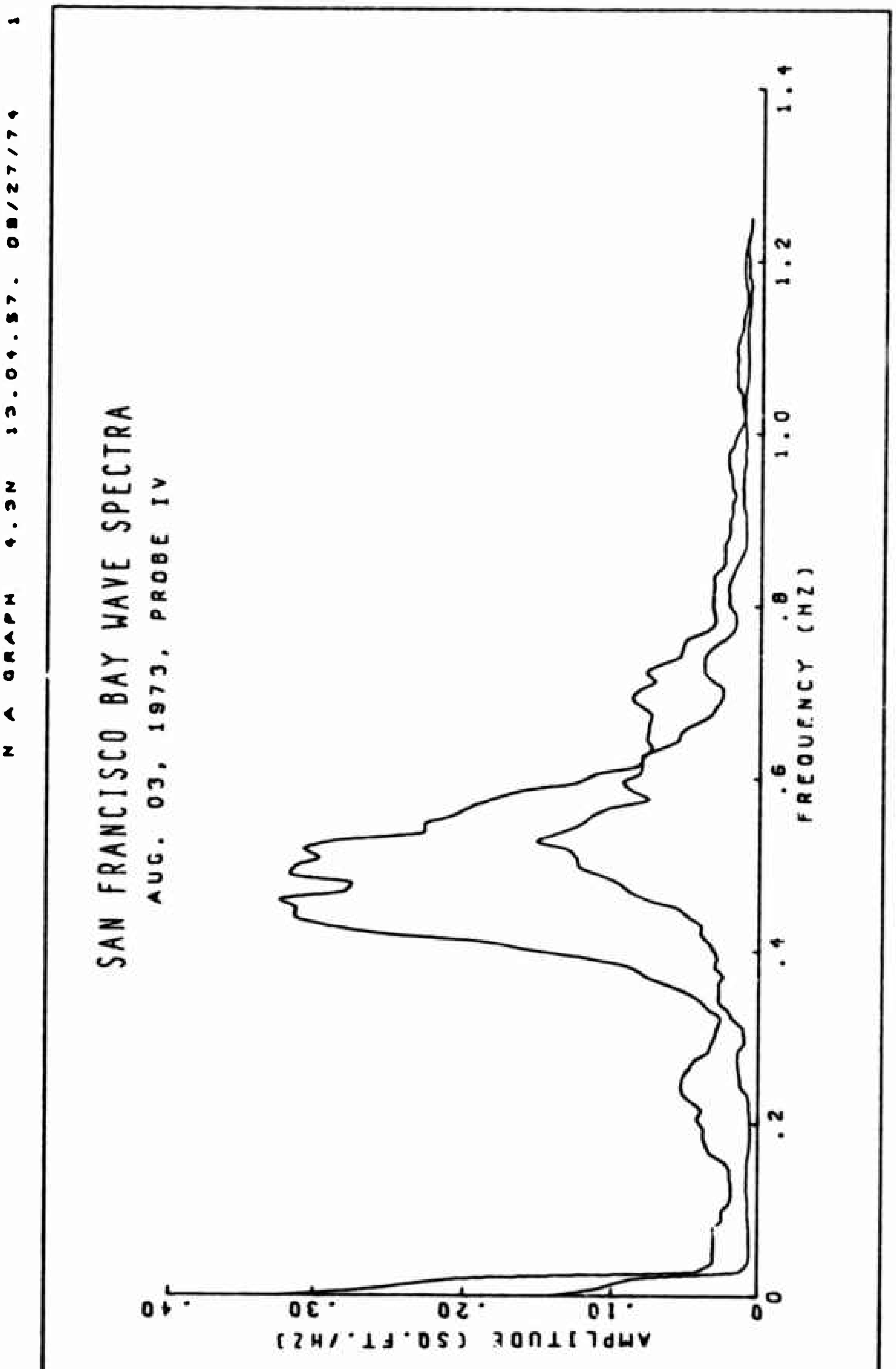
SAN FRANCISCO BAY WAVE SPECTRA
AUG. 03, 1973, PROBE IV
FREQUENCY (HZ)
AMPLITUDE (SQ.FT./HZ)
0
.10
.20
.30
.40
.2
.4
.6
.8
1.0
1.2
1.4

Figure E-2.1

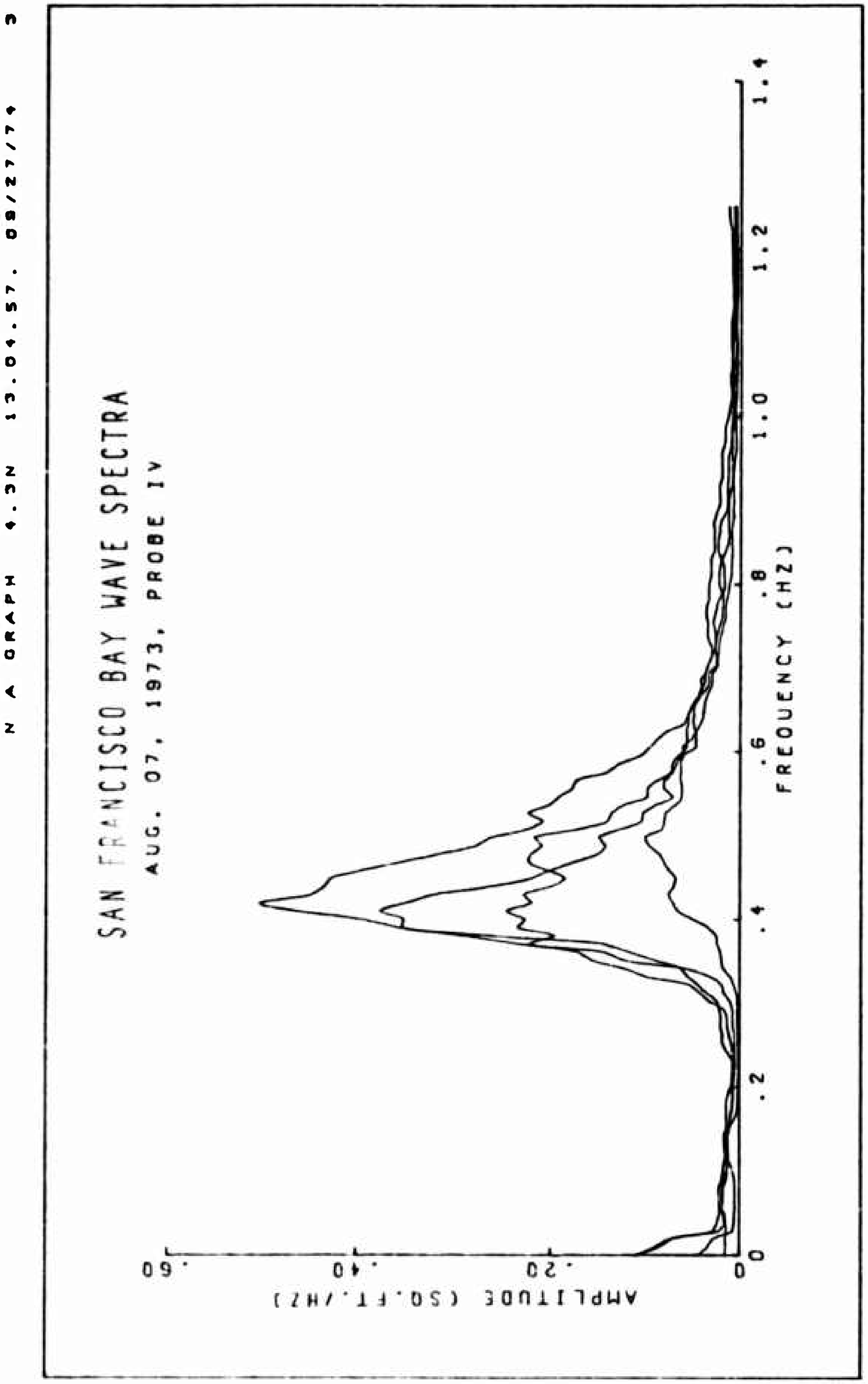
N A GRAPH 4.3N 13.04.57. 08/27/74 3
SAN FRANCISCO BAY WAVE SPECTRA
AUG. 07, 1973, PROBE IV
AMPLITUDE (SQ.FT./HZ)
0
.20
.40
.60
FREQUENCY (HZ)
0
.2
.4
.6
.8
1.0
1.2
1.4

Figure E-2.2

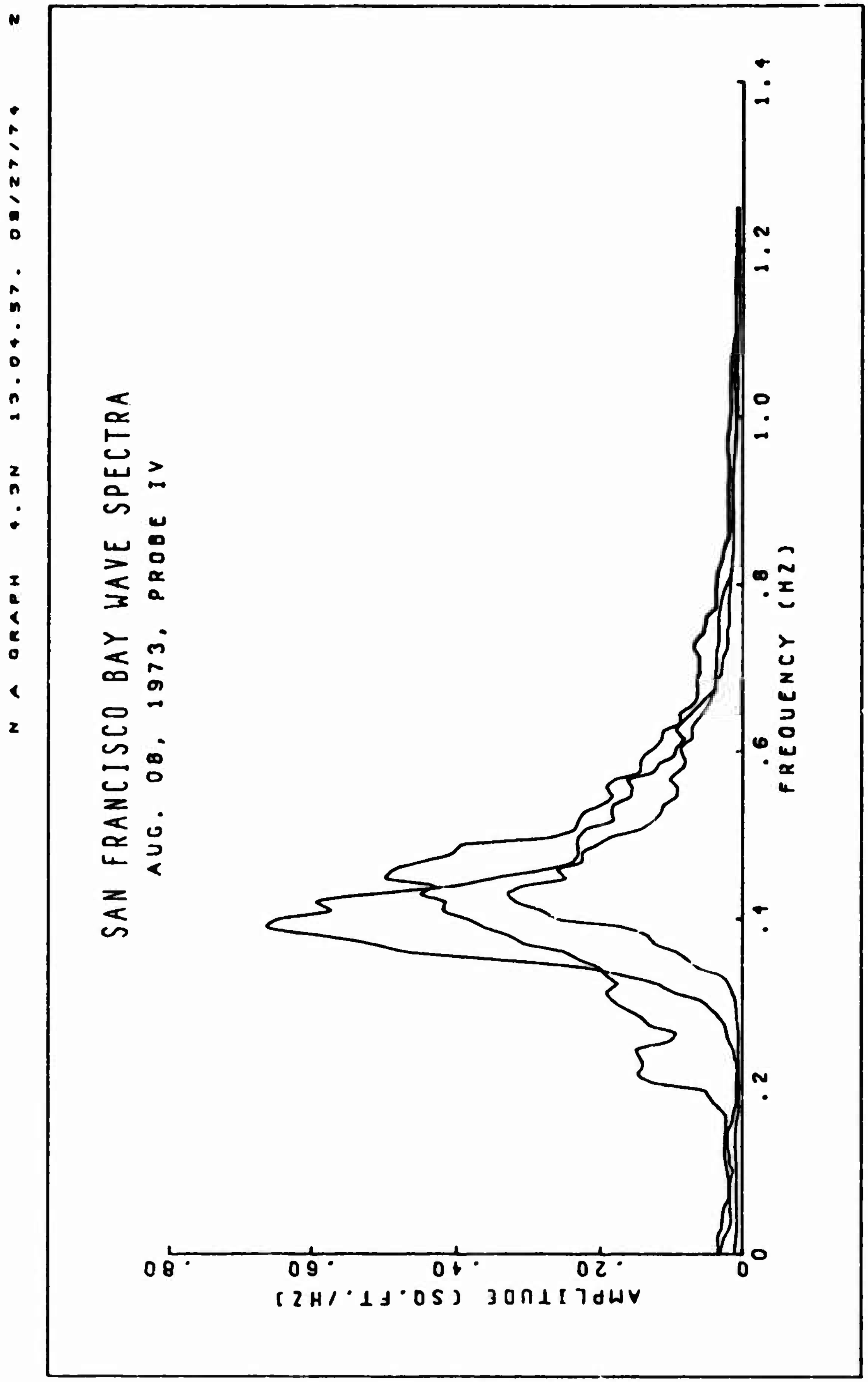
SAN FRANCISCO BAY WAVE SPECTRA
AUG. 08, 1973, PROBE IV
FREQUENCY (HZ)
AMPLITUDE (SQ.FT./HZ)
0
.2
.4
.6
.8
1.0
1.2
1.4
.20
.40
.60
.80

Figure E-2.3

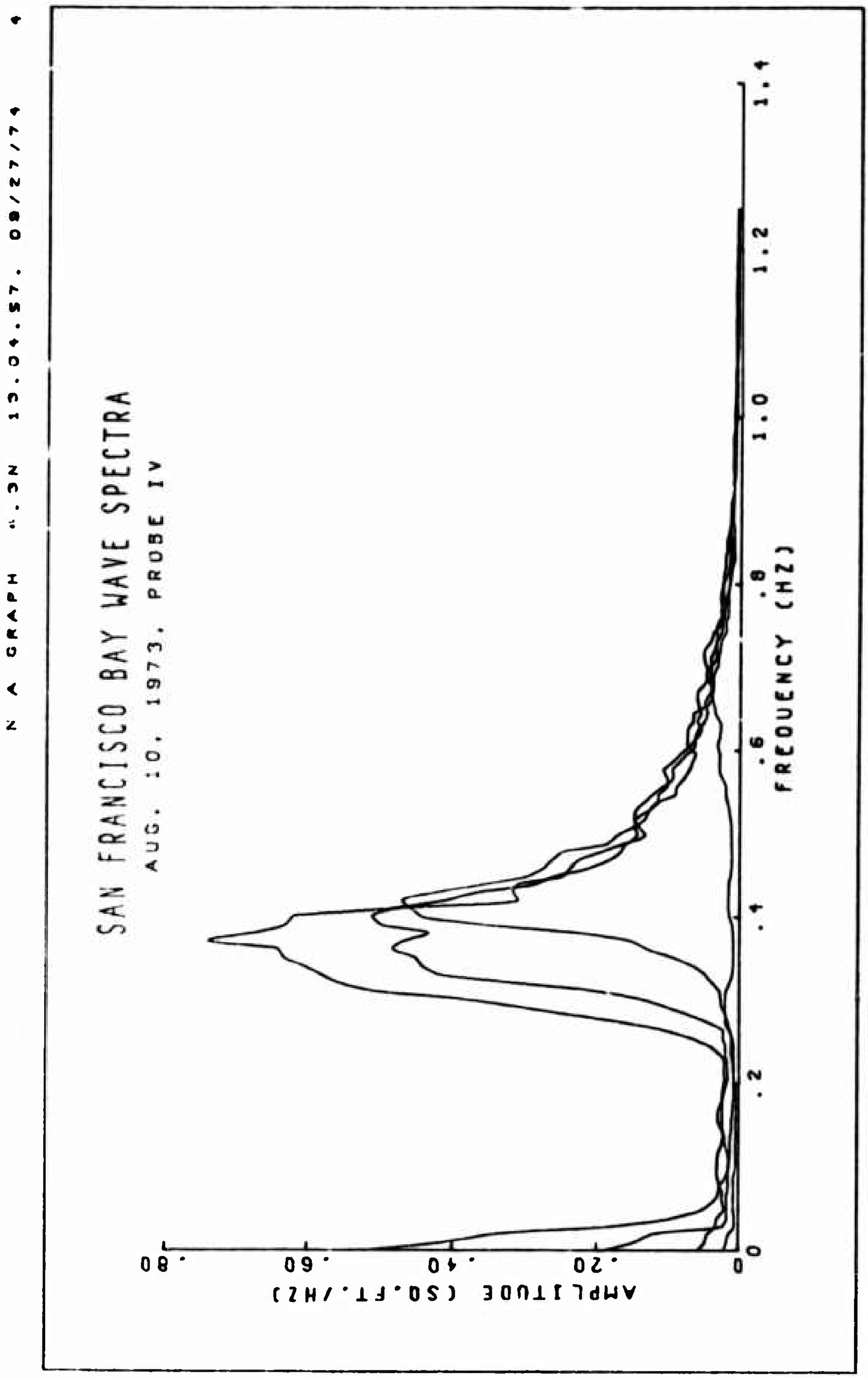
N A GRAPH 13.04.57. 08/27/74
SAN FRANCISCO BAY WAVE SPECTRA
AUG. 10, 1973, PROBE IV
AMPLITUDE (SQ.FT./HZ)
FREQUENCY (HZ)
0
.20
.40
.60
.80
.2
.4
.6
.8
1.0
1.2
1.4

Figure E-2.4

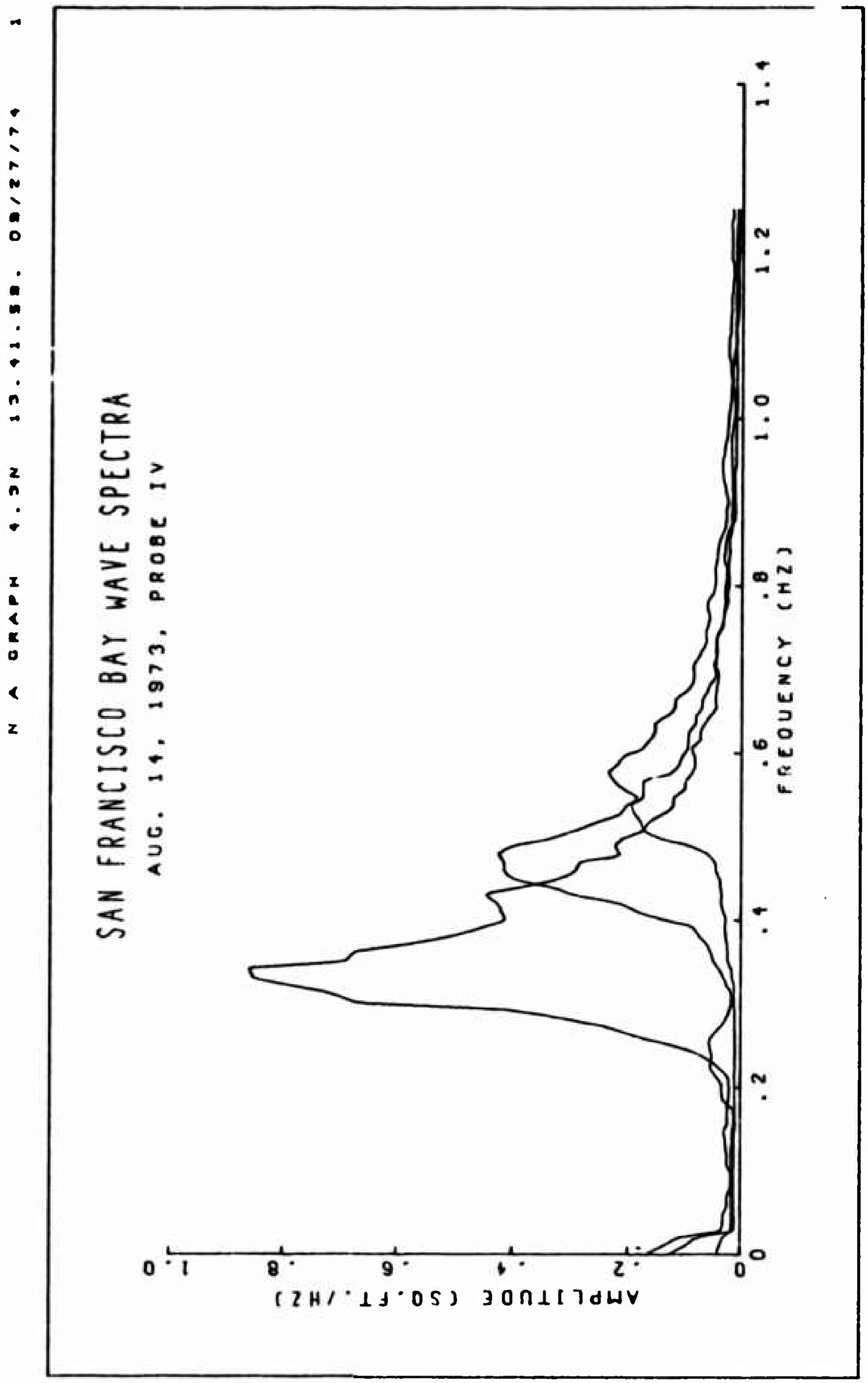
N A GRAPH 4.3N 13.41.58. 08/27/74 1
SAN FRANCISCO BAY WAVE SPECTRA
AUG. 14, 1973, PROBE IV
AMPLITUDE (SQ.FT./HZ)
0
.2
.4
.6
.8
1.0
FREQUENCY (HZ)
0
.2
.4
.6
.8
1.0
1.2
1.4

Figure E-2.5

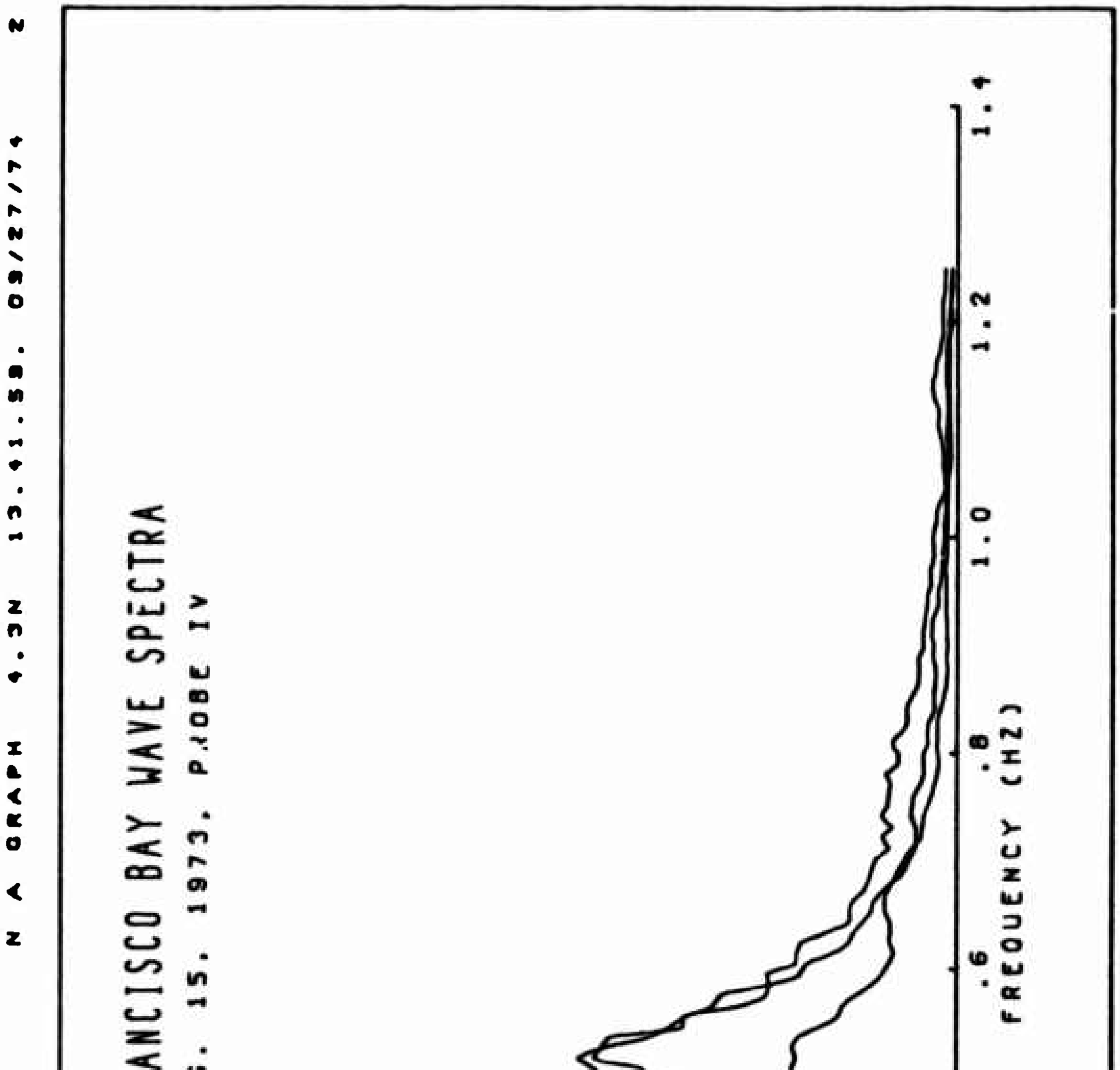
N A GRAPH 4.3N 13.41.58. 03/27/74 2
SAN FRANCISCO BAY WAVE SPECTRA
AUG. 15, 1973, PROBE IV
AMPLITUDE (SQ.FT./HZ)
0
.20
.40
.60
FREQUENCY (HZ)
.2
.4
.6
.8
1.0
1.2
1.4

Figure E-2.6

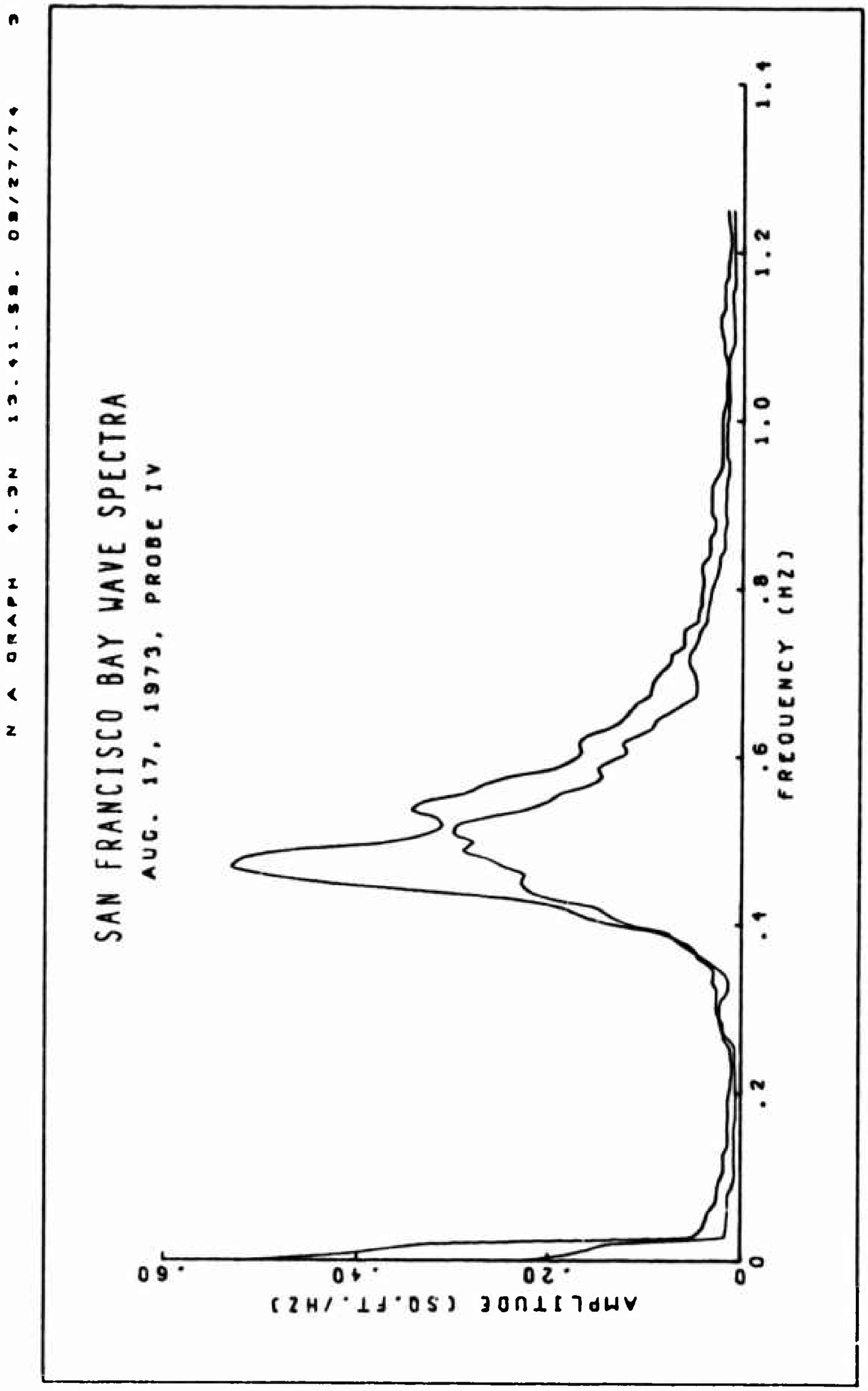
N A GRAPH 4.3N 13.41.58. 08/27/74 3
SAN FRANCISCO BAY WAVE SPECTRA
AUG. 17, 1973, PROBE IV
AMPLITUDE (SQ.FT./HZ)
0
.20
.40
.60
FREQUENCY (HZ)
0
.2
.4
.6
.8
1.0
1.2
1.4

Figure E-2.7

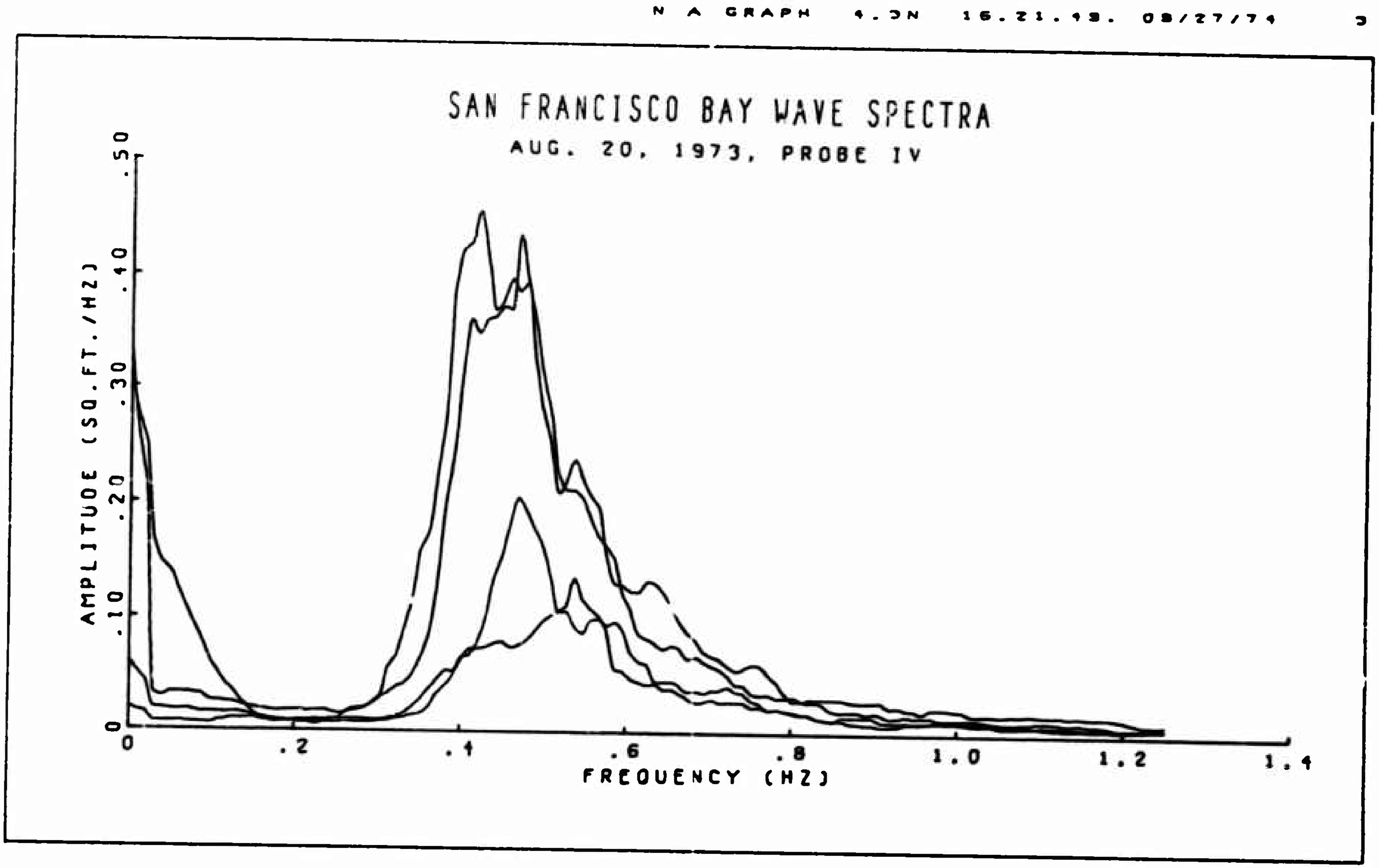
N A GRAPH 4.3N 16.21.43. 08/27/74
SAN FRANCISCO BAY WAVE SPECTRA
AUG. 20, 1973, PROBE IV
AMPLITUDE (SQ.FT./HZ)
0
.10
.20
.30
.40
.50
.2
.4
.6
.8
1.0
1.2
1.4
FREQUENCY (HZ)

Figure E-2.8

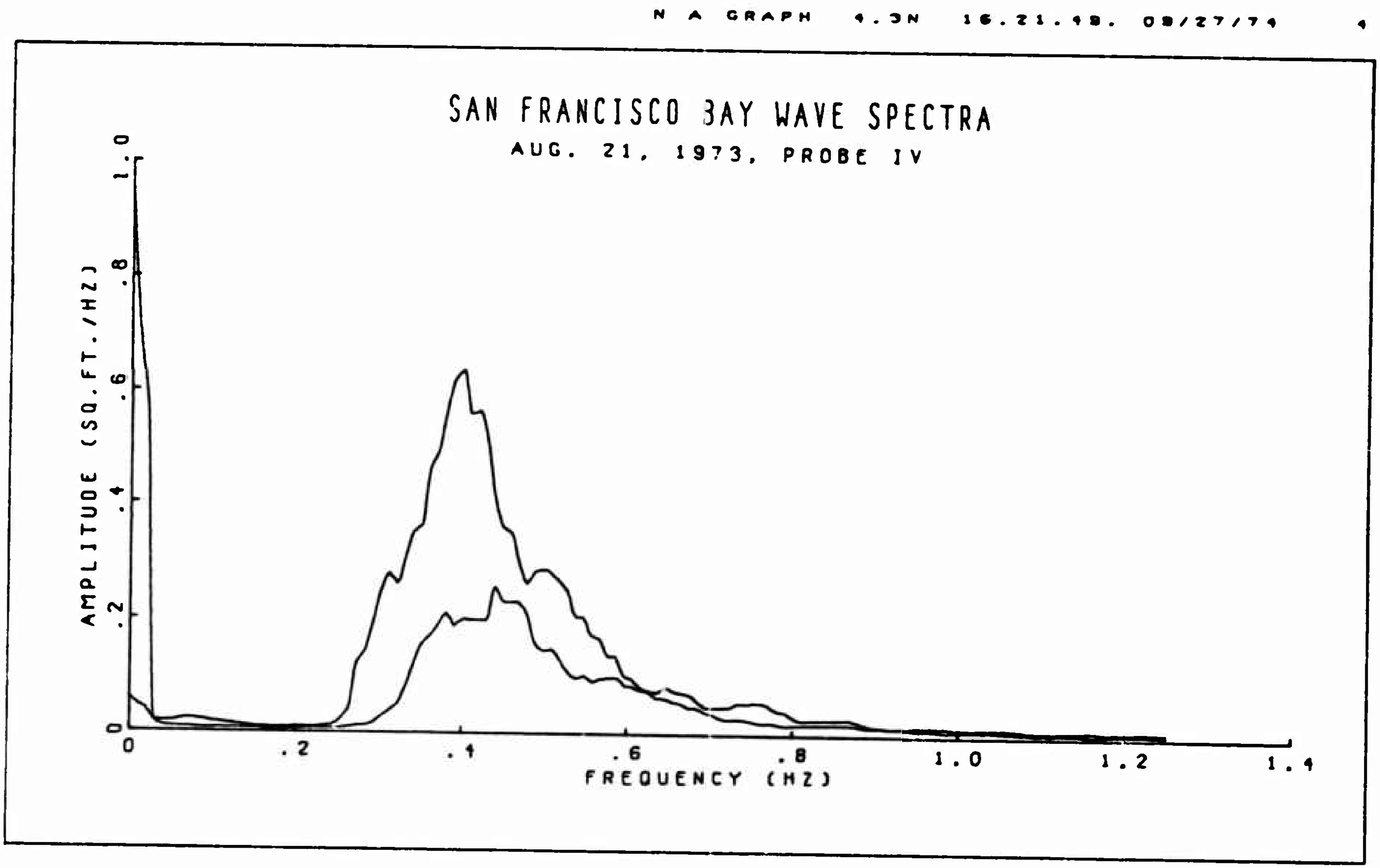
N A GRAPH 4.3N 16.21.49. 08/27/74 4
SAN FRANCISCO BAY WAVE SPECTRA
AUG. 21, 1973, PROBE IV
AMPLITUDE (SQ.FT./HZ)
0
.2
.4
.6
.8
1.0
FREQUENCY (HZ)
0
.2
.4
.6
.8
1.0
1.2
1.4

Figure E-2.9

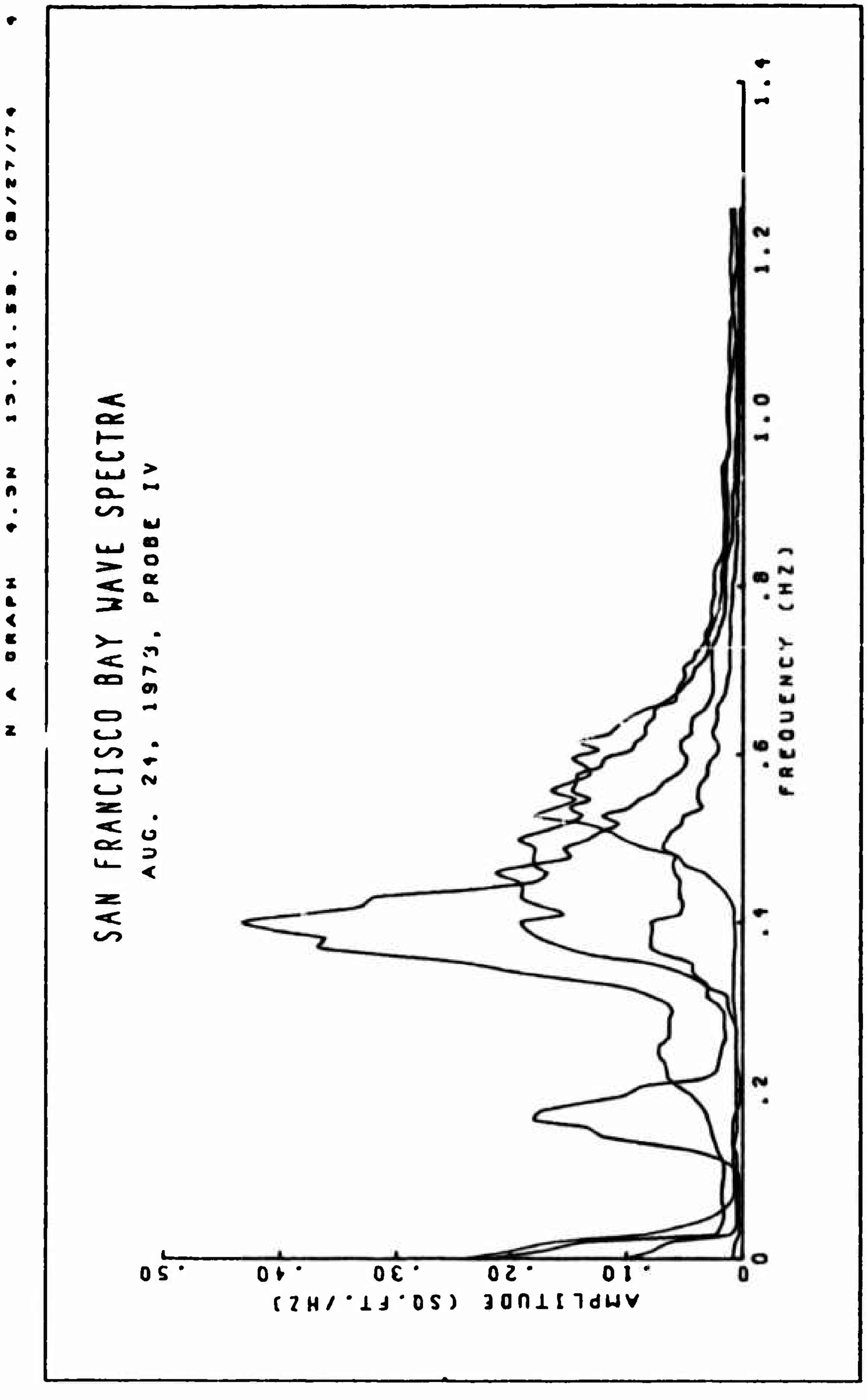
SAN FRANCISCO BAY WAVE SPECTRA
AUG. 24, 1973, PROBE IV
AMPLITUDE (SQ.FT./HZ)
FREQUENCY (HZ)
0
.10
.20
.30
.40
.50
.2
.4
.6
.8
1.0
1.2
1.4

Figure E-2.10

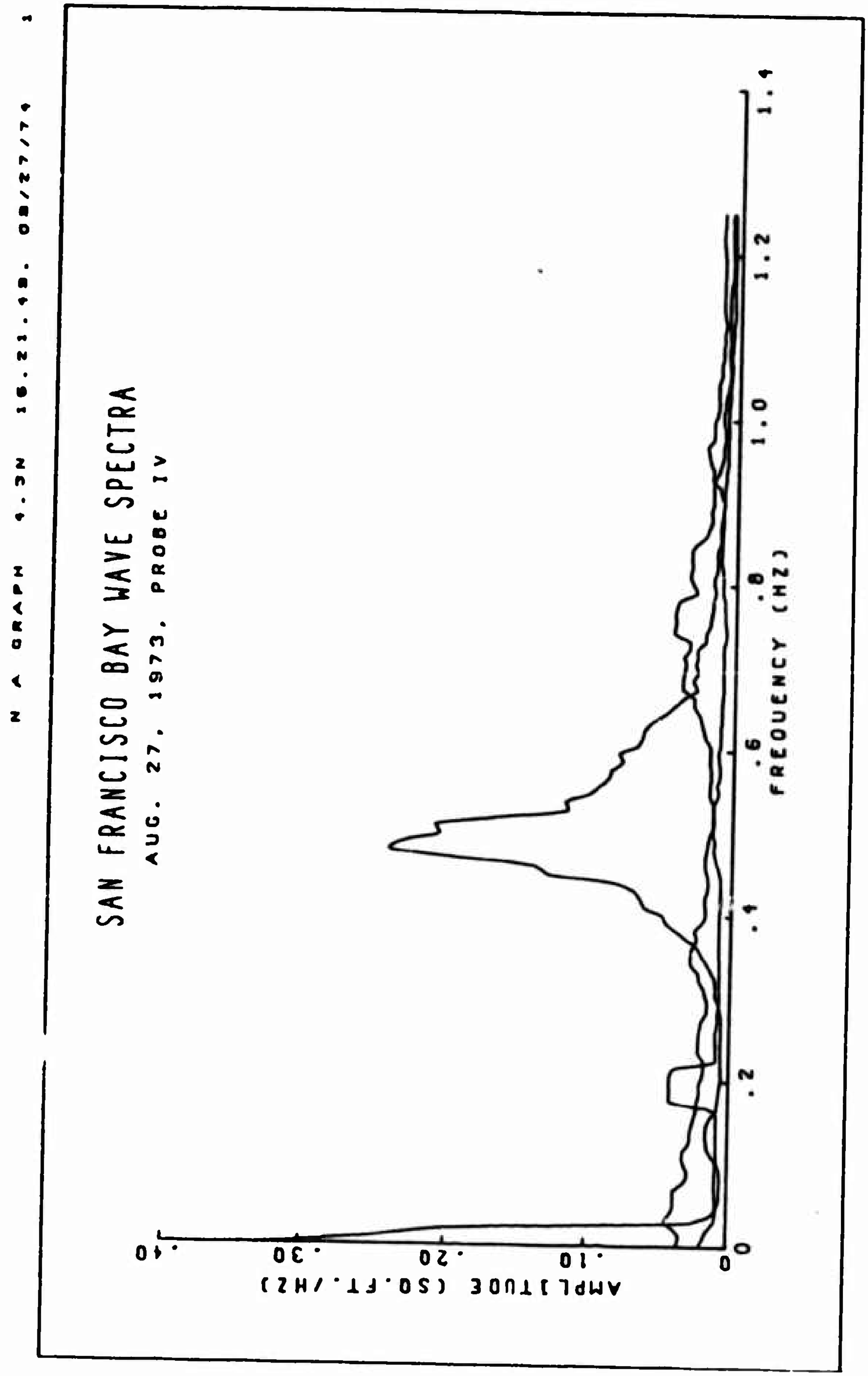
N A GRAPH 4.3N 16.21.48. 08/27/74 1
SAN FRANCISCO BAY WAVE SPECTRA
AUG. 27, 1973, PROBE IV
AMPLITUDE (SQ.FT./HZ)
0
.10
.20
.30
.40
.2
.4
.6
.8
1.0
1.2
1.4
FREQUENCY (HZ)

Figure E-2.11

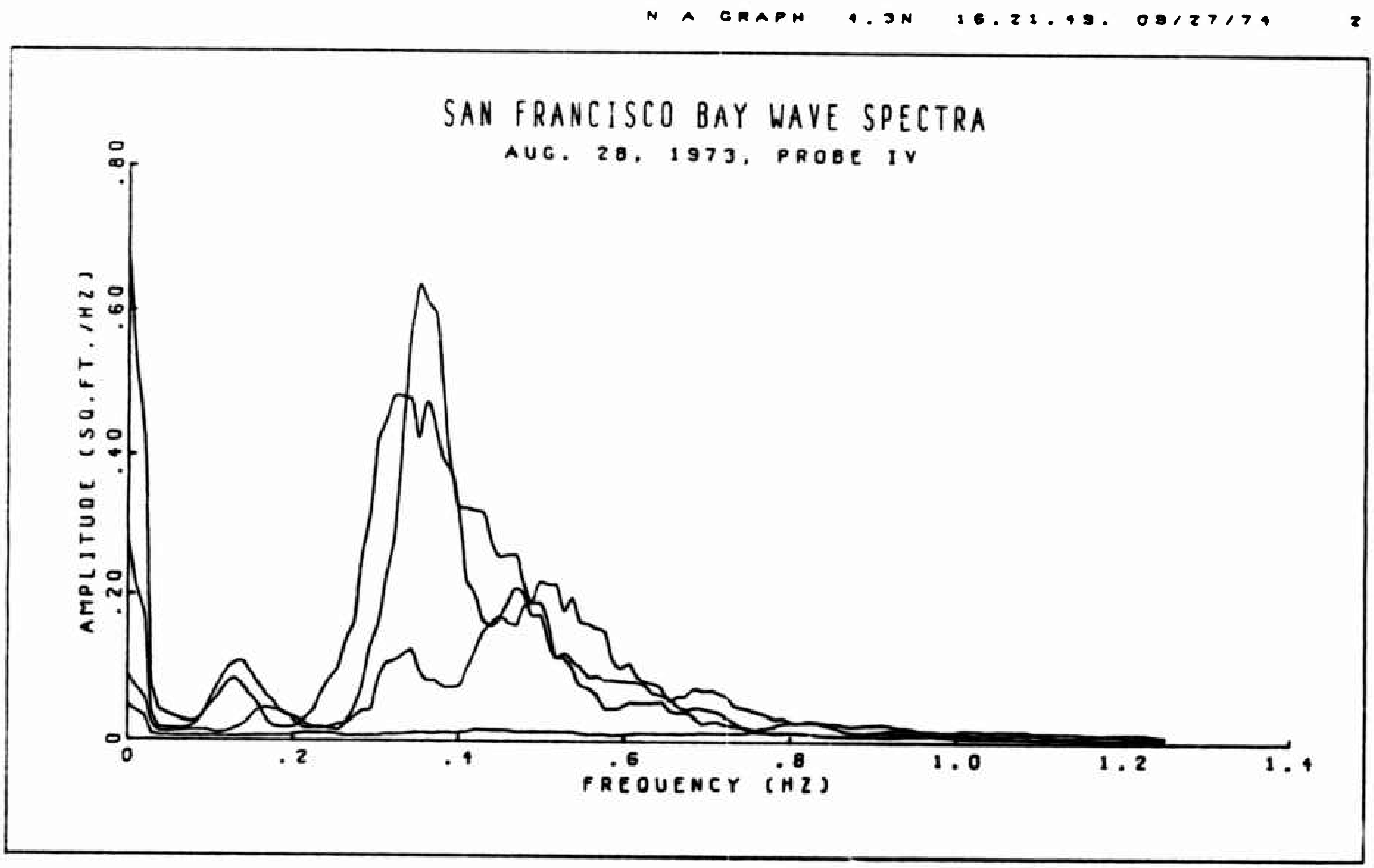
N A GRAPH 4.3N 16.21.49. 09/27/74 2
SAN FRANCISCO BAY WAVE SPECTRA
AUG. 28, 1973, PROBE IV
AMPLITUDE (SQ.FT./HZ)
0
.20
.40
.60
.80
.2
.4
.6
.8
1.0
1.2
1.4
FREQUENCY (HZ)

Figure E-2.12

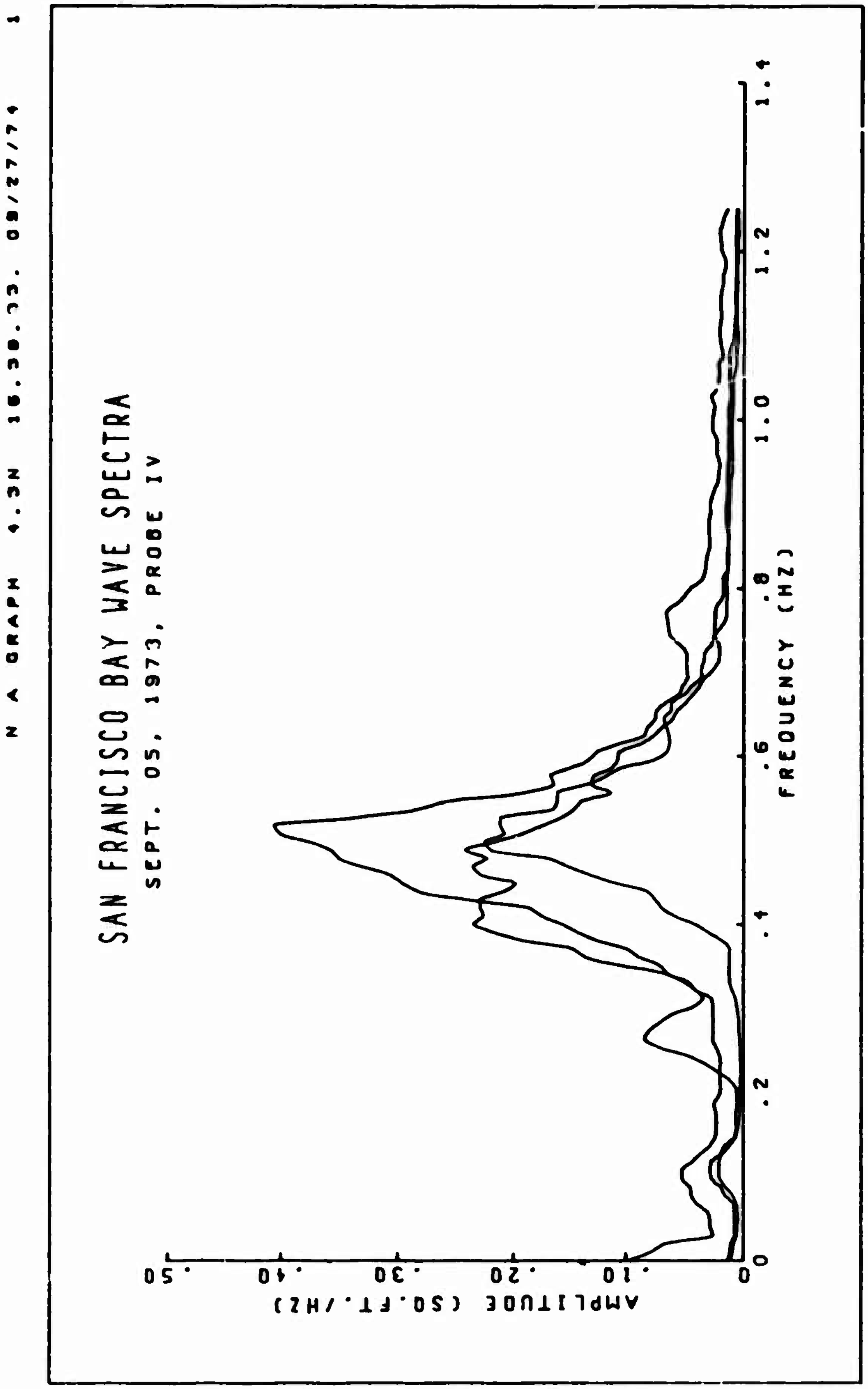
SAN FRANCISCO BAY WAVE SPECTRA
SEPT. 05, 1973, PROBE IV
AMPLITUDE (SQ.FT./HZ)
0
.10
.20
.30
.40
.50
FREQUENCY (HZ)
.2
.4
.6
.8
1.0
1.2
1.4

Figure E-2.13

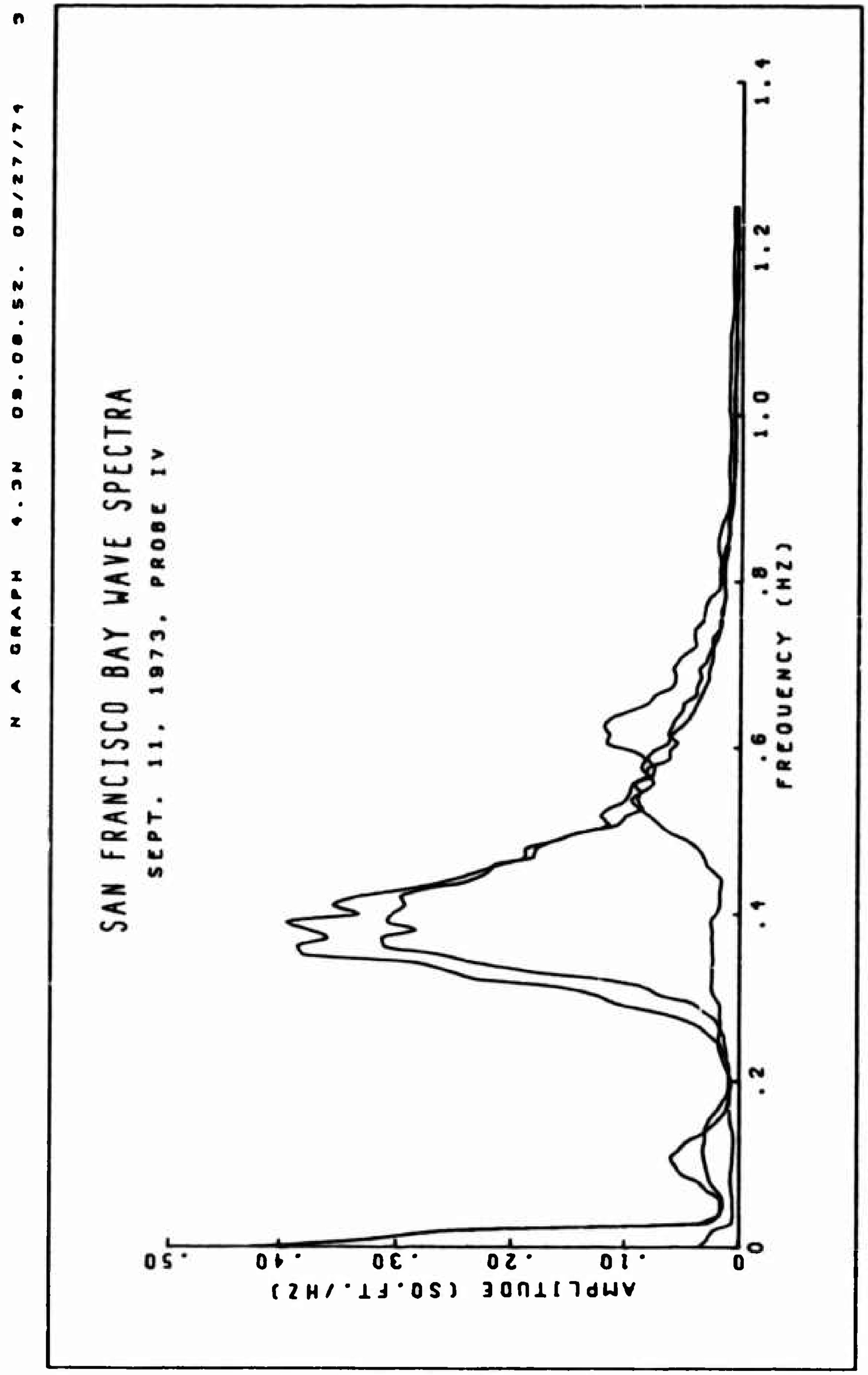
N A GRAPH 4.3N 03.08.52. 08/27/74
SAN FRANCISCO BAY WAVE SPECTRA
SEPT. 11, 1973, PROBE IV
AMPLITUDE (SQ.FT./HZ)
FREQUENCY (HZ)
0
.10
.20
.30
.40
.50
.2
.4
.6
.8
1.0
1.2
1.4

Figure E-2.14

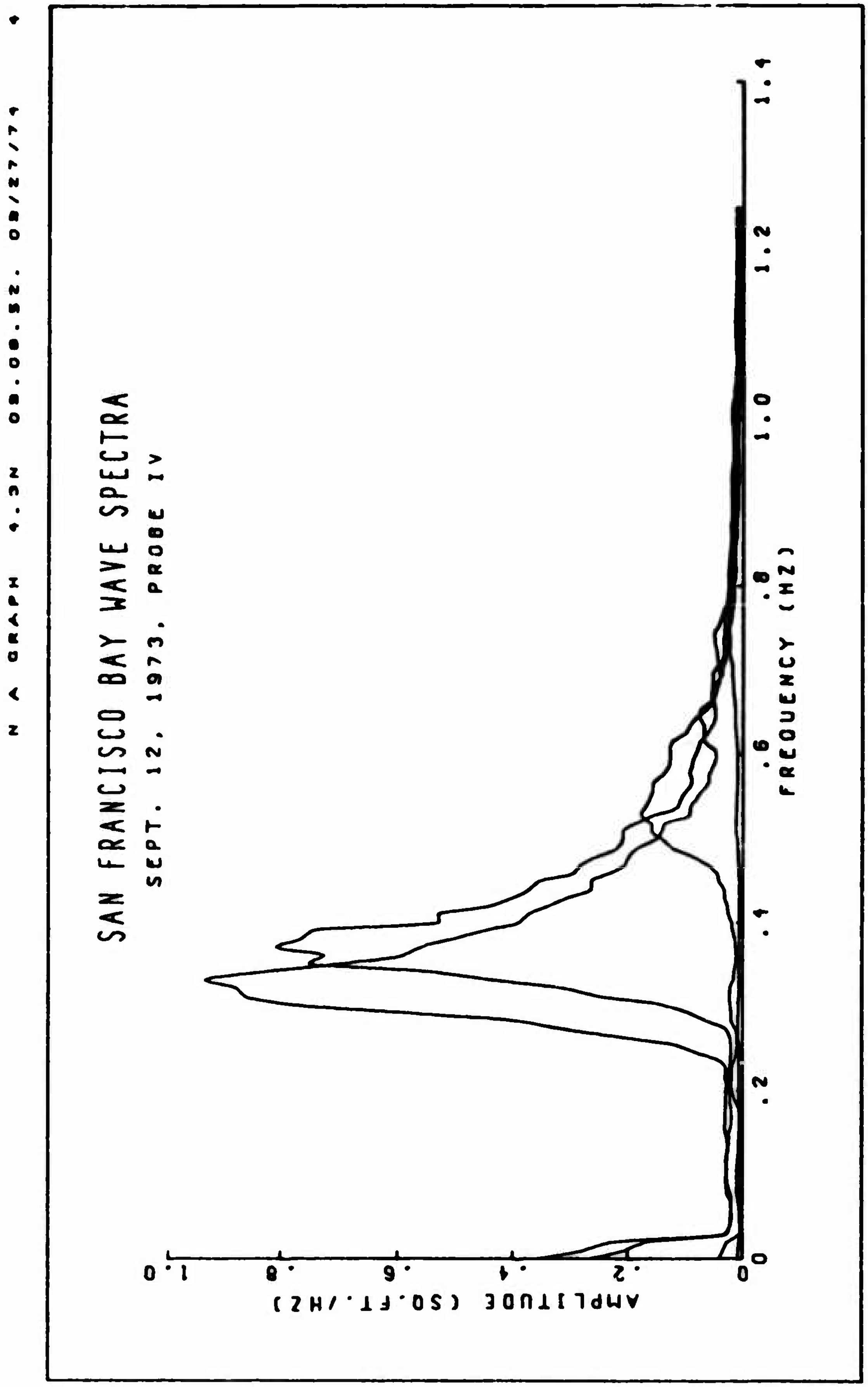
SAN FRANCISCO BAY WAVE SPECTRA
SEPT. 12, 1973, PROBE IV
FREQUENCY (HZ)
AMPLITUDE (SQ.FT./HZ)
0
.2
.4
.6
.8
1.0
1.2
1.4

Figure E-2.15

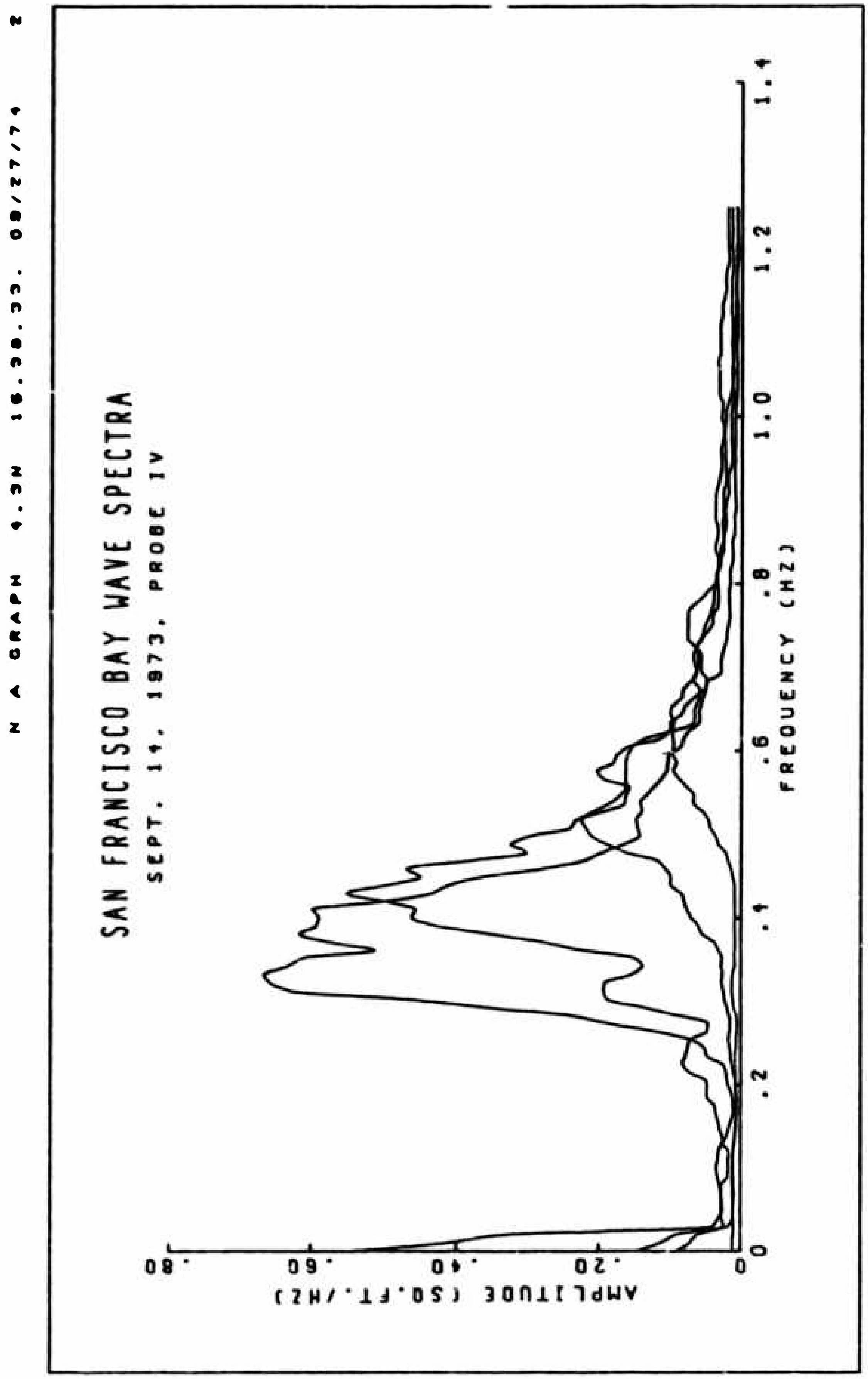
N A GRAPH 4.3N 16.38.33. 08/27/74
SAN FRANCISCO BAY WAVE SPECTRA
SEPT. 14, 1973, PROBE IV
AMPLITUDE (SQ.FT./HZ)
.80
.60
.40
.20
0
.2
.4
.6
.8
1.0
1.2
1.4
FREQUENCY (HZ)

Figure E-2.16

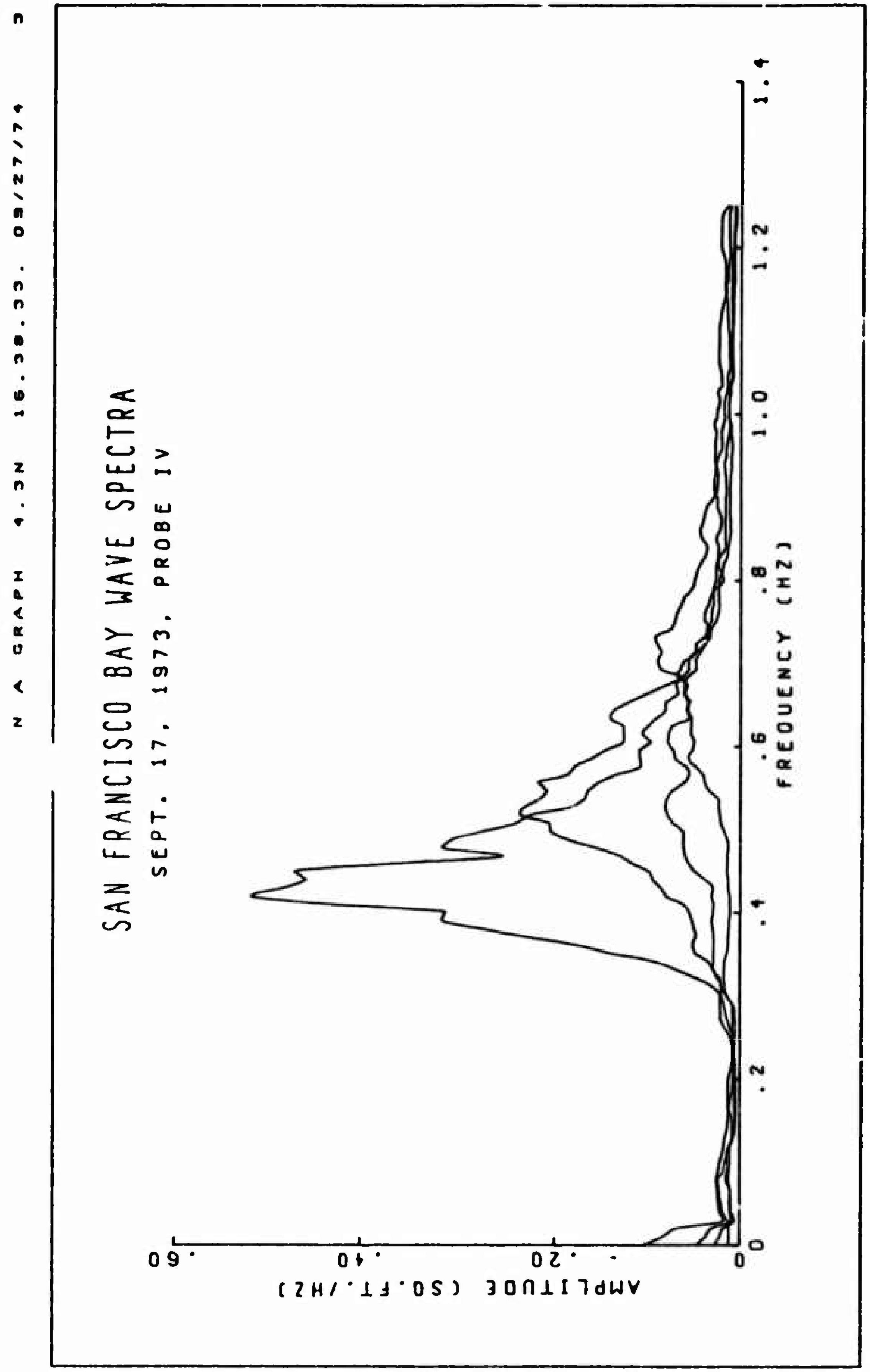
N A GRAPH 4.3N 16.38.33. 03/27/74 3
SAN FRANCISCO BAY WAVE SPECTRA
SEPT. 17, 1973, PROBE IV
FREQUENCY (HZ)
AMPLITUDE (SQ.FT./HZ)
0
.2
.4
.6
.8
1.0
1.2
1.4
0
.20
.40
.60

Figure E-2.17

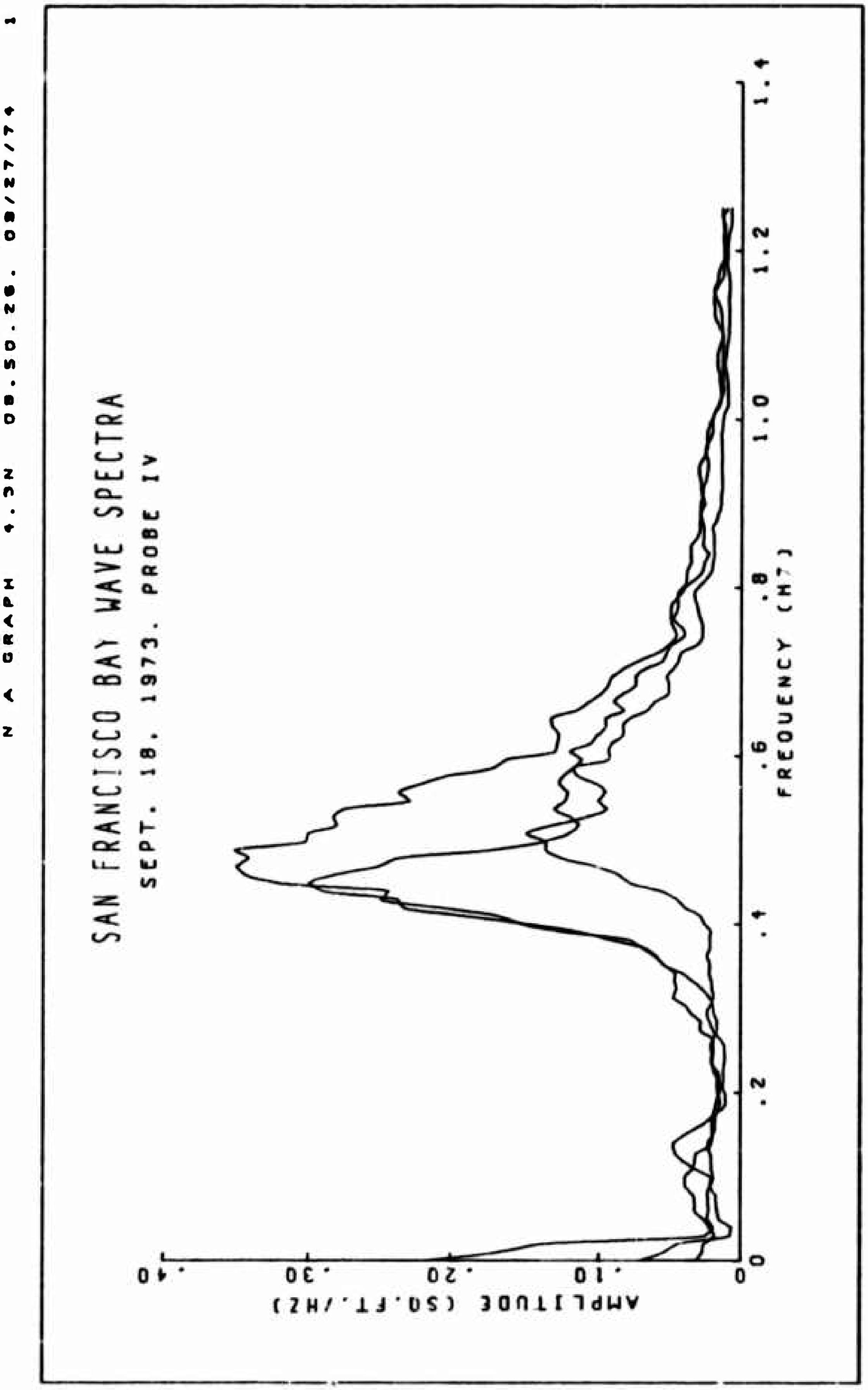
N A GRAPH 4.3N 08.50.26. 08/27/74 1
SAN FRANCISCO BAY WAVE SPECTRA
SEPT. 18, 1973, PROBE IV
FREQUENCY (HZ)
AMPLITUDE (SQ.FT./HZ)
0
.2
.4
.6
.8
1.0
1.2
1.4
.10
.20
.30
.40

Figure E-2.18

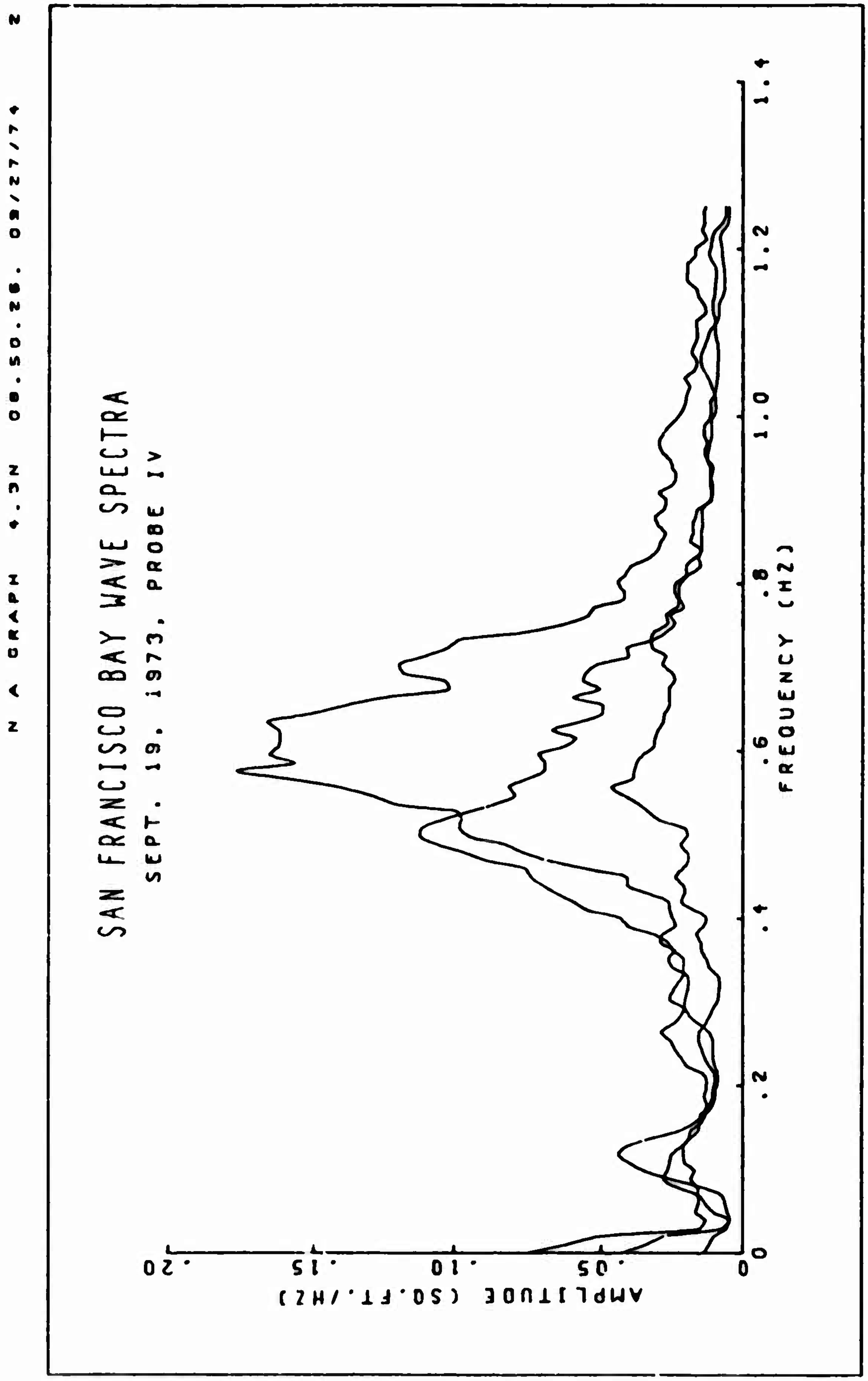
N A GRAPH 4.3N 08.50.28. 03/27/74 N
SAN FRANCISCO BAY WAVE SPECTRA
SEPT. 19, 1973, PROBE IV
AMPLITUDE (SQ.FT./HZ)
0
.05
.10
.15
.20
FREQUENCY (HZ)
0
.2
.4
.6
.8
1.0
1.2
1.4

Figure E-2.19

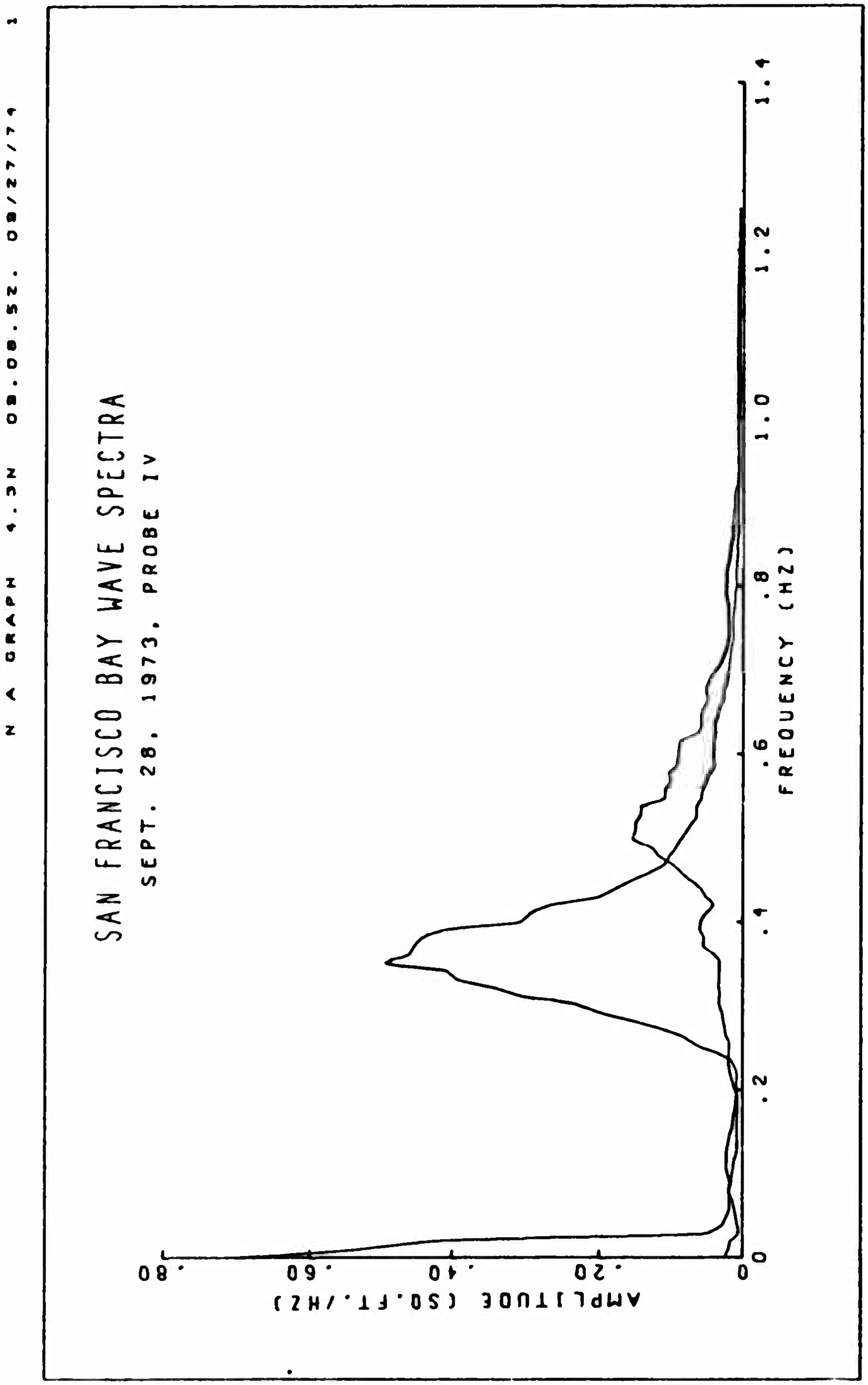
N A GRAPH 4.3N 08.08.52. 08/27/74 1
SAN FRANCISCO BAY WAVE SPECTRA
SEPT. 28, 1973, PROBE IV
FREQUENCY (HZ)
0
.2
.4
.6
.8
1.0
1.2
1.4
AMPLITUDE (SQ.FT./HZ)
.20
.40
.60
.80

Figure E-2.20

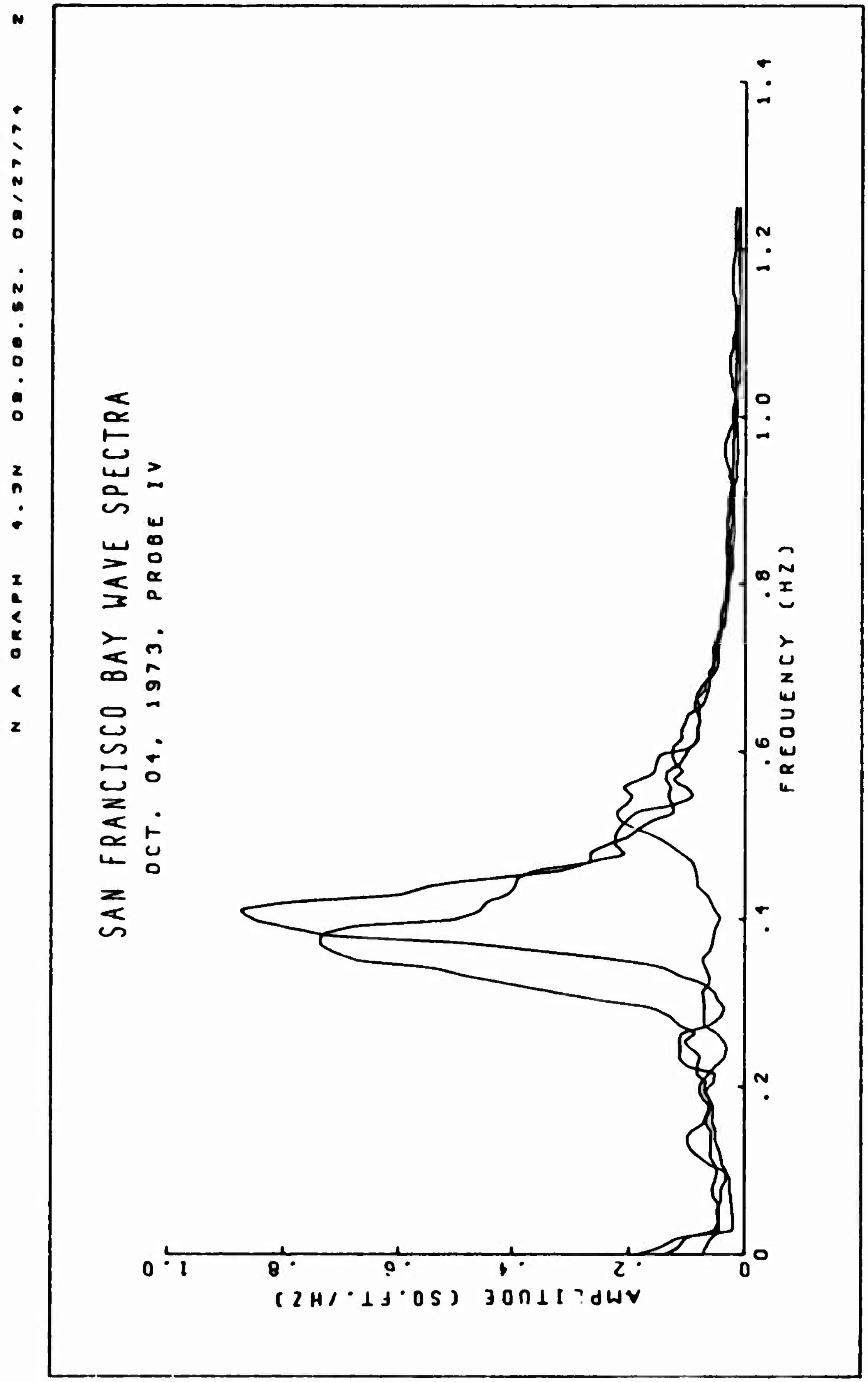
SAN FRANCISCO BAY WAVE SPECTRA
OCT. 04, 1973, PROBE IV
FREQUENCY (HZ)
AMPLITUDE (SQ.FT./HZ)
0
.2
.4
.6
.8
1.0
1.2
1.4

Figure E-2.21

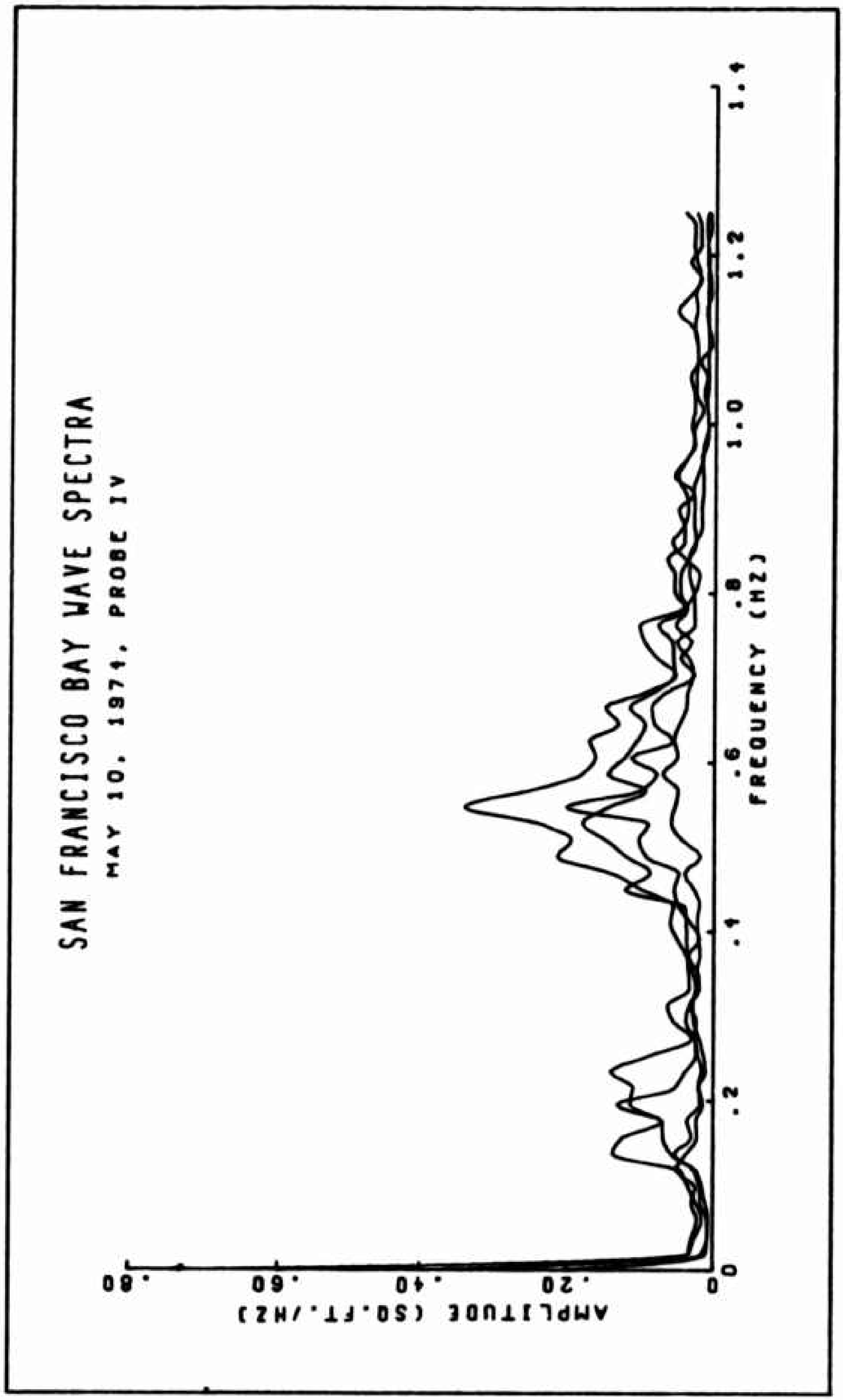
SAN FRANCISCO BAY WAVE SPECTRA
MAY 10, 1974, PROBE IV
FREQUENCY (HZ)
AMPLITUDE (SQ.FT./HZ)
0
.2
.4
.6
.8
1.0
1.2
1.4
.20
.40
.60
.80

Figure E-2.22

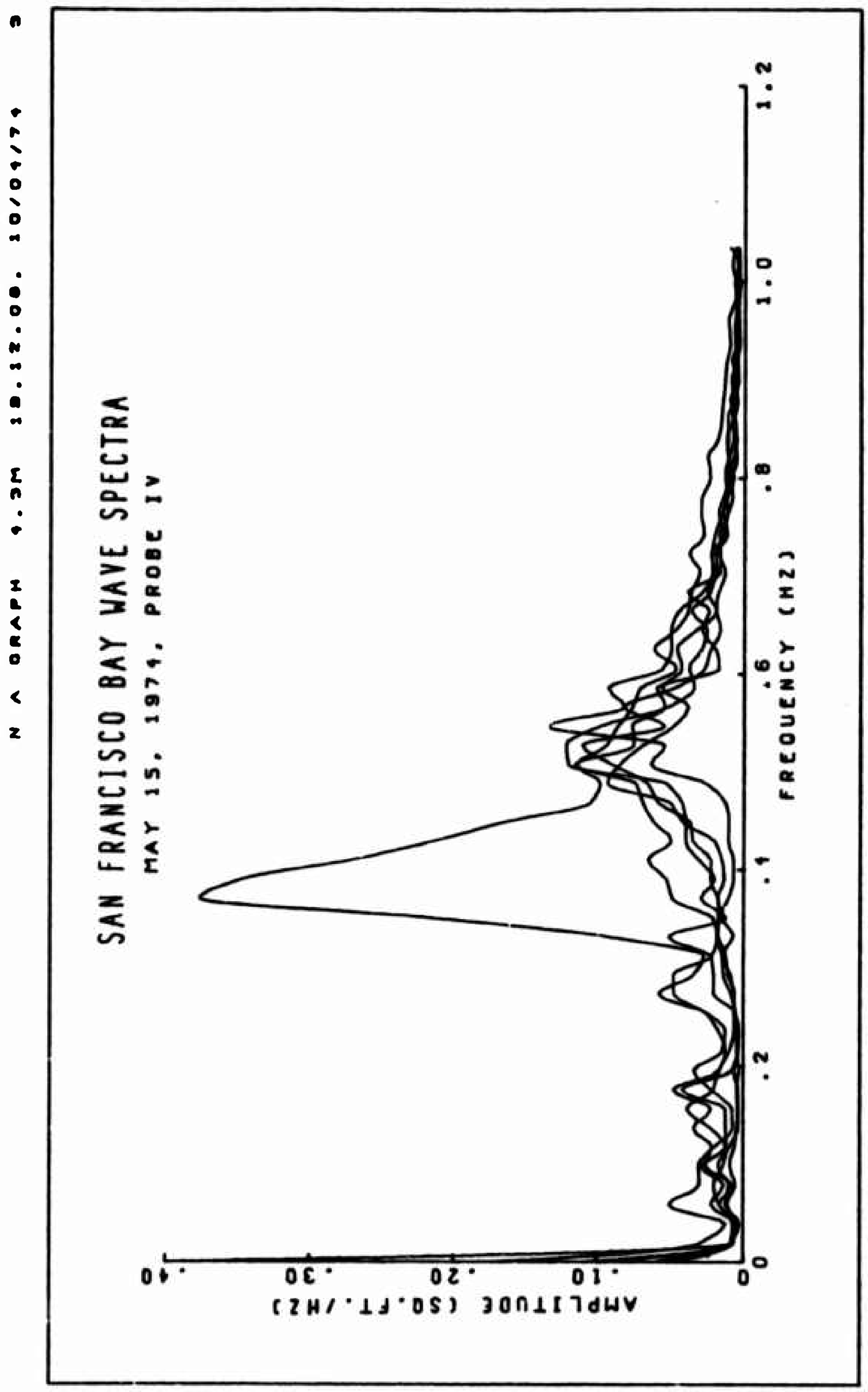
N A GRAPH
SAN FRANCISCO BAY WAVE SPECTRA
MAY 15, 1974, PROBE IV
FREQUENCY (HZ)
AMPLITUDE (SQ.FT./HZ)
0
.2
.4
.6
.8
1.0
1.2
.10
.20
.30
.40

Figure E-2.23

FIGURES E-3

DIRECTIONAL SPECTRA

The directional spectra, $S(\theta,f)$, are presented as contour polar plots with frequency in Hz in the radial direction. Note that the computations we carried out at constant frequency and may have resulted in too much spreading in θ. The contouring routine was not perfect and some small spurious contours are evident. The contour levels vary but not enough to include levels for the very low seastates. These appear as blanks in their respective locations.

DIRECTIONAL SPECTRA

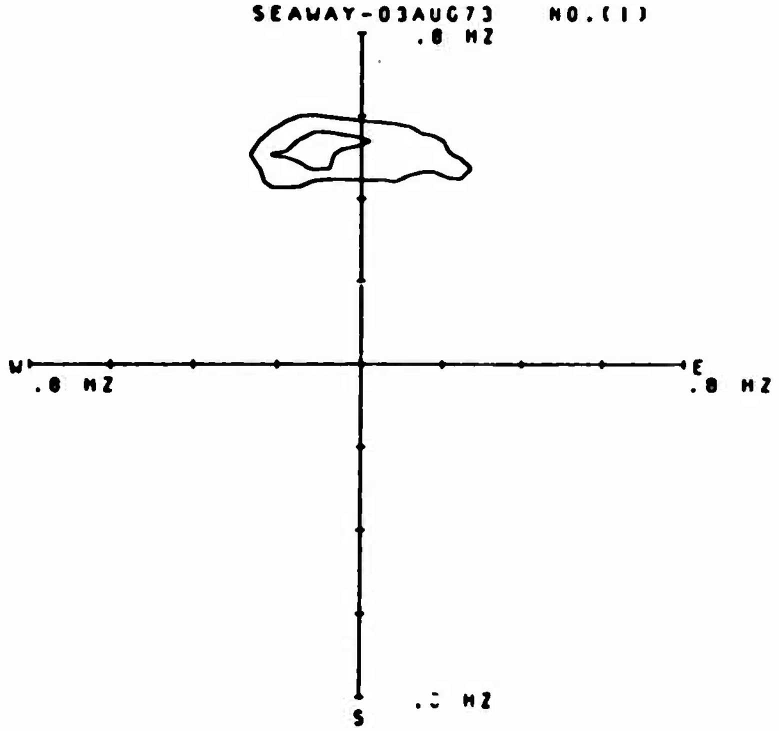

FIGURE E 3.1

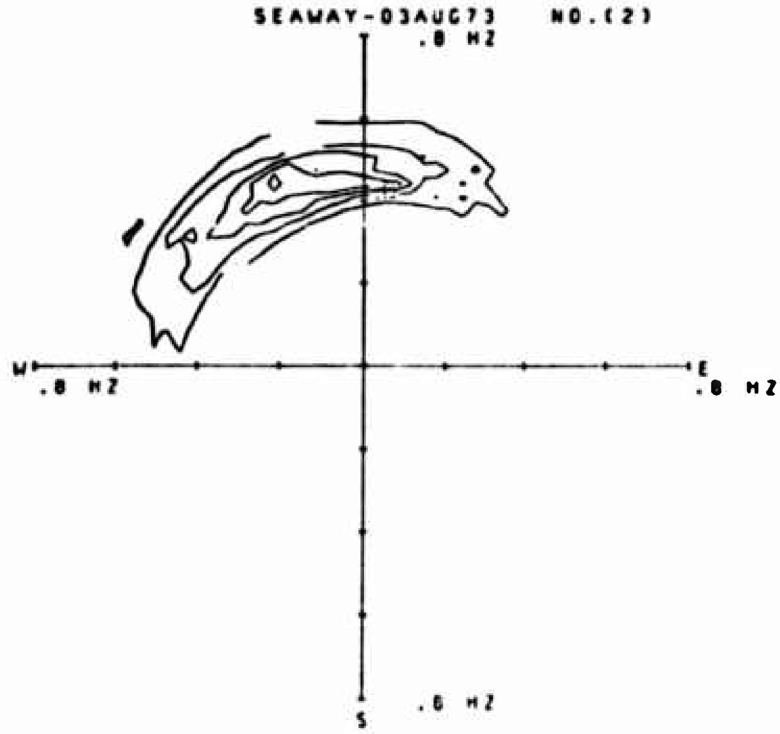

FIGURE E 3.2

DIRECTIONAL SPECTRA

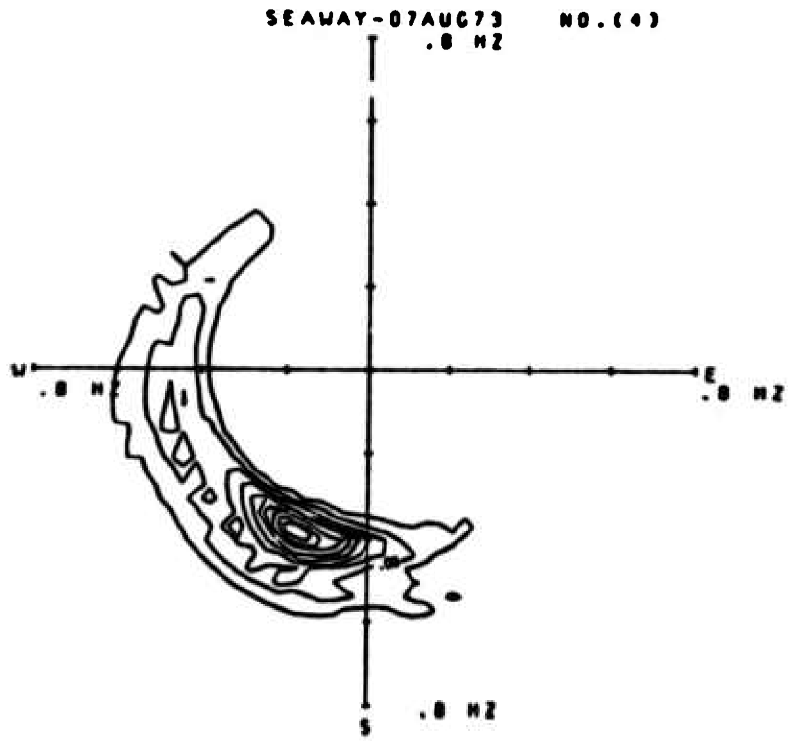

FIGURE E 3.3

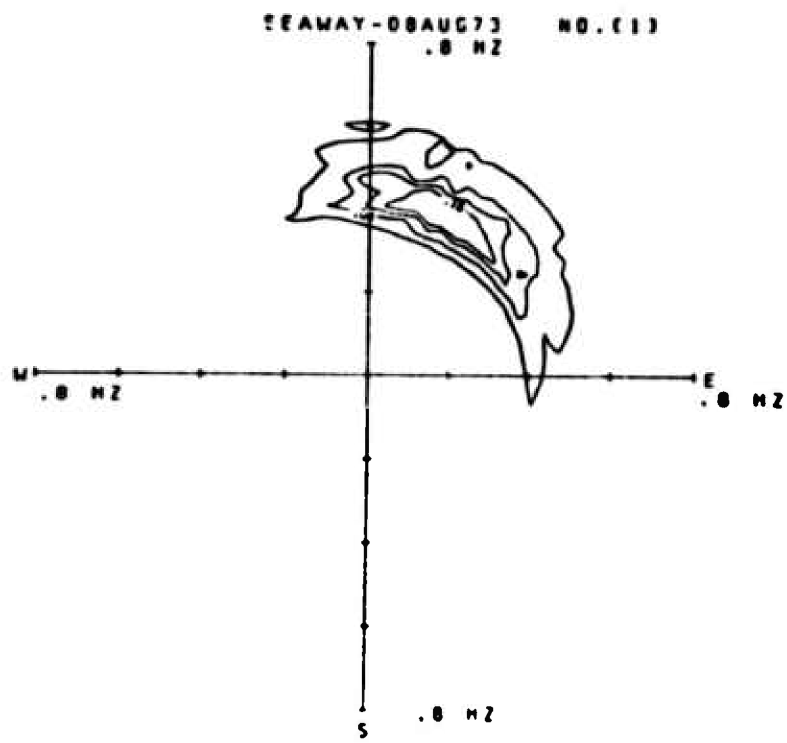

FIGURE E 3.4

DIRECTIONAL SPECTRA

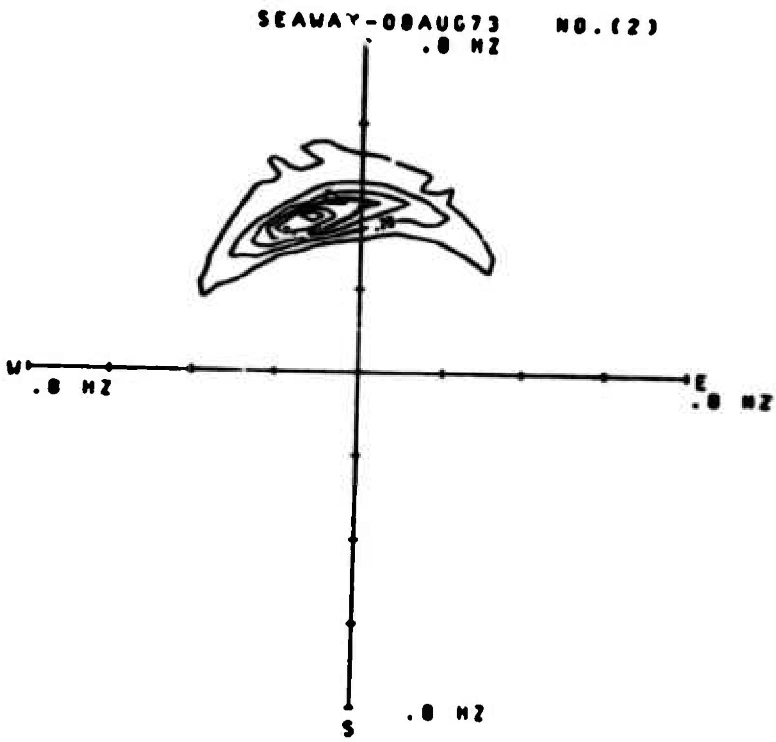

FIGURE E 3.5

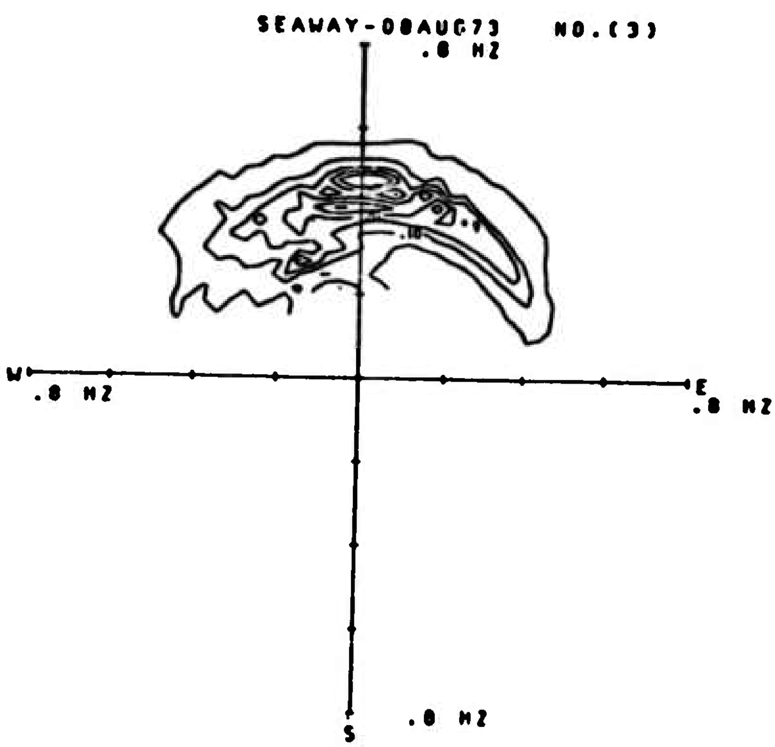

FIGURE E 3.6

DIRECTIONAL SPECTRA

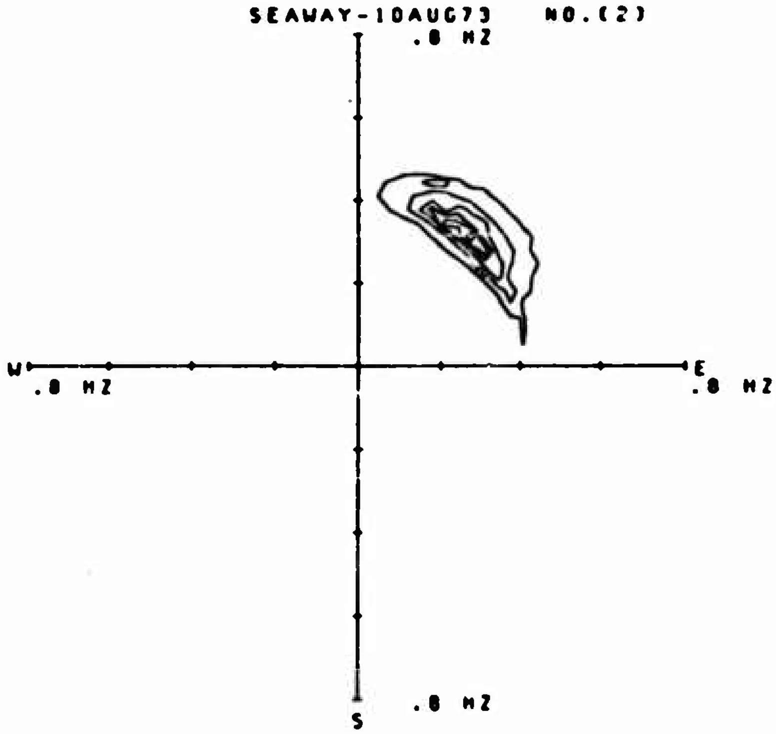

FIGURE E 3.7

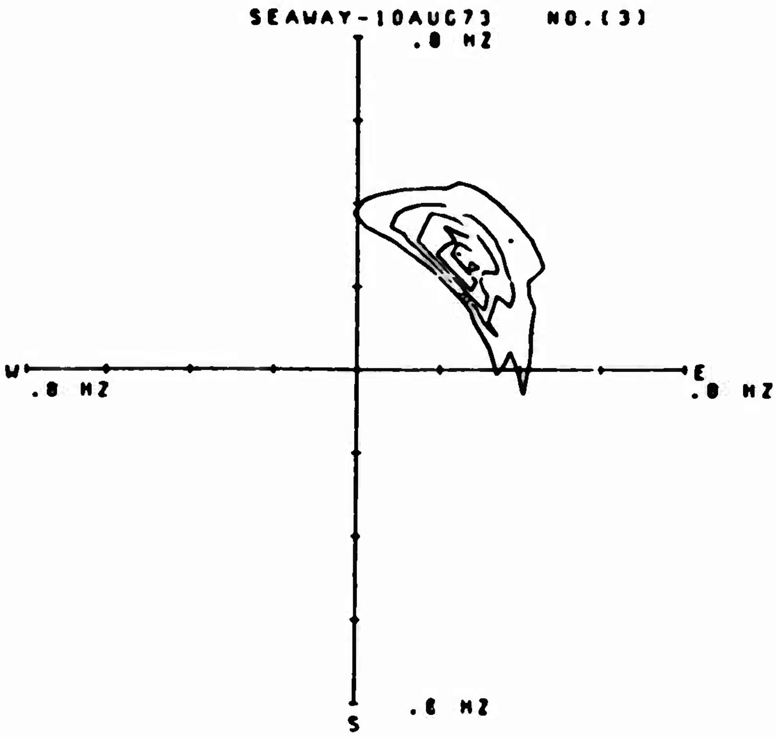

FIGURE E 3.8

DIRECTIONAL SPECTRA

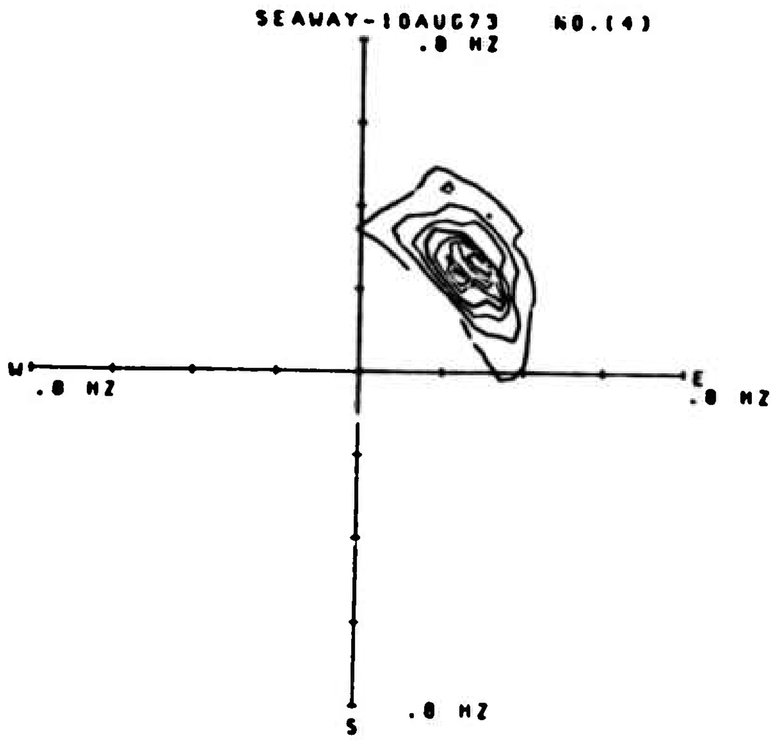

FIGURE E 3.9

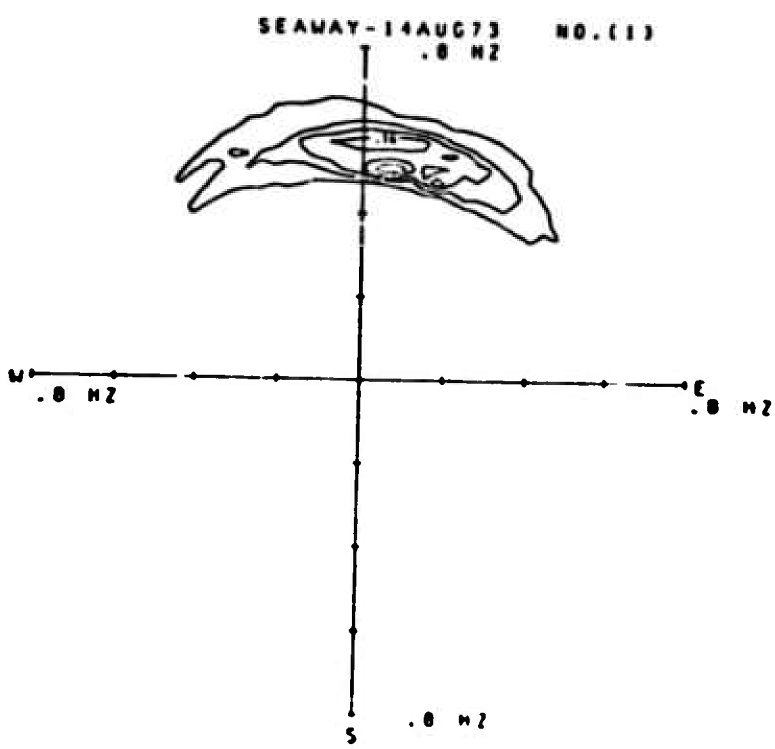

FIGURE E 3.10

DIRECTIONAL SPECTRA

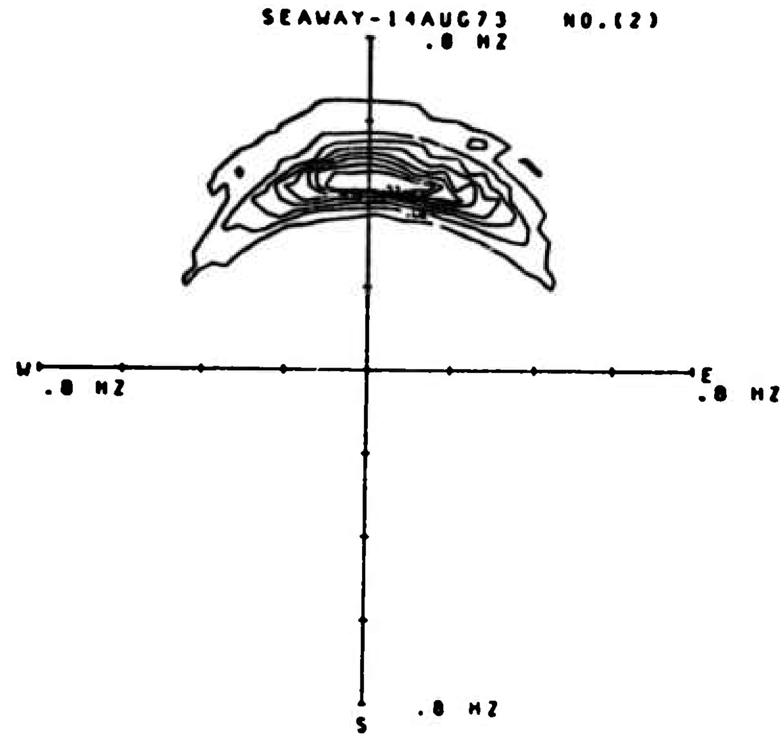

FIGURE E 3.11

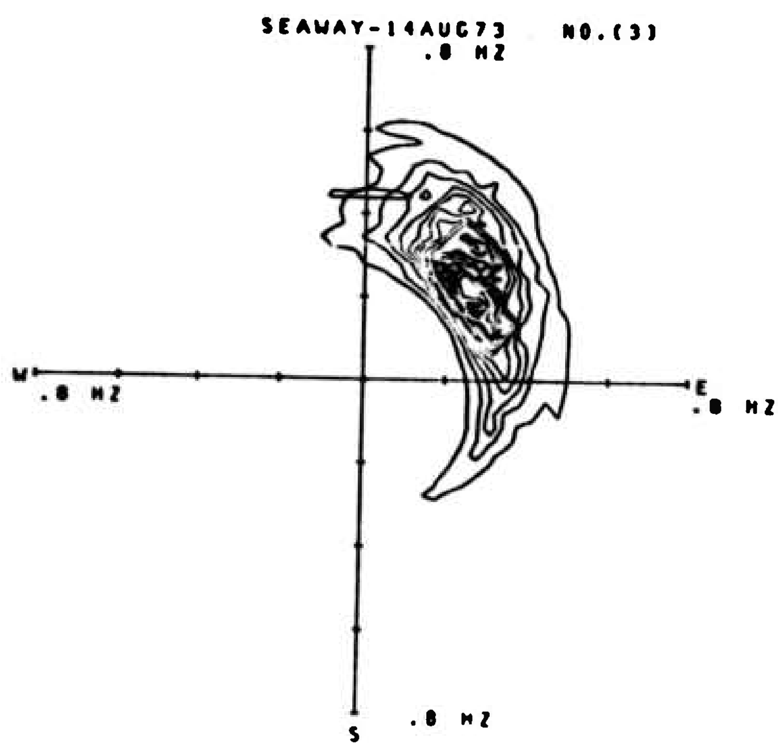

FIGURE E 3.12

DIRECTIONAL SPECTRA

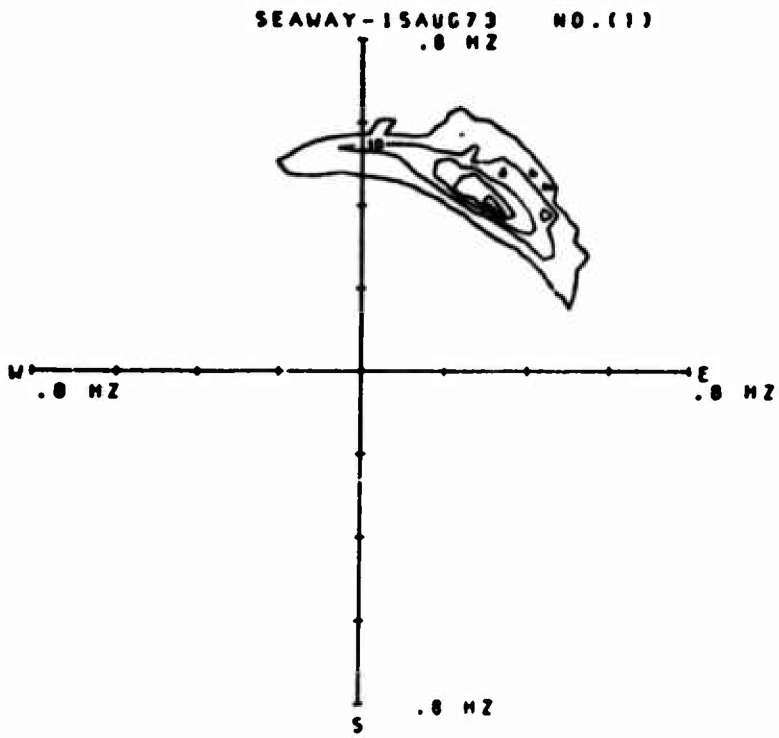

FIGURE E 3.13

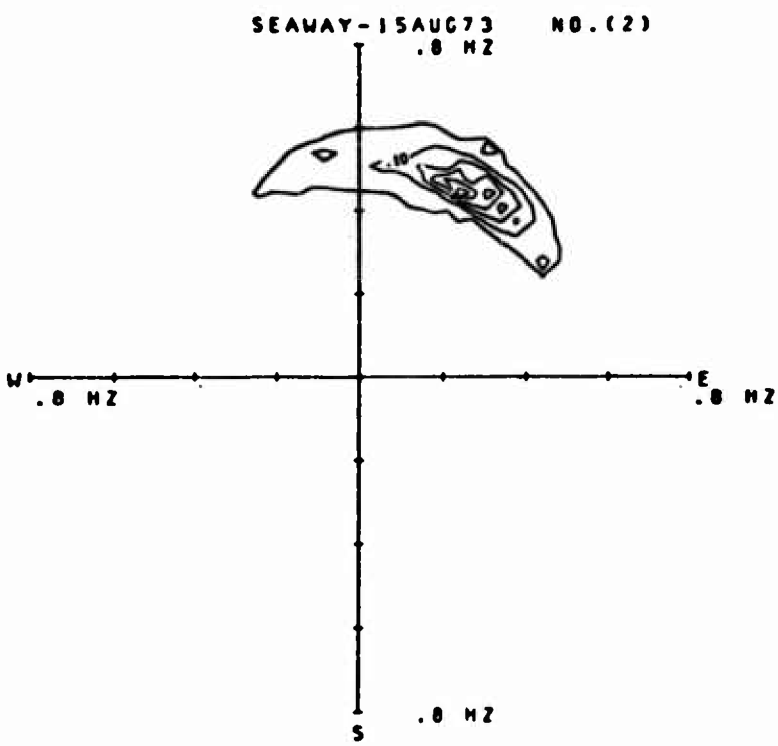

FIGURE E 3.14

DIRECTIONAL SPECTRA

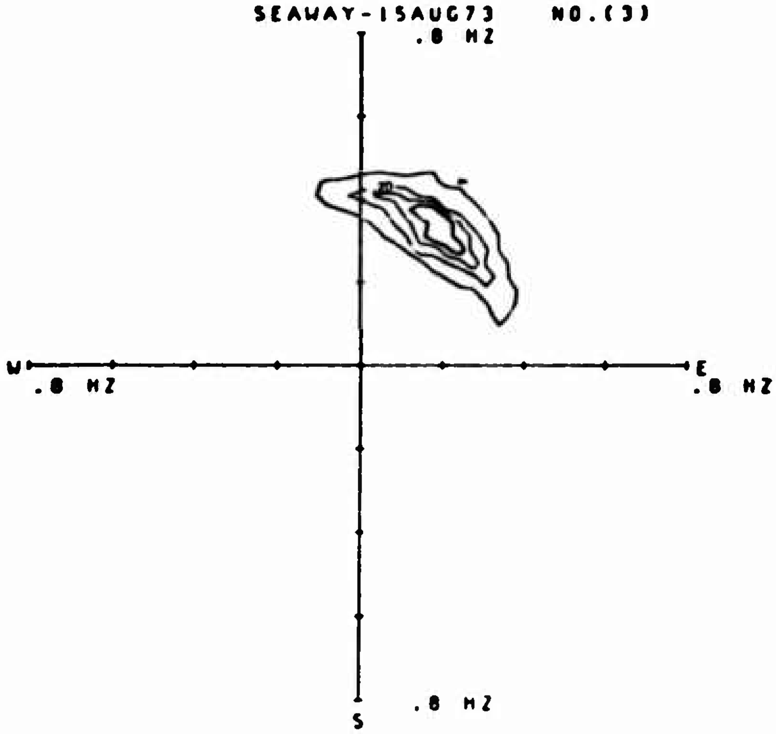

FIGURE E 3.15

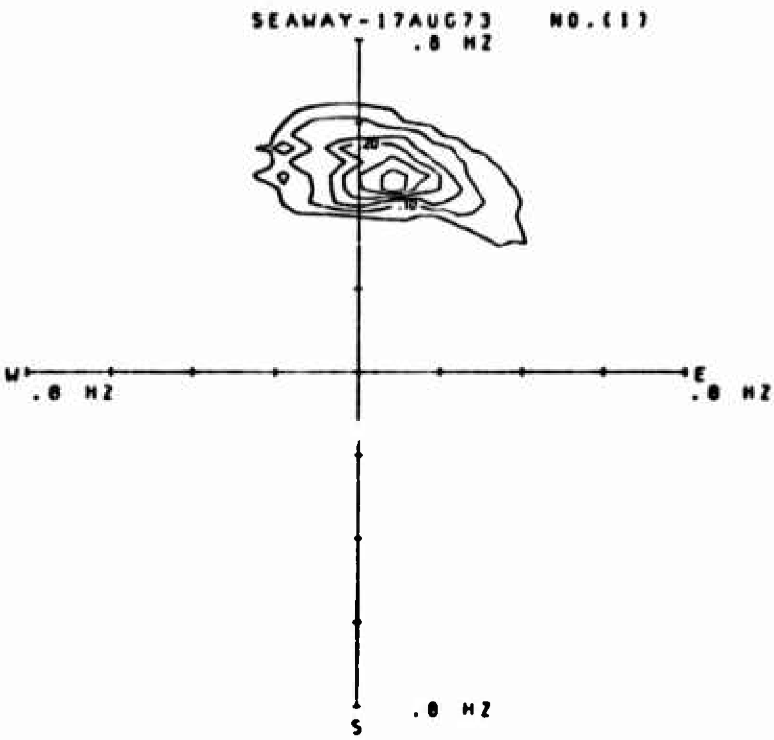

FIGURE E 3.16

DIRECTIONAL SPECTRA

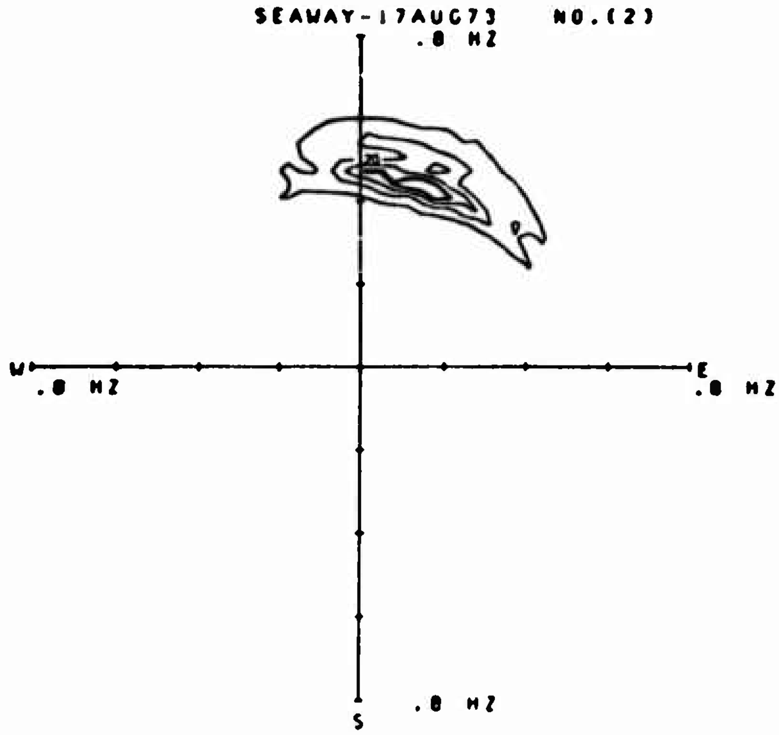

FIGURE E 3.17

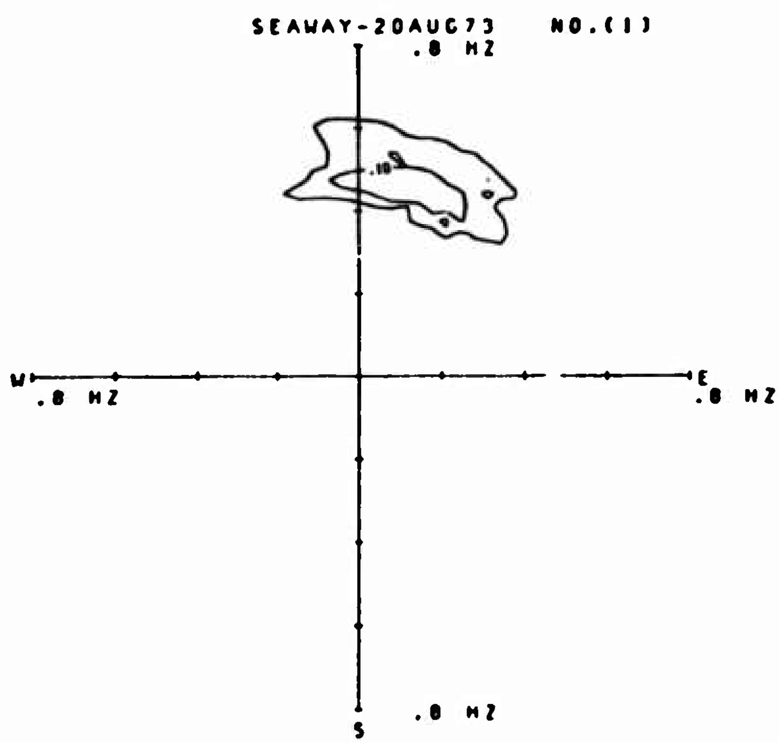

FIGURE E 3.18

DIRECTIONAL SPECTRA

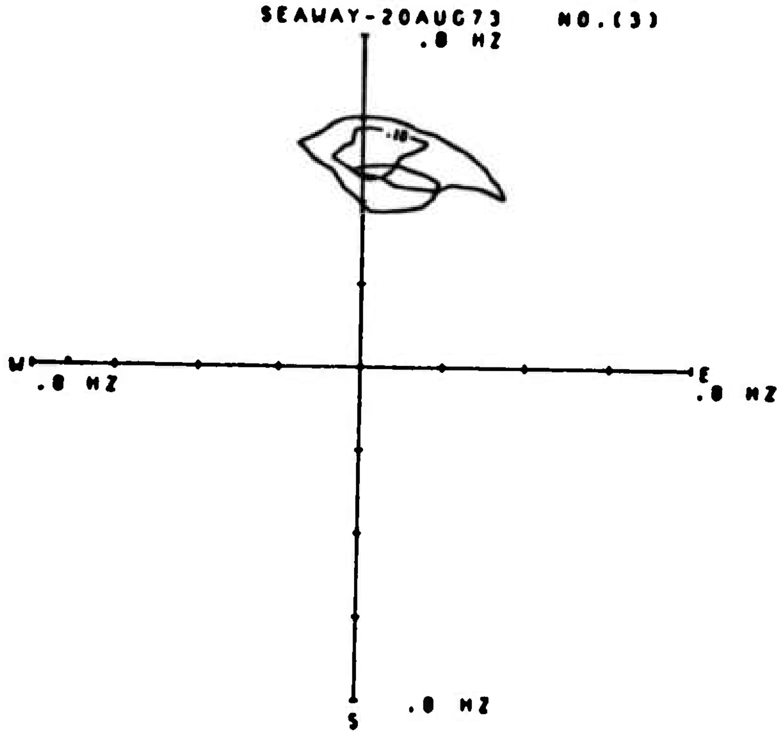

FIGURE E 3.19

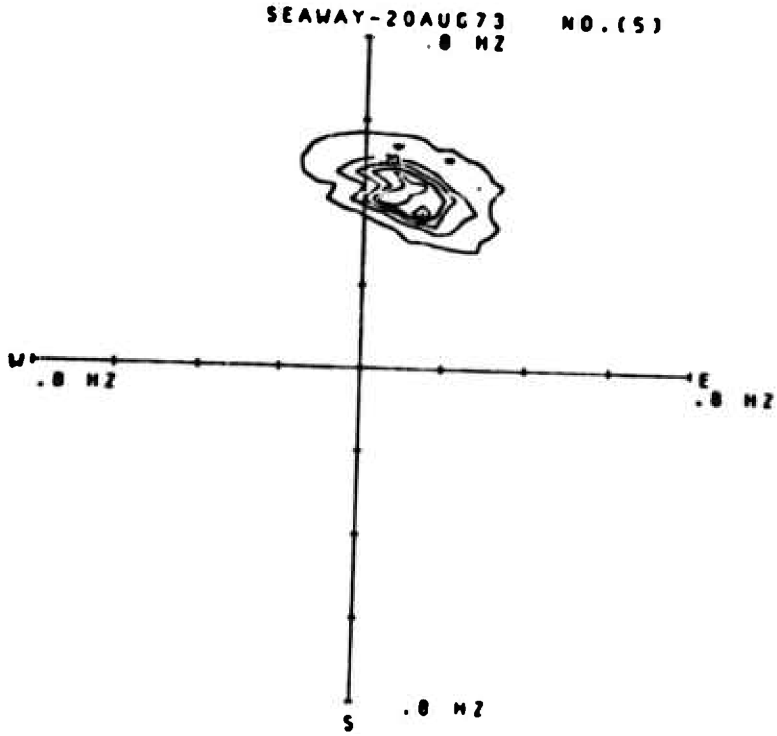

FIGURE E 3.20

DIRECTIONAL SPECTRA

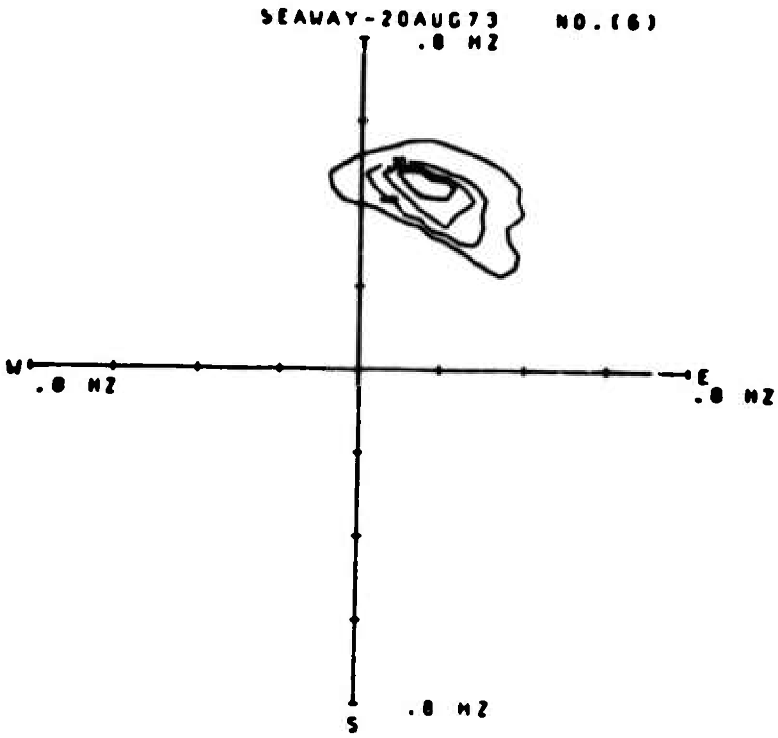

FIGURE E 3.21

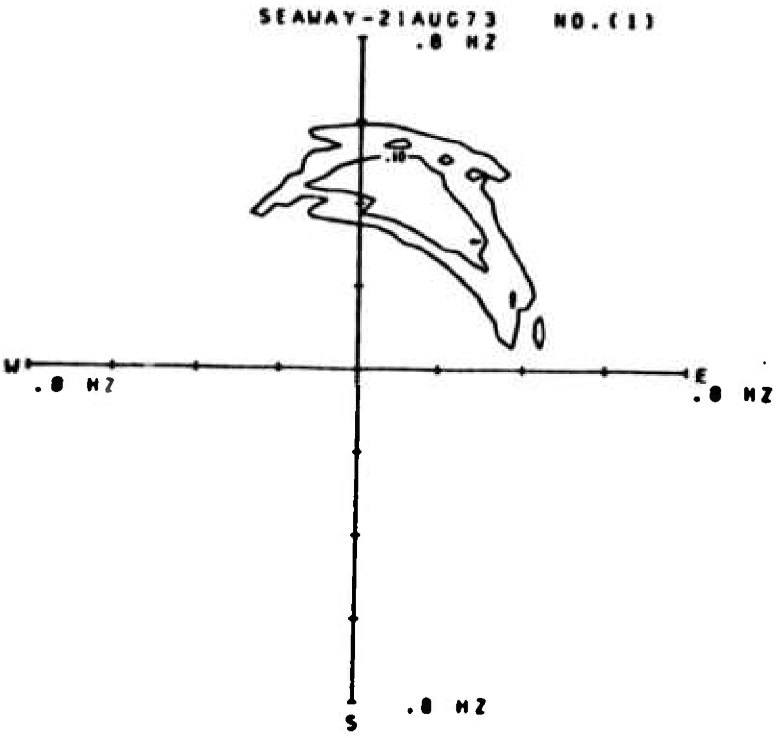

FIGURE E 3.22

DIRECTIONAL SPECTRA

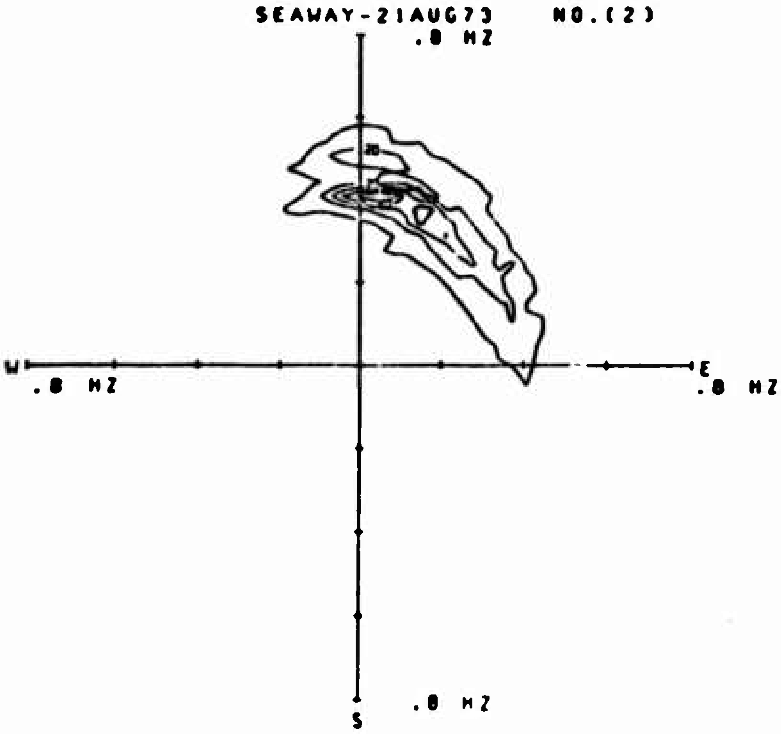

FIGURE E 3.23

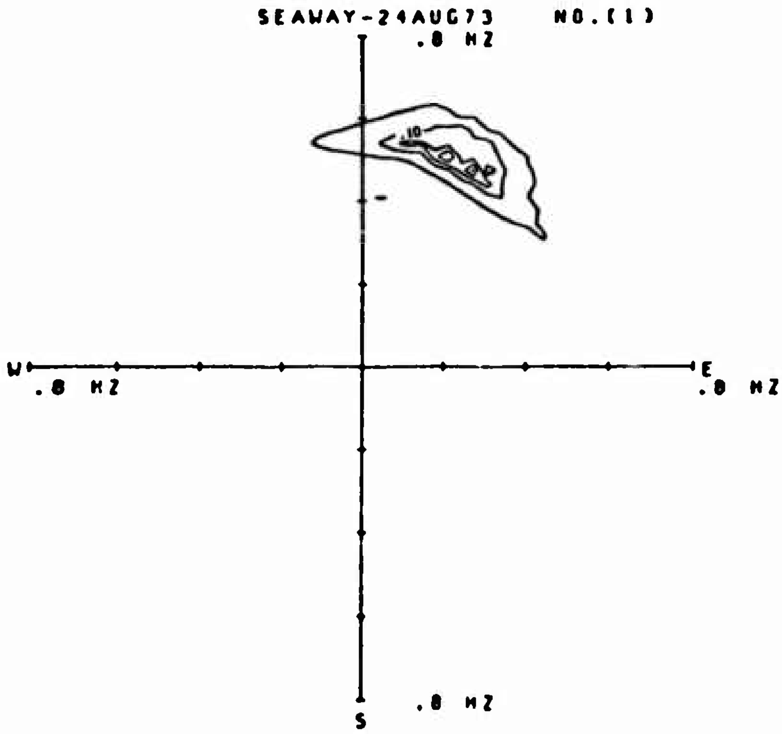

FIGURE E 3.24

DIRECTIONAL SPECTRA

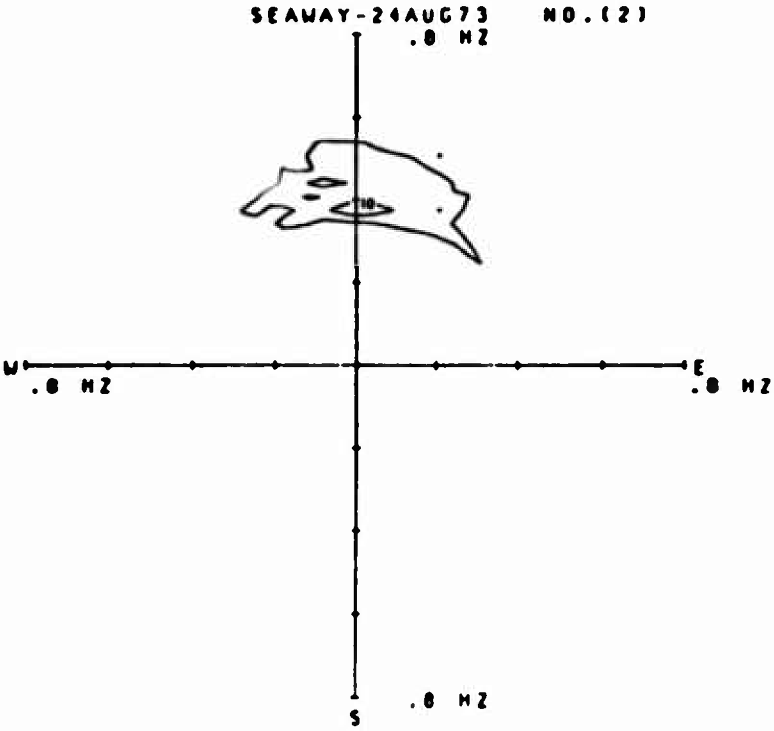

FIGURE E 3.25

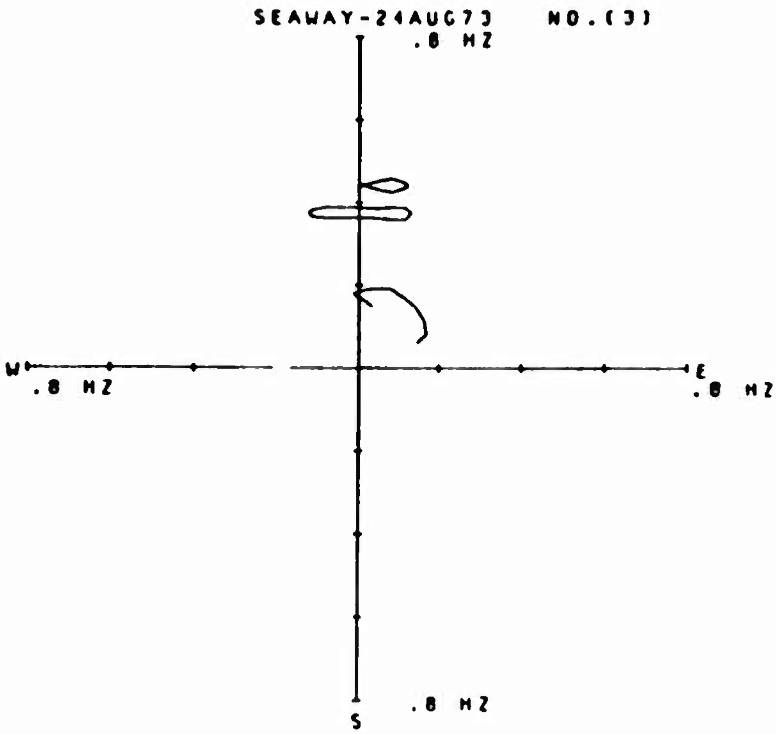

FIGURE E 3.26

DIRECTIONAL SPECTRA

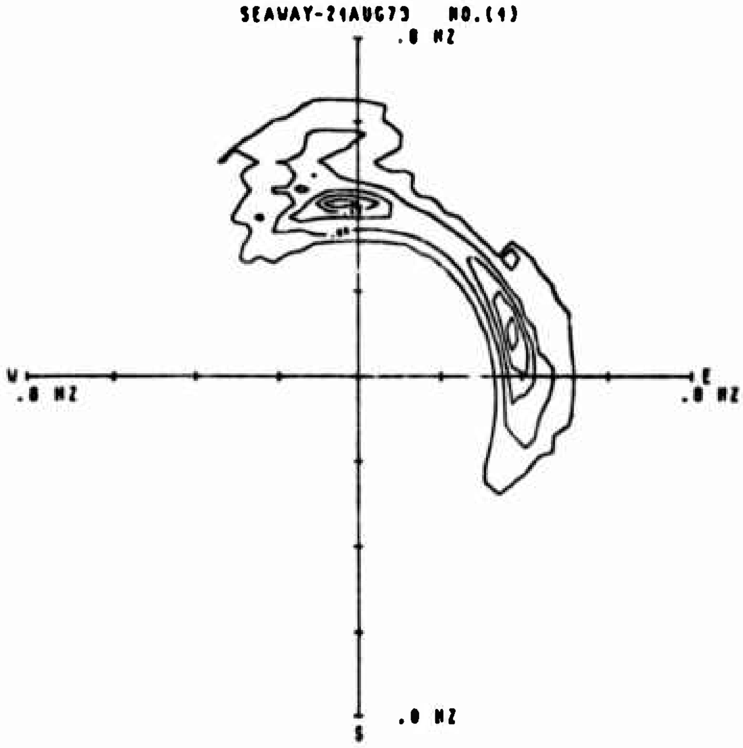

FIGURE E 3.27

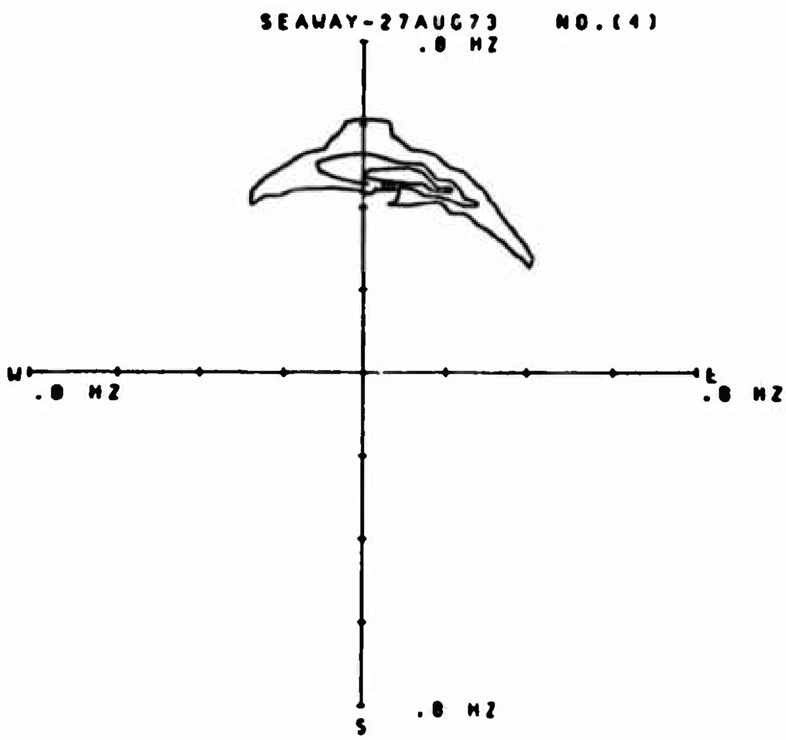

FIGURE E 3.28

DIRECTIONAL SPECTRA

SEAWAY-28AUG73 NO.(2)

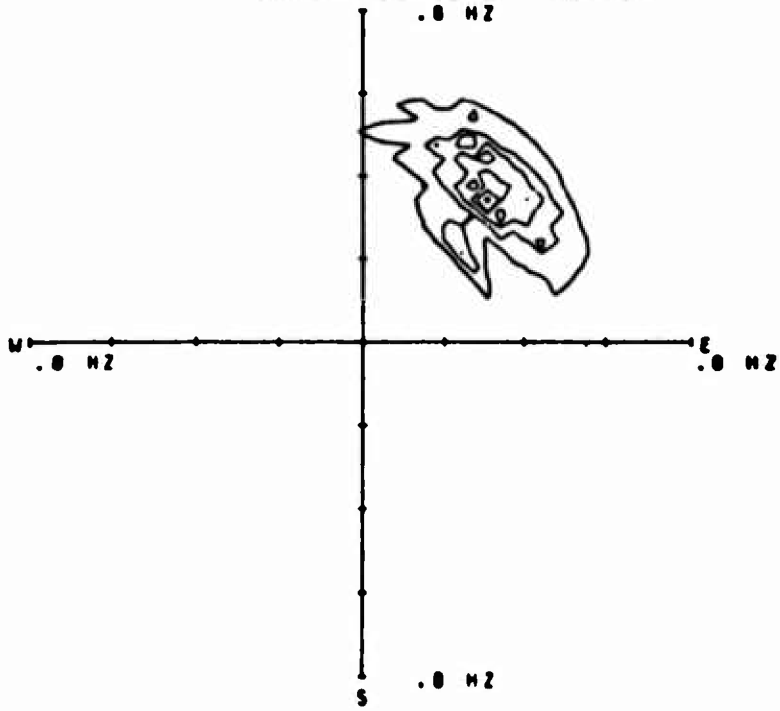

FIGURE E 3.29

SEAWAY-28AUG73 NO.(3)

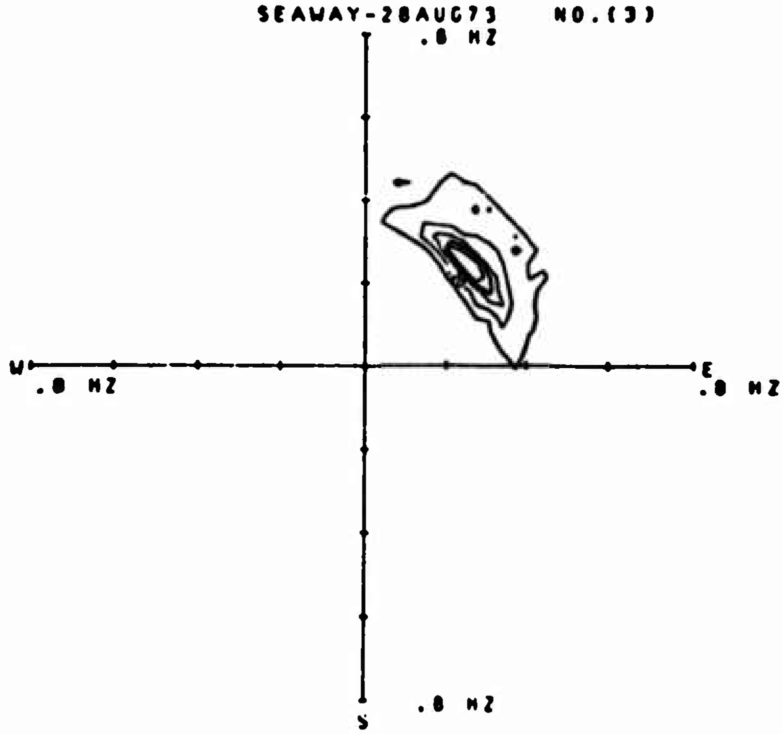

FIGURE E 3.30

DIRECTIONAL SPECTRA

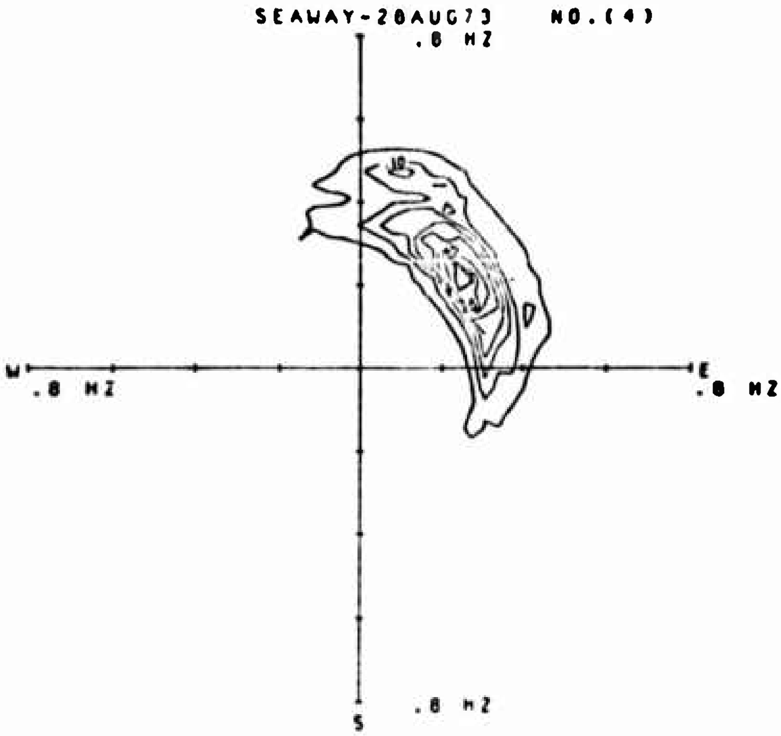

FIGURE E 3.31

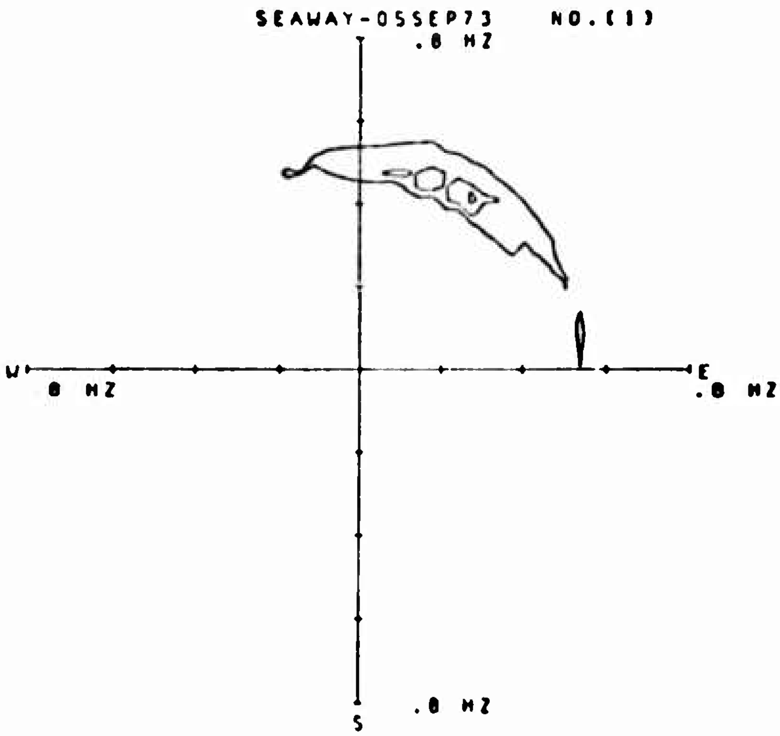

FIGURE E 3.32

DIRECTIONAL SPECTRA

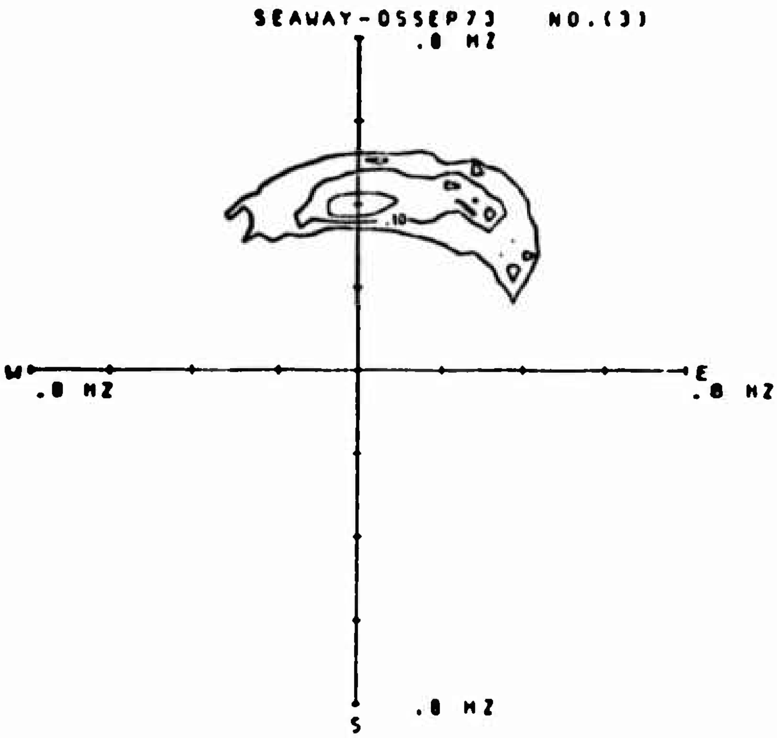

FIGURE E 3.33

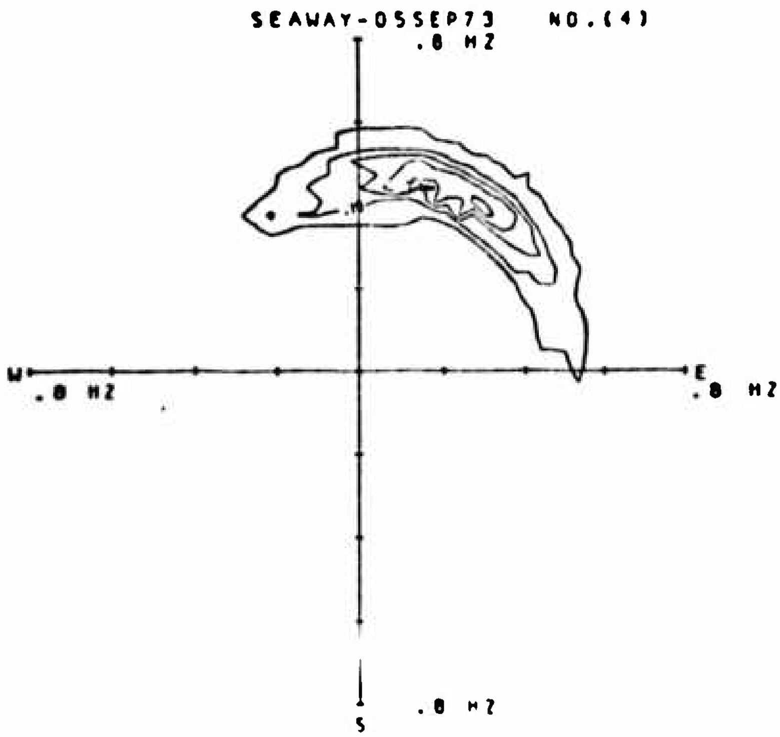

FIGURE E 3.34

DIRECTIONAL SPECTRA

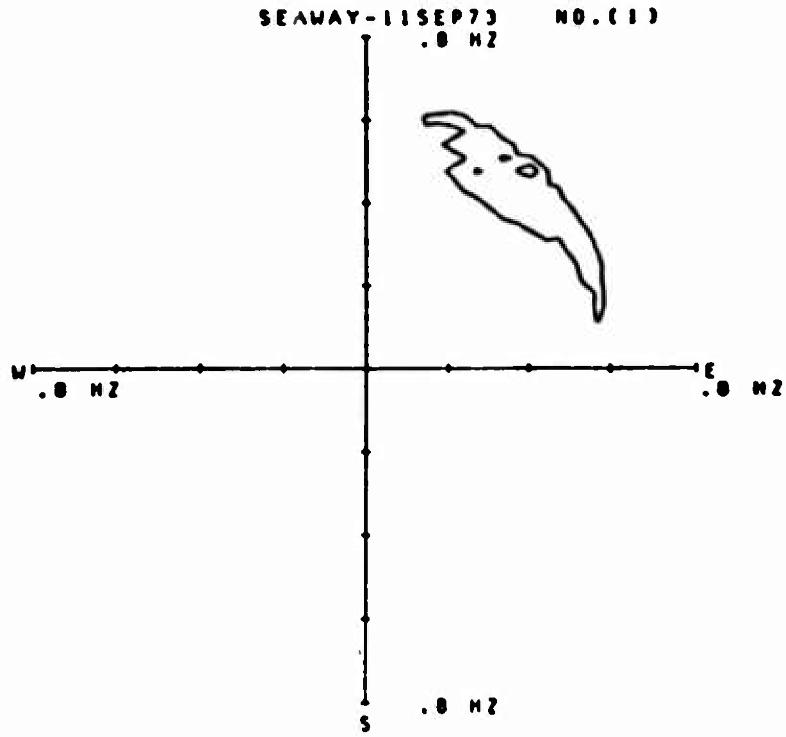

FIGURE E 3.35

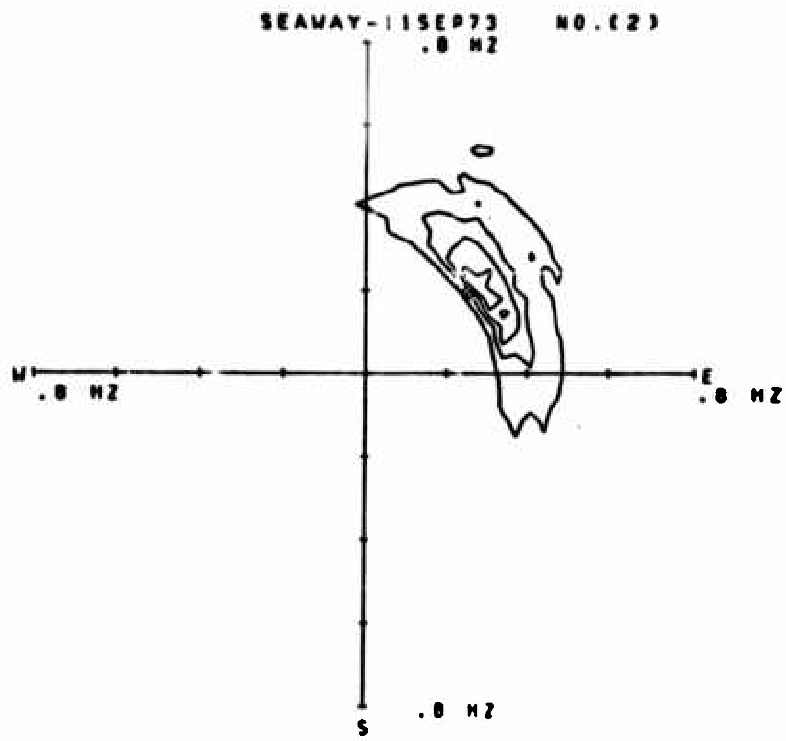

FIGURE E 3.36

DIRECTIONAL SPECTRA

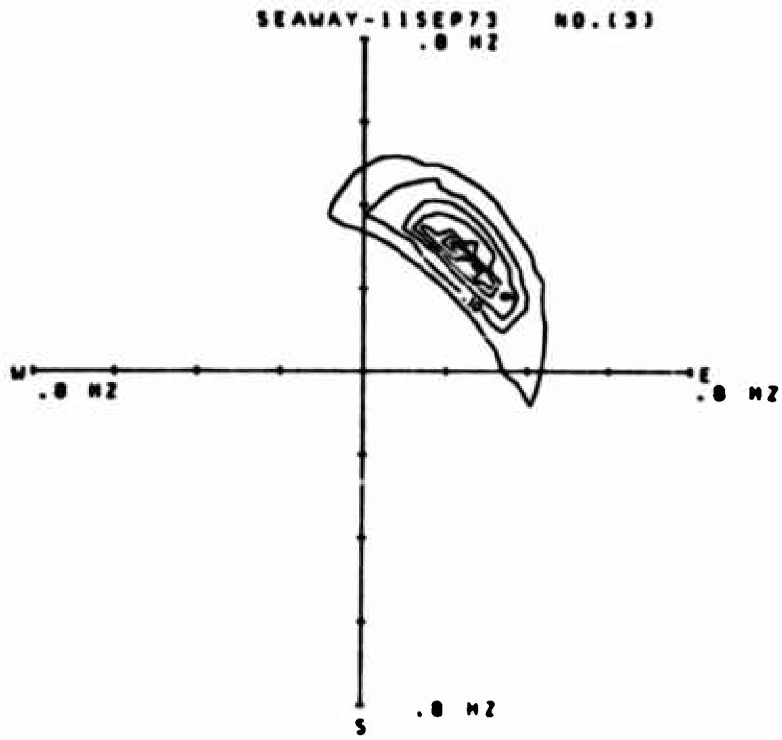

FIGURE E 3.37

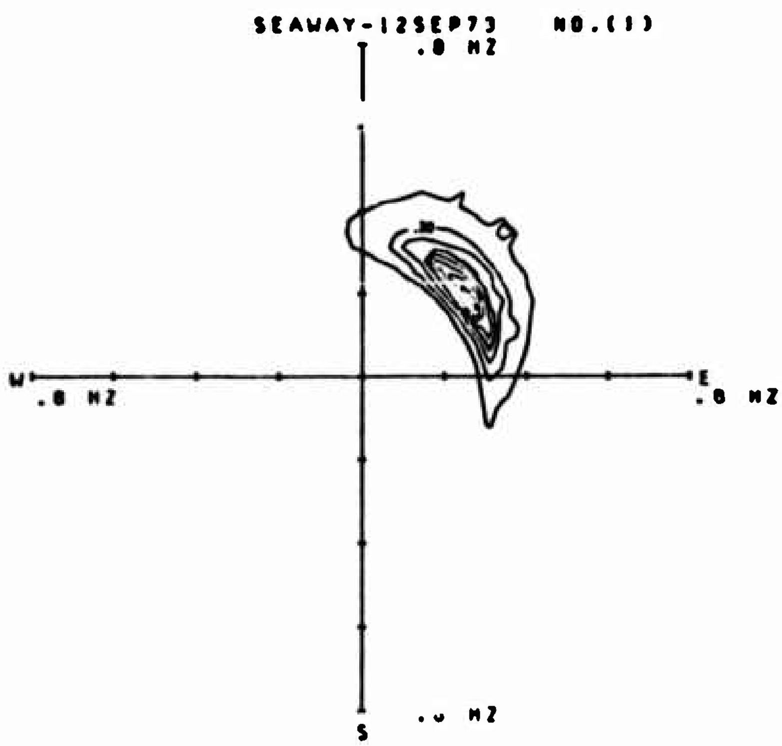

FIGURE E 3.38

DIRECTIONAL SPECTRA

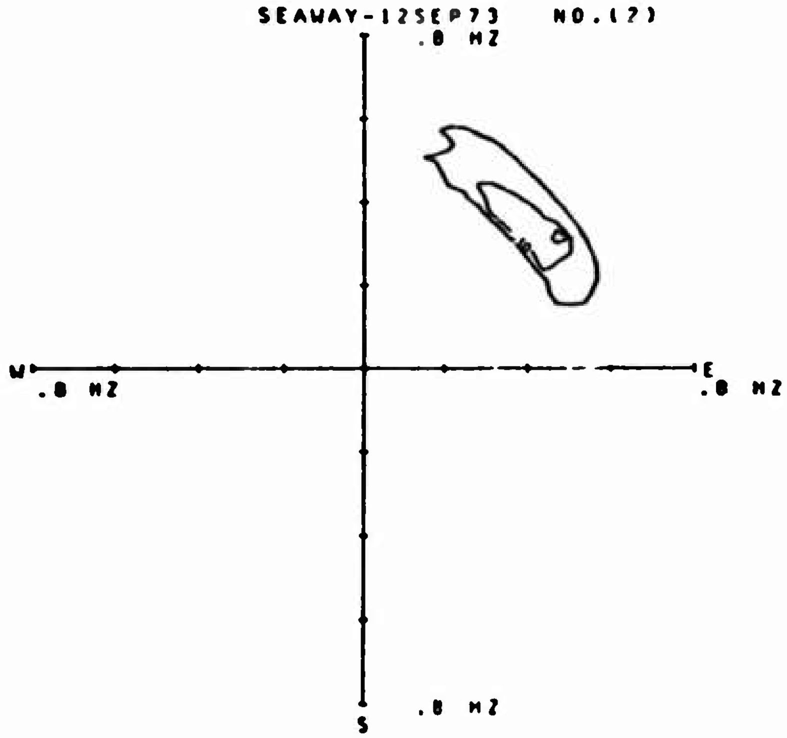

FIGURE E 3.39

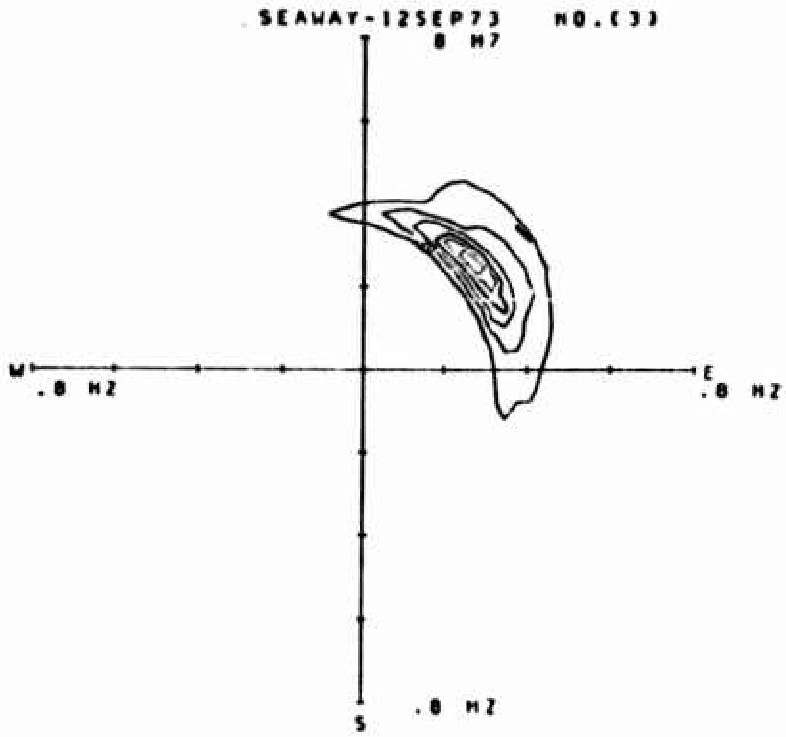

FIGURE E 3.40

DIRECTIONAL SPECTRA

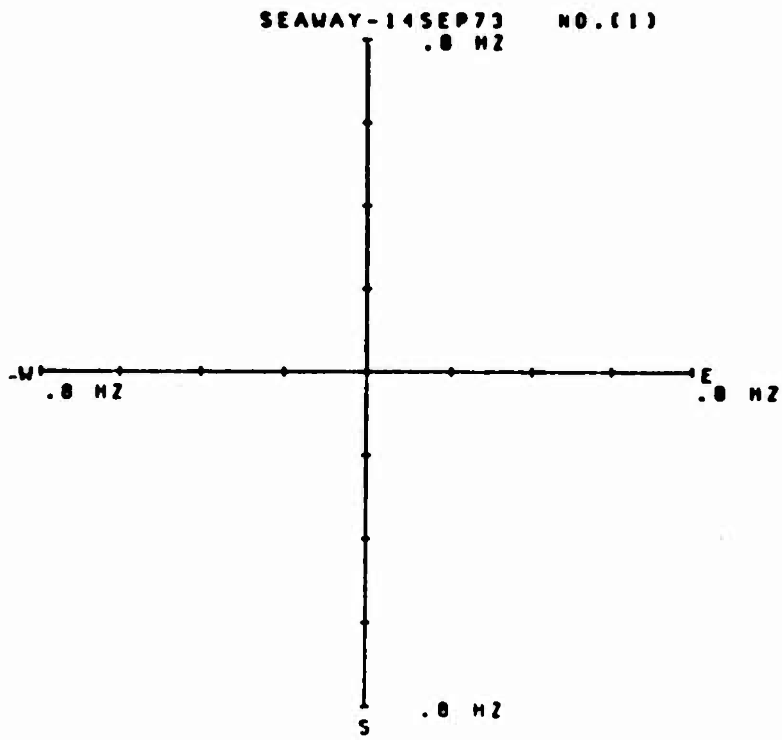

FIGURE E 3.41

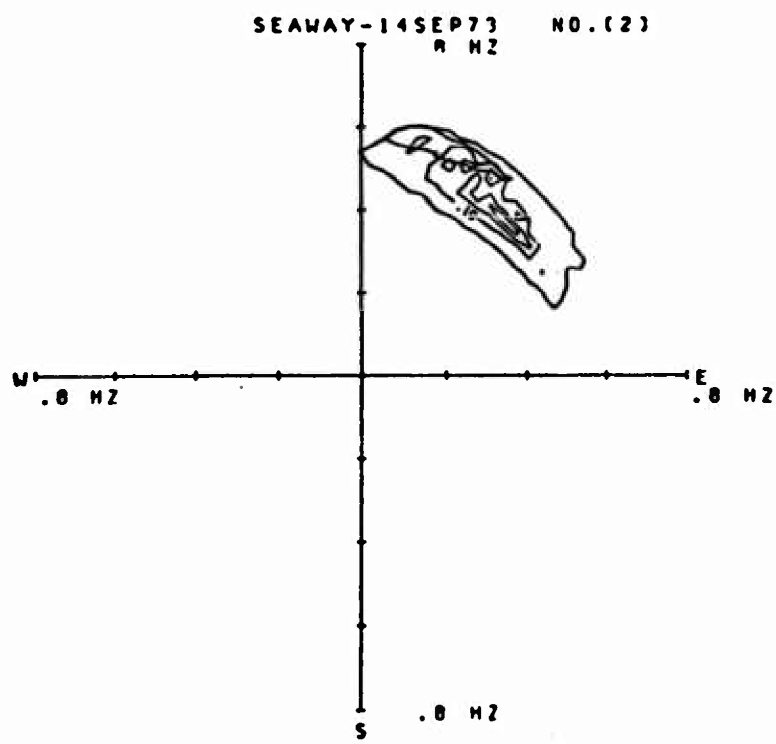

FIGURE E 3.42

DIRECTIONAL SPECTRA

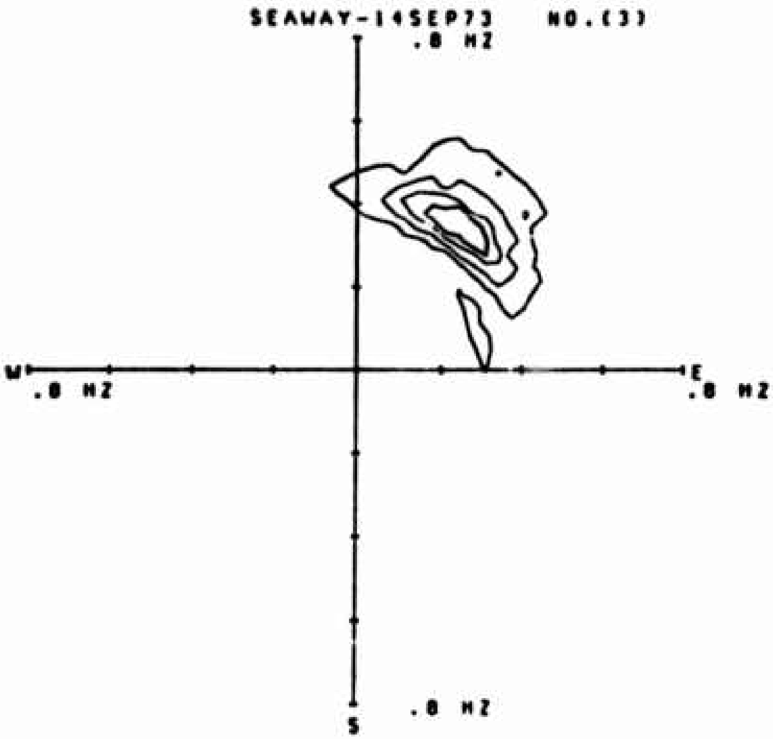

FIGURE E 3.43

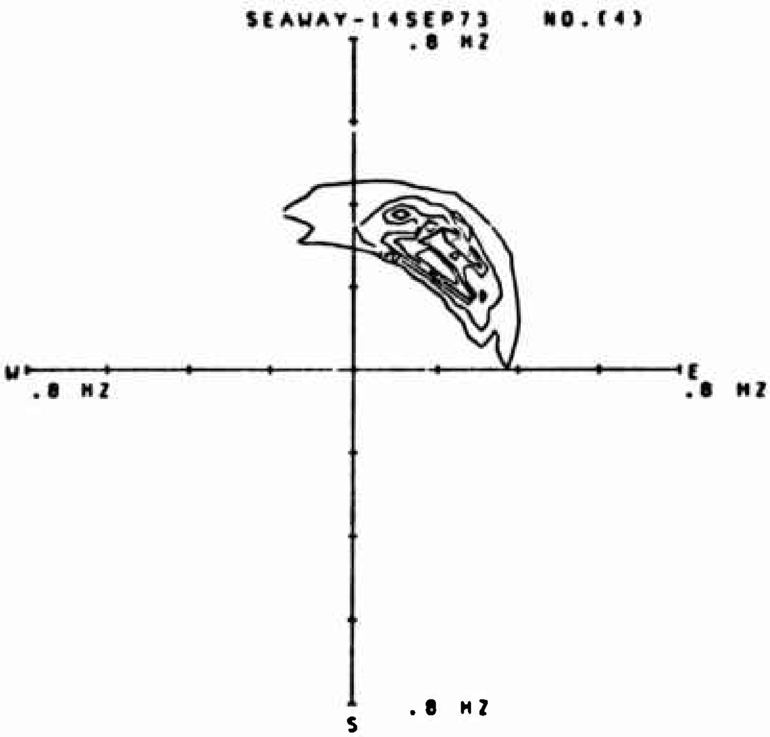

FIGURE E 3.44

DIRECTIONAL SPECTRA

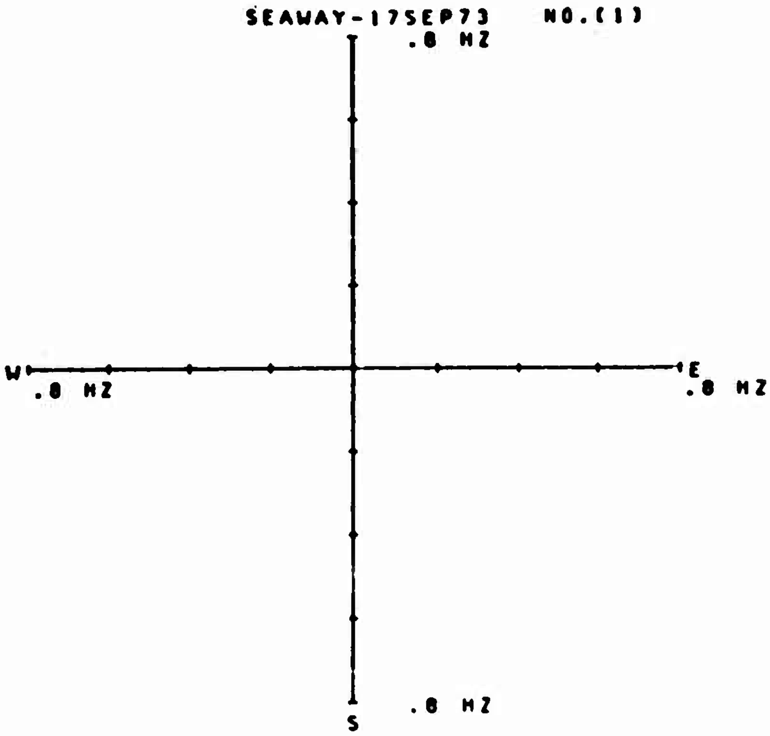

FIGURE E 3.45

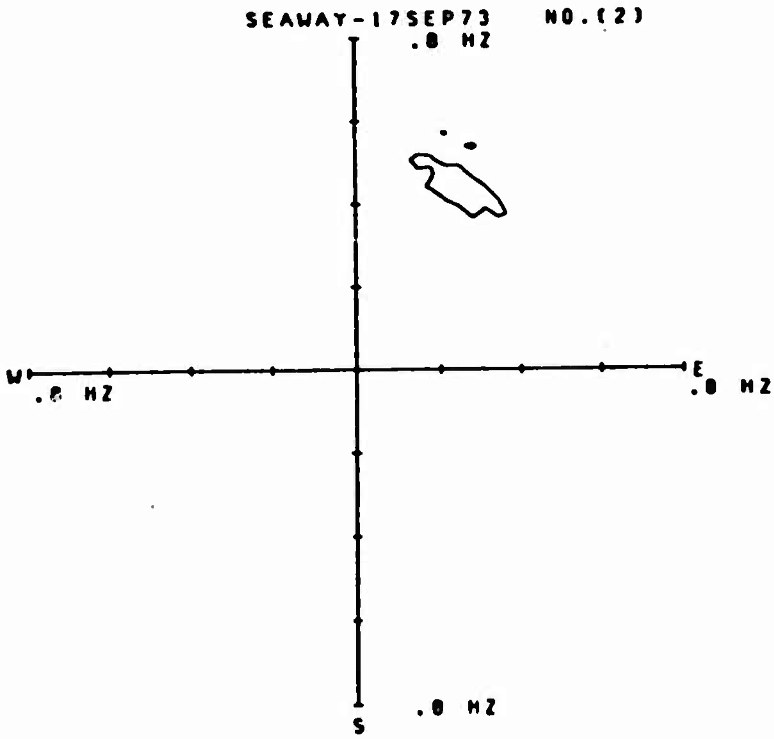

FIGURE E 3.46

DIRECTIONAL SPECTRA

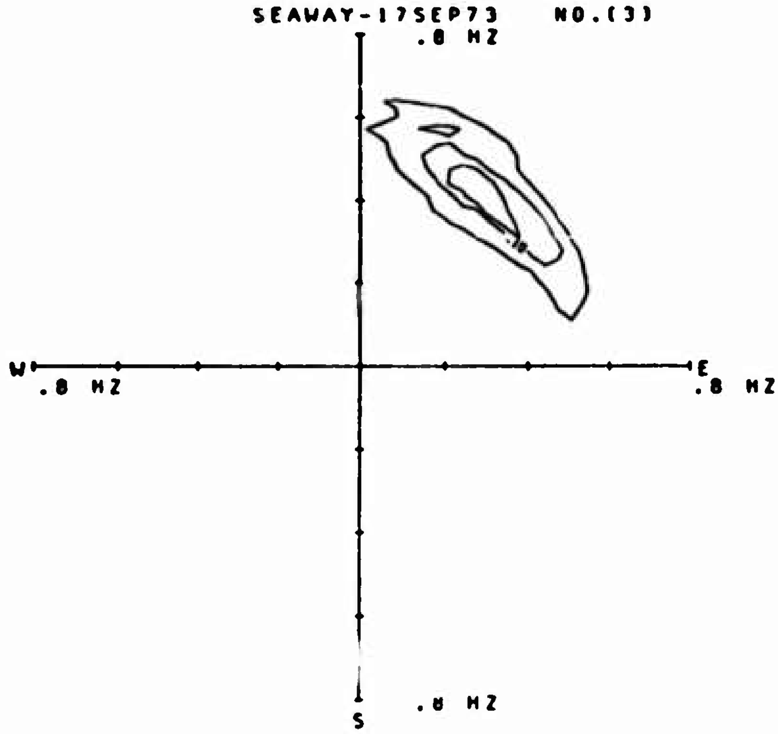

FIGURE E 3.47

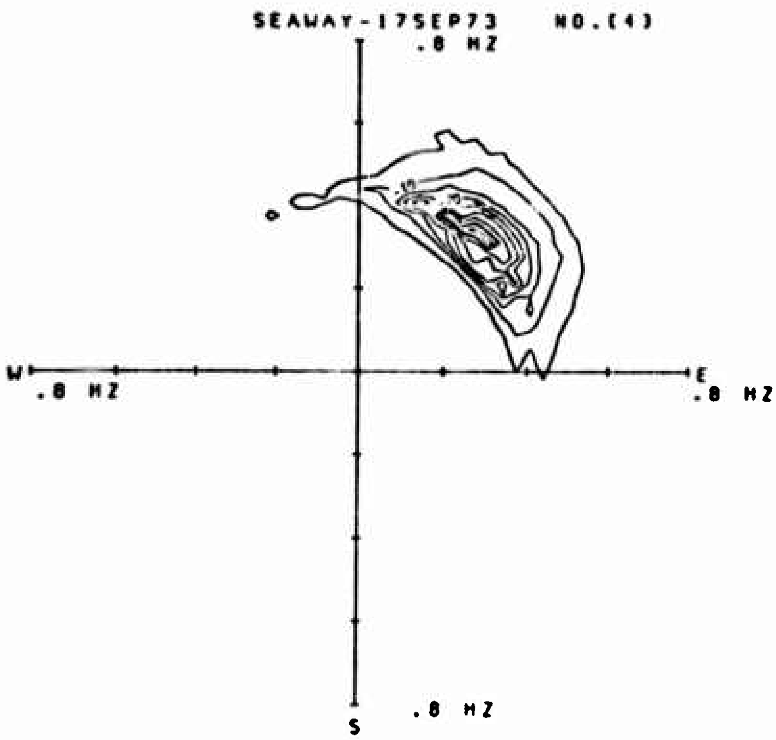

FIGURE E 3.48

DIRECTIONAL SPECTRA

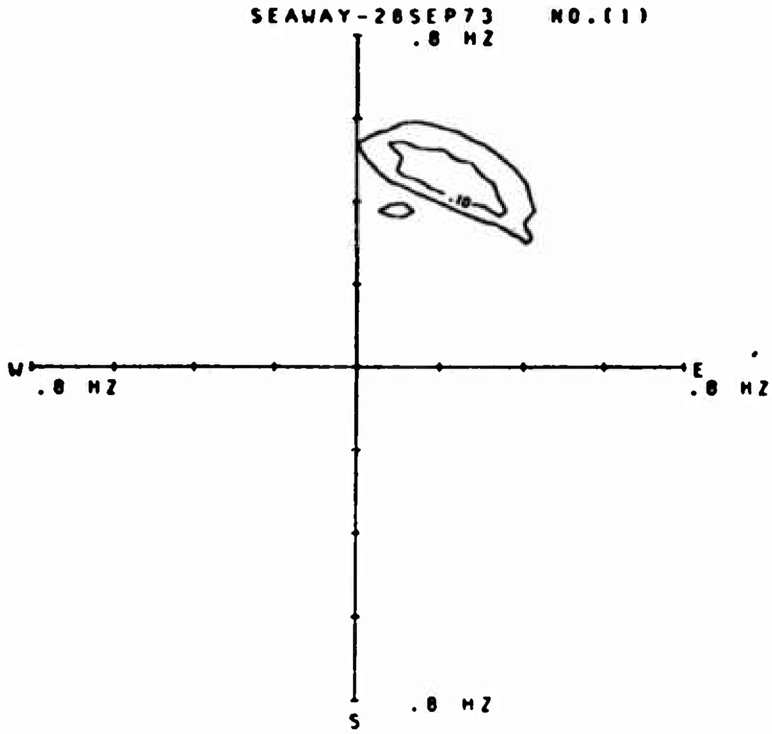

FIGURE E 3.49

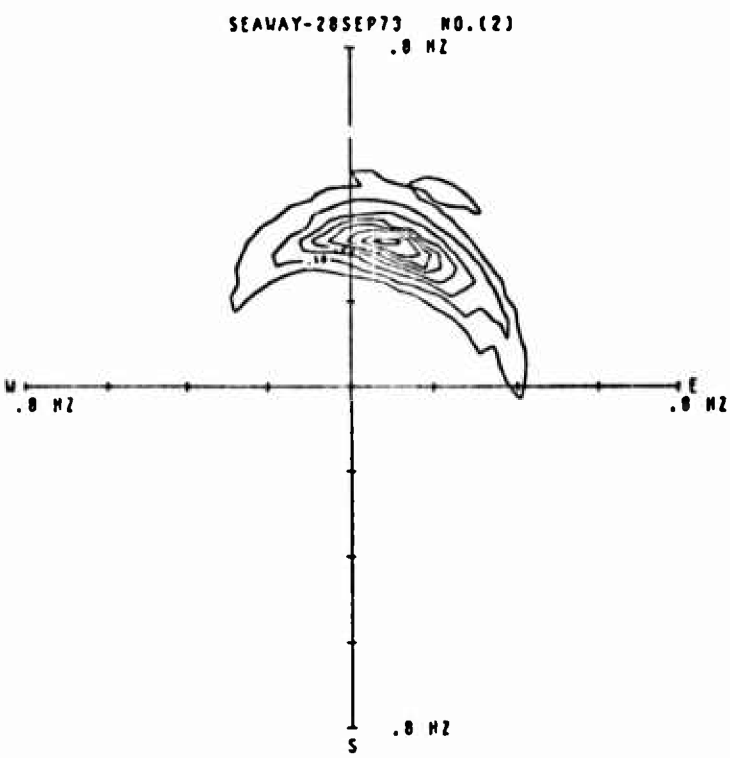

FIGURE E 3.50

DIRECTIONAL SPECTRA

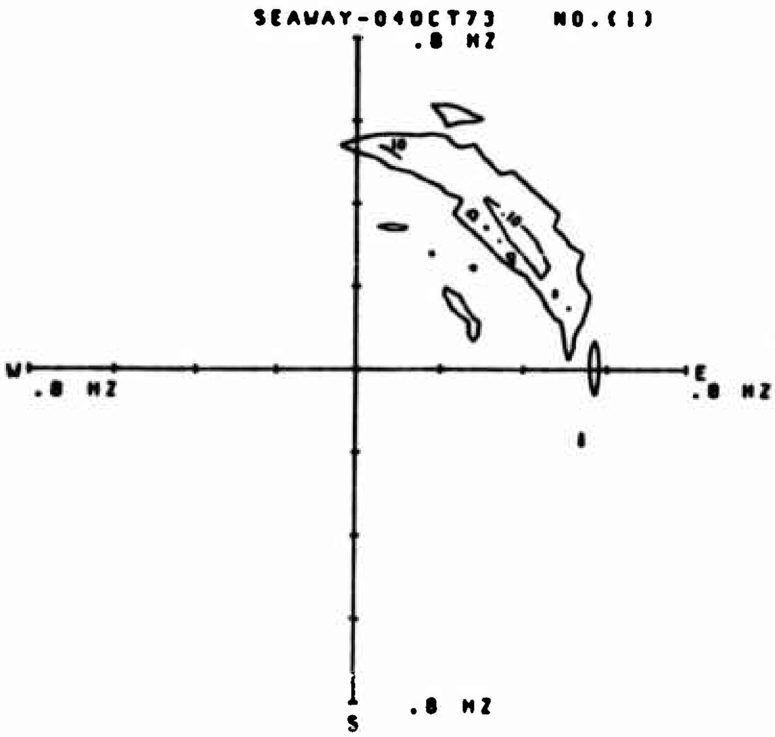

FIGURE E 3.51

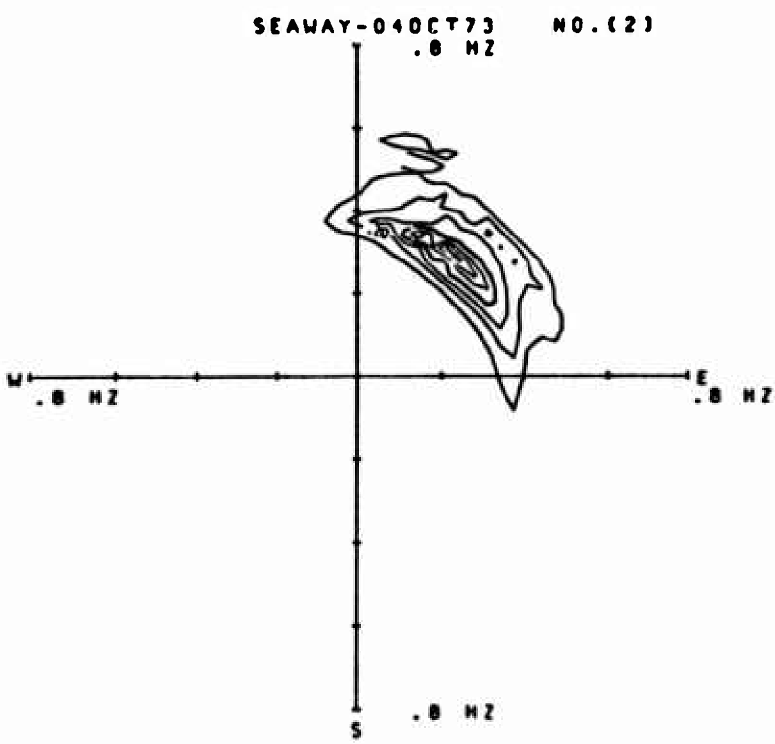

FIGURE E 3.52

DIRECTIONAL SPECTRA

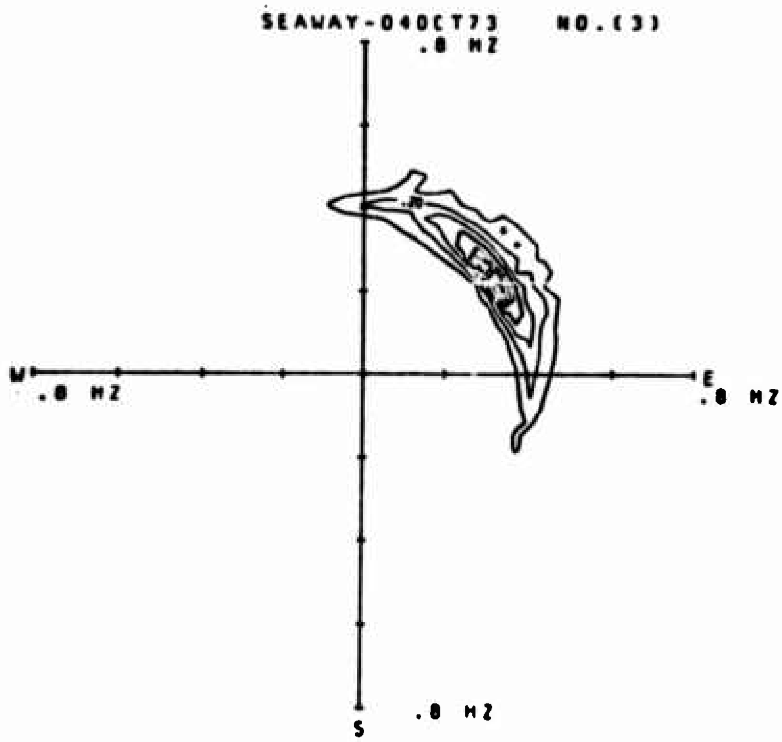

FIGURE E 3.53

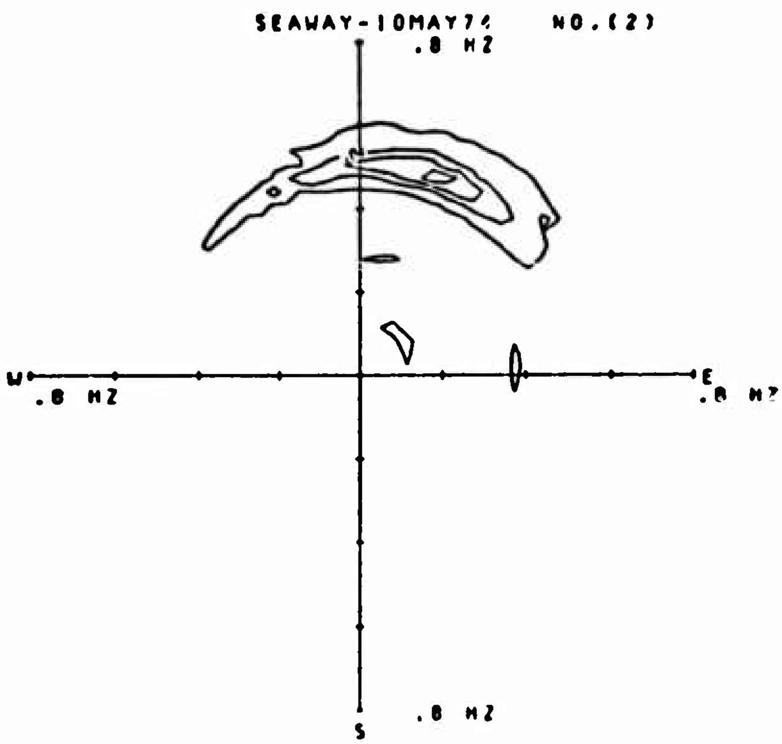

FIGURE E 3.54

DIRECTIONAL SPECTRA

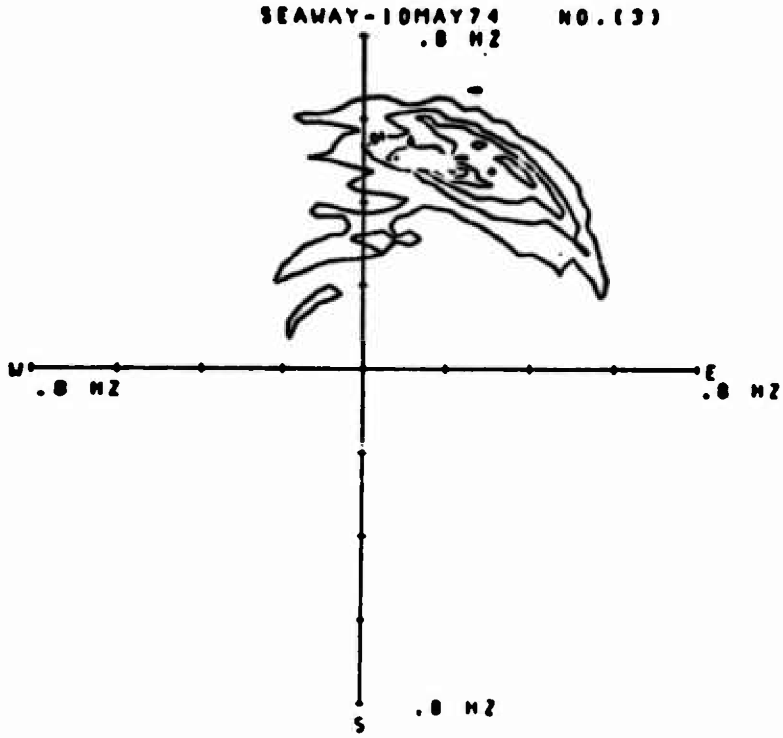

FIGURE E 3.55

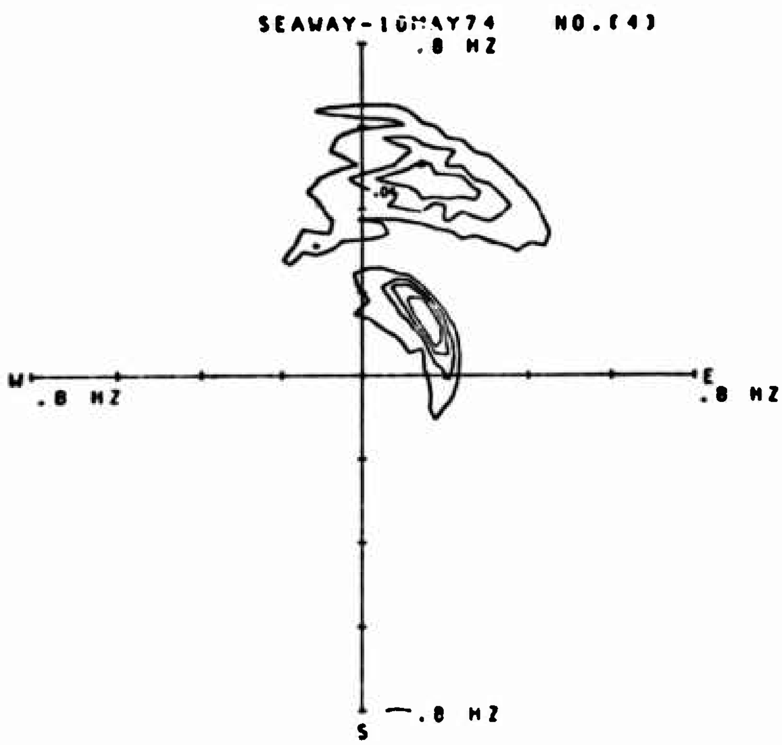

FIGURE E 3.56

DIRECTIONAL SPECTRA

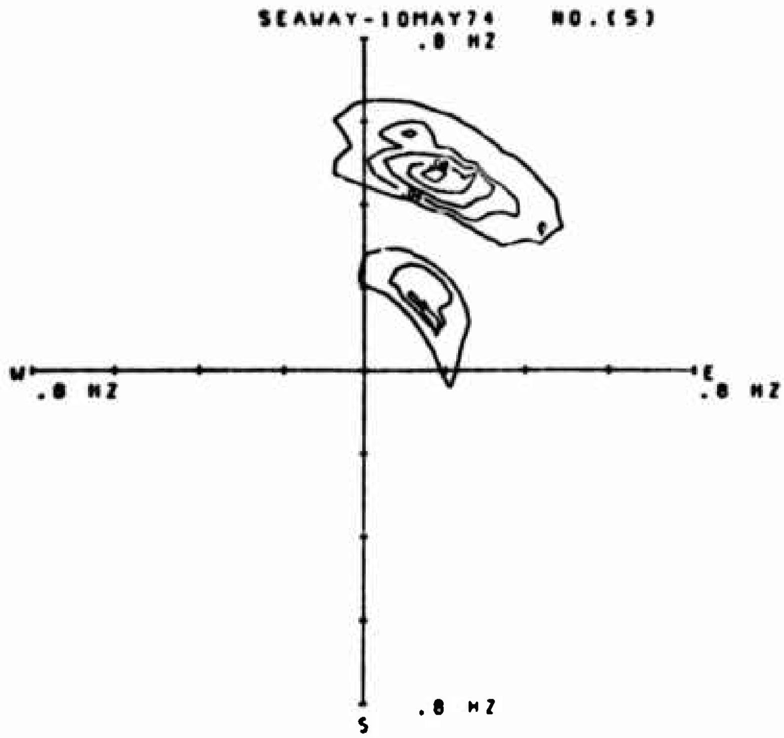

FIGURE E 3.57

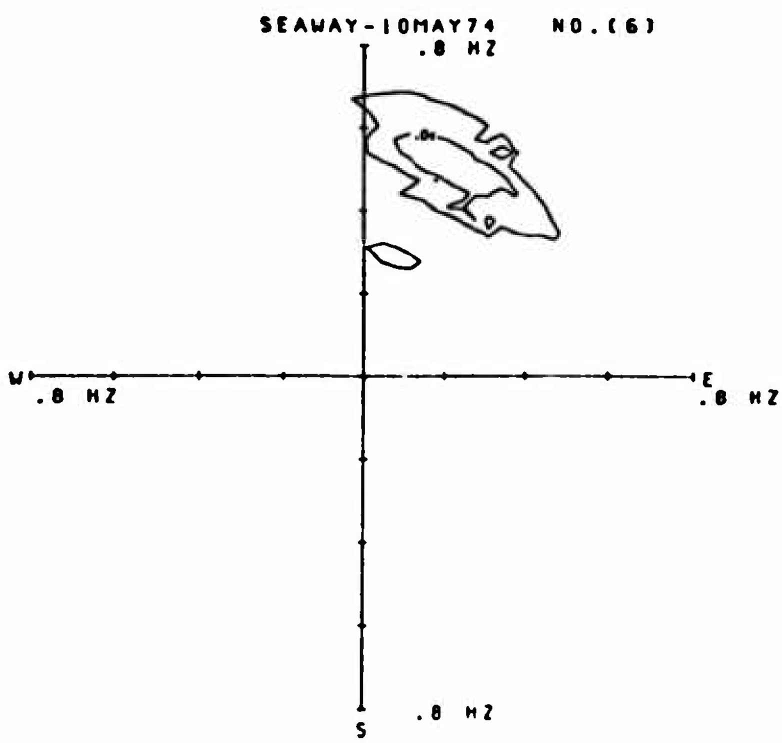

FIGURE E 3.58

DIRECTIONAL SPECTRA

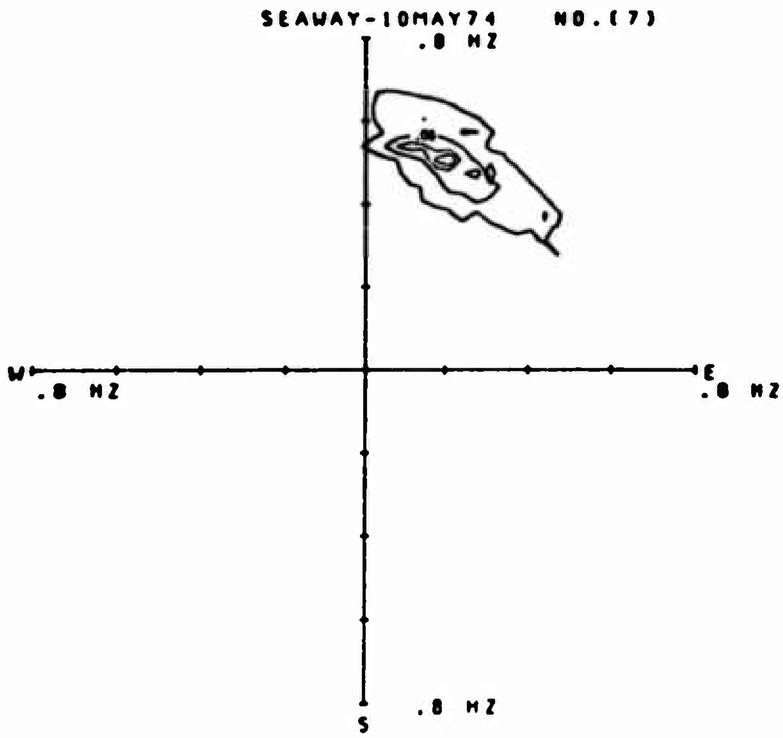

FIGURE E 3.59

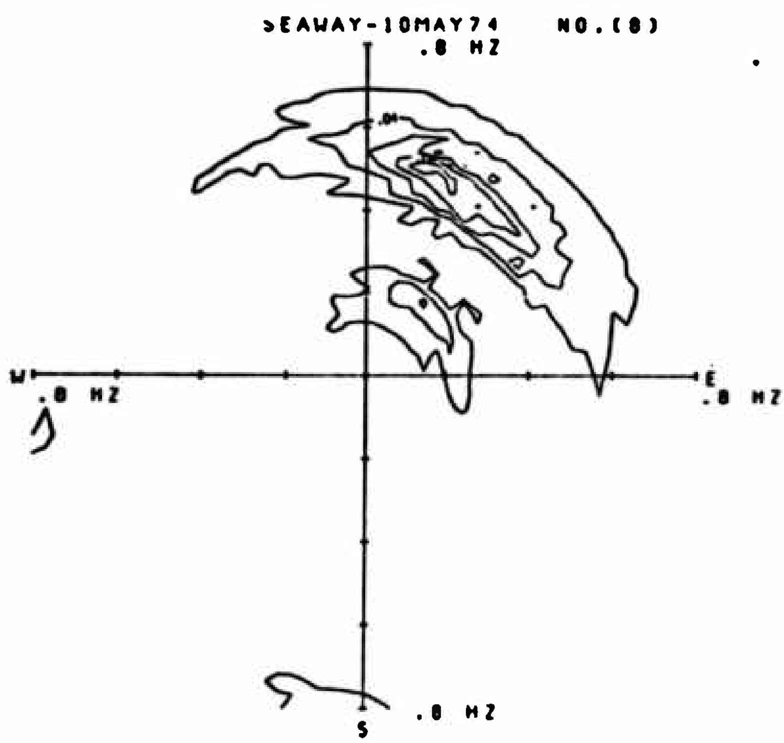

FIGURE E 3.60

DIRECTIONAL SPECTRA

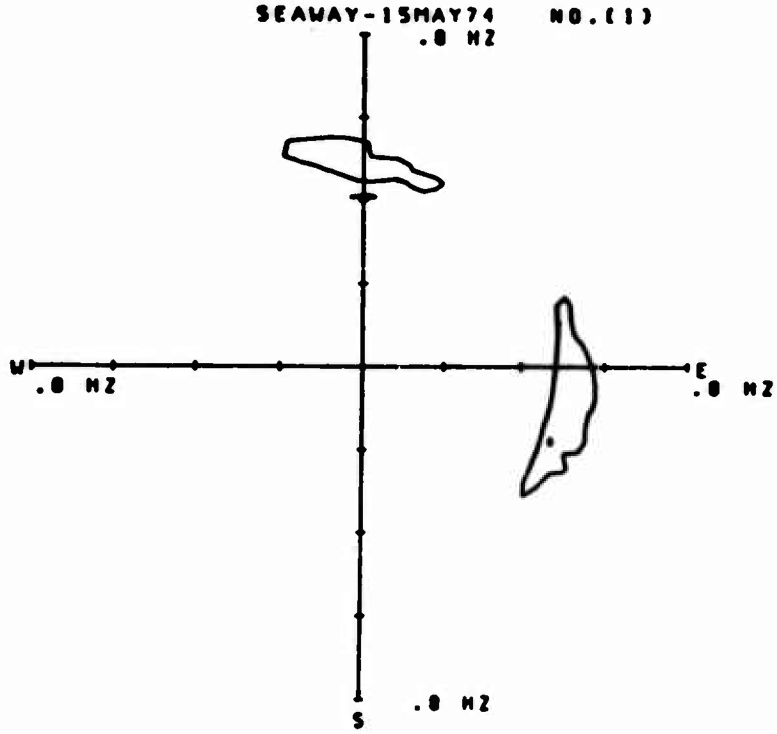

FIGURE E 3.61

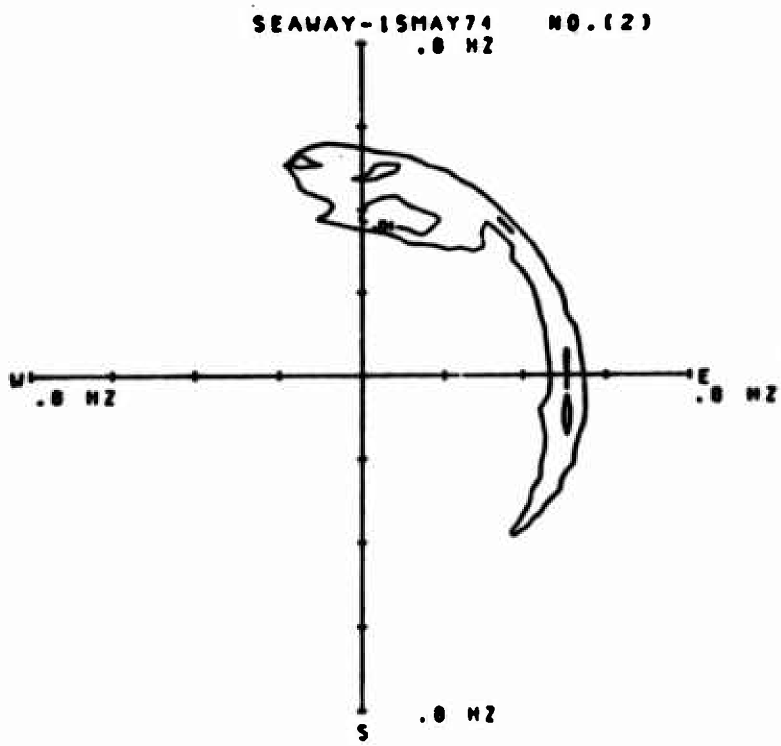

FIGURE E 3.62

DIRECTIONAL SPECTRA

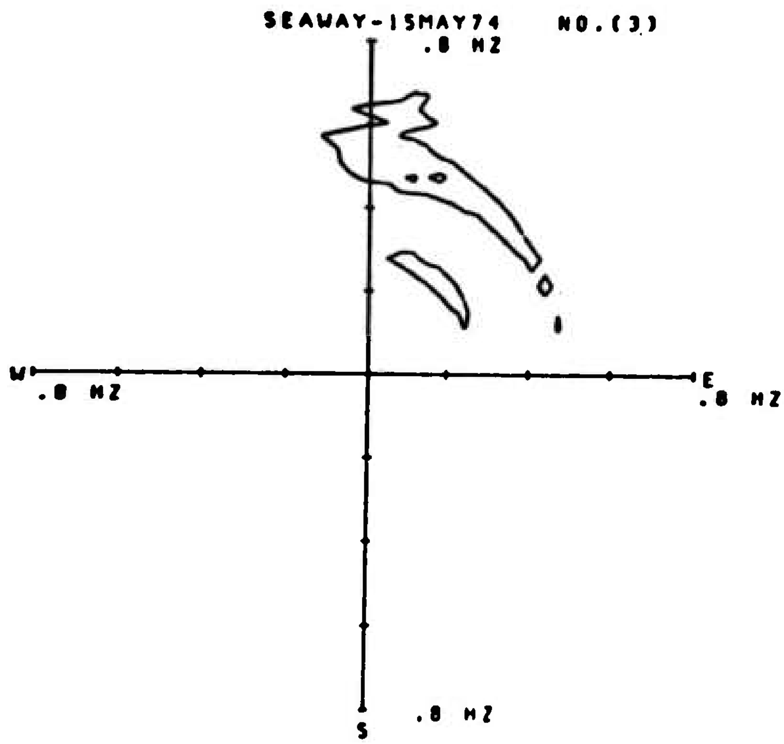

FIGURE E 3.63

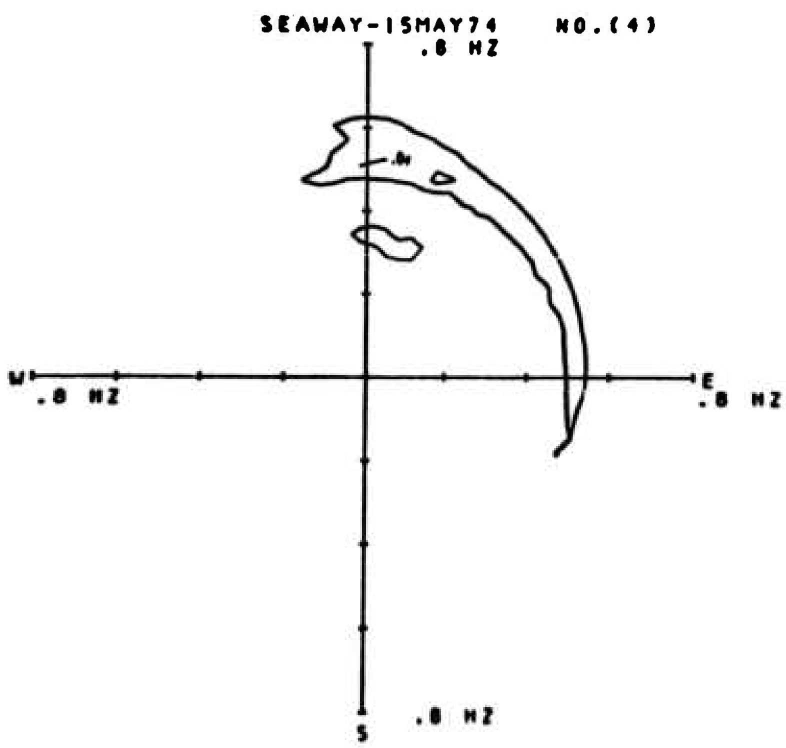

FIGURE E 3.64

DIRECTIONAL SPECTRA

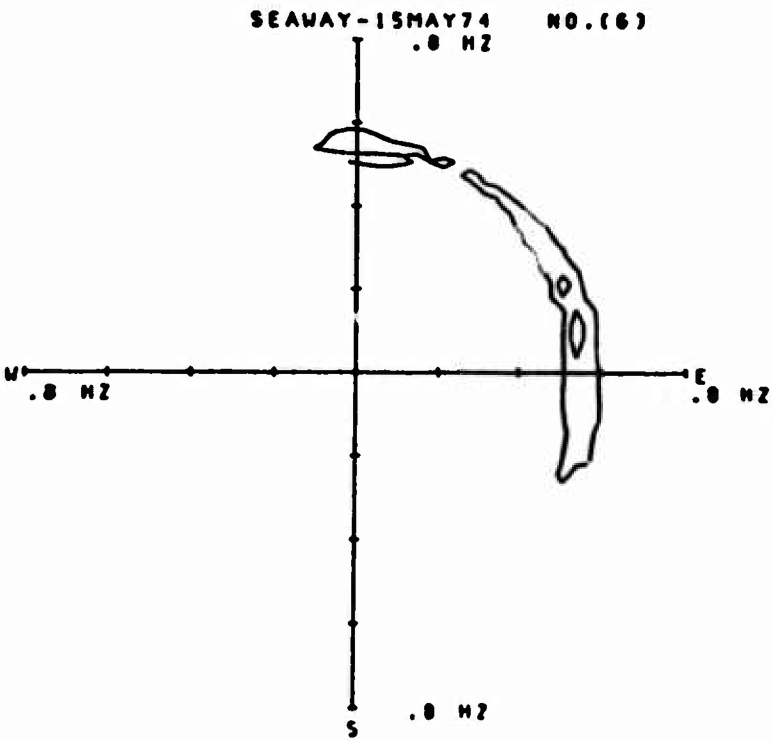

FIGURE E 3.65

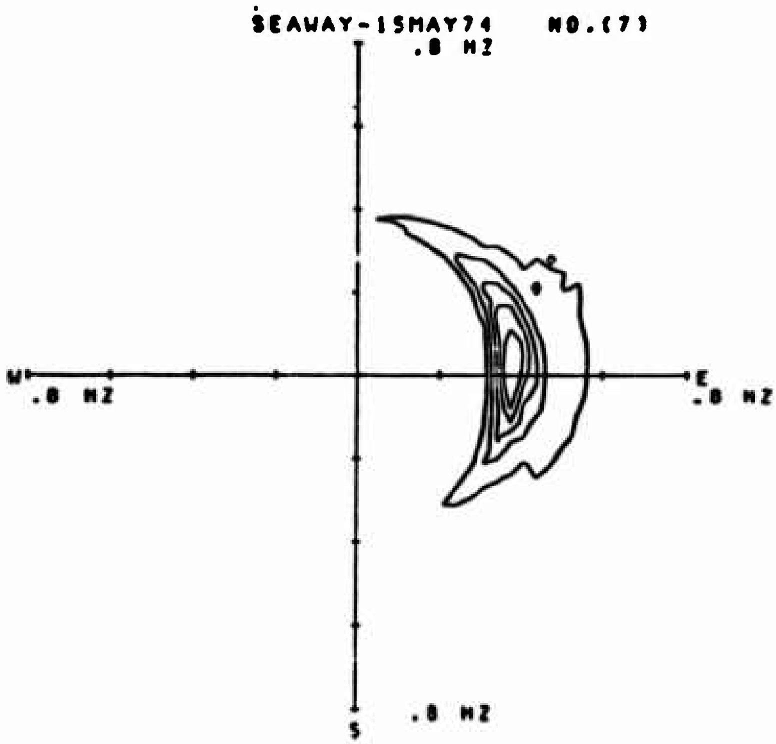

FIGURE E 3.66

TABLE E-I

OVERVIEW OF WAVE RECORDS 1973 and 1974

Abbreviations

BD	=	Depth of water at the buoy (ft).
BDR	=	Buoy direction from probe 1 to probe 2 unless otherwise noted (deg).
CDR	=	Current direction (deg).
CS	=	Current Speed (knots).
E	=	Ebb current.
F	=	Flood current.
$H_{1/3}$	=	Significant wave height.
S	=	Slack water.
WDR	=	Wave direction-visual estimate (deg).
WH	=	Wave height-visual estimate (ft.)

TABLE E-I

OVERVIEW OF WAVE RECORDS, 1973

DATE	RECORD NO.	TIME	OBSER[illegible] CONDITIONS WIND SPEED kt.	WIND DIR. deg.	CURRENT	COMMENTS	WAVE $H_{1/3}$	CALIBRATED DATA TAPE	FILE NO.	SEQ. NO.
03 AUG	1.1	10:53	12	210	F	WH=.65' WDR=190° CS=.5 CDR=0° WL=5-6' BDR=335°	0.665	8013	4	1
	1.2	1:03	16		F		1.010	"	5	2
07 AUG	2.1	11:34	10.5	192	E	WH=.6' WDR=202° CS=Low CDR=190° WL=10' BDR=147° BD=12'	0.571	8013	13	1
	2.2	1:05	16	205	E		0.899	"	14	2
	2.3	2:38	18	210	E	WH=1.4' WDR=210° CS=Low WL=20' BD=10'	0.973	"	15	3
	2.4	4:25	17	210	F	WH=1.0'	1.120	"	16	4
08 AUG	3.1	12:48	14	210	E	WH=.5' WDR=210°	0.856	8013	9	1
	3.2	2:31	17	216	E	WH=1.1' BD=10.5'	1.179	"	10	2
	3.3	4:15	17	210	S		1.222	"	11	3
10 AUG	4.1	11:01	10	210	F	WH=.6' CS=.5 CDR=210° No space between 4.1 and 4.2 on tape(analog)	0.443	8013	18	1
	4.2	1:03	13	210	E		1.002	"	19	2
	4.3	2:36			E		1.166	"	20	3
	4.4	3:50	18	210	E	WH=1.3' WDR=210°	1.338	"	21	4
14 AUG	5.1	11:20	13.5	200	F	WH=.8' WDR=211° CS=1 CDR=10° BD=11.2'	0.804	"	23	1
	5.2	12:55	17	200	F		0.989	"	24	2
	5.3	3:33	20	200	E	Damage to probe 2	1.357	"	25	3
15 AUG	6.1	11:32	12.5	177	F	WH=.8' BDR=148°, 1-2 initial BDR=105°, 4-2	0.811	"	27	1
	6.2	1:15	10	192	F	Severe noise before this record	0.786	"	28	2

TABLE E-I

OVERVIEW OF WAVE RECORDS, 1973

DATE	RECORD NO.	TIME	OBSERVED CONDITIONS			COMMENTS	WAVE $H^1/_3$	CALIBRATED DATA		
			WIND SPEED kt.	WIND DIR. deg.	CURRENT			TAPE	FILE NO.	SEQ. NO.
15 AUG	6.3	3:50	13.2	172	E	CDR= 172°	1.149	8013	29	3
17 AUG	7.1	10:30	17	165	F	WH=.91' BDR=100°, 1-2	0.915	8013	36	1
	7.2	12:05	17-18	185	F		1.099	"	37	2
20 AUG	8.1	11:00	10	205	E	WH=.5' WDR=185° WL=6' CS=.1 BDR=102°, 1-2	0.708	8013	39	1
	8.2				F	WL=8' Bad record, not digitized		"		
	8.3	12:22	10	200	S	WH=.5' WDR=180° WL=8' Ran out of tape	0.623	"	40	2
	8.4	1:25			F	WH=.7' WDR=180° to 0° WL=10' Channel 1 was not recording correctly, not digitized				
	8.5	1:28	13	190	F	WH=.7' WL=10' WDR=180° to 0° BDR=102°, 1-2 Passing silboat	1.127	"	41	3
	8.6	3:11	10.5	187	F		1.046	"	42	4
21 AUG	9.1	10:42	13	190	E	BDR=104°, 1-2	0.889	8013	44	1
	9.2	12:11	17	185	E		1.256	"	45	2
24 AUG	10.1	10:14	13		F	WH=.6' WDR=183° CS=.3 CDR=13° BDR=118°, 4-2	0.650	8013	47	1
	10.2	1:43	9.5	183	E		0.742	"	48	2
	10.3	3:13	8.5	193	E	WH=.4' to .5' WDR=140°	0.611	"	49	3
	10.4	4:56	8	196	S	WH=.5' WDR=140° Wave swells from 292°, wind increasing to 12.5 kt. and from 172°, Changed wave bouy position nearer to #14 rather than South Hampton Shoal	1.007	"	50	4

TABLE E-I

OVERVIEW OF WAVE RECORDS, 1973

DATE	RECORD NO.	TIME	OBSERVED CONDITIONS			COMMENTS	WAVE $H^{1}/_{3}$	CALIBRATED DATA		
			WIND SPEED kt.	WIND DIR. deg.	CURRENT			TAPE	FILE NO.	SEQ. NO.
12 SEP	15.4	3:30	17		E	CS=.25	1.348	5548	56	4
14 SEP	16.1	11:39	11.5	190	F	BDR=132°, 1-2 BD=12' Probe 1 was 1" in and probe 1 was moved prior to recording 16.02, 2"	0.621	8013	60	1
	16.2	12:50	13.5	168	F		0.790	"	61	2
	16.3	2:13	14.5	195-217	F	Waves look o.k., no particular Angel Island component; Probe 1 was in 1" to 2" after this run	1.190	"	62	3
	16.4	3:40	16	212	E		1.298	"	63	4
17 SEP	17.1	10:30	8.5	216	E	BDR=132°, 1-2	0.477	8013	65	1
	17.2	11:54	13-14	220	F		0.614	"	66	2
	17.3	2:01	13.5	208	F	BDR=128°, 1-2 BD=15'	0.860	"	67	3
	17.4	3:50	14-15	216	F		1.060	"	68	4
18 SEP	18.1	11:11	11	210	E	BDR=145°, 1-2 11:23 Boat passed close to wave bouy causing big waves	0.664	5548	58	1
	18.2	1:15	14-17	206	F		0.869	"	59	2
	18.3	2:40	14	215	F	BDR=174°, 1-2 BD=16' Swell moving toward south or southeast at 240° due to boat	0.992	"	60	3
19 SEP	19.1	12:43	8.5	215	E	BDR=135°, 1-2 Inverter blew up	0.629	"	62	1
	19.2	2:50	17	232	F	BD=14' Wind dropped to 10kt. quickly	0.765	"	63	2
	19.3	4:02	10	228	F		0.443	"	64	3

TABLE E-I

OVERVIEW OF WAVE RECORDS, 1973

DATE	RECORD NO.	TIME	OBSERVED CONDITIONS			COMMENTS	WAVE $H^{1}/_{3}$	CALIBRATED DATA		
			WIND SPEED kt.	WIND DIR. deg.	CURRENT			TAPE	FILE NO.	SEQ. NO.
28 SEP	20.1	1:59	13	202	F	WH=.7' BDR=258°, 2-4 BDR=302°, 1-2	0.684	5548	42	1
	20.2	4:34	16.5	210	E	BDR=305°, 4-1	1.046	"	43	2
04 OCT	21.1	2:17	13-14	220	E	BDR=178°, 2-3	0.843	5548	45	1
	21.2	3:30	15	215	F	WH=1.5' WDR=215° BDR=179°, 2-3	1.359	"	46	2
	21.3	5:33	12	220	F	BDR=178°, 2-3 BD=17'	1.252	"	47	3
01 NOV	22.1					No motion records, so wave records not digitized				
	22.2					" "				
	22.3					" "				
	22.4					" "				

TABLE E-I

OVERVIEW OF WAVE RECORDS, 1974

DATE	RECORD	TIME	OBSERVED CONDITIONS			COMMENTS	WAVE	CALIBRATED DATA		
			WIND SPEED kt.	WIND DIR. deg.	CURRENT		$H_{1/3}$	TAPE	FILE NO.	SEQ. NO.
10 MAY	30.1	10:38	7.5	215	E	WH=2.5" At 11:00 wind shifted to 190° and 9.5 kt.	0.357	3476	9	1
	30.2	11:11	10	200	E	WH=4" to 5" CS=1.3 CDR=108° At 11:19 wind shifted to 215°-220° and 14kt., at 11:45 the wind direction is 228° at 17kt	0.734	"	10	2
	30.3	11:48	17	228	E	WH=6" to 8" WDR=25° to 28° CS=1.6 BDR=130°, 1-2 Wind speed has dropped to 15 kt.	0.823	"	11	3
	30.4	12:12	12.6	196	F	WH=6" CDR=78° Wind shifting, at 12:20 it is from 204° and 11kt., at 12:18 it is from 200° at 10kt.	0.782	"	12	4
	30.5	12:40	13	198	F	WH=7" WL=8' to 10' CS=1.6 Wind speed dropping at 12:48 to 11kt. and at 12:52 to 10kt.	0.785	"	13	5
	30.6	1:15			F	CDR=62° BD=12'	0.667		14	6
	30.7	1:30	13	198	F	WH=8" to 1' WL=8' to 10' CDR=52° Wind speed is 15.5kt. at 1:38, Model capsized so wave recording stopped	0.878	"	15	7
	30.8	2:10	18	202	F	WDR=202° CS=1.4 CDR=44° Wind shifted at 2:23 to 224°	0.982	"	16	8
	30.9	2:26			F	Not digitized, False start				
	30.10	2:40	18	220	F	Wind shifted at 2:52 to 218° and 20kt., Power boat wake at 2:52 Not digitized, data is good		"	17	9
15 MAY	31.1	10:37	6		E	WH=5" WDR=270° WL=3' to 5' BDR=5°, 2-4 Wind shifting, at 10:38 to 270° and 8.5kt., and at 10:50 to 290° and 6.7kt.	0.539	3476	2	1
	31.2	10:55	6.5	290	E	Wave swell from 20°, Wind shifting, at 10:58 to 9.5kt., at 11:02 to 7-10kt. and at 11:08 to 270° and 9.3kt.	0.586	"	3	2
	31.3	12:12	6.5	200	E	CDR=265° Wave swell from 250° with a WH=.6" and WL=10', Wind waves from 170°	0.556	"	4	3

TABLE E-I

OVERVIEW OF WAVE RECORDS, 1974

DATE	RECORD NO.	TIME	OBSERVED CONDITIONS			COMMENTS	WAVE $H_{1/3}$	CALIBRATED DATA		
			WIND SPEED kt.	WIND DIR. deg.	CURRENT			TAPE	FILE NO.	SEQ. NO.
15 MAY	31.4	12:30	7-7.5	185	E	WDR=200° and 230° CS=.5 Wind shifting, at 12:36 to 220° and 5.5kt., and at 12:44 to 205° and 6kt.	0.575	3476	5	4
	31.5	12:55	6.5	200	E	At 1:03 the wind is from 220° at 7-10kt. Not digitized, false start				
	31.6	1:12	9	280°	E	WH=4" WL=3' The waves have very short crested tops which are almost breaking. At 1:17 the wind is from 270°	0.539	*	6	5
	31.7	2:20	13.5	270	E	WH=10" WDR=275° WL=8' to 18' BDR=223°, 1-2 Wind shifting, at 1:36 to 270° and 15kt., at 2:16 to 285° and 12.5kt. At 2:26 to 285-290° and 14.5kt. and at 2:32 to 285° and 13-14kt.	0.907	*	7	6
*19 JUL	32.1	10:49	13	214	F	BDR=150°, 4-2 B.D.=10' Wind speed increasing, at 11:03 to 15kt., at 11:12 to 16kt. Drop on channel 1				
	32.2	12:20	17	210	F					
	32.3	1:38	18.5	194	F	WDR=190° to 200° BDR=150°, 4-2 BD=11.5' Wind speed dropped, 1:45 to 17kt, 1:55 to 16kt. Jump on channel 3				
	32.4	2:41	18	210	S	WDR=20° BDR=135°, 4-2 Wind speed increased at 2:56 to 19.5kt.				
	32.5	4:23	17	209	E	At 4:38 the wind speed is 19kt.				
*23 JUL	33.1	10:00	13-14	214	E	WH=.5' WL=6' to 9' WDR=350° BDR=241°, 1-2 BD=7.3' Wind shifted at 10:10 to 200° and 12kt.				
	33.2	11:03	18	200	F	WH=1' to 1.5'				
	33.3	12:20	18	195	F	BDR=252°, 1-2 Jump on channel 1				
	33.4	1:45	18	200	F					
	33.5	2:35	18	195	F	WDR=20° BD=12.5'				

* Data not digitized, unless otherwise indicated, the data obtained is good.

TABLE E-II

WAVE STATISTICS FOR 1973 & 1974

η_{RMS}	RMS value for each probe.
$\bar{\eta}^2_{RMS}$	Average mean square value for the four probes.
S_E	Standard deviation of the mean square value.
$\bar{H}_{1/3}$	Average significant wave height.
$S_{\hat{\eta}}$	Standard deviation of the RMS.

NOT DIGITIZED

The data corresponding to the sequence number was not digitized. It was often either non-existent or defective and therefore not processed.

TABLE E-II

WAVE STATISTICS FOR 1973

DATE	RECORD NO.	η_{RMS} ft. PROBE NO. I	II	III	IV	$\overline{\eta^2_{RMS}}$ ft.^{2}	S_E ft.^{2}	$\overline{H}^{1/3}$ ft.	$S_{\hat{\eta}}$ ft.	SEQ. NO.
03 AUG	1.1	.211	.191	.189	.192	.038	.0036	0.665	.0301	1
	1.2	.327	.291	.290	.296	.091	.0093	1.010	.0463	2
07 AUG	2.1	.176	.169	.167	.162	.028	.0017	0.571	.0246	1
	2.2	.270	.260	.240	.248	.065	.0060	0.899	.0566	2
	2.3	.300	.271	.272	.251	.075	.0098	0.973	.0565	3
	2.4	.329	.322	.315	.302	.100	.0063	1.120	.0423	4
08 AUG	3.1	.251	.238	.241	.244	.059	.0024	0.856	.0133	1
	3.2	.342	.337	.319	.331	.110	.0056	1.179	.0287	2
	3.3	.371	.351	.343	.357	.126	.0074	1.222	.0422	3
10 AUG	4.1	.162	.118	.130	.134	.018	.0046	0.443	.0463	1
	4.2	.339	.293	.273	.286	.089	.0152	1.002	.0625	2
	4.3	.341	.332	.326	.318	.108	.0055	1.166	.0318	3
	4.4	.392	.379	.372	.362	.142	.0082	1.338	.0535	4
14 AUG	5.1	.245	.223	.248	.246	.058	.0048	0.804	.0322	1
	5.2	.255	.284	.309	.286	.080	.0107	0.989	.0842	2
	5.3	.391	.349	.377	.384	.141	.0118	1.357	.0556	3
15 AUG	6.1	.251	.233	.240	.247	.059	.0033	0.811	.0270	1
	6.2	.226	.227	.229	.243	.053	.0032	0.786	.0269	2
	6.3	.301	.314	.331	.316	.100	.0068	1.149	.0401	3
17 AUG	7.1	.263	.255	.273	.264	.070	.0033	0.915	.0191	1
	7.2	.310	.317	.320	.323	.101	.0030	1.099	.0177	2
20 AUG	8.1	.203	.192	.219	.206	.042	.0039	0.708	.0331	1
	8.2	NOT DIGITIZED								
	8.3	.229	.235	.250	.228	.055	.0041	0.623	.0199	2
	8.4	NOT DIGITIZED								
	8.5	.339	.313	.318	.332	.106	.0067	1.127	.0321	3
	8.6	.293	.296	.308	.300	.090	.0032	1.046	.0245	4
21 AUG	9.1	.267	.253	.276	.262	.070	.0043	0.889	.0286	1
	9.2	.359	.347	.362	.361	.128	.0043	1.256	.0268	2
24 AUG	10.1	.193	.188	.198	.206	.039	.0028	0.650	.0200	1
	10.2	.201	.215	.216	.216	.045	.0026	0.742	.0206	2
	10.3	.175	.181	.188	.182	.033	.0017	0.611	.0084	3
	10.4	.286	.296	.297	.302	.087	.0033	1.007	.0132	4
27 AUG	11.1	.127	.111	.113	.122	.014	.0015	0.356	.0192	1
	11.2	NOT DIGITIZED								
	11.3	.110	.112	.140	.159	.017	.0055	0.402	.0519	2
	11.4	.187	.205	.209	.199	.040	.0033	0.689	.0340	3
	11.5	NOT DIGITIZED								
28 AUG	12.1	.125	.118	.123	.131	.015	.0011	0.379	.0090	1
	12.2	.258	.245	.261	.263	.066	.0035	0.858	.0216	2
	12.3	.301	.326	.332	.328	.104	.0077	1.119	.0448	3
	12.4	.307	.329	.353	.320	.107	.0110	1.157	.0687	4
05 SEP	13.1	.198	.184	.223	.210	.042	.0060	0.704	.0463	1
	13.2	NOT DIGITIZED								
	13.3	.258	.247	.284	.262	.069	.0073	0.906	.0376	2

TABLE E-II

WAVE STATISTICS FOR 1973

DATE	RECORD NO.	η_{RMS} ft. PROBE NO. I	II	III	IV	$\overline{\eta}^2_{RMS}$ ft^2	S_E ft^2	$\overline{H}_{1/3}$ ft.	$S_{\hat{H}}$ ft.	SEQ. NO.
05 SEP	13.4	.298	.285	.300	.307	.089	.0047	1.018	.0341	3
11 SEP	14.1	.177	.171	.189	.184	.032	.0025	0.600	.0241	1
	14.2	.259	.255	.280	.265	.070	.0051	0.933	.0377	2
	14.3	.290	.273	.293	.287	.082	.0043	0.998	.0239	3
12 SEP	15.1	.122	.114	.122	.129	.015	.0013	0.373	.0179	1
	15.2	.196	.185	.212	.212	.041	.0045	0.670	.0348	2
	15.3	.350	.346	.356	.354	.352	.0027	1.255	.0206	3
	15.4	.362	.374	.383	.375	.140	.0054	1.348	.0231	4
14 SEP	16.1	.200	.179	.200	.203	.038	.0036	0.621	.0353	1
	16.2	.230	.238	.234	.244	.056	.0024	0.790	.0302	2
	16.3	.332	.338	.354	.346	.117	.0056	1.190	.0305	3
	16.4	.350	.353	.384	.369	.132	.0100	1.298	.0554	4
17 SEP	17.1	.142	.139	.160	.149	.022	.0024	0.477	.0267	1
	17.2	.193	.178	.199	.189	.036	.0030	0.614	.0252	2
	17.3	.265	.246	.264	.266	.068	.0042	0.860	.0362	3
	17.4	.313	.288	.307	.304	.102	.0056	1.060	.0277	4
18 SEP	18.1	.202	.194	.206	.209	.041	.0023	0.664	.0217	1
	18.2	.252	.235	.297	.266	.069	.0121	0.869	.1134	2
	18.3	.300	.267	.304	.304	.086	.0089	0.992	.0343	3
19 SEP	19.1	.187	.179	.193	.195	.036	.0024	0.629	.0208	1
	19.2	.224	.231	.238	.241	.055	.0031	0.765	.0218	2
	19.3	.134	.133	.150	.150	.020	.0024	0.443	.0214	3
28 SEP	20.1	.201	.191	.213	.206	.041	.0032	0.684	.0276	1
	20.2	.281	.272	.327	.284	.085	.0128	1.046	.0772	2
04 OCT	21.1	.268	.268	.245	.264	.068	.0048	0.843	.0279	1
	21.2	.416	.392	.380	.382	.154	.0115	1.359	.0577	2
	21.3	.377	.348	.356	.381	.134	.0101	1.252	.0397	3
01 NOV	22.1	NOT DIGITIZED								
	22.3	"	"							
	22.4	"	"							

TABLE E-II

WAVE STATISTICS FOR 1974

DATE	RECORD NO.	η_{RMS} ft. PROBE NO. I	II	III	IV	$\overline{\eta^2_{RMS}}$ ft^2	$\overline{H}$ $^1/_3$ ft.	SEQ NO.
10 MAY	30.1	.108	.111	.127	.114	.013	0.357	1
	30.2	.205	.207	.249	.226	.049	0.734	2
	30.3	.228	.228	.253	.235	.056	0.823	3
	30.4	.222	.225	.249	.233	.054	0.782	4
	30.5	.222	.231	.265	.246	.058	0.785	5
	30.6	.188	.193	.201	.193	.037	0.667	6
	30.7	.230	.242	.307	.240	.065	0.878	7
	30.8	.280	.284	.276	.298	.081	0.982	8
	30.9	NOT DIGITIZED						
	30.10	NOT DIGITIZED						
15 MAY	31.1	.161	.146	.162	.169	.025	0.539	1
	31.2	.158	.160	.176	.164	.027	0.586	2
	31.3	.142	.175	.163	.170	.026	0.556	3
	31.4	.146	.176	.165	.169	.027	0.575	4
	31.5	NOT DIGITIZED						
	31.6	.134	.154	.163	.158	.023	0.539	5
	31.7	.240	.270	.272	.263	.068	0.907	6

TABLE E-III

OVERVIEW OF MODEL TESTS IN SAN FRANCISCO BAY FOR 1973 AND 1974

Abbreviations

Heading	B	-	Beam	(Relative wave heading with respect to the model heading, obtained visually)
	Q	-	Quartering	
	F	-	Following	
	H	-	Head	

GM No. - See Table A-1 for the SL-7 model.

Model Heading - Degrees magnetic (approximate)

Capsize	S	-	Capsize to starboard
	P	-	Capsize to port

Movies X - Film records were taken but not necessarily of the entire run

4-STBD - The autopilot was "stepped" in two degree increments four times altering the course to starboard. These corrections were required to keep the model in the same relative encounter heading with the waves.

No. of Samples - Number of digitized samples.

TABLE E-III

MOTION DATA RECORDED FOR THE *SEALAND-7* MODEL DURING THE 1973 SEASON.

	YAW	RPM	SPEED	PITCH	ROLL	RUDDER	HEAVE	SWAY	SURGE
03 AUG - 10 AUG	1*	2	-	3	4	5	6	7	-
14 AUG - 27 AUG (Run 11.07)	1	-	2	3	4	5	6	7	-
(Run 11.08) 27 Aug - 14 SEP	1	-	2	3	4	5	-	6	7
17 SEP - 28 SEP	1	-	-	2	3	4	5	6	7
04 OCT	1	-	2	3	4	5	-	6	7
01 NOV	NO MOTIONS RECORDED								

* The number refers to the channel on which the data was recorded.

TABLE E-III

OVERVIEW OF MODEL TESTS IN SAN FRANCISCO BAY

EXPERIMENTS WITH MODEL SL-7, LIGHT CONDITION, 1973

DATE	RUN NO.	TIME	DURATION sec	HEADING	SPEED	GM POS	MODEL HEADING deg	CAPSIZE	MOVIES	COMMENTS	CALIBRATED DATA			
											TAPE NO.	FILE NO.	SEQ NO.	NO. SAMPLES
03 AUG	1.01	11:24	900	F	1	6	10			NOT DIGITIZED				
	1.02	12:13	900	F	2	6	6	S	X					
07 AUG	2.01	12:04	900	F	3	6	356			4-STBD	1156	29	1	2048
	2.02	12:39	394	F	3	6	8	S		7-STBD	"	30	2	985
	2.03	13:30	660	F	3	6	0	S		10-STBD	"	31	3	1650
	2.04	14:02	14	F	3	6		S			"	32	4	35
	2.05	14:18	269	F	3	6		S		3-STBD	"	33	5	672
	2.06	15:03	900	B	1	6				11-STBD	"	34	6	2048
	2.07	15:22	600	B	2	6				3-STBD Decreasing seas	"	35	7	1500
	2.08	15:54	390	Q	3	6		P		14-STBD	"	36	8	975
08 AUG	3.01	13:23	258	Q	3	6	60	P	X	Pure loss of stability	1156	39	1	651
	3.02	13:47	121	Q	3	6		P		Broaching	"	40	2	302
	3.03	14:03	31	Q	2	6		P			"	41	3	82
	3.04	14:19	83	Q	3	6		P	X		"	42	4	216
	3.05	14:57	525	Q	3	6		P		14-STBD	"	43	5	1320
	3.06	15:27	960	Q	1	6			X	5-STBD Autopilot unable to control model	"	44	6	2048
10 AUG	4:01	11:27	747	Q	3	6	36	P		10-STBD	1156	2	1	1889
	4:02	12:02	900	Q	2	6			X	5-STBD	"	3	2	2048
	4:03	12:37	650	Q	3	6		P		5-STBD	"	4	3	1612
	4:04	13:29	165	Q	2	6		P		4-PORT	"	5	4	407

TABLE F-III

OVERVIEW OF MODEL TESTS IN SAN FRANCISCO BAY

EXPERIMENTS WITH MODEL SL-7, LIGHT CONDITION, 1973

DATE	RUN NO.	TIME	DURATION sec	HEADING	SPEED	GM POS	MODEL HEADING deg	CAPSIZE	MOVIES	COMMENTS	CALIBRATED DATA			
											TAPE NO.	FILE NO.	SEQ NO.	NO. SAMPLES
10 AUG	4.05	13:45	16	Q	3	6		P			1156	6	5	26
	4.06									Bad run Autopilot malfunction				
	4.07	14:17	317	Q	2	6		S		23-STBD	"	7	6	801
	4.08	15:01	17	F	2	6		P			"	8	7	46
	4.09	15:15	3	F	2	6		P			"	9	8	14
	4.10	15:27	218	F	2	6		P	X	64 frames/sec	"	10	9	705
14 AUG	5.01	11:55	387	Q	2	6	330	S	X	9-STBD Good film of capsize	1156	12	1	964
	5.02	12:20	20	Q	2	6		S			"	13	2	48
	5.03	12:34	355	Q	2	6		S		8-STBD	"	14	3	884
	5.04	13:24	900	Q	1	6	315-20			18-STBD Almost beam sea	"	15	4	2048
	5.05	13:57	900	F	2	6					"	16	5	2048
	5.06	14:32	900	F	1	6				7-STBD Model out of control	"	17	6	2048
	5.07	15:08	165	B	3	6				Model hit wave buoy	"	18	7	455
15 AUG	6.01	11:59	900	F	1	6	335		X	15-STBD Wave train from 224°;major waves 195°	1156	21	1	2048
	6.02	12:30	900	F	2	6	350		X	13-STBD Wake from power boat	"	22	2	2048
	6.03	13:55	900	Q	1	6			X	16-STBD	"	23	3	1239
	6.04	14:35	690	B	3	6			X	16-STBD Significant change in sea state	"	24	4	1731
	6.05	15:05	10	Q	3	4		P	X		"	25	5	19

TABLE E-III

OVERVIEW OF MODEL TESTS IN SAN FRANCISCO BAY

EXPERIMENTS WITH MODEL SL-7, LIGHT CONDITION, 1973

DATE	RUN NO.	TIME	DURATION sec	HEADING	SPEED	GM POS	MODEL HEADING deg	CAPSIZE	MOVIES	COMMENTS	CALIBRATED DATA			
											TAPE NO.	FILE NO.	SEQ NO.	NO. SAMPLES
15 AUG	6.06	15:26	94	Q	2	4		P	X	8-PORT	1156	26	6	224
	6.07	15:34	358	F	2	4		P	X		"	27	7	893
17 AUG										Stbd catamaran engine blew up				
20 AUG	8.01	11:28	480	F	3	4	354	S	X		1156	46	1	1077
	8.02	11:53	108	F	3	4		S		Large violent broach to Stbd	"	47	2	260
	8:03	12:05	60	F	3	4		S	X		"	48	3	54
	8:04	12:56	180	Q	3	4		P	X		"	49	4	378
	8:05	13:15	180	Q	3	4		P	X		"	50	5	424
	8:06	13:51	60	Q	3	4		P	X	Most capsizes have occured near the wave buoy	"	51	6	162
	8:07	14:08	105	F	2	4		S			"	52	7	252
	8:08	14:24	50	F	2	4		P			"	53	8	70
	8:09	14:40	900	F	1	4			X	10-STBD Smaller waves at end of run ; NOT DIGITIZED				
21 AUG	9:01	11:11	900	Q	1	4	298			10-STBD	1156	56	1	2048
	9:02	11:44	897	F	1	4	340	S		Model went way off course, unable to correct;not digitized				
24 AUG	10:01	12:18	10	F	3	4			X	*Speed 3 looks like speed 2	1159	24	1	22
	10.02	13:06	541	F	2	4	354		X	5-STBD	"	25	2	1357

TABLE E-III

OVERVIEW OF MODEL TESTS IN SAN FRANCISCO BAY

EXPERIMENTS WITH MODEL SL-7, LIGHT CONDITION, 1973

DATE	RUN NO.	TIME	DURATION sec	HEADING	SPEED	GM POS	MODEL HEADING deg	CAPSIZE	MOVIES	COMMENTS	CALIBRATED DATA			
											TAPE NO.	FILE NO.	SEQ NO.	SAMPLES
24 AUG	10.03	14:28		F	3	4			X	Model off course; not digitized				
	10.04	14:47	900	F	3	4	342		X	5-PORT	1159	26	3	2048
	10.05	15:38	29	Q	3	4		P	X		"	27	4	75
	10.06	15:52	31	Q	3	4		S	X		"	28	5	77
	10.07	17:04	190	F	2	4		P		5-PORT	"	29	6	468
27 AUG	11.01	11:29	650	F	3	4				Swell from Treasure Island; Waves from Alcatraz	1159	32	1	1630
	11:02	11:40	98	STBD Turn	3	4			X	Manual control, maneuvering study - 1-3/4 turns to stbd.	"	33	2	234
	11:03	12:08	915	Q	3	4	325		X		"	34	3	2048
	11:04	12:24	210	STBD Turn	3	4			X		"	35	4	520
	11:05	13:08	900	F	2	4	15		X	8-STBD	"	36	5	2048
	11:06	13:50	880	Q	2	4	335	S	X	15-STBD	"	37	6	2048
	11:07	14:44	910	F	2	4	80		X	5-STBD	"	38	7	2048
	11:08	15:15	70	Q	2	4		S	X	Started in beam seas	"	39	8	140
	11:09	15:28	750	Q	2	4	320	S	X		"	40	9	1888
28 AUG	12:01	12:34	900	Q	2	4	347		X	5 - STBD Large rolls	1159	43	1	2048
	12:02		115	STBD Turn	2	4			X	Manual control, rudder hard over	"	44	2	272
	12:03	13:10	55	Q	3	4		S	X		"	45	3	107
	12:04	13:22	45	Q	3	4		S	X		"	46	4	67
	12:05	13:58	900	Q	1	4	330		X	18-STBD Less wind at end of run	"	47	5	2048

TABLE E-III

OVERVIEW OF MODEL TESTS IN SAN FRANCISCO BAY

EXPERIMENTS WITH MODEL SL-7, LIGHT CONDITION, 1973

DATE	RUN NO.	TIME	DURA-TION sec	HEAD-ING	SPEED	GM POS	MODEL HEAD-ING deg	CAP-SIZE	MOV-IES	COMMENTS	CALIBRATED DATA			
											TAPE NO.	FILE NO.	SEQ NO.	NO. SAMPLES
28 AUG	12:06		90	STBD turn	3	4			X			48	6	216
	12.07	14:34	30	F	3	4		S			"	49	7	40
	12.08	15:36	10	F	2	4	45	S	X	Capsize on film	"	50	8	16
	12.09	15:50	535	F	1	4		S	X		"	51	9	1056
09 SEP	13.01	13:55	195	F	2	3		P		P. Q. waves from Angel I. Following waves from Alcatraz I.	1159	2	1	465
	13.02	14:10	810	F	2	3		S		Large rolls - screws coming out; P.Q. Sea is small, longer waves from seas.	"	3	2	2008
	13.03	14:40	893	F	2	3	335	S		Small beam waves, larger following waves; large stbd roll- cliff-hanger; capsize, pure loss of stability	"	4	3	2048
11 SEP	14.01	12:53	160	Q	3	3	310	S		10-STBD P. Q. seas; big broach and roll	1159	58	1	392
	14.02	13:13	65	Q	3	3	320	S		Good broach	"	59	2	149
	14.03	13:30	925	Q	2	3	320			Waves look good	"	60	3	2048
	14.04	14.35	900	Q	2	3	335 330			5-STBD Waves sufficiently on the beam so that the model does not capsize.		61	4	2048
										Rolled the screws out	"			
	14.05	15:07	190	F	2	3		S		Good surge	"	62	5	464
	14.06	15:21	620	F	2	3		S		3-STBD Good waves; good surge; rolled screws out	"	63	6	1535
	14.07	16:34	700	B	1	8*				Very stiff, not very interesting	"	64	7	2017

TABLE E-III

OVERVIEW OF MODEL TESTS IN SAN FRANCISCO BAY

EXPERIMENTS WITH MODEL SL-7, LIGHT CONDITION, 1973

DATE	RUN NO.	TIME	DURATION sec	HEADING	SPEED	GM POS	MODEL HEADING deg	CAPSIZE	MOVIES	COMMENTS	CALIBRATED DATA			
											TAPE NO.	FILE NO.	SEQ NO.	NO. SAMPLES
12 SEP	15.01	11:55	336	F	3	3		S		Rate gyro died at some point during the day. Broaching and large rolls may be caused by rudder.	1159	7	1	818
	15.02	12:31	945	F	2	3	10			8-STBD Model is yawing quite a bit	"	8	2	2048
	15.03	13:30	170	F	2	3		S		Steering looks more reasonable, reduced yaw rate sensitivity.	"	9	3	409
	15.04	13:43	50	Q	2	3	60	P			"	10	4	118
	15.05	13:56	560	Q	1	3	110 50	P		Cannot come back from beam seas, rudder hard over; stbd screw mostly out of water; off course 110° heading, on course 50° heading; overwhelmed by one large wave.	"	11	6	1227
	15.06	14.51	900	F	1	3				3-STBD Screw coming way out	"	12	5	2048
14 SEP	16.01	12:07	372	F	3	3		S		New rate gyro calibrated to 71-72 auto pilot param.; over steering; almost cap., comb. wave and hard over rudder. Rate hooked up backwards; corrected for 16.03	5548	9	1	938
	16.02	12:33	90	F	3	3	10	S		Rate turned off - not steering as badly	"	10	2	210
	16.03	13:17	75	F	3	3	20	P		Rate gain OK; big seas		11	3	180

TABLE E-III

OVERVIEW OF MODEL TESTS IN SAN FRANCISCO BAY

EXPERIMENTS WITH MODEL SL-7, LIGHT CONDITION, 1973

DATE	RUN NO.	TIME	DURATION sec	HEADING	SPEED	GM POS	MODEL HEADING deg	CAPSIZE	MOVIES	COMMENTS	CALIBRATED DATA			
											TAPE NO.	FILE NO.	SEQ NO.	NO. SAMPLES
14 SEP	16.04	13.37	400	F	3	6	20	S		Good surge; 2 wave system - from astern and on stbd. quarter	5548	12	4	1005
	16.05	14:00	230	F	3	6	0	S		5-STBD Good surge & broach	"	13	5	564
	16.06	14:46	170	F	2	6	12	S		Good waves	"	14	6	420
	16.07	15:02	12	B	2	6		P		Too short to be digitized	"			
	16:08	15:12	900	B	1	6	65			Helm over; came around to course - lost again; monster beam seas; came close to capsizing	"	15	7	2048
17 SEP	17.01	11:07	700	F	3	4	10	S		3-STBD Small roll and broach	1159	14	1	1752
	17.02	11:39	660	F	3	4	20	S		5-PORT	"	15	2	
	17.03	12:35	467	Q	2	4	315	S		17-STBD Large roll - deck edge immersed	"	16	3	
	17.04	13:00	682	F	2	4	20	S		5-STBD	"	17	4	1708
	17.05	13:30	32	Q	2	4		P				18	5	57
	17.06	13:40	345	Q	2	4	50	P		8-STBD Good seas	"	19	6	855
	17.07	14:37	350	F	3	6	25	S		Very hard broach to port	"	20	7	870
	17.08	14:58	370	F	2	6	25	S		Good broach; rudder hard over to stbd	"	21	8	931
	17.09	15:23	930	F	1	6				15-STBD	"	22	9	2048
18 SEP	18.01	11:36	190	Q	3	4	325	S		5-STBD	1159	62	1	465

TABLE E-III

OVERVIEW OF MODEL TESTS IN SAN FRANCISCO BAY

EXPERIMENTS WITH MODEL SL-7, LIGHT CONDITION, 1973

DATE	RUN NO.	TIME	DURA-TION sec	HEAD-ING	SPEED	GM POS	MODEL HEAD-ING deg	CAP-SIZE	MOV-IES	COMMENTS	CALIBRATED DATA			
											TAPE NO.	FILE NO.	SEQ NO.	NO. SAMPLES
18 SEP	18.02	12:00	8	Q	3	4		S		To short to digitize				
	18.03	12:08	920	Q	2	4	345			13-STBD	1159	63	2	2048
	18.04	12:34	755	F	2	4	16	S		8-STBD	"	64	3	1881
	18.05	13:15	290	F	2	4	45-50	P		Difficulty in staying on course; low cycle resonance	"	65	4	723
	18.06	14:02	45	Q	2	4		S			"	66	5	104
	18.07	14:10	250	F	2	4		S		Watched, stopped, restarted slow cap	"	67	6	575
19 SEP	19.01	13:14	900	F	3	4	10			15-STBD	1159	70	1	2048
	19.02	13:54	640	F	3	4	30	S			"	71	2	1595
	19.03	14:21	52	F	3	4		S			"	72	3	112
	19.04	14:33	160	Q	3	4	347	S			"	73	4	411
	19.05	15:22	495	F	3	4	30-40	S		Big broach; lots of yawing	"	74	5	1288
	19.06	15:50	240	F	3	4	20	S			"	75	6	603

TABLE E-III

OVERVIEW OF MODEL TESTS IN SAN FRANCISCO BAY

EXPERIMENTS WITH MODEL SL-7, HEAVY CONDITION, 1973

DATE	RUN NO.	TIME	DURATION sec	HEADING	SPEED	GM POS	MODEL HEADING deg	CAPSIZE	MOVIES	COMMENTS	CALIBRATED DATA			
											TAPE NO.	FILE NO.	SEQ NO.	NO. SAMPLES
28 SEP	20.01	14:26	36	F	3	3	20	S			5548	25	1	82
	20.02	14:44	950	F	2	3	48		X	16-STBD	"	26	2	2048
	20.03	15:21	54	F	3	3		S	X		"	27	3	124
	20.04	15:34		F	2	3		?	X	Very steep wave - pure loss of stability. Not able to record - too short.				
	20.05	15:54	194	F	2	3	45	S	X		"	28	4	482
04 OCT	21.01	15:00	55	F	3	4	35	P			5548	31	1	124
	21.02	15:25	180	F	2	4		S		Good size seas; good surge; pure loss of stability. 9-STBD	"	32	2	445
	21.03	16:05	240	F	2	6	35	?			"	33	3	604
	21.04	16:27	145	Q	2	6	55-60	P			"	34	4	350
	21.05	16:48	50	Q	2	6		P			"	35	5	97
	21.06	17:03	325	Q	1	6	90-85	P			"	36	6	813
01 NOV	22.01	1:06	755	F	3	2	10-0	S		NOT DIGITIZED				
	22.02	1:49	910	Q	1	2	320							
	22.03	2:30	905	F	3	6	10							
	22.04	3:39	160	F	1	2	10-355	S						
	22.05	3:56	930	F	3	2			X					

TABLE E-III

OVERVIEW OF MODEL TESTS IN SAN FRANCISCO BAY

EXPERIMENTS WITH MODEL SL-7, HEAVY CONDITION, 1974

DATE	RUN NO.	TIME	DURATION sec	HEADING	SPEED	GM POS	MODEL HEADING deg	CAPSIZE	MOVIES	COMMENTS	CALIBRATED DATA			
											TAPE NO.	FILE NO.	SEQ NO.	NO. SAMPLES
10 MAY 74	30.01	9:35								Roll decay				
	30.02	11:15	450	H	1	6	200			10-STBD Green seas on deck, some slamming	3476	30	1	1024
	30.03	12:44	420	H	1	6	180			NOT DIGITIZED				
	30.04	13:15	420	H	3	6	200			Model off course at 13:18	"	31	2	513
	30.05	13:28	660	H	2	6	202				"	32	3	1024
	30.06	14:00	480	H	1	6	205				"	33	4	1024
15 MAY	31.01	10:58	420	H	3	6	280			Occasional slamming; larger seas during 2nd half of run	3476	19	1	966
	31.02	12:18	450	H	2	6	170-185				"	20	2	1024
	31.03	12:38	525	H	1	6	160-180				"	21	3	1024
	31.04	12:58	500	H	2	6	170				"	22	4	1024
	31.05	13:20	450	H	1	6	230-240			Good slamming	"	23	5	1024
	31.06	13:44	960	F	2	6	85	S		15-STBD Water depth=7', λ=18'; large rolling with water on deck, significant yawing, some surging, very long run.	"	24	6	2048
	31.07									Last 100 sec. of run 31.06	"	25	7	461

TABLE E-III

OVERVIEW OF MODEL TESTS IN SAN FRANCISCO BAY

EXPERIMENTS WITH MODEL SL-7, HEAVY CONDITION, 1974

DATE	RUN NO.	TIME	DURATION sec	HEADING	SPEED	GM POS	MODEL HEADING deg	CAPSIZE	MOVIES	COMMENTS	CALIBRATED DATA			
											TAPE NO.	FILE NO.	SEQ NO.	NO. SAMPLES
19 JUL	32.06	14:05	24	Q	2	6		S						
	32.07	14:24	395	Q	2	6		P		5-STBD Relative heading of model to waves is 60°				
	32.08	15:07	322	F	1	6	360			Model 20° off course 2-STBD Wave length slightly less than twice model length				
	32.09	15:41	31	Q	2	6		P	X	Relative heading of model to waves is 40°				
23 JUL	33.01	10:28	240	F	2	4	355	S	X	3-STBD Relative heading of model to waves is 10° Pure loss of stability				
	33.02	10:46	210	Q	2	4	315	S		5-STBD Relative heading of model to waves is 70° to 80° near capsize				
	33.03	11:30	930	F	1	4	355		X	10-STBD Wave length is 20', heading between model and waves is - 30°				
	33.04	12:04	90	F	3	4	0							

TABLE E-IV

STATISTICS OF MEASURED MODEL DATA

1973 AND 1974

TABLE E-IV

STATISTICS OF MEASURED MODEL DATA 1973

DATE AND RUN	1. YAW, degrees					2. RPM					3. PITCH, degrees					4. ROLL, degrees				
	MEAN	RMS	$H^{1}/_{3}$	$H^{1}/_{10}$	$H^{1}/_{100}$	MEAN	RMS	$H^{1}/_{3}$	$H^{1}/_{10}$	$H^{1}/_{100}$	MEAN	RMS	$H^{1}/_{3}$	$H^{1}/_{10}$	$H^{1}/_{100}$	MEAN	RMS	$H^{1}/_{3}$	$H^{1}/_{10}$	$H^{1}/_{100}$
8/3																				
1.01	NOT DIGITIZED																			
1.02	"	"																		
8/7																				
2.01	6.1	9.1	25.4	34.7	49.3	-1263	26.3	89.0	109.2	136.7	.8	1.4	5.4	6.4	7.8	-12.4	60.3	55.0	90.5	248.1
2.02	5.2	7.3	21.5	30.2		-1267	24.5	87.9	108.0	147.4	1.0	1.7	5.9	7.8	11.3	4.7	14.7	39.3	51.7	122.0
2.03	5.2	10.3	19.8	28.9	52.3	-1260	24.8	86.9	108.4	139.8	1.0	1.9	7.1	9.1	11.1	4.5	15.1	45.8	65.4	196.9
2.04	23.4	16.9				-1276	40.9				.7	2.4	7.0	8.8		-3.5	64.2	230.9	293.3	
2.05	2.9	10.1	34.1	64.9		-1241	132.4	62.5	79.8	113.2	1.1	2.6	8.7	13.3	40.9	1.6	19.9	54.0	93.4	270.6
2.06	-23.6	7.0	11.9	18.0	30.2	-787	10.0	28.7	40.4	151.9	.9	1.7	5.8	7.0	9.4	-142.8	56.2	75.8	168.9	
2.07	6.6	4.1	9.6	16.1	62.5	-1009	77.8	24.4	33.9	83.1	1.5	2.3	6.7	8.2	10.6	-220.5	0.1	0.3	0.3	0.3
2.08	-7.7	11.1	28.0	45.4		-1216	97.9	70.3	87.0	110.2	1.2	2.2	6.3	8.2	10.8	-220.5	0.1	0.3	0.3	0.3
8/8																				
3.01	-12.8	10.3	24.4	32.2		-1284	22.2	76.1	96.7	121.3	0.1	1.6	5.9	6.9	7.5	-7.2	13.1	39.0	46.0	57.3
3.02	-16.4	17.1	36.8	57.5		-1279	29.3	102.0	128.3		0.3	2.1	7.9	9.2		-7.9	17.0	44.9	51.5	

DATE AND RUN	5. RUDDER, degrees					6. HEAVE, ft./sec.^{2}					7. SWAY, ft./sec.^{2}					WAVE STATISTICS INTERPOLATED $H^{1}/_{3}$ ft.
	MEAN	RMS	$H^{1}/_{3}$	$H^{1}/_{10}$	$H^{1}/_{100}$	MEAN	RMS	$H^{1}/_{3}$	$H^{1}/_{10}$	$H^{1}/_{100}$	MEAN	RMS	$H^{1}/_{3}$	$H^{1}/_{10}$	$H^{1}/_{100}$	
8/3																
1.01	NOT DIGITIZED															
1.02	"	"														
8/7																
2.01	10.7	12.1	31.3	35.3	40.9	-5.0	14.7	5.7	12.1	53.9	-.7	5.0	3.0	5.6	25.6	0.67
2.02	9.9	11.0	29.4	38.0	45.3	-.9	3.7	3.8	5.1	7.0	.7	.8	2.2	2.7	3.4	0.78
2.03	9.8	11.7	28.5	34.6	40.7	-.9	3.2	3.8	5.0	10.6	.4	1.4	2.7	3.6	4.9	0.91
2.04	19.2	6.3	18.4			-10.4	16.0				1.8	5.4	24.3	34.0		0.93
2.05	6.5	12.8	38.0	54.4		-1.2	5.4	3.5	4.3	5.1	.6	2.1	2.8	4.0	11.2	0.94
2.06	-27.1	8.3	18.0	23.1	31.5	-35.9	15.1	12.8	22.2	56.2	-15.4	7.9	20.1	24.0	28.9	1.03
2.07	11.1	6.7	15.5	19.3	24.3	-56.7	3.1	9.6	11.6	14.7	-15.6	4.9	16.6	19.7	24.0	1.43
2.08	-6.2	13.9	34.7	48.0	93.9	-56.2	2.4	5.6	8.2	20.5	-21.9	7.9	26.3	31.7	55.9	1.13
8/8																
3.01	-11.1	11.6	29.6	35.2		-1.0	1.2	3.8	5.0	6.6	1.1	0.8	2.6	3.3	4.0	0.95
3.02	-12.5	14.9	34.2	46.4		-1.0	3.1	3.9	5.2	7.0	1.0	0.9	3.0	4.0	5.0	1.01

TABLE E-IV

STATISTICS OF MEASURED MODEL DATA 1973

DATE AND RUN	1. YAW, degrees					2. RPM					3. PITCH, degrees					4. ROLL, degrees				
	MEAN	RMS	$H^{1}/_{3}$	$H^{1}/_{10}$	$H^{1}/_{100}$	MEAN	RMS	$H^{1}/_{3}$	$H^{1}/_{10}$	$H^{1}/_{100}$	MEAN	RMS	$H^{1}/_{3}$	$H^{1}/_{10}$	$H^{1}/_{100}$	MEAN	RMS	$H^{1}/_{3}$	$H^{1}/_{10}$	$H^{1}/_{100}$
8/8																				
3.03	-20.9	12.2	12.1			-1010	6.8	23.5	26.0		0.2	2.0	7.6	9.3		-6.5	41.2	102.8	225.9	
3.04	-16.9	9.2	22.6	26.9		-1273	29.4	96.3	108.2		0.3	2.4	9.1	12.1		-8.5	17.8	43.3	46.4	
3.05	-22.0	18.3	21.7	33.9		-795	6.3	22.3	28.7	39.6	0.4	2.4	9.1	11.9	14.9	-5.6	13.6	43.0	50.7	61.3
3.06	-38.6	24.5	33.2	56.2		-788	13.4	42.0	53.9	78.9	0.7	2.2	7.9	10.6	15.1	-6.3	11.9	40.9	49.3	57.8
8/10																				
4.01	-12.9	9.6	23.8	34.3	52.4	-1366	20.6	68.5	83.8	109.8	0.6	1.1	3.8	4.7	5.4	-5.9	11.8	37.9	44.9	53.3
4.02	-14.7	7.9	17.3	27.6	40.5	-1082	6.3	23.3	32.7	47.3	0.7	1.5	5.4	6.9	8.6	-5.3	11.8	41.7	48.6	57.2
4.03	-17.2	10.0	30.8	39.4		-1348	24.7	87.5	105.9	135.1	0.9	1.8	6.6	8.7	11.5	-7.3	13.7	44.9	5[illegible].2	68.4
4.04	-24.7	9.4	22.2	35.3		-1077	7.7	27.5	35.2	41.1	0.6	1.7	6.1	8.1	10.8	-8.0	24.0	55.1	91.8	233.4
4.05	-27.1	13.0				1367	42.2	148.8			0.2	2.4	8.2			-14.1	75.7	232.4		
4.06	NOT DIGITIZED																			
4.07	8.9	11.1	19.4	27.2		-1081	16.0	38.5	72.7	348.2	0.8	1.8	6.6	8.0	9.4	5.9	18.2	44.2	57.4	120.9
4.08	33.0	11.2	33.8			-1075	10.6	38.6	41.7		-37.4	14.5				21.2	41.8	84.4		
4.09	60.5	15.3				-841	779.4				-34.4	19.8				-30.6	98.0			

DATE AND RUN	5. RUDDER, degrees					6. HEAVE, ft./sec.^{2}					7. SWAY, ft./sec.^{2}					WAVE STATISTICS INTERPOLATED $H^{1}/_{3}$ ft.
	MEAN	RMS	$H^{1}/_{3}$	$H^{1}/_{10}$	$H^{1}/_{100}$	MEAN	RMS	$H^{1}/_{3}$	$H^{1}/_{10}$	$H^{1}/_{100}$	MEAN	RMS	$H^{1}/_{3}$	$H^{1}/_{10}$	$H^{1}/_{100}$	
8/8																
3.03	-19.9	9.6	19.1	20.4		-4.3	12.2	7.8	12.3		1.1	2.0	3.4	4.6		1.06
3.04	-17.1	11.4	27.4	30.6		-1.2	3.9	4.2	5.0	5.4	0.9	1.2	4.3	5.4		1.11
3.05	-17.9	14.9	26.6	32.4		-1.0	2.6	4.3	6.0	8.6	0.8	1.4	4.7	6.4	10.0	1.20
3.06	-27.4	14.7	29.6	38.2		-0.6	1.9	6.5	8.5	10.5	0.3	1.9	6.6	8.6	11.0	1.21
8/10																
4.01	-10.1	11.8	31.0	37.4	43.6	-0.7	0.9	2.3	3.0	0.8	0.7	1.8	2.4	3.7		0.56
4.02	-12.8	11.1	24.7	29.2	37.1	-0.6	1.0	3.2	4.2	6.3	0.7	0.7	2.4	3.1	4.1	0.72
4.03	-16.2	12.9	34.1	41.7	52.4	-0.5	1.9	4.3	5.8	9.4	0.6	1.1	3.3	4.7	9.6	0.88
4.04	-26.3	10.3	25.0	34.0		1.7	7.4	6.1	7.4	8.4	0.8	2.1	4.9	6.5	11.6	1.04
4.05	-18.1	8.8				-13.5	16.1				2.4	4.9	16.2			1.07
4.06	NOT DIGITIZED															
4.07	17.1	10.9	24.3	30.2	40.2	-1.4	4.9	5.0	6.3	9.3	0.2	1.9	4.3	6.7	18.4	1.13
4.08	27.5	4.8	19.4			-23.6	10.4	36.2			5.6	14.0	46.6			1.22
4.09	34.8	11.5				-29.0	13.5				19.2	11.2	40.5			1.25

TABLE E-IV

STATISTICS OF MEASURED MODEL DATA 1973

DATE AND RUN	1. YAW, degrees					2. RPM					3. PITCH, degrees					4. ROLL, degrees				
	MEAN	RMS	H 1/3	H 1/10	H 1/100	MEAN	RMS	H 1/3	H 1/10	H 1/100	MEAN	RMS	H 1/3	H 1/10	H 1/100	MEAN	RMS	H 1/3	H 1/10	H 1/100
8/10 4.10	1.2	9.5	16.5	24.1		-1069	25.7	48.4	87.2	279.1	-40.4	0.4	1.2	1.5	2.1	-2.0	19.0	47.5	69.7	213.1

DATE AND RUN	5. RUDDER, degrees					6. HEAVE, ft./sec.^{2}					7. SWAY, ft./sec.^{2}					WAVE STATISTICS INTERPOLATED $H^1/_3$, ft.
	MEAN	RMS	H 1/3	H 1/10	H 1/100	MEAN	RMS	H 1/3	H 1/10	H 1/100	MEAN	RMS	H 1/3	H 1/10	H 1/100	
8/10 4.10	6.9	11.1	26.3	32.1		-8.5	4.0	3.9	5.1	6.7	2.5	1.7	5.6	7.3	14.[illegible]	1.28

TABLE E-IV

STATISTICS OF MEASURED MODEL DATA 1973

DATE AND RUN	1. YAW, degrees					2. RPM					3. PITCH, degrees					4. ROLL, degrees				
	MEAN	RMS	$H^1/_3$	$H^1/_{10}$	$H^1/_{100}$	MEAN	RMS	$H^1/_3$	$H^1/_{10}$	$H^1/_{100}$	MEAN	RMS	$H^1/_3$	$H^1/_{10}$	$H^1/_{100}$	MEAN	RMS	$H^1/_3$	$H^1/_{10}$	$H^1/_{100}$
8/14																				
5.01	10.7	7.9	20.4	31.7		5.2	0.6	1.7	2.0	2.3	2.0	1.5	5.6	6.8	8.1	6.8	12.7	42.8	51.9	76.3
5.02	16.5	11.8	56.5			4.8	0.6	1.6	1.8		2.2	1.9	4.7	6.3		14.5	21.7	74.9	111.8	
5.03	15.3	10.4	32.9	48.8		5.0	0.7	1.8	2.2	2.9	-29.8	2.4	6.8	8.1	10.3	18.2	15.9	49.7	59.1	86.8
5.04	15.0	7.2	13.5	19.6	27.5	3.9	0.4	1.2	1.4	1.8	2.0	1.9	6.9	8.6	10.4	7.9	10.0	36.3	42.8	49.9
5.05	6.2	12.3	26.1	45.6	62.2	5.6	0.7	2.1	2.5	3.0	1.8	2.2	7.8	10.0	12.9	5.0	12.9	44.2	53.1	64.4
5.06	23.3	24.7	36.9	52.7		4.2	0.7	1.9	2.3	2.7	2.6	2.6	9.2	11.4	13.4	6.1	11.2	38.0	45.9	57.7
5.07	17.6	11.8	24.4	44.2		5.6	1.0	1.9	2.3	2.7	2.3	2.1	6.8	8.0	9.3	16.8	12.2	42.8	55.7	69.2
9/15																				
6.01	0.5	7.6	19.0	25.1		2.2	0.0	0.1	0.1	0.1	2.0	1.7	6.4	8.2	10.9	0.7	10.8	39.9	46.5	50.8
6.02	3.0	3.2	18.8	28.9	40.2	2.3	0.0	0.0	0.1	0.1	2.1	1.7	6.3	8.0	10.1	3.0	11.6	40.7	47.8	54.4
6.03	11.8	5.3	12.0	16.6	24.0	4.0	0.4	1.3	1.6	1.8	2.0	1.9	7.1	9.1	11.9	6.0	9.9	36.4	43.8	52.2
6.04	6.2	3.9	9.6	13.2	17.0	6.6	0.6	1.9	2.2	2.6	2.3	1.7	5.6	7.2	9.1	8.8	10.6	38.2	46.9	61.2
6.05	-12.9	14.0				6.1	0.9	0.9			2.1	2.4				-16.4	29.1			
6.06	-13.1	5.1	11.3	12.9		5.4	0.6	1.8	2.0		32.1	0.1	0.2	0.3		-7.1	93.9	206.1	279.6	288.1

DATE AND RUN	5. RUDDER, degrees					6. HEAVE, ft./sec.[2]					7. SWAY, ft./sec.[2]					WAVE STATISTICS INTERPOLATED $H^1/_3$ ft.
	MEAN	RMS	$H^1/_3$	$H^1/_{10}$	$H^1/_{100}$	MEAN	RMS	$H^1/_3$	$H^1/_{10}$	$H^1/_{100}$	MEAN	RMS	$H^1/_3$	$H^1/_{10}$	$H^1/_{100}$	
8/14																
5.01	17.4	10.9	25.3	30.5	36.6	-0.9	1.4	4.4	5.6	7.5	0.2	1.0	3.2	4.1	5.6	0.86
5.02	25.4	5.5	18.3	21.7		-1.6	4.3	5.4	6.0		-0.6	1.2	3.5	4.1		0.91
5.03	22.7	11.0	26.4	31.1	38.0	-6.6	1.9	5.9	8.1	10.2	-3.3	3.1	7.1	9.7	12.4	0.94
5.04	23.5	8.7	20.1	23.3	30.6	-0.8	1.7	5.7	7.1	8.9	-0.6	1.6	5.5	6.8	8.8	1.05
5.05	10.3	13.9	26.3	33.5	46.2	-0.8	1.1	3.3	4.6	7.7	-0.3	0.8	2.6	3.7	6.7	1.12
5.06	19.8	15.5	23.8	29.9	41.6	-0.8	1.6	5.4	7.5	11.0	-0.4	1.6	6.0	8.2	12.2	1.20
5.07	23.0	9.1	22.5	31.0		-1.5	2.8	9.1	11.2	15.0	-2.3	2.2	7.6	9.1	11.2	1.30
8/15																
6.01	4.6	10.9	20.9	26.4	36.1	-0.8	0.9	2.7	3.4	4.5	0.2	0.7	2.4	2.9	4.0	0.81
6.02	6.6	11.2	23.0	30.4	43.5	-0.7	1.1	3.3	4.3	6.4	0.0	0.6	1.9	2.5	3.8	0.80
6.03	20.7	8.8	20.8	23.3	26.8	-0.9	1.6	5.2	6.6	8.8	-0.3	1.3	4.8	6.1	8.1	0.89
6.04	10.7	7.1	17.7	21.7	29.7	-0.9	3.0	9.5	12.0	16.1	-0.6	1.9	6.6	8.1	10.2	0.94
6.05	-8.9	8.0	14.6			-2.8	9.5	6.1				0.5	1.3	3.5		1.03
6.06	-12.4	8.7	23.5	27.6		-29.8	17.3	47.7	50.8	53.3	-0.8	22.1	58.4	66.6	80.2	1.09

TABLE E-IV

STATISTICS OF MEASURED MODEL DATA 1973

DATE AND RUN	1. YAW, degrees					2. RPM					3. PITCH, degrees					4. ROLL, degrees				
	MEAN	RMS	$H^1/_3$	$H^1/_{10}$	$H^1/_{100}$	MEAN	RMS	$H^1/_3$	$H^1/_{10}$	$H^1/_{100}$	MEAN	RMS	$H^1/_3$	$H^1/_{10}$	$H^1/_{100}$	MEAN	RMS	$H^1/_3$	$H^1/_{10}$	$H^1/_{100}$
8/15 6.07	-7.0	6.1	15.9	25.8		5.7	0.7	2.4	2.9	3.2	-41.1	0.3	0.9	1.2	1.7	-33.0	86.2	279.0	293.2	299.0
8/20																				
8.01	0.9	11.5	39.5	67.0		6.8	0.9	2.1	2.6	3.0	0.8	2.2	6.6	9.9	35.1	3.4	19.3	48.7	62.6	135.0
8.02	8.0	19.7	62.1			6.6	0.9	2.2	2.4		1.0	1.5	5.1	5.9		6.4	19.6	59.1	82.2	
8.03	8.1	14.1	51.0			6.4	0.9	1.7	2.1		0.9	1.6	6.1			8.8	30.6	85.1		
8.04	-11.0	12.2	41.0	47.0		6.8	0.8	2.3	2.8		0.7	1.5	5.1	6.2		-4.9	20.1	47.0	52.4	
8.05	-13.6	8.8	19.7	27.2		6.8	0.8	2.0	2.3	2.6	0.8	1.5	5.6	6.9	8.0	-7.6	18.2	43.9	52.5	
8.06	-28.9	17.5	56.9			5.9	0.9	2.0	2.3		0.7	1.9	6.6	7.8		-10.5	26.5	78.8	144.7	
8.07	16.6	17.5	56.9			5.3	0.9	2.3	2.6		0.9	2.0	7.0	8.0		5.1	24.6	60.2	81.4	
8.08	-18.0	13.1	23.0			5.3	0.8	1.4	1.5		0.4	1.6	5.2	6.5		-10.4	41.3	157.4	232.0	
8.09	NOT DIGITIZED																			
8/21 9.01	21.8	6.9	12.7	17.4	22.1	3.3	0.3	0.9	1.1	1.4	0.8	2.0	6.8	8.3	10.4	12.3	7.8	27.1	32.8	39.1
9.02	NOT	DIGITIZED																		

DATE AND RUN	5. RUDDER, degrees					6. HEAVE, ft./sec.²					7. SWAY, ft./sec.²					WAVE STATISTICS INTERPOLATED $H^1/_3$ ft.
	MEAN	RMS	$H^1/_3$	$H^1/_{10}$	$H^1/_{100}$	MEAN	RMS	$H^1/_3$	$H^1/_{10}$	$H^1/_{100}$	MEAN	RMS	$H^1/_3$	$H^1/_{10}$	$H^1/_{100}$	
8/15 6.07	-4.8	9.5	21.6	27.8	38.0	-30.7	13.9	41.9	45.3	49.8	7.5	19.0	56.2	61.9	64.9	
8/20																
8.01	4.6	13.6	32.5	44.7		-1.2	4.3	2.6	3.2	4.7	0.9	1.7	2.1	3.4	13.7	0.69
8.02	9.7	16.5	60.5	62.2		-1.0	3.7	3.6	5.7	8.8	0.7	1.0	2.4	3.4	4.5	0.67
8.03	11.8	8.9	27.5			-2.1	6.9	3.6			1.2	2.9	1.5	2.0		0.65
8.04	-8.8	13.9	49.4	56.9		-1.1	4.4	3.8	5.1	6.4	1.0	0.9	2.7	3.9	6.4	0.83
8.05	-12.2	10.6	29.7	34.9		-1.1	4.1	4.6	6.8	20.8	1.0	1.4	3.3	5.0	15.5	0.98
8.06	-24.0	10.3	28.9	35.3		-1.9	6.8	7.7	8.5		1.0	2.5	5.6	6.5		1.12
8.07	18.9	14.8	35.9	37.7		-1.8	6.3	4.5	5.9		0.7	1.5	3.3	5.2	15.8	1.11
8.08	-14.8	9.2	22.5			-4.3	11.2	9.3			1.3	3.2	4.6	10.3		1.09
8.09	NOT	DIGITIZED														
8/21 9.01	29.3	5.8	16.3	20.3	26.9	-0.8	2.1	7.1	8.7	11.5	0.7	1.7	6.0	7.3	9.1	1.03
9.02	NOT	DIGITIZED														

TABLE E-IV

STATISTICS OF MEASURED MODEL DATA 1973

DATE AND RUN	1. YAW, degrees MEAN	RMS	$H_{1/3}$	$H_{1/10}$	$H_{1/100}$	2. RPM MEAN	RMS	$H_{1/3}$	$H_{1/10}$	$H_{1/100}$	3. PITCH, degrees MEAN	RMS	$H_{1/3}$	$H_{1/10}$	$H_{1/100}$	4. ROLL, degrees MEAN	RMS	$H_{1/3}$	$H_{1/10}$	$H_{1/100}$
8/24																				
10.01	39.5	13.1				4.4	1.1				1.4	2.5				4.9	85.7			
10.02	-2.8	10.7	17.5	37.2		5.3	0.7	1.9	2.2	2.3	0.9	1.8	6.7	8.6	10.5	4.0	16.1	46.0	55.9	103.0
10.03	NOT DIGITIZED																			
10.04	-9.3	3.5	8.0	11.7	17.6	6.9	0.6	2.0	2.5	3.1	1.3	1.2	4.0	5.4	6.8	2.3	11.3	39.4	44.1	51.3
10.05	14.6	23.1				5.9	1.2	1.7	2.0		1.2	2.1	7.1	7.6		11.6	42.3	85.6	137.7	
10.06	-7.1	9.1				6.4	1.1	1.8	2.0		1.3	1.9	6.2	7.4		1.4	39.6	83.0	131.0	
10.07	-9.8	7.6	12.3	15.1		5.3	0.6	1.6	1.9	2.4	1.2	2.1	6.9	8.7	11.2	3.5	22.5	65.6	116.1	
8/27																				
11.01	-7.1	2.4	7.3	9.3	12.2	7.2	0.5	1.5	1.9	2.3	0.6	0.7	2.3	3.0	4.7	2.8	9.6	34.3	41.0	46.6
11.02	-6.5	55.4				5.6	0.7	1.6	2.1		0.8	1.0	3.4	4.4		-5.6	9.3	31.8	39.7	
11.03	-3.4	3.5	7.8	11.4	22.1	7.0	0.6	1.6	2.0	2.5	1.0	0.9	2.9	3.7	5.3	7.9	10.7	38.0	43.5	51.9
11.04	7.5	58.0	149.8			5.0	0.8	1.5	2.1		1.1	1.2	3.9	5.0	5.9	-0.9	13.6	39.6	52.6	
11.05	-9.0	2.9	6.7	9.6	16.3	5.8	0.4	1.2	1.5	1.9	0.7	0.7	2.2	2.8	3.6	0.4	10.1	36.0	43.3	50.2
11.06	-2.9	3.1	7.1	10.1	17.9	5.5	0.5	1.7	1.9	2.2	1.0	1.3	4.6	6.1	9.2	6.6	11.8	41.9	48.0	54.6

DATE AND RUN	5. RUDDER, degrees MEAN	RMS	$H_{1/3}$	$H_{1/10}$	$H_{1/100}$	6. HEAVE, ft./sec.^{2} MEAN	RMS	$H_{1/3}$	$H_{1/10}$	$H_{1/100}$	7. SWAY, ft./sec.^{2} MEAN	RMS	$H_{1/3}$	$H_{1/10}$	$H_{1/100}$	WAVE STATISTICS INTERPOLATED $H_{1/3}$ ft.
8/24																
10.01	14.7	6.4				-18.2	12.8				1.7	9.3				0.70
10.02	8.8	12.4	31.7	37.2	42.5	-1.0	3.3	3.1	4.0	5.9	0.3	0.9	2.3	3.2	7.6	0.72
10.03	NOT DIGITIZED															
10.04	1.9	11.1	34.3	41.3	48.1	-0.5	1.0	2.9	3.9	5.4	-0.2	0.9	2.7	3.2	4.0	0.65
10.05	25.1	12.9	44.0			-4.0	11.9	5.9	9.2		-0.3	2.9	4.1	8.9		0.70
10.06	7.0	11.2	31.7	36.0		-3.8	11.0	6.6	7.6		0.7	4.0	6.6	16.2		0.76
10.07	5.7	11.0	31.8	37.5		-1.7	6.3	7.6	9.2	11.1	-0.2	2.4	5.0	6.5	14.4	1.10
8/27																
11.01	3.5	8.6	24.9	31.3	40.5	-0.6	1.1	3.3	4.2	5.2	0.5	0.5	1.6	2.0	2.6	0.38
11.02	22.8	14.5				-0.4	1.6	5.3	7.1	9.0	0.1	0.8	2.3	2.9	3.5	0.38
11.03	9.0	9.0	26.5	32.5	40.9	-0.6	1.7	4.7	5.7	7.1	0.0	0.8	2.5	3.0	3.9	0.39
11.04	15.1	22.0	44.2	59.5		-0.4	2.1	6.6	8.5	10.8	0.0	1.0	3.3	4.4	5.8	0.39
11.05	0.1	8.6	25.0	31.2	40.0	-0.6	0.9	2.8	3.6	4.5	0.3	0.6	1.9	2.4	3.0	0.49
11.06	11.[illegible]	8.7	24.8	29.1	35.8	-0.8	1.5	4.5	6.2	11.0	0.0	0.9	3.0	4.0	5.5	0.64

TABLE E-IV

STATISTICS OF MEASURED MODEL DATA 1973

DATE AND RUN	1. YAW, degrees					2. RPM					3. PITCH, degrees					4. ROLL, degrees				
	MEAN	RMS	$H^1/_3$	$H^1/_{10}$	$H^1/_{100}$	MEAN	RMS	$H^1/_3$	$H^1/_{10}$	$H^1/_{100}$	MEAN	RMS	$H^1/_3$	$H^1/_{10}$	$H^1/_{100}$	MEAN	RMS	$H^1/_3$	$H^1/_{10}$	$H^1/_{100}$
8/27 11.07	-6.8	5.4	9.4	14.0	29.6	5.6	0.6	1.8	2.2	2.5	1.0	1.6	5.8	7.3	8.7	2.4	12.3	43.9	51.0	63.2
11.08	10.0	16.5	45.1	82.5		5.0	0.8	1.7	2.0		1.3	1.8	5.7	7.5		9.4	29.6	58.4	95.2	
11.09	-0.9	7.6	20.6	42.7	112.6	5.3	0.7	1.9	2.5	5.4	1.4	2.6	6.9	9.2	18.4	8.8	16.4	53.2	78.9	276.5

DATE AND RUN	5. RUDDER, degrees					6. HEAVE, ft./sec^2					7. SWAY, ft./sec^2					WAVE STATISTICS INTERPOLATED $H^1/_3$ ft.
	MEAN	RMS	$H^1/_3$	$H^1/_{10}$	$H^1/_{100}$	MEAN	RMS	$H^1/_3$	$H^1/_{10}$	$H^1/_{100}$	MEAN	RMS	$H^1/_3$	$H^1/_{10}$	$H^1/_{100}$	
8/27 11.07	4.0	10.7	29.6	35.5	42.4	-0.7	1.0	2.9	3.7	5.2	0.0	0.7	2.3	2.8	3.5	0.82
11.08	22.3	10.1	25.1	28.4		-2.3	8.8	7.0	7.9		-0.3	2.3	7.5	12.1		0.88
11.09	16.2	10.8	27.3	33.1	53.8	-1.0	3.4	5.2	6.4	8.2	-0.3	1.8	3.5	4.9	14.9	0.97

TABLE E-IV

STATISTICS OF MEASURED MODEL DATA 1973

DATE AND RUN	1. YAW, degrees					2. SPEED, ft./sec.					3. PITCH, degrees					4. ROLL, degrees				
	MEAN	RMS	$H^1/_3$	$H^1/_{10}$	$H^1/_{100}$	MEAN	RMS	$H^1/_3$	$H^1/_{10}$	$H^1/_{100}$	MEAN	RMS	$H^1/_3$	$H^1/_{10}$	$H^1/_{100}$	MEAN	RMS	$H^1/_3$	$H^1/_{10}$	$H^1/_{100}$
8/28																				
12.01	-3.0	2.8	7.3	9.4	13.1	5.5	0.5	1.7	1.9	2.1	0.7	1.0	3.5	4.5	5.5	4.1	11.2	40.0	46.3	54.4
12.02	7.9	62.7				4.2	0.9	1.0	1.2		1.0	2.9	4.6	5.9	7.4	-5.9	12.4	37.6	71.0	
12.03	-2.1	3.5				6.9	0.6	2.0	2.6		1.1	1.2	4.1	4.3		4.1	13.4	45.2	51.2	
12.04	9.9	12.9				6.1	0.9	1.9	2.2		0.9	1.8	4.5	5.9		9.7	18.5	53.9	79.6	
12.05	3.6	6.5	10.2	15.4	33.7	3.9	0.4	1.3	1.6	2.2	1.0	1.8	6.4	8.0	11.8	5.8	8.0	27.7	34.5	47.5
12.06	6.9	61.6				4.7	0.7	1.3	1.6		1.0	2.0	7.1	9.2		-6.2	12.1	38.4	42.9	
12.07	-1.2	15.4				6.9	1.0				1.2	2.0				9.5	24.5			
12.08	6.1	7.3				4.8	0.8				0.9	2.4				34.1	32.9			
12.09	-12.6	7.1	15.4			4.4	0.5	1.6	2.0	2.3	0.9	2.6	9.6	11.8	13.2	-1.6	13.0	42.8	54.6	96.2
9/5																				
13.01	-8.5	5.7	13.0	17.8		5.4	0.6	1.7	2.0	2.5	0.7	1.4	5.0	6.2	7.3	-0.1	14.4	45.0	52.4	
13.02	-4.4	6.1	13.8	22.4	63.4	5.3	0.6	1.8	2.1	2.6	0.8	1.7	6.1	7.4	8.8	3.3	14.5	51.7	62.5	83.2
13.03	-2.2	4.5	9.9	14.7	23.7	5.3	0.6	1.8	2.1	2.5	1.1	1.6	5.7	7.1	8.7	6.4	12.9	44.6	53.8	65.1

DATE AND RUN	5. RUDDER, degrees					6. SWAY, ft./sec.^{2}					7. SURGE, ft./sec.^{2}					WAVE STATISTICS INTERPOLATED $H^1/_3$ ft.
	MEAN	RMS	$H^1/_3$	$H^1/_{10}$	$H^1/_{100}$	MEAN	RMS	$H^1/_3$	$H^1/_{10}$	$H^1/_{100}$	MEAN	RMS	$H^1/_3$	$H^1/_{10}$	$H^1/_{100}$	
8/28																
12.01	10.4	8.8	25.1	29.5	35.2	1.2	0.8	2.5	3.[illegible]	3.7	-0.1	0.5	1.9	2.4	2.9	0.59
12.02	34.7	7.1	5.1	5.9		1.0	1.5	2.9	4.0	5.3	0.0	2.4	1.8	2.1	2.3	0.64
12.03	8.0	9.8	26.9	29.8		1.1	0.6	1.8	2.0		0.1	0.6	2.2	2.3		0.74
12.04	17.6	14.3				1.0	1.1	4.0	5.9		0.0	0.9	2.8	3.4		0.80
12.05	19.3	8.9	22.9	26.7	32.4	1.1	1.2	4.2	5.2	7.0	0.0	0.9	3.4	4.3	6.5	0.95
12.06	38.8	4.9	4.4	6.9		0.7	1.2	4.4	5.5		0.1	0.9	3.2	4.0		0.97
12.07	7.2	10.2	32.6			1.0	0.9	1.9	2.0		0.3	1.4				1.03
12.08	27.6	7.3				-0.4	2.1				0.6	1.6				1.16
12.09	-1.9	12.3	31.6	38.9	48.0	1.3	1.3	3.1	3.7	4.1						1.17
9/5																
13.01	4.0	10.6	28.2	35.2	48.5	0.7	0.9	2.6	3.3	4.2	-0.1	0.8	2.7	3.6	4.1	0.93
13.02	8.1	10.9	28.6	34.0	45.7	0.6	0.9	2.9	3.7	5.0	0.0	0.9	3.3	4.0	5.2	0.95
13.03	12.4	9.8	26.3	31.2	38.0	0.3	0.9	2.9	3.7	5.0	0.1	0.9	3.1	3.8	4.6	0.99

TABLE E-IV

STATISTICS OF MEASURED MODEL DATA 1973

DATE AND RUN	1. YAW, degrees					2. SPEED, ft./sec.					3. PITCH, degrees					4. ROLL, degrees				
	MEAN	RMS	H 1/3	H 1/10	H 1/100	MEAN	RMS	H 1/3	H 1/10	H 1/100	MEAN	RMS	H 1/3	H 1/10	H 1/100	MEAN	RMS	H 1/3	H 1/10	H 1/100
9/11																				
14.01	0.4	10.6	38.6	65.9		6.5	0.8	1.9	2.3	3.4	0.9	1.2	4.1	5.0	5.9	8.3	17.6	53.9	69.1	
14.02	0.4	10.0	42.8	76.5		6.5	0.7	1.8	2.4		1.1	1.6	5.6	7.0		11.8	20.4	63.5	92.5	
14.03	-2.4	3.8	8.8	12.0	16.7	5.3	0.6	1.8	2.1	2.4	1.1	1.6	5.5	6.8	8.3	5.9	12.3	43.6	49.1	55.9
14.04	[illegible]	6.3	11.8	16.9	31.6	5.2	0.6	1.8	2.1	2.5	1.1	1.7	6.3	9.5	6.6	13.1	45.5	51.9	60.4	60.4
14.05	-5.1	5.5	20.1	39.7		5.5	0.6	2.2	[illegible]	3.1	1.2	1.9	7.0	8.6		3.8	15.7	53.3	64.3	
14.06	-7.8	3.6	10.2	13.7	17.8	5.6	0.7	2.1	2.7	3.3	1.1	1.9	7.4	9.4	11.8	2.0	15.0	51.9	62.4	98.1
14.07	-2.5	3.9	6.8	10.4	19.9	3.6	0.2	0.7	0.9	1.1	1.2	1.5	4.9	6.1	8.3	6.3	7.5	27.5	33.7	40.8
9/12																				
15.01	-2.0	14.0	44.8	61.0		6.6	0.7	1.9	2.3	2.9	0.7	0.8	2.7	3.3	3.8	6.0	16.0	51.4	70.5	
15.02	-7.7	3.4	7.6	10.4	17.5	5.7	0.5	1.5	1.8	2.1	0.8	0.9	3.2	4.0	5.5	1.5	12.6	46.2	54.8	66.1
15.03	2.7	7.0	28.5	54.8		5.5	0.6	1.8	2.0	2.1	0.9	1.4	5.5	6.9		4.7	14.9	51.1	65.9	
15.04	-27.6	6.3	8.3	10.3		4.7	0.7	2.4	2.8		0.7	1.8	6.0	6.5		-13.0	22.1	28.5	29.8	
15.05	-44.1	15.6	13.6	23.8		3.6	0.5	1.3	1.6	2.1	0.9	1.7	6.0	7.7	11.5	-11.3	10.7	31.9	39.6	50.6
15.06	-5.3	7.1	14.5	22.5	30.4	4.5	0.5	1.7	2.1	2.4	1.2	2.6	9.6	11.7	16.7	1.5	11.2	40.0	46.4	55.6

DATE AND RUN	5. RUDDER, degrees					6. SWAY, ft./sec.²					7. SURGE, ft./sec.²					WAVE STATISTICS INTERPOLATED H 1/3 ft.
	MEAN	RMS	H 1/3	H 1/10	H 1/100	MEAN	RMS	H 1/3	H 1/10	H 1/100	MEAN	RMS	H 1/3	H 1/10	H 1/100	
9/11																
14.01	12.1	12.5	37.2	41.4		0.5	1.5	3.0	4.0	5.6	0.0	0.7	2.2	2.6	3.2	0.68
14.02	16.0	13.9	40.3	44.0		[illegible]	0.8	2.3	2.9		0.1	1.0	3.7	4.1		0.75
14.03	12.8	9.5	27.1	30.9	37.1	0.2	1.0	3.1	3.8	5.0	0.1	0.8	2.9	3.6	4.5	0.82
14.04	16.2	10.3	27.5	32.4	41.3	0.1	1.0	3.2	4.1	5.3	0.1	0.9	3.4	4.2	5.1	0.96
14.05	7.8	11.6	32.7	39.8		0.0	0.7	2.2	2.6	3.1	0.0	1.1	3.9	4.8		0.98
14.06	5.5	10.9	29.8	34.9	40.4	0.0	0.7	2.0	2.4	3.1	0.0	1.1	4.1	5.2	6.4	0.99
14.07	13.6	7.5	19.5	23.9	29.6	-0.3	2.0	6.8	8.5	11.0	0.0	0.7	2.2	2.7	3.9	1.04
9/12																
15.01	7.6	13.7	53.4	61.5		0.4	0.6	1.7	2.1	3.1	-0.1	0.4	1.5	2.0	3.3	0.46
15.02	3.4	8.7	26.1	31.3	36.5	0.3	0.5	1.5	1.9	2.3	0.0	0.4	1.7	2.1	2.8	0.60
15.03	9.5	10.0	25.8	30.2		0.3	0.6	1.7	2.1	2.4	0.0	0.8	2.9	3.8		0.88
15.04	-25.7	5.9	17.6	22.0		0.6	1.2	4.0	5.4		-0.1	1.2	3.9	4.2		0.96
15.05	-28.6	9.4	23.2	25.5		0.5	1.6	5.8	7.8	10.6	0.0	0.9	3.3	4.3	6.7	1.07
15.06	2.4	11.4	25.9	32.2	42.0	-0.1	1.1	3.7	4.6	6.1	0.0	1.4	5.2	6.3	8.8	1.29

TABLE E-IV

STATISTICS OF MEASURED MODEL DATA 1973

DATE AND RUN	1. YAW, degrees					2. SPEED, ft./sec.					3. PITCH, degrees					4. ROLL, degrees				
	MEAN	RMS	$H^1/_3$	$H^1/_{10}$	$H^1/_{100}$	MEAN	RMS	$H^1/_3$	$H^1/_{10}$	$H^1/_{100}$	MEAN	RMS	$H^1/_3$	$H^1/_{10}$	$H^1/_{100}$	MEAN	RMS	$H^1/_3$	$H^1/_{10}$	$H^1/_{100}$
9/14																				
16.01	0.9	16.5	59.2	67.8		6.3	0.7	2.0	2.3	2.6	0.7	1.0	3.4	4.4	5.6	0.6	16.2	48.6	57.9	76.2
16.02	1.9	12.4	47.5	69.6		6.8	0.7	1.9	2.2		0.9	1.2	4.3	4.8		2.1	18.2	55.1	77.8	
16.03	0.1	12.0	32.2			6.4	0.7	2.3	2.7		1.2	1.9	7.1	9.7		0.1	20.8	63.7	72.0	
16.04	-6.6	8.9	26.0	31.7		6.8	0.8	2.4	2.9	3.3	0.9	1.7	6.0	7.5	8.9	-4.2	11.2	36.3	42.5	53.3
16.05	7.5	11.6	26.0	38.5		6.8	0.9	2.6	3.1	3.5	0.9	1.9	6.4	7.7	9.3	4.0	12.5	41.7	49.6	57.5
16.06	2.2	9.0	27.3	45.7		5.4	0.7	2.3	2.6		0.9	2.5	9.5	11.0		0.8	12.8	42.1	55.3	
16.07	NOT DIGITIZED																			
16.08	-44.4	19.2	23.8	36.7		3.3	0.5	1.1	1.7	2.6	0.9	2.3	7.9	10.1	12.7	-9.4	10.7	36.9	45.8	57.2

DATE AND RUN	5. RUDDER, degrees					6. SWAY, ft./sec.^{2}					7. SURGE, ft./sec.^{2}					WAVE STATISTICS INTERPOLATED $H^1/_3$ ft.
	MEAN	RMS	$H^1/_3$	$H^1/_{10}$	$H^1/_{100}$	MEAN	RMS	$H^1/_3$	$H^1/_{10}$	$H^1/_{100}$	MEAN	RMS	$H^1/_3$	$H^1/_{10}$	$H^1/_{100}$	
9/14																
16.01	2.6	20.9	71.3	74.5		0.6	0.6	1.7	2.0	2.4	-0.2	0.5	1.9	2.4	3.0	0.68
16.02	2.6	13.3	51.3			0.4	0.8	2.6	3.1		-0.2	0.7	2.4	2.8		0.74
16.03	1.4	14.3	41.6	46.1		0.3	1.0	3.1	3.8		0.1	1.1	3.6	5.1		0.88
16.04	-7.5	12.6	33.0	40.7		0.4	0.8	2.3	2.8	3.5	-0.2	0.9	3.4	4.2	5.0	1.00
16.05	9.1	13.0	28.8	39.[illegible]		0.1	0.8	2.6	3.6	5.2	-0.1	1.0	3.5	4.2	4.7	1.11
16.06	3.7	10.5	28.7	34.2		0.3	0.7	2.2	2.7	3.3	-0.2	1.4	5.2	5.9		1.23
16.07	NOT DIGITIZED															
16.08	-34.2	8.9	22.9	35.4		0.4	1.9	6.7	8.6	11.5	-0.1	1.2	4.2	5.6	7.1	1.28

TABLE E-IV

STATISTICS OF MEASURED MODEL DATA 1973

DATE AND RUN	1. YAW, degrees					2. PITCH, degrees					3. ROLL, degrees					4. RUDDER, degrees				
	MEAN	RMS	$H^1/_3$	$H^1/_{10}$	$H^1/_{100}$	MEAN	RMS	$H^1/_3$	$H^1/_{10}$	$H^1/_{100}$	MEAN	RMS	$H^1/_3$	$H^1/_{10}$	$H^1/_{100}$	MEAN	RMS	$H^1/_3$	$H^1/_{10}$	$H^1/_{100}$
9/17																				
17.01	3.1	7.7	27.7	32.3		0.7	0.8	2.6	3.3	4.2	2.1	11.0	35.6	44.6	66.0	3.6	9.7	31.6	42.4	49.7
17.02	4.6	9.1	30.8	44.1		0.8	1.0	3.5	4.4	5.6	3.0	12.0	38.2	44.9	70.1	5.0	10.3	30.7	39.9	47.8
17.03	10.2	4.0	11.4	15.9	20.3	0.7	1.4	5.0	6.2	7.3	4.4	12.6	44.7	54.1	66.9	12.8	7.9	20.0	24.6	33.1
17.04	2.9	7.1	22.4	35.6		0.6	1.3	4.7	5.9	8.0	1.4	12.1	43.2	52.1	72.2	4.1	9.0	23.6	33.4	37.5
17.05	-13.6	11.2	10.2			0.5	1.6	5.0	5.3		-11.4	21.6	37.3	42.1		-12.1	7.6	16.2	19.1	
17.06	-10.0	7.3	16.0	25.1		0.6	1.3	5.0	6.2	7.2	-6.3	13.3	44.0	51.4	65.9	-10.4	10.1	23.4	30.1	
17.07	3.3	15.8	53.4	74.5		0.7	1.8	6.5	7.8	9.4	0.2	13.0	54.3	75.9	3.9	3.9	15.7	40.0	49.4	
17.08	6.3	11.9	28.8	46.5		.6	1.9	7.1	9.0	10.7	1.7	12.6	43.2	51.6	74.9	7.8	12.6	28.1	36.1	
17.09	0.1	7.3	13.9	20.2		0.7	2.1	7.9	10.0	13.1	-1.2	9.8	35.7	43.2	51.2	1.1	8.7	18.6	28.1	37.9
9/18																				
18.01	5.9	7.8	21.5	28.1		1.0	1.4	4.6	5.6	6.6	4.8	15.8	52.1	70.7		6.5	10.2	26.[illegible]	37.2	
18.02	NOT DIGITIZED																			
18.03	11.5	5.4	12.5	20.4	31.3	1.1	1.4	5.2	6.6	8.7	5.9	12.6	44.8	52.4	64.4	13.6	9.3	19.9	25.1	35.4
18.04	6.6	9.1	27.5	40.8		1.1	1.6	6.2	7.9	10.8	2.7	13.8	47.9	58.3	100.7	7.3	11.6	23.1	33.6	51.0

DATE AND RUN	5. HEAVE, ft./sec.^{2}					6. SWAY, ft./sec.^{2}					7. SURGE, ft./sec.^{2}					WAVE STATISTICS INTERPOLATED $H^1/_3$ ft.
	MEAN	RMS	$H^1/_3$	$H^1/_{10}$	$H^1/_{100}$	MEAN	RMS	$H^1/_3$	$H^1/_{10}$	$H^1/_{100}$	MEAN	RMS	$H^1/_3$	$H^1/_{10}$	$H^1/_{100}$	
9/17																
17.01	-0.8	0.8	2.4	3.1	4.3	0.4	0.6	1.9	2.3	3.0	-0.3	0.4	1.4	1.8	2.4	0.54
17.02	-1.4	0.6	2.0	2.6	3.5	0.3	0.6	1.8	2.2	2.9	-0.2	0.5	1.9	2.4	3.1	0.59
17.03	-1.6	0.9	2.8	3.9	5.5	0.2	0.9	3.0	3.6	4.3	-0.3	0.7	2.7	3.3	3.9	0.69
17.04	-1.5	0.5	1.6	2.1	2.7	0.3	0.6	2.0	2.7	3.5	-0.5	0.7	2.6	3.3	4.3	0.75
17.05	-2.5	6.0	2.6	3.0		0.8	2.0	5.5	11.2		-0.3	1.1	4.4	5.5		0.79
17.06	-1.7	0.6	1.8	2.3	2.9	0.5	0.7	2.3	3.0	3.9	-0.5	0.7	2.8	3.6	4.3	0.82
17.07	-1.6	0.6	2.1	3.0	5.3	0.3	0.7	2.1	2.8	4.6	-0.4	1.0	3.6	4.3	4.9	0.93
17.08	-1.7	0.6	1.9	2.7	5.0	0.2	0.8	2.6	3.5	5.5	-0.4	1.1	3.9	5.0	6.0	0.97
17.09	-1.7	0.5	1.7	2.2	2.8	0.1	0.6	2.1	2.5	3.1	-0.5	1.1	4.3	5.4	7.1	1.02
9/18																
18.01	-1.3	2.4	3.2	4.1	6.0	0.2	1.0	3.1	3.7	4.9	0.1	0.8	2.7	3.4	5.6	0.70
18.02	NOT DIGITIZED															
18.03	-1.2	0.9	3.1	3.9	5.0	0.1	1.0	3.4	4.3	5.4	0.0	0.8	2.9	3.6	4.6	0.78
18.04	-1.3	1.3	1.7	2.3	3.6	0.1	0.8	2.5	3.2	4.3	0.0	0.9	3.5	4.4	6.0	0.83

TABLE. E-IV

STATISTICS OF MEASURED MODEL DATA 1973

DATE AND RUN	1. YAW, degrees					2. PITCH, degrees					3. ROLL, degrees					4. RUDDER, degrees				
	MEAN	RMS	H1/3	H1/10	H1/100	MEAN	RMS	H1/3	H1/10	H1/100	MEAN	RMS	H1/3	H1/10	H1/100	MEAN	RMS	H1/3	H1/10	H1/100
9/18																				
18.05	-5.1	9.0	18.4	21.2		1.3	1.7	6.2	7.8	9.0	-4.0	14.9	47.0	53.0	57.9	-7.4	10.9	24.5	30.3	
18.06	27.9	13.8				1.4	1.6	5.3	6.8		15.0	20.1	66.2	104.8		27.5	10.4			
18.07	7.7	7.1	27.7	41.3		1.1	1.6	6.2	7.9	8.6	4.4	13.4	42.2	52.2	88.1	8.6	9.8	27.6	34.3	
9/19																				
19.01	7.7	6.5	21.3	27.3	34.9	1.1	1.1	3.7	4.6	5.5	5.9	11.5	38.4	45.6	57.1	7.9	9.4	25.1	34.2	44.5
19.02	5.6	6.7	24.8	30.4		1.2	1.0	3.3	4.4	6.3	4.3	11.4	38.5	46.4	68.4	5.2	8.5	27.4	39.7	45.8
19.03	5.8	5.9	14.2			1.1	1.4	4.2	5.4		5.8	10.5	32.2	34.5		5.8	7.0	15.1	20.1	
19.04	13.7	8.6	33.5	52.9		1.3	1.2	4.3	5.4	6.0	11.5	16.6	53.6	69.8		16.0	11.3	33.4	40.0	
19.05	-1.2	7.9	27.1	33.9		1.1	0.9	2.8	3.6	4.3	-1.5	12.4	39.3	44.3	50.5	-2.1	10.6	34.1	42.8	
19.06	4.9	7.6	30.4	52.4		1.2	0.9	3.1	3.8	4.4	3.2	11.5	37.4	51.2		4.3	8.5	26.3	32.0	
9/28																				
20.01	6.6	5.7				1.3	1.8	6.3	6.7		12.6	18.4	61.9	69.9		8.8	7.6	21.3		
20.02	-0.7	5.8	14.9	20.9	28.8	1.1	1.3	4.7	5.5	6.5	0.4	11.8	40.5	50.6	72.2	-0.7	6.3	17.1	23.8	32.9
20.03	4.3	9.2	30.3			1.4	1.6	4.9	6.1		6.8	21.6	61.2	66.4		5.7	11.7	28.1	36.6	

DATE AND RUN	5. HEAVE, ft./sec.^{2}					6. SWAY, ft./sec.^{2}					7. SURGE, ft./sec.^{2}					WAVE STATISTICS INTERPOLATED H1/3 ft.
	MEAN	RMS	H1/3	H1/10	H1/100	MEAN	RMS	H1/3	H1/10	H1/100	MEAN	RMS	H1/3	H1/10	H1/100	
9/18																
18.05	-1.2	1.9	2.0	2.7	3.7	0.2	1.0	2.6	4.0	12.1	0.2	1.0	3.6	4.6	5.9	0.89
18.06	-1.6	2.5	3.9	4.9		-0.1	1.2	4.0	5.7		0.3	1.0	3.4	4.5		0.93
18.07	-1.4	0.6	1.9	2.3	3.2	-0.1	0.8	2.3	2.8	3.4	-0.1	0.9	3.5	4.3	4.9	0.94
9/19																
19.01	-1.1	0.8	2.7	3.5	4.6	0.0	0.7	2.2	2.8	3.7	0.1	0.6	2.0	2.5	2.8	0.67
19.02	-1.1	0.7	2.2	2.8	3.6	0.0	0.6	1.8	2.2	3.0	0.2	0.5	1.8	2.4	3.3	0.71
19.03	-1.1	1.0	3.0	3.5		0.1	0.6	1.8	2.1		0.1	0.6	1.9	2.3		0.73
19.04	-1.4	2.4	3.5	4.6	6.1	-0.2	0.8	2.7	3.3	4.8	0.2	0.7	2.5	3.3	4.9	0.74
19.05	-1.1	0.6	1.9	2.5	4.2	0.1	0.7	2.1	2.6	3.2	0.2	0.5	1.6	2.0	2.3	0.64
19.06	-1.2	0.6	1.9	2.6	4.1	0.0	0.5	1.7	2.2	2.8	0.2	0.5	1.8	2.2	2.4	0.52
9/28																
20.01	-1.5	0.7	2.1	2.7		0.0	0.7	[illegible]	2.7		0.1	1.1	3.7	3.9		0.73
20.02	-1.2	0.5	1.7	2.3	4.7	-0.1	0.6	1.9	2.5	3.7	-0.1	0.7	2.7	3.2	3.8	0.79
20.03	-1.3	0.9	2.5	3.1		-0.2	0.9	2.7	3.6		0.4	0.9	2.7	3.3		0.86

TABLE E-IV

STATISTICS OF MEASURED MODEL DATA 1973

DATE AND RUN	1. YAW, degrees					2. PITCH, degrees					3. ROLL, degrees					4. RUDDER, degrees				
	MEAN	RMS	$H^1/_3$	$H^1/_{10}$	$H^1/_{100}$	MEAN	RMS	$H^1/_3$	$H^1/_{10}$	$H^1/_{100}$	MEAN	RMS	$H^1/_3$	$H^1/_{10}$	$H^1/_{100}$	MEAN	RMS	$H^1/_3$	$H^1/_{10}$	$H^1/_{100}$
9/28																				
20.04	NOT	DIGITIZED																		
20.05	-1.5	6.4	11.7	14.5		1.2	1.7	6.3	7.6	8.9	-0.3	15.0	44.6	51.4		-1.4	6.0	16.8	20.9	

DATE AND RUN	5. HEAVE, ft./sec.²					6. SWAY, ft./sec.²					7. SURGE, ft./sec.²					WAVE STATISTICS INTERPOLATED $H^1/_3$ ft.
	MEAN	RMS	$H^1/_3$	$H^1/_{10}$	$H^1/_{100}$	MEAN	RMS	$H^1/_3$	$H^1/_{10}$	$H^1/_{100}$	MEAN	RMS	$H^1/_3$	$H^1/_{10}$	$H^1/_{100}$	
9/28																
20.04	NOT	DIGITIZED														
20.05	-1.5	2.0	2.9	3.8	4.5	0.0	0.9	2.5	3.4	8.9	0.0	1.0	3.7	4.4	4.9	0.95

TABLE E-IV

STATISTICS OF MEASURED MODEL DATA 1973

DATE AND RUN	1. YAW, degrees					2. SPEED, ft./sec.					3. PITCH, degrees					4. ROLL, degrees				
	MEAN	RMS	$H^1/_3$	$H^1/_{10}$	$H^1/_{100}$	MEAN	RMS	$H^1/_3$	$H^1/_{10}$	$H^1/_{100}$	MEAN	RMS	$H^1/_3$	$H^1/_{10}$	$H^1/_{100}$	MEAN	RMS	$H^1/_3$	$H^1/_{10}$	$H^1/_{100}$
10/4																				
21.01	-3.0	5.5	20.9			2.9	0.7	2.2	2.2		-1.3	3.6	10.4	11.4		-4.8	12.6	42.0	48.9	
21.02	6.4	5.1	11.4	15.9		2.9	0.6	2.3	3.0		-0.3	3.6	13.3	15.8		13.0	15.3	38.4	49.0	
21.03	2.5	6.1	12.6	16.7		2.9	0.5	1.8	2.3	3.1	-0.8	3.2	10.3	12.4	14.3	6.4	15.8	41.5	49.9	
21.04	-11.4	6.2	12.4	20.0		2.9	0.5	1.6	2.0		-2.9	3.4	10.2	13.6		-24.4	16.8	41.3	55.8	
21.05	-12.4	8.5	11.7	12.5		2.9	0.6	2.1	2.7		-3.8	4.9	10.7	11.3		-26.9	14.5	44.8	50.1	
21.06	-14.4	4.2	9.4	12.2	16.6	2.9	0.6	2.1	2.7	3.3	-2.7	3.0	10.0	12.6	15.8	-35.0	13.1	38.0	43.5	
11/1																				
22.01	NOT DIGITIZED																			
22.02	"	"	"																	
22.03	"	"	"																	
22.04	"	"	"																	
22.05	"	"	"																	

DATE AND RUN	5. RUDDER, degrees					6. SWAY, ft./sec.[2]					7. SURGE, ft./sec.[2]					WAVE STATISTICS INTERPOLATED
	MEAN	RMS	$H^1/_3$	$H^1/_{10}$	$H^1/_{100}$	MEAN	RMS	$H^1/_3$	$H^1/_{10}$	$H^1/_{100}$	MEAN	RMS	$H^1/_3$	$H^1/_{10}$	$H^1/_{100}$	$H^1/_3$ ft.
10/4																
21.01	31.8	6.3	21.2	24.2		3.0	6.2	19.5	21.7		-1.5	1.9	5.7	6.8		1.11
21.02	25.4	4.8	15.6	18.5	22.2	-4.7	8.4	22.5	29.9		-0.9	2.1	7.4	8.9		1.28
21.03	25.7	4.1	13.2	16.5	20.4	-1.9	7.6	20.4	25.2		-1.2	1.7	5.8	7.1	8.0	1.35
21.04	24.2	4.2	13.1	16.0	18.4	10.0	7.9	22.2	30.3		-2.4	1.8	5.6	7.3		1.33
21.05	22.7	4.4	11.8	13.2		10.1	7.3	19.5	22.0		-2.7	2.4	5.5	5.8		1.30
21.06	10.7	2.8	8.5	10.3	12.3	15.5	6.6	18.6	23.1	29.6	-2.3	1.6	5.4	6.9	8.6	1.29
11/1																
22.01	NOT DIGITIZED															
22.02	"	"														
22.03	"	"														
22.04	"	"														
22.05	"	"														

TABLE E-IV

STATISTICS OF MEASURED MODEL DATA 1974

DATE AND RUN	1. YAW, degrees					2. PITCH, degrees					3. ROLL, degrees					4. RUDDER, degrees				
	MEAN	RMS	$H^1/_3$	$H^1/_{10}$	$H^1/_{100}$	MEAN	RMS	$H^1/_3$	$H^1/_{10}$	$H^1/_{100}$	MEAN	RMS	$H^1/_3$	$H^1/_{10}$	$H^1/_{100}$	MEAN	RMS	$H^1/_3$	$H^1/_{10}$	$H^1/_{100}$
10/5																				
30.01	ROLL	DECAY																		
30.02	-6.1	3.6	7.5	12.6		1.1	2.1	6.6	8.2	11.6	0.4	3.0	11.2	13.7	16.3	-4.2	4.3	8.2	11.4	18.7
30.03	NOT	DIGITIZED																		
30.04	-3.4	2.5	7.1	9.4		1.2	1.6	5.1	6.2	7.4	-0.1	1.6	4.8	5.7	6.3	-1.6	2.0	5.2	6.6	
30.05	0.2	3.0	8.2	11.9		1.4	2.2	6.9	8.3	10.4	3.8	2.0	6.3	7.6	9.6	0.6	1.7	8.4	11.7	
30.06	6.2	4.3	8.5	14.0		0.6	2.6	8.7	11.0	15.5	3.1	13.4	12.3	16.5	21.7	0.7	3.4	7.7	11.6	

DATE AND RUN	5. SPEED, ft./sec.					6. SWAY, ft./sec.²					7. SURGE, ft./sec.²					WAVE STATISTICS INTERPOLATED $H^1/_3$ ft.
	MEAN	RMS	$H^1/_3$	$H^1/_{10}$	$H^1/_{100}$	MEAN	RMS	$H^1/_3$	$H^1/_{10}$	$H^1/_{100}$	MEAN	RMS	$H^1/_3$	$H^1/_{10}$	$H^1/_{100}$	
10/5																
30.01	ROLL	DECAY														
30.02	3.3	0.4	0.7	0.9	1.1	-0.3	0.7	2.5	3.0	3.6	0.1	0.7	2.4	3.1	4.5	0.73
30.03	NOT	DIGITIZED														
30.04	5.4	0.3	0.9	1.0	1.2	-0.5	0.6	1.8	2.2	2.5	0.2	0.5	1.7	2.1	2.6	0.66
30.05	5.1	0.4	0.9	1.1	1.3	-0.7	0.5	1.6	1.9	2.5	0.3	0.8	2.5	3.1	4.0	0.87
30.06	3.3	0.3	0.7	0.9	1.2	-0.7	1.0	3.6	4.4	4.9	-0.2	1.1	3.6	4.5	6.5	0.97

TABLE E-IV

STATISTICS OF MEASURED MODEL DATA 1974

DATE AND RUN	1. YAW, degrees					2. PITCH, degrees					3. ROLL, degrees					4. SPEED, ft./sec.				
	MEAN	RMS	$H^1/_3$	$H^1/_{10}$	$H^1/_{100}$	MEAN	RMS	$H^1/_3$	$H^1/_{10}$	$H^1/_{100}$	MEAN	RMS	$H^1/_3$	$H^1/_{10}$	$H^1/_{100}$	MEAN	RMS	$H^1/_3$	$H^1/_{10}$	$H^1/_{100}$
10/15																				
31.01	-0.6	4.2	7.4	10.8		3.8	3.7	8.1	12.7	31.0	-6.3	5.4	7.7	10.6	20.5	6.4	0.5	1.3	1.6	3.9
31.02	-4.7	2.3	5.0	6.9	9.1	0.8	1.8	5.7	7.0	8.6	-0.4	2.7	9.8	13.2	20.3	5.6	0.3	0.9	1.1	1.4
31.03	-2.0	3.5	8.4	12.2		0.7	1.9	6.2	7.8	10.1	0.4	2.5	8.6	10.3	12.7	3.8	0.2	0.7	0.8	1.0
31.04	-5.3	2.1	4.1	6.4	11.6	0.6	1.5	4.7	5.7	6.9	-1.5	2.4	8.6	11.5	15.5	5.8	0.3	0.9	1.1	1.5
31.05	-2.5	4.2	12.5	16.5		0.7	1.9	5.9	7.5	9.7	0.2	2.7	9.9	12.8	16.7	3.5	0.3	0.7	0.9	1.1
31.06	0.6	7.0	16.1	22.5	37.4	0.2	1.9	7.1	8.8	11.1	2.1	11.5	37.2	44.9	64.8	5.9	0.6	2.0	2.4	2.8
31.07	1.4	9.1	20.5	33.5		0.2	2.0	7.1	9.0	11.3	3.4	14.5	43.1	62.8		5.9	0.7	2.0	2.4	2.9

DATE AND RUN	5. HEAVE, ft./sec.²					6. SWAY, ft./sec.²					7. SURGE, ft./sec.²					WAVE STATISTICS INTERPOLATED $H^1/_3$ ft.
	MEAN	RMS	$H^1/_3$	$H^1/_{10}$	$H^1/_{100}$	MEAN	RMS	$H^1/_3$	$H^1/_{10}$	$H^1/_{100}$	MEAN	RMS	$H^1/_3$	$H^1/_{10}$	$H^1/_{100}$	
10/15																
31.01	-1.6	2.8	8.3	10.4	13.8	3.5	1.4	3.8	5.4	14.4	1.5	2.1	4.6	9.7	33.8	0.58
31.02	-1.4	2.3	7.3	9.3	13.2	-0.4	1.2	4.0	5.2	7.2	-0.2	0.6	2.1	2.6	3.3	0.55
31.03	-1.3	1.9	6.3	8.4	11.0	-0.6	1.0	3.3	4.0	4.6	-0.3	0.7	2.3	3.0	3.8	0.57
31.04	-1.3	2.1	6.7	8.5	11.4	-0.7	0.9	3.0	4.0	5.7	-0.4	0.5	1.7	2.2	2.6	0.56
31.05	-1.4	1.8	5.8	7.4	10.1	-0.9	1.0	3.6	4.1	4.6	-0.3	0.7	2.2	2.3	3.6	0.53
31.06	-1.6	0.6	1.8	2.4	3.3	-0.8	0.7	2.2	2.7	3.6	-0.5	1.0	3.9	4.8	6.0	0.67
31.07	-1.8	1.7	1.8	2.2	2.8	-0.9	0.8	2.2	2.7	3.4	-0.5	1.1	3.8	4.9	6.3	0.74

☆ U.S. GOVERNMENT PRINTING OFFICE: 1975— 629-915/730